UNIVERSITY OF LIVERPOOL

PhD Thesis

Identification & Characterisation of Transcription Factors Affecting the Circadian System of *Arabidopsis thaliana*.

Author:
Andrew Tindall

Supervisor:
Prof. Anthony Hall

Thesis submitted in accordance with the requirements for the degree of Doctor of Philosophy

in the

Institute of Integrative Biology

June 2016

Abstract

Identification & Characterisation of Transcription Factors Affecting the Circadian System of *Arabidopsis thaliana*.

Doctor of Philosophy

by Andrew Tindall

ABSTRACT: Circadian clocks are endogenous, persistent, temperature-compensating timekeepers which provide temporal organization of biological processes from cyanobacteria to man. Within plants, the circadian clock plays an important role in controlling desirable agronomic traits, integrating a number of abiotic stress signalling pathways. Much of our current understanding of the plant clock has come from the model organism *Arabidopsis thaliana*, with the vast majority of studies using null mutants and transgenic luciferase reporters. However, whilst our models of the transcriptional-translational feedback loops underlying the clock have become increasingly complex in the last 20 years, the regulation of several key components of the clock on the transcriptional level remains unknown. There is a need for new components in the model to fill in these gaps.

Many known components of the plant clock are transcription factors. It was hypothesised therefore that the systematic screening and analysis of putative transcription factors would reveal novel circadian phenotypes. To this effect, a library of 338 hormone inducible transcription factor over-expression lines was screened with the novel delayed fluorescence assay to identify transcription factors giving circadian period phenotypes. Over-expression allows the investigation of partially redundant genes, and of those normally expressed within a hard-to-assay tissue. Twenty-one such genes were identified. Through the use of *in silico* tools to identify circadian expression patterns and promoter motifs, this shortlist was analysed for predicted interactions and modes of regulation. Traditional *pCAB2:LUC+* luciferase markers were used to further phenotype the TF lines, providing a deeper understanding of the effect of the gene on the circadian clock, whilst knock out libraries and hypocotyl elongation assays under monochromatic light were employed to further characterise the genes in question. In this way, the longlist was reduced to three putative transcription factors which gave a circadian phenotypes of interest: *INDOLE-3-ACETIC ACID INDUCIBLE 11*, the freezing-response regulator *MYBC1*, and *B-BOX DOMAIN PROTEIN/ CONSTANS-LIKE 15 (BBX13/COL15)*.

Acknowledgements

石の上に四年 (Four years on a rock)
Japanese Traditional.

I would like to thank many people who have helped me through the completion of this project. First amongst them, my supervisors: Prof Anthony Hall at the University of Liverpool, and Minami Matsui at RIKEN Yokohama, for their guidance and patience throughout the four year project. I was incredibly lucky to work in two dynamic, vibrant, and incredibly different laboratories, and will remember fondly all I have learned during my time with them.

Without the considerable help of Dr Peter Gould, Setsuko Shimada, Yoshito Oka and Takeshi Yoshizumi in the training and development of my practical laboratory skills, this project would not have been possible. Their hospitality, and warmth made me feel part of their dynamic research teams, whether at home or abroad. My time in RIKEN Yokohama was made far easier through the tireless work of Noboko Kimura and Mai Sato in the IPA office, and to them I am grateful. I'd also like to thank Mark Greenwood, Dr Jane Pulman, Patrick Diaz, and Dr Ben Wareham for their advice and assistance on the analysis and bioinformatics sections of the project.

A doctorate is not formed in a vacuum, and I am thankful for my friends both in the UK and in Japan for their support throughout the project and, in particular, towards the end. This includes (but is by no means limited to!) Dr Jordan Savage, Ben Murray, Jade Waller, The Bathers, Jessica Middleton-Pugh, Tobias Bardhun, Ambar Hegde, Victor Rambach, Rachel Amberg, the Iron Thieves, and all those who deserve my thanks for their support (and tolerance) throughout, and to whom I am eternally indebted. Special mention goes to everyone in the Tokyo Gaijin RFC, to whom I owe a large chunk of my sanity during the placement in Japan - Go You Good Thing!

I would finally like to say thank you to my parents, whose perennial support and consolation has been with me always, whether 200 or 6000 miles away.

Contents

List of Figures

List of Tables

Abbreviations

ANOVA	**An**alysis **O**f **Va**riance
CAB	**C**HLOROPHYLL **A**/B **B**INDING PROTEIN
CCA1	**C**IRCADIAN **C**LOCK **A**SSOCIATED **1**
CCD	**C**harge-**C**oupled **D**evice
CCA1	**C**IRCADIAN **C**LOCK **A**SSOCIATED **1**
CHE	**C**CA1 **H**IKING **E**XPEDITION
ChIP Seq	**Ch**romatin **I**mmuno-**P**recipitation **Seq**uencing
CRY	**CRY**PTOCHROME
DD	Constant **D**ark
Dex	**Dex**amethasone
DNA	**D**eoxyribo**N**ucleic **A**cid
EE	**E**vening **E**lement
ELF	**E**AR**L**Y **F**LOWERING
FFT-NLLS	**F**ast **F**ourier **T**ransform, **N**on-**L**inear **L**east **S**quares normalisation
GFP	**G**reen **F**luorescent **P**rotein
GI	**GI**GANTEA
GOF	**G**oodness **O**f **F**it
GR	**G**lucocorticoid **R**eceptor
Kan	**Kan**amycin
LD	**L**ight-**D**ark cycle
LHY	**L**ATE-ELONGATED **HY**POCOTYL
LOV	**L**ight, **O**xygen or **V**oltage
LUC	**Luc**iferase
LUX	**LUX** ARRYTHMO
mRNA	**M**essenger **R**ibo**n**ucleic **A**cid

MS	**M**urashige and **S**koog
MYB	**MYB** DNA-BINDING DOMAIN
NI	**N**ight **I**nhibitor loop
OX	**O**ver-e**X**pression
PCR	**P**olymerase **C**hain **R**eaction
Phy	**Phy**tochrome
PRR	**P**SEUDO **R**ESPONSE **R**EGULATOR
RAE	**R**elative **A**mplitude **E**rror
RO	**R**everse **O**smosis purification
RT-PCR	**R**everse **T**ranscriptase **P**olymerase **C**hain **R**eaction
RVE8	**RVE**ILLE **8**
SCF	**S**kp **C**ullin **F**-box
SD	**S**tandard **D**eviation
SMART	**S**election **M**arkers and **A**dvanced **R**eproductive **T**echnologies
SR	**S**pectrum **R**esampling
TOC1	**T**IMING **O**F **C**AB EXPRESSION **1**
WT	**W**ild **T**ype
ZTL	**Z**EI**TL**UPE

Chapter 1

Introduction

1.1 Introduction to Circadian Systems

1.1.1 Circadian Clocks Are Universal & Important Organisers of Biological Processes

"Everything changes and nothing stands still." - Heraclitus of Ephesus.

Life on planet earth is defined by diurnal changes. Light intensity, humidity, and ambient temperature all rise and fall throughout the twenty four hour period. Even in a mild, maritime climate like that of the UK, daily highs and lows in temperature can vary by ten to fifteen degrees. Fortunately such changes are rhythmic, regular and easily predictable as the earth turns on it's axis. Survival in such a constantly changing geophysical environment requires a similar daily physiological and behavioural periodicity from organisms. From sleep/wake cycles in humans to the opening and closing of flowers, we are all aware of how organisms possess biological rhythms. A large number of these rhythms are not merely reactionary responses to environmental changes, but persist in

the absence of external cues. Many of these endogenous rhythms are controlled by the circadian system - an internal timekeeper with an approximately 24 hour period.

For a timekeeper to be considered circadian, it must fulfil three essential criteria. Firstly, it must have an endogenous, free-running period of approximately 24 hours. All circadian clocks must persist in a constant environment in the absence of diurnal oscillations of exogenous cues. This is to distinguish circadian clocks to rhythms that are merely responses to environmental change.

Secondly, circadian clocks are "entrainable" (i.e. they can be adjusted and "re-set") by external stimuli called "zeitgebers" - most notably light and heat. Perhaps the most apparent manifestation of this is the phenomena of "jet-lag", which a person moving between two different time zones will generally exhibit before their circadian clock entrains and synchronises to local time.

Finally, circadian clocks must temperature compensate - that is, they must maintain their rhythm and periodicity over a range of temperatures. To demonstrate why this is significant, let us consider a ten degree Celsius increase in temperature. The resulting change in the rate of reaction can be calculated as so:

$$Q_{10} = \left(\frac{R_2}{R_1}\right)^{10/(T_2 - T_1)}$$

Where:

R is the rate.

T is the temperature, in celsius.

Typically in biological systems, the Q_{10} coefficient is 2 to 3 - in other words, a ten degree increase in temperature results in a doubling or trebling of the reaction rate. Obviously, for an endogenous timekeeper to run two to three times as fast at noon as it does at night is less than ideal for coordinating biological processes. As such, for a process to be considered circadian, its Q_{10} must remain approximately 1 as the temperature increases, corresponding with no net change in its rate with changing temperature (Reyes et al., 2008).

Circadian timekeepers organise biological processes from cyanobacteria (Xu et al., 2003) and plants (Harmer, 2009) to man (Ko and Takahashi, 2006). They are near-universal and indispensable organisers in eukaryotic organisms. Given that circadian clocks are essentially ubiquitous in nature, and their implications far-reaching, any understanding of physiology or biological signalling would be incomplete unless viewed and considered from a circadian perspective.

1.1.2 Auto-Regulatory Feedback Loops Form the "Gears" of the Circadian Clock

Auto-regulatory feedback loops lie at the core of circadian clockworks. Broadly speaking, an auto-regulatory feedback loop consists of two or more components that reciprocally regulate each other's function.

Let us consider a simple, abstracted auto-regulatory feedback loop. Component A induces component B, whether through controlling its abundance on the transcriptional, translational or post-translational level, through degradation of protein or RNA, by moving it spatially to its site of action, or through activating it (i.e. increasing the relative

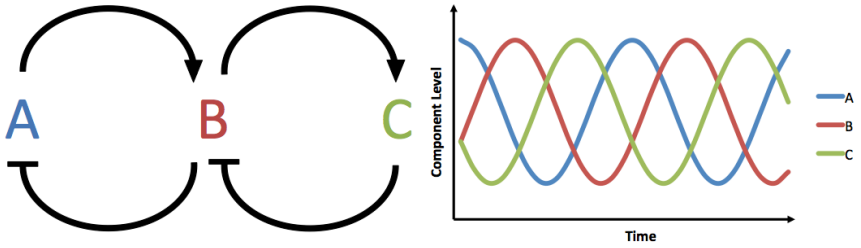

FIGURE 1.1: Overview of Interlocking Feedback Loops

Components A and B form a feedback loop, whereby Component A induces Component B which, in turn, suppresses Component A (Left). This results in sinosoidal oscillations of Components A and B. Component B also forms a feedback loop with Component C in much the same way. As the two loops contain a shared component, they are interlocking. This increases fidelity of the oscillator and allows multiple phasing of clock outputs, as seen in graph of relative abundance (Right).

abundance of its active form). Component B in turn suppresses Component A, through any of the previously suggested mechanisms. This turns off its own expression. In order to "close" the loop, the levels (or activity) of Component B must decrease over time (Figure 1.1). In biological systems, this can occur through passive denaturation of proteins, active degradation, or diffusion back into an inactive spacial domain. Taken together, this results in sinusoidally oscillating levels of the two components, with the two components being in anti-phase. Such an oscillator can be constructed artificially - a three-component oscillator consisting of repressor proteins (termed a "repressilator") been constructed on a single plasmid in *E. coli* (Elowitz and Leibler (2000), Figure 1.2). The protein LacI from *E. coli* inhibits the transcription of the second gene, *tetR*, which in turn inhibits the gene *cI* from the λ phage. CI protein inhibits *lacI* expression, closing the loop. This system oscillates with a regular period, as reported by a TetR-dependent GFP reporter system, and persists in *E. coli* over time. This shows that a transcription loop is sufficient to build an oscillatory system.

In living systems, these feedback loops can comprise of many components acting in synergy to perform an auto-regulatory function. Multiple components operating together allow extra levels of control - incorporating, for example, environmental inputs to the clock. Components may also participate in more than one auto-regulatory loop, facilitating crosstalk between different feedback loops in a phenomena referred to as "interlocking". These interlocking loops are analogous to the cogs in a mechanical clock - they oscillate, and as they do so they turn other cogs, driving the clock (Figure 1.1).

Increasing numbers of clock loops have been uncovered in circadian clockworks. A larger number of interlocking loops contributes to increased robustness (Brunner and Káldi, 2008, Cheng et al., 2001, Saithong et al., 2010). Connections between the loops perform a "pace-keeping" function, where the fidelity of one loop is dependent on the fidelity of the others (Brown et al., 2012, Gonze and Goldbeter, 2006). It also allows differential phasing of outputs. In other words, an increasingly byzantine clock architecture contributes to the functionality of the circadian clock.

1.1.3 External Stimuli "Entrain" the Circadian Clock

Whilst circadian clocks must be able to persist in the absence of a changing environment (known as "free-run"), effective clocks must also be capable of "resetting" and entraining by external stimuli (Roenneberg et al., 2003). Whilst 24hr day cycles are predictable, the actual hours of sunlight and the related variations in temperature differ with the cycle of seasons. Readjusting the circadian clock so that "dawn" correlates with the observed rising of the sun is of vital importance for proper phasing that is required in order for the clock to be of benefit. Clocks are entrained by "zeitgebers" (German for "time giver"), or external environmental cues. These cues consist primarily of diurnal cycles in light and temperature, with the hormone melatonin being important for clock resetting in

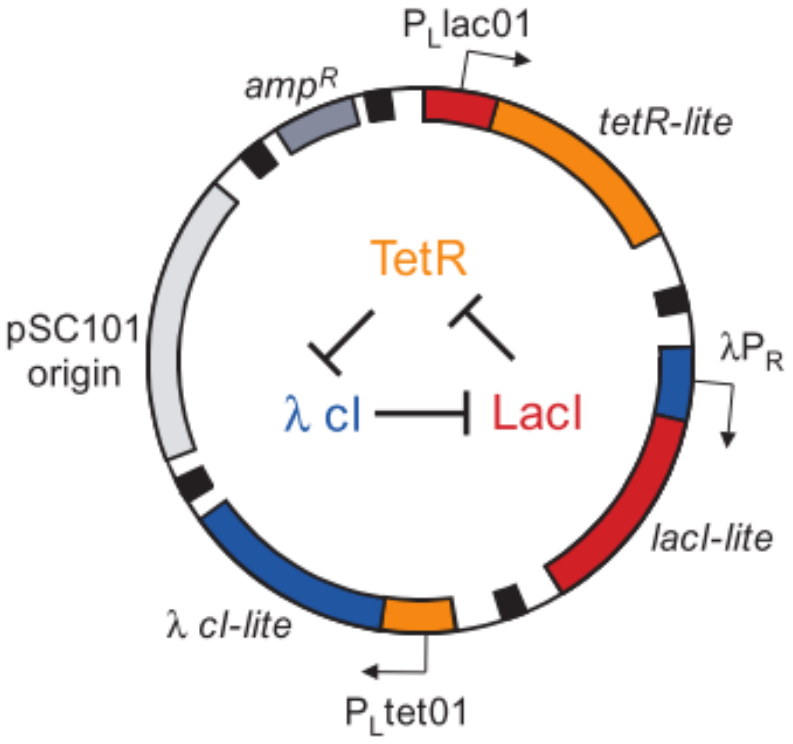

FIGURE 1.2: The Artificial Repressilator in *E. coli*

Three repressors of transcription, *LacI*, *tetR* and *λcI*, are incorporated in a single plasmid. These reciprocal repressors form a loop (see centre) that oscillates in level. The gene sequences were modified with a carboxyl terminal tag was placed at the 3' end of each repressor, which is recognised by proteases which target the proteins for degradation. Other plasmids carrying reporters under the control of each repressor (not shown) allow real-time imaging of the feedback loop, and are analogous to oscillator outputs. Modified from Elowitz and Leibler (2000).

animals (Cajochen et al., 2003) and a whole host of endogenous and exogenous cues in plants (discussed in detail below). In this manner, the clock is able to adapt and persist in a seasonally changing environment.

1.1.4 Many Organisms, Many Clocks

Circadian clocks have been found in practically all eukaryotes that have been investigated. Clocks have been observed and characterised throughout the animal kingdom: in mammals (Albrecht and Eichele, 2003), fish (Hirayama et al., 2005), birds (Gwinner and

Brandstätter, 2001), insects (Tomioka and Matsumoto, 2010) and nematodes (Hasegawa et al., 2005, Jones, 2010). Whilst there is considerable molecular and functional homology between the clocks in the animal kingdom, the clocks in the fungal (Liu and Bell-Pedersen, 2006, Salichos and Rokas, 2010) and plant kingdoms appear to have evolved independently (Harmer, 2009). Clocks have also been observed in single cell eukaryotes including yeast (Eelderink-Chen et al., 2010) and the algae *Chlamydomonas reinhardtii* (Mittag et al., 2005) and *Ostreococcus taurii* (Xu et al., 2003). In prokaryotes, too, circadian clocks have been observed in photosynthetic cyanobacteria from genuses as diverse as *Synechococcus* (Kondo et al., 1993), *Synechocystis* (Aoki et al., 1997), *Trichodesmium* (Chen et al., 1998), *Rhodospirillum* (Van Praag et al., 2000), and *Rhodobacter* (Min et al., 2005). These clocks are based around the KaiA/B/C gene cluster, and appear highly conserved, implying that circadian clocks evolved early in one of the oldest lineages extant on earth today (Dvornyk et al., 2003).

Circadian clocks are present in various kingdoms of life, and are highly conserved in those lineages. These clocks fulfil similar functions, yet their components show little to no homology across kingdoms. The major clock genes belong to entirely unrelated families (Cashmore et al., 1999). As such, circadian clocks in the various kingdoms of life are examples of convergent evolution. This, combined with the near ubiquity of the circadian clock, implies a strong pressure to evolve a circadian system and, once gained, retain it in order to thrive in the diurnally varying environments found on earth. Circadian biology stands at the crossroads between disparate signalling pathways, a master integrator, organiser and regulator that is integral to any understanding of a biological system.

1.2 The Clock in *Arabidopsis*

The clock in *Arabidopsis* consists of a number of interlocking feedback loops of various types. There are loops of proteins that function on the transcriptional, post-transcriptional and post-translational levels, as well as non-protein components which oscillate between different chemical states or different spacial configurations.

1.2.1 The Transcriptional Circadian Clock

The earliest identified *Arabidopsis* circadian components formed a transcriptional-translational feedback loop (TTL) that is the basis of all subsequent clock models. First amongst these was *TIMING OF CAB2-EXPRESSION 1 (TOC1)/PSEUDO RESPONSE REGULATOR 1 (PRR1)*, identified through imaging of the oscillation in transgenic luciferase driven by the circadian-regulated *CHLOROPHYLL A BINDING PROTEIN 2 (CAB)* promoter (Millar et al., 1995a). The *toc1-1* mutant conveyed a short period phenotype to circadian rhythms in *pCAB2:LUC* and stomatal CO_2 conductance in dark-grown seedlings (Somers et al., 1998b). TOC1 was later shown to have transcription factor function, negatively regulating a wide range of genes (Gendron et al., 2012), and is aided in this process by the accessory components LUX ARRHYTHMO (LUX) (Hazen et al., 2005, Helfer et al., 2012, Onai and Ishiura, 2005), CCA1-HIKING EXPEDITION 1 (CHE) (Pruneda-Paz et al., 2009), EARLY FLOWERING 3 (ELF3) (Nusinow et al., 2011) and ELF4 (McWatters et al., 2007).

Two more transcription factors were identified as part of this loop. Constitutive overexpression of the MYB-domain transcription factor *CIRCADIAN CLOCK ASSOCIATED 1 (CCA1)* abolished the circadian rhythm of several genes with dramatically different phases and resulted in plants with lengthened hypocotyls and delayed flowering

(Wang and Tobin, 1998). These two phenotypes are known clock outputs (Johansson and Staiger, 2014, Nusinow et al., 2011). Furthermore, the expression of both the endogenous *CCA1* and the related *LATE ELONGATED HYPOCOTYL (LHY)* gene was suppressed in the knock-out, demonstrating that these genes were co-regulated in a feedback loop. Similarly, the dominant *lhy* mutant exhibited late hypocotyl and flowering time phenotypes as well the abolition of circadian expression rhythms in *LHY* transcript levels (Schaffer et al., 1998). Increased *LHY* expression from a transgene caused the endogenous gene to be expressed at a constant level, suggesting that *LHY* was part of a feedback circuit that regulated its own expression. These two related genes are partially redundant and are required to maintain circadian rhythms (Mizoguchi et al., 2002).

These three components form a self-regulatory feedback loop. Both CCA1 and LHY are transcriptional factors that bind to and negatively regulate the the promoter region of *TOC1* (Alabadí et al., 2001). Conversely, TOC1 regulates *CCA1* and *LHY* expression. These three core clock genes and suite of accessory proteins form the first transcriptional loop of the *Arabidopsis* circadian clock, named the "Morning Loop" due to its role co-ordinating expression of dawn-related transcription events.

TOC1 is the mediator of interlocking crosstalk between the Morning Loop and the "Evening Loop", the second we will consider. Modelling *in silico* showed that the single-loop model was unable to account for all experimental observations (Locke et al., 2005a). Extension of the model to fit observed data introduced a hypothetical component with mRNA peak at dawn, repressed through the action of TOC1, that fitted the expression profile of flowering-time regulator *GIGANTEA (GI)*(Locke et al., 2005b). GI was initially identified as a late flowering mutant (Rédei, 1962), and was subsequently shown to have a role in the circadian clock distinct from that in regulating flowering time (Lee

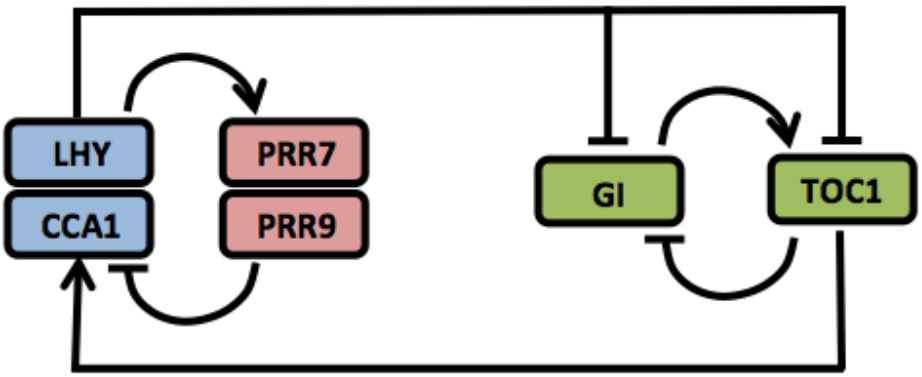

FIGURE 1.3: Model of the Transcriptional/Translational Clock in Arabidopsis.

Elements of the night inhibitor and evening oscillators are shown in red and green, respectively. The morning loop forms the outer loop with *CCA1/LHY* and *TOC1*, and is woven into the other two loops. Based on Pokhilko et al. (2010).

et al., 2005).

The third and final transcriptional loop represses CCA1/LHY through the activity of *PSEUDO-RESPONSE REGULATOR 7 (PRR7)* and *PRR9* - two genes within the same family as *TOC1* (Makino et al., 2000). These two genes are partially redundant, with the *prr7-3 prr9-1* double mutant showing dramatic and more than additive period lengthening in the light and becoming arrhythmic in constant darkness (Salomé and McClung, 2005). This final loop is known as the "Night Inhibitor (NI), due to arresting the perception of dawn through suppression of *CCA1/LHY* transcription during the subjective night (Pokhilko et al., 2010).

Several transcriptional activators have been identified as important accessory clock components, with subtler circadian defects as mutant phenotypes. The *REVEILLE (RVE)*

genes , similarly to their homologues *CCA1/LHY*, bind to the evening element (EE) (Rawat et al., 2011), a motif over-represented in the promoters of evening phased clock-regulated genes (Harmer et al., 2000). Unlike CCA1 and LHY, which act as repressors of the evening element, RVE8 directly induces the transcription of EE-containing genes (Farinas and Mas, 2011, Hsu et al., 2013), associates with the *PRR5* and *TOC1* promoters (Farinas and Mas, 2011, Rawat et al., 2011), and thus forms a negative feedback loop. Two close homologues RVE4 and RVE6 play partially redundant roles with RVE8, with multiple null-mutants having more severe phenotypes (Hsu et al., 2013), and protein levels which peak in the afternoon (Rawat et al., 2011). CCA1 and LHY have also been shown to repress several other evening genes which are circadian clock components required for the maintenance and sustenance of rhythms, including the night-time repressor of clock gene expression *LUX ARRHYTHMO (LUX)* (Hazen et al., 2005, Helfer et al., 2012), the CCA1-activating *BROTHER OF LUX ARRHYTHMO (BOA, aka NOX)* (Dai et al., 2011), and the repressors *EARLY FLOWERING 3 (ELF3)* and *ELF4*, known as the Evening Complex (Herrero et al., 2012).

Whilst the transcriptional-translational loops formed the core of the earliest clock models (Figure 1.3), they are insufficient to describe all observed phenotypes (Pokhilko et al., 2010, Seo and Mas, 2014). Evidently, additional parts of the clockwork must exist. Furthermore, the investigations that have lead to the development of this clock model have all considered whole plants, averaging and pooling phenotypes across different tissues and/or groups of plants. This assumes that the circadian clock is identical in all tissue types, and at different developmental phases. Whilst the TTL model forms the cornerstone of our understanding, there is a significant amount of the circadian network which is built around this foundation.

1.2.2 Post-Transcriptional Regulation in the Circadian Clock

This transcriptional-level model is a far from complete picture. Component levels and functionality can be controlled on multiple levels, as can their outputs, and not only through differential timing of transcript abundance. A solely transcription model is incapable of explaining the observed levels of clock protein abundance and the mutant phenotypes observed in a variety of environments. Protein level can be adjusted through control of messenger RNA (mRNA) translation or through protein degradation. The activation of proteins through cofactors or covalent modification can regulate the pool of active, effective protein within the cell. Additionally, the subcellular location of proteins is manipulated throughout the diurnal cycle to regulate the clock and its outputs.

1.2.2.1 Regulation on the RNA Level

Degradation of mRNA provides a powerful means for controlling gene expression. Whilst transcription-level control proceeds at a more leisurely pace, when fast responses are to be achieved the rapid decay of mRNAs is necessary to alter the level of gene expression. This is implicated as a key factor in generating the sharp, transient peak of LHY protein levels at dawn, necessary for the robustness and resetting of the circadian clock. Translational induction of LHY mRNA and, hence, increased levels of LHY protein, coincides with acute down regulation of *LHY* transcription (Kim et al., 2003). mRNA degradation is also key in the induction and regulation of clock outputs (Gutierrez et al., 2002, Lidder

et al., 2005).

1.2.2.2 Physical Interaction & Direct Binding

Physical interaction and recruitment of clock proteins through direct binding is also implicated in clock control. ELF4 and ELF3 proteins are capable of forming a complex *in vivo* and *in planta*, as demonstrated via yeast two-hybrid assay and fluorescence resonance energy transfer (FRET) respectively, with the central domain of ELF3 required for this interaction (Herrero et al., 2012). This central domain is required for mutant phenotype complementation, with ELF4 localising ELF3 into nuclear bodies.

In *Arabidopsis thaliana* a tripartite complex composed of ELF4, ELF3, and LUX - known as the evening complex - modulates daily rhythms in gene expression and growth through transcriptional regulation. These three genes are coexpressed, with peak transcript levels around dusk (Doyle et al., 2002, Onai and Ishiura, 2005). They associate with one another to form a complex, proper complex formation of which is required for correct phasing of downstream transcripts, including *PRR9* (Herrero et al., 2012). ELF4 and ELF3 code for sequence-unrelated proteins with no known functional domains, whilst LUX is a GARP transcription factor (Hazen et al., 2005, McWatters et al., 2007, Onai and Ishiura, 2005, Thines and Harmon, 2010). The recruitment and cooperation of these disparate factors is essential in granting them their circadian function.

Yet more core oscillator genes are regulated as a result of physical interactions. Perhaps the best known is that of ZTL and TOC1, resulting in the degradation and gating of TOC1 (discussed in detail below in section 1.2.2.3). Additionally, TOC1 has been shown to physically interact with PRR3 (Para et al., 2007) as well as several members

of the PHYTOCHROME INTERACTING FACTOR bHLH transcription factor family (Yamashino et al., 2003). Further, the ability of CCA1 and LHY to form hetero- and homo-dimers is of notable importance for the circadian clock. As each contains a single *MYB* domain yet two such domains are required for DNA binding, it seems likely that, for CCA1/LHY as well as several other proteins, the formation of alternate complexes at different points in the diurnal cycle will be found to have wide implications for clock function and its communication with its outputs.

1.2.2.3 Regulation of Protein Level

The abundance of many clock proteins is under post-translational control, and the evening loop in particular shows considerable amounts of regulation at the protein level. The GI protein regulates the evening loop through direct binding and stabilization of the F-box protein ZEITLUPE (ZTL) in the presence of light (Kim et al., 2007). ZTL is part of a Skp/Cullin/F-box (SCF) E3 ubiquitin ligase complex which binds proteins and tags them with one or more molecules of ubiquitin, which targets them for degradation (Han et al., 2004, Kiba et al., 2007). Other homologues of ZTL within the ADO/FKF/LKP/ZTL family have been implicated as required for this process, including LOV KETCH PROTEIN 2 (LKP2/FKL2/ADO3) (Schultz et al., 2001, Yasuhara et al., 2004) and ADO3/FKF1. Indeed, similar GI interactions through the LOV domain in a light-dependent manner have been observed for FKF1 (Fore et al., 2001, Nelson et al., 2000) and LKP2 (Kim et al., 2007). Stabilised ZTL directly interacts with TOC1 and PRR5 and is necessary for the targeting for their degradation by the proteosome ubiquitination pathway (Fujiwara et al., 2008, Kiba et al., 2007, Más et al., 2003). Additionally, TOC1

binds directly with PRR3 in a manner that interferes with ZTL, preventing its recruitment to the SCF complex and its subsequent degradation by the proteosome (Para et al., 2007). In this way ZTL both regulates the clock, and is regulated itself by the clock, through protein-protein interaction.

1.2.2.4 Phosphorylation & Covalent Modification

Phosphorylation can regulate the clock through regulating the functionality of CCA1. Phosphorylation is required for homodimer formation and normal function of CCA1, a process mediated by the Ser/Thr protein kinase CASEIN KINASE II (CK2) (Sugano et al., 1998, 1999), with lines constitutively expressing an engineered form of CCA1 that cannot be phosphorylated by CK2 exhibiting an as-wild type circadian phenotype, effectively rescuing the overexpression phenotype (Daniel et al., 2004). Furthermore, the over-expression of CK2 regulatory subunits (and, hence, the upregulation of CK2 activity) results in a shortening of circadian period (Portolés and Más, 2007). In this way, covalent modification of clock genes can result in their activation and up-regulation, not only their degradation, providing "fine-tuning" of the clock and providing the system with a faster response to stimuli than through transcriptional control alone.

Phosphorylation also regulates clock proteins through a degradation pathways independent from ZTL. PRR3, 7 and 9 protein levels are modulated in a post-translational manner that does not involve ZTL or its homologues. Kinase-mediated phosphorylation has been implicated in the regulation of their degradation (Farré and Kay, 2007, Gallego and Virshup, 2007) however the causative agents still remain elusive. Additionally, 102 phosphorylated peptide residues exhibit changes in abundance in response to circadian

rhythms, with oscillatory phosphorylation quantified in ELF4 and PRR3 (Choudhary et al., 2015). These include proteins influencing transcriptional regulation, translation, metabolism, stress and phytohormones-mediated responses. Furthermore, the *elf4-211* allele, wherein a serine-to-leucine substitution removes a kinase substrate (Kolmos et al., 2009), has no circadian rhythms in phosphorylation and as a consequence is unable to form the evening complex through interaction with ELF3 (Choudhary et al., 2015). This interaction is vital for clock function (McWatters et al., 2007). It seems possible that post-translational control will emerge as an increasingly complex dimension of the circadian clock, especially in efforts to understand the integration of the entrainment and output pathways into the core oscillator.

Circadian rhythms can persist in the presence of transcriptional inhibitors. In the unicellular pico-alga *Ostreococcus tauri*, which possesses many circadian features homologous to that in *Arabidopsis* including a *CCA1/TOC1* feedback loop, rhythms persist in the absence of transcription, as demonstrated through translational reporters, the rhythmic oxidation of peroxiredoxin proteins and the absence of phase "resetting" following transitive inhibition of transciption in free run (O'Neill et al., 2011). Peroxiredoxins are conserved markers of circadian rhythms across bacteria and archaea, as well as being found in all three eukaryotic kingdoms (Edgar et al., 2012). Oscillations in the oxidation state of peroxiredoxins probably reflect an endogenous rhythm in the generation of reactive oxygen species (O'Neill and Reddy, 2011)

In the cyanobacteria *Synechococcus*, a cluster of three genes within the *KaiA/B/C* operon has been implicated as a circadian oscillator (Ishiura et al., 1998), operating in complex to phosphorylate each other (changing their function), and this phosphorylation loop can

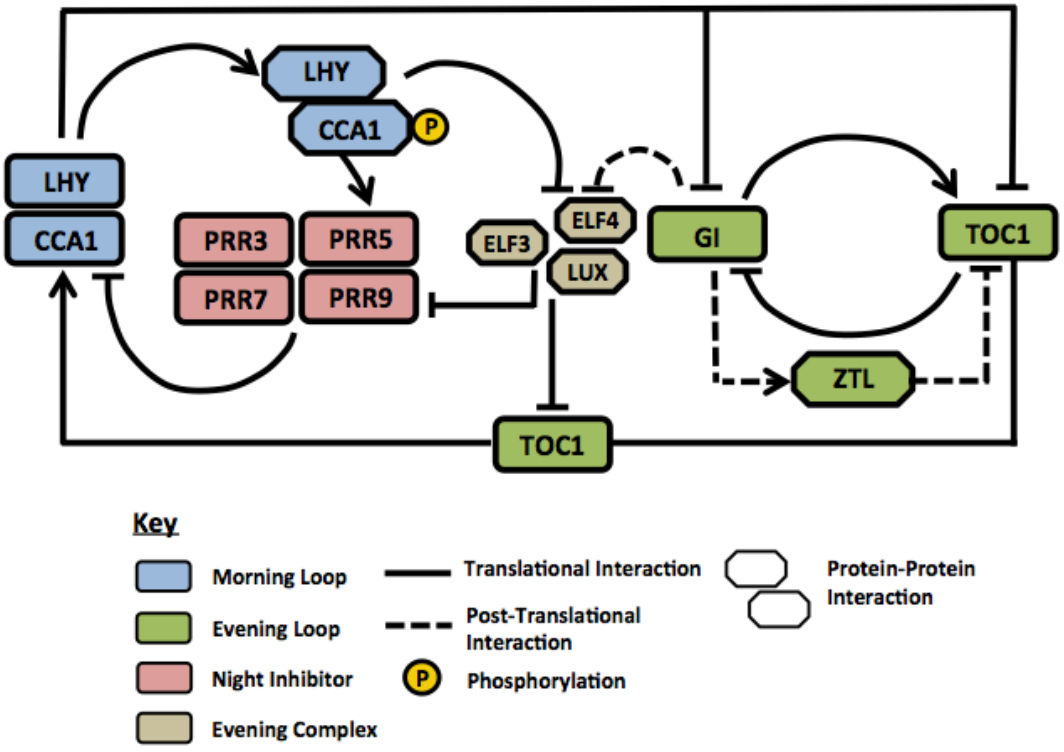

FIGURE 1.4: Model of the Transcriptional/Translational/Post-Translational Circadian Clock in Arabidopsis.

As Fig 1.3, expanded to incorporate post-transcriptional elements. Post-translational modification of CCA1/LHY and the formation of heterodimer is required for the formation of the PRR NI complex. ZTL suppresses TOC1 through proteosomal degradation, and is in turn stabilised by GI through direct binding. ELF3/4 and LUX aid TOC1 in its suppression of *LHY/CCA1*, and do form protein complexes. Based on Pokhilko et al. (2010).

be reconstituted from protein components alone without transcription *in vitro* (Nakajima et al., 2005). In light of this, it seems possible that the original, basal clock was primarily a non-transcriptional one based on cycles of protein modification, which has subsequently been expanded and adorned with additional loops on different levels, increasing clock fidelity and resulting in the highly divergent clocks we observe today in plants, insects and mammals.

1.2.3 Non-Protein Oscillators of the Circadian Clock

The oscillators of the circadian system are not only limited to protein components. The intracellular and subcellular levels of several small organic and inorganic molecules fluctuate throughout the diurnal cycle in a manner that persists in free-run conditions and affects the clock itself, implicating them as part of the circadian system.

Calcium signals have long been implicated as second messengers and signal integrators in multiple branches of the plant signalling network, regulating stomatal closure and opening (Allen et al., 2001, Sanders et al., 2002), the establishiment of symbiosis in root hairs in legumes (Gleason et al., 2006, Shaw and Long, 2003), tip growth patterning in pollen tubes (Hepler et al., 2001, Sanders et al., 1999) and root hair cells (de Montaigu et al., 2014, Monshausen et al., 2008), as well as heat shock (Saidi et al., 2009, Zhang et al., 2009) and salt stress responses (Kiegle et al., 2000, Tracy et al., 2008). Calcium, too, has a place in the circadian clock. Through the use of imaging systems based on the transgenic calcium-sensitive luminescent protein aequorin, whereby fluorescence intensity is directly proportional to the concentration and availability of free calcium ions (Hearn and Webb, 2014), circadian oscillations of cytosollic and chloroplastic free calcium can be observed in free-run, and the peaks of these signals can be shifted by re-entrainment with light-dark signals (Johnson et al., 1995). Once entrained, chloroplastic free calcium oscillates with a circadian period in constant darkness, although not in constant light. Additionally, the mutant *toc1-1* has differential effects on rhythms in free cytosolic calcium concentration and on rhythms in *CAB2* expression (Xu et al., 2007).

Calcium ions can affect and regulate intracellular events through binding with calmodulin proteins which, in turn, regulate many processes. Calmodulin-dependent protein kinases have been shown to directly phosphorylate the *Drosophilla melanogaster* circadian gene *CLOCK (CLK)* in the presence of calcium and are integral to light entrainment of the clock in that organism (Butcher et al., 2002). In *Arabidopsis* and other plants, the role of these circadian calcium signals is unclear but the amplitude of the oscillations (c. 350 nM) is sufficient to activate signalling pathways regulating both physiology and gene expression (Dodd et al., 2010, Love et al., 2004). It has therefore been posited that calcium signals form a distinct loop of the circadian clock, integrating stress signals and in turn regulating outputs through calmodulin-dependent kinases.

Cyclic ADP-Ribose (cADPR) is an intracellular signalling molecule that forms a loop within the circadian clock. cADPR is a cytosolic agent promoting calcium ion release from internal vacuolar stores (Allen et al., 1995) cADPR-regulated transcript sets obtained by microarray analysis correlate with the known circadian-regulated transcriptome, in both abundance and phase (Dodd et al., 2009). Internal cADPR concentration oscillates with a circadian rhythm and the cADPR signaling antagonist nicotinamide inhibits circadian cytoplasmic Ca^{2+} oscillations. Additionally, the circadian clock and its outputs are altered by disruption of cADPR signalling, as demonstrated through transcript abundance analysis of *CCA1*, *TOC1* and *LHY*, as well as through imaging with the *pCAB2:LUC* reporter (Dodd et al., 2009).

1.2.4 Entrainment Pathways in the Circadian Clock

1.2.4.1 Light is the Principle Zeitgeber

Circadian clocks are entrainable by external stimuli. This provides the biologically essential function of clock resetting within a diurnal environment that changes in length with the cycle of seasons. These stimuli range from diurnally-oscillating abiotic stimuli to signals from within the plant. By far the most influential zeitgeber in field conditions, light modulates the circadian clock in multiple ways. There are three distinct types of light signals which plants sense and respond to - red (600-700nm wavelength), far red (>700nm) and blue light (400-500nm). All three types of light modulate and entrain the circadian clock.

Blue light is capable of entraining the circadian clock. Cryptochromes are a family of principle blue-light sensors in many signalling processes, and both *CRY1* and *CRY2* are required for phytochrome signalling into the clock (Devlin and Kay, 2000). However, they are not required for rhythmicity - in contrast to the mammalian clockwork, where cryptochromes form part of the core oscillator (Kume et al., 1999) and mice lacking functional cryptochromes are completely arrhythmic (van der Horst et al., 1999). Mutants in *phyB* also have lengthened periods by up to 3 hrs when grown under constant low fluence blue light (i.e. 3-5 μmolm^{-2} s^{-1})(Somers et al., 1998a); however this occurs indirectly through suppression of CRY2 through physical binding (Más et al., 2000).

In addition to cryptochromes, blue light mediates the circadian clock through the action of phototropins, a family of blue-light dependent sensors. Phototropins are required for the maintenance of certain kinds of circadian rhythms in constant low-intensity blue

light. The rhythm of chloroplastic Photosystem II (PSII) efficiency, as measured through Chlorophyll a Fluorescence, is a reporter of the circadian clock in the chloroplast, and is affected by the nuclear oscillator. Phototropins are required for the persistence of this oscillation in constant low-intensity blue light, however they have no effect on the levels of circadian gene expression in the nucleus (Litthauer et al., 2015). This demonstrates the differences between the modulation of circadian outputs in distinct subcellular compartments - phototropins are required for these rhythms in the chloroplast, yet are not apparently required for oscillations in the nuclear clock, suggesting further levels of complexity in regulation of clock within distinct organelles.

Red and far-red (FR) light is sensed primarily through phytochromes. Limiting red light input, either by reducing fluence rate or the abundance of photoreceptors, lengthens the period of the circadian clock in *Arabidopsis* (Millar et al., 1995b). Phytochrome B (PhyB) is the primary high-intensity red light photoreceptor involved in entraining the circadian clock, with null mutants losing their responsiveness to RL (Somers et al., 1998a).

Tissue-specific expression of Phy A, B, C, D, and E is tightly regulated by the clock (Toth et al., 2001). PhyC protein levels, as reported through a PHYC::LUC+ construct, have very weak rhythms with extremely low amplitude; however PHYC has clear circadian oscillations on the mRNA level, implicating regulation on the post-transcriptional level (Toth et al., 2001). As such, the expression of additional phytochromes is indicative of a multi-directional crosstalk between the clock, light signalling and other as-yet unclear pathways.

PhyA is the only phytochrome transducing the FR light input into the circadian clock

(Yanovsky et al., 2001). Resetting of the clock by FR light requires *PHYA*, *FHY1* and *FHY3* (Yanovsky et al., 2000, 2001). FHY1/3 are downstream signalling components in the PhyA-mediated FR response pathway, and are required for nuclear localisation of phyA (Lin et al., 2007). FHY3 forms a complex activating *ELF4* transcription during the day to regulate its diurnal expression (Li et al., 2011). Whilst there is evidence that this activating complex may contain phyA (Saijo et al., 2008), HY5 (a component of the blue-light response) also associates with FHY3 at the *ELF3* promoter, suggesting integration of FR and blue light signalling (Li et al., 2010).

In addition to the canonical light sensor pathways, light directly regulates the levels of circadian clock components. ZTL contains a Light-Oxygen-Voltage domain, and its activity is regulated by light levels. Light-dependent auto-phosphorylation of the LOV domain modulates ZTL's ability to associate with the stabilising protein GI (Kim et al., 2007). *ZTL* is constitutively expressed at the translational level, but clock regulated at a post-translational level via GI binding and stabilisation (Demarsy and Fankhauser, 2009, Kim et al., 2007). As ZTL is a component of a SCF ubiquitin ligase complex responsible for marking proteins for degradation, blue light stabilisation has a far reaching effect on the levels of multiple circadian clock components. ZTL protein accumulates in the late evening and, following nightfall, provides a strong dusk signal that brings about a rapid decrease in the levels of various proteins via the SCF-Ubq complex. GI-mediated, light-dependent stabilisation of ZTL is required for TOC1 degradation at the onset of night(Han et al., 2004), and the ZTL-mediated degradation of other PRR proteins, and PRR5 in particular, is also highly dependent on light quality and intensity (Kiba et al., 2007, Para et al., 2007).

Whilst phytochromes and cryptochromes are "universal" light sensors involved in numerous circadian-independent light signalling events, as opposed to light sensing clock components like *ZTL*, they cannot simply be grouped together and labelled as clock "inputs". Expression of both families of light sensor is regulated by the circadian clock (Bognár et al., 1999, Harmer et al., 2000, Toth et al., 2001). In this sense they are much more like light-sensing clock components, blurring the already fuzzy boundaries between clock input components and clock outputs considerably. Perhaps these overlapping classifications are unnecessary; either way, the regulation of phytochrome and cryptochrome expression by the clock is valuable in demonstrating how deeply integrated the circadian clock is in the plant, influencing major pathways and with control integrated across multiple levels.

1.2.4.2 Temperature Compensation & Entrainment

Along with the variance in light, the most apparent diurnally variable stimulus for plants is temperature. As previous noted, circadian clocks must temperature compensate (that is to say, they must run at comparable speeds across a biologically relevant range of temperatures). Although the circadian system's response to temperature is mostly one of compensation, *Arabidopsis* clocks are also capable of entrainment by diurnal thermocycles. Rhythms in several clock related genes can be reset or entrained by thermocycles, and this process requires *PRR7/9* (Salomé and McClung, 2005) and *ELF4* (McWatters et al., 2007). However, separate loops of the circadian clock are differentially regulated by temperature, with cycles of the clock output *CAT3* being entrainable by temperature cycles, but not the TOC1-dependent loops regulating expression of *CAB2* (Michael and McClung, 2003). It appears that, whilst the circadian clock responds to short-term

changes in temperature through compensation, it is capable of "remembering" trends of temperature change throughout the diurnal cycle and integrating them to increase clock fidelity.

1.2.4.3 Soluble Sugars Entrain the Circadian Clock

Sugar has been shown to directly entrain the circadian clock, and by far the most characterised example of this occurs in roots. Sucrose perturbs expression of clock genes in root far more severely than in shoots, and the root clock is synchronised by diurnal changes in sucrose phloem traffic from the shoot (James et al., 2008). The addition of sucrose to the growth medium shortens the circadian period when grown in continuous-light free-run conditions by c. 1 hr (Knight et al., 2008). Throughout the day, sucrose levels within the plant increase and decrease diurnally in line with photosynthetic rates which, in turn, are affected by light availability. Carbon fixation, assimilation and starch metabolism are under circadian control at the transcriptional level in *Arabidopsis* (Dodd et al., 2005, Graf et al., 2010, Lu et al., 2005, Noordally et al., 2013, Stitt and Zeeman, 2012), and there is also evidence from microarray analysis that sucrose solutes directly affect clock genes on the transcriptional level (Bläsing et al., 2005). Sucrose thus functions as a long-range signalling molecule for entraining the clock and, in the absence of light, is the primary zeitgeber in the root.

Mathematical studies putatively identified *GIGANTEA* as associated with sucrose sensing, and experiments confirmed that *gi* mutants could not sustain sucrose-dependent circadian oscillations in continuous dark (Dalchau et al., 2011). Additionally, *gi* mutants have elevated amplitude oscillations in sucrose concentration in *Arabidopsis* and rice,

implying that this role of GI within sugar entrainment may be conserved in the plant kingdom (Eimert et al., 1995, Izawa et al., 2011). However, more recently, PRR7 has been implicated as a possible regulator of sugar-dependent regulation of the circadian clock. PRR7 transcript abundance was increased following photosynthetic supression through CO_2 depletion or treatment with the photosynthetic inhibitor DCMU, and *prr7* mutants are insensitive to the effects of sucrose on the circadian period, implying that the PRR7 promoter is coordinately modulated by the zeitgebers light and sugar and, through it, so is the clock (Haydon et al., 2013a).

1.2.4.4 Additional Entrainment Signals

Phytohormones are major players in plant signalling, and are under direct regulation by the circadian clock. Auxin sensitivity peaks in the morning (Went and Thimann, 1937), auxin-dependent stem extension is circadian gated (Jouve et al., 1999), and auxin signal transduction is directly regulated by the circadian clock (Covington and Harmer, 2007). Ethylene emmission is also circadian controlled in *Arabidopsis* , but rhythms in ethylene are not required for rhythmic growth (Thain et al., 2004). The clock component TIME FOR COFFEE (TIC) acts as a negative factor in jasmonate signalling, gating JA responses to the early morning (Shin et al., 2012). Additionally, application of phytohormones can in turn affect the circadian oscillator: cytokinins delay circadian phase, auxins regulate circadian amplitude, and brassinosteroids and abscisic acid modulate circadian periodicity (Hanano et al., 2006).

Elicitors of pathogenesis can also reset the circadian clock. Misexpression of *CCA1* and *LHY* increases susceptibility to the bacterial pathogen *Pseudomonas syringae* (Bhardwaj

et al., 2011, Wang et al., 2011) and, futhermore, it has been shown that defense activation by the *P.syringae* elicitor flg22 can feedback and shorten the period of *pCCA1:LUC+* reporter activity (Zhang et al., 2013). Treatment with salicylic acid, a plant immune response inducing signal, increases the amplitude and average levels of *TOC1* expression irrespective of application time but, curiously, does not affect its phasing or period length (Zhou et al., 2015). This suggests that elicitors of pathogen attack affect the clock through phase resetting as well as re-enforcing the existing rhythms.

Additional nutrient levels are influenced by and, in turn, reset the clock (Haydon et al., 2015). Iron is an essential micronutrient for plants, having a vital structural and catalytic roles in the chloroplast, yet iron levels have to be tightly regulated as it is cytotoxic in high concentrations (Clemens et al., 2002, Shcolnick and Keren, 2006). Iron transport and storage is under circadian control, with defects in *PRR7* and *TIC* expression leading to increased sensitivity to excess iron (Concerte et al., 2009, Liu et al., 2013). Closing the loop, iron deficiency affects the circadian clock, lengthening period by c. 2-3hrs (Chen et al., 2013, Salomé et al., 2012). This process is light dependent, requires protein translation in the plastids, and is separable from the circadian effects of inhibition of photosynthesis. Additionally, nitrate availability affects the circadian period. Nitrate assimilation to organic glutamate and glutamine is controlled through *CCA1*, and pulses of glutamine are capable of inducing stable phase shifts in *CCA1* expression (Gutiérrez et al., 2008). Whilst the availability of these nutrients in the soil does not vary throughout the diurnal cycle, the plant's need for the end products of their assimilation waxes and wanes with photosynthetic activity. As several other macro and micronutrient homeostasis pathways are known to be under diurnal regulation, it seems possible that more will shown to feed back and regulate the clock in turn.

1.2.5 The Plant Circadian System - One Clock or Many?

Whilst the mammalian circadian clock consists of cellular "slave" oscillators coordinated and synchronised by a master circadian clock in the suprachiasmatic nucleus (SCN) within the hypothalamus (Herzel et al., 2007), plant clocks were long believed to be entirely cell autonomous. Plant clocks have been observed in antiphase between tissues, between leaves and, through the use of foil covers to entrain distinct halves to antiphase LD cycles, within a single leaf with no apparent corrective crosstalk between them (Thain et al., 2000).

Contrary to this assumption, increasing amounts of evidence has emerged suggesting that inter cellular communication between circadian clocks is a feature in plants. Weak communication between individual circadian clocks has been observed in leaves, whereby distinct "waves" of reporter intensity move from base to tip (Wenden et al., 2012). Comparative assay of clock-driven luciferase expression in roots and leaves has provided evidence of phased "waves" of coordination through the tissue from root to shoot (Fukuda et al., 2012).

Furthermore, there is emerging evidence that circadian clocks can communicate over longer ranges. Using tissue-specific luciferase assays, it has been demonstrated that there is significant communication between the vascular and mesophyll clocks, with the vascular clock serving as the dominant coordinator (Endo et al., 2014). As outlined before above, it had been proposed that circadian clocks in the leaves are master-regulators of

the simplified oscillators in roots, exerting control through sucrose transport through the vasculature (James et al., 2008). It seems possible that the vasculature may have an even larger role in the circadian network, communicating between tissues in the mesophyll and the roots and beyond. Additionally, in the succulent *Kalanchoe daigremontiana*, independent localised oscillators in the leaves are responsible for variations in crassulacean acid metabolism (CAM), yet they eventually co-operate to produce a whole leaf circadian CAM response in a manner that heavily implies coordination (Rascher et al., 2001), suggesting that intercellular communication does not rely on vascular propagation.

Comparisons with animal circadian signalling networks, however, should not be overstated. Plants do not require the rapid responses and central coordination of the animal system because their growth-dominated lifestyle moves at a slower pace than that of animals. Conversely, plants are far more dependent on and sensitive to elemental extremes than animals, as they are stationary and vegetative.

A defining feature of animal circadian clocks is a hierarchical network of semi-autonomous cellular clocks under the centralised control of the suprachiasmatic nucleus (SCN), a small cluster of cells in the hypothalamus of the brain which synchronises circadian rhythms through secretion of hormones. For a long time, plants were thought to lack an analogous master circadian coordinator, however recent evidence has emerged to suggest that the plant shoot apex may function in this manner (Takahashi et al., 2015). Live-imaging of single cells, desynchronization of dispersed protoplasts, and mathematical analysis all demonstrated the dominant role of the shoot apex in circadian synchronisation. The increased synchrony confers robustness of morning and evening oscillations and capabilities for phase readjustment, much akin to the role of the SCN in animals. Rhythms in roots are altered by shoot apex ablation and micrografting, further demonstrating that

the shoot apex acts to coordinate clocks in distant organs.

1.2.6 The Circadian Clock Is a Key Regulator & Signal Coordinator in Plants

It is becoming increasingly clear that robust circadian rhythms are integral to control of expression and overall fitness, and are linked to important agronomic traits in multiple crop species. Clock outputs have clear roles to play in the regulation of multiple pathways and developmental events.

The clock is a key regulator of transcription in almost every biological process, with a large proportion of plant genes falling under circadian control. Early microarray time course experiments in *Arabidopsis* estimated that between 6% and 15% of the transcriptome is circadian regulated (Covington et al., 2008, Edwards et al., 2005, Harmer et al., 2000); later *in vivo* luciferase enhancer trap studies predicted that the clock regulates expression of a much higher 36% of *Arabidopsis* genes (Michael and McClung, 2003). This suggests that clock control through transcriptional outputs contributes significantly to the regulation of gene expression, however it is important to view this in context - compared with the estimated 30–50% of the transcriptome that cycles under diurnal photocycles with continuous temperature (Bläsing et al., 2005), and the 89% of genes that cycle in expression level under at least one diurnal condition (Michael et al., 2008), a relatively small proportion of the genome is under circadian control. However, its involvement in key agronomic traits suggests that the clock's importance as a regulator cannot merely be measured by the size of the regulome.

Robust circadian rhythms convey a pleiotropic fitness advantage. It has long been known that tomato plants grown in 12hr-12hr light/dark cycles outgrow those in 6hr-6hr or 24hr-24hr conditions, controlling for light exposure such that photoinhibition is not a concern (Highkin and Hanson, 1954). Systematic studies with mutant lines of *Arabidopsis* have shown that plants grow best when the period of their circadian clock coincides with that of the surrounding environment, and that this is true for fast- and slow-running clocks (Dodd et al., 2005). The wild type (period = 24hrs), long-period mutant *ztl-27* (period = 28hrs) and short period mutant *toc1-2* (period = 20hrs) all produce more chlorophyll, fix more carbon, grow faster and survive better than the mutants when grown in diurnal light-dark cycles with the same period as their clocks. This phenomena has also been observed in cyanobacteria (Ouyang et al., 1998, Woelfle et al., 2004), whereby strains with clock periods that resonated with the diurnal conditions out-competed those that did not. Interestingly, it has also been shown that, in cyanobacteria, clock-disrupted (i.e. arrhythmic) strains are out-competed in diurnal conditions but show no difference to wild type when grown in constant light (Ouyang et al., 1998). The advantages of resonance observed in these three species are likely due to the optimum phasing of clock outputs - the timing of an output event (e.g. the expression of a gene or suite of genes) would coincide with the correct environmental time when it is optimal for plant growth and survival.

A robust circadian clock conveys resistance to the related environmental stresses drought and temperature. In cotton, heat-shock proteins are differentially expressed throughout the day cycle in a circadian-dependent manner (Rikin, 1992), and their resistance to cold shock was similarly dependent in part on the time of day the chilling stress was induced

(Rikin et al., 1993). In *Arabidopsis*, clock regulation of cold stress response was first implicated after finding that stress transcriptome results varied significantly depending on the time of sampling (Bieniawska et al., 2008). The induction of the cold and drought resistance pathway regulatory genes *C-PROTEIN BINDING FACTOR/ DEHYDRATION RESPONSE ELEMENT BINDING-FACTOR (CBF/DREB) 1, 2* and *3* by cold-shock is gated by the clock (Fowler et al., 2005), with arrhythmic mutants having constitutive expression of *CBF1, 2, 3* and, hence, increased freezing tolerance. The promoter regions of these and many other cold-response factors contain the circadian regulated Evening-Element motif (Mikkelsen and Thomashow, 2009). Transcription at these promoters is further enhanced by the cold-dependent alternate splicing of *CCA1* into a form that shows increased affinity for, recruitment to, and transcription from these particular promoters (James et al., 2012, Seo et al., 2012). Similarly its partner clock gene *LHY* is also alternatively spliced, but its high affinity form is preferentially spliced at higher temperatures (James et al., 2012). Additionally, *TOC1* appears to be the key integrator between cold, drought and ABA signalling (Legnaioli et al., 2009). In these ways, the circadian clock is a key regulator in the perception of and response to environmental stresses.

The clock also plays a role in the response to biological stress. Circadian variations in immune function and disease susceptibility have long been reported in *Drosophila melanogaster*, with innate immunity factors peaking in expression throughout the day in a manner that persists in constant darkness (Mcdonald, 2001). In plants, there is increasing amounts of evidence for a similar role for the circadian clock in disease resistance. As previously outlined, disruption of the *Arabidopsis* clock results in extreme susceptibility to the bacterial pathogen *Pseudomonas syringae* (Zhang et al., 2013) and the oomycete

Hyaloperonospora arabidopsidis (Wang et al., 2011). In free-run conditions, a suite of genes related to pathogen resistance are expressed only at night, peaking just prior to dawn, with the timing corresponding with the formation of spores of the fungal pathogen (Wang et al., 2011). Similarly, *Arabidopsis* plants are more resistant to the generalist herbivore *Trichoplusia ni* (cabbage looper caterpillar) when both plants and caterpillars are entrained to the same LD cycles when compared to plants entrained in antiphase to the insects (Goodspeed et al., 2012). The underlying mechanisms of these phenomena are still unclear, however the master immune regulator NPR1 (NON-EXPRESSOR OF PATHOGENESIS-RELATED GENE 1) regulates transcription of core circadian clock genes. Following pathogen attack, NPR1 re-enforces the circadian clock by regulating both morning- and evening-expressed clock genes, and tightly gates the immune responses (Zhou et al., 2015). Whilst the method of control and the responses seem to be stress- and pathogen/pest-specific, it seems likely that circadian regulation of biological stress is widespread and organises the timing defence to coincide with high-risk environmental conditions and peak times of attack.

The photoperiodic induction of flowering is regulated by a coincidence mechanism between light signalling and the circadian clock (Hayama et al., 2004, Sawa et al., 2008, Yanovsky and Kay, 2003). Flowering in *Arabidopsis* is induced when levels of the inducer of flowering CONSTANS (CO) in leaves reach a critical threshold (Onouchi et al., 2000, Putterill et al., 1995) which is sufficient to induce transcription of the florigen *FLOWERING LOCUS T (FT)*, a mobile long-range flowering hormone that propagates a from leaves to the meristem and triggers the floral transition (Corbesier and Coupland, 2006, Samach and Gover, 2001). The timing of CONSTANS transcription is under circadian control in a light-dependent manner , with the formation of the FLAVIN-BINDING,

KELCH REPEAT, F-BOX 1 (FKF1) and GIGANTEA (GI) protein complex being required for transcription (Imaizumi et al., 2003, Lee et al., 2005). The expression of these genes is controlled by the circadian clock (Fowler et al., 1999, Nelson et al., 2000), yet the complex formation is dependent on blue-light signalling - the complex forms only when the FKF1 LOV domain absorbs blue light in a manner not dissimilar to its relative ZTL (Fore et al., 2001, Imaizumi et al., 2003). CO protein stabilisation is also light- and clock-gated. CO is degraded at night through the ubiquitination pathway (Ishikawa et al., 2006, Valverde et al., 2004), however this is prevented by blue-light dependent FKF1 binding and stabilisation in the afternoon in LD (Song and Noh, 2012). This provides a narrow window for CO accumulation and FT induction when *CO* mRNA transcription and translation in the evening coincides with blue-light activation of FKF1 binding. As the clock controlled CO/FT pathway is highly conserved in angiosperms (Greenup et al., 2009, Song et al., 2010a), and timing of flowering is a key factor in determining yield, it is of great practical agronomic importance.

Evidently, the clock provides the plant with the facility to be anticipatory of, rather than merely reactive to, changes in its environment - to be prepared for changes in light quality, water availability, temperature or pest activity throughout the day, and in the longer term to integrate multiple cues on a longer time-scale to anticipate and respond to changing seasons. It is the cornerstone of plant signalling, and the *Arabidopsis* model is excellent preparation for studies in other species.

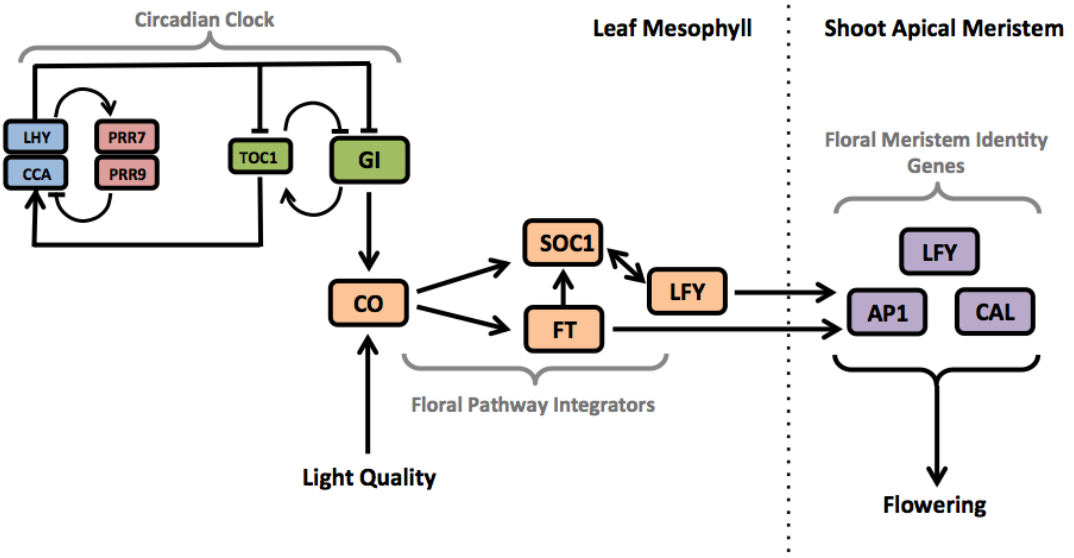

FIGURE 1.5: The Circadian Clock is Required for Photoperiodic Flowering in Arabidopsis.

Photoperiodic flowering through CONSTANS accumulation is determined through a coincidence mechanism between light quality signalling and the expression of the clock gene GI. Once CO protein reaches a critical threshold in leaves, it induces a suite of floral pathway integrators which are in turn regulated by gibberellins, vernalisation and the autonomous pathway (ommitted for clarity). the mobile florigen FT moves to the apical meristem where it induces the transcription of floral identity genes and marks the transition to flowering. This pathway is conserved in higher plants (Johansson and Staiger, 2014, Laurie, 1997, Liew et al., 2014).

1.2.7 The Circadian Clock is Of Agronomic Significance

Our understanding of the central oscillator in *Arabidopsis* is rapidly increasing yet it is not in itself an economically or agriculturally important plant. its main value is as a reference model on which to base our understanding of multiple species - *Arabidopsis* is fairly representative of the plant kingdom as a whole, and the circadian clock seems well conserved. A large number of *Arabidopsis* clock genes have direct homologues or paralogues in the distantly related monocot barley, with the common ancestor proposed to have around two thirds of the key clock components identified in *Arabidopsis* prior

to the dicot-monocot split (Cristiane et al., 2015). There is considerable conservation of clock components, architecture and function throughout the angiosperms (Song et al., 2010b) in species as diverse as soybean (Hudson, 2010, Liu et al., 2009), *Brassica rapa* (Kim et al., 2012, Lou et al., 2012), tomato (Facella et al., 2008), poplar (Takata et al., 2008, 2010) and rice (Murakami et al., 2003, 2007a,b).

Whilst the monocot-dicot split dates back a mere 100-150 million years (Chaw et al., 2004), there is also a surprising degree of conservation between the *Arabidopsis* and bryophyte clock, as categorised by the moss *Physcomitrella patens* despite over 420 million years of divergent evolution. *P.patens* has multiple *CCA1/LHY* and *PRR* homologues, although it lacks homologous *TOC1*, *GI* and the LOV-KELCH domain containing proteins in the *ZTL* family (Holm et al., 2010, Okada et al., 2009). Furthermore, the green alga *Ostreococcus taurii* possesses a basal circadian clock, centred around a homologue of *TOC1* (Djouani-Tahri et al., 2010).

It appears, therefore, that *P.patens* and *O.taurii* have a streamlined version of the circadian clock, and its conservation lends credence to the claim that the circadian clock is vital for plants.

1.2.7.1 Ppd-1 & Other PRR Homologues

The circadian clock is a key regulator of various agriculturally important traits in a range of crop species, and loci linked to these traits frequently encode homologues of the *Arabidopsis* TOC1/PRR family. Chiefly, a homologue of *Arabidopsis PRR7*, *Photo-Period 1 (Ppd-1)*, is of key agricultural importance in wheat (*Triticum aestivum*) and is a so-called "elite" gene (Beales et al., 2007, Le Couviour et al., 2011). Varieties with

mutant forms of *Ppd-1* are photoperiod insensitive, flowering under both long and short days. This is critical as it allows cultivation in a broad variety of latitudes and climates (Seki et al., 2011, Shaw et al., 2013). Indeed, photoperiod insensitivity was one of the key traits introduced by Norman Borlaug in the 1950s that facilitated the "Green Revolution" (Borlaug, 1983). As wheat is a highly adaptable crop grown in virtually all countries, between which daylengths vary dramatically, multiple alleles of this gene have been selected for by breeders. Late flowering *Ppd-A1* and *Ppd-D1* alleles are common in wheat varieties cultivated for Northern Europe, but not the Mediterranean or East Asia (Shaw et al., 2013). Different alleles and haplotypes have been cultivated independently by breeders around the world, and there is broad conservation of alleles in independently generated varieties cultivated at the same latitudes (Guo et al., 2010). Similarly, *Ppd-1* alleles in barley are important in conveying photoperiod insensitivity to spring varieties (Turner et al., 2005). The genes *Hv CIRCADIAN CLOCK ASSOCIATED 1(HvCCA1)* and *Hv PHOTOPERIOD H1*, which are most similar to *Arabidopsis CCA1* and *PRR7* respectively, are both transcriptional regulators that affect expression of *AtCCA1, AtLHY* and *AtTOC1* when cloned into *Arabidopsis*, and furthermore are capable of rescuing the circadian phenotypes of null mutants (Kusakina et al., 2015). This illustrates that the clock components are conserved across the plant kingdom, and that homologues are functionally equivalent in the circadian clock.

Many *PRR*-family genes underlie important quantative trait loci (QTLs) for cultivation at northern latitudes in crops besides wheat and barley. In sugar beet, a *PRR* orthologue is responsible for the photoperiod insensitivity underlying the important switch from annual to biennial growth habits in modern cultivars (Boudry et al., 1994). Similarly, alleles of the *OsPRR* family are the underlying genes for QTLs required for rice

cultivation in long days as found in summers away from the equator (Koo et al., 2013). These five genes are expressed in a diurnal, sequential manner that mirrors that seen in *Arabidopsis* and suggesting that they might form part of the circadian clock, or its closely related outputs, in rice (Murakami et al., 2003). In sorghum, *SbPRR37* plays a major role in regulating photoperiodic flowering, with mutants no longer exhibiting short-day dependent heading which is especially critical in the cultivation of this species outside the tropics (Murphy et al., 2011). In summary, the pseudo response-regulator family is key in controlling photoperiodic flowering in a range of crops. It remains to be seen how the circadian clock regulates outputs in these species, and how our understanding of the circadian clock in *Arabidopsis* can guide crop breeding.

1.2.7.2 *GIGANTEA* Homolgoues

Much like in wheat and barley, there is a large degree of natural variation in the circadian clock between cultivars of *Brassica rapa*. *B. rapa* is widely cultivated, with great phenotypic difference between cultivars - the species incorporates turnips, an oilseed crop, napa cabbage and several other leaf vegetable varieties. As a member of the *Brassicaceae* family along with *Arabidopsis* it is perhaps unsurprising that *B. rapa* possesses a closely related circadian clock (Lou et al., 2011, 2012). Different cultivars possess variability in circadian period length, phase and even response to temperature (Lou et al., 2011). Water use efficiency, an important trait for agriculture, is under circadian control in *B. rapa*(Edwards et al., 2011) as a result of circadian gating of gas exchange and stomatal conductance (Edwards et al., 2012). Additionally, allelic polymorphism in *BrGI* is responsible for circadian variation and increased freezing and salt tolerance within cultivated varieties (Xie et al., 2015). In this way, circadian gating of abiotic stress responses

increases fitness of cultivars.

Homologues of *GI* have considerable influence in other species too. GI has a dual role as a clock gene and a regulator of flowering time, giving it diverse effects eventual heading date and seed/fruit yield (Mishra and Panigrahi, 2015). A comparative analysis of *Solanaceae* transcriptomes indicated a role for *GI* in tomato seed germination and potato tuber formation (Rutitzky et al., 2009). In rice, *OsGI* is required for robust diurnal expression of up to 75% of transcripts in leaves, affecting heading date but having little to no effect on net photosynthetic rates (Izawa et al., 2011). Maize possesses two *GI* homologues, with *ZmGI1* the more highly expressed. Mutants in *gi1* flower early in long-day photoperiods, but not short days, indicating its differential involvement in these two flowering time pathways. Furthermore, *gi1* mutants undergo vegetative phase change earlier and grow taller than non-mutant plants in field conditions (Bendix et al., 2013). It appears that the capacity of GI to integrate several inputs to the clock and act as the link between the circadian system and the flowering time network has resulted in its implication in many desirable crop traits.

1.2.7.3 Other Clock Genes

There is evidence of the clock genes influencing heading date independent of *GI/PRR* homologues. In soybean the transgenic *AtBBX32* increases grain yield through altering transcript levels of the soybean clock genes *GmTOC1* and *LHY-CCA1-LIKE2 (GmLCL2)* (Preuss et al., 2012). Quantitative trait loci linked to timing of flowering in barley have also been mapped to clock gene homologues. The cultivar Mari (*mat-a.8*) is

an early flowering, photoperiod-insensitive variety that has greatly increased the cultivation range of two-row spring barley since its introduction in the early 1960s. The gene underlying this short-season adaptation was a homologue of *Arabidopsis Early Flowering 3 (HvElf3)* (Zakhrabekova et al., 2012). Photoperiod insensitive alleles of *HvElf3* have altered expression profiles of *HvGI*, indicating that *HvElf3* affects the clock and could be an oscillator component in barley much like in *Arabidopsis*. *OsELF3-1* is a floral activator in long days in rice, with mutants showing altered expression of clock gene homologues and flowering time regulators (Yang et al., 2013). *OsELF3-1* is a known component of the rice circadian clock, showing positive regulation of *OsLHY* expression and negative regulation of the *OsPRR* quintet (Zhao et al., 2012). Similarly, alleles of *LUX, ELF3*, and *ELF4* homologues are tightly associated with natural variations in heading date between northern and equatorial cultivars in the legumes lentil (Sarker et al., 1999) and pea (Liew et al., 2009, Weller et al., 2012). As such, a whole host of clock genes influence heading date, allowing photoperiod independent flowering in all seasons, and extending the reproductive period so plants are more mature at the time of flowering and so able to commit more resources to seed or fruit growth.

1.2.8 Conclusion

In summary, an understanding of the circadian clock is vital for putting a wide variety of biological pathways into the whole-plant context. The clock is an integrator of multiple pathways, and as such is able to respond to stress and perturbations within cells, across tissues, or even (with vascular transport of hormones) across the whole plant. It responds to and gates the outputs of various signalling pathways. Better models of the clock will, therefore, result in better understandings of plant signalling and development.

Conventional crop breeding has selected for allelic variety in core circadian clock genes and its outputs in many plants and processes, although this has mostly focused on heading date. Elite wheat varieties are closely linked with *Ppd-1* alleles, as manipulation of flowering time greatly increases crop productivity by allowing multiple crops per year, or allowing harvest before seasonal phenomena (e.g. monsoons or late-season floods). With the circadian clock regulating almost every pathway in *Arabidopsis* it seems likely that pairing a greater understanding of the circadian clock with modern breeding techniques will result in increased yields, stress resistance and drought tolerance in myriad agricultural crops. However, currently our understanding of the circadian system limits this work. We do not know, for example, how the circadian clock is segregated throughout the plant - the discovery of "slave oscillators" in crop plants akin to those in *Arabidopsis* would allow fine manipulation of growth independent of grain or tuber formation, greatly increasing yield.

However, the model of the circadian clock is incomplete. So far, the vast majority of our knowledge of the plant circadian is of the transcriptional-translational clock, in leaves. Ironically, of the core oscillator genes identified, relatively few appear to be transcription factors. This is a glaring hole in our knowledge implying that either there are unknown factors driving transcription, or the products of these genes form as-yet unidentified complexes with known general transcription factors. Recent work has begun to investigate the clock outside the leaves, and within cells; however this is in its infancy. Incorporation of different drought and temperature regimes begins to challenge the limits of the described models. Additionally, there is very little characterisation of the clock in developmental contexts - how, if at all, does the clock interact in the determination of the cell fates in the meristem? Is the circadian clock the same in all tissues throughout their development? Moreover, despite knowing that the circadian clock regulates 30% of

the transcriptome, relatively few of these genes have been observed to be directly under the control of *CCA1/LHY*. Understanding the circadian clock, and how it fits into the broader context of the whole plant, requires new components to connect the pathways and provide a better model for further research and plant breeding.

1.3 Circadian Screening Techniques in *Arabidopsis*

Over the last two decades, the development of high-throughput techniques has enabled us to probe the plant circadian clock, a key coordinator of vital biological processes, in ways previously impossible. With the circadian clock increasingly implicated in key fitness and signalling pathways, this has opened up new avenues for understanding plant development and signalling. Our tool-kit has been constantly improving through continual development and novel techniques that increase throughput, reduce costs and allow higher resolution on the cellular and subcellular levels. Increasingly, with costs falling and the power of assays rising, the emergent challenge for researchers is choosing the best platform for dissecting their phenotypes of interest.

1.3.1 Molecular Assays & The Need for Non-Invasive Assays in Screening.

The circadian system can be probed in considerable depth through the use of molecular techniques such as quantitative-PCR and Northern blotting to assay clock gene expression directly over a sampling time-course. Indeed, these techniques are used extensively in circadian studies alongside high-throughput techniques, having been used to characterise numerous clock components, most notably *CCA1* (Wang and Tobin, 1998) and

LHY (Schaffer et al., 1998). More recently, the proliferation of micro-arrays and RNA-seq technology has expanded the molecular toolkit, allowing us to view the abundance and splicing patterns of multiple mRNAs simultaneously (Filichkin et al., 2010, Schaffer et al., 2001). They are still vital tools for in-depth characterisation and investigation of the mechanism of action for individual circadian genes, and for teasing apart the roles of separate clock loops.

However, molecular techniques are considerably time and resource consuming, requiring the researcher to perform multiple, regular samplings over several days. They also require destructive sampling – the harvest of leaf tissue, whole plants or groups of plants– which not only requires lots of plant growth space, but involves large amounts of resource-consuming wet-work at the bench following the time-course. This necessarily reduces the resolution and throughput of the assay, limiting not only the sampling frequency but also the number of parallel and consecutive experiments that the lab's finances (and level of fatigue) can support. Additionally, destructive sampling raises issues with averaging biological variation between tissues as well as between plants, making observation of an individual plant or tissue throughout a time-course impossible. Together, this makes molecular techniques unsuitable for the wide-scale screening and initial identification of clock genes.

By means of contrast, non-destrictive are far better suited to screening as they allow concurrent sampling on the same plant without perturbing the clock through stress or killing it. They also allow a high level of automation. As opposed to physical harvest, the assays outlined below can be set up and left to run with minimal human intervention, compared with methods where harvest have to be performed regularly over several days.

This has resulted in a paradigm shift in recent years, whereby the limiting factor in the throughput of circadian investigations has become the data handling and preparation of plant materials, and the scale of these experiments is limited only by the capacity and number of assay machines. This allows researchers to carry out broader, further-reaching experiments investigating the influence of several factors on the clock to identify candidates for future in-depth study.

1.3.2 Indirect Circadian Assays

The circadian clock is a key signal coordinator in plants. As such, circadian genes can be identified by searching for mutant phenotypes in processes that are regulated by the clock. Hypocotyl elongation and flowering time are two such processes that have a long history in circadian research. Both have easily scoreable phenotypes, which allows incredibly high throughput - thousands of seeds can be mutagenised and screened on a single plate for hypocotyl elongation, whilst the ease of identifying flowering time phenotypes means the only limiting factor is the size of the greenhouse. However, these techniques are not without their shortcomings.

1.3.2.1 Hypocotyl Elongation

Circadian dysfunction frequently results in aberrant hypocotyl elongation phenotypes, and this can be used to investigate circadian defects. This phenomenon occurs shortly after seedling germination, where the initial hypocotyledonous stem (henceafter "hypocotyl") grows and elongates. This process regulated by a complex and involved coincidence mechanism between internal and external cues (Nozue et al., 2007). Elongation is rhythmically

controlled, with a daily growth arrest coinciding with perceived dawn and a rapid growth phase at subjective dusk (Dowson-Day and Millar, 1999).

Many canonical circadian genes are implicated in the control of hypocotyl elongation. The core morning loop gene *LATE ELONGATED HYPOCOTYL* draws its name from the delayed elongation phenotype of the mutant (Schaffer et al., 1998). The *toc1-1* mutant shows a shortened elongation cycle in line with its shortened circadian period (Somers et al., 1998b). *ELF3* is required for the daily arrest of hypocotyl elongation, and mutants in this gene abolish rhythmic patterns of elongation (Dowson-Day and Millar, 1999). Hypocotyl elongation frequently forms the base of investigative tools in a wide variety of plants for investigation of signalling pathways that cross-talk with the clock, including light (Cashmore et al., 1999, Cerdán et al., 1999, Mazzella et al., 1997), hormones (Cary et al., 1995, Chory and Li, 1997, Collett et al., 2000, Jensen et al., 1998, Su and Howell, 1995) and sucrose (Stewart et al., 2011, Zhang et al., 2010). As such, mutations that affect the circadian system have wide-reaching effects on regulating the signalling pathways that control hypocotyl elongation, making it a key phenotype for prospective circadian mutants.

Unfortunately, as hypocotyl elongation is controlled by a complex multi-factor coincidence mechanism, phenotypes frequently have non-circadian explanations. Light has a role in regulating hypocotyl elongation distinct from its role as a zeitgeber(Mockler et al., 1999). Perceived by the red-light sensitive phytochomes and blue light sensitive cytochromes, exogenous light severely suppresses hypocotyl extension in the wild type (Chen et al., 2004). The phytohormones ethylene, cytokinin (Cary et al., 1995), auxin (Jensen et al., 1998), giberellins and brassinosteroids (Chory and Li, 1997) all too have regulatory roles on hypocotyl elongation. As such, whilst hypocotyl screening remains

a valuable tool for identifying mutants for circadian screening due to its incredibly high throughput, it cannot implicate the clock without further characterisation.

1.3.2.2 Flowering Time

As outlined previously (Figure 1.5), photoperiodic flowering is a result of a coincidence mechanism between light and the circadian clock. Perturbation of one half of this equation results in altered flowering time and, as such, circadian mutants have flowering time phenotypes. Many core clock genes were initially discovered through flowering time screens. Mutant *gigantea* results in delayed flowering and increased vegetative growth (Araki and Komeda, 1993) and, as their names imply, mutants in *EARLY FLOWERING 3/4* were identified by their hypersensitivity to photoperiod (Doyle et al., 2002, Zagotta et al., 1996). As these pathways are highly conserved in plants, this screen is suitable for a wide variety of species.

Whilst all clock mutants have flowering time phenotypes, it is not true that all flowering time mutants also have circadian defects. The other side of the photoperiodic equation - light sensing and signal transduction - affects heading date in a manner distinct from the clock (Cerdán and Chory, 2003, Mockler et al., 1999). Additionally, flowering time is regulated by pathways distinct from photoperiod. Gibberellins can directly induce expression of *CONSTANS (CO)* independently of GI or light (Blazquez et al., 1998). FLOWERING LOCUS C (FLC) is a key integrator of non-photoperiodic flowering pathways, mediating vernalisation and the autonomous pathway. FLC suppresses expression of the floral pathway integrator *LEAFY (LFY)* and the florigen *FLOWERING LOCUS T (FT)* and preventing the floral transition. Expression of FLC is suppressed following exposure to cold, alleviating its repression of flowering and allowing the shift to floral transition (Michaels et al., 2003, Schmitz and Amasino, 2007, Sheldon et al., 2000a,b).

This is the "vernalisation pathway", which promotes early heading after exposure to cold and ensures seasonal flowering. Additionally, FLC is one of many targets of the "autonomous pathway" - an RNAi and epigenetic pathway that induces flowering in the absence of any other stimuli (Simpson, 2004).

Mutants in any one of these pathways, in the pathway integrators or in the meristem identity genes could result in flowering time phenotypes that are non-circadian in nature. Much like hypocotyl elongation, a flowering time phenotype alone is insufficient to identify clock genes. Whilst the clock may be a key integrator and coordinator of multiple processes, many of the outputs are in turn tightly regulated by multiple genes

1.3.3 Direct Assays of the Circadian Clock

Direct assays of the circadian clock directly measure rhythms in almost real-time, as opposed to long-term outputs. Resolutions are on the scale of minutes and hours, as opposed to days as with indirect assays. Whilst this is possible through real-time imaging of rhythmic hypocotyl elongation (Nusinow et al., 2011) or the molecular techniques outlined previously they are both low-throughput techniques that do not lend themselves to screening. Instead, in this section rhythmic leaf movement, delayed fluorescence and transgenic clock-driven luciferase reporters will be considered and compared as phenotyping platforms.

1.3.3.1 Leaf Movement

Along with diel rhythms in stem and root elongation, leaf movement is a well-characterised, growth-dependent circadian clock output (Farré, 2012). Circadian-regulated oscillations

in leaf position are a result of differential patterns of growth in cells on opposing adaxial and abaxial sides of the petiole (the structure that connects the leaf blade to the stem, which causes the positions of young leaves to rise and fall throughout the 24 hour period (Dornbusch et al., 2014, Engelmann and Johnsson, 1998)). This movement is differentially phased from petiole elongation, and requires a functional *ELF3* and evening complex for proper phasing (Dornbusch et al., 2014).

Although the biological importance of leaf movement remains unproven, it has long been used as a circadian reporter. The plant clock was first described through the study of rhythmic pulvinus-driven opening and closing of leaves in *Mimosa pudica* (d'Ortous De Mairan, 1792). Low-throughput leaf movement assays have also provided insight into the clock in *Arabidopsis*, with the absence of leaf movement rhythms in *lhy* mutants helping to implicate that gene in the circadian system (Schaffer et al., 1998). Measuring directly the clock controlled physiological outputs such as leaf movement provides a non-invasive assay that, unlike luciferase reporters, does not require transformation. Leaf movement is favoured over other physiological outputs due to the increased rhythm robustness and ease of assay (Dowson-Day and Millar, 1999). Computer-automated image capture by CCD within the growth chamber can be performed throughout the time-course (Edwards and Millar, 2007). Over the past decade several straight-forward systems have been developed based on computer-automated capture of leaf position (Kim and Nam, 2009), whilst advancements in digital camera technology has reached a point where consumer-level cameras are suitable for circadian imaging, dramatically driving down the hardware costs of such systems (Bours et al., 2012), and the relatively cheap digital cameras have removed a major barrier to entry for circadian phenotyping. The more recent development of sophisticated machine vision algorithms and reliable computer automation have

helped automate the leaf tracking analysis, previously a time-consuming bottleneck in the pipeline for the researcher. Together this has gone a long way to enabling the use of leaf movement as a high throughput clock assay.

Whilst this system can be used in non-transformable plants, it cannot be used for species with sessile leaves (i.e. those that lack petioles). This makes the vast majority of monocots, including all major cereal crops, unsuitable for this technique. Furthermore, in *Arabidopsis*, leaf movements halt once the leaves are mature which equates to a window for assay of approximately one week (Edwards and Millar, 2007). Regardless, leaf movement is a robust and accurate assay that, with further development and ever-reducing hardware costs, is an attractive and valuable tool for investigating circadian function. However, the number of plants that can be viewed in parallel is relatively limited which, for the initial broad screening required for the project, is undesirable for the initial stages of this investigation.

1.3.3.2 Transgenic Luciferase

A large number of investigations of the transcriptional circadian oscillator have used transgenic luciferase reporters to probe clock period and robustness (Millar et al., 1992, Southern et al., 2006). This technique has been used to identify several core clock genes, most notably *TOC1* (Millar et al., 1995a). A plant containing a transgenic luciferase circadian reporter was mutagenised, and the subsequent mutant progeny assayed for phenotypes in the rhythm of the reporter. From this screen, a mutant was identified which routinely had earlier peaks of the luciferase reporter, indicating a shorter period, fast-running clock. This semi-dominant mutant in timing of cab2-driven luciferase was

FIGURE 1.6: Photolytic Oxidation of Luciferin by Luciferase

$$Luciferin + ATP \rightarrow LuciferylAdenylate + PP_i \quad (1.1)$$

$$LuciferylAdenylate + O_2 \rightarrow Oxyluciferin + AMP + Light \quad (1.2)$$

named *toc1*. The technique has since used as a screen to identify new circadian mutants (Onai et al., 2004), to characterise the expression patterns and transcriptional phasing of known clock components (Farré and Kay, 2007), and to investigate the roles external entraining stimuli such as temperature (Kusakina et al., 2014, Nagel et al., 2014, Thines and Harmon, 2010) and sucrose (Dalchau et al., 2011) play in clock function.

Luciferase is an enzyme that catalyses the oxidation of luciferin, a compound with which test plants are dosed. Typically, the brighter, modified *LUC+* gene sourced from the firefly *Photinus pyralis* is used (Sherf and Wood, 1994). The oxidative reaction occurs in two stages: the first is ATP-dependent, and results in the production of the unstable intermediate luciferyl adenylate (Figure 1.6, Equation 1.1); whilst the second consumes oxygen and is light emitting (Figure 1.6, Equation 1.2). In a typical cell, following saturation with luciferin, oxygen and ATP are provided by internal pools; as such the amount of luminescence observed is directly dependent on how much luciferase is present (Millar et al., 1992, Ow et al., 1986). As luciferase is an unstable enzyme that rapidly loses function (Van Leeuwen et al., 2000), the amount of functional luciferase is directly determined by the rate of luciferase expression. Luminescence intensity can be recorded through the use of photo-multiplier tubes attached to detectors, as in the TopCount system, or, increasingly, high sensitivity charge-coupled cameras enclosed within light-tight growth chambers with automated lights (Southern et al., 2006). As such, luciferase luminescence is indicative of the level of luciferase expression *in planta*.

When under the control of a circadian-regulated promoter, the observed luminescence provides a quantitative measure of promoter-driven gene expression. This makes luciferase, when placed under the control of a circadian-regulated promoter such as *CAB2* or *CCR2* (Millar and Kay, 1991), an excellent reporter of clock transcriptional output (Hall and Brown, 2007, Millar et al., 1992, 1995b).

Interestingly, in recent years the sensitivity of luminescence imaging cameras has increased to the point where more specific resolution is now possible. In the duckweed *Lemna gibba*, circadian rhythms in *AtCCA1:LUC+* have been detected within individual cells following transient transformation by particle bombardment (Muranaka et al., 2013). In *Arabidopsis*, the identification of tissue-specific clocks in the leaf mesophyll and vasculature was possible through the use of split-luciferase assays, wherein half of the luciferase protein is driven by a clock promoter and another half by a tissue-specific promoter, which are only luminous when expressed together in the same cell (Endo et al., 2014).

However, whilst luciferase has been used successfully to assay clock function in various species, most notably tobacco, *Arabidopsis* (Millar et al., 1992) and rice (Sugiyama et al., 2001), the need to introduce transgenic luciferase into the plants is a time-consuming step that greatly reduces throughput. For an initial library screen, it this loss of throughput undesirable. That said, the data is of higher quality than other phenotyping techniques, and is still considered the "gold standard" of circadian research. Luciferase allows direct investigation of promoter transcription and, as such, allows us to probe transcriptional feedback loops and investigate the effects of the circadian defect on individual components of the clockwork, whilst endogenous assays only give a broad overview of clock phenotype. Luciferase remains a vital tool for the confirmation of phenotypes but, for

this investigation, it will not provide the initial screening platform.

1.3.3.3 Delayed Fluorescence is an Endogenous Assay For Screening

First described in 1951 (Strehler and Arnold, 1951), delayed fluorescence is the emission of light from plants, algae and cyanobacteria following their transfer from light to dark conditions resulting from charge recombination in the photosynthetic machinery (Rutherford et al., 1984), primarily within the P680 light harvesting complex of photosystem II (Arnold and Davidson, 1954, Jursinic, 1986, Van Wijk et al., 1999). This emission is under clock control and can be used as an indicator for circadian phenotyping (Gould et al., 2009).

Normally in photosynthesis, incoming photons excite electron pairs in the light harvesting complexes of the photosystems, raising them to higher energy states (Figure 1.8). These electrons are passed to receiver molecules further down the photorespiratory chain which use their stored energy to generate a membrane potential, pump protons across the thylakoid membrane, and do biological work (Blankenship, 2002). Charge-recombination between the receiver molecule plastoquinone QA re-excites the P680 complex (Figure 1.7), which produces fluorescence as it returns to the ground state through the release of stored energy in the form of a photon (Jursinic, 1986). Approximately 0.03% of absorbed solar energy is re-emitted in this manner (Jursinic, 1986). The intensity of the delayed fluorescence emission decays rapidly to undetectable near-background levels over the course of a minute (Berden-zrimec et al., 2010, Goltsev et al., 2003); it is therefore critical that images are taken over exactly the same period following lights off in order to observe rhythmicity. This persistence allows the long exposure windows required for detailed

imaging. However, because the intensity decays exponentially and rapidly, accurate and precise control of the light source and length of delay is required to acquire accurate data.

The intensity of delayed fluorescence has been shown to be under the control of the circadian clock. The periods and robustness of known clock mutants *lhy-21*, *cca1-11*, *gi-11* and *toc1-2* as detected by delayed fluorescence agree with those previously determined by other techniques (Gould et al., 2009). Whilst the exact nature of the relationship between the clock and delayed fluorescence is still unclear, many of the key genes that make up the light harvesting complexes within PSI and II are under circadian control at the transcriptional level (Harmer et al., 2000), providing a possible link between the nuclear transcriptional clock and this particular output.

As a platform for circadian phenotyping, delayed fluorescence provides a non-transgenic system that can be used to assay the clock in a vast number of species. The CCD cameras used for luciferase imaging are sufficiently sensitive for delayed fluorescence assays, provided that the growth chamber and lights are under accurate precision control (Gould et al., 2009). To date, it has been used to investigate plant species including *Arabidopsis*, the C3 monocots barley (Gould et al., 2009) and einkorn wheat (Gawroński et al., 2014), the C4 monocot maize (Gould et al., 2009), the model CAM species *K. fedtschenkoi* (Gould et al., 2009), and the coniferous gymnosperm Norway spruce (*Picea abies*) (Gyllenstrand et al., 2014).

The system provides a quick and simple, non-invasive, universal platform for phenotyping plant clocks across species and taxa without the need for transformation. For our

FIGURE 1.7: Delayed Fluorescence in Photosystem II

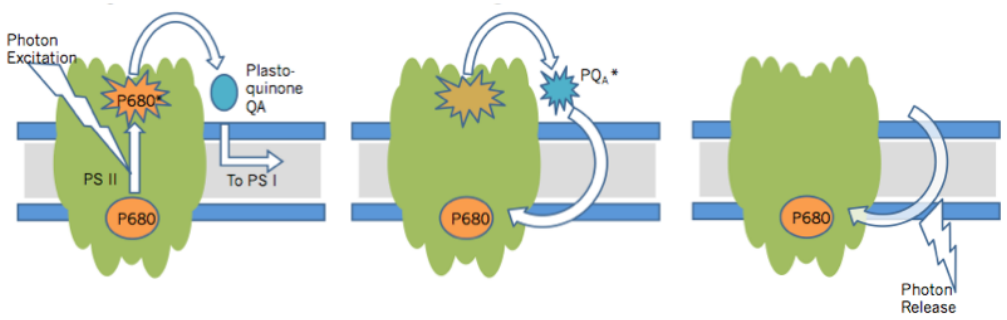

Normally, in photosystem II of the chloroplast, energy from photons excites electrons in the light-harvesting complex P680 . The energy of these excited electrons usually passes to plastiquinone A (PQ_A) and on to downstream components in the photophosphorylitic electron transport chain (ETC, Left) (Nelson et al., 2004). However, a small proportion of excited electrons return to the ground state state of P680 (Centre), releasing a photon (Right). This photon, with a wavelength of 680 nm, is delayed fluorescence (Christen et al., 2000)

purposes, delayed fluorescence is well suited to initial screening - it is non-invasive unlike molecular techniques, it does not require transformation like luciferase assays, and it is higher throughput than leaf movement - and it will provide the initial screening platform for the screening of RIKEN TF library lines.

1.3.4 Summary

Non-destructive, high-throughput assays are vital for circadian research in the genomic age. Nowadays, the number breadth of libraries of mutant and/or transgenic plants is staggering - the main hurdle for research is deciding which lines to investigate. High-throughput assays, especially those that require little plant material, allow circadian phenotypes to be identified quickly and set the stage for the next phase in the functional characterisation of these genes. We have access to a vast quantity of genomic resources,

and through broad platform screening we are able to capitalise upon this.

This project revolves around the characterisation of transcription factors that affect the clock in subtle ways. There are 1500-2800 putative transcription factors in *Arabidopsis* (Davuluri et al., 2003, Guo et al., 2005, Iida et al., 2005, Riaño-Pachón et al., 2007, Riechmann et al., 2000), of which a handful have been investigated on the circadian level. We know that the clock regulates transcription of between 6% and 36% of the genome (Covington et al., 2008, Edwards et al., 2005, Harmer et al., 2000, Michael and McClung, 2003), however we have little evidence as to which transcription factors are responsible for this regulation. A systematic analysis of *CCA1* binding targets using ChIP and deep sequencing revealed that CCA1 plays an important role in regulating a large subset of the rhythmic transcriptome (Nagel et al., 2015). Although many of these target genes were evening expressed and contained the EE motif, as might be expected, a significant subset were morning phased and enriched for previously unrecognized motifs associated with CCA1 function. This demonstrates that the picture of the underlying mechanisms for regulating transcription still remain hazy. It is therefore necessary to assay the clock for a large number of mutants in a large number of genes in order to identify transcription factors responsible for clock outputs and for the coordination of the oscillator with the broader signalling context. Without high-throughput assays, this would be impossible. Without direct clock assays, this would still be incredibly difficult - a large number of genes influence hypocotyl elongation and flowering time that are merely downstream of, or have no connection to, the clock. With tools like delayed fluorescence, leaf movement and transgenic luciferase assays, investigation of large numbers of genes is possible and, as such, so is the identification of new circadian factors.

In conclusion, delayed fluorescence will provide the initial screen. It has considerably higher throughput than leaf movement, allowing more samples to be imaged simultaneously, and does not require transformation which would delay the initial phase of the investigation. Leaf movement and luciferase phenotyping will be used to confirm and further investigate the phenotypes of lines initially identified by the initial screen.

1.4 Strategies for the Generation of Mutant Lines

With high throughput screening techniques, large numbers of mutants can be phenotyped rapidly. By perturbing the expression level of a gene and viewing whether this affects the clock, it is possible to identify circadian components. However, before phenotyping is possible, these mutants first have to be generated. Several approaches have been used in the past, which are reviewed briefly here.

Exposure of *Arabidopsis* to mutagens generates random mutations in the underlying genome. Plants are exposed to mutagens typically as embryos within the seed, with mutants in the future germ line cells persisting into the subsequent generation. Ethylmethane sulphonate (EMS) is the most commonly used mutagen. It alkylates guanine bases, resulting G/C to A/T transitions. These substitutions can lead to amino acid substitution (and, hence, protein misfunction), lead to constitutively active versions of the gene (e.g. those lacking a residue needed for degradation) or even introduce premature stop codons resulting in truncated proteins (Maple and Møller, 2007). Deletions can be generated through bombardment with slow neutrons, resulting in 1kb deletions which can completely eliminate genes from the genome (Li and Zhang, 2002, Li et al., 2001). However, in both techniques the identification of the mutated gene in question can be

laborious - insertions are introduced into the plant at random, and identification of their location is only possible through mapping, positional cloning or extensive sequencing, all of which are considerably time consuming.

Mutants can also be generated through the random insertion of a known genetic sequence into the genome, terminating transcription and knocking out the gene, or disrupting the expression of the gene to various other effects. One way of achieving this is through the use of transposons - the so-called "jumping genes" - first identified in maize. Two transposable element systems from maize have been widely used in *Arabidopsis*: *Suppressor-mutator*, also called Enhancer (*Spm/En*) (Aarts et al., 1993); and *Activator/ Dissociation* (*Ac/Ds*) (Altmann et al., 1995, Bhatt et al., 1996, Long et al., 1997). In each case, the transposase genes, encoded by the autonomous elements *Ac* and *Spm*, are required to mobilize non-autonomous elements, *Ds* and *dSpm*, respectively. Mobilised transposons are capable of inserting themselves into the genome pseudo-randomly - as a general rule, they preferentially insert into the more available euchromatin upstream region of genes. Plants carrying the mobile elements are crossed with those carrying transposases (typically, these are introduced by T-DNA transformation). The F1 progeny is self-fertilised, and F2 plants selected that have inherited a transposed element, but have lost the transposase gene by segregation.

Transposon insertion was used to identify *LHY*. The original *lhy-1* allele was generated by a transposon insertion into the 5' untranslated leader, leading to over-expression of the mRNA (Schaffer et al., 1998). As transposons have a known DNA sequence, their insertion sites can be identified through sequencing outwards from primers within the transposon, allowing quick and easy identification of the knocked-out gene. However, most transpositions are short range (Bancroft and Dean, 1993, Keller et al., 1993),

meaning the majority of insertions are into relatively few genes.

In a similar way, transformation by *Agrobacterium* inserts a known DNA sequence at random into the genome, and can be used to generate mutants. This allows sequencing out for quick identification of the insertion site much like transposons; however they are advantageous as they insert at random into the genome (as opposed to close to their initial site), allowing far more genes to be knocked out. A T-DNA carrying a stop codon and an antibiotic resistance marker was generated by the Salk Institute Genomic Analysis Laboratory to this end (Alonso et al., 2003). The institute has created a library of these lines, with insertions into known genes, which can be ordered on demand. Such lines were instrumental in characterising the circadian function of *PRR5/7/9* (Salomé and McClung, 2005). However, unlike EMS and neutron mutagens, T-DNA and transposons occur at a significantly lower frequency (transformation rates are typically 1%), necessitating the testing of a far larger number of plants before mutants become apparent.

The majority of mutant generating techniques produce predominantly loss-of-function (null) mutants. Recently, T-DNA based techniques have been used to generate libraries of over-expression lines. One such approach was the RIKEN **F**ull-length cDNA **O**ver-e**X**pressing gene (FOX) hunting system, whereby a normalised full-length *Arabidopsis* cDNA library was introduced individually into the plant (Ichikawa et al., 2006). These cDNAs were driven by the 35S promoter - a global and constitutive over-expression promoter sourced from the Cauliflower Mosaic Virus (Odell et al., 1985). Insertion of these constructs results in constitutive high-level expression of the cDNA.

This resource has proved invaluable, however the identification of the genes is slow.

Transformation of plants is performed from a mixed *Agrobacterium* culture containing roughly equal proportions of 10,000 cDNAs. Sequencing is subsequently performed on the FOX lines to identify which cDNA they carry, a time-consuming process carried out at significant expense. As such, the library remains incomplete, with many genes lacking a representative FOX line (including, at the commencement of this project, all canonical clock genes). Additionally, the *p35S::cDNA* constructs have severe effects - a large number are seedling-lethal or result in considerable developmental phenotypes.

Current mutant libraries allow us a degree of investigation into the circadian system. Through knock-out and overexpression mutants, we are able to observe circadian defects for the core clock genes. However, the peripheral components and subtle feedback loops have remained thusfar elusive. Both techniques are crude measures for altering gene levels - for a diurnally oscillating or active gene, locking expression in the peak or trough from the moment the seed germinates in all tissues may be problematic as many circadian genes, as well as those regulating pathways which affect or are affected by the clock, have multiple roles at different developmental phases and in different tissues. A gene mutant may well give a circadian phenotype in adult plants, but will remain elusive if it is also require for proper embryogenesis. Compromising the ability of a plant to correctly express a transcript in any and all developmental and anatomical contexts may result in severe consequences.

Being able to choose when and where we alter expression would allow better investigation of the circadian clock. Seedling lethal genes could be investigated, potentially revealing the pathway for circadian inititation with germination. Expressing genes out of their usual anatomical context would allow us to visualise them better, especially for genes typically expressed in small tissues, by bringing them into the leaf where reporters can

be easily assayed. Finally, being able to choose when we "turn on" a mutant would allow investigation of circadian gating on the response - by inducing genes at different times during circadian phase, we can fully understand their roles in the oscillator. Fortunately, the Transcription Factor - Glucocorticoid Receptor (TF) Library addresses these issues and has recently been developed by RIKEN, Yokohama.

1.5 The RIKEN Transcription Factor - Glucocorticoid Receptor (TF) Library

1.5.1 Transcription Factors in *Arabidopsis*.

Transcription factors are DNA-binding proteins which regulate transcription. Plant transcription factors are notable for the large number of genes and the variety of gene families when compared with those of animal models. Of 25,498 predicted protein coding genes in *Arabidopsis* (The Arabidopsis Genome Initiative., 2000), of which 1500-2600 are predicted to possess transcription factor function (based on DNA binding domain (DBD) sequence conservation) (Davuluri et al., 2003, Guo et al., 2005, Iida et al., 2005, Riaño-Pachón et al., 2007, Riechmann et al., 2000). These genes fall into 72 distinct families and show far more diversity than transcription factors in animals. For example, zinc-finger TFs represent more than half of all transcription factors in *Drosophilla melanogaster* or the model nematode *Caenorhabditis elegans*, whereas in *Arabidopsis* they are still the most populous group yet represent only around 20% of the total (Riechmann et al., 2000). It is perhaps unsurprising that around half of all *Arabidopsis* transcription factors belong to families and contain DBDs that are unique to plants.

1.5.2 Glucocorticoid Hormones Induce Transcription Factor Function In Animals.

Glucocorticoids are a class of animal steroid hormones found almost universally in vertebrates. The family consists of many members including cortisol and dexamethasone, which cause pleiotrophic effects in humans and animals (Rhen and Cidlowski, 2005), although there are no glucocorticoid hormones or receptors in the plant kingdom.

Glucocorticoid hormones function through the glucocortioid receptor (GR), a protein sequence located in the cytoplasm of mammalian cells. As lipid-soluable steroid molecules, glucocorticoids are capable of passing through the phospholipid membrane into the cytoplasm, without need for an import protein. They activate the receptor through ligand binding.

In its native form, the GR is modular in structure and consists of six domains: the N-terminal regulatory domains (A/B), a DNA-binding domain (C), the hinge region (D), the ligand-binding domain (E), and the C-terminal domain (F) (Kumar and Thompson, 2005). The unbound GR exists in a cytosollic complex with the highly conserved heat shock proteins 90 and 70, with the hydrophobic ligand-binding cleft is opened to access by steroid (Pratt et al., 2006). Upon ligand binding, the GR undergoes a conformation change and dissociates from the heat shock proteins, facilitating its dynein-dependent translocation to the nucleus and import across the nuclear membrane.

The GR functions as a transcriptional activator. its main nuclear function in mammalian cells is the regulation of transcription of a suite of anti-inflammatory genes through its DNA binding domain (Buckingham, 2006, Hayashi et al., 2004). The hormone-dependent

FIGURE 1.8: Dexamethasone Induces Nuclear Import & Activity of Transcription Factors in the RIKEN TF-GR Library.

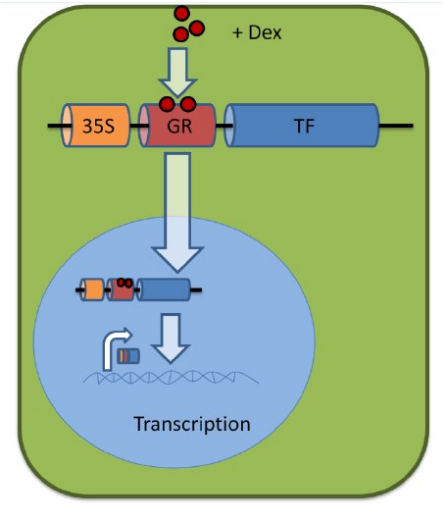

Dexamethasone binds to GR cassette, facilitating nuclear import of the protein. Upon co-localisation of transcription factor and DNA, transcription occurs. The 35S promoter drives high levels expression in all plant tissues.

import of GR into the nucleus brings the transcriptional activator into the same organellar domain as its target DNA sequences. In this way, glucocorticoids are capable of inducing transcriptional responses in mammalian cells.

1.5.3 The GR Cassette Has Been Incorporated Into Plants.

Glucocorticoid induction of transcription factors has been a tool in plant molecular biology for over two decades (Aoyama and Chua, 1997, Lloyd et al., 1994). As proteins which induce DNA transcription, native transcription factors are functionally active within the nucleus where they are able to bind DNA. Fusion of the mouse or rat GR ligand-binding domain to a transcription factor localises it within the cytoplasm and segregates it from its site of action. Treatment with a glucocorticoid hormone facilitates its import into the nucleus and, thus, transcription factor function. This import can clearly be demonstrated

through the use of GFP-GR fusion proteins in tobacco and *Arabidopsis* (Brockmann et al., 2001).

Induction of transcription factor activity through dexamethasone binding is sufficient to induce downstream gene expression. This was clearly demonstrated with the synthetic GVG (*35S:GAL4-GR*) system. In this, a transgenic construct consisting of the yeast GAL4 transcription factor bound to the GR ligand binding (E) domain is expressed under the 35S promoter from cauliflower mosaic virus, which conveys constitutative global over-expression in plants. Following treatment with dexamethasone, this construct is capable of inducing luciferase constructs driven by the *GAL4* promoter (Aoyama and Chua, 1997).

In addition to transactivation through an exogenous non-plant transcription factor, direct fusion of a transcription factor to a GR cassette can be sufficient to investigate the downstream targets. The use of a GR-cassette fused APETALA3/PISTILLATA (AP3/PI) led to the discovery of the downstream gene *NAC-LIKE, ACTIVATED BY AP3/PI (NAP)*, which was induced at the mRNA level following induction of the AP3-GR construct with dexamethasone (Sablowski and Meyerowitz, 1998). *SUPPRESSOR OF OVER-EXPRESSION OF CO 1 (SOC1)* and *FLOWERING LOCUS T (FT)* were also identified as direct targets of CONSTANS (CO) by this approach (Samach et al., 2000). A similar approach has been used in circadian studies, with induction of the *p35S:PRR5-GR* construct by dexamethasone elucidating *CCA1* and *LHY* as immediate downstream targets of PRR5 in the Night Inhibitor loop (Nakamichi et al., 2010). Use of the same construct was used to demonstrate the role of epigenetic marks (namely histone H3K4 trimethylation) in the circadian system. Dexamethasone application alongside treatment with nicotinamide, a histone H3K4 trimethylation suppressor, resulted in a significant increase of PRR5 binding to the *CCA1* and *LHY* promoters compared with

plants treated with dexamethasone alone (Malapeira et al., 2012).

The GR cassette provides an inducible transcription system in plants, allowing quicker responses to induction with less perturbation through stress than with the alternative alcohol- or heatshock-inducible promoter systems.

1.5.4 The RIKEN TF Library Of Inducible Transcription Factors.

The TF library is a genetic resource for *Arabidopsis* developed by the Matsui team in RIKEN Yokohama allowing rapid induction of over-expression function for a variety of transcription factors (Hong et al., 2013). It forms the backbone of this investigation, and unmodified provides the plant material for the initial screens.

RIKEN's TF library consists of transcription factor full-length cDNAs, driven by the constitutive 35S over-expression promoter, fused to the rat GR ligand binding domain (hence after GR). To construct binary vectors for over-expression of each transcription factor, a previously-generated entry clone library of Arabidopsis transcription factors was used (Mitsuda et al., 2010), and each open reading frame of a transcription factor recombined individually into the destination plasmid pBI35S-GW-GR through the GATEWAY cloning method (Invitrogen). This generated a vector containing the cDNA in-frame with the GR (glucocorticoid receptor) domain, under the control of the 35S promoter.

Each vector was transformed into *Agrobacterium* and, subsequently, into *Arabidopsis thaliana* (Columbia ecotype). TF library lines are T1 seed stocks, consisting of TF

homo- and heterozygotes along with wild types in a 1:2:1 ratio. As the 35S promoter results in over-expression (and, thus, gain-of-function) this results in a 3:1 stock of TF to wild type seed. Whilst a total of approximately 800 transcription factor vectors were successfully generated, due to failures in the transformation stages and time/space constraints the TF library remains incomplete at the time of writing, with no plans to generate the missing lines.

The TF line library provides advantages over alternative seed libraries (e.g. the SALK knock-out library, the RIKEN FOX 35S:mRNA over expression library in two ways. Firstly, and perhaps most obviously, the GR cassette allows us to manipulate the induction of the transcription factor (and, hence, downstream targets) at different points throughout the circadian or developmental cycle. Control of timing within the circadian cycle allows us to disrupt different loops of the circadian oscillator, and could result in differing effects and their immediacy. Induction late in the developmental cycle allows us to investigate over-expression phenotypes that may otherwise be seedling- or embryo-lethal.

The TF library transgenes are driven by the ectopic over-expression 35S promoter and this provides further advantages. Over-expression should reveal mild and redundant phenotypes that would be elusive to traditional loss-of-function mutant screens. It is already known that overlapping and partially redundant gene function is core to the clock function; whilst *cca1* null mutants only show mild short phenotypes due to redundancy of function with *LHY*, over-expression leads to arrhythmia (Wang and Tobin, 1998). Similarly in the *LOV-KETCH PROTEIN* family genes (*ZTL, LKP2, LKP3/FKF1*), individual loss-of-function mutations in *LKP3* are milder and are partially compensated by the other two members (Baudry et al., 2010). Over-expression allows us to investigate

the circadian network in a wider context than knock-out mutagenesis, and can reveal interesting gene families and complexes that might otherwise go undetected through complete or partial compensation.

The TF library is T1 seed. As these are over-expression lines, this allows screening of hetero and homozygous lines side by side - especially in techniques which pool seed. However, due to the differing copy number within the seed stocks, for some lines this may pose a problem regarding dosage compensation of the transcripts. It is important to remember this limitation alongside the relative convenience of the library in order to correctly interpret the results.

The 35S promoter has another interesting advantage over knock-out mutagenesis in that it is a global overexpressor affecting all tissues. As previously outlined, there is debate over whether the whole clock is present in all cells and all tissues (Endo et al., 2014, James et al., 2008). The global nature of the 35S promoter allows us to use leaf-specific reporters (be they *pCAB2:LUC*, *pCCR2:LUC* or chloroplast-driven delayed fluorescence) to identify phenotypes in components that would normally only occur outside the leaf mesophyll by bringing the causative gene and the reporter into the same cell.

1.6 Project Summary & Overview

In this project, delayed fluorescence was further developed as a circadian screening platform. The entirety of the RIKEN TF library (268 genes at the time of writing) was recovered, and initial *in silico* predictions made for this selection of genes. The lines

were treated with dexamethasone and screened for circadian phenotype through delayed fluorescence. 21 genes were identified as giving circadian phenotypes through this method.

These phenotypes were confirmed through delayed fluorescence and *pCAB2:LUC+* assays, and the effects of dexamethasone induction investigated. The SALK T-DNA databases were searched for homologous knock-out lines for these genes, their genotypes confirmed, and the knock outs analysed for circadian defects by delayed fluorescence. Further *in silico* analysis was carried out on these lines to enrich them for direct circadian clock involvement - specifically promoter region analysis, microarray data-mining, and consideration of anatomical context. The involvement of light in these circadian defects was investigated through hypocotyl elongation assays for a subset of these genes in multiple light regimes.

This resulted in the identification of three putative transcription factors which gave a circadian phenotype of interest: *INDOLE-3-ACETIC ACID INDUCIBLE 11*, the freezing-response regulator *MYBC1*, and *B-BOX DOMAIN PROTEIN/ CONSTANS-LIKE 15 (BBX13/COL15)*.

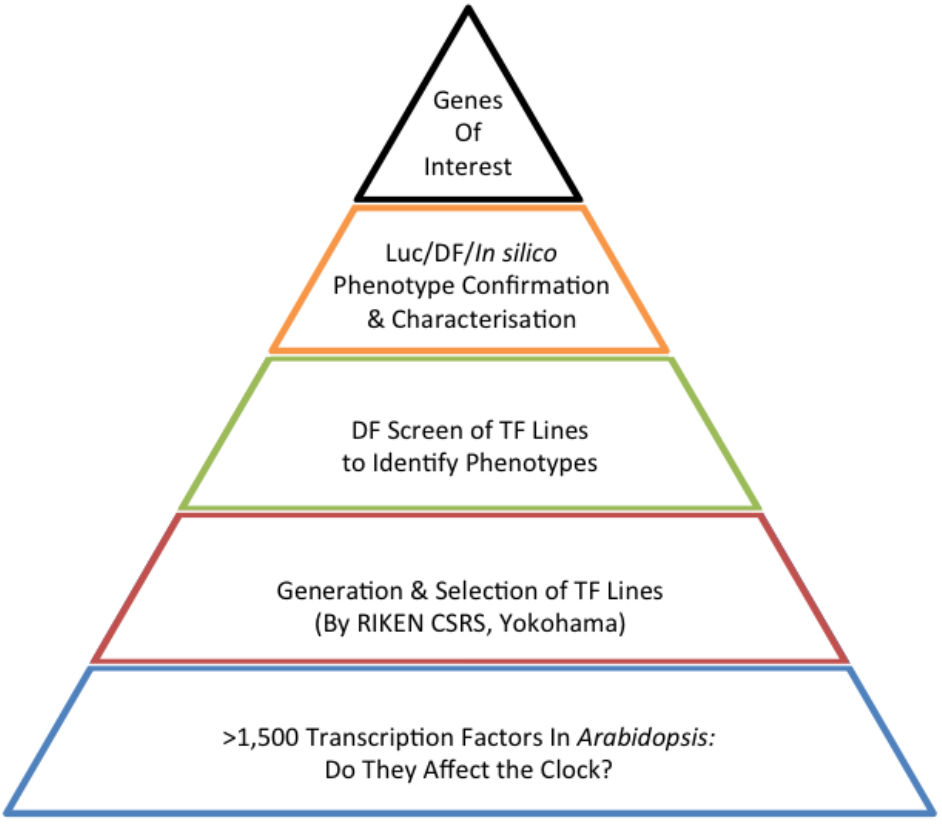

FIGURE 1.9: Workflow Overview of the Project.

Chapter 2

Materials & Methods

2.1 Plant Material & Provenance

2.1.1 RIKEN TF Lines

TF library lines were obtained from RIKEN Yokohama Institute, generated previously by Hong et al. (2013).

These lines were generated through the *Agrobacterium*-mediated transformation of Col-0 background wild type *Arabidopsis* with a TF-binary vector library. Binary vectors were generated using the GATEWAY cloning system (Invitrogen), whereby each open reading frame of a transcription factor (incorporated into a pDONR207 entry plasmid, sourced from the library generated in Mitsuda et al., 2010) was recombined individually into the destination plasmid, *pBI35S-GW-GR*, in-frame with the glucocorticoid receptor (GR). The destination plasmid was constructed by replacing the GUS gene of pBI121 with the GR fragment of a pMON721 derivative, and insertion of the 'reading frame B cassette'

for the GATEWAY cloning system between the 35S promoter and the GR of the pBI121 derivative (Aoyama and Chua, 1997, Rusconi and Yamamoto, 1987). The library was subsequently introduced into *A. tumefaciens* (GV3101pMP90) by electroporation, and Col-0 *Arabidopsis* transformed as outlined below.

Unless otherwise stated, all TF library lines are T1 stocks, of homozygous-heterozygous-homozygous mix in a 1:2:1 ratio (i.e. functionally 3:1 over-expression).

2.1.2 SALK lines

The Salk Institute Genomic Analysis Laboratory (SIGnAL) has generated a library of knock-out lines through random transformative insertion into the genome of a T-DNA construct containing a *p35S:NOS* terminator and the *NTPII* kanamycin-resistance marker. Insertion sites were confirmed by SIGnAL through DNA sequencing out from the flanking regions. All lines used in this investigation were selected through querying the SALK library by AtG gene code for stable T3 homozygous knockouts and ordering relevant seed stocks from the Nottingham Arabidopsis Stock Centre (NASC) repository (http://arabidopsis.info/). Ordered seeds were grown on MS media + 1.5% BactoAgar + 50μM kanamycin to to confirm homozygocity of the parent stock by segregation, and surviving lines allowed to set seed. It is these T4 generation seeds that were used for subsequent experiments, hereafter referred to as "SALK lines".

2.2 Plant Growth Conditions

2.2.1 Seed Sterilisation

2.2.1.1 Vapour-Phase Chlorine Surface Sterilisation

Vapour-phase surface-sterilisation was achieved by placing open Eppendorf tubes containing the loose seed (c. 50-1000 seeds per tube) into a large desiccation jar. Two chlorine tablets (CLO-TABS, Arrow Solutions) were dissolved in 500ml of RO water. This was vapourised through the addition of 5ml concentrated hydrochloric acid and the jar sealed. This was then left for 3 hours before seeds were removed from the desiccation jar and moved to a sterile flow hood for an additional 30 minutes to remove the remaining chlorine. Seeds were then imbibed and suspended in 0.15% agar. (Protocol modified from Clough and Bent, 1998)

2.2.1.2 Liquid-Phase Chlorine Surface Sterilisation

Liquid-phase surface sterilisation was achieved through washing c. 50-500 seeds per Eppendorf tube with 500-800μl 70% (v/v) ethanol and 0.05% (v/v) Triton X-100, turning periodically, for 2 minutes. Ethanol was removed and seeds bathed in 500-800μl 10% sodium hypochlorite bleach (commerical household bleach, diluted in autoclaved RO water) for 5mins with periodical shaking. Bleach was removed and seeds washed in 4 changes of sterile H_2O . Seeds were then imbibed and suspended in 0.15% agar.

2.2.2 Growth Media

Unless otherwise stated, "MS media/MS agar" refers to 1X Murashige & Skoog (MS) salts media dissolved in RO H_2O , adjusted to pH 5.8 with 5M potassium hydroxide, with 1.5% Agar. If used, drug supplements were added following autoclaving and cooling to 60°C . Standard drug supplement concentrations, to be assumed unless otherwise stated, are: 50μg /ml kanamycin, 20μg /ml hygromycin/

2.2.2.1 GM Agar

Germination Media (GM) Agar refers to 1X Murashige & Skoog (MS) salts in RO H_2O , pH 5.8, 0.8% Agar, supplemented with Gamborg's B5 vitamins (Sigma Aldrich, final concentration 1X) following autoclaving and cooling to 60°C .

2.2.2.2 Soil

Plants grown to seed were transferred from agar media to soil. Soil media was made by combining John Innes No. 1 with pearlite in a 2:1 ratio. All soils were autoclaved and treated with Intercept 60WP insecticide (imidacloprid).

2.3 General Protocols

2.3.1 Transformation of E.coli

Unless otherwise stated, all *Escherichia coli* strains are DH5α. 100ng of plasmid DNA was added to 50μl chemically competent DH5α cells, mixed gently, and incubated on ice for 30mins. Cells were then "heat shocked" by placing at 42°C for 45 seconds before returning to ice for a further 2 minutes. Samples were incubated at 37°C in a shaking incubator with 1ml pre-warmed LB media broth (10g/L tryptone, 5g/L yeast extract, 10g/L NaCl; adjusted pH 7.5) for 1hr prior to plating (20μl and 200μl) on LB media + 1% agar plates laced with selection antibiotics. Plates were incubated at 37°C for 2 days.

The following concentrations of antibiotics were used: 50μg /ml ampicillin, 50μg /ml kanamycin and 20μg /ml hygromycin.

2.3.2 DNA Extraction from Bacteria

Plasmids were extracted from overnight cultures, grown in the presence of antibiotics, through Miniprep with Wizard Plus SV Minipreps DNA Purification System (Promega) according to the manufacturer's instructions and the elution diluted to 100 ngμl .

2.3.3 Ethanol DNA cleanup

DNA was cleaned through ethanol precipitation. For a given volume of DNA, 1/10th of that volume of 5M ammonium acetate was added before adding 2-3 volumes of ice-cold 100% ethanol. The sample was mixed by pipette and incubated at -80°C for 1 hour. The sample was then centrifuged at 13,000rpm for 2 minutes to precipitate DNA. The

supernatant was removed and the DNA pellet washed with a volume of ice cold 70% ethanol followed by centrifugation. The wash was repeated, and the DNA pellet allowed to dry for 15 minutes at room temperature before being resuspended in 50μl water. Samples were diluted to 150ng/μl .

2.3.4 PCR

PCR was carried out with Kod FX Neo (Toyobo Biosciences) according to manufacturer's instructions. Unless otherwise stated, PCR was performed with 35 cycles, with an annealing temperature 5°C below the mean *T(m)* for the primer pair.

2.3.5 Agarose Gels

PCR samples were run on 1.2% agarose TBE gels for 40 minutes at 120V. Gels were transferred to an ethidium bromide bath (0.02mg/L) for 20 minutes before imaging on a UV imaging bed.

2.4 Dexamethasone Treatments

2.4.1 Preparation of Dexamethasone Stocks

Dexamethasone stock solutions were made by dissolving with 1ml absolute ethanol per milligram of anhydrous dexamethasone salt (Sigma Aldrich). Dexamethasone stocks were stored at 4°C in the dark.

2.4.2 Topical Treatment

Topical treatment solutions were made by diluting stock solutions 1:49ml with 0.01% Tween 20 in sterile water and passing through a 25μm syringe filter to give a 50μM dexamethasone solution. Solutions, if stored at 4°C , were allowed to reach room temperature before application to plants. Treatments were applied as an aerosol through the use of a 24mm atomiser pump, administered from 20cm away from the plates. Approximately 1 pump of the applicator nozzle was used per 20cm^2 of sample area (for 96 well plates, this was 6 pumps per plate using a standard applicator atomiser). Pumps were sterilised by soaking overnight in absolute ethanol, spray bottles were sterilised through autoclave. Mock treatments consisted of filtered 0.01% Tween 20 in sterile water, 2% ethanol, applied in the same manner. Unused working stocks were sealed, wrapped in foil and stored at 4°C for up to two weeks.

Unless otherwise stated, dexamethasone was applied at seven hours after dawn. This time was chosen as, in the Hall lab, this is the time used for application of luciferase. Plates of plants were removed from their growth chamber and transferred to a sterile flow hood. Room-temperature dexamethasone was applied as outlined above, and the plates re-sealed. The plates of plants were returned to the LD growth chamber. Imaging began at dawn the following day.

2.4.3 Media Infiltration

Growth media were supplemented with dexamethasone by adding stock solution to media, after autoclaving and allowing to cool to c. 60°C , to give a final concentration of

5μM dexamethasone.

2.5 Generation of Transgenic Lines

2.5.1 Generation of Missing TF Line Vectors

The transcription factor library constructed by RIKEN is incomplete with lines missing due to failure to generate colonies following the GATEWAY vector construction, failure to transform plants, a failure to recover transgenic progeny or death of the T0 plants before they could set seed. Notably, the circadian transcription factors *CCA1* and *LHY* were missing from the TF library. These were generated by transforming the gateway vectors constructed by Hong et al. (2013) and stored at RIKEN in deep freeze into *E.coli*, plating onto kanamycin selection LB media, recovering the plasmid by miniprep, confirming the identity through sequencing, and transforming into *Agrobacterium* for floral dip. The same Col-0 seed stocks as used to generate the RIKEN TF library were used. Selection was carried out as described below.

All TF library lines carry kanamycin resistance markers.

2.5.1.1 Transformation of *E.coli* and Recovery of Gateway Plasmids By Miniprep

E.coli were transformed with the protocol outlined above.

Resistant *E.coli* colonies were inoculated into 10ml LB broth and incubated with shaking at 37°C overnight. Plasmids were extracted through Miniprep with Wizard Plus SV Minipreps DNA Purification System (Promega) according to the manufacturer's instructions and the elution diluted to 100 ngμl . Identity of vectors was confirmed through RIKEN's in-house sequencing service, using primers generated for the vector backbone using Primer3 (Untergasser et al., 2012).

2.5.1.2 Transformation of *A. tumefasciens*

Vectors were transformed into *Agrobacterium* strain GV3101 (a strain resistant to gentamycin and rifampicin) through electroporation. 50μl of competent cells were mixed on ice with 1μl 100ng/μl plasmid DNA and transferred to a pre-chilled sterile 2mm electroporation cuvette. Cells were electroporated (BioRad electroporator; capacitance = 25 μF, voltage: 2.4 kV, resistance = 200 ω, pulse length = 5 msec), combined with 1ml LB liquid media, transferred to a 15ml culture tube and incubated for 4hrs at 30°C in a shaking incubator). Culture was spread on an LB agar selection plate (50 μg /ml gentamycin, 10 μg /ml rifampicin, 50μg /ml kanamycin) and incubated for 4 days to isolate individual colonies. (Protocol modified from Weigel and Glazebrook, 2006.)

2.5.2 Provenance & Preparation of *pCAB2:LUC+* Vector

The *pCAB2:LUC+* vector was sourced from Andrew Millar's lab (Millar et al., 1992), and arrived in RIKEN Yokohama as a stab culture in *Agrobacterium* strain GV3101 (resistant to gentamycin and rifampicin). This vector carries a hygromycin resistance

marker. Transformed stab culture was streaked onto LB media +1% agar plates supplemented with 50 μg /ml gentamycin, 10 μg /ml rifampicin and 20μg /ml hygromycin, and incubated at 28°C for 4 days to isolate individual colonies.

2.5.3 Transformation of *Arabidopsis*

2.5.3.1 Preparation of *Arabidopsis* for Transformation

Plants to be transformed were grown on MS agar plates as outlined above. When transgenic plants (TF lines and SALK lines) were to be transformed, the MS media was supplemented with 50μg /ml kanamycin to select for transformants. After 14 days plants were transferred to 3" diameter soil pots, with a density of 8 plants per pot, and the soil covered with netting. Plants were then grown under long day (18hr light/6hr dark) conditions until bolting and where visible flowers were present.

2.5.3.2 *Agrobacterium*-Mediated Transformation

Plants were transformed using the double floral dip method outlined in Davis et al., 2009. *Agrobacterium* colonies carrying a suitable transformation plasmid were grown in 50ml YEBS liquid media (1 g/L yeast extract, 5 g/L beef extract, 5 g/L sucrose, 5 g/L bacto-peptone, 0.5 g/L magnesium sulphate; adjusted pH 7, supplemented with 50 μg /ml gentamycin, 10 μg /ml rifampicin and an appropriate concentration of the *Arabidopsis* transformation vector selection antibiotic) at 28°C , 250 rpm for 3 days until cells had reached saturation. This culture was added to 450ml YEBS liquid media and incubated

for a further 8 hrs before the addition of 200μl Silwett L77.

The aerial parts of the plants (i.e. the internodal stems, bracts and floral tissues) were dipped in the *Agrobacterium* culture. Plants were sealed in plastic bags for 24hrs to increase humidity. This process was repeated with a fresh culture four days later to increase the transformation rate.

Plants were then placed in paper sleeves (to keep the seeds with their associated pots without affecting humidity), left to go to seed and allowed to dry completely before seed harvesting.

2.5.4 Selection of Transformants

T_0 seed was selected by plating liquid-phase surface sterilised seed at a density of approximately 200-500 seeds per 12cm x 12cm plate on MS + 1.5% agar. MS media was supplemented with relevant antibiotics (50μg /ml kanamycin for TF library transformation; 20μg /ml hygromycin for luciferase transformation; 50μg /ml kanamycin + 20μg /ml hygromycin for transformation of TF library lines and SALK lines with luciferase constructs). Following 2 days imbibition at 4°C in constant dark and 12 days growth, seedlings were selected for antibiotic resistance phenotypes. For kanamycin, this manifested as a resistance to bleaching of cotyledons and leaves (Harrison et al., 2006), wheras with hygromycin we observe no arrest of development prior to emergence of the first pair

of true leaves (Nakazawa and Matsui, 2003). Typical transformation rates were 0.8%-1.2%.

Transformed T_0 seedlings were transferred to soil pots and grown to seed. The resulting T_1 seed was retained (and screened in the case of luciferase transformation), and the selection procedure repeated to generate stable T_2 stocks. Zygocity of the lines was ascertained through germination segregation assay.

2.6 Circadian Imaging

2.6.1 Preparation of Plant Material For Delayed Fluorescence Imaging

Seed for delayed fluorescence analysis was vapour-phase surface sterilised, imbibed at 4°C for 48 hours prior to planting. 96-well plates were prepared by filling with MS agar to a total volume of 300μl per well. Seeds were planted in groups of 15-20 into the wells. An empty, inverted 96-well plate was place over the top to act as a lid and provide "headroom" for growing seedlings. The plates were sealed with a double layer of microporous tape. The plates were transferred into a Sanyo MLR350 plant growth chamber, and were grown under 80 μmolm^{-2} s^{-1} 12-h light/12-h dark cycles at 22°C for 14 days. These LD 12:12 light cycles, in addition to promoting growth, entrain the circadian oscillator. Plates were transferred to the imaging cabinet at dawn of day 15.

2.6.2 Preparation of Plant Material for Luciferase Imaging

Plate design and set-up was identical to that of delayed fluorescence imaging with the following modifications:

Seeds were planted in 96 well plates to the lower density of 10-15 seeds per well. Plants were grown for 7 days, and were removed from the chambers in the evening of d7 for luciferase treatment. Plates were re-sealed with microporous tape and returned to the growth chamber, and transferred to the imaging cabinet at dawn of day 8.

2.6.3 Experimental Conditions

Circadian screens were carried out in Sanyo MIR-553 incubators (Sanyo Gallenkamp, UK) set to the desired experimental temperature. Image acquisition was performed using a top mounted ORCA-II-BT 1024 16-bit camera (Hamamatsu Photonics, Japan) cooled to -80°C (Gould et al., 2009, Southern et al., 2006). This setup allowed for the simultaneous imaging of six 96-well microtitre plates per cabinet.

Lighting inside the cabinets was supplied by red/blue light emitting diode (LED) arrays (MD Electronics, UK). These arrays were controlled using WASABI imaging software (Hamamatsu Photonics, Japan) and, later, μManager (www.micro-manager.org/, Edelstein et al., 2010). This software also captured images from the cameras. Light intensity was set to a total of 40 μmol m^{-2} s^{-1}, split equally as 20 μmol m^{-2} s^{-1} from each red and blue channel.

2.6.4 Camera Settings & Image Capture

Identical cameras and lenses were used for both types of imaging, set up as described in Gould et al., 2009, Southern et al., 2006, with the following acquisition programs:

2.6.4.1 Delayed Fluorescence

Delayed fluorescence images were captured in the dark with a 2 min exposure. A 300 microsecond delay was inserted between switching off the lights and image capture to allow the extinction of any residual light, autofluorescence of plastics, etc. Following image capture, lights were switched back on to give functional constant light (LL) conditions. Image acquisition occurred at hourly intervals for 7 days.

2.6.4.2 Luciferase

Luciferase luminescence images were captured in the dark with a 20 min exposure. A five minute delay was inserted between switching off the lights and image capture to allow the extinction of any residual light and damping of delayed fluorescence to zero. Following image capture, lights were switched back on to give functional constant light (LL) conditions. Image acquisition occurred at two-hourly intervals for 7 days.

2.7 Hypocotyl Elongation Assays

Wavelength-specific hypocotyl elongation protocols were modified from those developed by Setsuko Shimada at the RIKEN Yokohama institute. Seeds were liquid-phase surface sterilised and planted on GM agar plates (10cm x 10cm), supplemented with 5μM dexamethasone, to a density of c. 40 seeds per plate. Plates were incubated in the dark for 3

days at 4°C before inducing germination through exposure to red light (1μmol m^{-2}) for 3 hours and then subjecting them to the test light treatment for 11 days. These were: red (1μmol m^{-2}), blue (10μmol m^{-2}) and dark (wrapped in aluminium foil, and placed in the same growth cabinets as the light conditions to ensure a stable temperature). All light conditions were constant (LL), with a temperature of 22°C . Hypocotyls were imaged using a Nikon D50 DSLR camera (Nikon Corporation, Japan) and the hypocotyls measured from the root/shoot junction to the point at which the cotyledon petioles branch from the shoot using the measure tools in FIJI/ImageJ (Abràmofff et al., 2005).

2.8 Gateway Cloning

2.8.1 Plant gDNA extraction

DNA was harvested from 5mm diameter leaf samples, which were ground in 400μl extraction buffer (200mM Tris-Cl, 250mM NaCl, 25mM EDTA, 0.5% SDS, pH 7.5). Ground lysate was centrifuged at 13,000rpm for 5 minutes to precipitate insoluble plant material, and the supernatant retained. An equal volume of propan-2-ol was added and the sample mixed by invertion. Centrifugation was repeated to pellet the DNA and the supernatant discarded. The DNA pellets were washed with 70% ethanol as outlined previously before suspension in 100μl water.

2.8.2 TOPO/BP Cloning

100ng of fresh PCR product was combined with 1μl salt solution an 1μl TOPO vector in a final volume of 6μl and mixed gently. Reactions were incubated at room temperature for 5 minutes before transformation into chemically competent *E.coli*

2.8.3 LR Cloning

300ng of entry vector was combined with 300ng of destination vector in 8μl of TE buffer, pH 8.0. 2μl LR Clonase II enzyme mix was added and mixed by vortexing briefly. Reactions were incubated at 25°C for 1 hour before 1μl Proteinase K was added to terminate the reaction. The samples were incubated at 37°C for 10 minutes before transformation into *E.coli.*

2.8.4 *XhoI* Linearisation

2μl 10X buffer, 1μl of *XhoI* (Takara Biosciences) and 1μg of vector DNA were combined and made up to a final volume of 20μl with water. The reaction vlume was incubates at 37°C for 5 minutes before denaturing the enzyme at 80°C for 5 minutes.

2.9 Yeast 2-Hybrid

2.9.1 Yeast Media

Unless grown on selection media, yeast was grown on YPDA media. After autoclaving, 15 ml of filter-sterilized 0.2% adenine hemisulfate (Sigma Cat. No. A-9126) was added to 1 L of YPD Medium (Bactopeptone 20g/L, yeast extract 10g/L, glucose 2.5%) to a final concentration of 0.003%.

SD minimal media (2% glucose, 6.7 g/L yeast nitrogen base without amino acids) was autoclaved, allowed to cool, and supplemented with drop-out supplement mixes (Clontech).

In both cases, agar media was made by addition of 2.5% BactoAgar before autoclavation.

X-α-gal plates were surface-infused with 100μl 5-bromo-4-chloro-3-indolyl alpha-D-galactopyranoside (4mg/ml, dissolved in dimethylformamide), and incubated overnight at 30°C to drive off solvent.

2.9.2 Transformation of AH109 Yeast

First, competent yeast cells were prepared. Yeast was grown in YPDA overnight at 30°C . From this overnight culture, 30 ml was transferred to a flask containing 300 ml of YPDA and adjusted to OD600 = 0.2 to 0.3. The sample was incubated at 30°C for 3 hours with shaking (230rpm) before centrifugation at 1,000 x g for 5 min at room temperature. The supernatant was discarded and the cells re-suspended in 50ml sterile TE buffer. Centrifugation was repeated, and the pellet resuspended in 1.5ml TE buffer.

Next, 1μg of plasmid DNA was combined with 0.1mg of sonicated salmon sperm DNA and 0.1ml of yeast competent cells and mixed by vortexing briefly. This was combined with 0.6ml of freshly prepared PEG/LiAc solution (40% PEG 3350 + 100mM LiAc in 1x TE) and incubated for 30 minutes at 30°C with shaking (200rpm). Cell walls were permeated by adding 70μl DMSO and mixing gently. Samples were then heat shocked (42°C for 15 minutes, on ice for 1-2 mins). Cells were centriuged at top speed for 5 seconds. The pellet was re-suspended in 0.5ml TE buffer and plated onto agar media and 1:1000, 1:100 and 1:10 dilutions.

2.10 Microarray

2.10.1 RNA Extraction

Plant samples were ground in pestle and mortars pre-chilled with liguid nitrogen. RNA extractions were performed using Qiagen RNeasy Plant kits, according to the manufacturer's protocol.

2.10.2 DNase I Clean-Up

DNA was removed from RNA samples through the action of DNase I. 20-50μg RNA was combined with 2μl Recombinant DNaseI in DEPC-treatetd 1X buffer (total volume = 50μl) and incubated at 37°C for 1 hour. DNase I was inactivated byincubation at 70°C for 10 mins, before dilute to 100μl with DEPC-treated water.

2.10.3 Phenol-Chloroform Clean-Up

In order to remove contaminating sugars and proteins, the entire sample of DNA-cleaned RNA was mixed with an equal volume of phenol: chloroform (pH 4.5), vortexed for 1 minute and spun at top speed in a micro-centrifuge for 2 minutes. The upper, aqueous phase was transferred to a fresh tube. Any errantly transferred chloroform was removed by centrifugation 10 seconds at top spin followed by removal of the bottom phase with a micropipette. Another volume of phenol-chloroform was added, vortexed, spun and the upper, aqueous layer reserved as before. This layer was combined with 20μl of 3M Sodium Acetate (pH 5.2) and 2.5 volumes of ice cold 90% ethanol, and placed on ice for 2–5 minutes before spinning at top speed in a microcentrifuge for 10 minutes. The supernatant was removed and the pelleted RNA washed with 1ml 70% ethanol. Pellets

were dried under a vacuum before resuspension in 25μl DEPC-treated water. RNA concentrations were confirmed by nanodrop.

2.10.4 Agilent One-Color Spike-In

RNA samples were labelled for microarrays using the One-Color Spike In kit (Agilent Technologies), according to the manufacturer's instructions for 200ng of RNA. Quality was confirmed with BioAnalyzer®chip-based capillary electrophoresis (Agilent Technologies). 500ng of RNA was denatured at 70°C for 2 minutes and loaded into BioAnalyzer RNA Nano chips, prepared and loaded with gel according to the manufacturer's protocol. Gels were run with the default settings for RNA Nano chips imaging eukaryotic total RNA. Data was analysed with 2100 Expert software (Agilent Technologies).

2.10.5 Labelling

Samples were labelled using Agilent Quick Amp labelling kits according to the manufacturer's instructions.

2.10.6 Microarray

Microarray samples were loaded into Agilent RNA Nano LabChips and run in the Agilent RNA 6000 Nano machine, according to manufacturer's instructions.

Data were analysed using Genespring GX (Agilent Technologies). Samples were baselined to median of all samples. Quality control thresholds from the Spike in mix were set to the default/recommended values (0.8 and 1.2) and were: detection limit, Ela slope, gSpatial, gNeg CH/Met, gNeg sub Sig.

Chapter 3

Delayed Fluorescence Screening of TF-GR Library Lines

3.1 Introduction

Constitutive overexpression of transcription factors can result in circadian phenotypes. This has been well-characterised within the core circadian oscillator, Overexpression of *CCA1* is known to result in arrhythmia (Wang and Tobin, 1998), whilst transient over-expression of *TOC1* supresses *CCA1/LHY* expression and results in a shortened period (Gendron et al., 2012). However, over-expression of genes outside of the canonical "core" clock can also result in circadian phenotypes, through up-regulating signalling pathways or through directly inducing clock genes. *FLOWERING BASIC-LOOP-HELIX 1 (FBH1)*, a transcriptional activator of *CONSTANS* in photoperiod-independent flowering (Ito et al., 2012), results in circadian period shortening when overexpressed through binding to and activating transcription at the *CCA1* promoter (Nagel et al., 2014). Over-expression of *HEAT SHOCK FACTOR B2b (HsfB2b)*, a gene responsible for responses to

biotic and abiotic stress, is capable of sustaining circadian rhythms at high temperatures that would normally induce arrhythmia (Kolmos et al., 2014). Overexpression of the light signal transduction pathway components *FHY3, FAR1* and *HY5* induces the promoter of *ELF4* (Li et al., 2011). Over-expression is advantageous in allowing the elucidation of otherwise elusive genes - knock-out lines, for example, may lackphenotypes dueto overlapping egen function and redundancy within the genome. Whilst overexpression lines may have pleitrophic effects which complicate analysis, it seems not only possible but likely that overexpression of additional transcription factors will result in circadian phenotypes.

Broad screening has been used to identify clock genes and circadian-regulating elements in the past. A forward-genetic screen using a *Ds* transposon carrying the *35S* constitutive over-expression promoter was used to identify *LHY*. This DNA transposon consists of two flanking regions surrounding a central *35S* promoter and is activated by the *Ac* transposase carried at an alternate locus (Long et al., 1993). Activation of the *Ds* transposon causes it to transpose and insert pseudo-randomly into the genome, preferring to insert itself in the regions upstream of genes. This, effectively, generates dominant gain-of-function mutants at random. An *LHY* gain-of-function mutant was generated in this manner, identified in a flowering type screen, and further characterised as a circadian transcription factor (Schaffer et al., 1998).

The screen employed in this study differs conceptually from this in two ways - firstly, it will be a direct circadian screen as it will measure delayed fluorescence rather than a multi-factor phenotype like flowering time which is only partially under clock control. This will allow more direct identification of factors that affect the clock, without the need to sift through those which function through other pathways. Furthermore, it is a reverse genetic screen whereby known genes are screened to discover novel phenotypes

rather than phenotypes screened to identify novel genes. The RIKEN TF library, like the *Ds* transposon, employs the *35S* promoter to grant dominant, gain-of-function phenotypes through over-expression. In each library line, the promoter drives a known cDNA sequence. The screen will identify whether over-expression of these genes results in a circadian phenotype.

Preparation of the RIKEN TF library lines was achieved through gateway cloning at RIKEN Yokohama (Hong et al., 2013, Mitsuda et al., 2010), which took place prior to the onset of this investigation. This is a three-stage process - first, an entry plasmid library containing the cDNA sequences of transcription factors from *Arabidopsis* was incorporated one by one into a destination plasmid pBI35S-GW-GR, inserting the cDNA sequence in-phase and in fusion with the GR cassette, driven by the CaMV 35S promoter. The GR cassette is a mammalian-derived sequence that associates to the cytoplasm, unless treated with a glucocorticoid hormone whereby it facilitates nuclear import (see Chapter 1.5). The destination plasmid also carries the sequences required for *Agrobacterium* mediated transformation into *Arabidopsis*.

Whilst this was attempted for over 1500 genes, plasmids were only successfully constructed for 934 samples. The plasmids were confirmed in the correct orientation for 800 of these genes. Of these, transformed T0 plants, and T1 seed stocks thereof, were only generated for 388 genes. Between 5 and 12 independent transformants were generated for each gene. From these, 4 independent transformants for each of the 388 genes were selected for this screen- a compromise had to be made between the degree of replication and the number of genes to be assayed as the number of lines that could be brought from RIKEN to Liverpool was limited by the amount of time available to collect seed samples and by departmental policy. Four independently-transformed lines is a suitable

number of replicants, providing suitable control for the potentially disruptive effects of random T-DNA insertion knocking out genes that result in or mask phenotypes, whilst still allowing the whole library to be collected and assayed.

Delayed fluorescence was selected as the screening technique for this assay, for reasons previously outlined in detail in Chapter 1.3. To summarise, DF provides a versatile screen that allows the highest throughput - it allows more parallel samples in a single experiment than leaf movement, IRGA or low-throughput molecular methods, yet unlike luciferase screening does not require transformation that would dramatically slow the initial screen. It is becoming increasingly common in plant investigations (Gould et al., 2009, Haydon et al., 2013b, MacGregor et al., 2013) and, with 2100 TF lines in total to screen, is well suited to the task in hand.

In order to gain an insight into the effects of overexpressing transcription factors on the circadian clock, the RIKEN TF library lines were collected from RIKEN Yokohama. First, predictions were made for these lines *in silico* - published microarray datasets were examined for diurnal expression profiles, and the promoter motifs were considered. Next, the lines were assayed for circadian phenotypes through delayed fluorescence. The periods of the lines were calculated through FFT-NLLS, and genes of interest selected for the next stage of the analysis.

As a result of this screen, 21 TF lines were identified as giving circadian phenotypes in the presence of dexamethasone.

3.2 Predicting Circadian Phenotypes *In Silico*

Ideally, a complete, unbiased screen would be carried out for every transcription factor in *Arabidopsis*. Unfortunately, this is not possible as the RIKEN TF library is incomplete - it does not have representative lines for 75% of the putative transcription factors. Systematic construction of the library has halted, and will not resume due to cost constraints of building the library wholesale. Individual transcription factor lines can, however, be constructed and plants generated on special order, if they are deemed necessary. Developing tools for predicting which genes would give circadian phenotypes is important as it allows us to select which of the remaining lines should have their generation prioritised for circadian study.

One method for approaching this problem is mining the wealth of circadian expression data already published. There are various databases containing plant gene expression data and tools for analysing published microarray data, including AtGenExpress (Schmid et al., 2005), GENEVESTIGATOR (Zimmermann et al., 2004), GEO (Barrett et al., 2007), VirtualPlant (http://virtualplant.org), and DIURNAL (Mockler et al., 2007). The last of these is geared towards identifying diurnal and circadian rhythmic patterns, and will be used for mining microarray data.

From expression data, it is possible to predict whether a gene is circadian regulated. For a gene to be part of the circadian clock, it must in turn be regulated by it. Whilst this regulation may be at the translational or post-translational, the microarray data captures the transcriptional level. Although not not all, clock genes are transcriptionally regulated, transcriptional feedback loops are still considered a "prime mechanism" driving the plant circadian clock (McClung, 2014, Staiger and Köster, 2011). Furthermore we know that many circadian inputs are in turn clock gated on the expression level. It

stands to reason that genes closely related to the circadian clock will be more likely to influence it, and vice-versa. Identifying these genes will, therefore, be used to predict future phenotypes.

3.2.1 Selecting & Testing Prediction Criteria

DIURNAL v 1.2 contains microarray data for over 20 different experimental conditions. (Table 3.1). These can be divided into two categories - diurnal experiments (where samples were entrained and sampled in diurnal light or heat conditions) and circadian ones (where samples were entrained in diurnal conditions but sampled in constant conditions). These samples include a range of different daylengths, growth media, light regimes, genotypes and age of plant at the start of the experiment (Table 3.1).

These datasets were probed for rhythmicity through the DIURNAL/HAYSTACK front-end provided by Mockler et al. (2007). This method takes gene expression data for microarrays over a timecourse and compares them to pre-determined HAYSTACK model expression profiles. The correlation is calculated through a modified Pearson correlation coefficient, with the threshold for rhythmicity set at 0.8 (as recommended by the system's developers). Analysis was carried out for the two experimental types outlined in Table 3.1. Out of 388 genes, 355 oscillated in one or sampling environment with diurnally alternating conditions. 351 genes oscillated in one or more circadian experiment. A more stringent criteria is therefore needed for making predictions.

Next, corresponding diurnal and circadian microarray datasets were compared to each other. Pairings were selected where all conditions are the same except for a single clock-pertinent variable. There are four such pairings offered by DIURNAL. In LDHC and

TABLE 3.1: Datasets Accessible Through DIURNAL & Their Experimental Conditions

Diurnal

Name	Age (Days)	Genotype	Media	Tissue	Light (μE)	Daylength	Temp (°C)
LLHC	7	Col-0	Agar, no suc	Seedling	100	12/12 LL	22/12
LDHC	7	Col-0	Agar, no suc	Seedling	100	12/12 LD	22/12
LDHH-Stitt	35	Col-0	Soil	Leaf	130	12/12 LD	22
LDHH-Smith	29	Col-0	Soil	Leaf	180	12/12 LD	20
Short Day	7	Ler	Agar, 3% suc	Seedling	180	8/16 LD	22
Long Day	7	Ler	Agar, 3% suc	Seedling	90	16/8 LD	22
COL SD	7	Col-0	Agar, no suc	Seedling	100	8/16 LD	22
COL LDHH	7	Col-0	Agar, 3% suc	Seedling	120	12/12 LD	22
LER SD	7	Ler	Agar, no suc	Seedling	100	8/16 LD	22
phyB9 SD	7	*phyB-9*	Agar, no suc	Seedling	100	8/16 LD	22

Circadian

Name	Age (days)	Genotype	Media	Tissue	Light (μE)	Daylength	Temp (°C)
LL (LLHC)	7	Col-0	Agar, no suc	Seedling	100	LL	22
LL(LDHC)	7	Col-0	Agar, no suc	Seedling	100	LL	22
LL12(LDHH)	7	Col-0	Agar, 3% suc	Seedling	100	LL	22
LL23(LDHH)	8	Col-0	Agar, 3% suc	Seedling	60	LL	22
DD(DDHH)	8	Col-0	Agar, 3% suc	Seedling	0	DD	22
lhyox SD	7	*lhy-ox*	Agar, no suc	Seedling	101	8/16 LD	22
lux-2 LDHH	7	*lux-2*	Agar, 3% suc	Seedling	120	12/12 LD	22

Genotypes - Columbia (Col-0), Landsberd-ereta (Ler). Both *phyB-9* and *lux-2* are null mutants in Col-0 backgrounds. Light intensity measured in microeinsteins per second per meter squared (μE).

LL(LDHC), samples are grown and entrained by 12hr light/heat cycles in both experiments, with LL(LDHC) being transferred to an environment with constant heat and light - and hence placed in circadian free-run - prior to sampling. LLHC/LL(LLHC) is similar, entrained by heat alone. COL SD/*lhyOX* SD and COL(LDHH)/*lux-2*(LDHH), conversely, represent two identically prepared samples of two different genotypes - a wild type and a clock mutant. Comparison of these paired conditions will allow the separation of genes responding to their environment from those that are driven by the circadian clock.

In order to test these prediction metrics, a list of circadian clock components with transcriptional regulation activities was used. The hypothesis tested was whether the prediction criteria outlined above would select the known clock genes - i.e. are the clock genes rhythmic in diurnal conditions and arrhythmic in free run? Eight genes were used for

TABLE 3.2: Comparison of Microarray Expression Profiles

		Conditions		Number of Genes		
Exp.	Description	Con. 1	Con. 2	Arrhythmic	Diurnal	Circadian
1	Light- & Temp.-Entrainment	LDHC	LL(LDHC)	92	99	61
2	Temp.-Entrainment	LLHC	LL(LLHC)	116	75	73
3	*LHY* OX	Col-0 SD	*lhyOX* SD	17	216	22
4	*LUX* Knockout	Col-0 LD	*lux-2* LD	19	207	31

In experiments 1 and 2, diurnally expressed genes are those which are rhythmic in Condition 1 only (i.e. they are rhythmic in the presence of the zeitgeber). Circadian expressed genes are those that are rhythmic in both conditions (i.e. rhythms persist in free-run). In experiments 3 and 4, circadian expression is taken to mean genes which are rhythmic in the wild type but this rhythm is abolished in the circadian mutant. Diurnal expression in these conditions is for lines for which rhythm persists in the mutant (i.e. where circadian perturbation does not abolish rhythm). In both groups, the arrhythmic samples are those that do not return a rhythmic expression profile in both conditions

this: *CCA1, LHY, PRR3, PRR5, PRR7, PRR9, TOC1,* and *LUX*. In the comparisons between diurnal conditions and free-run (Exp. 1 & 2), the prediction criteria stand up well. All eight genes are expressed rhythmically in both diurnal conditions (i.e. P >0.8). All are also rhythmic in both free-run conditions, with the exception of *PRR9* which is not rhythmic in LL(LDHC). As such, seven clock genes are predicted as being implicated in the circadian clock in both experiments, and one is predicted in a single condition. This criteria, therefore, can be used to make reliable predictions.

Predictions from the mutant/wild type comparisons (Exp 3 & 4) do not fare so well. All eight clock genes are rhythmically expressed in both wild type and both mutant conditions. This at first seems surprising, especially for *LHY* which would be expected to be arrhythmic in the constitutive over-expresser *lhyOX*. However, *LHY* transcript levels have been shown tobe rhythmically regulated even in the over-expressor, albeit at low amplitude, due to gating of the oscillator Schaffer et al. (1998). Furthermore, in Experiment 3 the over-expressor is sampled in diurnal (short day) light, further allowing gating of the transcripts through the actions of e.g. phytochromes and cryptochromes. Either way, none of the eight clock genes were predicted as giving clock phenotypes by

these methods, which is obviously incorrect.

Arrhythmia is a very severe clock phenotype - indeed, the most severe - and perhaps it is unfair to use it as the only criteria for predicting circadian involvement. In addition to identifying whether genes are rhythmically expressed, DIURNAL also provides a quantification of circadian phase. As an alternative prediction method, phases were compared between the two conditions in each experiment (Table 3.3). A threshold of >2hrs phase difference was chosen as the biological significance cut-off. In the two diurnal/free-run comparisons, none of the genes show a phase shift of >2hrs, as expected. In the mutant experiments, phase shifts are expected between the wild-type and aberrant circadian clocks. In *lhyOX*, all clock genes queried had a phase shift of >2hrs except for *PRR9*. In *lux-2*, only *LUX* itself showed a phase shift of >2hrs.

In summary, different criteria will be used to make predictions in the two experiment types. For zeitgeber experiments, rhythmicity in both entraining and free-run conditions identifies circadian-regulated genes. In the mutant experiments, the loss of rhythmia in the mutant will be used alongside phase shifts of more than 2 hrs. Genes flagged in 3 or more conditions as having circadian involvement will be selected as being intimately involved in the clock and predicted to give a phenotype in the over-expresser.

3.2.2 Summary & Predictions

A total of 194 genes were identified and flagged as having circadian involvement in one or more condition set.

In Experiments 1 and 2, where expression patterns are compared between diurnal conditions and entrained free run, 61 and 73 genes respectively were flagged. As these were free-run experiments, this means that rhythms persisted when entrained plants were

transferred to free-run. Far fewer genes (92) were arrhythmic when entrained by both light- and heat-cycles than in heat cycles alone (116), which is to be expected. There were also genes which were circadian regulated in one entrainment condition but arrhythmic in the other (Exp1=26, Exp2=38), suggesting and demonstrating the differential entrainment pathways by heat and light.

The remaining two experiments compare clock mutants to the wild type, where circadian phenotypes manifest as rhythms in the wild type but arrhythmia in the clock mutant, even in the presence of a zeitgeber. A total of 22 genes rhythmic in the wild type were arrhythmic in *lhyOX*, and 30 were so in *lux-2*. In addition, 53 genes showed a phase shift of >2hrs in the *lhyOX*. In *lux-2*, this was the case for 71 genes.

A total of 30 genes were flagged as being of circadian interest in three or more experiments. These genes were predicted to have a deep circadian involvement, and their over-expression may well have interesting consequences for the clock (Table 3.4).

TABLE 3.3: In Silico Prediction Testing Using Known Clock Genes

Exp1 (Are genes rhythmic in diurnal and free run?)

	LDHC		LL(LDHC)		Predictions	
Gene	Rhythm	Phase	Rhythm	Phase	Rhythm	Phase
LHY	Yes	23	Yes	1	Yes	-22 (2)
PRR9	Yes	4	No	n/a	No	n/a
CCA1	Yes	1	Yes	1	Yes	0
LUX	Yes	11	Yes	13	Yes	2
PRR7	Yes	7	Yes	7	Yes	0
PRR5	Yes	8	Yes	8	Yes	0
PRR3	Yes	12	Yes	13	Yes	1
TOC1	Yes	12	Yes	14	Yes	2

Exp2 (Are genes rhythmic in diurnal and free run?)

	LLHC		LL(LLHC)		Predictions	
Gene	Rhythm	Phase	Rhythm	Phase	Rhythm	Phase
LHY	Yes	2	Yes	2	Yes	0
PRR9	Yes	7	Yes	7	Yes	0
CCA1	Yes	2	Yes	2	Yes	0
LUX	Yes	13	Yes	15	Yes	2
PRR7	Yes	8	Yes	8	Yes	0
PRR5	Yes	10	Yes	10	Yes	0
PRR3	Yes	13	Yes	13	Yes	0
TOC1	Yes	13	Yes	14	Yes	1

Exp3 (Are lines arrhythmic OR >2hr phase-shifted in free run?)

	WT (SD)		*lhyox* (SD)		Predictions	
Gene	Rhythm	Phase	Rhythm	Phase	Arrhythmic	Phase
LHY	Yes	23	Yes	17	No	-6
PRR9	Yes	4	Yes	4	No	0
CCA1	Yes	23	Yes	7	No	-16
LUX	Yes	9	Yes	20	No	11
PRR7	Yes	6	Yes	19	No	13
PRR5	Yes	8	Yes	19	No	11
PRR3	Yes	8	Yes	20	No	12
TOC1	Yes	14	Yes	21	No	7

Exp4 (Are lines arrhythmic OR >2hr phase-shifted in free run?)

	WT (LDHH)		*lux-2* (LDHH)		Predictions	
Gene	Rhythm	Phase	Rhythm	Phase	Arrhythmic	Phase
LHY	Yes	0	Yes	1	No	1
PRR9	Yes	4	Yes	4	No	0
CCA1	Yes	1	Yes	1	No	0
LUX	Yes	11	Yes	15	No	4
PRR7	Yes	7	Yes	7	No	0
PRR5	Yes	8	Yes	8	No	0
PRR3	Yes	12	Yes	11	No	-1
TOC1	Yes	13	Yes	14	No	1

TABLE 3.4: Predicted Circadian-Linked Genes (Microarray Mining)

TF	AtG	Exp1 Circ	Exp2 Circ	Exp3 Arr.	Exp4 Arr.	Exp3 Phase	Exp4 Phase
T0142	AT5G61590	Yes	Yes	No	No	Yes	Yes
T0171	AT1G04550	Yes	Yes	No	No	Yes	No
T0195	AT1G05805	Yes	Yes	No	Yes	Yes	No
T0222	AT2G18300	Yes	Yes	No	No	Yes	Yes
T0223	AT2G20180	No	Yes	No	No	Yes	Yes
T0281	AT5G12330	No	No	Yes	Yes	Yes	Yes
T0294	AT5G62610	No	Yes	No	No	Yes	Yes
T0301	AT1G03970	Yes	Yes	No	Yes	No	No
T0309	AT1G22070	Yes	Yes	No	No	No	Yes
T0366	AT5G11260	No	Yes	No	No	Yes	Yes
T0393	AT2G02080	Yes	No	No	No	Yes	Yes
T0490	AT5G60850	Yes	Yes	No	No	Yes	Yes
T0491	AT5G62430	No	Yes	No	No	Yes	Yes
T0492	AT5G62940	No	No	No	Yes	Yes	Yes
T0530	AT1G70510	No	No	Yes	No	Yes	Yes
T0534	AT1G79840	No	No	No	Yes	Yes	Yes
T0575	AT5G41410	Yes	Yes	No	No	Yes	Yes
T0580	AT5G65310	Yes	No	No	No	Yes	Yes
T0875	AT5G05090	Yes	No	No	No	Yes	Yes
T0909	AT5G59450	No	No	No	Yes	Yes	Yes
T1005	AT5G08330	Yes	Yes	No	No	Yes	Yes
T1034	AT5G28300	No	Yes	No	No	Yes	Yes
T1103	AT5G15850	Yes	Yes	No	No	Yes	Yes
T1106	AT5G57660	Yes	Yes	No	No	Yes	Yes
T1116	AT5G14960	Yes	Yes	No	No	Yes	Yes
T1146	AT1G10200	Yes	Yes	No	No	Yes	No
T1254	AT5G50010	Yes	No	No	No	Yes	Yes
T1356	AT1G70000	Yes	Yes	No	No	Yes	No
T1438	AT5G07690	No	Yes	No	No	Yes	Yes
T1440	AT5G08520	Yes	Yes	No	No	Yes	Yes

3.3 Analysis & Data Pipeline Construction

3.3.1 Introduction & Test Data Provenance

A multitude of data analysis tools exist for use in plant circadian biology. In this section the relative benefits of different analysis techniques are assessed and compared, their limitations considered, and the analysis approach for the project selected. The data analysis pipeline is constructed, incorporating existing software, new uses of applications, and the writing of novel software for processing and interpreting data.

For comparison of techniques, a previously published test data set was sourced from the lab group and analysed through each method. The data consists of wild type, *phyE*,*toc1-101*,*lhy*, *prr5-1*, *ztl-105* and *phyD* lines carrying *pCAB2:LUC+* or *pCCR2:LUC+* markers.

3.3.2 Period Analysis Techniques

With the development of high-throughput assays, developing large data-sets in ever decreasing time frames, quantitative period identification has increasingly become a time-consuming and rate-reducing step in circadian investigation. Fortunately, several methods for estimating the underlying period have been developed that can reduce and simplify this process. With a variety of different techniques and algorithms of varying complexity, choosing which is most applicable can prove challenging.

Broadly, period prediction and quantification approaches can be split into two categories: curve-fitting algorithms and stochastic modelling approaches.

The related curve-fitting algorithms mFourfit and Fast Fourier Transform Non-Linear Least Squares (FFT-NLLS), long the central period estimators in circadian investigations, both function by constructing a model wave-form from the sum of several cosine functions (up to five for mFourfit; up to 25 for FFT-NLLS) with a primary period within a user-defined biologically significant range (Edwards et al., 2010, Martin Straume et al., 1991). In this investigation, this range is assumed as 15h to 35h.Of these, FFT-NLLS is preferred as it is capable of identifying and returning arrhythmic results and providing the confidence intervals for the predicted periods, phases and amplitudes, allowing us to identify arrhythmic samples in a manner that mFourfit cannot. It is the stronger method for working with messy, noisy data such as delayed fluorescence outputs.

Alternative techniques, Maximum Entropy Spectral Analysis (MESA) and Spectrum Resampling (SR), have been developed using a stochastic modelling approach (Burg, 1972, Costa et al., 2013, Dowse and Ringo, 1989). Although the particulars differ, both methods function by repeating the cycle of fitting a model, adding noise, smoothing and taking period measurements. The resulting measurements are used to calculate a biological period and its confidence limits. Whilst MESA and SR especially are designed to be more robust when confronted with observational noise (Costa et al., 2013), they are considerably more computationally taxing than other methods, with SR being particularly noise tolerant and extremely mathematically demanding.

3.3.3 Comparison & Selection of Period Prediction Techniques

It is recommended by Zielinski et al. (2014) to, where possible, perform simultaneous analysis with techniques from both curve-fitting and stochastic spectrum schools for analysing data . All four proceedures outlined above can be run remotely on a server

TABLE 3.5: Comparison of Period Estimation Methods

	FFT		MFF		MESA		SR	
Line	Mean	Median	Mean	Median	Mean	Median	Mean	Median
Wild Type:CCR2	23.40	23.39	23.43	23.46	23.08	23.15	22.34	22.38
Wild Type:CAB2	22.43	22.43	22.40	22.32	22.38	22.34	23.35	23.39
lhy:CCR2	22.41	22.59	22.73	22.47	22.10	22.05	22.53	22.52
phyD:CCR2	22.90	22.88	22.66	22.62	22.30	22.34	22.70	22.77
phyE:CAB2	22.59	22.66	22.54	22.60	22.61	22.65	22.53	22.62
prr5-1:CAB2	21.72	21.65	21.73	21.64	21.53	21.49	21.49	21.43
prr5-1:CCR2	21.25	21.29	21.02	21.40	20.85	20.63	20.83	20.86
toc1-101:CAB2	19.87	19.04	19.91	19.19	19.32	19.22	19.56	19.20
toc1-101:CCR2	19.46	19.42	19.63	19.26	19.65	19.39	19.71	19.27
ztl-105:CCR2	22.74	23.28	22.71	22.73	22.41	22.32	22.79	23.00

Comparison of the same set of luciferase data (See Section 3.3.1). Seeds were surface-sterilised, vernalised for 2 days in constant darkness at 4°C before being planted on MS + 1.5% agar in 96-well plates at a density of c 10 seeds per sample, sealed with micropore tape and grown under 100μmol m^{-2} s^{-1} 12:12 22°C conditions for 7 days. Samples were saturated with luciferase through topical application on the evening of day 7 before transfer to the CCD imaging camera. Samples analysed through four period estimation methods hosted on BioDARE. For all samples, n = 8.

TABLE 3.6: Comparison of Goodness-of-Fit By Analysis Method

	FFT GOF		MFF GOF		MESA GOF		SR GOF	
Line	Mean	Median	Mean	Median	Mean	Median	Mean	Median
Wild Type:CAB2	0.450	0.450	0.440	0.439	0.417	0.412	0.381	0.400
Wild Type:CCR2	0.632	0.604	0.703	0.720	0.618	0.606	0.602	0.592
lhy:CCR2	0.698	0.734	0.826	0.838	0.709	0.697	0.700	0.708
phyD:CCR2	0.718	0.706	0.820	0.840	0.678	0.683	0.700	0.713
phyE:CAB2	0.441	0.457	0.447	0.474	0.409	0.413	0.355	0.361
prr5-1:CAB2	0.621	0.634	0.742	0.754	0.686	0.712	0.610	0.622
prr5-1:CCR2	0.732	0.697	0.882	0.870	0.793	0.778	0.793	0.782
toc1-101:CAB2	0.675	0.674	0.870	0.863	0.830	0.840	0.721	0.784
toc1-101:CCR2	0.796	0.754	0.965	0.965	0.865	0.867	0.880	0.874
ztl-105:CCR2	0.791	0.795	0.931	0.932	0.832	0.846	0.794	0.813

Comparison of the same set of luciferase data (See Section 3.3.1). Seeds were surface-sterilised, vernalised for 2 days in constant darkness at 4°C before being planted on MS + 1.5% agar in 96-well plates at a density of c 10 seeds per sample, sealed with micropore tape and grown under 100μmol m^{-2} s^{-1} 12:12 22°C conditions for 7 days. Samples were saturated with luciferase through topical application on the evening of day 7 before transfer to the CCD imaging camera. Samples were analysed through four period estimation methods hosted on BioDARE. For all samples, n = 8.

TABLE 3.7: Comparison of Period Error Estimation Methods

	FFT Err.		MFF Err.		MESA Err.		SR Err.	
Line	Mean	Median	Mean	Median	Mean	Median	Mean	Median
Wild Type:CCR2	0.311	0.308	0.618	0.606	0.703	0.720	0.021	0.021
Wild Type:CAB2	0.188	0.169	0.417	0.412	0.440	0.439	0.027	0.027
lhy:CCR2	0.415	0.369	0.709	0.697	0.826	0.838	0.112	0.024
phyD:CCR2	0.397	0.425	0.678	0.683	0.820	0.840	0.028	0.027
phyE:CAB2	0.169	0.169	0.409	0.413	0.447	0.474	0.020	0.020
prr5-1:CAB2	0.330	0.328	0.686	0.712	0.742	0.754	0.026	0.027
prr5-1:CCR2	0.493	0.442	0.793	0.778	0.882	0.870	0.028	0.028
toc1-101:CAB2	0.454	0.448	0.830	0.840	0.870	0.863	0.039	0.030
toc1-101:CCR2	0.671	0.589	0.865	0.867	0.965	0.965	0.050	0.040
ztl-105:CCR2	0.593	0.620	0.832	0.846	0.931	0.932	0.034	0.030

Comparison of the same set of luciferase data (See Section 3.3.1). Seeds were surface-sterilised, vernalised for 2 days in constant darkness at 4°C before being planted on MS + 1.5% agar in 96-well plates at a density of c 10 seeds per sample, sealed with micropore tape and grown under 100μmol m^{-2} s^{-1} 12:12 22°C conditions for 7 days. Samples were saturated with luciferase through topical application on the evening of day 7 before transfer to the CCD imaging camera. Samples analysed through four period estimation methods hosted on BioDARE. For all samples, n = 8.

hosted by the BioDARE service (University of Edinburgh), which will form part of the pipeline.

The test data (outlined in Section 3.3.1) was analysed through four period analysis techniques - FFT-NLLS, MFourfit, MESA and Spectrum Resampling. Biologically relevant period thresholds were set at 15hrs and 35hrs. Mean and median values for predicted period, error and goodness-of-fit were calculated and are recorded in Tables 3.5, 3.7 and 3.6 respectively. Mean intensity traces as well as period vs error plots were plotted for each sample comparing it to the wild-type are are shown in full in Appendix A

There is no large difference in the mean periods returned by any of the methods, although spectrum resampling has a tendency to return slightly shorter periods (Table 3.5). Goodness-of-Fit is comparable across the four techniques, with FFT and SR tending towards slightly lower GOF values and, hence, better model fit (Table 3.6). The error estimates corresponding to are far more divergent between the four methods. MFourFit

and MESA return far higher error values than FFT-NLLS. Spectrum resampling produces far smaller error values, by a factor of 10 or more. (This can be clearly seen in the period vs error charts in Appendix A, Figures A.1 & A.2). It should be noted that these differences are due to the fundamentally different approaches of the analysis methods. MFourFit gives preference to simpler models over those with lower error and GOF, whilst FFT-NLLS allows greater curve fitting to reduce these metrics at the cost of over-fitting. Likewise, spectrum resampling seeks to minimise error, and employs an iterative process to decrease it and hence gives low error values typically <0.1.

For this study, FFT-NLLS will be the main period prediction technique used. It has a longer history in plant circadian research than SR, and is more widely accepted than any other technique. SR analysis will be carried out, as doing so with BioDARE is relatively trivial, and used to confirm FFT-NLLS phenotypes - when FFT-NLLS cannot confidently identify a period within the biologically acceptable range, or cannot choose between two periods, SR will be used to clarify whether this sample is rhythmic and what period it has.

3.4 Dexamethasone and the Empty GR Vector Have No Effect on the Circadian Clock

Whilst there are no native glucocorticoid receptors in the plant kingdom, there is no guarantee that the hormones do not affect native plant components. Indeed, there is evidence that treatment with dexamethasone induces a whole suite of genes in the wild type and in lines transformed with the empty vector and, furthermore, in high concentration is sufficient to elicit significant stress responses and cause developmental and growth defects (Kang et al., 1999). Additionally, dexamethasone induces an enlargement of the nuclear pore complex in animals that may allow non-specific transport of large solutes and proteins across the nuclear membrane (Kastrup et al., 2006). Taken together this indicates that glucocorticoids may have a series of non-specific effects on gene transcription independent of the GR cassette. Whilst dexamethasone induction of a transgenic GR construct is a well-established protocol (Aoyama and Chua, 1997, Brockmann et al., 2001, Kang et al., 1999, Onouchi et al., 2000, Pautot et al., 2001, Sablowski and Meyerowitz, 1998), its effects on the sensitive circadian clock in wild-type *Arabidopsis* is as-yet unknown.

Additionally, an empty vector line was obtained from RIKEN Yokohama, containing the GR vector fused to no additional residues driven by the CaMV 35S promoter. This line was used to see whether the GR cassette is sufficient to induce a circadian phenotype, with or without dexamethasone.

In order to demonstrate the effects of dexamethasone on the native *Arabidopsis* clock, wild type and empty vector seeds were planted in groups of 15-20 on MS media as outlined in 2 and grown for 14 days in LD 12:12 cycles before treating with topical

dexamethasone or mock-treatment with the dexamethasone solvent solution. Treatment was applied at ZT+7, and the plants returned to the LD growth cabinets. Imaging began at the subsequent dawn. These plants were then imaged through delayed fluorescence in LL, and their periods calculated through FFT-NLLS.

There was no significant difference in mean period between dexamethasone treated and untreated wild type plants ($Period_{treated}$ = WT - 0.51, p= 0.104). The empty *p35S::GR* vector had no significant effect on period, both following mock (p = 0.104) and dexamethasone treatment (p= 0.218, Figure 3.1b). In addition, there are no phase shift effects (Table 3.1a). In conclusion, the induction system does not interfere with the circadian clock or delayed fluorescence output.

FIGURE 3.1: Dexamethasone and the Empty GR Vector Have No Effect on the Clock.

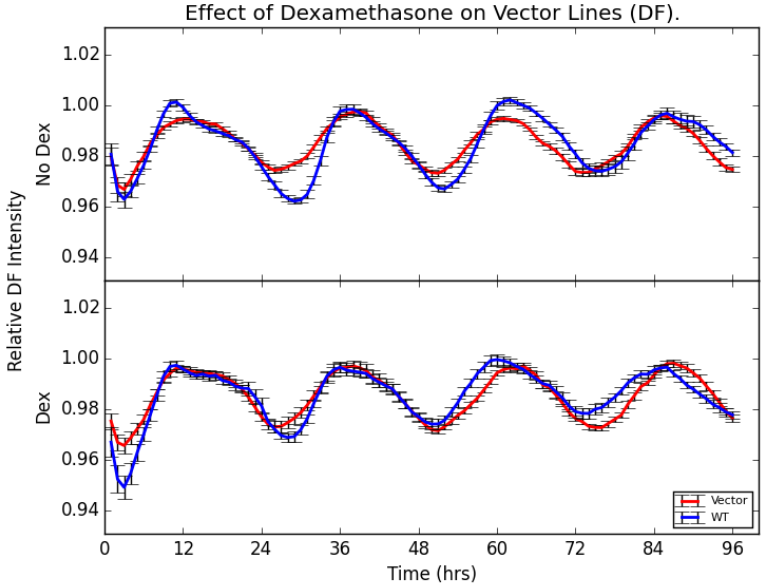

(A) Mean DF Relative Intensity.

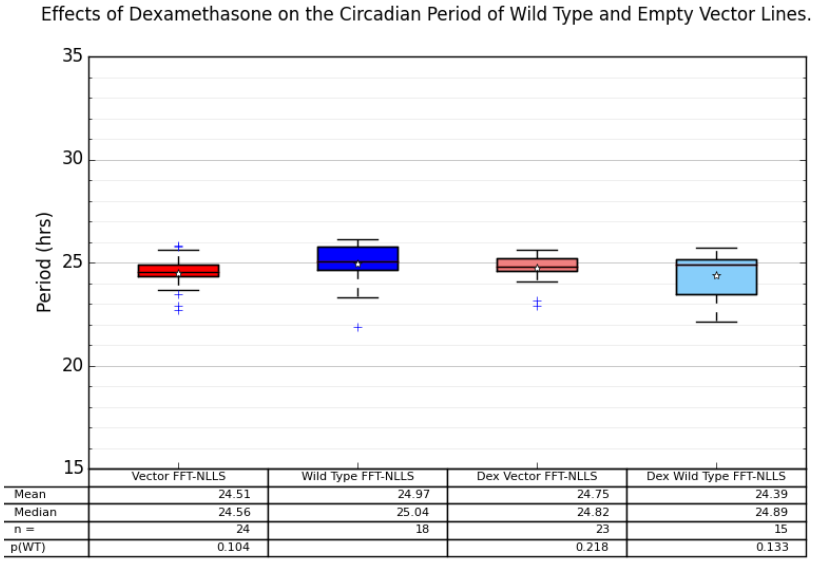

	Vector FFT-NLLS	Wild Type FFT-NLLS	Dex Vector FFT-NLLS	Dex Wild Type FFT-NLLS
Mean	24.51	24.97	24.75	24.39
Median	24.56	25.04	24.82	24.89
n =	24	18	23	15
p(WT)	0.104		0.218	0.133

(B) FFT-NLLS Analysis Summary.

Data were collected as outlined in Section 2, baseline detrended and normalised before analysis. All statistics are two-way Student's T-Test comparisons. Vectors are compared to the wild type in their respective treatment regime, wild types are compared to each other. The Empty GR Vector line was kindly donated by Prof Matsui from RIKEN Yokohama.

3.5 Screening Results

3.5.1 Experimental Design

T1 seed from the RIKEN TF library was selected for the screen. This seed is a mix of heterozygote/homozygote/wildtype seed in a 2:1:1 ratio so, with 20-25 seeds per well, the transgenic over-expression phenotype will drown out the small amount of wild type. Moreover, the over-expression phenotype conveyed by the 35S promoter will be dominant or semi-dominant, meaning a phenotypic segregation of 3:1. Carrying out antibiotic selection to remove wildtype seed was ruled out as a viable option both prior to and during the screen. Kanamycin is cytotoxic even to resistant plants which could perturb the circadian system during the screen, and prior generation of T2 seed would have taken significant amounts of time and space which was at a premium.

TF independently lines were screened with 2x replication (giving a total of eight samples per transcription factor) on MS agar through delayed fluorescence according to the protocols given in Chapter 2. A total of 268 genes were represented in the library of TF lines recovered (which, at the time of writing, represents all the library that had been transformed into *Arabidopsis* and confirmed through PCR).

The decision was taken to initially treat all screened plants with topical dexamethasone and compare TF lines to the wild-type, as opposed to comparing them to the wild type and the untreated TF lines. Again, this was in part due to time constraints - library screening already requires considerable amounts of CCD camera time - but also due to material considerations, as only a small aliquot of each seed line was collected from the RIKEN library stocks.

Dexamethasone was applied using the topical spray protocol in Chapter 2. The spray was applied at ZT + 7 of the 13th day of growth. Plants were then returned to the diurnal growth chamber. Transfer to free-run and imaging began the next day at dawn. This time was chosen for several reasons. The first was purely practical - an afternoon application was far more convenient than a late evening or night time application in terms of lab access and scheduling. Furthermore, the timing of dexamethasone treatment may well affect the circadian clock phenotypes observed. As it is important to have a regularly timed application, for reproducibility between the batches, a time was chosen which could reliably be kept to.

3.5.2 Data Handling & Selection Criteria

A data handling pathway was constructed to identify phenotypes of interest. A semi-quantitative definition was selected for this for multiple reasons. Firstly, there were concerns about the differences in expression level between plants. The transformation process used to generated the TF lines inserts the sequence at random into the genome regardless of how transcriptionally "active" the region is, and can insert multiple copies of the T-DNA (Gelvin, 2003, Honda et al., 2002, Jorgensen et al., 1987). As such, it is likely that different independently transformed lines will have different expression levels and, possibly, different phenotypes. Furthermore, as this was an initial screen where the protocol is still being optimised and developed by an inexperienced researcher, a number of wells gave questionable results due to plating errors or powdery mildew infection (there was an outbreak of this fungal infection at the time, making it a real concern). The technique that follows allows the elimination of compromised wells (referred to as "dead") by their mean DF intensity before analysing their periods through FFT-NLLS. Phenotypes were identified by looking at the difference in period relative to that of the

wild type (found to be 24.47hrs across all plates, n = 430). Genes where this was the case for the majority of samples were selected as having phenotypes of interest and were carried over for further analysis.

A total of 60 individual 96 well plates were assayed across four experimental runs in the ORCAII cabinets. Dexamethasone was applied as ZT+7 the day prior to imaging, and plants returned to LD growth chambers overnight, as outlined in Chapter 2. All experiments began within 20 mins of 9am (subjective dawn).

FIGURE 3.2: Flowchart of Screening Selection Methodology.

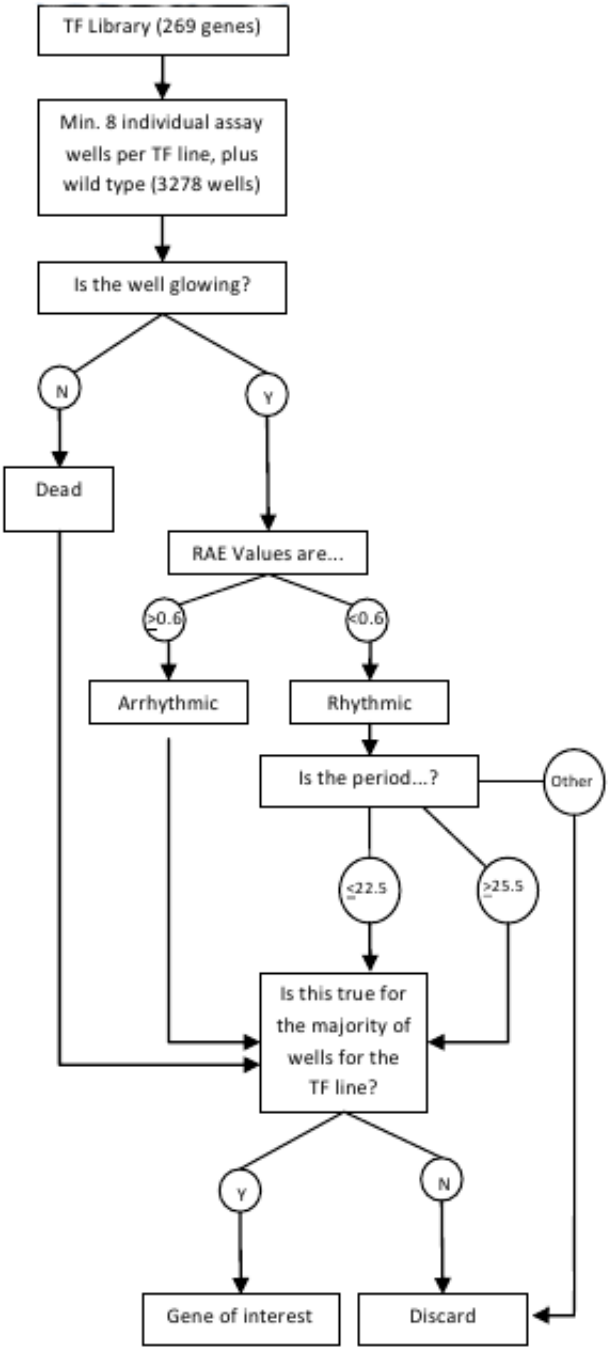

3.5.3 Identification of Genes-of-Interest

In summary: from 3,278 FFT result-giving test wells, 378 rhythmic wells were identified with abnormal periods (Period <22.5hr, >25.5, or RAE $\geq$ 0.6). Genes where several wells gave similar long or short (but robust) periods were selected from this short-list as genes of interest. This identified a list of 21 candidate genes (Table 3.5). Eight of these selected TF lines had long-period phenotypes when compared to the wild type, seven of which statistically significantly different from the wild type when analysed through Student's T-Test. Thirteen had short-period phenotypes, of which all were statistically significant.

T0052 encodes *CYTOKININ RESPONSE FACTOR 8 (CRF8)/ETHYLENE RESPONSE FACTOR 70 (ERF070).* The FFT-NLLS results show a tight cluster with a short period and a low RAE (Figure 3.3b). There is no prior indication that CRF8 might be involved with the circadian clock. *CRF8* is rhythmically expressed in diurnal LD conditions, with a peak at 4hrs after dawn, but not in free-run conditions. It is typically involved in root development and phosphate starvation responses (Ramaiah et al., 2014), and has been shown to exhibit protein-protein interactions with the other 6 members of the CRF family (Cutcliffe et al., 2011).

Dehydration response has long been linked with the circadian clock, so it is perhaps unsurprising that *DEHYDRATION RESPONSE ELEMENT-BINDING 2B (DREB2B)*, as encoded by T0082, shows a circadian phenotype in the overexpressor. T0082 has a short period phenotype (WT - 1.38, p <0.001, Figure 3.4a) and the periods calculated by FFT-NLLS group fairly tightly to the left of the wild type. This phenotype is less

TABLE 3.8: Genes of Interest Obtained from DF Screening

TF	Names	Gene	Mean Period (hrs)	Phenotype
T0052	CRF8	AT1G71130	22.88***	Short
T0082	DREB2B	AT3G11020	23.33***	Short
T0189	IAA11	AT4G28640	22.88*	Short
T0213	FBH3	AT1G51140	23.46*	Short
T0314	ABF1	AT1G49720	22.37***	Short
T0527	BUM1	AT1G62360	24.70*	Long
T0530	KNAT2	AT1G70510	25.66***	Long
T0576	HAT2	AT5G47370	24.97*	Long
T0591	SOG1	AT1G25580	23.12***	Short
T0592	ANAC010	AT1G28470	26.20**	Long
T0593	SND1	AT1G32770	22.55***	Short
T0638	RD26	AT4G27410	21.10***	Short
T0649	ANAC087	AT5G18270	21.22***	Short
T0760	WRKY3	AT2G03340	22.82*	Short
T0811	NF-YC10	AT1G07980	24.67*	Long
T0825	HAP2B	AT3G05690	26.02***	Long
T0840	HRS1	AT1G13300	22.75**	Short
T0856	MYBC1	AT2G40970	25.91	Long
T0910	n/a	AT5G66770	22.88***	Short
T1082	BBX13/COL15	AT1G28050	23.42*	Short
T1268	ZFHD2	AT5G65410	25.50*	Long

All samples were planted at a density of 8-12 seedlings on MS + 1.5% agar in wells of 96 well plates. Seedlings were grown for 14 days in 12:12 LD, treated with dexamethasone, and imaged in LL as outlined in Chapter 2. Periods were calculated by FFT-NLLS. Wild type period was 24.47hrs (n = 430). n = 8 for all samples except for T0592, T0910 and T1082 where n=7; T0638, T0825 and T1268 where n = 6; and T0840 where n = 14.
Statistics: Student's T-Test, two-tailed comparison with wild type from the same experimental run. * $p \leq 0.05$, ** $p \leq 0.01$, *** $p \leq 0.001$.

clear in the mean intensity plot (Figure 3.4a), *DREB2B* is as yet unimplicated in the circadian clock, however there is evidence that it is under clock control. It is rhythmically expressed in free-run conditions, as shown via DIURNAL, and its upregulation in response to droughting is enhanced in *LKP2* over-expressing plants (Miyazaki et al., 2015). It has also been reported that the *DREB* family are constitutively over-expressed in arrhythmic mutants (Fowler et al., 2005). If over expression of *DREB* conversely affects the clock, it could be indicative of feedback in the clock gating of drought response.

T0189 has a phenotype tending towards being short (WT-0.81, Figure 3.5b) and, although this is a slight shift it is statistically significant ($p = 0.037$). By T+132hrs, the peaks of DF intensity have clearly shifted out of sync with the wild type (3.5a). T0189 encodes *INDOLE-3-ACETIC ACID INDUCIBLE 11 (IAA11)*, a member of a family of negative transcriptional regulators that are degraded in response to auxin (IAA) signalling (Liscum and Reed, 2002). Each member of this family regulates a different suite of genes; whilst we know that the circadian clock gates auxin signalling (Voß et al., 2015), *IAA11* has not been directly implicated in these, or as yet any, auxin signalling events.

T0213, corresponding to *FLOWERING B HELIX-LOOP-HELIX 3 (FBH3)*, was found to have a short period phenotype (WT-1/25, $p = 0.002$, Figure 3.6b). The timing of the peaks of delayed fluorescence intensity drift clearly in and out of phase with those of the wild type in the intensity traces (Figure 3.6a). *FBH3* is a nuclear localised transcription factor (Riechmann et al., 2000) expressed in multiple tissues (Schmid et al., 2005), and is an activator of *CONSTANS* in photoperiodic flowering (Ito et al., 2012). Furthermore, *FBH3* is in the same family as *FBH1*, and exhibits high conservation on the amino acid level (WU-BLAST 2.0: Identities = 56/86, 65% Positives = 76/86, 88%. Altschul et al. (1990), Gish and States (1993)) which when over-expressed results in circadian period shortening upon temperature changes from 22°C to 28°C (Nagel et al., 2014). *FBH1* and *CCA1* form a reciprocal feedback loop, binding each other's promoters and regulating each other's expression.

It is also known as *ABA-RESPONSIVE KINASE SUBSTRATE 1 (AKS1)* as it is phosphorylated in response to ABA treatment in guard cells (Takahashi et al., 2013). The unphosphorylated form induces the transcription of inwardly rectifying potassium ion channels, and AKS1/FBH3 directly binds the promoter of *KAT1*, a major channel of

this sort in guard cell. This was alleviated following ABA-induced phosphorylation. Guard cell stomatal aperture has been well documented as under circadian control (Gorton et al., 1989, Holmes and Klein, 1986, Hubbard et al., 2007), with daily cycles of opening and closing maintaining transpiratory balance, as well as ABA being a known inducer of stomatal closure following drought stress (MacRobbie, 2000, Schroeder et al., 2001). If *AKS1* truly does affect the circadian system, it could act as a signal integrator between the clock and ABA signalling in the guard cell and beyond.

T0314 encodes *ABA RESPONSE ELEMENT BINDING FACTOR 1 (ABF1)*, a known transcriptional activator that binds the *cis*-activating abscisic acid-responsive elements (ABREs) (Choi et al., 2000) and responds to ABA, cold and heat (Sharma et al., 2011). It shows a short period phenotype in the screen, a statistically significant shortening of 1.64hrs compared to the wild type (Figure 3.7b). In addition to its regulatory roles in stress responses, *ABF1* has been implicated in the circadian clock. Microarray data from DIURNAL shows that *ABF1* is rhythmically expressed in free run following entrainment by light and heat with an expression peak of ZT+12. Computational modelling using co-clustering to sort genes into biological function "modules" predicted that *ABF1* could potentially be involved in the circadian clock (Heyndrickx and Vandepoele, 2012). Whilst these predictions are limited (38.1% of known gene functions are correctly identified by the clustering modules), it seems promising that *ABF1* is circadian-regulating or circadian-adjacent and, thus, that this observed phenotype is real and a result of direct action on the clock.

Encoded for by T0527, *BUMBERSHOOT/SHOOT MERISTEMLESS (BUM/STM)* is a key transcription factor required for shoot apical meristem maintenance throughout the

lifetime of the plant by preventing the incorporation of cells in the "central zone" of the meristem into leaf primordia (Clark et al., 1996, Endrizzi et al., 1996, Long et al., 1996, Scofield et al., 2007). In the delayed fluorescence screen, there is a tendency towards a long period phenotype in five of the samples investigated, representing 3 independently transformed lines (WT + 0.69hrs, p=0.016, Figure 3.8b). Two show robust periods within the wild-type range and correspond to a single independently transformed line, which may indicate insertion into a region of the genome with low transcriptional activity and availability.

T0530 encodes *KNOTTED-LIKE FROM ARABIDOPSIS THALIANA 2 (KNAT2)*, a homeobox transcription factor. A long period phenotype was observed alongside a loss in robustness (Figure 3.9b ZT+1.82). Expressed in the vegetative apical meristem and in developing carpels *KNAT2* is not typically found in the leaves. Ectopic expression of *KNAT2* results in altered leaf morphology, with curled lobed leaves and downwards-bending cotyledons (Pautot et al., 2001). By bringing this gene into the same tissue as a circadian reporter it is possible that the meristem clock can be investigated.

The homeodomain-leucine zipper (HD-ZIPII) family of transcription factors are mostly known to be involved in the regulation of adaptive responses to the environment and are induced as part of the shade avoidance response (Ariel et al., 2007, Bou-Torrent et al., 2012, Ciarbelli et al., 2008). Represented by T0576, a member of this family *HAT2* had a statistically significant long period phenotype (WT+0.86, p =0.012, Figure 3.10b) that can clearly be seen in the intensity trace, beginning in phase with the wild type and become gradually more delayed with each peak (Figure 3.10a). *HAT2* is induced by auxin, but not by other phytohormones, and is a transcriptional suppressor (Sawa et al., 2002).

The *p35S:HAT2* over expresser also has a long hypocotyl phenotype, which scanning electron microscopy reveals to be due to cell elongation and not cell division - whilst this is a phenotype shared by auxin response mutants *sur2* (Delarue et al., 1998), *yucca* (Zhao et al., 2001), and transgenic plants that overexpress the *iaaM* auxin-synthesizing gene from *Agrobacterium* (Romano et al., 1995), it may also be indicative of a clock effect.

T0591 encodes *ARABIDOPSIS NAC DOMAIN CONTAINING PROTEIN 8/SUPPRESSOR OF GAMMA RADIATION 1 (ANAC008/SOG1)*, a transcription factor and master regulator of plant responses to DNA damage, including cell cycle arrest, DNA repair, programmed cell death and endoreduplication (Yoshiyama et al., 2009, 2014). T0591 has a short period phenotype (WT -0.89hrs) that is statistically significant ($p < 0.001$, Figure 3.11b). Two additional genes in the NAC-Domain containing family were found to have period phenotypes. *SECONDARY WALL-ASSOCIATED NAC DOMAIN 1/3 (SND1/3)* are regulators of secondary cell wall formation, a woody structure which provides considerable strength and rigidity to plants, allowing them to grow and remain upright under their own weight (Mitsuda et al., 2007). T0593 encodes *SND1/ANAC012* which was shown to have a short period phenotype (WT - 1.46hrs, $p < 0.001$, Figure 3.13b), whilst T0592 encodes *ANAC010/SND3* which has a long period phenotype (WT + 0.86hrs, $p = 0.008$, Figure 3.12b). It is interesting that three members of this large family which have no previous circadian implication were flagged as giving clock phenotypes, although *Arabidopsis* has over 100 members of the family it is perhaps less surprising (The Arabidopsis Genome Initiative., 2000). Despite no previous recorded involvement in the clock, there is evidence that NAC domain proteins are in part responsible for ABA signalling (Ernst et al., 2004) and, as ABA and its associated stresses affect the clock, this may indicate a putative mechanism for the observed phenotypes.

A severely short period phenotype was observed for T0638 (WT - 3.24hrs, $p < 0.001$, Figure 3.14b), which encodes *RESPONSIVE TO DESICCATION 26 (RD26)*. The delayed fluorescence intensity peaks begin out-of-phase with the wild type, drift into phase by T + 60hrs, and back out of phase by 120hrs (Figure 3.14a). Note that the "uptick" in the intensity trace after 120hrs is an artefact of the detrending process that is present on in the last day's worth of data for all samples, as the DF signal damps. In most other graphs this is not plotted as these experiments were carried out for 168hrs, however this particular experimental run was only carried out for 144hrs. As FFT-NLLS analysis is carried out on the 24-144hr window, this has no effect on the period prediction analysis. *RD26*, also known as *ANAC072*, is a transcriptional regulator that responds to drought and ABA treatement (Fujita et al., 2004, Tran et al., 2004), although it has not as yet been implicated in, or being under, circadian regulation. From the same experiment, T0649 has a similar short period (WT - 3.08hrs, $p < 0.001$, Figure 3.15b). Encoding *ANAC087*, this gene is yet another member of this large the NAC-domain containing family.

T0760 encodes *WRKY DNA-BINDING PROTEIN 3 (WRKY3)*, which shows a short period phenotype (WT - 1.24hrs, $p = 0.021$, Figure 3.16b). In this particular experiment, there is no tight clustering of wild type periods in the RAE plot, which can obscure the phenotype; however when the clustering of FFT results for T0760 is compared with those of e.g. T0593, the phenotype becomes clearer. *WRKY3* is nuclear-localised, specifically recognises the W-box (TTGACC) *in vitro*, is rhythmically expressed in diurnal and free-run conditions, and is involved in pathogen defence responses (Lai et al., 2008, Skibbe

et al., 2008).

T0811 was selected as a long period phenotype, which whilst mild was statistically significant (WT+0.85, p =0.018, Figure 3.17b). T0811 encodes *NUCLEAR FACTOR Y, SUBUNIT C10 (NF-YC10.* Nuclear Factor Y is highly conserved in eukaryotes, although investigation of this family's phenotypes in *Arabidopsis* have been limited by redundancy and the fact that 35S overexpressing lines exhibit extreme growth retardation. It is known that the NF-Y complex binds to CCAAT boxes, cis-acting elements present in 25% of eukaryotic promoters, whereby it acts as a transcriptional activator (Edwards et al., 1998, Mantovani, 1999, Wenkel et al., 2006a). The dexamethasone induction system is therefore well suited to study of these kinds of genes. There are three subunits of nuclear factor Y - A, B and C. A member of the *NUCLEAR FACTOR Y, SUBUNIT A/HEME ACTIVATOR PROTEIN (YEAST) HOMOLOGUE* family, T0825 (*NF-YA2/HAP2B*) also has a long period phenotype with a mean period of 26.02hrs (WT + 1.8, $p < 0.001$, Figure 3.18b). Whilst there is a single sample with a considerably longer period than the other five sample wells, the median period is still long at 25.49 (WT median +1.17). The peaks of DF intensity do not align with those of the wild type, suggesting that the phase phenotype was present during the entrainment conditions. *HAP2B* is not rhythmically expressed in any condition searchable via DIURNAL, whilst *NF-YC10* is diurnally expressed in LLHC conditions but not free run.

Typically expressed in roots, expression of *HYPERSENSITIVITY TO LOW PI-ELICITED PRIMARY ROOT SHORTENING 1 (HRS1)* in leaves resulted in a short period DF phenotype (T0840, WT - 1.33hrs, p = 0.002, Figure 3.19b). *HRS1* is transcriptionally regulated by nitrate and post transcriptionally by phospate, and functions to integrate

these two nutrient signalling pathways in the root (Liu et al., 2009, Medici et al., 2015). It is not rhythmically expressed. As a typically root expressed gene, any circadian phenotypes of *HRS1* would have gone unnoticed, as assays predominantly focus on aerial tissues. However the use of a 35S promoter has allowed the phenotype to be investigated.

Whilst T0856, encoding *MYB FAMILY TRANSCRIPTION FACTOR C1 (MYBC1)*, does not have a period length phenotype (WT - 0.35, $p = 0.225$, Figure 3.20b), it shows a loss of robust rhythmia, indicated by a rise in the RAE value (RAE = WT + 0.2, $p < 0.001$). *MYBC1* is a negative regulator of freezing tolerance in *Arabidopsis* (Zhai et al., 2010). Additionally, *MYBC* is one of 5 genes in the same family as *LUX ARRHYTHMO* Hazen et al. (2005). As its name suggests, over-expression of *LUX* results in arrhythmia in a wild-type background (Onai and Ishiura, 2005), although some OX lines have shown to be rhythmic presumably due to a dosage-response effect (Helfer et al., 2012). As such, it makes sense to select T0856 for this increase in RAE value.

T1082 encodes *CONSTANS-LIKE 15/B-BOX DOMAIN PROTEIN 13 (COL15/BBX13)*, which has a short-period phenotype (WT - 1.09, $p = 0.013$, Figure 3.22b). This results in a clear drifting out of phase with the wild type as the experiment continues, with the peaks a clear 6hrs our of phase by 120hrs (Figure 3.22a). *COL15* is expressed rhythmically in diurnal and free run conditions, with a peak around midday. Implicated as circadian *in silico* by module clustering (Heyndrickx and Vandepoele, 2012), COL15 also exhibits protein-protein interactions with the circadian regulator LKP2 and a weak interaction with its homologue ZTL (Fukamatsu et al., 2005). The role of *COL15* is unknown - CONSTANS and the COL family are typically implicated in CCAAT-box binding and the regulation of flowering, however is also suggestion of a putative role for COL15 in

RNA processing within nuclear speckles, as shown through its interactions with COLD SHOCK DOMAIN PROTEIN 3 (CSP3) (Kim et al., 2013b). COL15 also interacts with AtHAP3/5 subunits, which may mediate its activity (Ben-Naim et al., 2006, Wenkel et al., 2006a).

T1268 encodes *ZINC FINGER HOMEODOMAIN 1/2 (ZFHD1/2)*, which gives a statistically significant long period phenotype (WT + 0.99, p = 0.035, Figure 3.23b). ZFHD1/2 directly binds the ZFHD recognition sequence (ZFHDRS) found upstream of the dehydration-inducible expression of the *EARLY RESPONSIVE TO DEHYDRATION STRESS 1 (ERD1)* gene in response to drought (Tran et al., 2007).

In summary, a series of TF lines were selected through the delayed fluorescence screen in the presence of dexamethasone, representing transcription factors from various gene families and implicated in many processes, although response to abscisic acid and drought/-cold stress was common. For all the TF lines, the phenotype was observable in multiple independently transformed lines - four independently transformed lines were assayed, in duplicate, for each member of the library - indicating that these phenotypes are a result of the transgene and not genetic disruption caused by random insertion during *Agrobacterium* transformation. These selected TF lines will be further studied throughout the rest of the investigation.

FIGURE 3.3: DF Results for *CYTOKININ RESPONSE FACTOR 8 (CRF8)* / T0052.

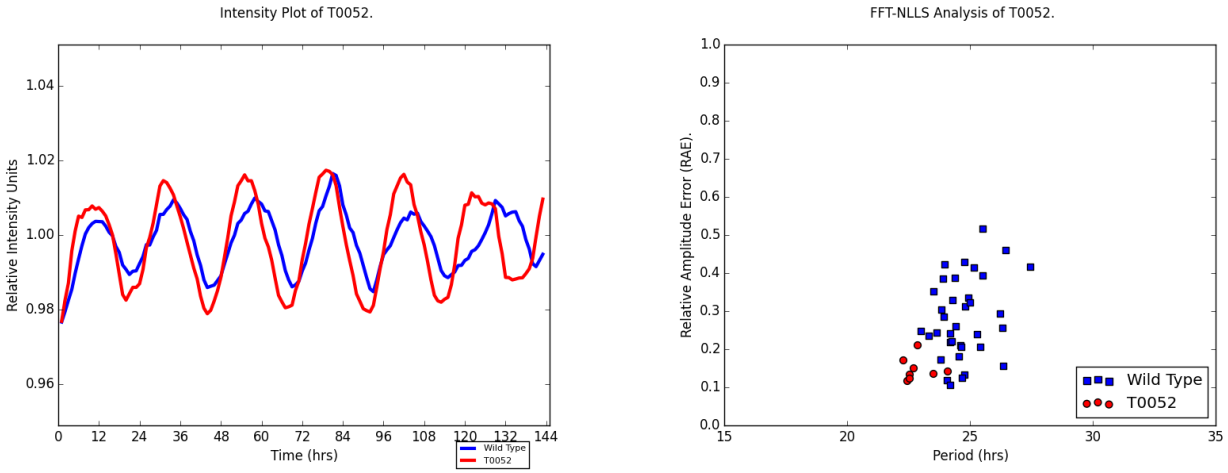

(A) Mean Relative Intensity Plot. (B) Mean Relative Intensity Plot.

The data was amplitude- and baseline-detrended and normalised to the mean in BioDARE. Period analysis was carried out via FFT-NLLS for the 24-144hrs experimental window. Mean period = 22.88hrs (WT-1.83, p <0.01, n = 8).

FIGURE 3.4: DF Results for *DEHYDRATION RESPONSE ELEMENT-BINDING 2B (DREB2B)* / T0082.

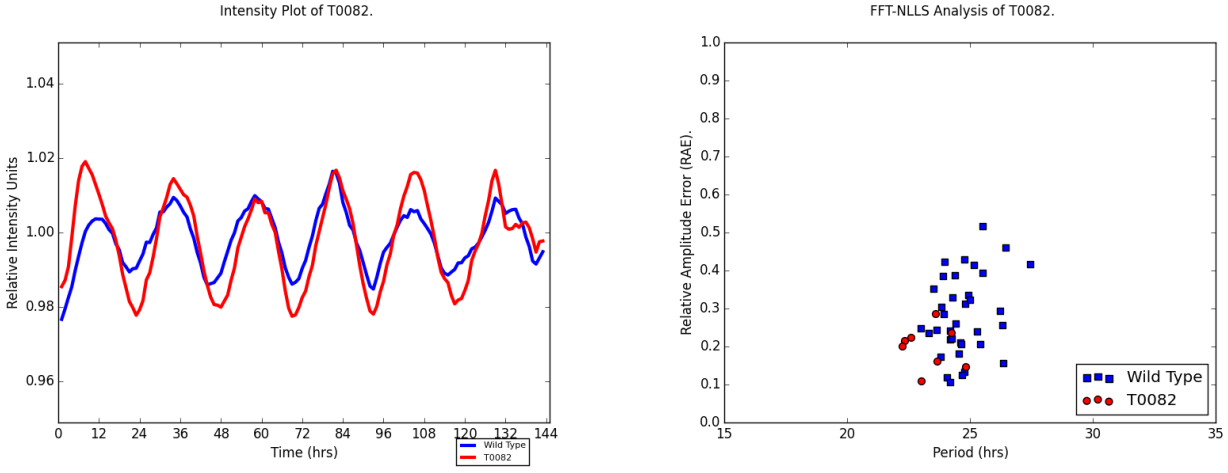

(A) Mean Relative Intensity Plot. (B) Mean Relative Intensity Plot.

The data was amplitude- and baseline-detrended and normalised to the mean in BioDARE. Period analysis was carried out via FFT-NLLS for the 24-144hrs experimental window. Mean period = 23.33hrs (WT-1.38, p <0.001, n = 8).

FIGURE 3.5: DF Results for *INDOLE-3-ACETIC ACID INDUCIBLE 11 (IAA11)* / T0189.

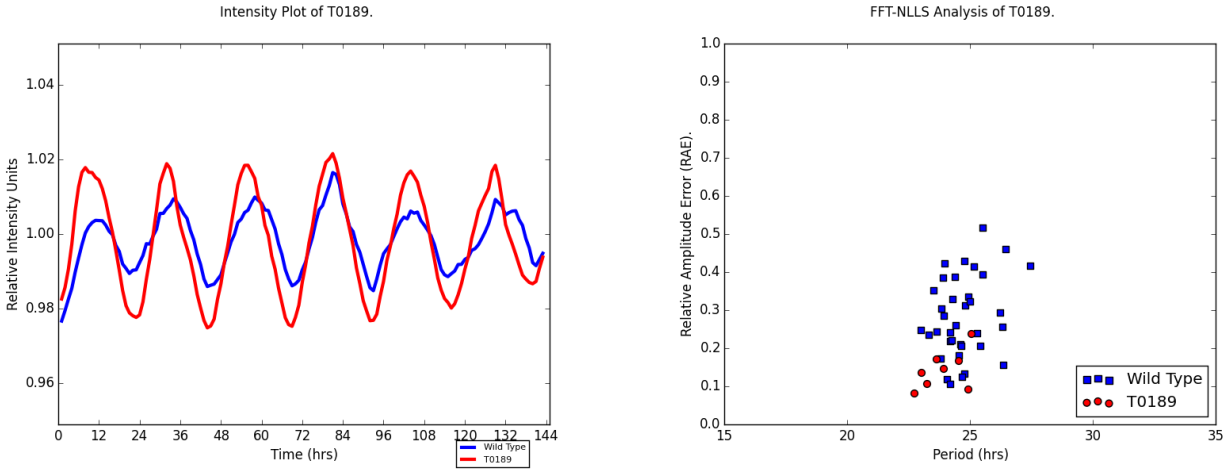

(A) Mean Relative Intensity Plot. (B) Mean Relative Intensity Plot.

The data was amplitude- and baseline-detrended and normalised to the mean in BioDARE. Period analysis was carried out via FFT-NLLS for the 24-144hrs experimental window. Mean period = 22.88hrs (WT-0.81, p <0.037, n = 8).

FIGURE 3.6: DF Results for *FLOWERING B HELIX-LOOP-HELIX 3 (FBH3)* / T0213.

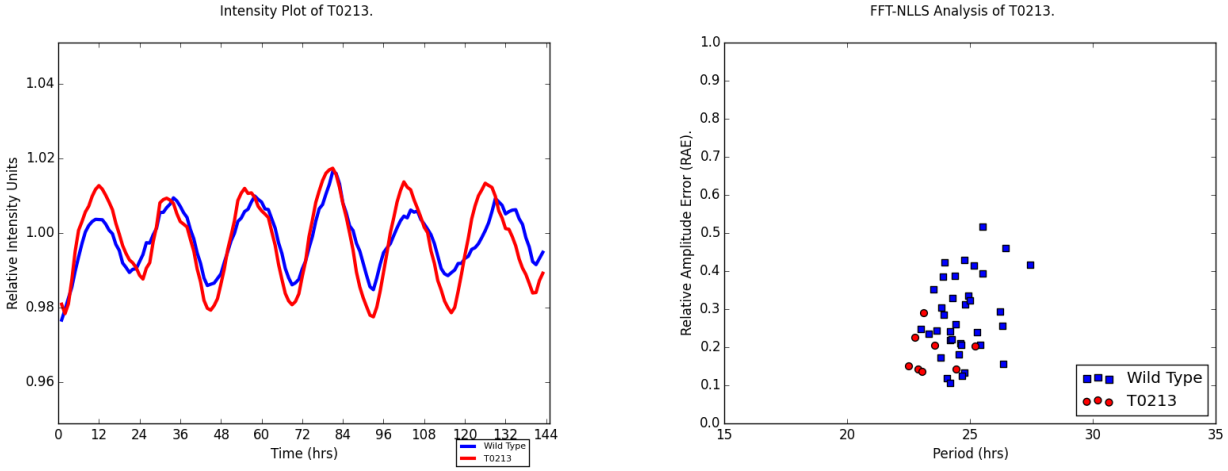

(A) Mean Relative Intensity Plot. (B) Mean Relative Intensity Plot.

Plants were grown for 13 days in LD 12:12 cycles before treating with dexamethasone at ZT+7. Plants were returned to the growth chamber, and imaging began the next day at dawn. The data was amplitude- and baseline-detrended and normalised to the mean in BioDARE. Period analysis was carried out via FFT-NLLS for the 24-144hrs experimental window. Mean period = 23.46hrs (WT-1.25, p = 0.002, n = 8).

FIGURE 3.7: DF Results for *ABA RESPONSE ELEMENT BINDING FACTOR 1 (ABF1)* / T0314.

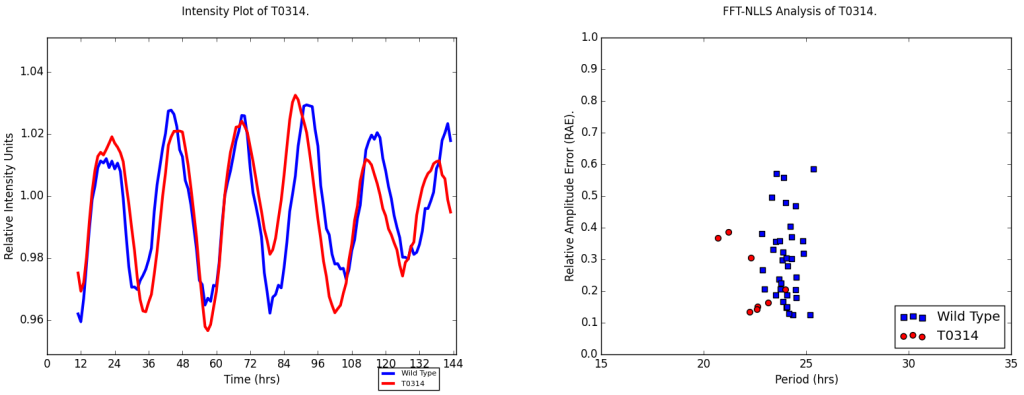

(A) Mean Relative Intensity Plot. (B) Mean Relative Intensity Plot.

Plants were grown for 13 days in LD 12:12 cycles before treating with dexamethasone at ZT+7. Plants were returned to the growth chamber, and imaging began the next day at dawn. The data was amplitude- and baseline-detrended and normalised to the mean in BioDARE. Period analysis was carried for the 24-144hrs experimental window. Mean period = 22.37 (WT-1.64, p = 0.001, n = 8).

FIGURE 3.8: DF Results for *BUMBERSHOOT 1 (BUM1)/ SHOOT MERISTEMLESS (STM)* / T0527 .

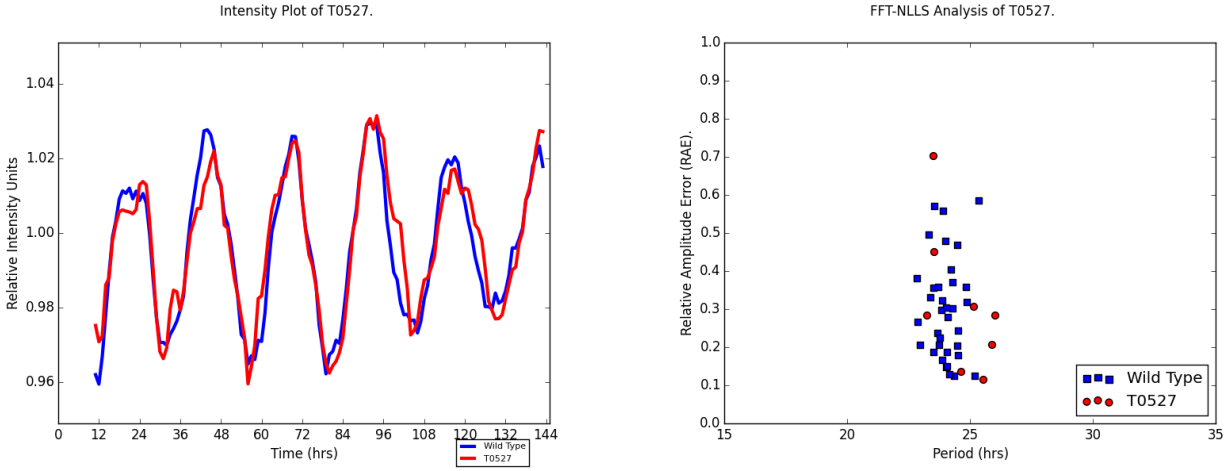

(A) Mean Relative Intensity Plot. (B) Mean Relative Intensity Plot.

Plants were grown for 13 days in LD 12:12 cycles before treating with dexamethasone at ZT+7. Plants were returned to the growth chamber, and imaging began the next day at dawn. The data was amplitude- and baseline-detrended and normalised to the mean in BioDARE. Period analysis was carried out via FFT-NLLS for the 24-144hrs experimental window. Mean period = 24.70hrs (WT+0.69, p = 0.016, n = 8).

FIGURE 3.9: DF Results for *KNOTTED-LIKE FROM ARABIDOPSIS THALIANA 2 (KNAT2)* / T0530.

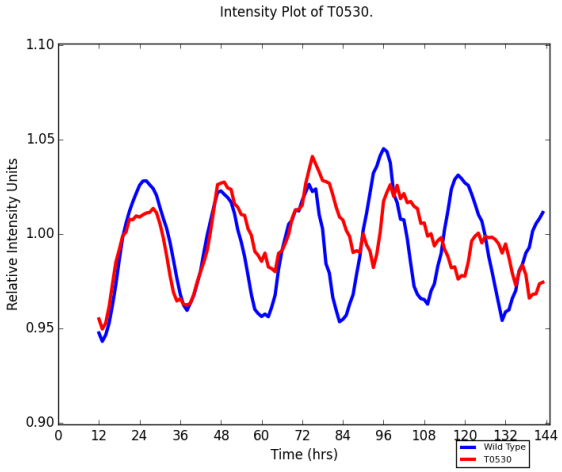

(A) Mean Relative Intensity Plot.

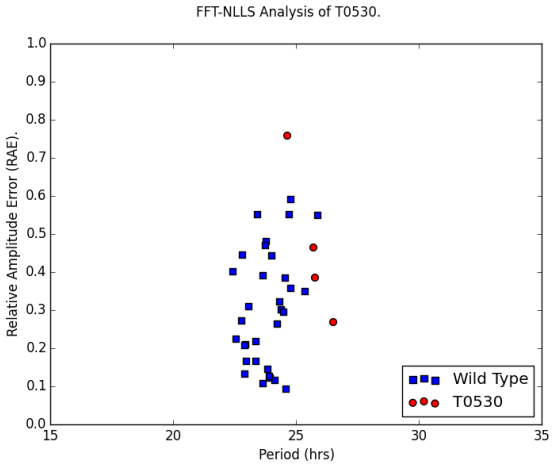

(B) Mean Relative Intensity Plot.

Plants were grown for 13 days in LD 12:12 cycles before treating with dexamethasone at ZT+7. Plants were returned to the growth chamber, and imaging began the next day at dawn. The data was amplitude- and baseline-detrended and normalised to the mean in BioDARE. Period analysis was carried for the 24-144hrs experimental window. Mean period = 25.66 (WT +1.82, $p < 0.001$, n = 8).

FIGURE 3.10: DF Results for T0576 *(HD-ZIPII FROM A.THALIANA 2 (HAT2)* / T0576.

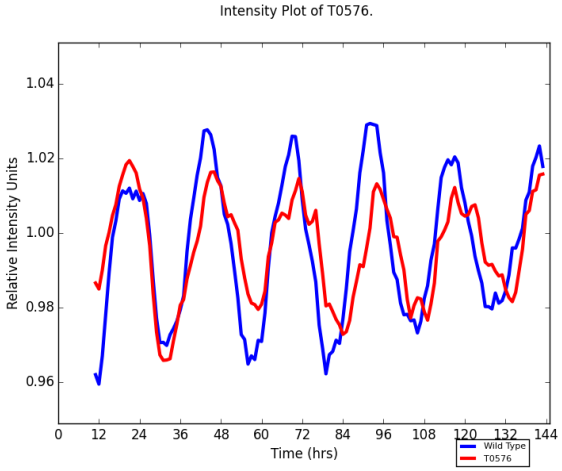

(A) Mean Relative Intensity Plot.

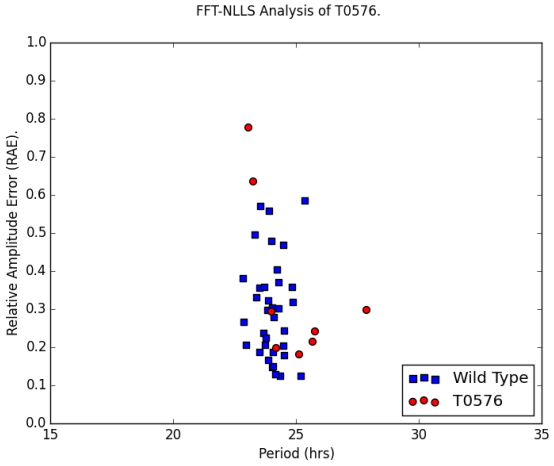

(B) Mean Relative Intensity Plot.

Plants were grown for 13 days in LD 12:12 cycles before treating with dexamethasone at ZT+7. Plants were returned to the growth chamber, and imaging began the next day at dawn. The data was amplitude- and baseline-detrended and normalised to the mean in BioDARE. Period analysis was carried for the 24-144hrs experimental window. Mean period = 24.97 (WT + 0.86, $p = 0.012$, n = 8).

FIGURE 3.11: DF Results for *SUPPRESSOR OF GAMMA RADIATION 1 (SOG1)* / T0591).

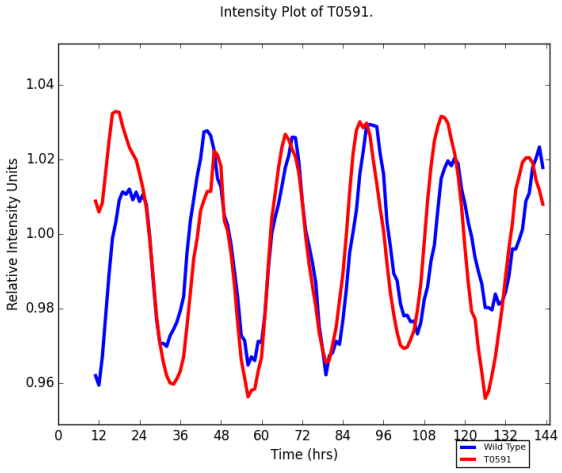

(A) Mean Relative Intensity Plot.

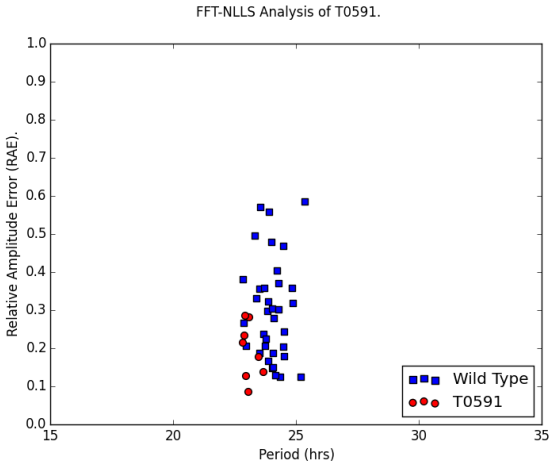

(B) Mean Relative Intensity Plot.

Plants were grown for 13 days in LD 12:12 cycles before treating with dexamethasone at ZT+7. Plants were returned to the growth chamber, and imaging began the next day at dawn. The data was amplitude- and baseline-detrended and normalised to the mean in BioDARE. Period analysis was carried for the 24-144hrs experimental window. Mean period = 23.12 (WT - 0.89, $p < 0.001$, n = 8).

FIGURE 3.12: DF Results for *ARABIDOPSIS NAC DOMAIN CONTAINING PROTEIN 10 (ANAC010)* / T0592.

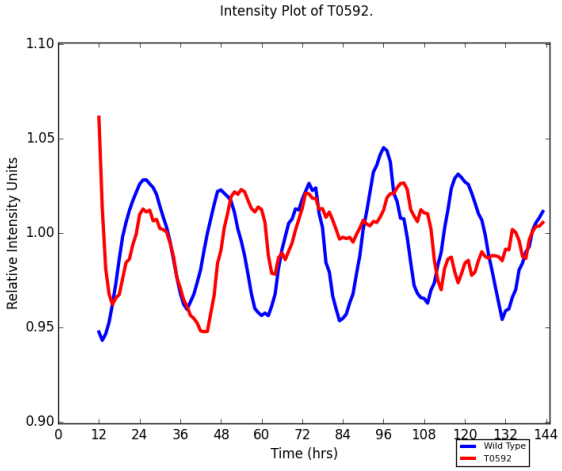

(A) Mean Relative Intensity Plot.

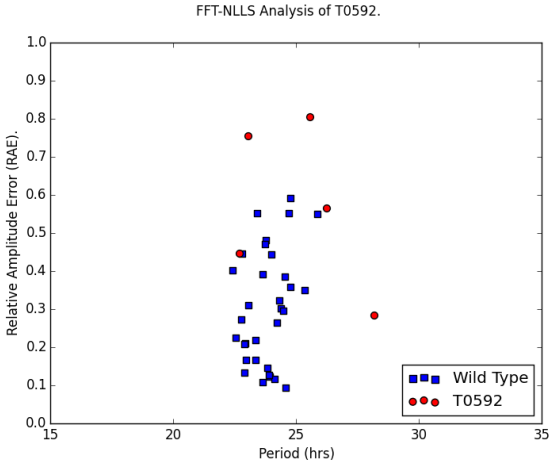

(B) Mean Relative Intensity Plot.

Plants were grown for 13 days in LD 12:12 cycles before treating with dexamethasone at ZT+7. Plants were returned to the growth chamber, and imaging began the next day at dawn. The data was amplitude- and baseline-detrended and normalised to the mean in BioDARE. Period analysis was carried for the 24-144hrs experimental window. Mean period = 26.20 (WT + 0.86, p = 0.008, n = 7).

FIGURE 3.13: DF Results for *SECONDARY WALL-ASSOCIATED NAC DOMAIN 1 (SND1)* / T0593.

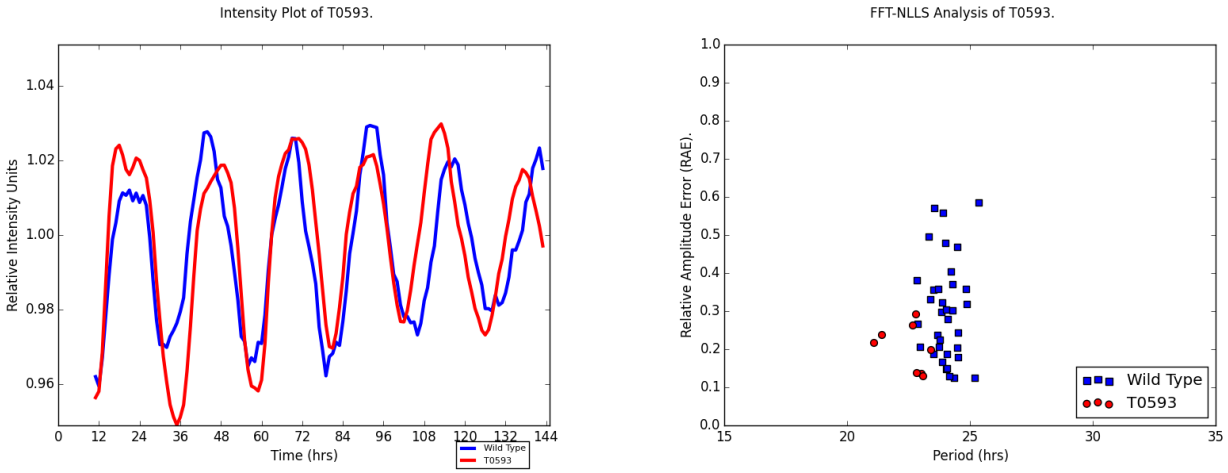

(A) Mean Relative Intensity Plot. (B) Mean Relative Intensity Plot.

Plants were grown for 13 days in LD 12:12 cycles before treating with dexamethasone at ZT+7. Plants were returned to the growth chamber, and imaging began the next day at dawn. The data was amplitude- and baseline-detrended and normalised to the mean in BioDARE. Period analysis was carried for the 24-144hrs experimental window. Mean period = 22.55 (WT - 1.46, $p < 0.001$, n = 8).

FIGURE 3.14: DF Results for *RESPONSIVE TO DESICCATION 26 (RD26)* T0638.

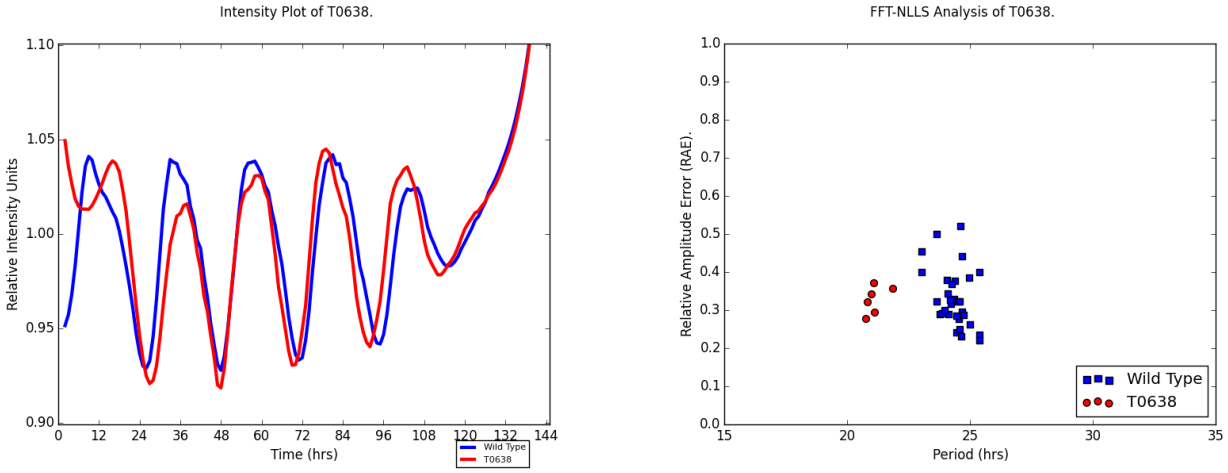

(A) Mean Relative Intensity Plot. (B) Mean Relative Intensity Plot.

Plants were grown for 13 days in LD 12:12 cycles before treating with dexamethasone at ZT+7. Plants were returned to the growth chamber, and imaging began the next day at dawn. The data was amplitude- and baseline-detrended and normalised to the mean in BioDARE. Period analysis was carried for the 24-144hrs experimental window. Mean period = 21.1 (WT - 3.24, $p < 0.001$, n = 6).

FIGURE 3.15: DF Results for *ARABIDOPSIS NAC DOMAIN CONTAINING PROTEIN (ANAC087)* / T0649.

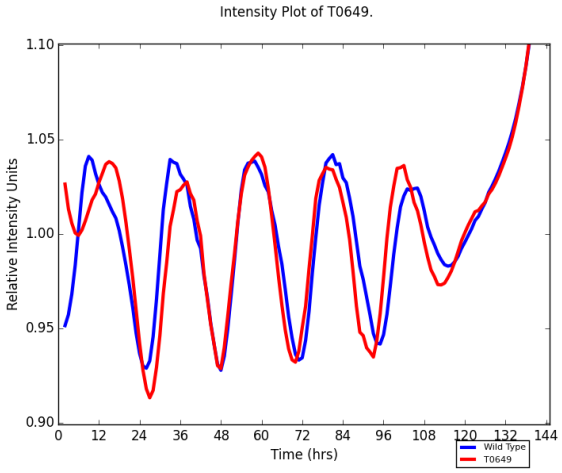

(A) Mean Relative Intensity Plot.

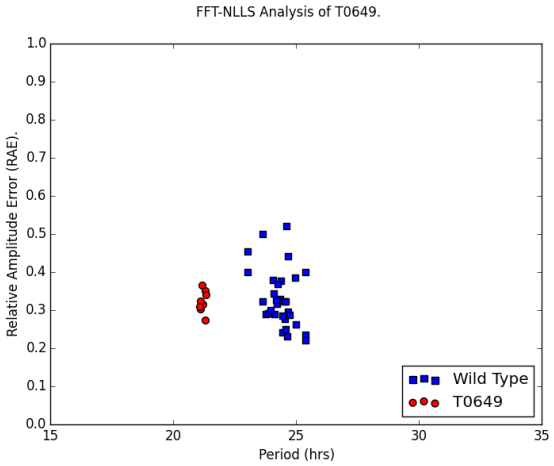

(B) Mean Relative Intensity Plot.

Plants were grown for 13 days in LD 12:12 cycles before treating with dexamethasone at ZT+7. Plants were returned to the growth chamber, and imaging began the next day at dawn. The data was amplitude- and baseline-detrended and normalised to the mean in BioDARE. Period analysis was carried for the 24-144hrs experimental window. Mean period = 21.22 (WT - 3.08, $p < 0.001$, n = 8).

FIGURE 3.16: DF Results for *WRKY DNA-BINDING PROTEIN 3 (WRKY3)* / T0760.

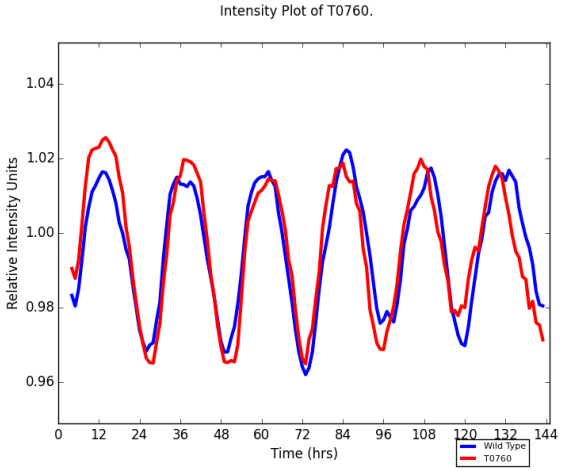

(A) Mean Relative Intensity Plot.

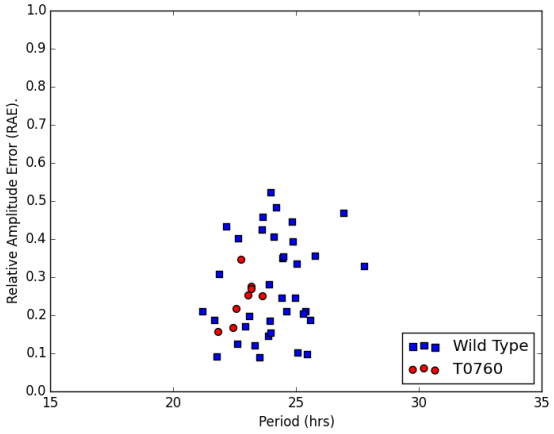

(B) Mean Relative Intensity Plot.

Plants were grown for 13 days in LD 12:12 cycles before treating with dexamethasone at ZT+7. Plants were returned to the growth chamber, and imaging began the next day at dawn. The data was amplitude- and baseline-detrended and normalised to the mean in BioDARE. Period analysis was carried for the 24-144hrs experimental window. Mean period = 22.84 (WT - 1.24, $p = 0.021$, n = 8).

FIGURE 3.17: DF Results for *NUCLEAR FACTOR Y, SUBUNIT C10 (NF-YC10)* / T0811.

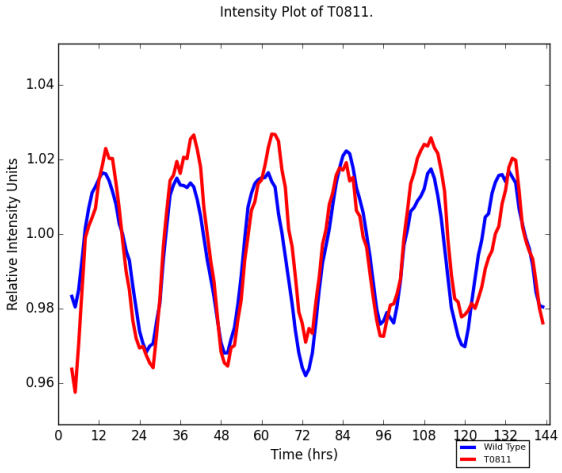

(A) Mean Relative Intensity Plot.

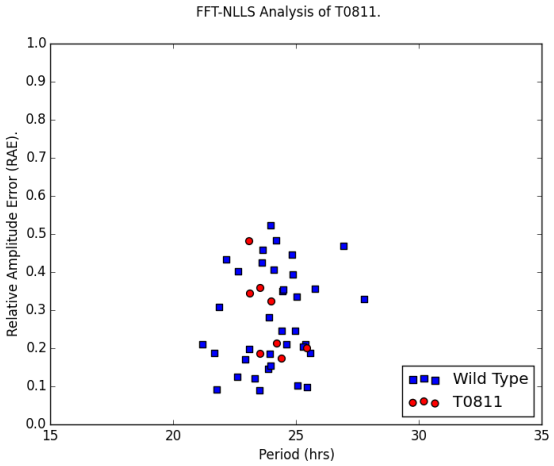

(B) Mean Relative Intensity Plot.

Plants were grown for 13 days in LD 12:12 cycles before treating with dexamethasone at ZT+7. Plants were returned to the growth chamber, and imaging began the next day at dawn. The data was amplitude- and baseline-detrended and normalised to the mean in BioDARE. Period analysis was carried out via FFT-NLLS for the 24-144hrs experimental window. Mean period = 24.67hrs (WT+0.85, p =0.018).

FIGURE 3.18: DF Results for *HEME ACTIVATOR PROTEIN HOMOLOG 2B (HAP2B)* / T0825.

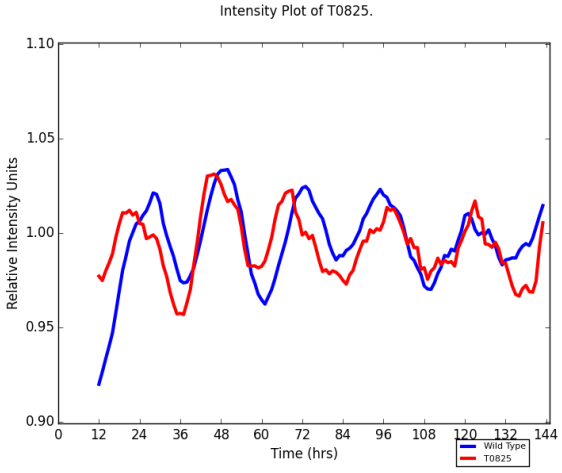

(A) Mean Relative Intensity Plot.

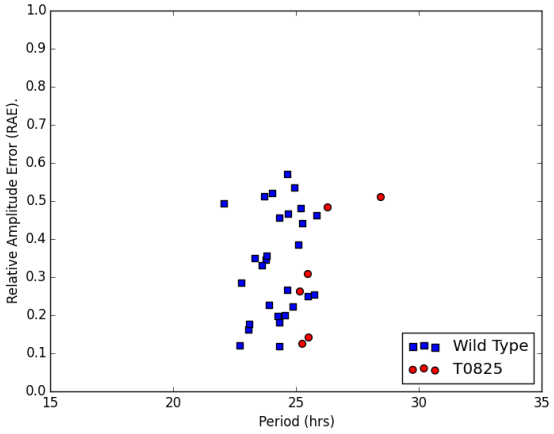

(B) Mean Relative Intensity Plot.

Plants were grown for 13 days in LD 12:12 cycles before treating with dexamethasone at ZT+7. Plants were returned to the growth chamber, and imaging began the next day at dawn. The data was amplitude- and baseline-detrended and normalised to the mean in BioDARE. Period analysis was carried for the 24-144hrs experimental window. Mean period = 26.02 (WT + 1.8, $p < 0.001$, n = 6). N.B. Median period = 25.49 (WT+1.17).

FIGURE 3.19: DF Results for *HYPERSENSITIVITY TO LOW PI-ELICITED PRIMARY ROOT SHORTENING 1 (HRS1)* / T0840.

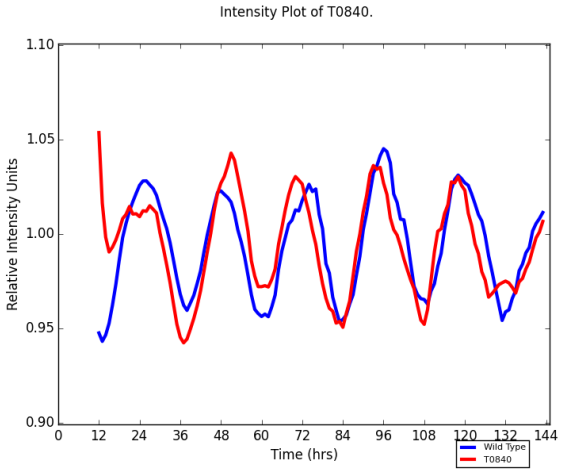

(A) Mean Relative Intensity Plot.

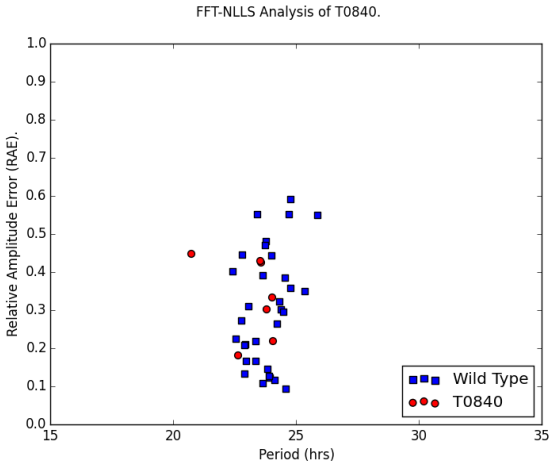

(B) Mean Relative Intensity Plot.

Plants were grown for 13 days in LD 12:12 cycles before treating with dexamethasone at ZT+7. Plants were returned to the growth chamber, and imaging began the next day at dawn. The data was amplitude- and baseline-detrended and normalised to the mean in BioDARE. Period analysis was carried for the 24-144hrs experimental window. Mean period = 22.75 (WT - 1.33, p = 0.002, n = 14).

FIGURE 3.20: DF Results for *MYB FAMILY TRANSCRIPTION FACTOR C1 (MYBC1)* / T0856.

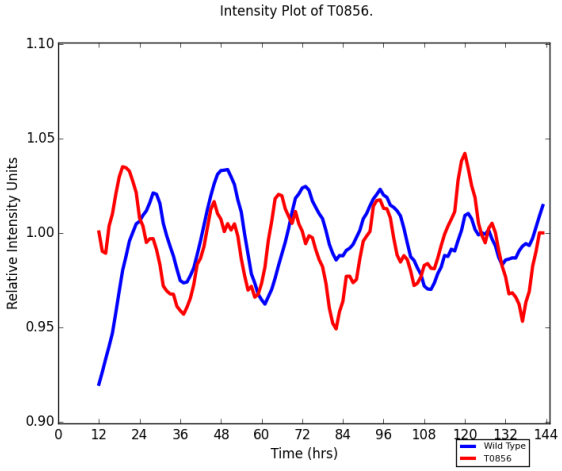

(A) Mean Relative Intensity Plot.

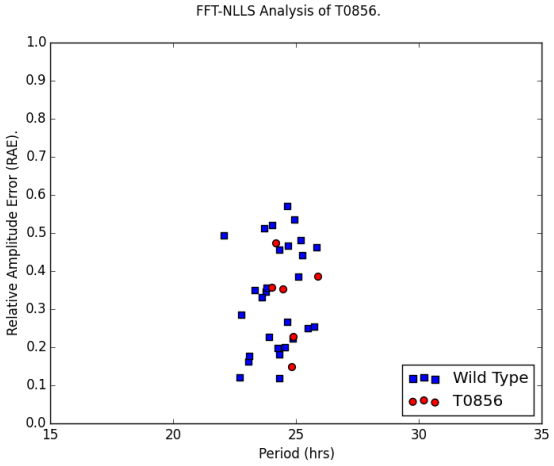

(B) Mean Relative Intensity Plot.

Plants were grown for 13 days in LD 12:12 cycles before treating with dexamethasone at ZT+7. Plants were returned to the growth chamber, and imaging began the next day at dawn. The data was amplitude- and baseline-detrended and normalised to the mean in BioDARE. Period analysis was carried for the 24-144hrs experimental window. Mean period = 24.73 (WT - 0.35, p = 0.225, n = 8).

FIGURE 3.21: DF Results for AT5G66770 / T0910.

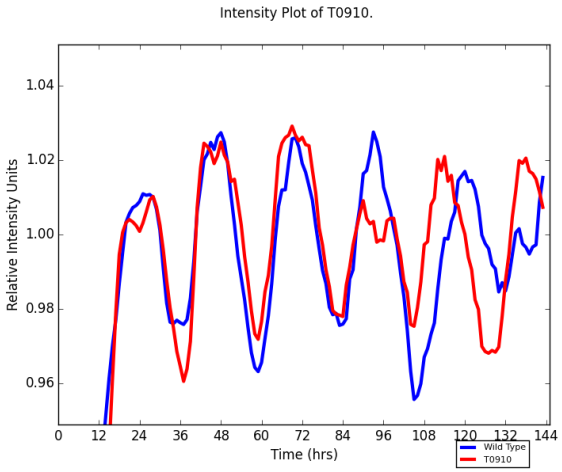

(A) Mean Relative Intensity Plot.

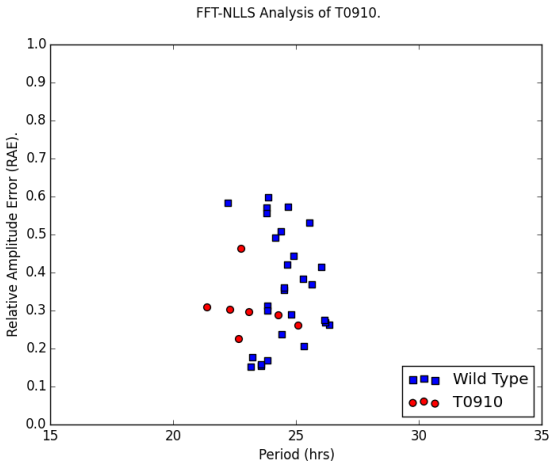

(B) Mean Relative Intensity Plot.

Plants were grown for 13 days in LD 12:12 cycles before treating with dexamethasone at ZT+7. Plants were returned to the growth chamber, and imaging began the next day at dawn. The data was amplitude- and baseline-detrended and normalised to the mean in BioDARE. Period analysis was carried out via FFT-NLLS for the 24-144hrs experimental window. Mean period = 22.88hrs (WT-1.83, p <0.001, n = 7).

FIGURE 3.22: DF Results for *BBOX DOMAIN 13/ CONSTANS-LIKE 15 (BBX13/COL15)* / T1082.

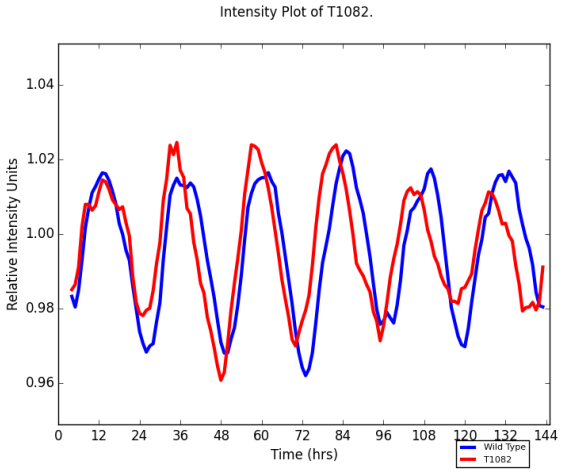

(A) Mean Relative Intensity Plot.

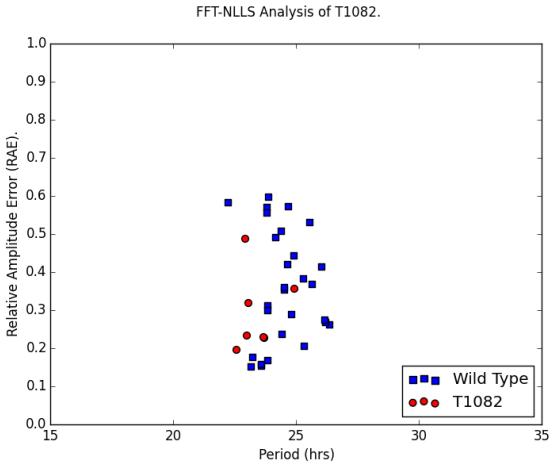

(B) Mean Relative Intensity Plot.

Plants were grown for 13 days in LD 12:12 cycles before treating with dexamethasone at ZT+7. Plants were returned to the growth chamber, and imaging began the next day at dawn. The data was amplitude- and baseline-detrended and normalised to the mean in BioDARE. Period analysis was carried for the 24-144hrs experimental window. Mean period = 23.42 (WT - 1.09, p = 0.013, n = 7).

FIGURE 3.23: DF Results for *ZINC FINGER HOMEODOMAIN 2 (ZFHD2)* / T1268.

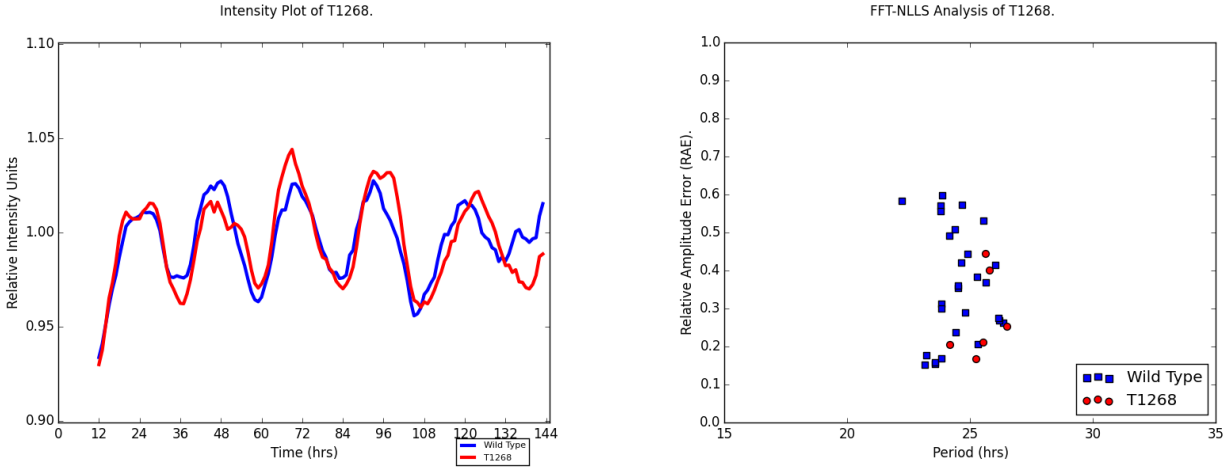

(A) Mean Relative Intensity Plot.

(B) Mean Relative Intensity Plot.

Plants were grown for 13 days in LD 12:12 cycles before treating with dexamethasone at ZT+7. Plants were returned to the growth chamber, and imaging began the next day at dawn. The data was amplitude- and baseline-detrended and normalised to the mean in BioDARE. Period analysis was carried for the 24-144hrs experimental window. Mean period = 25.50 (WT + 0.99, p = 0.035, n = 6).

3.6 Discussion

The RIKEN TF library was screened following dexamethasone treatment on Day 14, at ZT+8. Due to limits on the number of seeds that could be sent from RIKEN, there was insufficient material to carry out the initial screen under multiple dexamethasone treatment conditions. Only c. 50-80 seeds of each line were retrieved, meaning there were not enough for multiple treatment regimes. Phenotypes were defined through comparisons between the treated TF lines and wild types, which operates on the assumption that the empty vector has no effect on the clock, the GR cassette completely excludes transcription factors from the nucleus, and that the transcription factors have no additional cytosollic functions/do not act as kinase substrates or otherwise undergo cytosollic modification. Whilst the evidence gathered in the preliminary experiments means that the first can be discounted, the rest remain problematic.

Furthermore a single time-point for dexamethasone treatment was selected, again due to material constraints. The timing of over-expression induction may well result in different phenotypes. Over-expression in the evening of typically morning-phased components is likely to be more immediately severe than evening induction of evening-phased components. Previous work with the GR cassette in *Arabidopsis* has shown that induction is relative fast, with transcript levels being affected within 4hrs, which is within the boundaries of a circadian relevant timeframe (Nakamichi et al., 2010). Changing the timing of gene induction would be an interesting avenue for further research.

The distribution of wild type samples was far less tightly clustered than those of the TF lines, with a larger interquartile range of periods and RAE values. Why is this the case? Whilst the wild type seed was of the same background as the TF lines (Col-0), it was

grown and stored in Liverpool rather than RIKEN. It will have also been a different age, which depending on storage conditions could have compromised the germination rates, the age and health of the seedlings following 15 days growth and, hence, the quality of the delayed fluorescence readings. Indeed, the Liverpool-grown seed routinely had a paler testa (seed coat) than that of the seed sourced from RIKEN. The testa is a vital organ determining seed germination, being water- and oxygen-impermeable in most conditions, and *Arabidopsis* mutants in testa pigmentation are known to show reduced dormancy (Debeaujon et al., 2000). To control for this in subsequent experiments, a sample of RIKEN Col-0 seed will be grown and bulked along with any future seed generation in order to provide a reference of the same age. Additionally, in the 96 well plates, the wild type references were planted in the first column (A1 - H1), which is adjacent to the edge of the plate. These samples are more likely to be subject to dessication and, indeed, the cornermost wells (A1, H1, A12, H12) were occasionally dry by the end of the experiment. In these circumstances, they were ommitted from analysis. Sealing the plates more tightly brings its own problems, denying oxygen from the central wells of the plates and reducing their growth and intensity. The "fisheye" effect of the camera lens, the shallow focal length of the wide aperture lens, and the lower light intensity at the edges of the cabinet (where these wild type samples were located) could have also contributed as equipment error. In future cabinet experiments, the wild type references will be planted in different positions within the plates to help control for this.

The selection criteria were chosen to select genes that showed measurable divergence from the expected period of the wild type. Amplitude was ignored as a criteria. The reason for this was that DF signal intensity very quickly damps throughout the experiment, which adversely affects period estimates (Zielinski et al., 2014). This project

focuses mostly on period phenotypes. In order to clearly visualise and investigate the data obtained towards the end of the experiment (i.e. those after the plants have been in free run for several circadian cycles, after which any period shift phenotypes would be more pronounced), data were amplitude normalised to improve the accuracy of period estimates. However, as a consequence, the amplitude does not contain any meaningful data.

Published microarray data were used to produce a series of predictions of circadian phenotype. From these 44 predictions, 3 gave circadian phenotypes when assayed with delayed fluorescence as identified by the selection criteria (KNAT2, ANAC010, MYBC1, COL15). Comparing the rhythmicity of microarray expression profiles in this way does not appear to give good, reliable predictions of the over-expression phenotype. The wealth of microarray data provides a valuable resource, allowing the examination of expression profiles in detail over many different conditions; however for circadian prediction an alternative prediction method is clearly needed. Whilst it provides an essential insight as to how a gene is expressed in a perturbed circadian condition, it is of limited use in predicting what will affect the clock.

In total 21 TF lines were selected as genes of interest by their delayed fluorescence phenotype. With 268 distinct RIKEN transcription factor lines, this represents 7.8% of the lines screened. This at first seems quite high, as it is in the same region of magnitude as the conservative microarray-based estimations that 6-15% of the *Arabidopsis* transcriptome was circadian regulated (Covington et al., 2008, Edwards et al., 2005, Harmer et al., 2000). Conversely, the finding that over expression of gene affects a single output of the circadian system does not in itself indicate that the gene is part of the clockwork

or directly affecting it. For example, a number (4) of the selected genes have previously been implicated in ABA signalling. ABA is heavily involved in the propagation of cold and drought signalling which along with the hormone itself have all been well documented as affecting, and being affected by, the circadian system (Bieniawska et al., 2008, Hanano et al., 2006, Legnaioli et al., 2009). Whether the over expression of the transcription factor is directly causative of the phenotype, or whether it begins a chain of more general ABA- or stress-response signalling which perturbs the clock remains to be seen.

In order to characterise these transcription factors, first the phenotypes must be shown to be replicable. The effect of dexamethasone, and the lack of phenotype in its absence, needs to be ascertained. Furthermore, as delayed fluorescence is a general output of the circadian clock's overall phenotype, the transcriptional nature of the TF lines and the extent to which the directly (as in the case of a clock gene) or indirectly (as in general stress signalling) affect the clock cannot be investigated without directly observing the transcriptional outputs of the circadian clock.

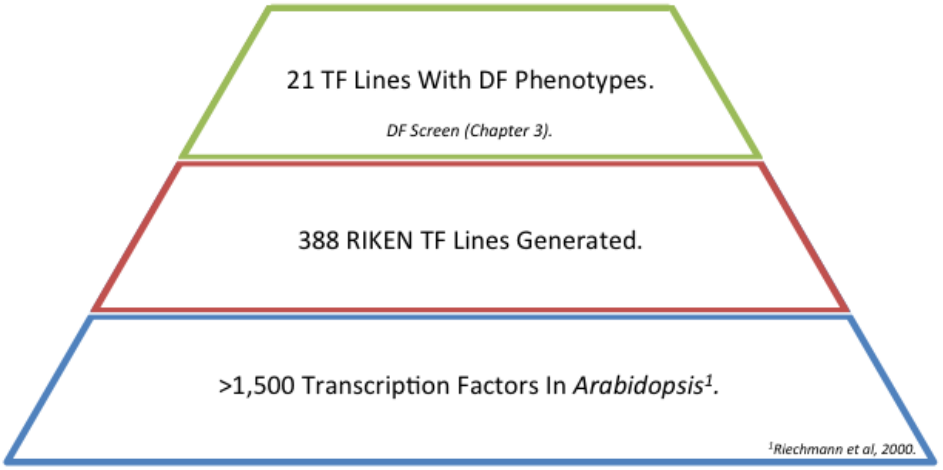

FIGURE 3.24: Workflow Overview: 21 Lines Identified by DF Screen.

Chapter 4

Further Characterisation of Genes of Interest

4.1 Introduction

From the RIKEN TF library, 21 genes were identified as giving circadian phenotypes. Treated with dexamethasone, these lines showed delayed fluorescence circadian phenotypes relative to those of the wild type. Delayed fluorescence was selected for this screen due to the high throughput afforded by its lack of a transformation requirement and the capability to observe hundreds of test samples simultaneously. However, these phenotypes were only investigated in the presence of dexamethasone, and with only one reporter system.

In this chapter, the phenotypes were further investigated by DF as well as by the additional technique of transgenic luciferase. The induction of transcription factor activity also came under scrutiny, with the phenotypes characterised when treated and mock-treated with dexamethasone. Finally, in order to view the genes in a wider genetic

context, the investigation moved beyond over-expression by examining native expression *in silico* and characterising the phenotypes of knock-out, null mutant lines for these transcription factors.

Dexamethasone Induction

TF lines were screened only in the presence of dexamethasone, administered at the day prior to the transfer to LL and the start of image capture. As a glucorticoid hormone, dexamethasone is capable of facilitating the nuclear import of GR-fusion proteins (Aoyama and Chua, 1997), and it has been demonstrated to have no other effects on the circadian system (See Chapter 3.4). Compared to other inducible systems in *Arabidopsis*, which are predominately two-component systems like the alcohol-inducible *35S::AlcR/ pAlcR::Target* where the induction of target gene function is mediated through an inducible transgenic regulator of transcription (Knowles et al., 2014), dexamethasone induction of the TF lines does not require transcription, responds quickly to induction, does not have pleiotropic effects, and is highly dose sensitive.

However, the GR system is not well characterised in a circadian context, and may lead to phenotypes even in the absence of dexamethasone. Native GR in mammals continuously shuttles between cytoplasm and nucleus via the nuclear pore complex (NPC) with glucocorticoid treatment moving the equilibria and resulting in a net shift from cytoplasm to nucleus (Madan and DeFranco, 1993, Savory et al., 1999). As such, the high level of gene expression from the 35S promoter (Benfey and Chua, 1990, Jefferson et al., 1987, Odell et al., 1985), potentially transcribed from multiple copies in homozygous or multiple-insertion lines, combined with this nuclear pore "leak" may result in nuclear TF levels sufficient to induce transcription even in the absence of dexamethasone. This

is especially possible for genes that are normally expressed at low copy number - which includes many diurnally oscillating genes in their "trough" phase.

Additionally, it is not unreasonable to assume that some of genes may have cytoplasmic associations that result in circadian phenotypes. CCA1 has been detected in the cytoplasm, where it undergoes post-translational phosphorylation (Yakir et al., 2009); similarly in *Drosophilla* and mouse the shuttling of genes between the nucleus and cytoplasm, where they undergo modification and activity regulation, is a key feature of the clock and its regulation (Bae and Edery, 2006). Some clock components are effective in the cytoplasm rather than the nucleus - ZTL stabilisation occurs predominantly in the cytoplasm, whilst GI has distinct roles in the cytoplasm and the nucleus (Kim et al., 2013a). The GR protein sequence is also capable of native co-importation of bound proteins, both chaperones and protein fusions (Vandevyver et al., 2012), which could in turn affect compartmentalisation of other genes. Regulation of or interference with these processes could have dramatic effects on the circadian system in a manner that is distinct from the transcriptional over expression of the transcription factor targets.

This raises several questions. Are the observed phenotypes dexamethasone-dependent? Do the phenotypes require dexamethasone-facilitated nuclear import? Or is 35S over-expression of the TF line sufficient to affect the circadian system? Are our proposed transcription factors functioning within the nucleus, or are they affecting the clock whilst in the cytoplasm? To begin to answer these questions, it is important to characterise the TF line phenotypes in the presence and absence of dexamethasone induction. It is imperative, and feasible now that the pool of lines for consideration is smaller, to carry out this investigation.

Alternative Phenotyping Methods

Delayed fluorescence is a general clock output with complex multi-level circadian control as many of the key genes that make up the light harvesting complexes are under circadian control at the transcriptional level (Harmer et al., 2000). As such, it gives an indication of the overall clock phenotype in the leaves (i.e. the majority of the aerial tissue where the LHCs are located). However, as an emerging technique, any phenotypes through delayed fluorescence must be additionally investigated through other methods. The other techniques also bring certain advantages, and allow investigation of aspects of the clock that delayed fluorescence cannot probe.

Luciferase remains the "gold standard" of plant circadian phenotyping investigations. Unlike delayed fluorescence, luciferase reporters allow us to investigate specific components of the clock due to the fact that they are direct and specific transcriptional outputs of the circadian system. They do not merely give a general measure of overall clock health; instead they reveal the clock function at the level of whichever promoter the luciferase construct is being driven by (typically *pCAB2* or *pCCR2*). It is possible to probe different loops and, as such, gain insight into the place of the gene within the circadian network. Directly investigating the transcriptional clock is vital in the study of transcription factors.

It has been observed previously that delayed fluorescence circadian phenotypes broadly agree with those from luciferase reporter studies. Luciferase phenotypes for the short-period *gi-11* (Park et al., 1999), *lhy-21* (Mizoguchi et al., 2002), *cca1-11* (Alabadí et al., 2002) and *toc1-2* (Strayer et al., 2000) mutants, as well as the long period *prr7-3* and *prr9-1* alleles (Farré et al., 2005), are comparable to their delayed fluorescence phenotypes, although not as severe (Gould et al., 2009). This, however, is not a foregone

conclusion. The nucleus and chloroplast are distinct compartments and there is emerging evidence that the roles of certain genes may be compartment specific. Phototropins are required for circadian rhythms off Chlorophyll a Fluorescence in chloroplasts but not transcriptional rhythms in the nucleus Litthauer et al. (2015), indicating that the clock and its regulation may not be universal to all compartments. Confirmation of circadian phenotype through luciferase reporters remains a necessary and important step in characterising circadian mutants. To this end, TF lines were transformed with the luciferase reporter *pCAB2:LUC+* and phenotyped in this way.

Phenotypes Beyond The TF Lines

The RIKEN TF lines are all constitutive over-expression lines - they consist of cDNAs driven by the 35S promoter from Cauliflower Mosaic Virus. A hypothesis of this investigation is that 35S-driven global over expression can reveal otherwise elusive circadian phenotypes. There are several reasons for this assertion. Genes will be expressed in leaves, even if this is not normally the case, where they will be introduced to a reporter (*pCAB2*-driven luciferase or, in DF experiments, chlorophyll) within a large tissue by area, which forms the dominant signal in lumino-fluorescent imaging. Additionally, partially redundant genes or those with overlapping functions can be identified as having phenotypes that might otherwise be missed if there is another to compensate. However, over-expression is not the only mutant context, especially for a gene in a diurnally oscillating system. Mutant or insertional knock-outs were obtained, "switching off" the genes in order to see how they relate phenotypically to the TF lines where genes are permanently "switched on".

In this chapter, the circadian phenotypes of the selected genes of interest were analysed with CCD imaging of transgenic *pCAB2:LUC+* reporters. The SALK knockouts for the lines of interest, where available, were also analysed through delayed fluorescence and luciferase technique in order to uncover the effects of permanently "switching off" the genes and seeing how they relate to the TF lines where genes are "switched on". Finally, *in silico* tools were used to further probe the genes of interest, to predict their functions and features of regulation, as well as to invesgiate their expression from the wild-type promoters.

In this way, the list of genes-of-interest was reduced to 3, with further phenotypic characterisation, and avenues of future research opened up.

4.2 *In Silico* Investigation

In this section, *in silico* tools were used to investigate the genes of interest, with the intention of further characterising their phenotypes and putting them in the context of the whole plant.

4.2.1 Microarray Analysis

The GENEVESTIGATOR software was used to explore published microarray data for the genes of interest(Hruz et al., 2008). GENEVESTIGATOR provides a wealth of tools for interpreting microarray data. It also allows filtering by meta-profile: in contrast to normal expression profiles where each signal value denotes the expression level of one gene in one sample, each signal value in a meta-profile corresponds to the average expression level of one gene over a set of samples sharing the same biological context. This allows the user to restrict the search to samples from the same tissue type, or following a particular class of treatment.

4.2.1.1 COL15/BBX3 Is Co-Expressed & Co-Regulated With Core Clock Genes

We can hypothesise that genes tightly co-expressed with clock components may in some way interact with them (directly or indirectly), or be under the same kinds of regulation. These interactions may have so far remained elusive due to subtle phenotypes, or partial redundancy. The co-expression data for all samples was filtered for canonical clock genes *CCA1*, *LHY*, *TOC1* (Alabadí et al., 2001), *PRR3/5/7/9* (Zeilinger et al., 2006), *GI*,

ELF3/4 (Nusinow et al., 2011), *LUX* (Hazen et al., 2005) and *RVE8* (Rawat et al., 2011). Members of the gene of interest short-list which are co-expressed with one or more clock genes were selected for further study.

In this way, only a single gene was selected. The highly co-expressed partners for AT1G28050 (*COL15/BBX13*) includes several circadian genes: *LUX* (Pearson's Correlation Coefficient R=0.61), *TOC1* (R=0.60), *ELF4* (R=0.60), and *PRR3/5* (Pearson's Correlation Coefficient R=0.54; see Figure 4.1). These are all evening phased genes. LUX and ELF4, along with ELF3, form the evening complex (Nusinow et al., 2011) that repressess the expression of genes through binding LUX binding sites (LBS) in promoter regions (Chow et al., 2012). The evening complex, however, contains many peripheral proteins. As one of the major promoter binding circadian complexes, its recruitment of additional proteins to the promoter is important for understanding the integration of circadian and other signalling responses. We can therefore select AT1G28050 (*COL15/BBX13*/T1082) as a prime candidate gene.

When we filter by "*Perturbation*", selecting those experiments where treatment or mutagenesis was carried out to disrupt or otherwise affect the circadian clock, we get similar results (see Figure 4.2). Of our 21 gene shortlist, only COL15/BBX13 has any clock genes within the top 25 candidates when sorted by Pearson's coefficient. We find it co-expressed with the evening complex forming genes *LUX* (Pearson's Correlation Coefficient R=0.68), *ELF4* (Pearson's Correlation Coefficient R=0.55) and *ELF3* (Pearson's Correlation Coefficient R=0.54), as well as *TOC1* (Pearson's Correlation Coefficient R=0.62). The high correlation with these genes following disruption of circadian control of gene expression, further suggests co-regulation with the evening complex.

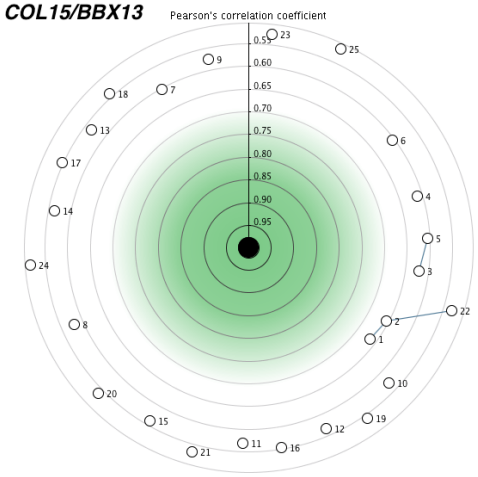

Description of the most correlated genes (top 25)

	Gene	Score	Description
1	253322_at	0.67	BEST Arabidopsis thaliana protein match is: cold regulated gene 27 (TAIR:A...
2	COR27	0.66	cold regulated gene 27
3	248744_at	0.62	B-box type zinc finger protein with CCT domain
4	PCL1, LUX, BOA	0.61	[AT5G59570, Homeodomain-like superfamily protein]:[AT3G46640, Home...
5	TOC1, AtTOC1, A...	0.60	CCT motif -containing response regulator protein
6	ELF4	0.60	Protein of unknown function (DUF1313)
7	PDC2	0.60	pyruvate decarboxylase-2
8	CIPK21, SnRK3.4	0.58	CBL-interacting protein kinase 21
9	267036_at	0.57	unknown protein; FUNCTIONS IN: molecular_function unknown; INVOLVED IN:...
10	260688_at	0.57	unknown protein; FUNCTIONS IN: molecular_function unknown; INVOLVED IN:...
11	SSADH1, ENF1, AL...	0.57	aldehyde dehydrogenase 5F1
12	264045_at	0.57	riboflavin biosynthesis protein, putative
13	256221_at	0.57	Chaperone DnaJ-domain superfamily protein
14	249850_at	0.56	DNAJ heat shock N-terminal domain-containing protein
15	PBL1	0.56	PBS1-like 1
16	249456_at	0.55	Saccharopine dehydrogenase
17	245319_at	0.55	cAMP-regulated phosphoprotein 19-related protein
18	APRR5, PRR5	0.54	pseudo-response regulator 5
19	APRR3, PRR3	0.54	pseudo-response regulator 3
20	ERD7	0.54	Senescence/dehydration-associated protein-related
21	248410_at	0.53	SPFH/Band 7/PHB domain-containing membrane-associated protein family
22	COL9	0.53	CONSTANS-like 9
23	BT4, ATBT4	0.53	BTB and TAZ domain protein 4
24	HSFA8, AT-HSFA8	0.52	heat shock transcription factor A8
25	260674_at	0.52	unknown protein; LOCATED IN: endoplasmic reticulum; EXPRESSED IN: 22 pl...

FIGURE 4.1: COL15 Coexpression Data (Samples)

Analysis of expression data across all microarray data (Samples). Data scored by Pearson's Correlation Coefficient. The top 25 genes are selected. Circadian genes highlighted in yellow. Coexpression scores are calculated on log2-scaled expression data that is processed from the GENEVESTIGATOR database. The closer the dots are to the centre, the higher their coexpression with COL15. Linked dots form their own coexpression clusters, indicating a possible coregulatory complex. Graphs generated with GENEVESTIGATOR.

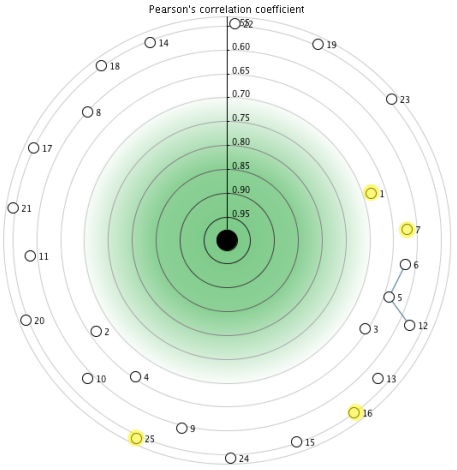

Description of the most correlated genes (top 25)

	Gene	Score	Description
1	PCL1, LUX, BOA	0.68	[AT5G59570, Homeodomain-like superfamily protein]:[AT3G466...
2	DGAT1, TAG1, ATDGAT, RD...	0.66	membrane bound O-acyl transferase (MBOAT) family protein
3	248744_at	0.66	B-box type zinc finger protein with CCT domain
4	249456_at	0.65	Saccharopine dehydrogenase
5	COR27	0.64	cold regulated gene 27
6	253322_at	0.62	BEST Arabidopsis thaliana protein match is: cold regulated gene 2...
7	TOC1, AtTOC1, APRR1, PRR1	0.62	CCT motif -containing response regulator protein
8	CYCT1;3	0.60	cyclin T 1;3
9	264045_at	0.59	riboflavin biosynthesis protein, putative
10	SSADH1, ENF1, ALDH5F1, SS...	0.59	aldehyde dehydrogenase 5F1
11	ATBET9, BET9	0.59	bromodomain and extraterminal domain protein 9
12	COL9	0.58	CONSTANS-like 9
13	260688_at	0.57	unknown protein; FUNCTIONS IN: molecular_function unknown; INV...
14	CIPK21, SnRK3.4	0.55	CBL-interacting protein kinase 21
15	249850_at	0.55	DNAJ heat shock N-terminal domain-containing protein
16	ELF4	0.55	Protein of unknown function (DUF1313)
17	245600_at	0.55	CBS domain-containing protein with a domain of unknown function...
18	245319_at	0.55	cAMP-regulated phosphoprotein 19-related protein
19	254580_at	0.55	Uncharacterised protein family (UPF0114)
20	249989_at	0.54	protein serine/threonine kinases;protein tyrosine kinases;ATP bin...
21	260674_at	0.54	unknown protein; LOCATED IN: endoplasmic reticulum; EXPRESSE...
22	259354_at	0.54	Heavy metal transport/detoxification superfamily protein
23	251494_at	0.54	Protein kinase superfamily protein
24	ELF3, PYK20	0.54	hydroxyproline-rich glycoprotein family protein
25	CCR2, GRP7, ATGRP7, GR-...	0.54	cold, circadian rhythm, and rna binding 2

FIGURE 4.2: COL15 Coexpression Data (Perturbations)

Analysis of expression data across all microarray data (Perturbations). Sample data was restricted to that from experiments with a circadian-related perturbation experiment (i.e. clock mutants, circadian calcium inhibition, etc). Data scored by Pearson's Correlation Coefficient. The top 25 correlated genes are selected. Circadian genes highlighted in yellow. Scores are calculated on log2-scaled expression data that is processed from the GENEVESTIGATOR database. The closer the dots are to the centre, the higher their coexpression with COL15. Linked dots form their own coexpression clusters, indicating possible coregulatory complexes. Graphs generated with GENEVESTIGATOR.

4.2.2 ATHENA Promoter Analysis

Over-expression of the genes of interest has been show to lead to abnormal circadian phenotypes, implying that there is a direct or indirect interaction between the transcription factor proteins represented by the TF lines and the clock. In order to form a transcriptional feedback loop, there must be a corresponding interaction between transcription factor expression and the clock. This can be due to a clock-controlled degradation of mature protein, as in ZTL-mediated F-box degradation of TOC1 (Harmer, 2009), or through control of transcription through promoter binding.

In order to analyse the promoters of the genes of interest, the tool ATHENA was used (O'Connor et al., 2005). Provided by Washington State University, ATHENA can predict motifs in a putative promoter sequence. It was used to analyse the 1000bp upstream regions from the 21 genes with clock phenotypes and searched for known circadian related motifs - Evening Elements (Consensus Sequence: AAAATATCT) and CCA1 binding elements (Consensus Sequence: AAMAATCT). This resulted in 8 genes that possessed at least one putative circadian-regulated motif within the queried region. Perhaps unsurprisingly there was no statistically significant enrichment of either site in the promoter set queried (CCA1 Binding-Site P= 0.5719; Evening Element P= 0.1426), nor for any other except the CACGTG motif ($P < 10^{-3}$) indicating that these 21 transcription factors were not under the control of any single regulatory factor.

The best candidate promoter, T1082 (*COL15/BBX13*), possessed 3 EE motifs (2 in the CpG island) and was previously flagged for co-expression alongside known repressors of *CCA1* expression (*TOC1* and *PRR5*), and its short period phenotype in the initial

screen. The putative promoter of *IAA11* also bears mentioning, possessing a predicted CCA1 binding site in the regulatory region between the CpG island and the start of the gene (Figure 4.3a.

FIGURE 4.3: ATHENA Promoter Analysis Results.

(A) T0189/At4g28640 (*IAA11*).

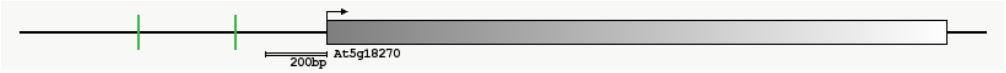

(B) T0649/At3g05690 (*ANAC087*).

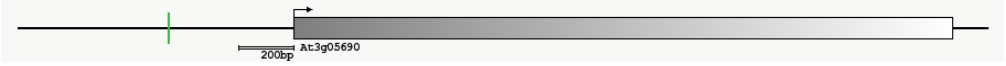

(C) T0825/At3g05690 (*HAP2B*).

(D) T0840/At1g13300 (*HRS1*).

(E) T1082/At1g28050 (*COL15/BBX13*).

Full length genomic sequences + 1000bp upstream were analysed with ATHENA for putative transcription factor binding site motifs. The navy blue vertical lines represent predicted evening element motifs (AAAATATCT). Green verticle lines represent predicted CCA1 binding site motifs (AA[A/C]AATCT). The predicted gene sequence is represented as a gray rectangle; an arrow indicates the start of transcription. Aqua rectangles indicate predicted CpG islands.

4.3 Delayed Fluorescence Analysis of SALK Knock-Out Lines

Following the identification of 21 TF lines yielding clock phenotypes of interest in the over-expresser (see Chapter 3), it is important to investigate the null phenotype of these selected genes. Key circadian genes may yield clock phenotypes in the null mutant, and this is certainly true of the transcription factors *CCA1* (Wang and Tobin, 1998), *LHY* (Schaffer et al., 1998) and *TOC1* (Millar et al., 1995a). A converse phenotype in the null mutant and over-expresser would further implicate a gene in the circadian network and help towards elucidating its function.

One of the advantages of the global constitutive 35S promoter used to drive the TF lines is that it allows us to investigate phenotypes that would not normally be visible through delayed fluorescence (see Chapter 1.5). Foremost, it allows us to phenotype partially redundant genes. Overlapping function and partial (or total) redundancy is commonplace in *Arabidopsis*; indeed it has been claimed that the majority of loss-of-function genes do not give readily-apparent phenotypes (Bouché and Bouchez, 2001). A circadian phenotype in the over-expresser but not the null mutant could identify the component as having an overlapping role with another gene or genes. Similarly, the 35S promoter is global, bringing genes into the assay tissues that are normally expressed in tissues not probed by delayed fluorescence (i.e. outside the leaf). Furthermore, when imaging and assaying groups of whole seedlings, expression and phenotypes outside of the leaf can be lost and "swamped out" by the stronger signals coming from the (relatively much larger) leaves. The tissue-specificity of the phenotypes are worth investigation, in order to characterise the genes and provide clues as to their method of action.

Knock-out libraries for *Arabidopsis* have already been generated and made accessible to the scientific community. The Salk Institute Genomic Analysis Laboratory (SIGnAL) has generated a library of knock-out lines through agrobacterium-mediated transformation and random insertion into the genome of a T-DNA construct containing a *p35S:NOS* terminator and the *NTPII* kanamycin-resistance marker. Insertion sites were identified by SIGnAL through DNA sequencing of the flanking regions.

The SALK library was queried for homozygous knockouts for the 21 line long-list identified by the initial delayed fluorescence screen in Chapter 3.5. The resulting list of SALK lines (18 lines representing 16 genes) was ordered, grown on kanamycin selective media to confirm homozygocity (through non-segregation of the resistance phenotype) and bulked for seed. Of these 20 SALK lines, 2 failed to germinate (*knat2*,*hat2*) leaving 16 lines representing 14 genes (Table 4.1).

The circadian systems of these 14 homozygous knock-out lines were probed through delayed fluorescence assay. The data were analysed using the pipeline developed in Chapter 3, as well as through the additional analytic technique of spectrum resampling.

TABLE 4.1: SALK Lines Analysed By Delayed Fluorescence

SALK code	TF	AtG	Other Names
N681541	T0082	AT3G11020	*dreb2b*
N665722	T0189	AT4G28640	*iaa11*
N670552	T0213	AT1G51140	*aks1/fbh3*
N664035	T0314	AT1G49720	*abf1*
bum	T0527	AT1G62360	*bum*
N665077	T0592	AT1G28470	*nac010*
N673916	T0593	AT1G32770	*snd1/anac012*
N665270	T0649	AT5G18270	*anac087*
N678916	T0811	AT1G07980	*nf-yc10*-1
N664846	T0811	AT1G07980	*nf-yc10*-2
N683262	T0825	AT3G05690	*nf-ya2*
N671533	T0856	AT2G40970	*mybc1*
N664486	T0910	AT5G66770	*at5g66770*
N655685	T1082	AT1G28050	*col15/bbx13*-1
N666438	T1082	AT1G28050	*col15/bbx13*-2
N655321	T1268	AT5G65410	*athb25/zhd2*

4.3.1 Results

All of the SALK lines analysed returned predicted periods within the biologically relevant 15-35hr range through both FFT-NLLS (Table 4.3) and spectrum resampling (Table 4.4).

The periods of three SALK lines were statistically significantly different to the wild type by one analysis technique, all tending towards a period lengthening. FFT-NLLS identified N681541 (period = WT + 0.81, p = 0.013), whilst *at5g66770* (period = WT + 0.47, p = 0.041) and *iaa11* (period = WT + 0.50, p = 0.039) were flagged through spectrum resampling. One line, *col15/bbx13*-1, was identified as having a period with a statistically significant difference to the wild type by both FFT (period = WT + 1.60, p = 0.039) and SR (period = WT + 2.06, p = 0.030). No lines returned a statistically significantly different FFT-NLLS RAE value, indicating that none of the SALK lines showed a significant loss of clock robustness observable through delayed fluorescence.

It is important to consider the intensity traces for the individual experimentally tested samples, in order to view the phenotype and ascertain whether or not it is a result of a few atypical readings distorting the curve.

dreb2a was identified as having a statistically signficant period lengthening relative to the wild type by FFT-NLLS (period = WT + 0.81, p = 0.013). In the DF intensity traces, there is a regular periodicity for all the 8 sample lines (Figure 4.5b). Initially, the peaks of the lines begin broadly in phase with the wild type phase and remain so for the first 24hrs of free run conditions. As the experiment continues, the lines shift out of phase and begin to show peaks after those of the wild type by 108hrs (notably N681541_3, N681541_4 and N681541_7 in the figure).

In *nf-yc10*-2 (Period$_{SR}$ = WT + 0.47, p = 0.041), the peaks again begin in phase with the wild type for the first 24hrs, however they generally stay in phase for the entire 144hr experimental window used for period analysis (Figure 4.6b). Individual samples drift gradually out of phase, with peaks being clearly out-of-phase with the wild type by 84hrs (notably N664486, N664486_5).

The same phenomena can be observed for *iaa11* (Period$_{SR}$ = WT + 0.50, p = 0.039). Most sample peaks begin broadly in-phase, drifting gradually out of phase as the experimental free-run conditions continue (Figure 4.7b). However, one sample (N665722_7) begins with its peak significantly out of phase with the wild type, and remains so for the entire experiment.

bbx13/col15-1 was the only line to have a statistically significant difference from the wild type by both period prediction methods (Period$_{FFT}$ = WT + 1.60, p = 0.039; Period$_{SR}$ = WT + 2.06, p = 0.030). Whilst there are two unusually long periods (Figure 4.4c) which may affect the mean, the median period is still longer than the wild type (WT + 1.02hrs). Samples begin broadly in phase with the wild type peaks. By 48hrs, samples are showing peaks out-of-phase with the wild type (notably N655685_ 2, which has its second peak at around 42 hrs. By 72 hrs, the peaks are all out of phase with the wild type as well as with each other. By 120hrs, the lines appear to have lost all synchronised periodicity (Figure 4.4b). This was true for both replicate plates.

4.3.2 Summary

In conclusion, 16 SALK lines were analysed for a circadian phenotype via delayed fluorescence in free run constant light conditions following entrainment to 12:12hr LD cycles. Experiments were performed with 8 replicates. *col15/bbx13*-1 had a statistically

TABLE 4.2: Summary of SALK Lines With Phenotypes Identified By DF Analysis

Line	Corresp. TF	Period (FFT)	Diff.	P=	Period (SR)	Diff.	P=
dreb2b	T0082	24.34	+0.81	0.013	24.01	+0.41	0.124
at5g66770	T0910	23.94	+0.41	0.137	24.07	+0.47	0.041
iaa11	T0189	24.21	+0.66	0.057	24.10	+0.50	0.039
bbx13/col15	T1082	25.13	+1.60	0.039	25.66	+2.06	0.030

TABLE 4.3: Summary of SALK Lines Analysed By Delayed Fluorescence, FFT-NLLS Analysis, Comparison to Wild Type.

Line	n	Mean Period	Median Period	Mean vs WT	P_{period}		Mean RAE	Median RAE	Diff. vs WT	P_{RAE}
bum	8	23.70	23.85	0.17	0.537		0.191	0.195	-0.049	0.220
athb25/zhd2	8	23.95	24.03	0.42	0.124		0.227	0.231	-0.013	0.737
*col15/bbx13*6		25.13	24.51	1.60	0.039	*	0.323	0.319	0.082	0.109
1										
abf1	8	23.59	23.64	0.05	0.900		0.207	0.184	-0.033	0.431
at5g66770	8	23.94	23.84	0.41	0.137		0.192	0.176	-0.049	0.240
nf-yc10-	8	23.49	23.63	-0.04	0.888		0.177	0.164	-0.063	0.124
2										
nac010	8	23.11	23.04	-0.42	0.110		0.181	0.174	-0.060	0.140
anac087	8	23.01	23.09	-0.52	0.061		0.201	0.208	-0.039	0.341
iaa11	8	24.19	24.21	0.66	0.057		0.225	0.214	-0.016	0.700
*col15/bbx13*8		24.01	23.45	0.48	0.368		0.234	0.210	-0.007	0.888
2										
aks1/fbh3	7	23.14	23.19	-0.39	0.168		0.168	0.185	-0.072	0.105
mybc1	8	23.60	23.26	0.07	0.858		0.170	0.170	-0.071	0.094
nf-yc10-	8	23.46	23.17	-0.07	0.831		0.219	0.206	-0.022	0.644
1										
nf-yc10-	8	23.82	23.66	0.29	0.343		0.206	0.210	-0.035	0.372
1										
dreb2b	8	24.34	24.41	0.81	0.013	*	0.223	0.218	-0.018	0.679

Continued on next page

Table 4.3 – *Continued from previous page*

Line	n	Mean Period	Median Period	Mean vs WT	P_{period}	Mean RAE	Median RAE	Diff. vs WT	P_{RAE}
nf-ya2	8	23.43	23.44	-0.10	0.705	0.187	0.191	-0.054	0.183

Summary of SALK Lines Analysed By Delayed Fluorescence, FFT-NLLS Analysis, Comparison to Wild Type.
Samples were planted, grown, delayed fluorescence assayed and analysed via FFT-NLLS as outlined previously. Statistical significance was calculated against wild type through Student's T-Test (two-tailed, unpaired). Significance thresholds: p $<$ 0.0001 ***, p $<$0.001 **, p $<$0.05 *. Wild Type mean period = 23.53, mean RAE = 0.241, n = 10.

significant phenotype when analysed through both FFT-NLLS and SR. The observed phenotype of this line was appreciably longer than that of the other three lines, with a mean calculated period of WT+1.6hrs. This long period phenotype in the knock out is converse to the short-period phenotype observed in the corresponding over-expressing TF line T1082.

FIGURE 4.4: Delayed Fluorescence Analysis for SALK N655685 (*bbx13/col15*).

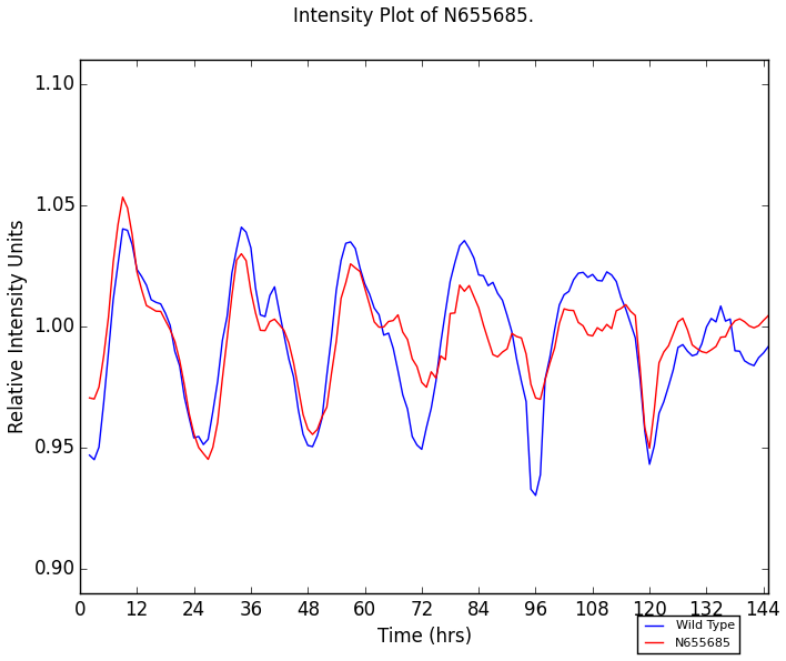

(A) Mean DF (Relative Intensity) Plot.

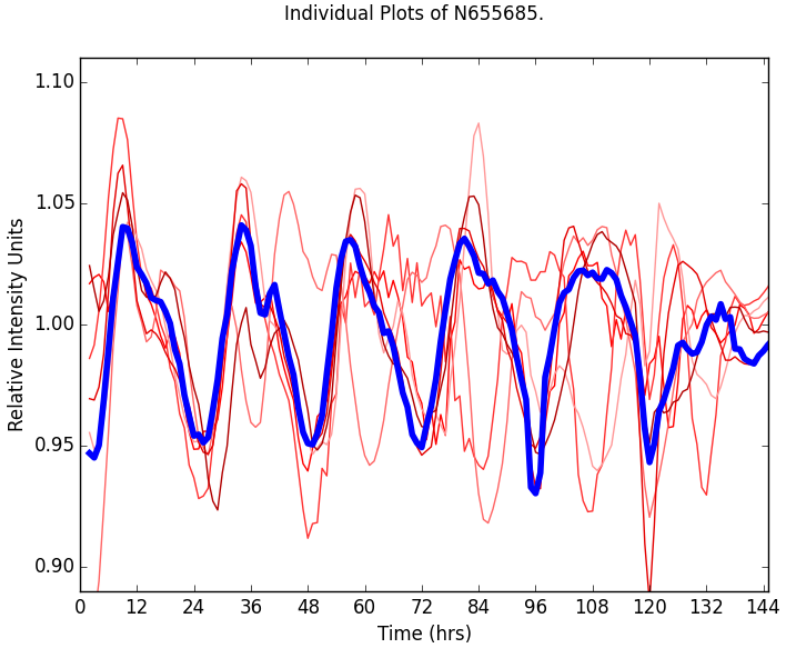

(B) Individual DF (Relative Intensity) Plot, vs Mean WT.

Results were obtained through imaging imaging 14-day old LD (12:12hr) entrained groups of 20 seedlings for 7 days in constant light and temperature (22°C) conditions. Line N655685 gave a statistically significant long period phenotype when analysed through FFT-NLLS (Mean_{sample} = 25.13hrs vs Mean_{WT} = 23.53hrs, Student's T-test p = 0.039) and spectrum resampling (Mean_{sample} = 25.66hrs vs Mean_{WT} = 23.6hrs, Students T-Test p = 0.03). There is no statistically significant change in mean RAE when calculated through FFT-NLLS analysis (change = + 0.082, Students T-Test p = 0.109) and there is a small but statistically significant increase in RAE when calculated by SR (change = + 0.009, Students T-Test p = 0.019)

Figure 4.4, Continued...

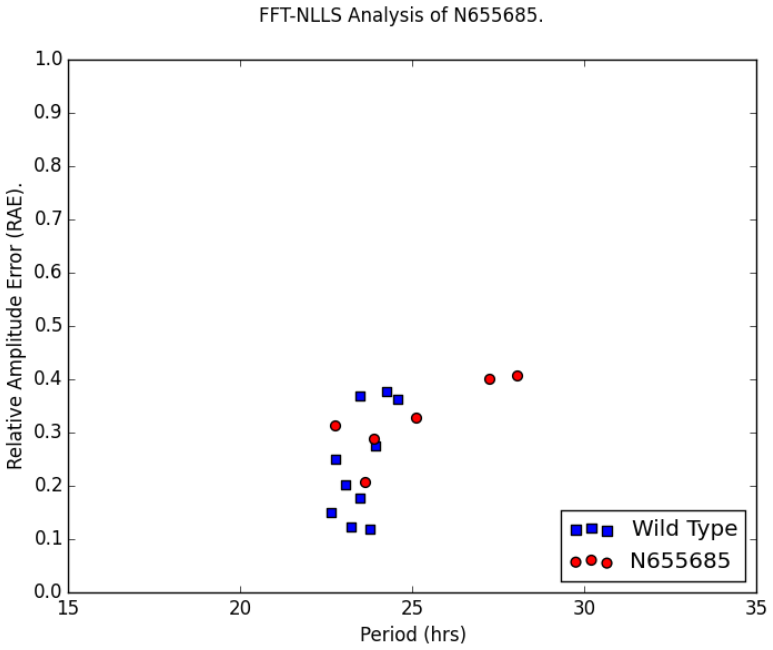

(C) FFT-NLLS Analysis (Period vs RAE).

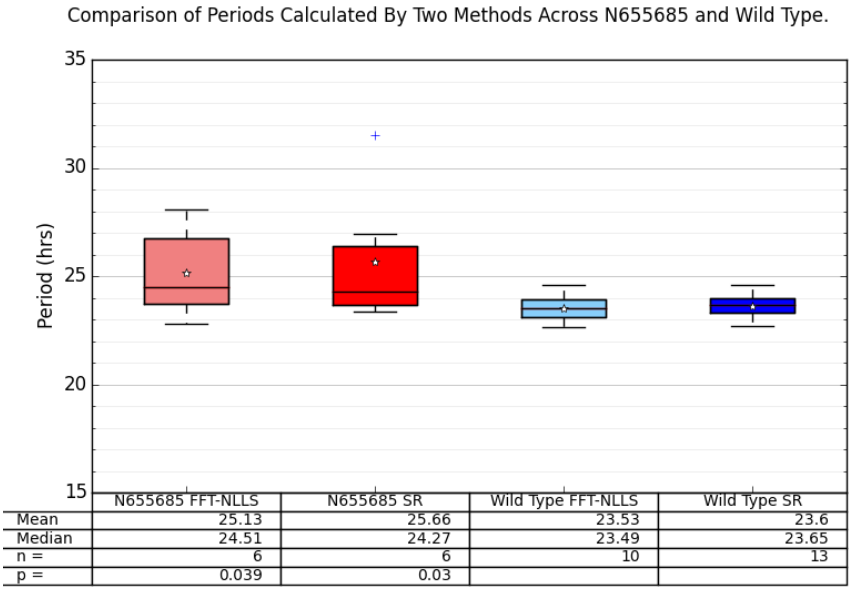

	N655685 FFT-NLLS	N655685 SR	Wild Type FFT-NLLS	Wild Type SR
Mean	25.13	25.66	23.53	23.6
Median	24.51	24.27	23.49	23.65
n =	6	6	10	13
p =	0.039	0.03		

(D) Spectrum Resampling Analysis (Period vs GOF).

FIGURE 4.5: Delayed Fluorescence Analysis for SALK N681541 (*dreb2a*).

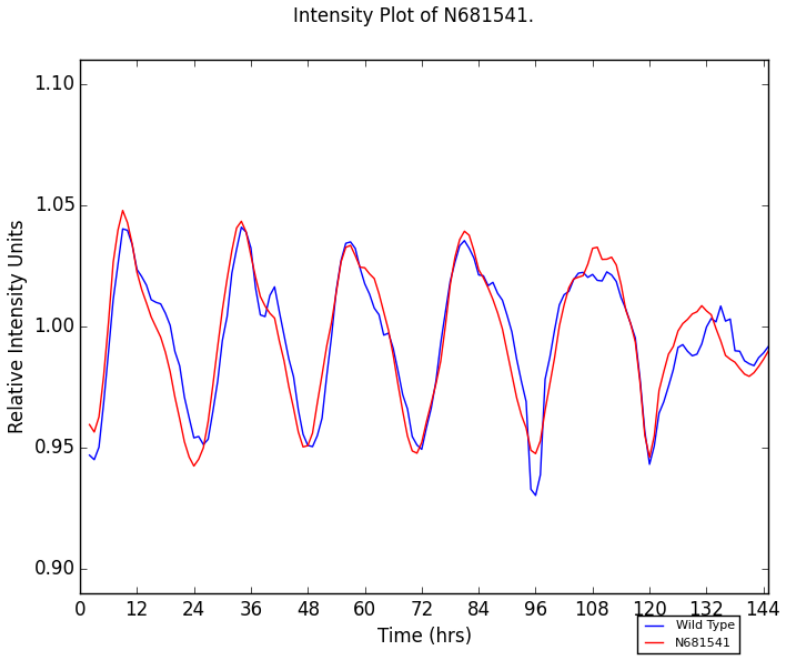

(A) Mean DF (Relative Intensity) Plot.

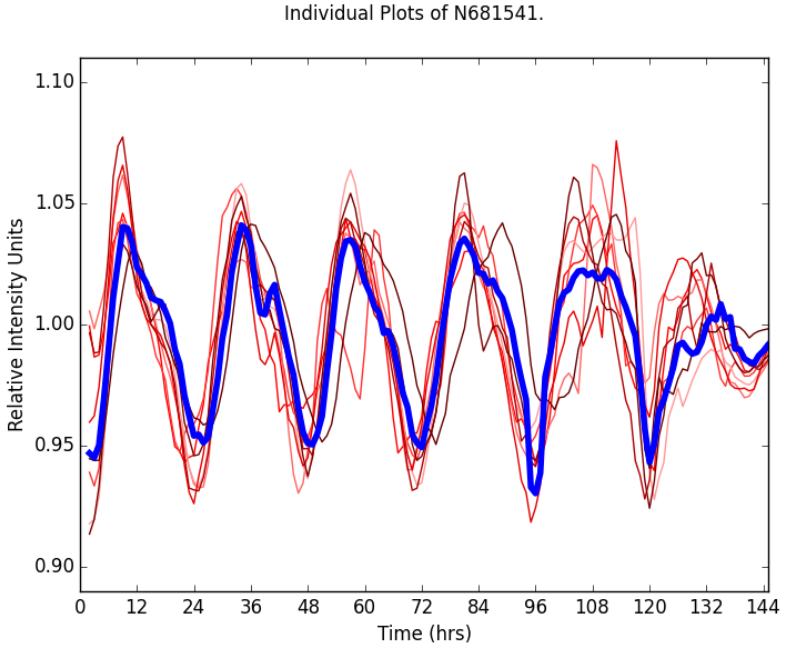

(B) Individual DF (Relative Intensity) Plot, vs Mean WT.

Results were obtained through imaging imaging 14-day old LD (12:12hr) entrained groups of 20 seedlings for 7 days in constant light and temperature (22°C) conditions. Line N681541 gave a statistically significant long period phenotype when analysed through FFT-NLLS (Mean_{sample} = 24.34hrs vs Mean_{WT} = 23.53hrs, Student's T-test $p = 0.013$) but and a long but not statistically significant period when analysed through spectrum resampling (Mean_{sample} = 24.01hrs vs Mean_{WT} = 23.6hrs, Students T-Test $p = 0.124$). Neither analysis technique returned a statistically significant change in mean RAE value compared to the wild type.

Figure 4.5, Continued...

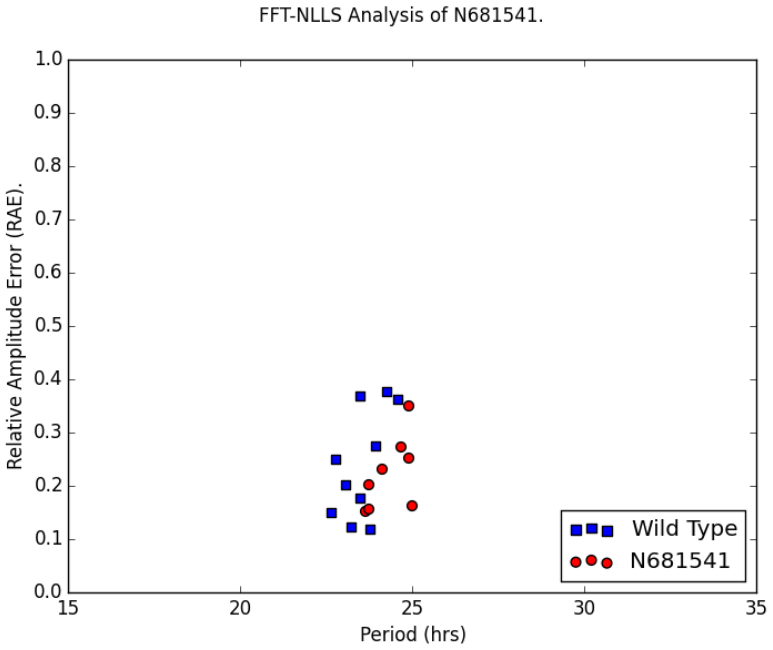

(C) FFT-NLLS Analysis (Period vs RAE).

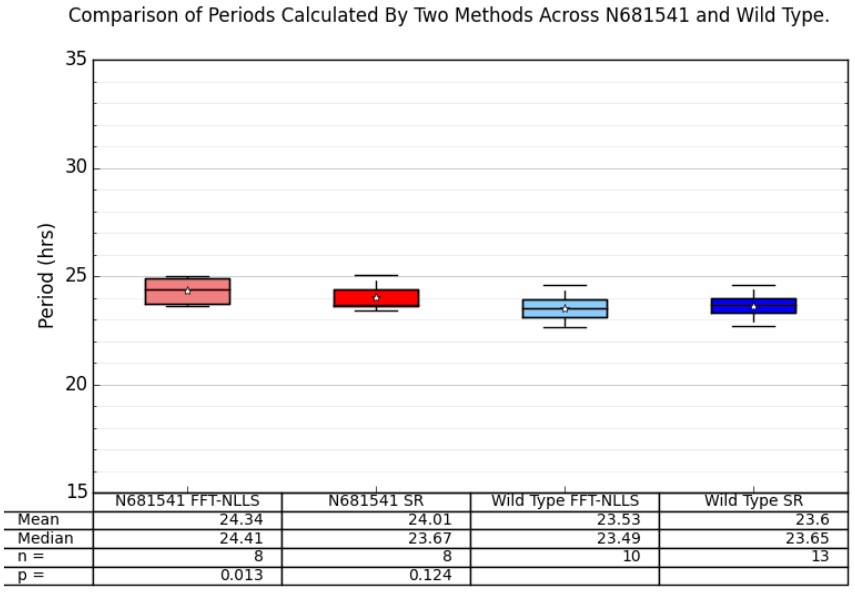

	N681541 FFT-NLLS	N681541 SR	Wild Type FFT-NLLS	Wild Type SR
Mean	24.34	24.01	23.53	23.6
Median	24.41	23.67	23.49	23.65
n =	8	8	10	13
p =	0.013	0.124		

(D) Spectrum Resampling Analysis (Period vs GOF).

FIGURE 4.6: Delayed Fluorescence Analysis for SALK N664486.

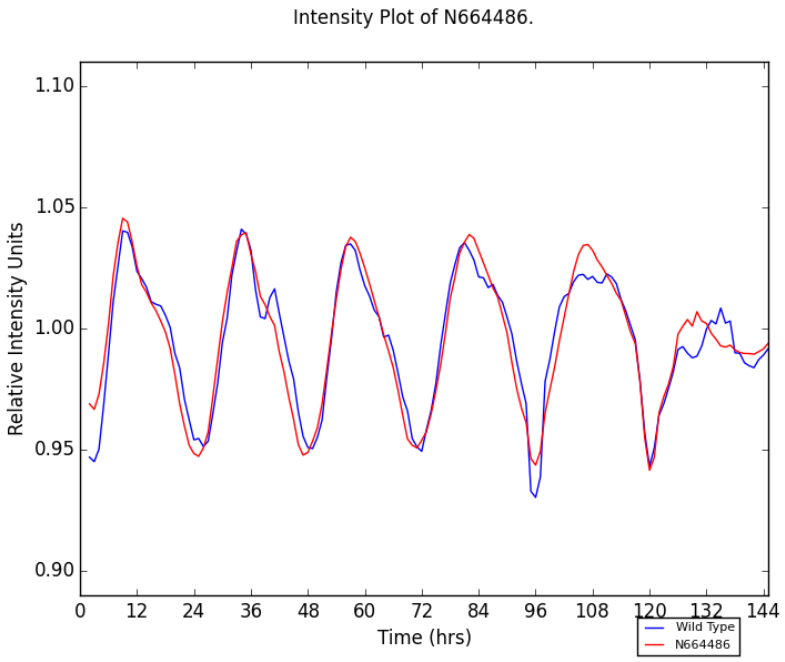

(A) Mean DF (Relative Intensity) Plot.

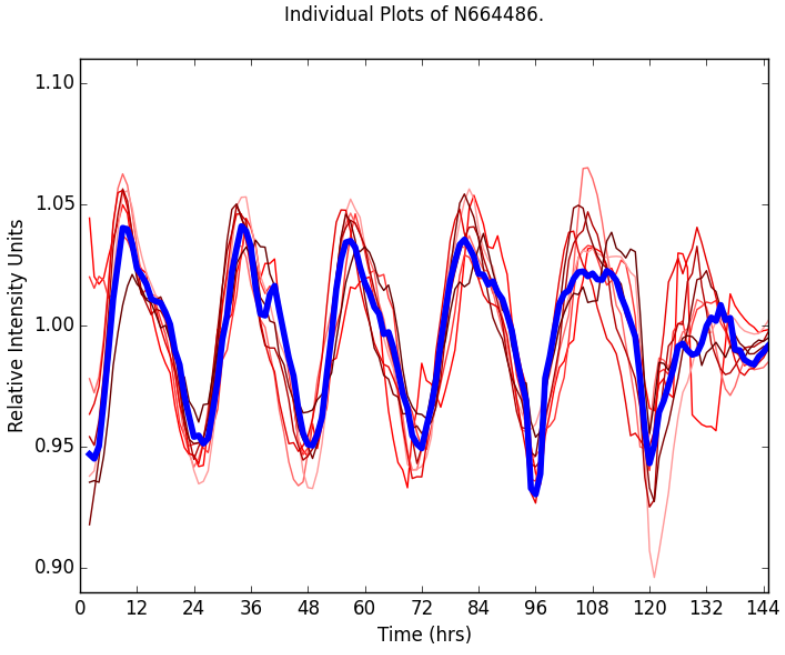

(B) Individual DF (Relative Intensity) Plot, vs Mean WT.

Results were obtained through imaging imaging 14-day old LD (12:12hr) entrained groups of 20 seedlings for 7 days in constant light and temperature (22°C) conditions. Line N664486 gave a statistically significant long period phenotype when analysed through spectrum resampling (Mean_{sample} = 24.07hrs vs Mean_{WT} = 23.6hrs, Students T-Test p = 0.041) but not when analysed through FFT (Mean_{sample} = 23.94hrs vs Mean_{WT} = 23.53hrs, Students T-Test p = 0.137). Neither analysis technique returned a statistically significant change in mean RAE value compared to the wild type.

Figure 4.6, Continued...

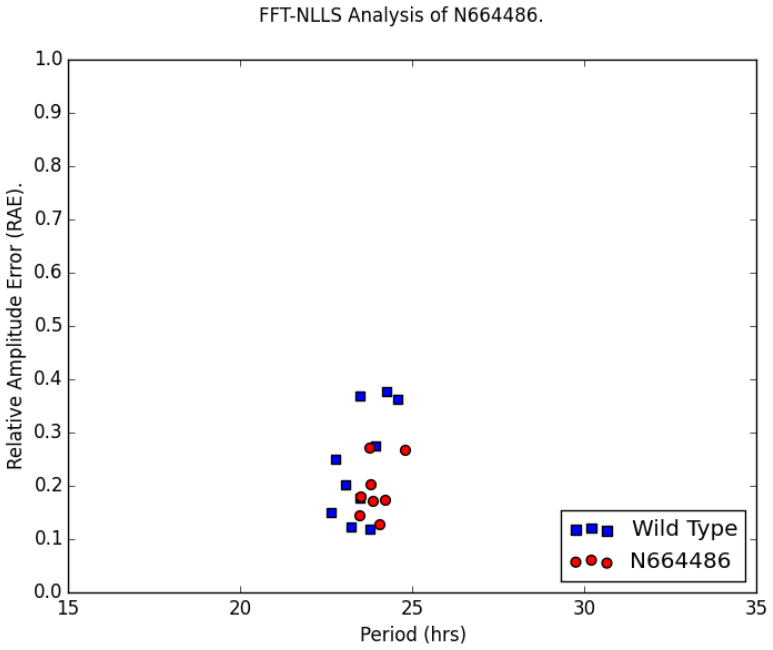

(C) FFT-NLLS Analysis (Period vs RAE).

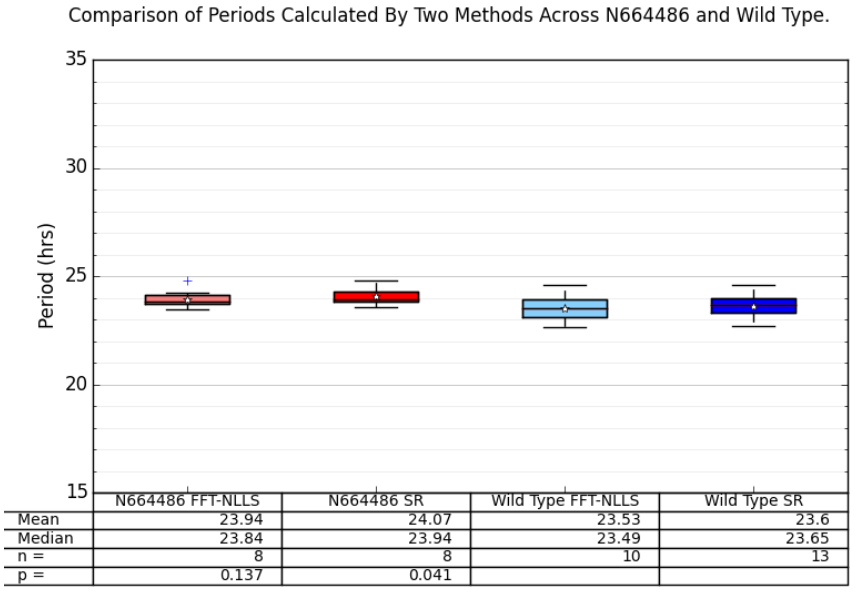

	N664486 FFT-NLLS	N664486 SR	Wild Type FFT-NLLS	Wild Type SR
Mean	23.94	24.07	23.53	23.6
Median	23.84	23.94	23.49	23.65
n =	8	8	10	13
p =	0.137	0.041		

(D) Spectrum Resampling Analysis (Period vs GOF).

FIGURE 4.7: Delayed Fluorescence Analysis for SALK N665722 (*iaa11*).

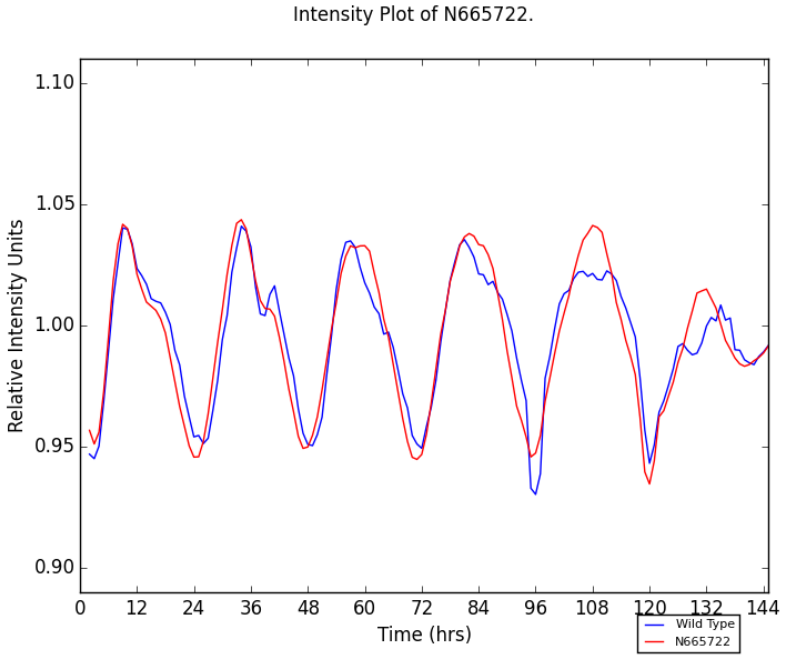

(A) Mean DF (Relative Intensity) Plot.

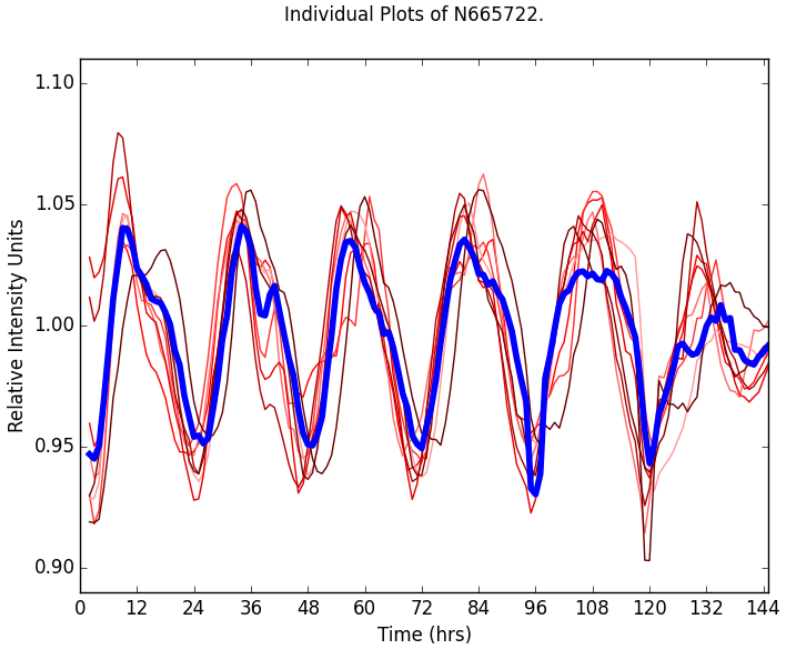

(B) Individual DF (Relative Intensity) Plot, vs Mean WT.

Results were obtained through imaging imaging 14-day old LD (12:12hr) entrained groups of 20 seedlings for 7 days in constant light and temperature (22°C) conditions. Line N665722 gave a statistically significant long period phenotype when analysed through spectrum resampling (Mean_{sample} = 24.10hrs vs Mean_{WT} = 23.6hrs, Students T-Test p = 0.039) but not when analysed through FFT (Mean_{sample} = 24.19hrs vs Mean_{WT} = 23.53hrs, Students T-Test p = 0.057). Neither analysis technique returned a statistically significant change in mean RAE value compared to the wild type.

Figure 4.7, Continued...

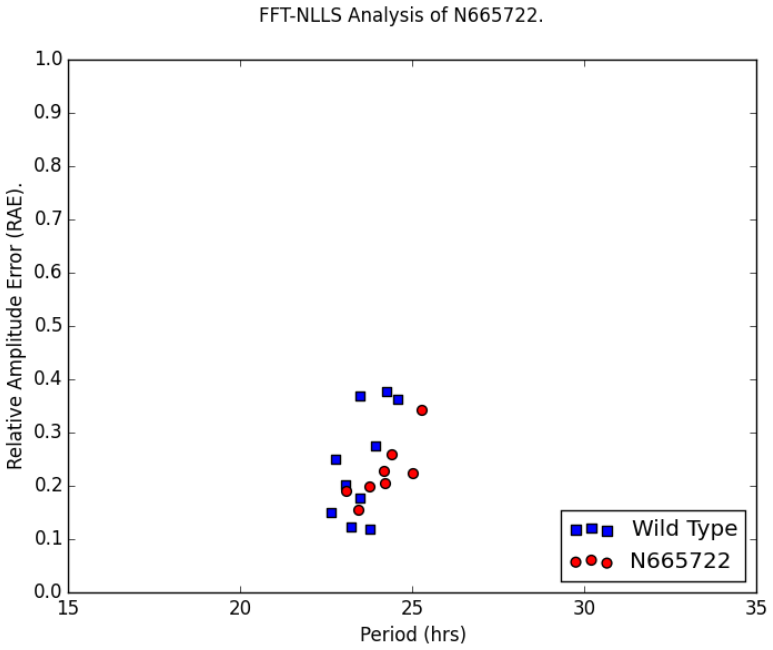

(C) FFT-NLLS Analysis (Period vs RAE).

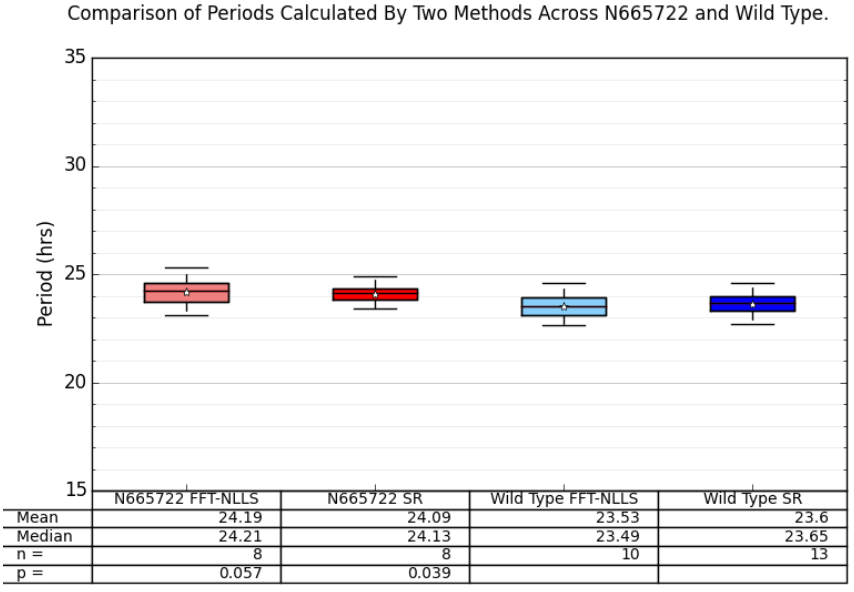

	N665722 FFT-NLLS	N665722 SR	Wild Type FFT-NLLS	Wild Type SR
Mean	24.19	24.09	23.53	23.6
Median	24.21	24.13	23.49	23.65
n =	8	8	10	13
p =	0.057	0.039		

(D) Spectrum Resampling Analysis (Period vs GOF).

TABLE 4.4: Summary of SALK Lines Analysed By Delayed Fluorescence, Spectrum Resampling Analysis, Comparison to Wild Type.

Line	n	Mean Period	Median Period	Mean vs WT	P_{period}		Mean RAE	Median RAE	Diff. vs WT	P_{RAE}	
bum	8	23.75	23.88	0.15	0.484		0.044	0.044	0.000	0.921	
athb25/zhd2	8	24.01	23.97	0.41	0.092		0.047	0.046	0.003	0.189	
col15/bbx136	6	25.66	24.27	2.06	0.030	*	0.053	0.054	0.009	0.019	*
1											
abf1	8	23.54	23.81	-0.05	0.870		0.043	0.043	-0.001	0.605	
at5g66770	8	24.07	23.94	0.47	0.041	*	0.044	0.045	0.000	0.992	
nf-yc10-	8	23.56	23.70	-0.03	0.879		0.042	0.042	-0.002	0.414	
2											
nac010	8	23.31	23.25	-0.29	0.192		0.041	0.041	-0.003	0.201	
anac087	8	23.20	23.22	-0.40	0.062		0.042	0.041	-0.003	0.323	
iaa11	8	24.10	24.13	0.50	0.039	*	0.044	0.045	0.000	0.853	
col15/bbx138	8	24.16	23.65	0.56	0.260		0.050	0.047	0.006	0.142	
2											
aks1/fbh3	7	23.30	23.33	-0.29	0.198		0.044	0.044	0.000	0.895	
mybc1	8	23.73	23.48	0.13	0.691		0.042	0.043	-0.002	0.475	
nf-yc10-	8	23.58	23.53	-0.01	0.944		0.066	0.045	0.022	0.211	
1											
nf-yc10-	7	23.91	23.69	0.31	0.302		0.043	0.044	-0.001	0.788	
1											
dreb2b	8	24.01	23.67	0.41	0.124		0.043	0.044	-0.001	0.753	
nf-ya2	8	23.70	23.70	0.10	0.645		0.046	0.047	0.002	0.399	

Summary of SALK Lines Analysed By Delayed Fluorescence, SR Analysis, Comparison to Wild Type.

Samples were planted, grown, delayed fluorescence assayed and analysed via SR as outlined previously. Statistical significance was calculated against wild type through Student's T-Test (two-tailed, unpaired). Significance thresholds: $p < 0.0001$ ***, $p < 0.001$ **, $p < 0.05$ *. Wild Type mean period = 23.60, mean RAE = 0.043, n = 13.

4.4 Dexamethasone-Dependent TF Line Phenotyping

In the initial screen (Chapter 3.5), phenotypes were measured by delayed fluorescence in the presence of dexamethasone and compared to the wild type. As mentioned previously, there are three problems with this approach - that the action of the GR cassette to exclude the TF line from the nucleus may be incomplete; that the dexamethasone treatment does not induce the full import of the TF protein; and that the cytosollic TF proteins may have an effect on the circadian clock. In order to investigate these questions, the TF lines flagged previously need re-phenotyping through delayed fluorescence in the presence and absence of dexamethasone.

Additionally, phenotypes were identified through delayed fluorescence screening, which is an indirect assay of the transcriptional circadian clock. Previously, the advantages of delayed fluorescence were outlined as a platform for screening large numbers of genes quickly, and being able to integrate a lot of circadian signal processing as a general output of clock function; however, it has a series of drawbacks that necessitate further investigation. It is not as well established in the literature as luciferase reporters are, and it is not capable of directly observing alterations in the nuclear clock. As this study is focusing on transcription factors, it would be desirable to be able to directly investigate transcriptional outputs. To this end, luciferase reporters were transformed into TF line *Arabidopsis* plants, and the resulting progeny analysed in the presence and absence of dexamethasone.

The goals of these experiments are to confirm the phenotypes by replication and through an alternative method, to characterise the effects of dexamethasone on these phenotypes (both to demonstrate the transcriptional nature of the phenotypic effectsf and to identify

any possible dexamethasone independent phenotypes), and to investigate any differential effects of the TF lines on the two reporter systems.

4.4.1 TF-CCA1 Construction

At the time of the initial DF screen, there were no known clock transcription factors in the RIKEN TF library. Between the construction of gateway plasmids, the generation of *Agrobacterium* stocks, the recovery of transformed seedlings and their survival of these transgenic plants to maturity, there are many steps at which line construction can fail. It is essential that one is used as a control line, to test the effectiveness of dexamethasone induction, and to provide a phenotype reference for analysis.

The RIKEN institute retains the gateway vectors used for generating the TF library, as well as the binary vectors used in turn to build them. Currently at the time of writing, there are three circadian clock genes that have been demonstrated to have direct, known transcription factor ability. Of these, one (*TOC1*) was identified as a transcription factor fairly recently by Gendron et al. (2012), long after the normalised transcription factor cDNA library used to generate the TF lines. This leaves the related *MYB* transcription factors *CCA1* and *LHY*. Both of these vectors were successfully constructed, with the previous failure occurring during the subsequent transformation stages. T1 heterozygous seed stocks were successfully obtained for TF-CCA1, but unfortunately not TF-LHY (which was attempted, but the plants died before setting seed). These were subsequently assayed in this section.

4.4.2 Luciferase Library Construction

The TF LUC lines were constructed through *Agrobacterium*-mediated transformation of the RIKEN TF T1 and T2 plants with a T-DNA vector containing the *pCAB2:LUC+* reporter as outlined in Chapter 2. Whilst multiple reporter constructs under the control of different-phased circadian promoters were considered, due to time and space constraints in the growth facilities at RIKEN only a single reporter could be transformed into the plants. *pCAB2:LUC+* was selected as the morning phased *pCAB2* promoter is well-established in the existing literature, and due to the fact that some alternative reporters carried unsuitable selection markers. Prior to transformation, lines were selected through sowing on MS agar laced with kanamycin, as the TF vectors carry the *NPTII* kanamycin resistance gene between the T-DNA flanking sequences.

This generated *pCAB2:LUC+* T1 seed with homozygous, heterozygous and wild-type seed in a 1:2:1 ratio.

TABLE 4.5: TF x *pCAB2::LUC+* Line Construction

TF	Names	Number of Independently Transformed Lines	Number of Plants Recovered
T0052	CRF8	2	4 (2,2)
T0082	DREB2B	2	4 (2,2)
T0189	IAA11	1	1
T0213	FBH3	1	1
T0314	ABF1	0	
T0527	BUM1	0	
T0530	KNAT2	1	2
T0576	HAT2	0	
T0591	SOG1	1	2
T0592	ANAC010	2	6 (1, 5)
T0638	RD26	0	
T0649	ANAC087	2	4 (2,2)
T0760	WRKY3	0	
T0825	HAP2B	0	
T0840	HRS1	1	4
T0856	MYBC1	0	
T0910	n/a	1	2
T1082	BBX13/COL15	1	5

Summary of TF luciferase library construction. Lines were transformed as per the protocol outlined in Chapter 2. Two independently transformed TF lines were used for each transformation. The number of independently transformed TF lines successfully transformed with luciferase is recorded in column 3. The number of plants recovered from the selection plates (i.e the number of independent luciferase transformations) is recorded in column 4.

4.4.3 Results

For delayed fluorescence re-screening, each line was planted in a well on a 1X MS + 1.5% agar plate. Each plate itself was replicated, and alternate plates treated with dexamethasone or mock treated with the dexamethasone solvent mixture at ZT + 7 on day 14. For luciferase phenotyping, the same growth conditions were used except treatment with dexamethasone or the mock solvent was performed at ZT + 7 on day 7. At the same time as dexamethasone treatment, luciferase was applied to the plates. This was performed to minimise stress to the plants, and to reduce the risk of contaminating the plates. For both experiments, plates were imaged in CCD cabinets and analysed as outlined previously, under LL/22°C conditions. Data were pooled following experiments and across replications, and analysis carried out as before.

In total, 18 genes were investigated. 11 were investigated by delayed fluorescence and luciferase, whilst 7 were analysed by DF alone. As plant transformation and vector construction took place in RIKEN Yokohama while imaging took place in Liverpool, omitted lines could not easily be re-generated. Additionally, the TF-CCA1 line (generated above) was also assayed.

4.4.3.1 Wild Type Data

Wild type plants were treated identically to the TF line plants. In 96 well test plates, wild type plants were planted in the left-most column.

In the luciferase experiments, there is no significant difference between the wild type references in the two drug treatments (WT_{Mock}=24.45, WT_{Dex}=24.48; p= 0.926). In the delayed fluorescence experiments, there is a slightly larger difference between two drug treatments, however this is still not statistically significant (WT_{Mock}=25.05, WT_{Dex}=25.39;

p= 0.08). It should be noted that the wild type periods for the DF experiments here are longer than those obtained from the initial screen. Summary Figure 4.8 shows dexamethasone and mock treated wild type plants in both conditions.

FIGURE 4.8: Comparisons of dexamethasone and mock treated wild type plants

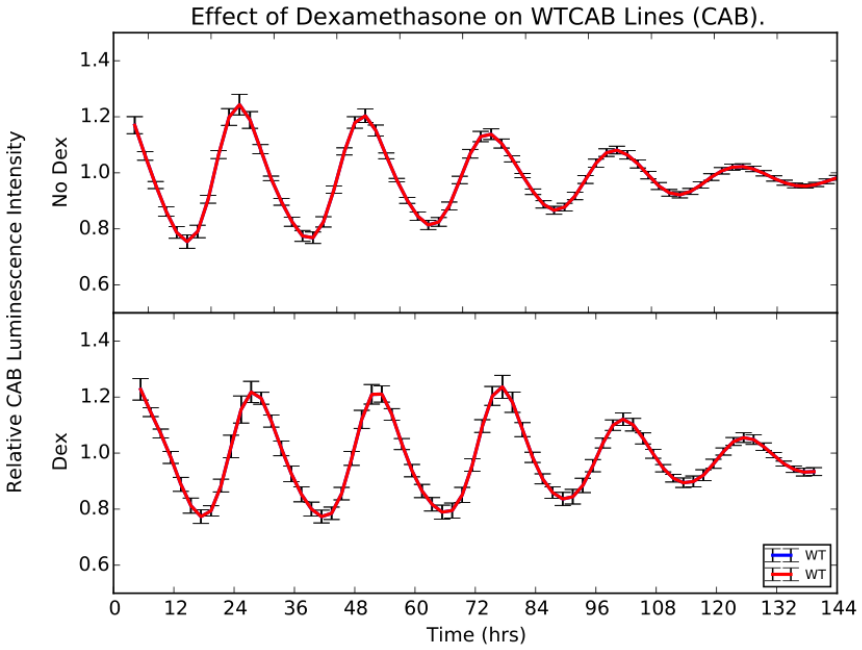

(A) Luciferase Wild type

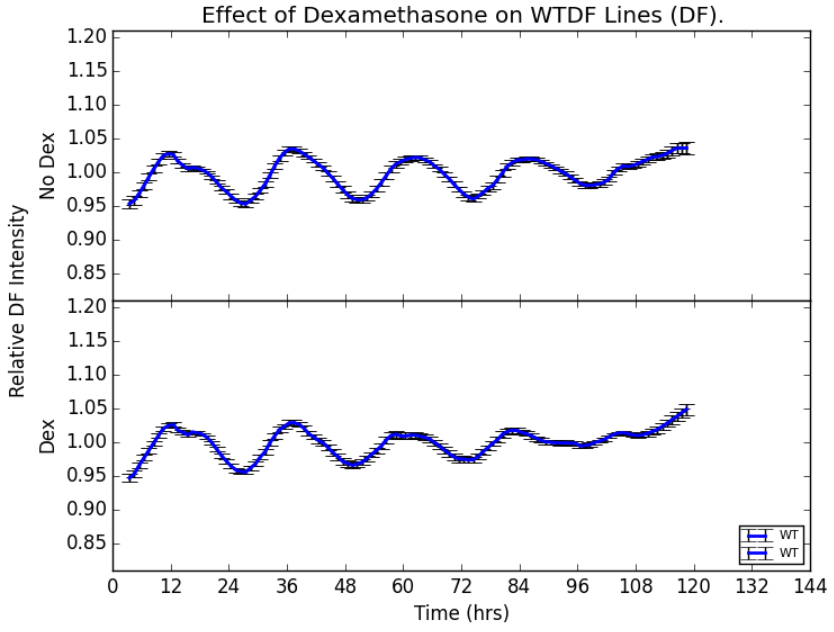

(B) DF Wild type

Seedlings were grown at a density of 15-20 per sample in 12/12 LD cycles as outlined above before treating with dexamethasone or mock solution at ZT+7. Transfer to free-run and imaging began at the subsequent dawn. Luciferase periods: WT_{Mock}=24.45, WT_{Dex}=24.48; p= 0.926, n = 40; DF periods: WT_{Mock}=25.05, WT_{Dex}=25.39; p= 0.08, n = 62.

4.4.3.2 CYTOKININ RESPONSE FACTOR 8 (CRF8)/ T0052

Samples of 3 independently transformed T1 T0052 lines were assayed by delayed fluorescence in the absence and presence of dexamethasone. In both treatment conditions, the mean period is longer than that of the wild type - however, this seems to be the norm for the TF lines in these experiments. The mean period of the dexamethasone-treated samples is slightly shorter than that of the mock-treated plants, but this difference is not statistically significant (Mean difference: -0.43hrs, p= 0.469, Table 4.6). There is a wider distribution of periods returned from this condition, increasing the overlap with the other sample sets, as is made clear by the standard error bars on Figure 4.20b. Looking at the line-graph, it is clear that for the first 24hrs, T0052 remains in-phase with the wild type in both conditions (Figure 4.20a). Over the following days of free-run, in the absence of entrainment signals, the mock treated samples drift slightly out of phase with the shorter-period wild type periods. The treated sample, however, appears to shift and "re-set", delaying the increase in DF intensity and resuming with a longer period. This effect is more severe for lines T0052-2 and T0052-3 (Figure 4.20c).

Two independently transformed non-segregating T0052 lines were successfully transformed with *pCAB2:LUC+*. In the mock treated condition, both lines show shortening compared to the wild type, and this is statistically significant for T0052-1 but not T0052-2. When dexamethasone is applied, these periods become shorter statistically significant for both lines (Mean shift: -0.7hrs, p = 0.001, Table 4.6). However, there is no significant change in the observed periods between the two conditions, and likely explained by the slightly longer wild-type period in this condition.

Periods (Luc)

		Mock Treatment vs WT				Dex Treatment vs WT				Mock vs Dex	
Line	n	Period	Diff.	p =		Period	Diff.	p =		Diff	p =
T0052-1	16	23.52	-0.93	0.009	**	23.86	-0.61	0.038	*	0.34	0.174
T0052-2	16	24.03	-0.43	0.216		23.69	-0.78	0.008	**	-0.34	0.053
T0052	**32**	**23.77**	**-0.68**	**0.009**	****	**23.78**	**-0.7**	**0.001**	****	**0**	**0.987**

Periods (DF)

		Mock Treatment vs WT				Dex Treatment vs WT			Mock vs Dex	
Line	n	Period	Diff.	p =		Period	Diff.	p =	Diff	p =
T0052-1	4	25.96	1.2	0.022	*	25.64	0.88	0.36	-0.32	0.459
T0052-2	6	25.38	0.61	0.207		24.93	0.17	0.853	-0.45	0.694
T0052-3	2	25.39	0.63	0.374		24.71	-0.04	0.975	-0.68	0.727
T0052	**12**	**25.58**	**0.81**	**0.023**	****	**25.15**	**0.39**	**0.531**	**-0.43**	**0.469**

TABLE 4.6: Phenotypes of *CYTOKININ RESPONSE FACTOR 8 (CRF8)/ ETHYLENE RESPONSE FACTOR 70 (ERF070)*/T0052) Lines

Plants were analysed in LL conditions following 12:12 LD entrainment. Dexamethasone treatment was performed the day prior to imaging as outlined previously. Images were captured and period analysis was performed on baseline detrended data, normalised to the mean, as outlined in Section 2. All statistical tests are Student's T-Test (two-tailed, unpaired); significance thresholds: p $\leq$ 0.001 ***, p $\leq$0.01 **, p $\leq$0.05 * Mean results for all independently-transformed lines are in **bold**.

4.4.3.3 DEHYDRATION-RESPONSIVE ELEMENT BINDING PROTEIN 2 (DREB2B) / T0082

Two independently transformed T0082 lines were transformed in turn with *pCAB2:LUC+*, and multiple resistant seedlings rescued for each line. Periods of both lines were statistically significantly shorter than the wild types in both treated and untreated conditions (WT_{NoDex} - 0.64hrs, p=0.015; WT_{Dex} - 0.67hrs, p= 0.002; Table 4.7).

Three independently transformed lines were assayed through delayed fluorescence. There appears to be little difference between the delayed fluorescence lines and the wild type in either condition, all tending to a longer period as seems to be the trend for this particular experiment. The exception is T0082-3, which following dexamethasone treatment has a dramatically shortened period (WT-2.62hrs), although this is not statistically significant. There are relatively few T0082-3 samples (n=2), which may explain this. When considering the RAE plots, it is clear that there is a considerable difference between these samples in both period and RAE, as exhibited by the large error bars in the dex-treated

condition (Figure 4.21d). In fact, T0082-3 appears to be a distinct outlier (Figure 4.21c), likely due to it's low level of replication.

Treatment with dexamethasone did not appear to have any statistically significant effect on the periods of the LUC lines, with the mean dexamethasone-treated periods for T0082-1 and -2 being equivalent to the untreated mean periods +0.16hrs and -0.18hrs respectively. In contrast, the delayed fluorescence lines show a mean shortening of $P_{Untreated}$ -0.49 (Table 4.7), however a single line (T0082-3) appears to be largely responsible for this effect. Regardless, this effect is statistically insignificant. We can with a degree of confidence state that any observed differences in periods for T0082 lines are independent of dexamethasone.

Periods (Luc)

		Mock Treatment vs WT				Dex Treatment vs WT				Mock vs Dex	
Line	n	Period	Diff.	p =		Period	Diff.	p =		Diff	p =
T0082-1	16	23.61	-0.85	0.017	*	23.77	-0.71	0.017	*	0.16	0.445
T0082-2	16	24.02	-0.44	0.221		23.84	-0.63	0.032	*	-0.18	0.513
T0082	**32**	**23.81**	**-0.64**	**0.015**	*****	**23.81**	**-0.67**	**0.002**	******	**-0.01**	**0.968**

Periods (DF)

		Mock Treatment vs WT				Dex Treatment vs WT				Mock vs Dex	
Line	n	Period	Diff.	p =		Period	Diff.	p =		Diff	p =
T0082-2	6	25.7	0.93	0.028	*	25.63	0.87	0.269		-0.06	0.837
T0082-3	2	25.28	0.51	0.467		22.66	-2.1	0.132		-2.62	0.207
T0082-5	4	25.63	0.86	0.089		25.98	1.22	0.372		0.36	0.425
T0082	**12**	**25.6**	**0.84**	**0.006**	******	**25.11**	**0.35**	**0.59**		**-0.49**	**0.293**

TABLE 4.7: Phenotypes of *DEHYDRATION-RESPONSIVE ELEMENT BINDING PROTEIN 2 (DREB2B)*/T0082 Lines

Plants were analysed in LL conditions following 12:12 LD entrainment. Dexamethasone treatment was performed the day prior to imaging as outlined previously. Images were captured and period analysis was performed on baseline detrended data, normalised to the mean, as outlined in Section 2. All statistical tests are Student's T-Test (two-tailed, unpaired); significance thresholds: $p \leq 0.001$ ***, $p \leq 0.01$ **, $p \leq 0.05$ *. Mean results for all independently-transformed lines are in **bold**.

4.4.3.4 INDOLE-3-ACETIC ACID INDUCIBLE 11 (IAA11) / T0189

Whilst transformation of two independent T0189 lines was attempted, luciferase-expressing plants were only successfully generated for one such line. In untreated conditions, T0189-2 had an as-wild type period (24.00, p=0.40, Table 4.8). Following dexamethasone treatment, this period shortened by 0.54hrs. Whilst this was statistically significant from the wild type (p=0.025), the difference between the untreated and treated periods was not.

The DF data for T0189-2 does not agree. Both periods are slightly longer than those of the wild type, with no statistically significant change in period following dexamethasone treatment. Two other independently transformed lines were assayed that did show period shortening following dexamethasone treatment, although again this is not statistically significant (Table 4.8). On average across the three lines, there is a dexamethasone-dependent shortening of similar scale (-0.44hrs), and yet again this is not statistically significant. It is clear from the RAE that the main difference following dexamethasone treatment is a loss of robustness as indicated by an increase in relative amplitude error (Figures 4.22b, 4.22d), although this is also not statistically significant (p=0.26).

4.4.3.5 FLOWERING B HELIX-LOOP-HELIX 3 (FBH3) / T0213

A single independently transformed T0213 line was successfully analysed with a luciferase reporter. There was no significant difference in period between the untreated T0213 lines and the wild type, although there was in the treated condition (-0.697hrs, p=0.0195, Table 4.9). However, the mean shortening of TF line period following dexamethasone treatement was small (-0.35hrs) and not statistically significant (p=0.33).

Periods (Luc)

		Mock Treatment vs WT				Dex Treatment vs WT				Mock vs Dex	
Line	n	Period	Diff.	p =		Period	Diff.	p =		Diff	p =
T0189-2	8	24	-0.46	0.394		23.46	-1.01	0.028	*	-0.53	0.586

Periods (DF)

		Mock Treatment vs WT				Dex Treatment vs WT				Mock vs Dex	
Line	n	Period	Diff.	p =		Period	Diff.	p =		Diff	p =
T0189-1	5	25.69	0.92	0.044	*	24.59	-0.17	0.874		-1.1	0.446
T0189-2	5	25.12	0.35	0.451		25.22	0.46	0.633		0.1	0.862
T0189-3	2	24.59	-0.17	0.807		24.53	-0.23	0.866		-0.06	0.91
T0189	**12**	**25.27**	**0.5**	**0.107**		**24.83**	**0.07**	**0.914**		**-0.44**	**0.464**

TABLE 4.8: Phenotypes of *INDOLE-3-ACETIC ACID INDUCIBLE 11 (IAA11)* / T0189 Lines

Plants were analysed in LL conditions following 12:12 LD entrainment. Dexamethasone treatment was performed the day prior to imaging as outlined previously. Images were captured and period analysis was performed on baseline detrended data, normalised to the mean, as outlined in Section 2. All statistical tests are Student's T-Test (two-tailed, unpaired); significance thresholds: $p \leq 0.001$ ***, $p \leq 0.01$ **, $p \leq 0.05$ *. Mean results for all independently-transformed lines are in **bold**.

Similarly, in the DF investigation, there is no significant difference between the wild type and untreated T0213 samples (WT+0.01hrs, p= 0.970, Table 4.9), whilst following dexamethasone treatment the TF line mean period shortens (WT-0.377, p= 0.024), but the difference between the TF lines in the two conditions is not significant (p= 0.332). This shortening can be observed in all three independently transformed lines, and is accompanied by a rise in RAE (Figure 4.23d).

4.4.3.6 ABA RESPONSE ELEMENT BINDING FACTOR 1 (ABF1) / T0314

No T0314 plants were rescued from the selection plates following luciferase transformation. Two independently-transformed T0314 T1 lines were assayed through delayed fluorescence. These two lines do no agree phenotypically: T0314-1 is longer than the wild type in both conditions (1hr in each), with no sizeable change between the two drug conditions. The mock treated T0314-2 is also longer than the wild type, but not

Periods (Luc)

		Mock Treatment vs WT				Dex Treatment vs WT				Mock vs Dex	
Line	n	Period	Diff.	p =		Period	Diff.	p =		Diff	p =
T0213-3	16	24.17	-0.29	0.445		23.81	-0.67	0.024	*	-0.36	0.332

Periods (DF)

		Mock Treatment vs WT			Dex Treatment vs WT			Mock vs Dex	
Line	n	Period	Diff.	p =	Period	Diff.	p =	Diff	p =
T0213-1	6	24.54	-0.22	0.665	23.81	-0.95	0.303	-0.74	0.659
T0213-2	4	25.03	0.26	0.599	24.7	-0.06	0.949	-0.34	0.776
T0213-3	2	24.99	0.23	0.744	23.73	-1.02	0.453	-1.26	0.177
T0213	**12**	**24.78**	**0.01**	**0.97**	**24.09**	**-0.67**	**0.325**	**-0.69**	**0.431**

TABLE 4.9: Phenotypes of *FLOWERING B HELIX-LOOP-HELIX 3 (FBH3)*/ T0213 Lines

Plants were analysed in LL conditions following 12:12 LD entrainment. Dexamethasone treatment was performed the day prior to imaging as outlined previously. Images were captured and period analysis was performed on baseline detrended data, normalised to the mean, as outlined in Section 2. All statistical tests are Student's T-Test (two-tailed, unpaired); significance thresholds: p ≤ 0.001 ***, p ≤0.01 **, p ≤0.05 *. Mean results for all independently-transformed lines are in **bold**.

by as much. Dexamethasone-treated T0314-2 appeared to shorten considerably (Mock-0.87hrs), however this was not statistically significant (Table 4.10).

Periods (DF)

		Mock Treatment vs WT				Dex Treatment vs WT			Mock vs Dex	
Line	n	Period	Diff.	p =		Period	Diff.	p =	Diff	p =
T0314-1	6	25.68	0.91	0.031	*	25.82	1.06	0.182	0.15	0.706
T0314-2	5	25.45	0.68	0.139		24.58	-0.18	0.833	-0.87	0.429
T0314	**11**	**25.57**	**0.81**	**0.012**	*****	**25.2**	**0.44**	**0.469**	**-0.37**	**0.505**

TABLE 4.10: Phenotypes of *ABA RESPONSE ELEMENT BINDING FACTOR 1 (ABF1)*/T0314 Lines

Plants were analysed in LL conditions following 12:12 LD entrainment. Dexamethasone treatment was performed the day prior to imaging as outlined previously. Images were captured and period analysis was performed on baseline detrended data, normalised to the mean, as outlined in Section 2. All statistical tests are Student's T-Test (two-tailed, unpaired); significance thresholds: p ≤ 0.001 ***, p ≤0.01 **, p ≤0.05 *. Mean results for all independently-transformed lines are in **bold**.

4.4.3.7 KNOTTED-LIKE FROM ARABIDOPSIS THALIANA 2 (KNAT2) / T0530

Whilst two independently transformed lines were transformed with the luciferase marker, resistant plants were only rescued from one selection plate. Two transformed plants in the T0530-1 background were rescued, seed collected and assayed. The T0530 LUC lines had shorter periods than the wild type in both the dex- and mock-treated conditions, and these differences were statistically significant (Table 4.11). Whilst the dexamethasone treated samples had a shorter mean period than the mock treated ones (Period = Mock -0.345hrs), this difference was not statistically significant (p=0.125).

The delayed fluorescence results are more confusing. On average, the periods are longer than the wild type, and exhibit a non-significant lengthening of +0.17hrs following dexamethasone treatment. However, this trend is not uniform across the assayed lines: T0530-1, for example, shows a shortening in period following dexamethasone treatment (-0.33hrs), in line with the phenotype observed through luciferase. This is refuted by T0530-3, which has the opposite phenotype of a large increase in period following dexamethasone treatment- although this may be the result of little replication (n=2). In contrast, T0530-2 appears to have no difference between the periods in either condition. Regardless, there is not a clear trend besides a tendency for TF lines to have periods longer than the wild-type in all conditions (observed for the majority of lines in this experiment) and the mean changes in period are neither considerably large nor statistically significant.

Periods (Luc)

		Mock Treatment vs WT				Dex Treatment vs WT				Mock vs Dex	
Line	n	Period	Diff.	p =		Period	Diff.	p =		Diff	p =
T0530-1	15	23.63	-0.83	0.021	*	23.42	-1.06	0	***	-0.21	0.247

Periods (DF)

		Mock Treatment vs WT				Dex Treatment vs WT				Mock vs Dex	
Line	n	Period	Diff.	p =		Period	Diff.	p =		Diff	p =
T0530-1	5	25.7	0.93	0.041	*	25.37	0.61	0.482		-0.33	0.337
T0530-2	6	25.98	1.22	0.005	**	25.98	1.22	0.124		0	1
T0530-3	2	25.56	0.79	0.262		26.69	1.93	0.161		1.13	0.119
T0530-4	2	25.18	0.41	0.564		26.41	1.65	nan		1.23	nan
T0530	**15**	**25.72**	**0.96**	**0.001**	***	**25.89**	**1.13**	**0.033**	*	**0.17**	**0.474**

TABLE 4.11: Phenotypes of *KNOTTED-LIKE FROM ARABIDOPSIS THALIANA 2 (KNAT2)*/T0530 Lines

Plants were analysed in LL conditions following 12:12 LD entrainment. Dexamethasone treatment was performed the day prior to imaging as outlined previously. Images were captured and period analysis was performed on baseline detrended data, normalised to the mean, as outlined in Section 2. All statistical tests are Student's T-Test (two-tailed, unpaired); significance thresholds: p $\leq$ 0.001 ***, p $\leq$0.01 **, p $\leq$0.05 *. Mean results for all independently-transformed lines are in **bold**.

4.4.3.8 HOMEOBOX-LEUCINE ZIPPER PROTEIN HAT2 (HAT2) / T0576

No T0576 lines were successfully transformed with the luciferase marker. Four lines were investigated through delayed fluorescence, which on average showed shortening following dexamethasone treatment (Mean change= -0.7hrs; Table 4.12). T0576-1 shows no real change in period or RAE in the two conditions, however the other three lines investigated showed a period shortening accompanied by a loss of robustness (Figure 4.26d). There is also a considerable de-sychnronisation between the timing of DF peaks in TF lines and the wild type in the dexamethasone-treated condition (Figure 4.26c).

4.4.3.9 ARABIDOPSIS NAC DOMAIN CONTAINING PROTEIN 8 (ANAC008) / T0591

T0591-2 was successfully transformed with luciferase. There was no statistically significant difference between the period of the untreated T0591 luciferase line and those

		Periods (DF)								
		Mock Treatment vs WT				Dex Treatment vs WT			Mock vs Dex	
Line	n	Period	Diff.	p =		Period	Diff.	p =	Diff	p =
T0576-1	6	26.06	1.29	0.004	**	26.08	1.33	0.099	0.03	0.955
T0576-2	6	25.66	0.9	0.033	*	24.6	-0.16	0.853	-1.06	0.318
T0576-3	2	25.37	0.6	0.391		25.13	0.37	0.788	-0.24	0.573
T0576-4	2	25.09	0.33	0.643		24.39	-0.37	0.789	-0.7	0.717
T0576	**16**	**25.7**	**0.94**	**0.001**	**	**25.2**	**0.44**	**0.426**	**-0.51**	**0.297**

TABLE 4.12: Phenotypes of *Homeobox-leucine zipper protein HAT2*/T0576 Lines

Plants were analysed in LL conditions following 12:12 LD entrainment. Dexamethasone treatment was performed the day prior to imaging as outlined previously. Images were captured and period analysis was performed on baseline detrended data, normalised to the mean, as outlined in Section 2. All statistical tests are Student's T-Test (two-tailed, unpaired); significance thresholds: p $\leq$ 0.001 ***, p $\leq$0.01 **, p $\leq$0.05 *. Mean results for all independently-transformed lines are in **bold**.

of the wild type (Table 4.13). Following dexamethsone treatment, the period shortens. Relative to the wild type, this is statistically significant (p= 0.004), but the shortening between the two conditions is not significiant (-0.73hrs, p=0.096).

Four lines were investigated through delayed fluorescence. All four show large shortening between the mock- and dexamethasone-treated conditions (Mean change= -1.02, p=0.092; Table 4.13), whilst there is considerable desynchronisation between the peaks of DF intensity for TF and wild-type plants towards the end of the experiment (Figure 4.27a). This broadly agrees with the observations from the luciferase experiment (Figures 4.14a & 4.14b).

4.4.3.10 ARABIDOPSIS NAC DOMAIN CONTAINING PROTEIN 10 (ANAC010) / T0592

Two independently transformed T0592 lines were transformed with luciferase. Both showed period shortening relative to the wild type in both treated and untreated conditions, and this effect was both larger and statistically significant for T0592-2 but not T0592-1 (Table 4.14). The differences between treated and untreated samples was small

Periods (Luc)

		Mock Treatment vs WT				Dex Treatment vs WT				Mock vs Dex	
Line	n	Period	Diff.	p =		Period	Diff.	p =		Diff	p =
T0591-2	16	24.3	-0.16	0.673		23.57	-0.91	0.005	**	-0.73	0.096

Periods (DF)

		Mock Treatment vs WT				Dex Treatment vs WT			Mock vs Dex	
Line	n	Period	Diff.	p =		Period	Diff.	p =	Diff	p =
T0591-1	6	25.75	0.98	0.025	*	25.16	0.4	0.682	-0.59	0.402
T0591-2	6	26.01	1.24	0.005	**	25.44	0.68	0.43	-0.56	0.615
T0591-3	2	24.95	0.18	0.794		22.45	-2.31	0.095	-2.5	0.093
T0591-4	2	26.97	2.2	0.005	**	25.05	0.3	0.829	-1.91	0.438
T0591	**16**	**25.9**	**1.13**	**0**	***	**24.88**	**0.12**	**0.843**	**-1.02**	**0.092**

TABLE 4.13: Phenotypes of *ARABIDOPSIS NAC DOMAIN CONTAINING PROTEIN 8/ SUPPRESSOR OF GAMMA RADIATION 1 (ANAC008 / SOG1)*/T0591 Lines

Plants were analysed in LL conditions following 12:12 LD entrainment. Dexamethasone treatment was performed the day prior to imaging as outlined previously. Images were captured and period analysis was performed on baseline detrended data, normalised to the mean, as outlined in Section 2. All statistical tests are Student's T-Test (two-tailed, unpaired); significance thresholds: $p \leq 0.001$ ***, $p \leq 0.01$ **, $p \leq 0.05$ *. Mean results for all independently-transformed lines are in **bold**. For all samples, n = 16.

and not statistically significant for either line. Curiously, these samples do not appear to begin in-phase with the wild type (Figure 4.15a)

Of the four lines assayed by DF, all showed lengthening when exposed to dexamethasone (Mean diff. 0.63hrs, p=0.838, Table 4.14), however this effect is not statistically significant. This is appears particulary severe in T0592-3 and -4, however it should be noted that relatively few replicates are performed for these two samples. The samples with higher replication have far more modest period shifts.

4.4.3.11 RESPONSE TO DESSICATION 26 (RD26) / T0638

No T0638 lines were successfully transformed with luciferase, however three TF lines were assayed by delayed fluorescence. These are unlike those discussed so far in that the periods of mock treated samples are not all considerably longer than the wild type - indeed, the mean wild-type and T0638 lines have the same period (24.28hrs, 4.15).

Periods (Luc)

		Mock Treatment vs WT				Dex Treatment vs WT				Mock vs Dex	
Line	n	Period	Diff.	p =		Period	Diff.	p =		Diff	p =
T0592-1	8	23.85	-0.61	0.208		23.95	-0.53	0.191		0.1	0.673
T0592-2	40	23.36	-1.1	0	***	23.3	-1.17	0	***	-0.05	0.728
T0592	**48**	**23.44**	**-1.02**	**0**	*******	**23.41**	**-1.07**	**0**	*******	**-0.03**	**0.838**

Periods (DF)

		Mock Treatment vs WT				Dex Treatment vs WT				Mock vs Dex	
Line	n	Period	Diff.	p =		Period	Diff.	p =		Diff	p =
T0592-1	7	25.8	1.03	0.028	*	25.89	1.13	0.081		0.1	0.873
T0592-2	10	25.91	1.14	0.001	***	26.74	1.98	0.005	**	0.83	0.225
T0592-3	2	25.52	0.76	0.284		26.32	1.56	0.256		0.79	0.334
T0592-4	2	25.66	0.89	0.21		27.48	2.72	0.056		1.82	0.427
T0592	**21**	**25.81**	**1.04**	**0**	*******	**26.44**	**1.68**	**0.001**	*******	**0.63**	**0.122**

TABLE 4.14: Phenotypes of *ARABIDOPSIS NAC DOMAIN CONTAINING PROTEIN 10/ SECONDARY WALL-ASSOCIATED NAC DOMAIN (ANAC010 / SND3)*/T0592 Lines

Plants were analysed in LL conditions following 12:12 LD entrainment. Dexamethasone treatment was performed the day prior to imaging as outlined previously. Images were captured and period analysis was performed on baseline detrended data, normalised to the mean, as outlined in Section 2. All statistical tests are Student's T-Test (two-tailed, unpaired); significance thresholds: p $\leq$ 0.001 ***, p $\leq$0.01 **, p $\leq$0.05 *. Mean results for all independently-transformed lines are in **bold**.

Following dexamethasone treatment, there is on average a period shortening (-0.56hrs) although, again, this is not statistically significant (p=0.513, 4.15). There is little overlap of the distribution of periods, and peaks of DF intensity are visibly shorter than that of the wild type (Figures 4.29a, 4.29d).

Periods (DF)

		Mock Treatment vs WT			Dex Treatment vs WT			Mock vs Dex	
Line	n	Period	Diff.	p =	Period	Diff.	p =	Diff	p =
T0638-1	5	23.95	-0.81	0.147	24.28	-0.48	0.617	0.33	0.846
T0638-2	6	25.24	0.47	0.278	23.92	-0.84	0.376	-1.32	0.302
T0638-4	2	25.41	0.65	0.357	24.76	0	0.998	-0.66	0.722
T0638	**13**	**24.77**	**0**	**0.994**	**24.21**	**-0.55**	**0.416**	**-0.56**	**0.513**

TABLE 4.15: Phenotypes of *RESPONSE TO DESSICATION 26 (RD26)*/T0638 Lines

Plants were analysed in LL conditions following 12:12 LD entrainment. Dexamethasone treatment was performed the day prior to imaging as outlined previously. Images were captured and period analysis was performed on baseline detrended data, normalised to the mean, as outlined in Section 2. All statistical tests are Student's T-Test (two-tailed, unpaired); significance thresholds: p $\leq$ 0.001 ***, p $\leq$0.01 **, p $\leq$0.05 *. Mean results for all independently-transformed lines are in **bold**

4.4.3.12 ARABIDOPSIS NAC DOMAIN CONTAINING PROTEIN 87 ANAC087) / T0649

Two independently transformed T0649 lines were in turn transformed with luciferase, and two of these rescued plants were assayed. The periods of untreated samples are not statistically significantly different from those of the wild type. The periods of both lines shorten when treated with dexamethasone, and are statistically significantly shorter than the wild types for both genotypes. This effect is more acute for T0649-2, as can clearly be see in the timing of luciferase intensity peaks in Figure 4.16a and the spread of periods in the RAE plot (Figure 4.16b). Although the dex-treated lines have shorter periods than the untreated ones, this difference is not statistically significant - perhaps due to the slight shortening of the untreated samples compared to the wild type, and the subsequent smaller difference between it and the treated samples, meaning that the distributions of treated- and untreated-periods overlap so much as to be statistically insignificant (Table 4.16).

The delayed fluorescence screens give broadly similar results. Dexamethasone treated samples are on average 0.55hrs shorter than those of the mock treated condition, and this is true for all three lines investigated. This is much more severe for T0649-3, which shows far more period shortening, however this is accompanied by a wider distribution of periods and RAE values (Figures 4.30c, 4.30d).

Periods (Luc)

		Mock Treatment vs WT				Dex Treatment vs WT				Mock vs Dex		
Line	n	Period	Diff.	p =		Period	Diff.	p =		Diff	p =	
T0649-1	16	24	-0.45	0.194		23.87	-0.6	0.039	*	-0.13	0.535	
T0649-2	16	23.79	-0.66	0.057		23.49	-0.99	0.001	***	-0.3	0.088	
T0649	**32**	**23.9**	**-0.56**	**0.028**	*****	**23.68**	**-0.79**	**<0.001**	*******	**-0.22**	**0.12**	

Periods (DF)

		Mock Treatment vs WT				Dex Treatment vs WT				Mock vs Dex		
Line	n	Period	Diff.	p =		Period	Diff.	p =		Diff	p =	
T0649-1	7	24.96	0.2	0.608		24.83	0.07	0.927		-0.13	0.877	
T0649-2	7	25.24	0.47	0.246		24.91	0.16	0.831		-0.32	0.683	
T0649-3	7	25.11	0.34	0.367		23.59	-1.17	0.182		-1.52	0.007	**
T0649	**21**	**25.1**	**0.34**	**0.163**		**24.55**	**-0.21**	**0.686**		**-0.55**	**0.197**	

TABLE 4.16: Phenotypes of *ARABIDOPSIS NAC DOMAIN CONTAINING PROTEIN 87 (ANAC087)*/T0649 Lines

Plants were analysed in LL conditions following 12:12 LD entrainment. Dexamethasone treatment was performed the day prior to imaging as outlined previously. Images were captured and period analysis was performed on baseline detrended data, normalised to the mean, as outlined in Section 2. All statistical tests are Student's T-Test (two-tailed, unpaired); significance thresholds: $p \leq 0.001$ ***, $p \leq 0.01$ **, $p \leq 0.05$ *. Mean results for all independently-transformed lines are in **bold**.

4.4.3.13 HEME ACTIVATOR PROTEIN (YEAST) HOMOLOG 2B (HAB2B) / T0825

Of the four T0825 lines investigated, all had slightly longer periods in the dexamethasone treated period (Average +0.3hrs, p= 0.359). This difference is small, and is not apparent in the RAE or line-intensity plots (Figure 4.31). Unfortunately, no T0825 lines were successfully transformed with luciferase and as such no phenotype can be observed for this line.

		Periods (DF)								
		Mock Treatment vs WT				Dex Treatment vs WT			Mock vs Dex	
Line	n	Period	Diff.	p =		Period	Diff.	p =	Diff	p =
T0825-1	7	25.52	0.76	0.064		25.76	1	0.188	0.24	0.726
T0825-2	3	24.87	0.1	0.861		25.45	0.69	0.536	0.58	0.389
T0825-3	3	24.88	0.11	0.843		25.27	0.51	0.643	0.39	0.168
T0825-4	3	25.76	0.99	0.092		25.76	1	0.304	0	0.997
T0825	**16**	**25.32**	**0.56**	**0.046**	*	**25.62**	**0.86**	**0.082**	**0.3**	**0.359**

TABLE 4.17: Phenotypes of *HEME ACTIVATOR PROTEIN (YEAST) HOMOLOG 2B (HAB2B)*/T0825 Lines

Plants were analysed in LL conditions following 12:12 LD entrainment. Dexamethasone treatment was performed the day prior to imaging as outlined previously. Images were captured and period analysis was performed on baseline detrended data, normalised to the mean, as outlined in Section 2. All statistical tests are Student's T-Test (two-tailed, unpaired); significance thresholds: p $\leq$ 0.001 ***, p $\leq$0.01 **, p $\leq$0.05 *. Mean results for all independently-transformed lines are in **bold**

4.4.3.14 HYPERSENSITIVITY TO LOW PI-ELICITED PRIMARY ROOT SHORTENING 1 (HRS1) / T0840

One T0840 line was successfully transformed with luciferase. Six plants were rescued from the selection media and their seed assayed. However, there was no statistically significant difference in period from the wild type in either condition, or between the treatment conditions (Table 4.18). In the DF experiments, two of the three lines investigated gave statistically significant period lengthening in the mock treated condition

(Table 4.18), but this is not the case following dexamethasone treatment. The plots also do not suggest any period change between the two conditions - the FFT-NLLS periods are longer than wild type for both conditions, although there is a small increase in RAE following dexamethasone treatment (Figures 4.32b & 4.32d), and there is no distinct difference in the timing of DF intensity peaks and the shape the wave form between the two conditions or their respective wild types (Figures 4.32a, 4.32c).

Periods (Luc)

		Mock Treatment vs WT			Dex Treatment vs WT			Mock vs Dex	
Line	n	Period	Diff.	p =	Period	Diff.	p =	Diff	p =
T0840-3	32	24.13	-0.33	0.255	23.98	-0.49	0.052	-0.14	0.641
T0840	**32**	**24.13**	**-0.33**	**0.255**	**23.98**	**-0.49**	**0.052**	**-0.14**	**0.641**

Periods (DF)

		Mock Treatment vs WT				Dex Treatment vs WT			Mock vs Dex	
Line	n	Period	Diff.	p =		Period	Diff.	p =	Diff	p =
T0840-1	8	25.8	1.04	0.007	**	25.83	1.07	0.145	0.03	0.94
T0840-2	5	25.08	0.31	0.484		24.98	0.22	0.803	-0.09	0.918
T0840-3	9	25.64	0.87	0.013	*	25.32	0.56	0.418	-0.32	0.408
T0840	**22**	**25.57**	**0.8**	**0.001**	***	**25.41**	**0.66**	**0.16**	**-0.16**	**0.59**

TABLE 4.18: Phenotypes of *HYPERSENSITIVITY TO LOW PI-ELICITED PRIMARY ROOT SHORTENING 1 (HRS1)*/T0840 Lines

Plants were analysed in LL conditions following 12:12 LD entrainment. Dexamethasone treatment was performed the day prior to imaging as outlined previously. Images were captured and period analysis was performed on baseline detrended data, normalised to the mean, as outlined in Section 2. All statistical tests are Student's T-Test (two-tailed, unpaired); significance thresholds: $p \leq 0.001$ ***, $p \leq 0.01$ **, $p \leq 0.05$ *. Mean results for all independently-transformed lines are in **bold**.

4.4.3.15 MYB-FAMILY TRANSCRIPTION FACTOR C1 (MYB1C) / T0856

T0856 shows a statistically significant period lengthening relative to the wild type following dexamethasone treatment (WT +2.45hrs, p= 0.003), but not mock treatment (WT +0.56hrs, p= 0.125). Furthermore, there is a statistically significant period lengthening in the dexamethasone treated T0856 plants relative to the mock treated ones (Mock +1.89hrs, p= 0.02, Table 4.19). This period shift is particularly noticeable in the DF intensity trace, where the peaks drift clearly out-of-phase with the wild type in the dex-

but not mock-treated condition (Figures 4.31a & 4.33c), as well as the RAE plots where the dex-treated samples are clearly divergent from the mock-treated (Figures 4.31b & 4.33c).

T0856 was selected from the initial screen due to a high RAE value, in line with the over-expression phenotype of it's homologue *LUX ARRHYTHMO*. There is indeed a statistically significant increase in mean RAE between the treated and untreated conditions (Mock = 0.27, Dex = 0.45; Diff= +0.18, p= 0.024) and can clearly be seen in the RAE plot (Figure 4.31b).

Unfortunately, no T0856 lines were successfully transformed with luciferase so this phenotype cannot be confirmed through this method.

Periods (DF)

		Mock Treatment vs WT			Dex Treatment vs WT				Mock vs Dex		
Line	n	Period	Diff.	p =	Period	Diff.	p =		Diff	p =	
T0856-1	2	25.95	1.18	0.098	25.89	1.13	0.431		-0.06	0.985	
T0856-2	2	25.2	0.43	0.542	27.41	2.66	0.056		2.22	0.01	*
T0856-4	2	24.98	0.22	0.757	27.66	2.91	0.038	*	2.68	0.099	
T0856	**8**	**25.32**	**0.56**	**0.125**	**27.21**	**2.45**	**0.003**	**	**1.89**	**0.02**	*

TABLE 4.19: Phenotypes of *MYB-FAMILY TRANSCRIPTION FACTOR C1 (MYBC1)*/T0856 Lines

Plants were analysed in LL conditions following 12:12 LD entrainment. Dexamethasone treatment was performed the day prior to imaging as outlined previously. Images were captured and period analysis was performed on baseline detrended data, normalised to the mean, as outlined in Section 2. All statistical tests are Student's T-Test (two-tailed, unpaired); significance thresholds: p $\leq$ 0.001 ***, p $\leq$0.01 **, p $\leq$0.05 *. Mean results for all independently-transformed lines are in **bold**

4.4.3.16 AT5G66770/T0910

T0910-1 was transformed with *pCAB2:LUC+*. In both the dexamethasone and mock treated conditions, the periods of luciferase intensity were significantly short (Table 4.20). There was, however, no significant difference between the two treatment regimes.

Conversely, in the delayed fluorescence experiments periods of T0910 lines are longer than the wild type in all conditions. There is no significant difference between the two treatment regimes (Dex = Mock + 0.15hrs, p= 0.798, Table 4.20).

Periods (Luc)

		Mock Treatment vs WT				Dex Treatment vs WT				Mock vs Dex	
Line	n	Period	Diff.	p =		Period	Diff.	p =		Diff	p =
T0910-1	16	23.5	-0.96	0.006	**	23.69	-0.78	0.008	**	0.19	0.075

Periods (DF)

		Mock Treatment vs WT				Dex Treatment vs WT			Mock vs Dex	
Line	n	Period	Diff.	p =		Period	Diff.	p =	Diff	p =
T0910-1	5	25.59	0.82	0.072		26.23	1.47	0.092	0.64	0.101
T0910-2	6	25.72	0.95	0.023	*	24.83	0.07	0.945	-0.89	0.527
T0910-3	2	25.53	0.76	0.28		26.59	1.83	0.182	1.06	0.068
T0910	**13**	**25.64**	**0.87**	**0.003**	**	**25.79**	**1.03**	**0.12**	**0.15**	**0.798**

TABLE 4.20: Phenotypes of *AT5G66770*/T0910 Lines

Plants were analysed in LL conditions following 12:12 LD entrainment. Dexamethasone treatment was performed the day prior to imaging as outlined previously. Images were captured and period analysis was performed on baseline detrended data, normalised to the mean, as outlined in Section 2. All statistical tests are Student's T-Test (two-tailed, unpaired); significance thresholds: p $\leq$ 0.001 ***, p $\leq$0.01 **, p $\leq$0.05 *. Mean results for all independently-transformed lines are in **bold**.

4.4.3.17 CONSTANS-LIKE 15 (COL15) / T1082

One independently transformed T1082 line was successfully transformed with luciferase. Multiple luciferase-transformed plants were rescued from the selection plate and assayed. The mean period in both the mock- and dexamethasone-treated conditions was slightly shorter than the wild type (0.5hrs, Table 4.21) as clearly visible in Figure 4.18b, and this difference is statistically significant in both cases (p = 0.028, 0.005 respectively). There is no significant difference between the two treatment conditions (p = 0.780).

Five T1082 lines were analysed by delayed fluorescence. In the mock treated condition, there is no difference between T1082 lines and the wild type (WT +0.06hrs). This is especially clear in the DF intensity traces in Figure 4.35c - the peaks of T1082-2, -6 and

-7 are all clearly in-phase with the wild type throughout the experimental window, whilst T1082-1 and -3 slightly anticipate the reference.

However, following dexamethasone treatment, the period shortens relative to the wild type (-0.80hrs, p=0.066) and relative to the mock-treated condition (-0.87hrs, p= 0.006, Table 4.21). The mean period for the dex-treated DF lines is comparable to those from the luciferase period (23.96hrs compared to 23.92hrs).This shortening is observed for all five lines (Figure 4.35d.

Periods (Luc)

		Mock Treatment vs WT				Dex Treatment vs WT				Mock vs Dex		
Line	n	Period	Diff.	p =		Period	Diff.	p =		Diff	p =	
T1082-1	40	23.95	-0.50	0.028	*	23.92	-0.56	0.005	**	-0.03	0.780	

Periods (DF)

		Mock Treatment vs WT				Dex Treatment vs WT				Mock vs Dex		
Line	n	Period	Diff.	p =		Period	Diff.	p =		Diff	p =	
T1082-1	11	24.93	0.16	0.608		24.30	-0.46	0.465		-0.63	0.261	
T1082-2	2	24.57	-0.2	0.78		22.66	-2.1	nan		-1.91	nan	
T1082-3	12	24.81	0.04	0.9		24.15	-0.61	0.316		-0.65	0.154	
T1082-6	2	24.54	-0.23	0.743		23.95	-0.81	0.552		-0.59	0.303	
T1082-7	2	24.95	0.18	0.793		21.70	-3.06	0.029	*	-3.25	0.005	**
T1082	**29**	**24.83**	**0.06**	**0.777**		**23.96**	**-0.80**	**0.066**		**-0.87**	**0.006**	******

TABLE 4.21: Phenotypes of *CONSTANS-LIKE 15/ B-BOX DOMAIN PROTEIN 13 (COL15/BBX13)*/T1082 Lines

Plants were analysed in LL conditions following 12:12 LD entrainment. Dexamethasone treatment was performed the day prior to imaging as outlined previously. Images were captured and period analysis was performed on baseline detrended data, normalised to the mean, as outlined in Section 2. All statistical tests are Student's T-Test (two-tailed, unpaired); significance thresholds: $p \leq 0.001$ ***, $p \leq 0.01$ **, $p \leq 0.05$ *. Mean results for all independently-transformed lines are in **bold**.

4.4.3.18 TF-CCA1

There was no significant difference in period between TF-CCA1 luciferase lines and the wild type, regardless of the dexamethasone treatment (Table 4.22). However, there is a statistically significant loss of robustness, as indicated by an increase in RAE value, in both treatment conditions. Given the tight clustering and low RAE values given by

the *pCAB2:LUC+* wild types, this is especially striking. *CCA1* over-expressing lines are known to lose rhythmicity in free-run conditions, which in FFT-NLLS analysis manifests as an increase in RAE (Green et al., 2002). Whilst the observed luciferase phenotype of this line does not match up completely with that previously observed, the TF-CCA1 lines still possess two functional copies of *CCA1* under native control. These may remain rhythmic, which may explain loss of robustness over the less severe abolition of rhythms.

In the delayed fluorescence experiments, the phenotype is more unusual. Mock-treated samples are statistically significantly longer than the wild type (WT +0.84hrs, p= 0.026, Table 4.22). Following dexamethasone treatment, the period shortens considerably (-1.61hrs), but this is not a statistically significant difference relative to either the wild type or the mock-treated samples. The RAE values are of a similar size with the comparable luciferase experiments, however as the wild type RAE values from DF are higher than luciferase, these do not represent large nor statistically significant changes in robustness.

As the TF lines used for these DF experiments were T1 seed (much like the rest of the TF library), transformed with luciferase to give T2 plants. It is possible that the mixture of homo-, hetero- and wild-type TF-CCA1 plants in the DF experiments resulted in the unexpected phenotypes observed.

Periods

		Mock Treatment vs WT				Dex Treatment vs WT				Mock vs Dex	
Line	n	Period	Diff.	p =		Period	Diff.	p=		Diff	p =
TF-CCA1 (Luc)	22	24.44	-0.012	0.970		24.72	0.243	0.360		0.276	0.376
TF-CCA1 (DF)	9	25.61	0.84	0.026	*	24.00	-0.76	0.319		-1.61	0.146

RAEs

		Mock Treatment vs WT				Dex Treatment vs WT				Mock vs Dex	
Line	n	RAE	Diff.	p =		RAE	Diff.	p =		Diff	p=
TF-CCA1 (Luc)	22	0.33	0.087	<0.001	***	0.27	0.06	0.002	**	-0.06	0.071
TF-CCA1 (DF)	9	0.30	0	0.905		0.36	0.02	0.654		0.06	0.158

TABLE 4.22: Phenotypes of TF-CCA1 Lines

Plants were analysed in LL conditions following 12:12 LD entrainment. Dexamethasone treatment was performed the day prior to imaging as outlined previously. Images were captured and period analysis was performed on baseline detrended data, normalised to the mean, as outlined in Section 2. All statistical tests are Student's T-Test (two-tailed, unpaired); significance thresholds: $p \leq 0.001$ ***, $p \leq 0.01$ **, $p \leq 0.05$ *. Mean results for all independently-transformed lines are in **bold**. For luciferase experiments, n =40.

FIGURE 4.9: Effects of Dex-Induction of CRF8 on *pCAB2:LUC+* Intensity

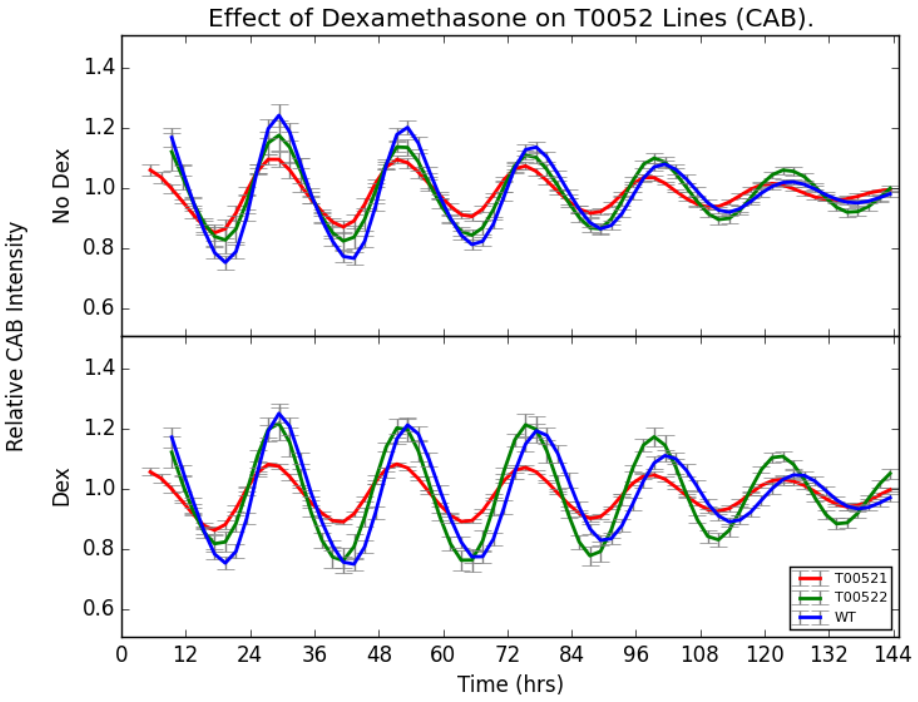

(A) Luciferase Intensity

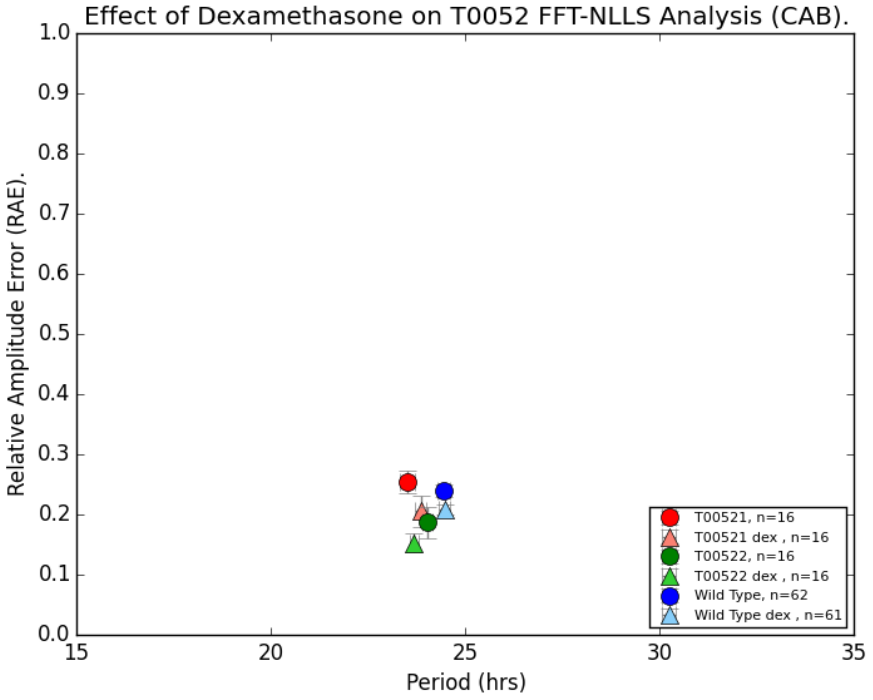

(B) Luciferase Periods

Seedlings were surface sterilised and grown at a density of 15-20 per sample for a total of 7 days in 12/12 LD cycles before treatment with dexamethasone at ZT+7, using the protocol outlined in Chapter 2. Treated plants were returned to the diurnal growth conditions. Experimental imaging began at dawn day 8 with transfer into LL. All seeds are T1 luciferase, T3 TF-GR, unless otherwise stated.

FIGURE 4.10: Effects of Dex-Induction of DREB2B on *pCAB2:LUC+* Intensity

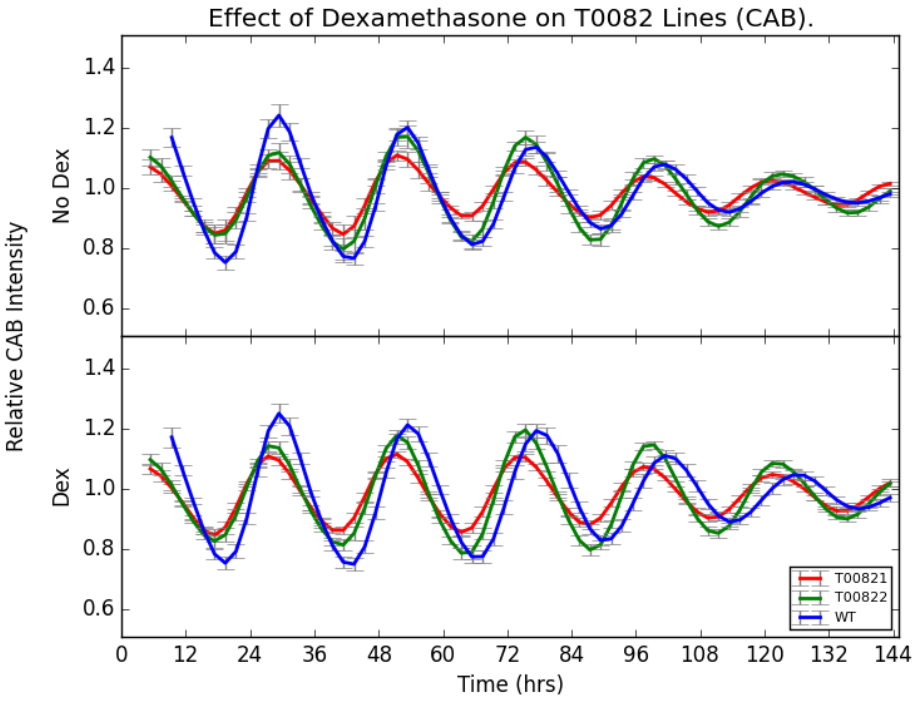

(A) Luciferase Intensity

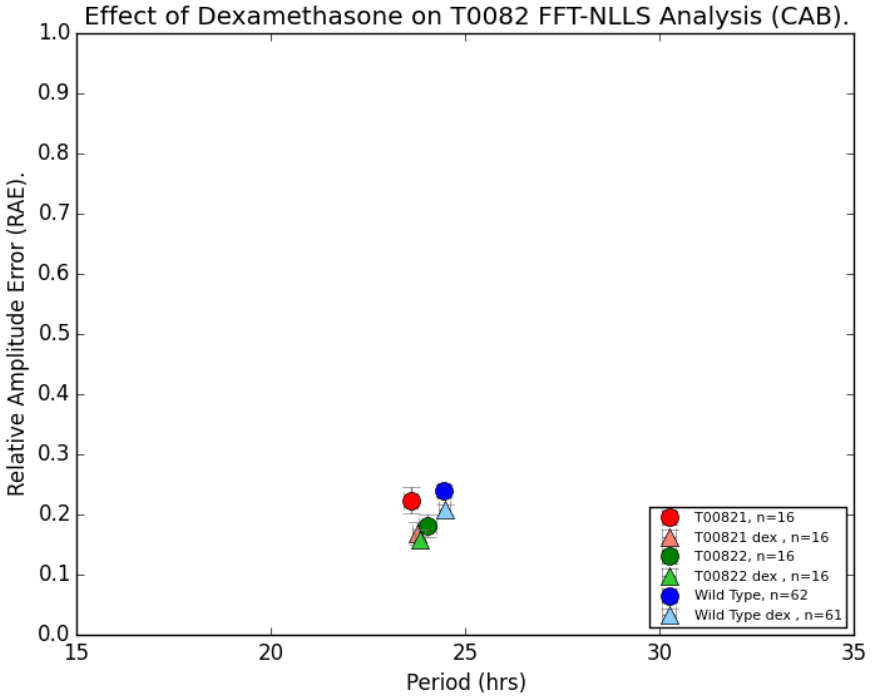

(B) Luciferase Periods

Seedlings were surface sterilised and grown at a density of 15-20 per sample for a total of 7 days in 12/12 LD cycles before treatment with dexamethasone at ZT+7, using the protocol outlined in Chapter 2. Treated plants were returned to the diurnal growth conditions. Experimental imaging began at dawn day 8 with transfer into LL. All seeds are T1 luciferase, T3 TF-GR, unless otherwise stated.

FIGURE 4.11: Effects of Dex-Induction of IAA11 on *pCAB2:LUC+* Intensity

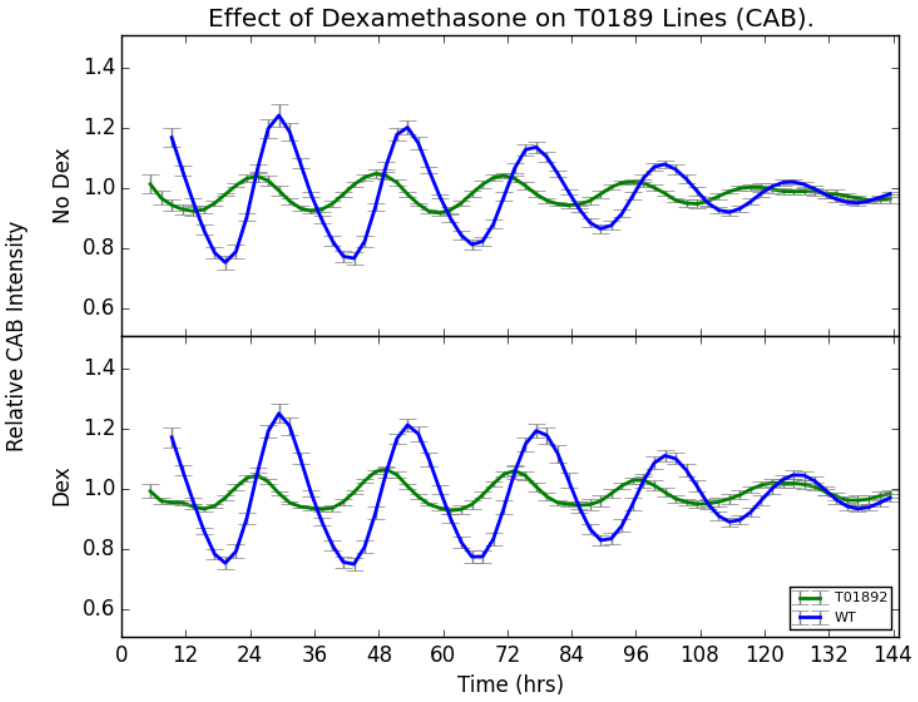

(A) Luciferase Intensity

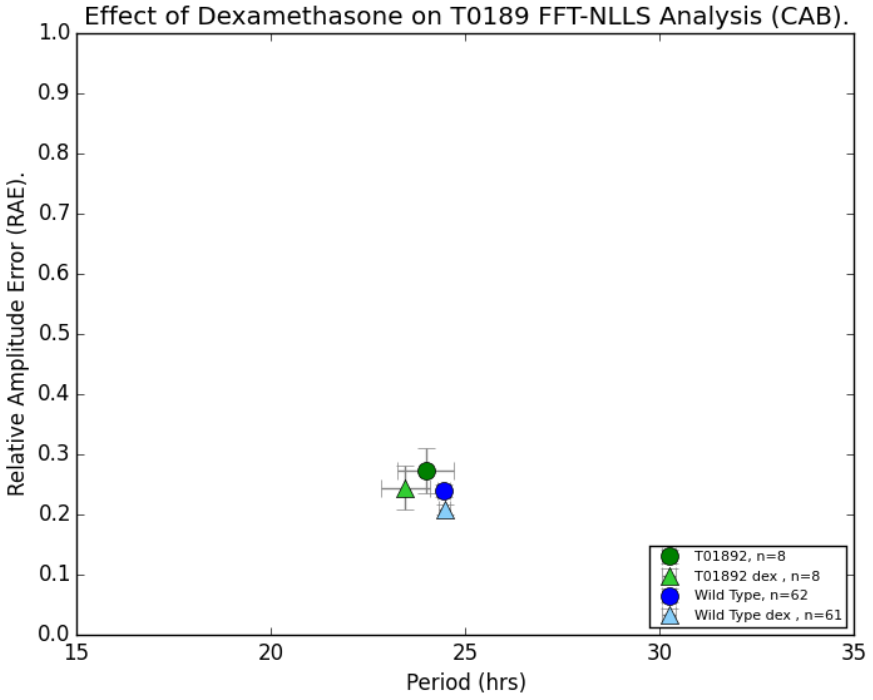

(B) Luciferase Periods

Seedlings were surface sterilised and grown at a density of 15-20 per sample for a total of 7 days in 12/12 LD cycles before treatment with dexamethasone at ZT+7, using the protocol outlined in Chapter 2. Treated plants were returned to the diurnal growth conditions. Experimental imaging began at dawn day 8 with transfer into LL. All seeds are T1 luciferase, T3 TF-GR, unless otherwise stated.

FIGURE 4.12: Effects of Dex-Induction of FBH3 on *pCAB2:LUC+* Intensity

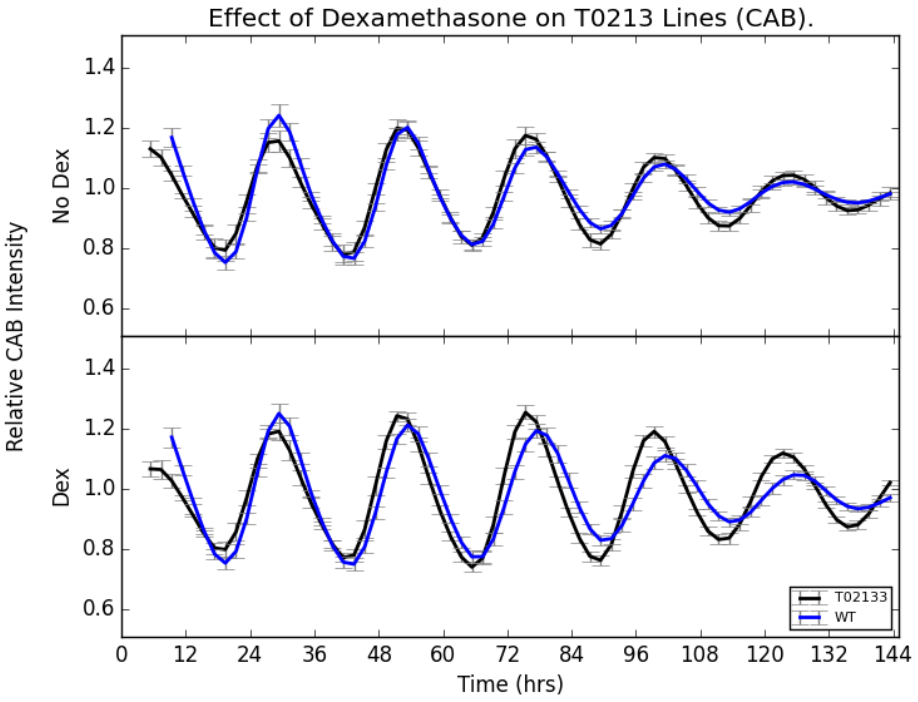

(A) Luciferase Intensity

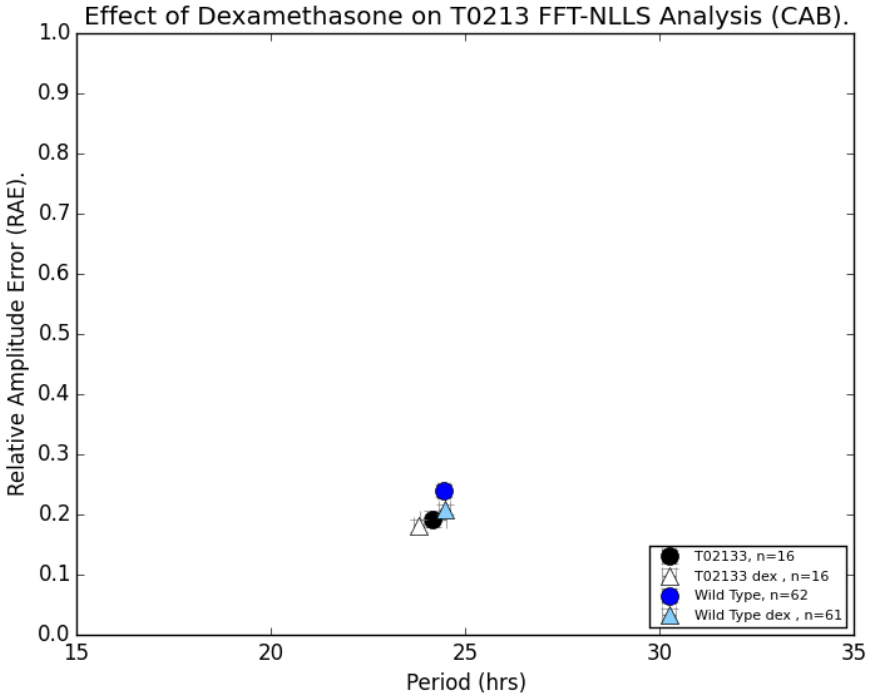

(B) Luciferase Periods

Seedlings were surface sterilised and grown at a density of 15-20 per sample for a total of 7 days in 12/12 LD cycles before treatment with dexamethasone at ZT+7, using the protocol outlined in Chapter 2. Treated plants were returned to the diurnal growth conditions. Experimental imaging began at dawn day 8 with transfer into LL. All seeds are T1 luciferase, T3 TF-GR, unless otherwise stated.

FIGURE 4.13: Effects of Dex-Induction of ABF1 on *pCAB2:LUC+* Intensity

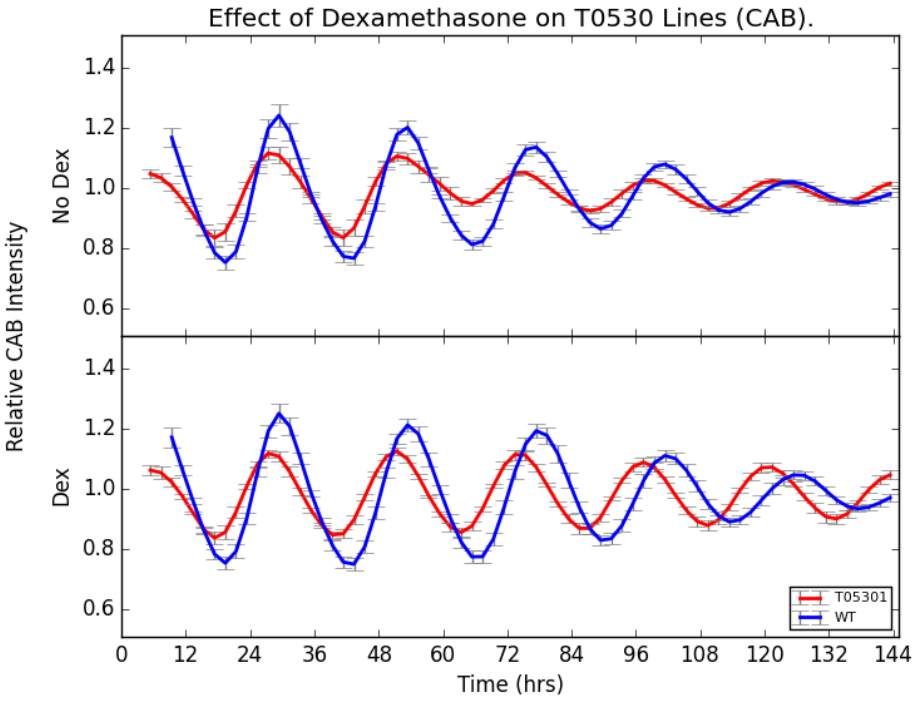

(A) Luciferase Intensity

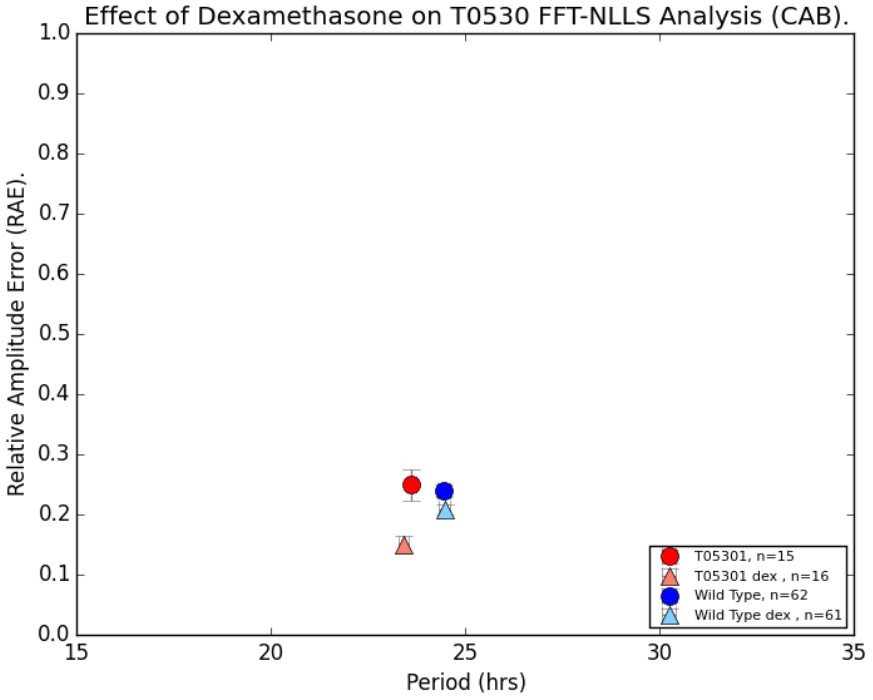

(B) Luciferase Periods

Seedlings were surface sterilised and grown at a density of 15-20 per sample for a total of 7 days in 12/12 LD cycles before treatment with dexamethasone at ZT+7, using the protocol outlined in Chapter 2. Treated plants were returned to the diurnal growth conditions. Experimental imaging began at dawn day 8 with transfer into LL. All seeds are T1 luciferase, T3 TF-GR, unless otherwise stated.

FIGURE 4.14: Effects of Dex-Induction of SOG1 on *pCAB2:LUC+* Intensity

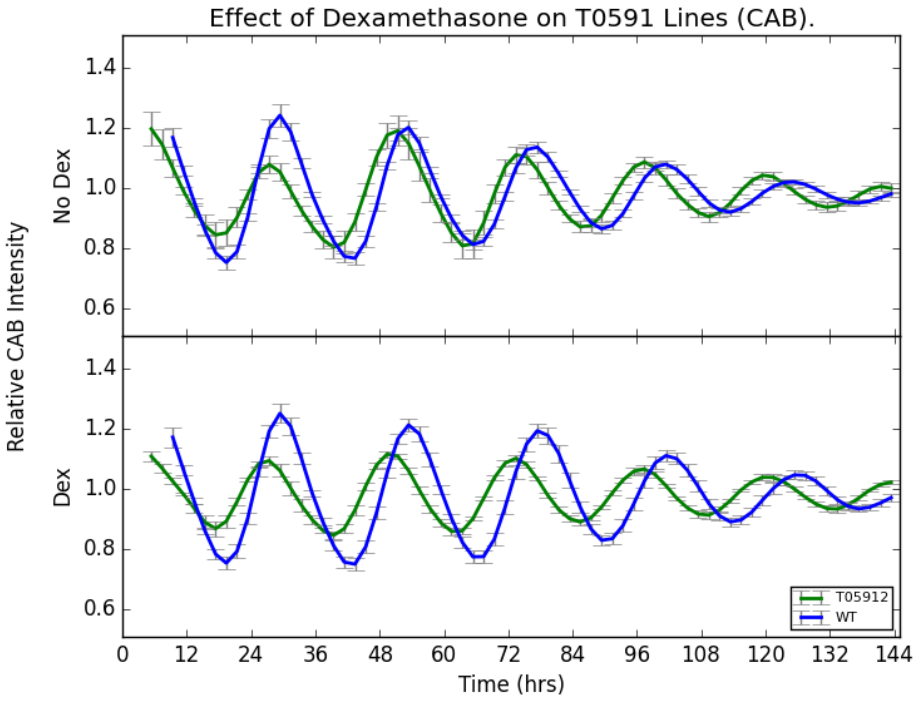

(A) Luciferase Intensity

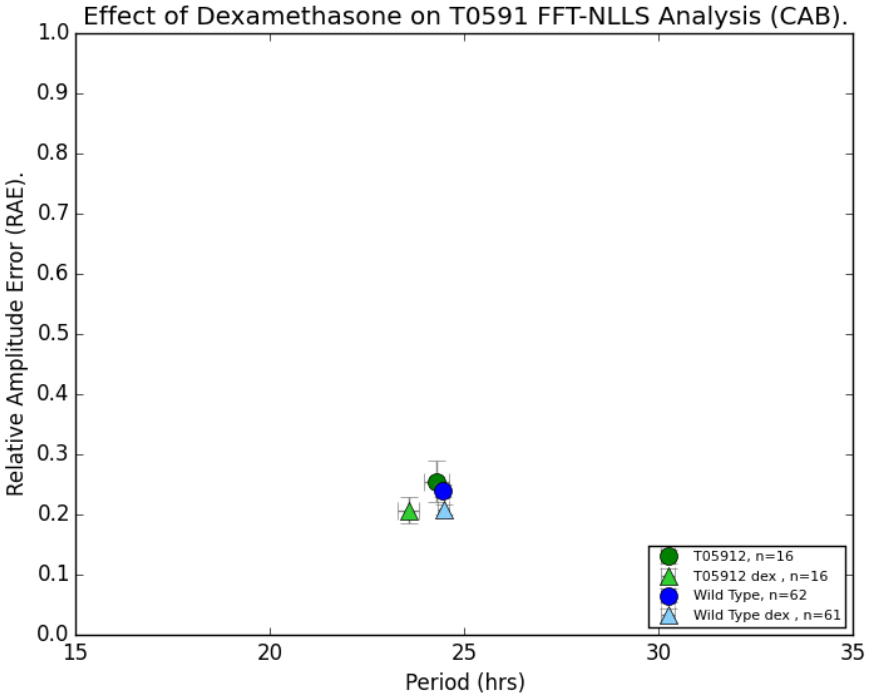

(B) Luciferase Periods

Seedlings were surface sterilised and grown at a density of 15-20 per sample for a total of 7 days in 12/12 LD cycles before treatment with dexamethasone at ZT+7, using the protocol outlined in Chapter 2. Treated plants were returned to the diurnal growth conditions. Experimental imaging began at dawn day 8 with transfer into LL. All seeds are T1 luciferase, T3 TF-GR, unless otherwise stated.

FIGURE 4.15: Effects of Dex-Induction of ANAC010 on *pCAB2:LUC+* Intensity

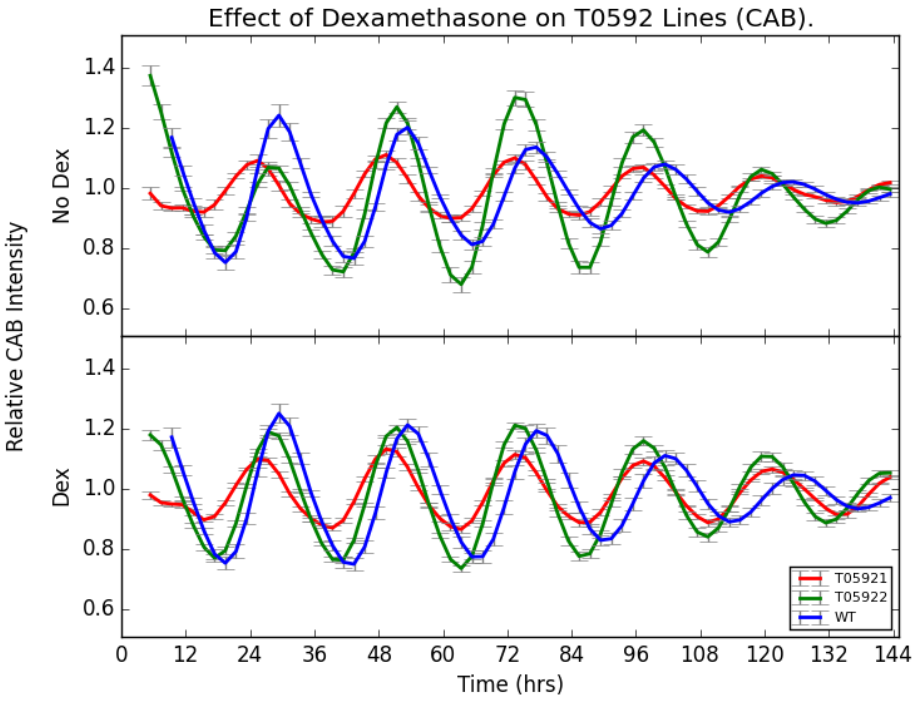

(A) Luciferase Intensity

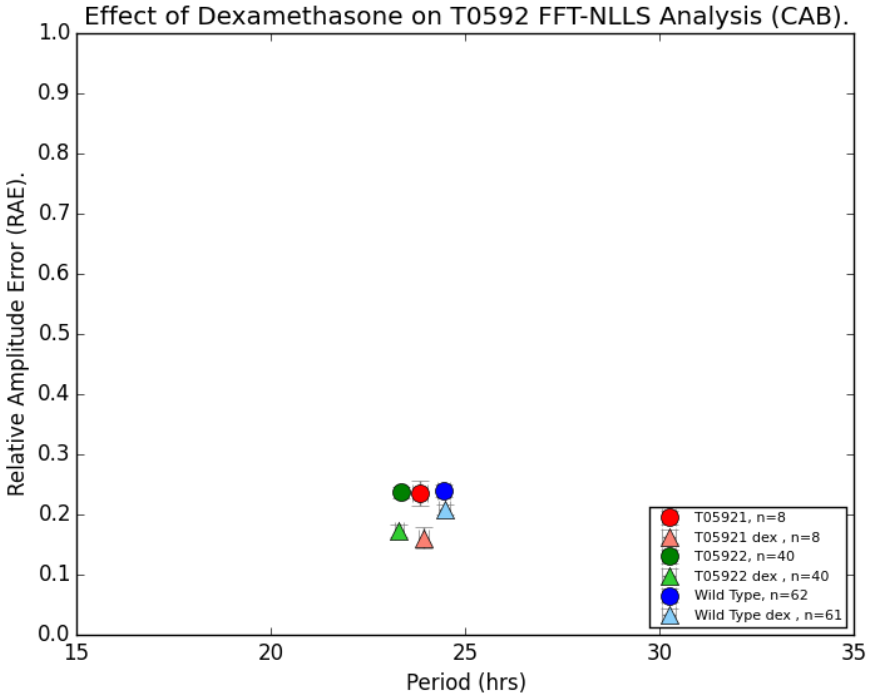

(B) Luciferase Periods

Seedlings were surface sterilised and grown at a density of 15-20 per sample for a total of 7 days in 12/12 LD cycles before treatment with dexamethasone at ZT+7, using the protocol outlined in Chapter 2. Treated plants were returned to the diurnal growth conditions. Experimental imaging began at dawn day 8 with transfer into LL. All seeds are T1 luciferase, T3 TF-GR, unless otherwise stated.

FIGURE 4.16: Effects of Dex-Induction of ANAC087 on *pCAB2:LUC+* Intensity

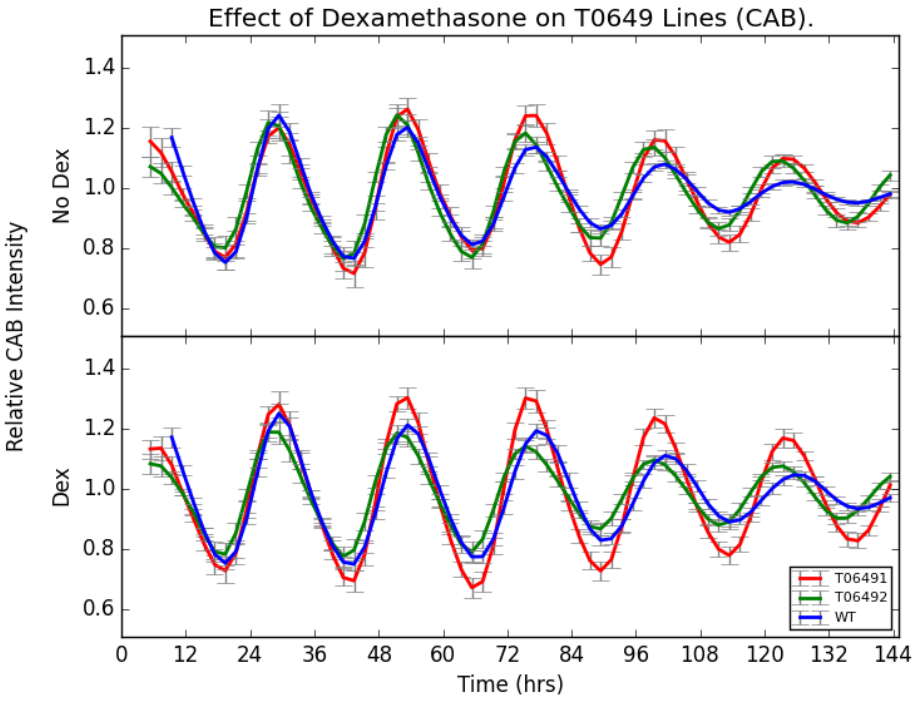

(A) Luciferase Intensity

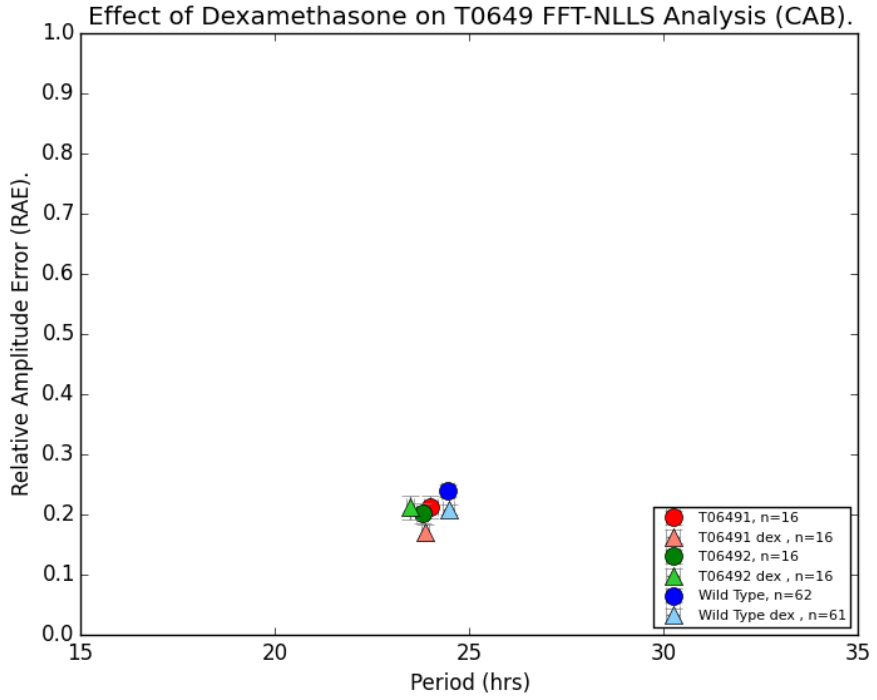

(B) Luciferase Periods

Seedlings were surface sterilised and grown at a density of 15-20 per sample for a total of 7 days in 12/12 LD cycles before treatment with dexamethasone at ZT+7, using the protocol outlined in Chapter 2. Treated plants were returned to the diurnal growth conditions. Experimental imaging began at dawn day 8 with transfer into LL. All seeds are T1 luciferase, T3 TF-GR, unless otherwise stated.

FIGURE 4.17: Effects of Dex-Induction of AT5G66770 on *pCAB2:LUC+* Intensity

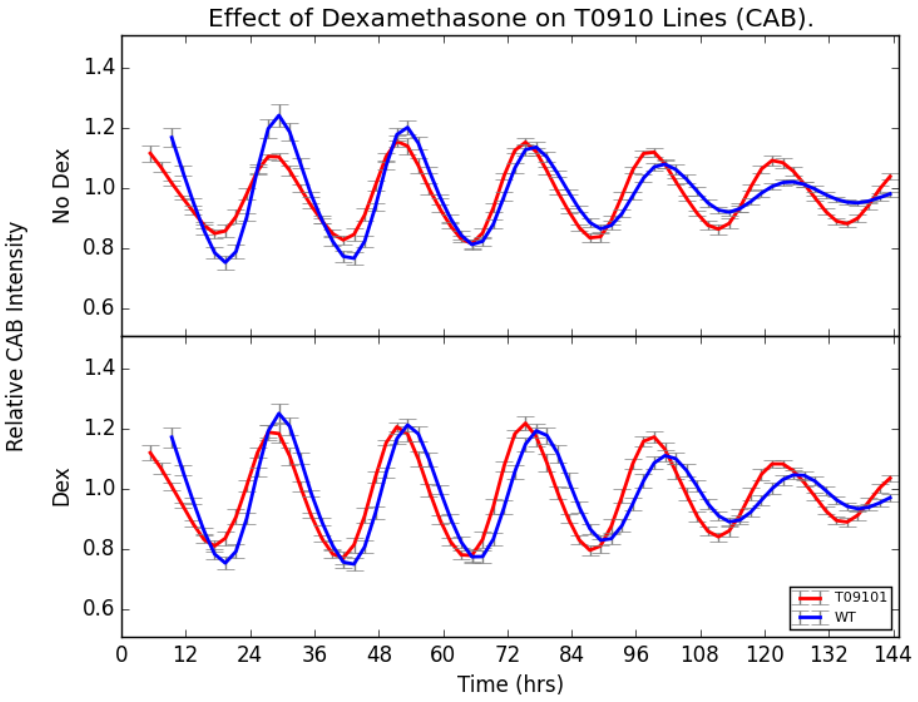

(A) Luciferase Intensity

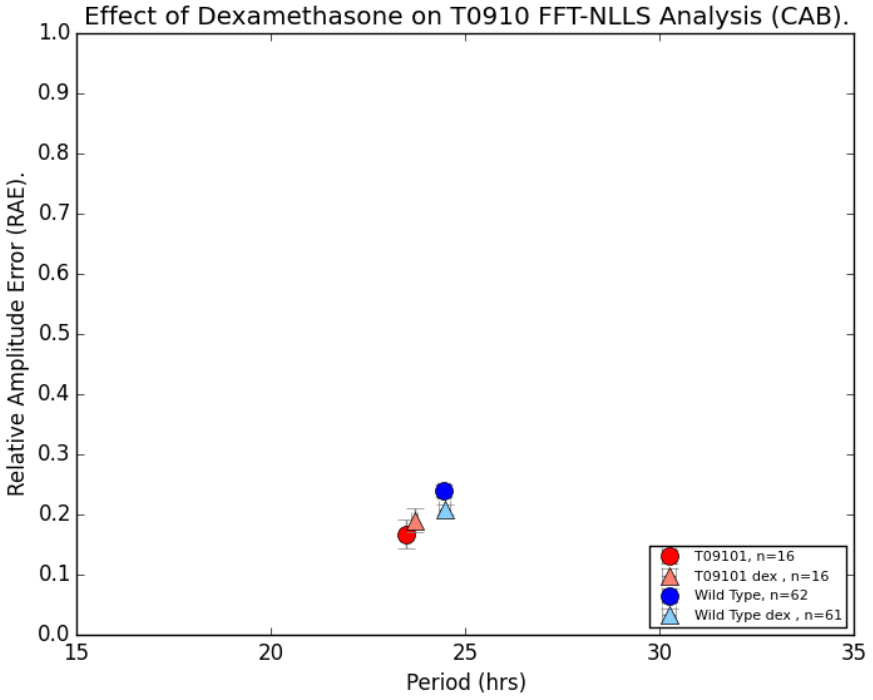

(B) Luciferase Periods

Seedlings were surface sterilised and grown at a density of 15-20 per sample for a total of 7 days in 12/12 LD cycles before treatment with dexamethasone at ZT+7, using the protocol outlined in Chapter 2. Treated plants were returned to the diurnal growth conditions. Experimental imaging began at dawn day 8 with transfer into LL. All seeds are T1 luciferase, T3 TF-GR, unless otherwise stated.

FIGURE 4.18: Effects of Dex-Induction of COL15 on *pCAB2:LUC+* Intensity

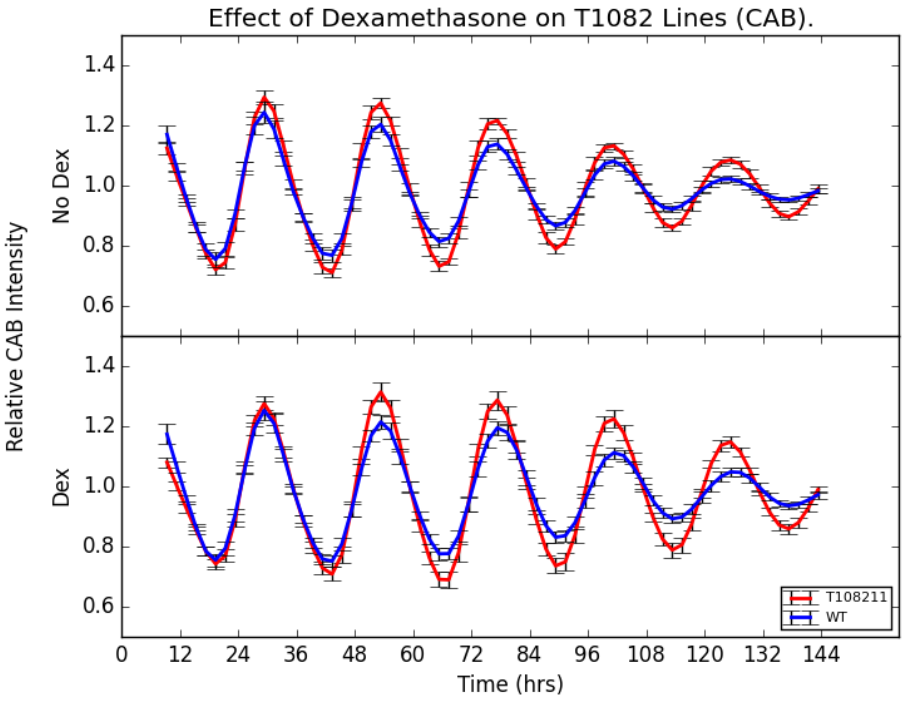

(A) Luciferase Intensity

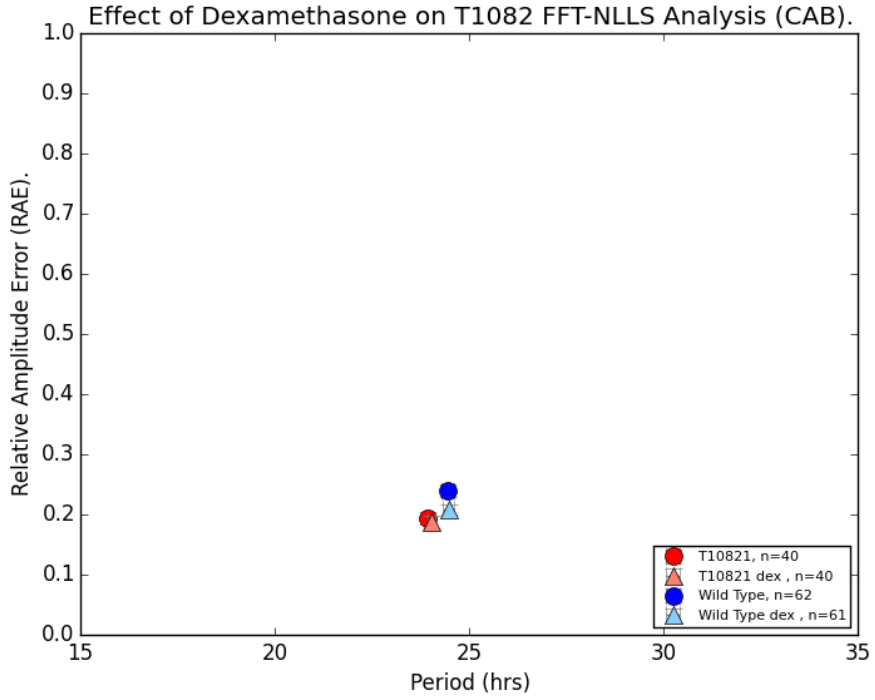

(B) Luciferase Periods

Seedlings were surface sterilised and grown at a density of 15-20 per sample for a total of 7 days in 12/12 LD cycles before treatment with dexamethasone at ZT+7, using the protocol outlined in Chapter 2. Treated plants were returned to the diurnal growth conditions. Experimental imaging began at dawn day 8 with transfer into LL. All seeds are T1 luciferase, T3 TF-GR, unless otherwise stated.

FIGURE 4.19: Effects of Dex-Induction of CCA1 on *pCAB2:LUC+* Intensity

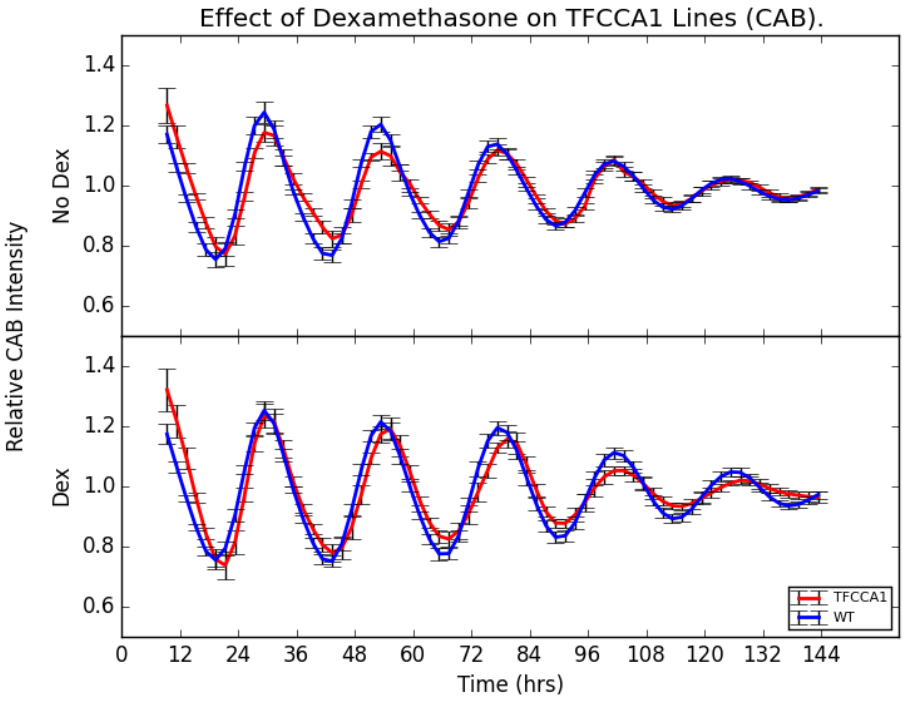

(A) Luciferase Intensity

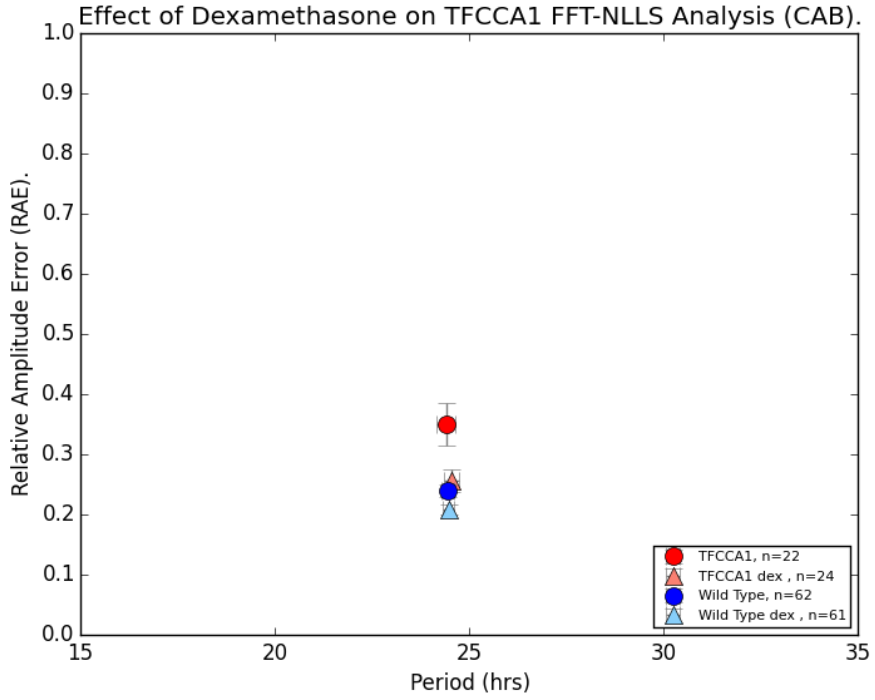

(B) Luciferase Periods

Seedlings were surface sterilised and grown at a density of 15-20 per sample for a total of 7 days in 12/12 LD cycles before treatment with dexamethasone at ZT+7, using the protocol outlined in Chapter 2. Treated plants were returned to the diurnal growth conditions. Experimental imaging began at dawn day 8 with transfer into LL. All seeds are T1 luciferase, T3 TF-GR, unless otherwise stated.

FIGURE 4.20: Effects of Dex-Induction of *CRF8* (T0052) on DF Intensity

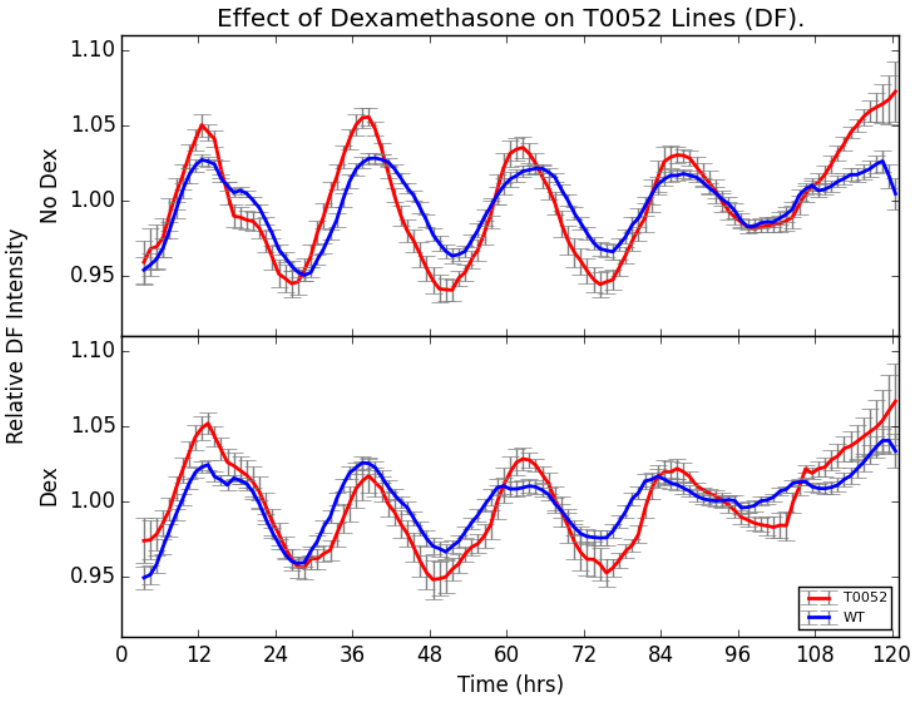

(A) DF Intensity, Averaged

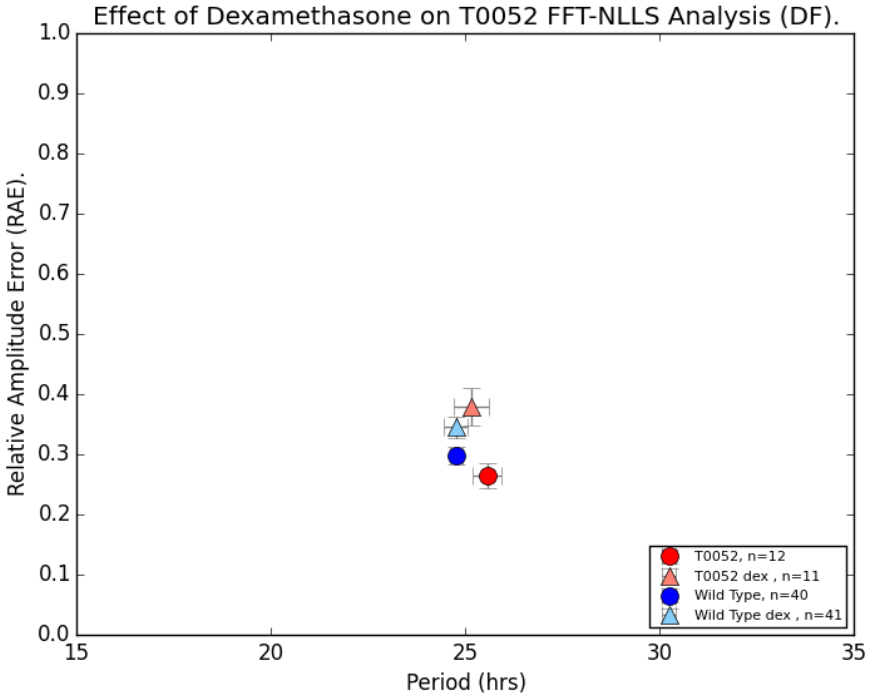

(B) DF Periods, Averaged

Seedlings were grown at a density of 15-20 per sample for a total of 15 days in 12/12 LD cycles before treatment with dexamethasone at ZT+14. Experimental imaging began at dawn day 16 with transfer into LL.

Figure 4.20, Continued...

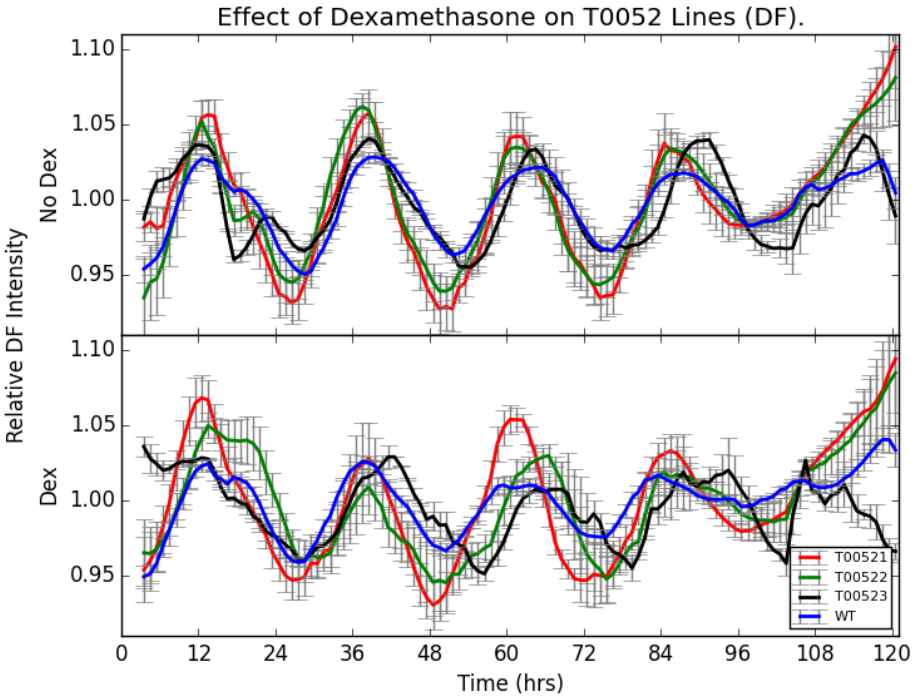

(C) DF Intensity, by Independently-Transformed Lines

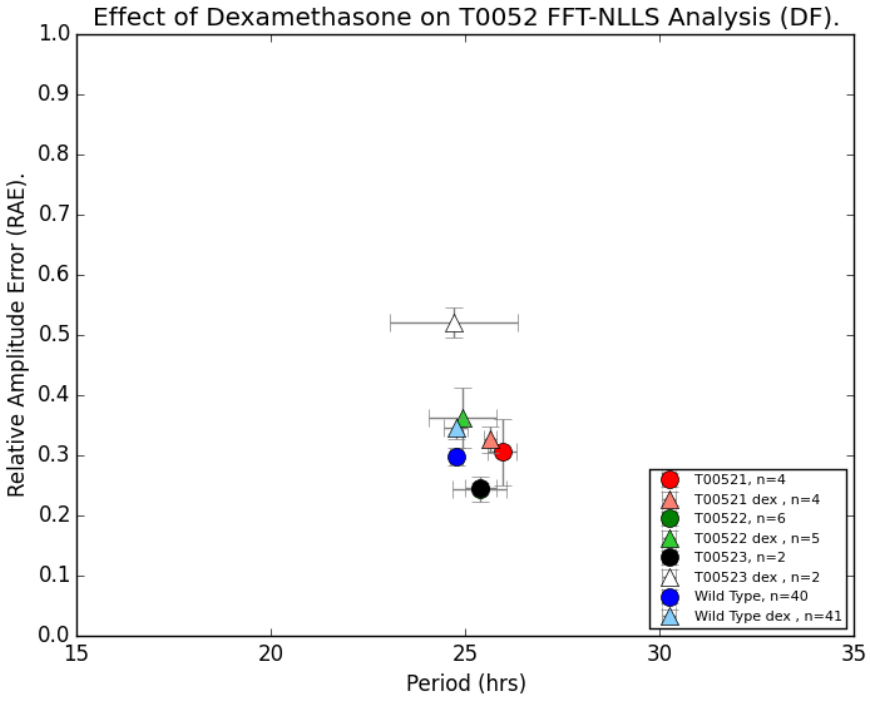

(D) DF Periods, by Independently-Transformed Lines

FIGURE 4.21: Effects of Dex-Induction of *DREB2B* (T0082) on DF Intensity

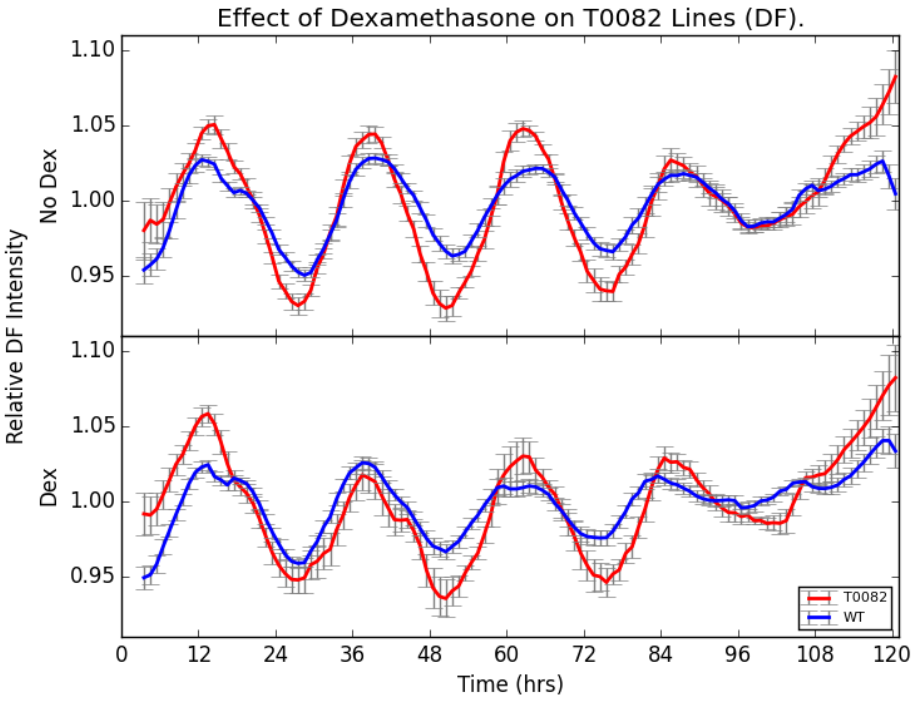

(A) DF Intensity, Averaged

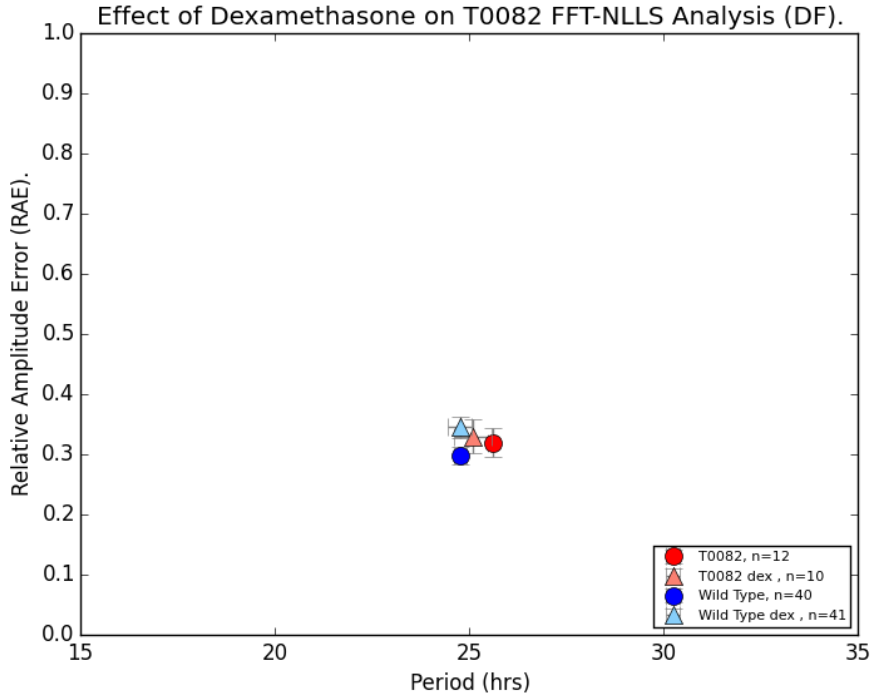

(B) DF Periods, Averaged

Seedlings were grown at a density of 15-20 per sample for a total of 15 days in 12/12 LD cycles before treatment with dexamethasone at ZT+14. Experimental imaging began at dawn day 16 with transfer into LL.

Figure 4.21, Continued...

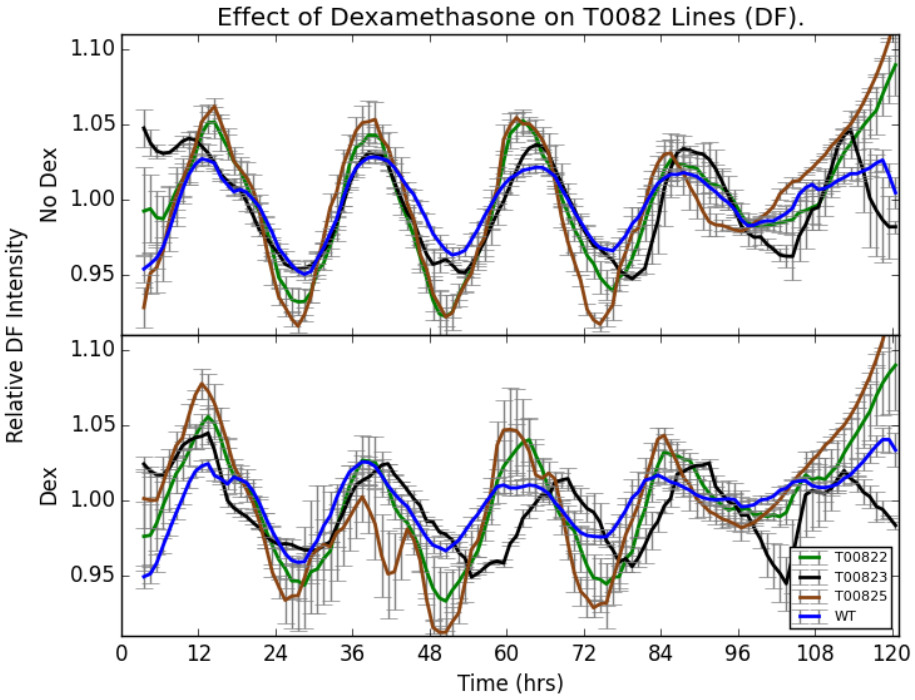

(C) DF Intensity, by Independently-Transformed Lines

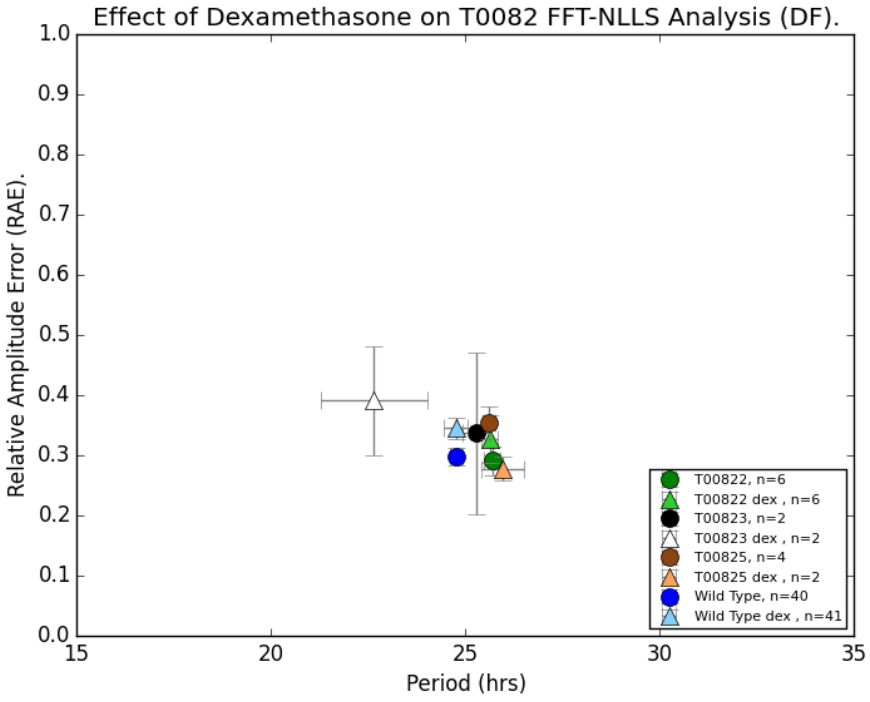

(D) DF Periods, by Independently-Transformed Lines

FIGURE 4.22: Effects of Dex-Induction of *IAA11* (T0189) on DF Intensity

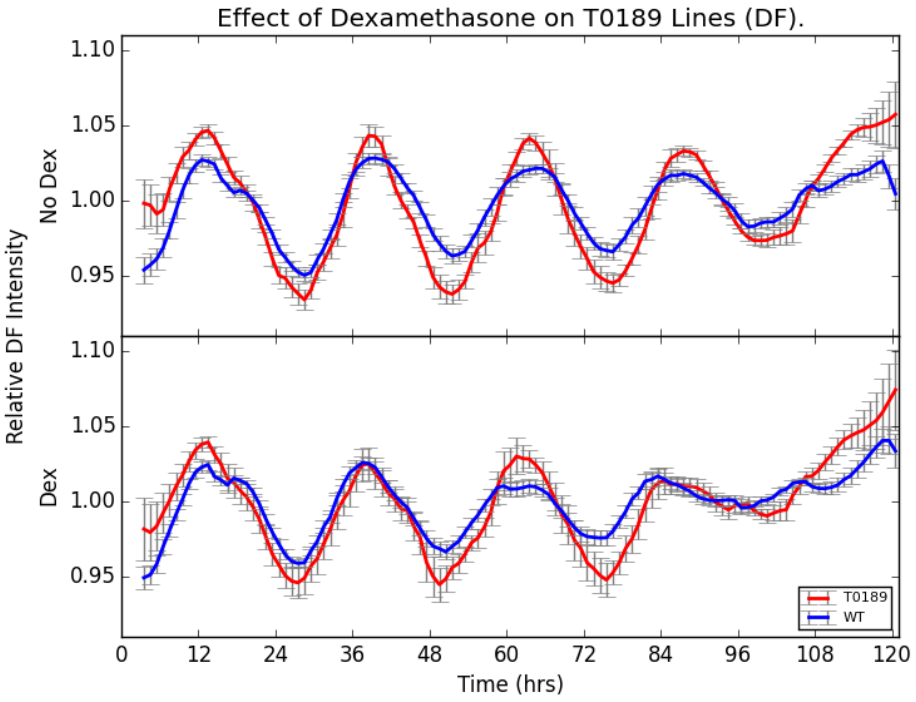

(A) DF Intensity, Averaged

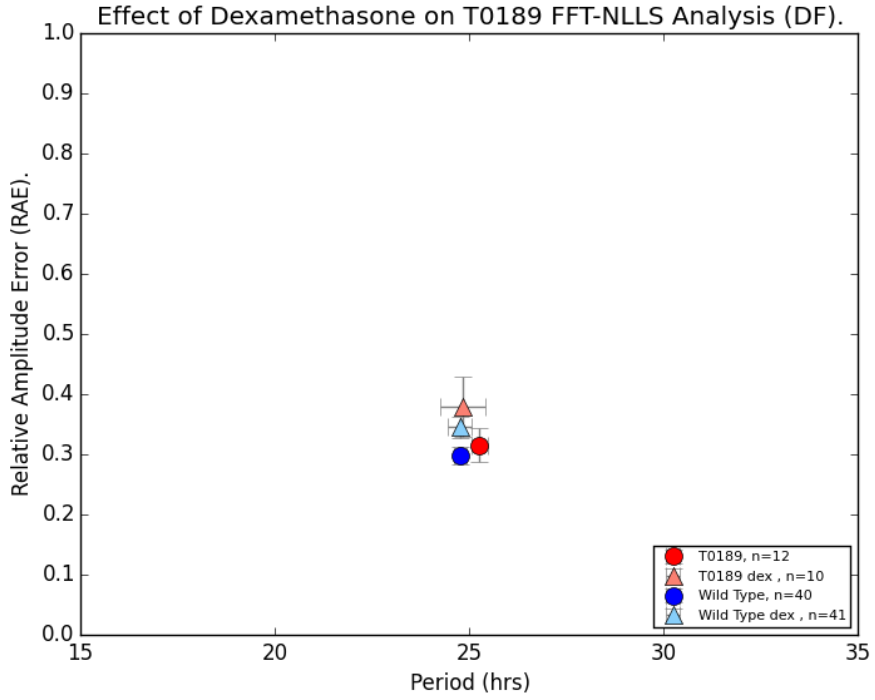

(B) DF Periods, Averaged

Seedlings were grown at a density of 15-20 per sample for a total of 15 days in 12/12 LD cycles before treatment with dexamethasone at ZT+14. Experimental imaging began at dawn day 16 with transfer into LL.

Figure 4.22, Continued...

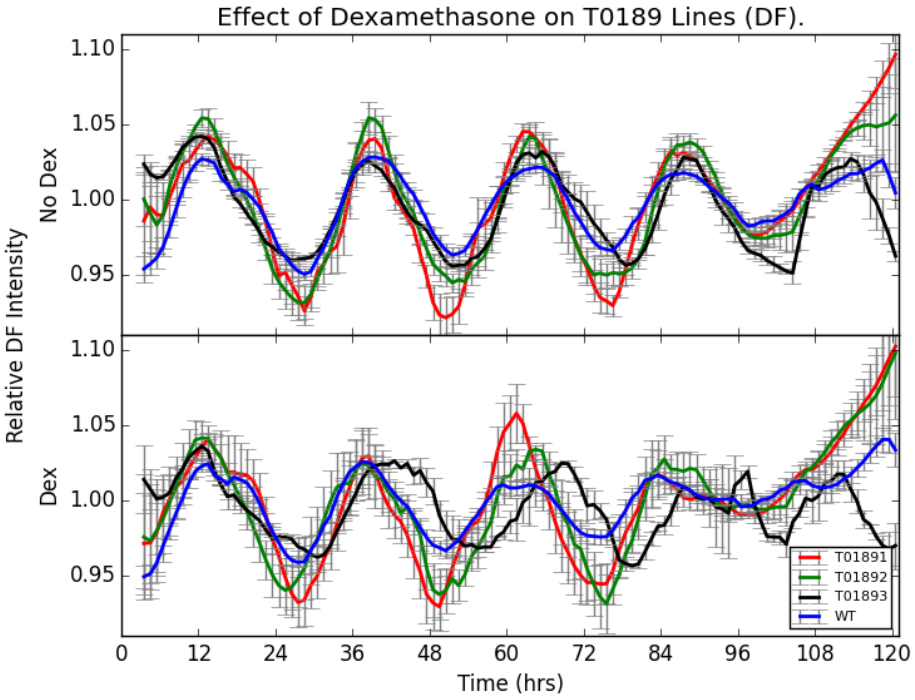

(C) DF Intensity, by Independently-Transformed Lines

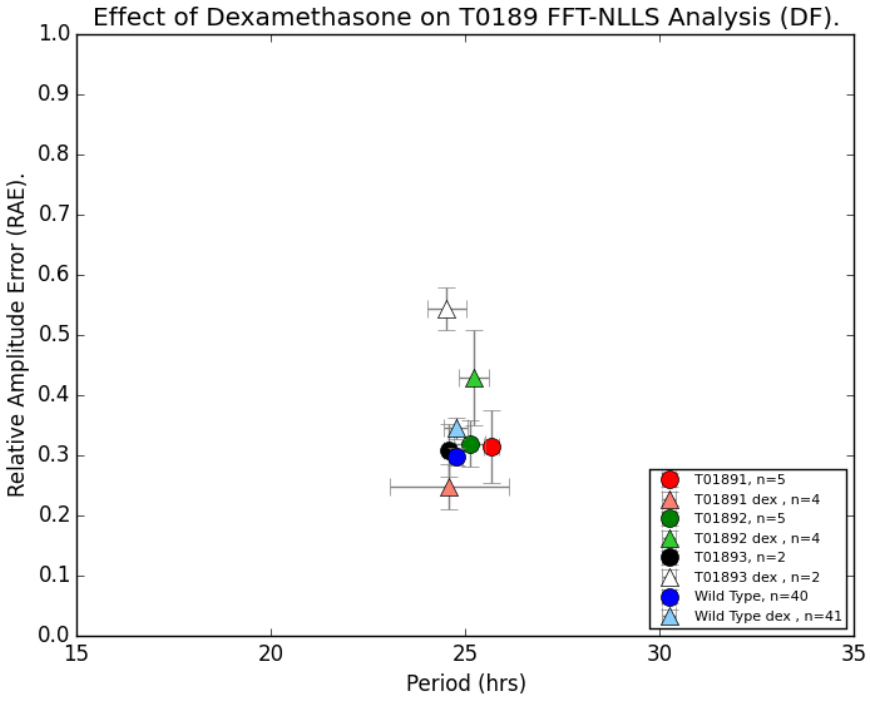

(D) DF Periods, by Independently-Transformed Lines

FIGURE 4.23: Effects of Dex-Induction of *FBH* (T0213) on DF Intensity

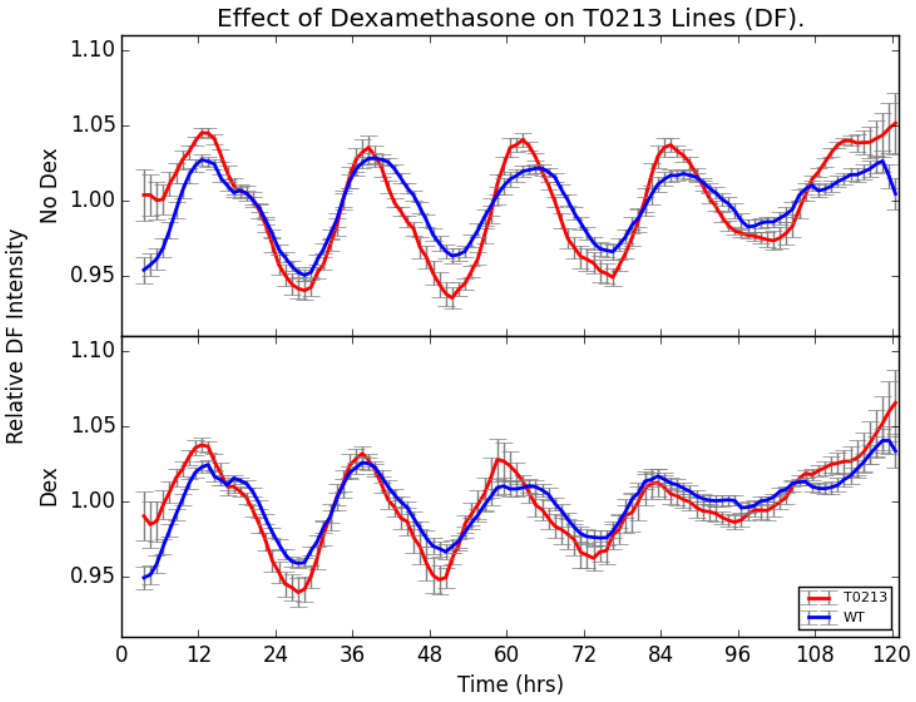

(A) DF Intensity, Averaged

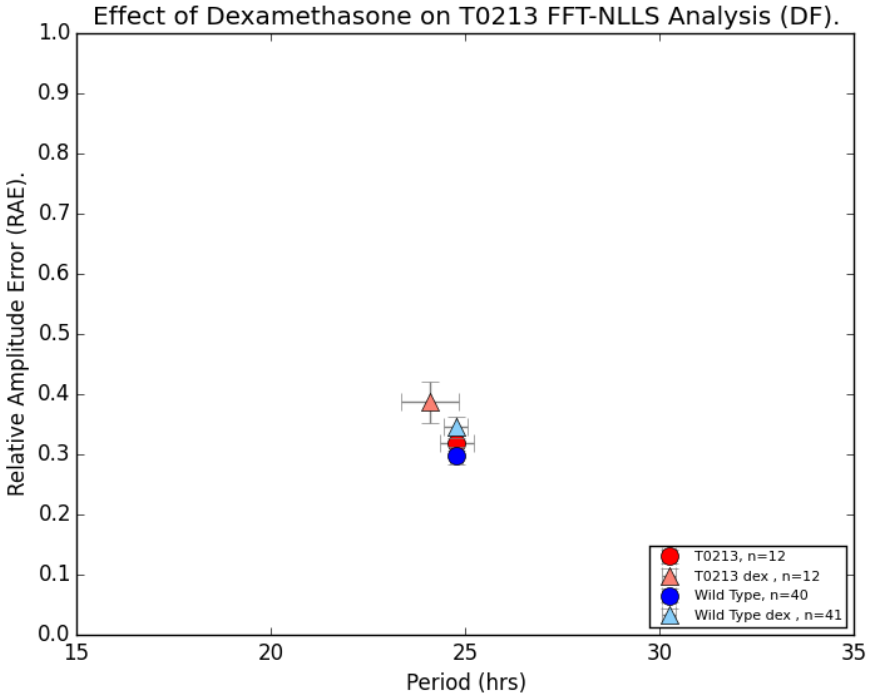

(B) DF Periods, Averaged

Seedlings were grown at a density of 15-20 per sample for a total of 15 days in 12/12 LD cycles before treatment with dexamethasone at ZT+14. Experimental imaging began at dawn day 16 with transfer into LL.

Figure 4.23, Continued...

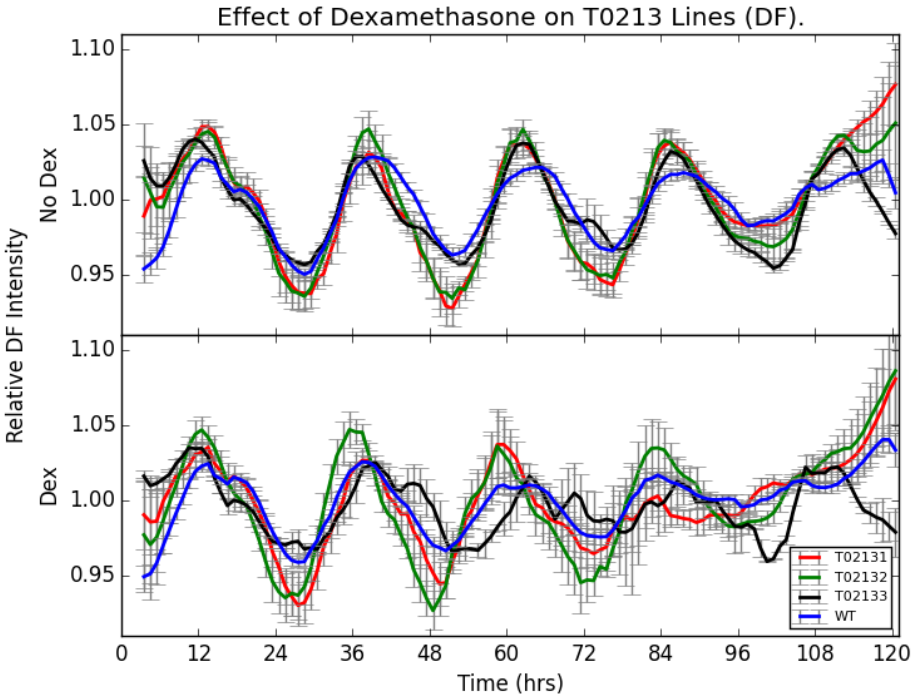

(C) DF Intensity, by Independently-Transformed Lines

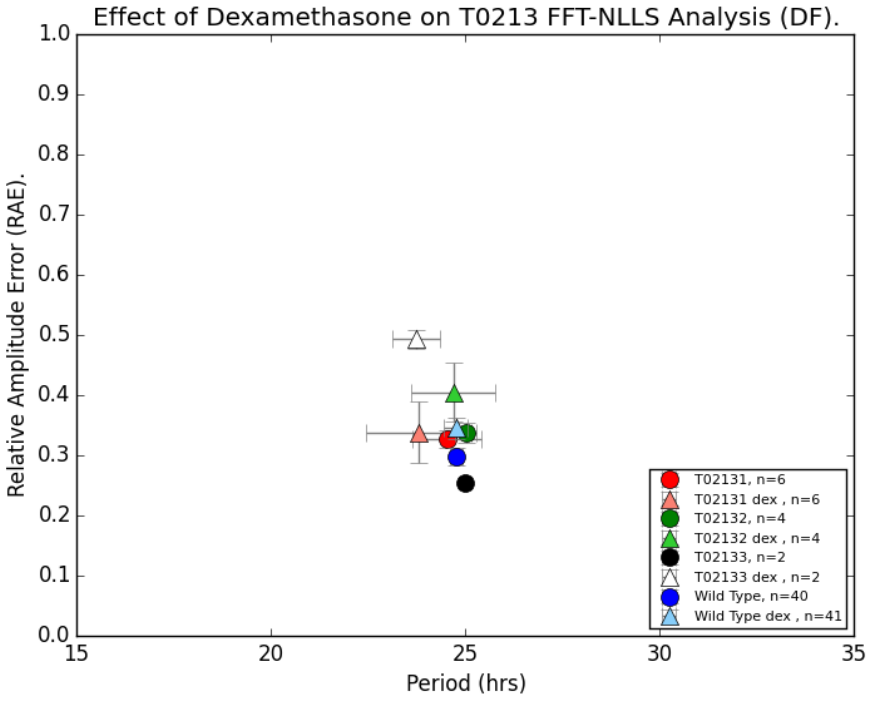

(D) DF Periods, by Independently-Transformed Lines

FIGURE 4.24: Effects of Dex-Induction of *ABF1* (T0314) on DF Intensity

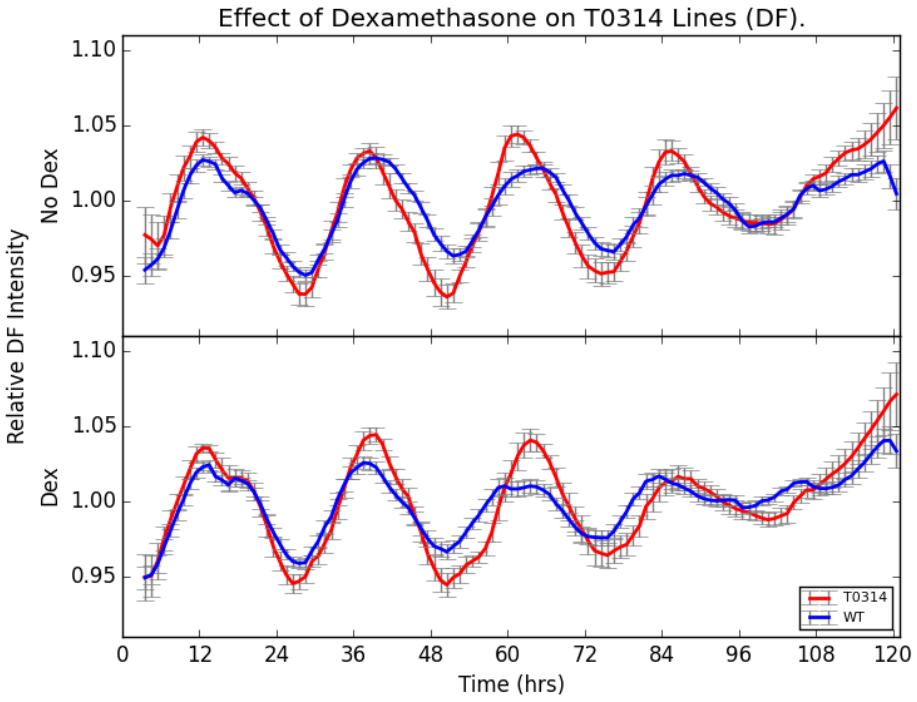

(A) DF Intensity, Averaged

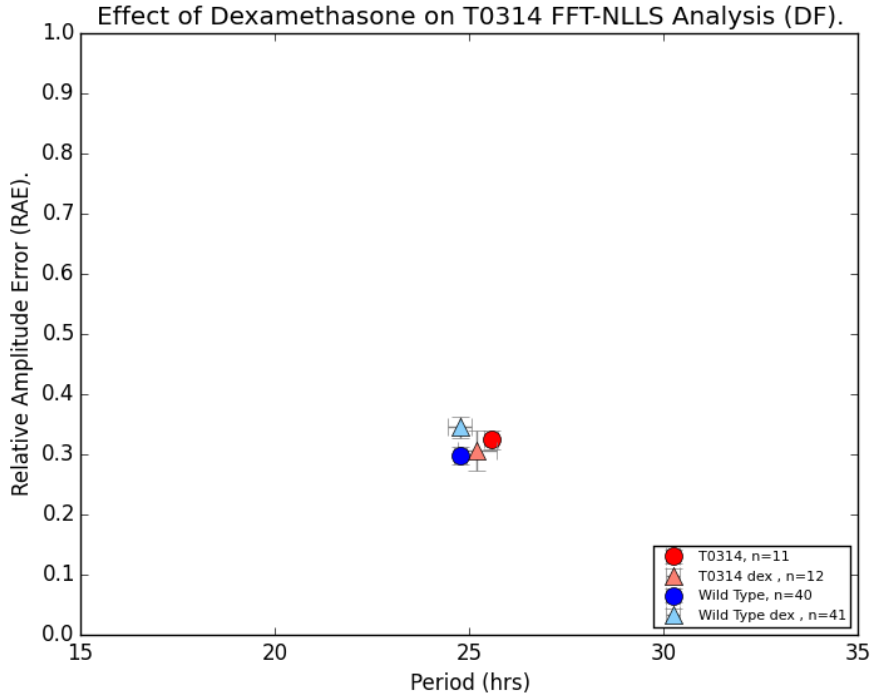

(B) DF Periods, Averaged

Seedlings were grown at a density of 15-20 per sample for a total of 15 days in 12/12 LD cycles before treatment with dexamethasone at ZT+14. Experimental imaging began at dawn day 16 with transfer into LL.

Figure 4.24, Continued...

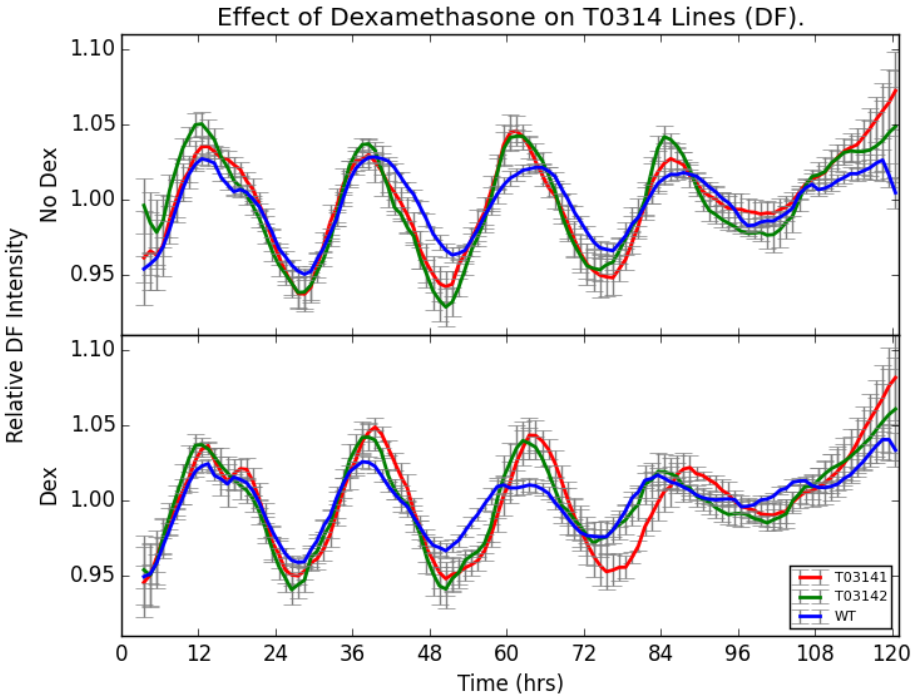

(C) DF Intensity, by Independently-Transformed Lines

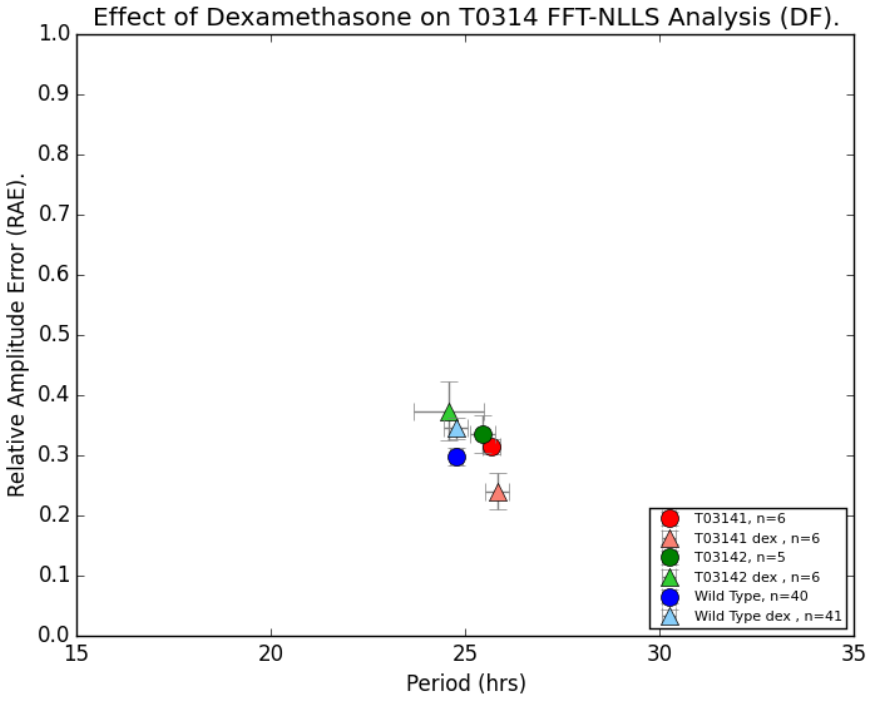

(D) DF Periods, by Independently-Transformed Lines

FIGURE 4.25: Effects of Dex-Induction of *KNAT2* (T0530) on DF Intensity

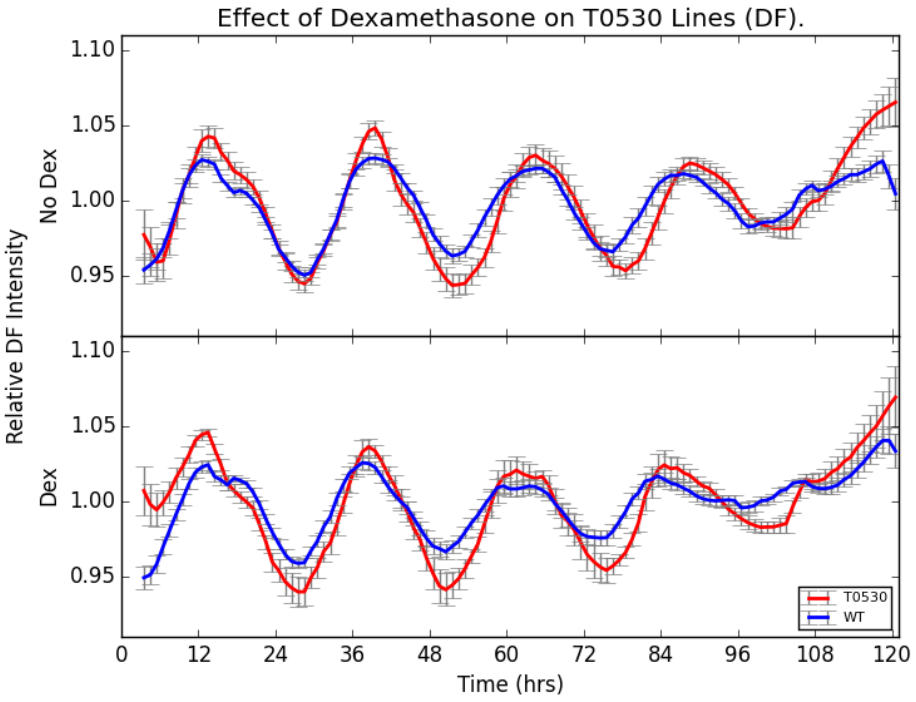

(A) DF Intensity, Averaged

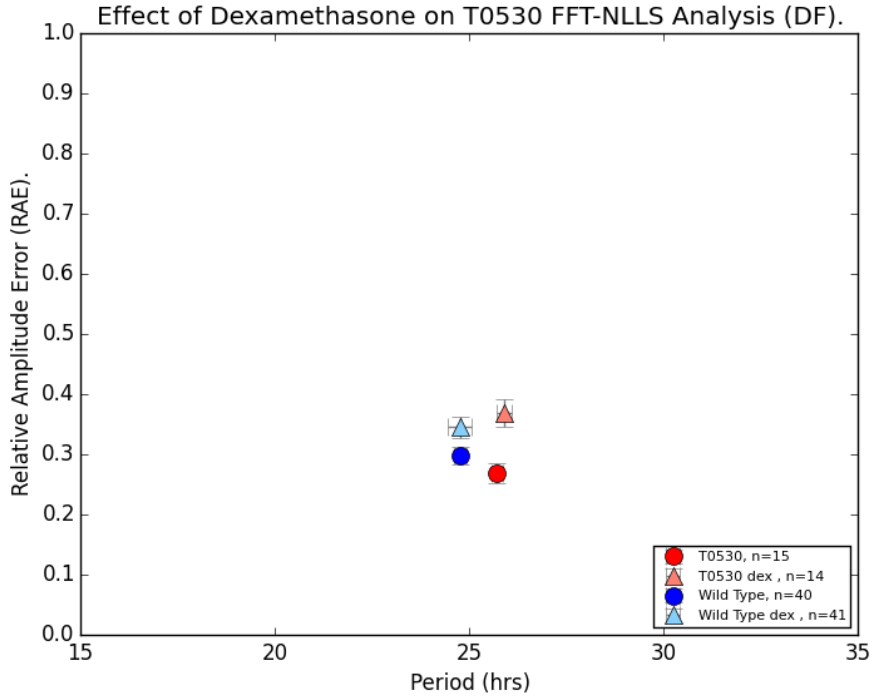

(B) DF Periods, Averaged

Seedlings were grown at a density of 15-20 per sample for a total of 15 days in 12/12 LD cycles before treatment with dexamethasone at ZT+14. Experimental imaging began at dawn day 16 with transfer into LL.

Figure 4.25, Continued...

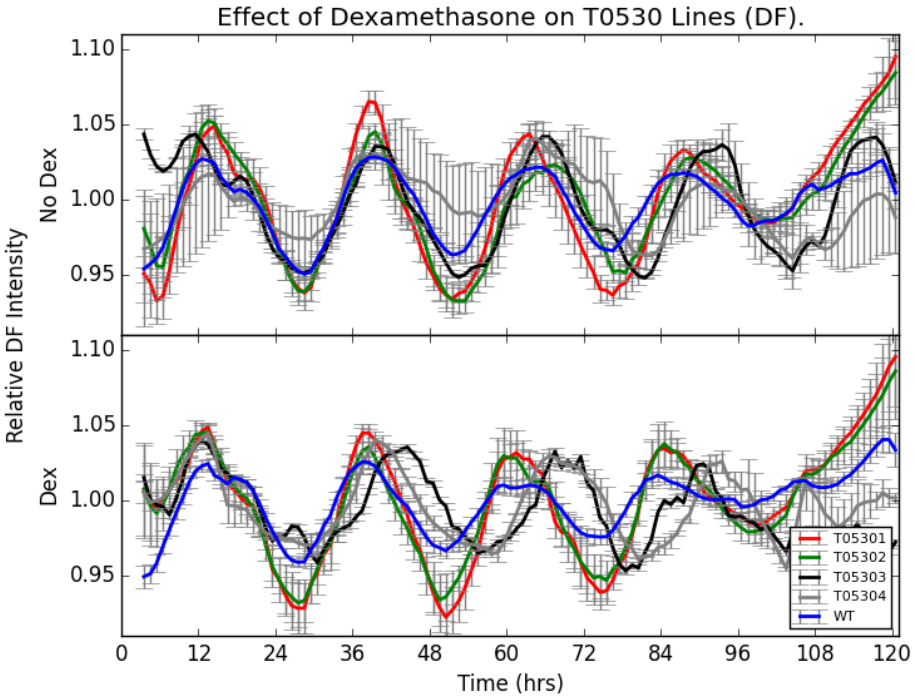

(C) DF Intensity, by Independently-Transformed Lines

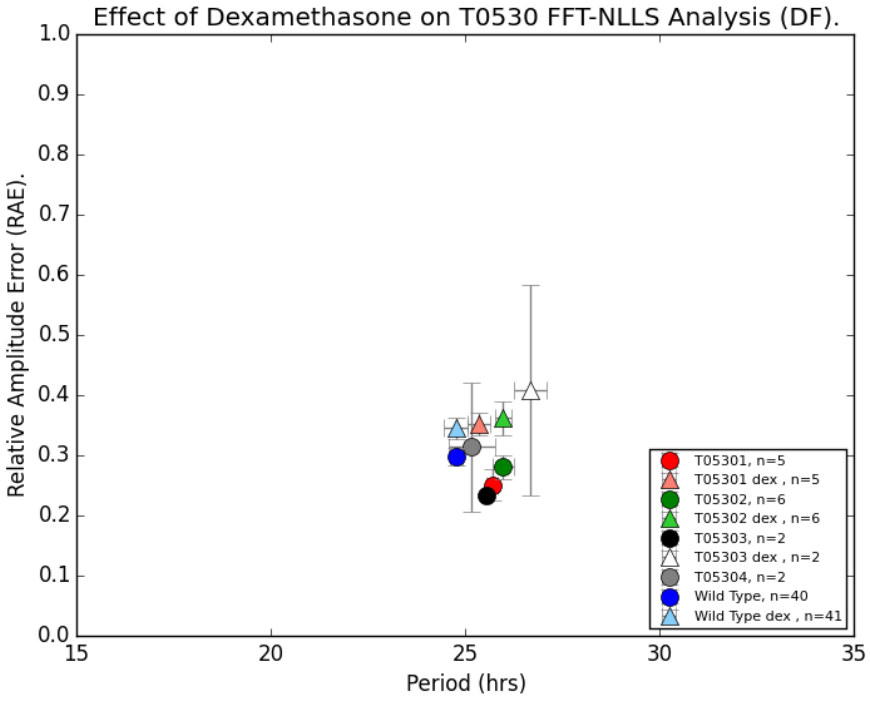

(D) DF Periods, by Independently-Transformed Lines

FIGURE 4.26: Effects of Dex-Induction of *HAT2* (T0576) on DF Intensity

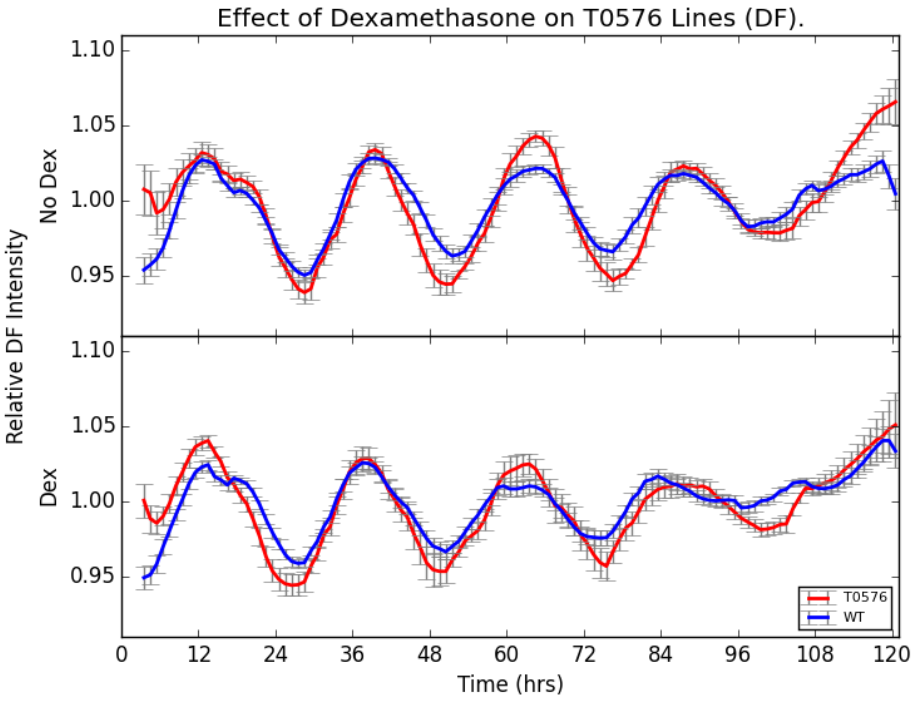

(A) DF Intensity, Averaged

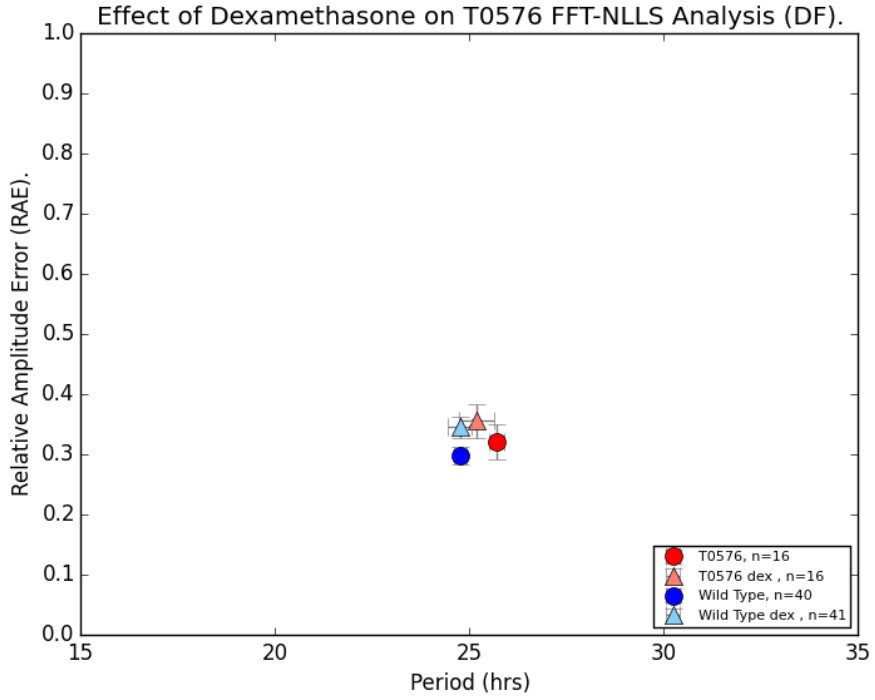

(B) DF Periods, Averaged

Seedlings were grown at a density of 15-20 per sample for a total of 15 days in 12/12 LD cycles before treatment with dexamethasone at ZT+14. Experimental imaging began at dawn day 16 with transfer into LL.

Figure 4.26, Continued...

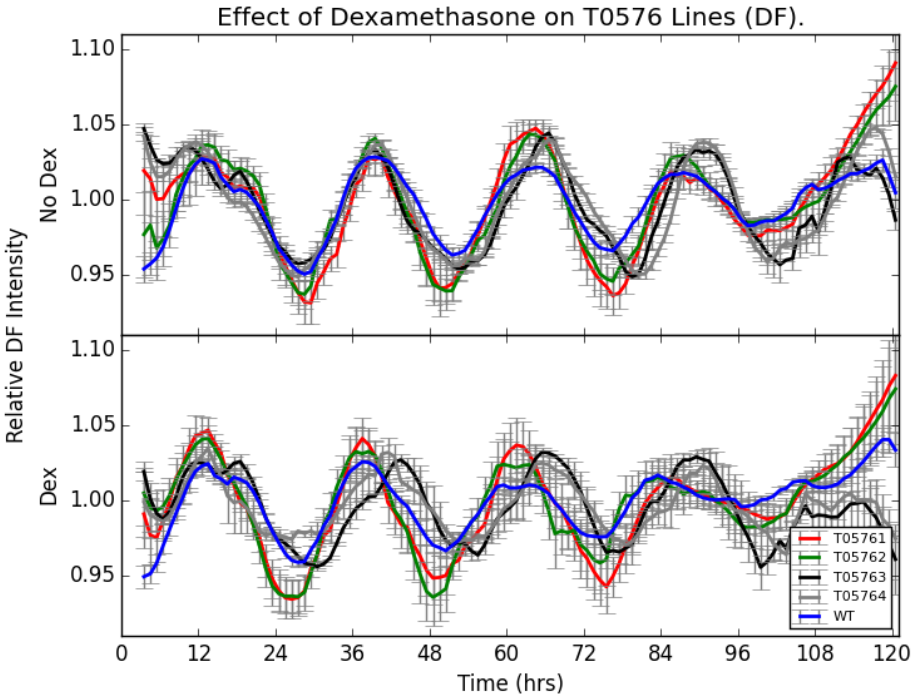

(C) DF Intensity, by Independently-Transformed Lines

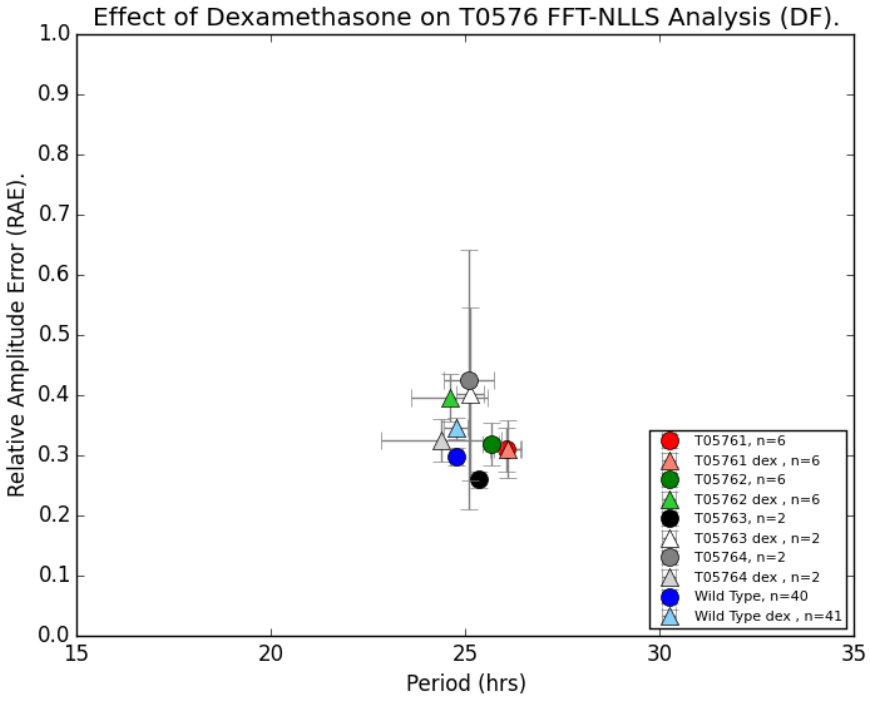

(D) DF Periods, by Independently-Transformed Lines

FIGURE 4.27: Effects of Dex-Induction of *SOG1* (T0591) on DF Intensity

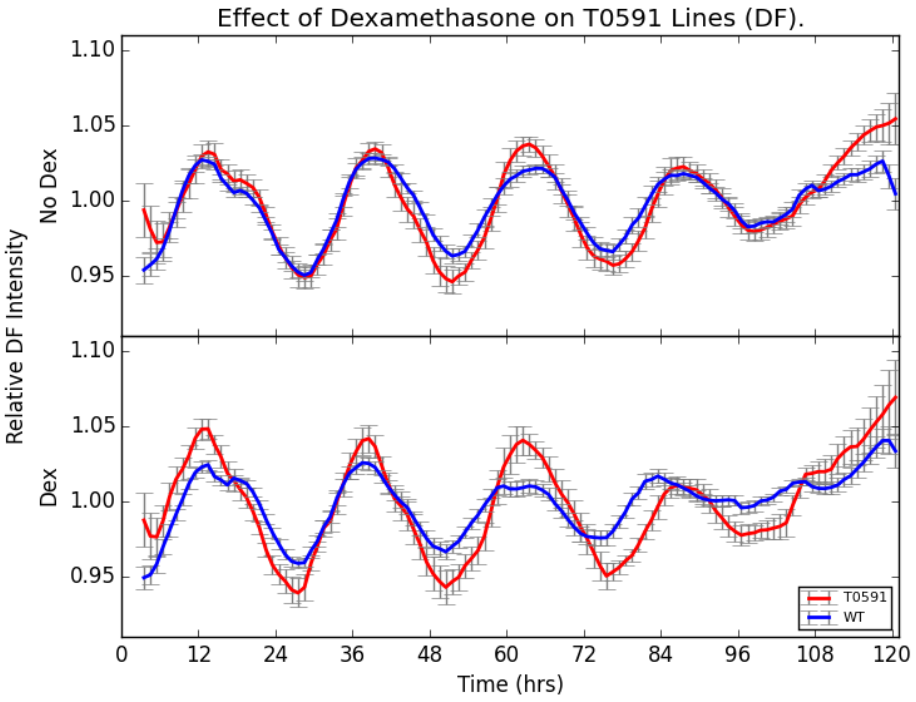

(A) DF Intensity, Averaged

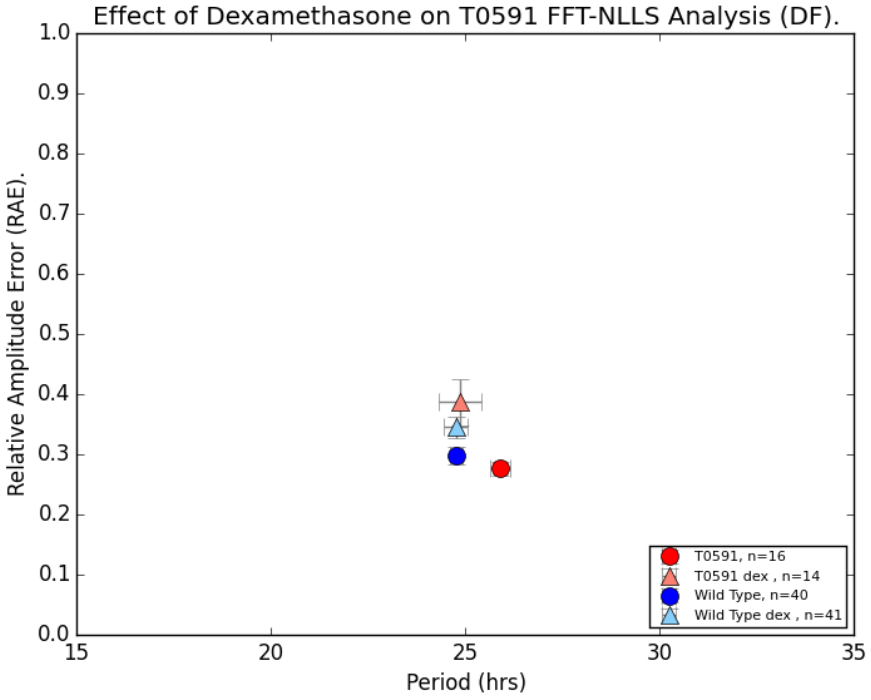

(B) DF Periods, Averaged

Seedlings were grown at a density of 15-20 per sample for a total of 15 days in 12/12 LD cycles before treatment with dexamethasone at ZT+14. Experimental imaging began at dawn day 16 with transfer into LL.

Figure 4.27, Continued...

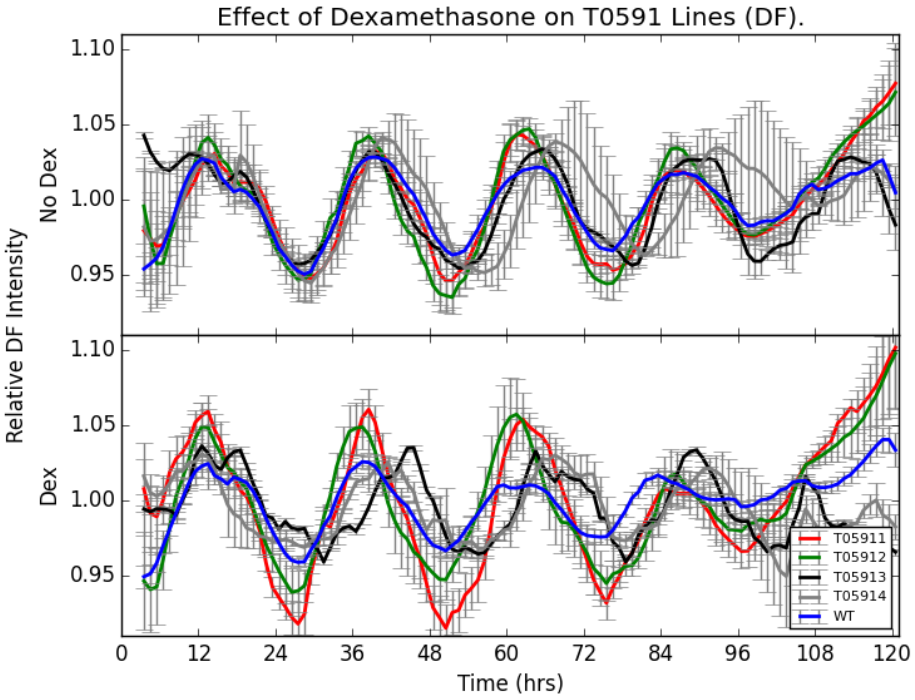

(C) DF Intensity, by Independently-Transformed Lines

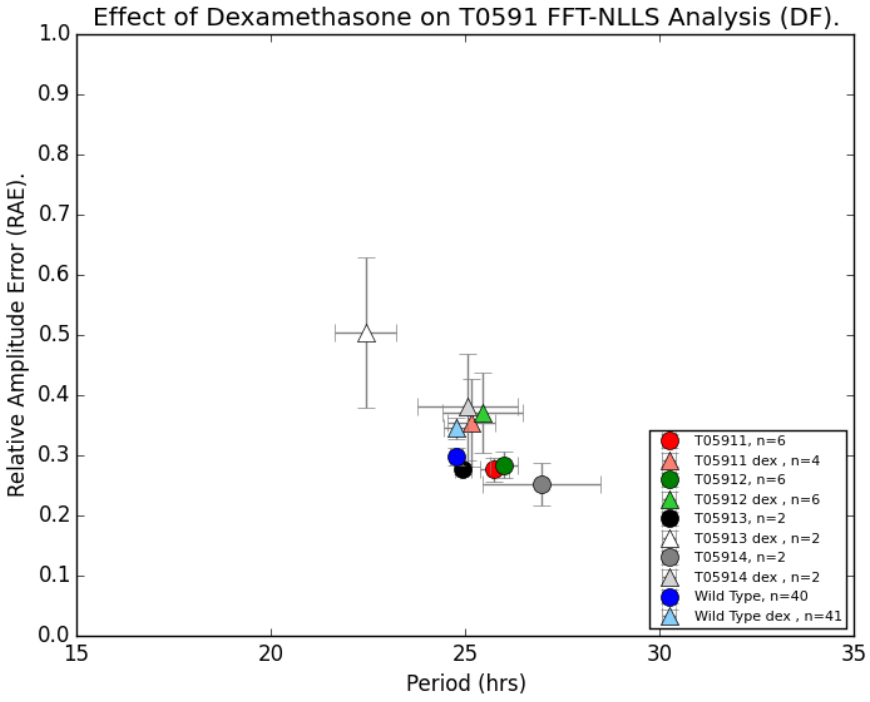

(D) DF Periods, by Independently-Transformed Lines

FIGURE 4.28: Effects of Dex-Induction of *ANAC010* (T0592) on DF Intensity

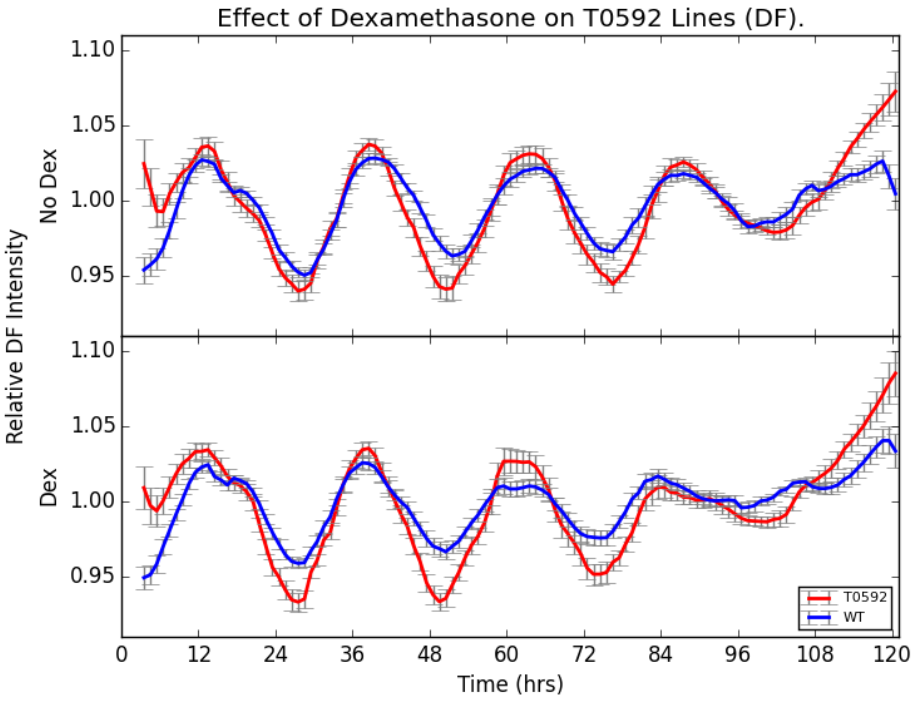

(A) DF Intensity, Averaged

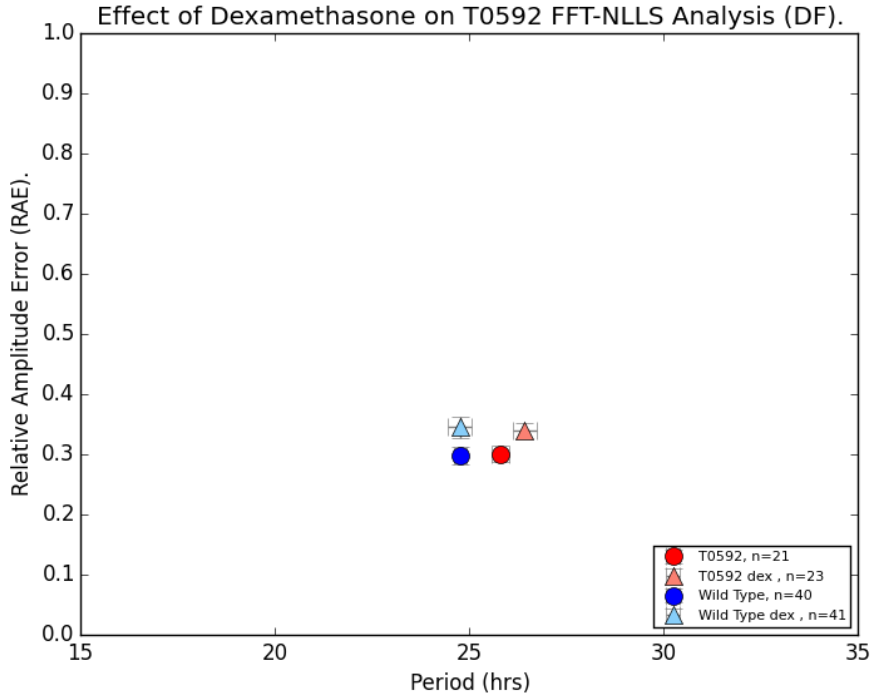

(B) DF Periods, Averaged

Seedlings were grown at a density of 15-20 per sample for a total of 15 days in 12/12 LD cycles before treatment with dexamethasone at ZT+14. Experimental imaging began at dawn day 16 with transfer into LL.

Figure 4.28, Continued...

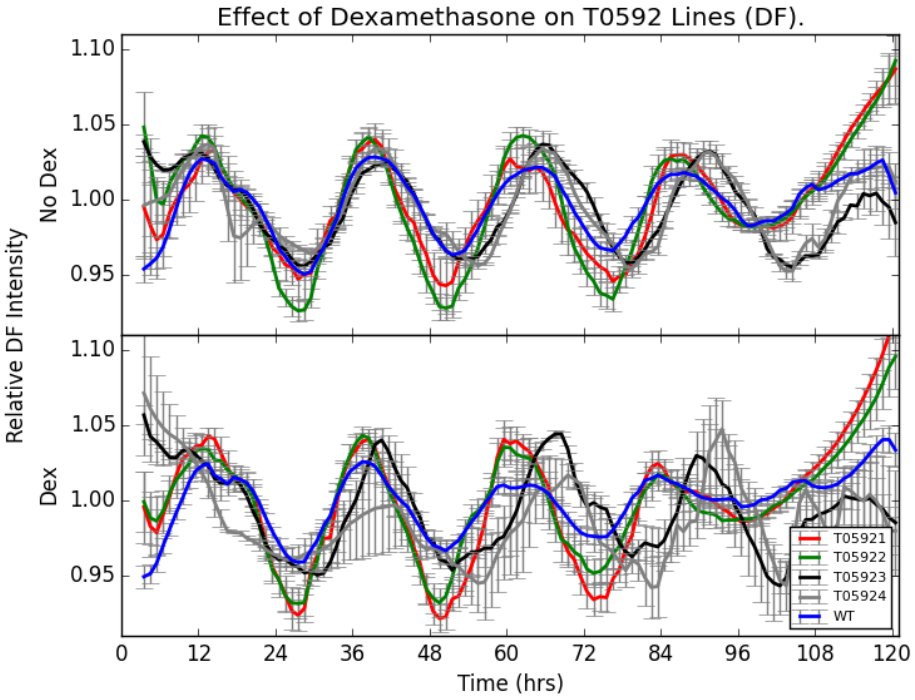

(C) DF Intensity, by Independently-Transformed Lines

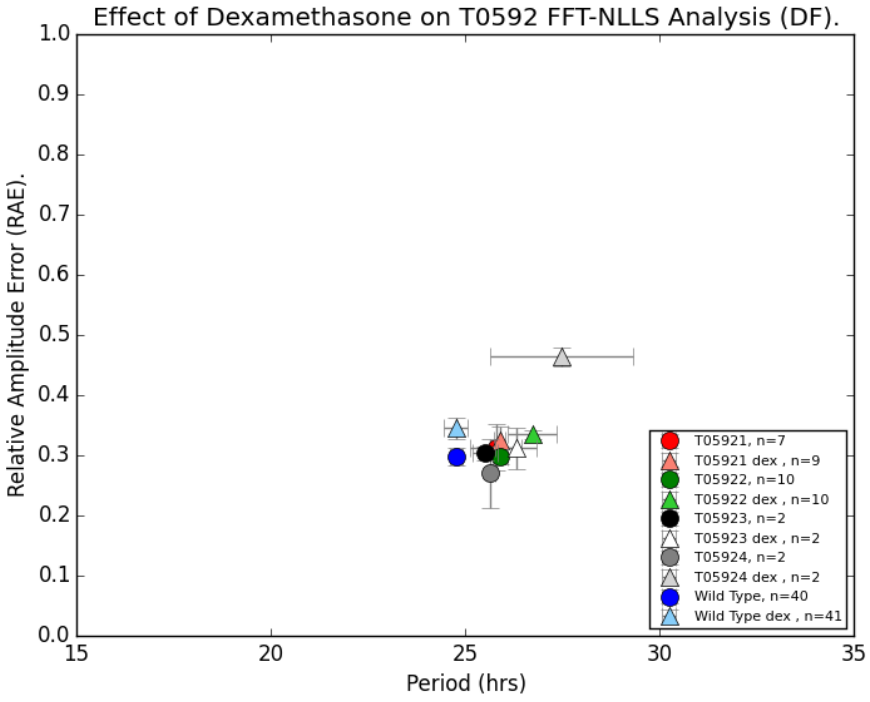

(D) DF Periods, by Independently-Transformed Lines

FIGURE 4.29: Effects of Dex-Induction of *RD27* (T0638) on DF Intensity

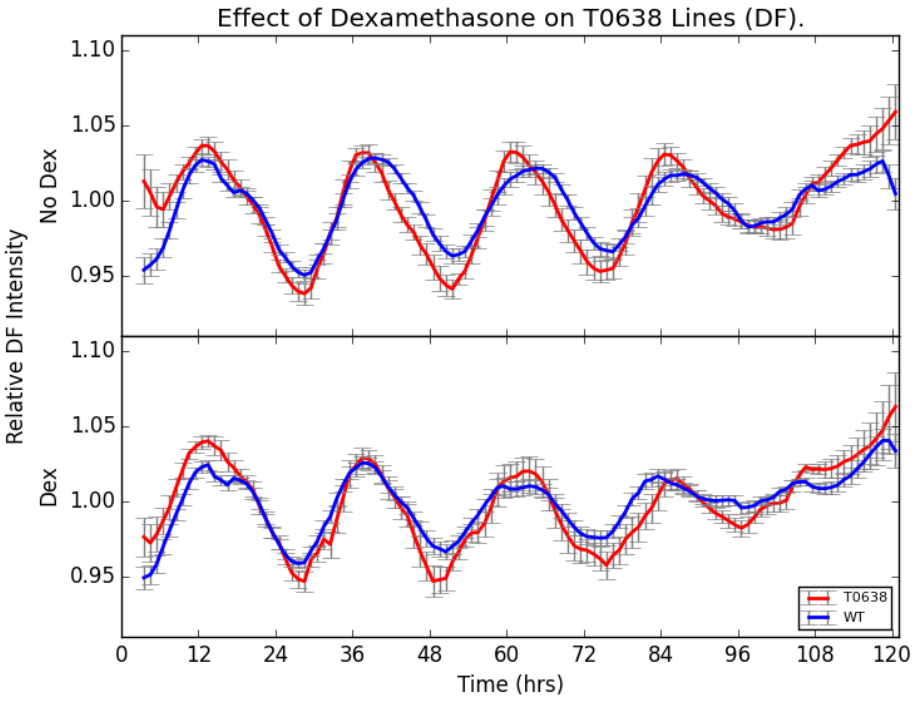

(A) DF Intensity, Averaged

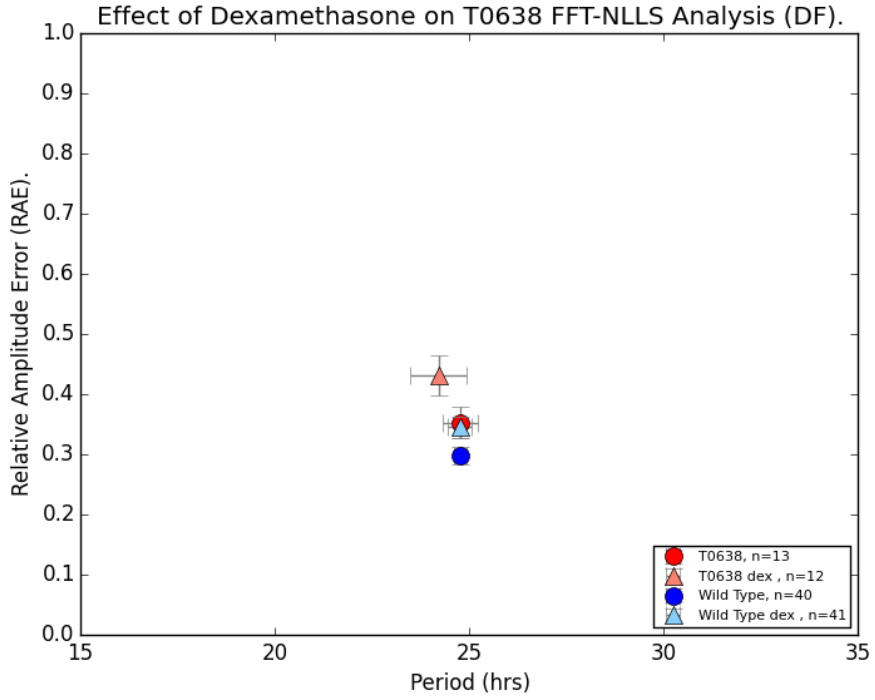

(B) DF Periods, Averaged

Seedlings were grown at a density of 15-20 per sample for a total of 15 days in 12/12 LD cycles before treatment with dexamethasone at ZT+14. Experimental imaging began at dawn day 16 with transfer into LL.

Figure 4.29, Continued...

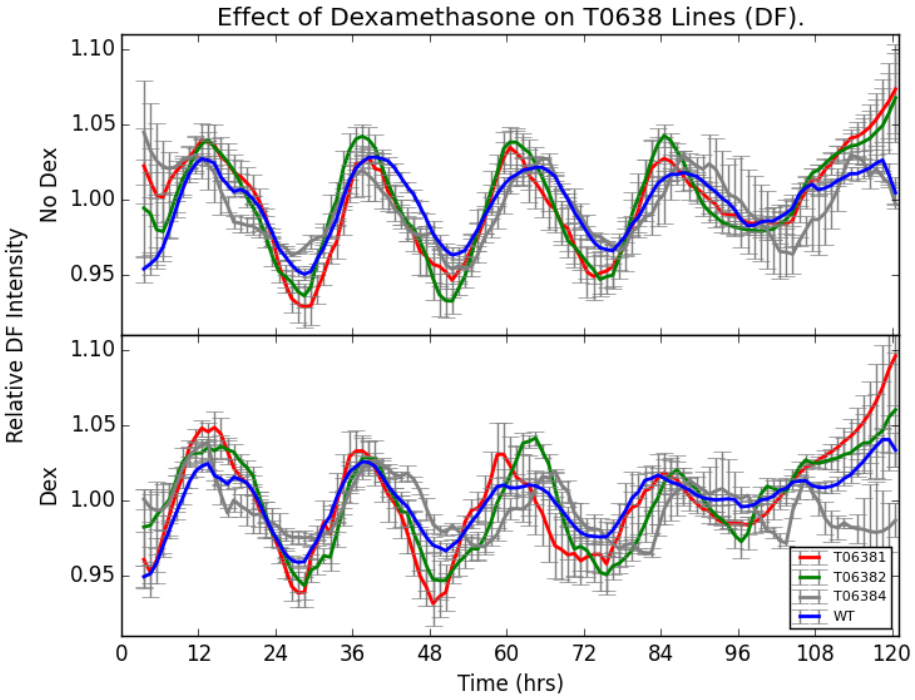

(C) DF Intensity, by Independently-Transformed Lines

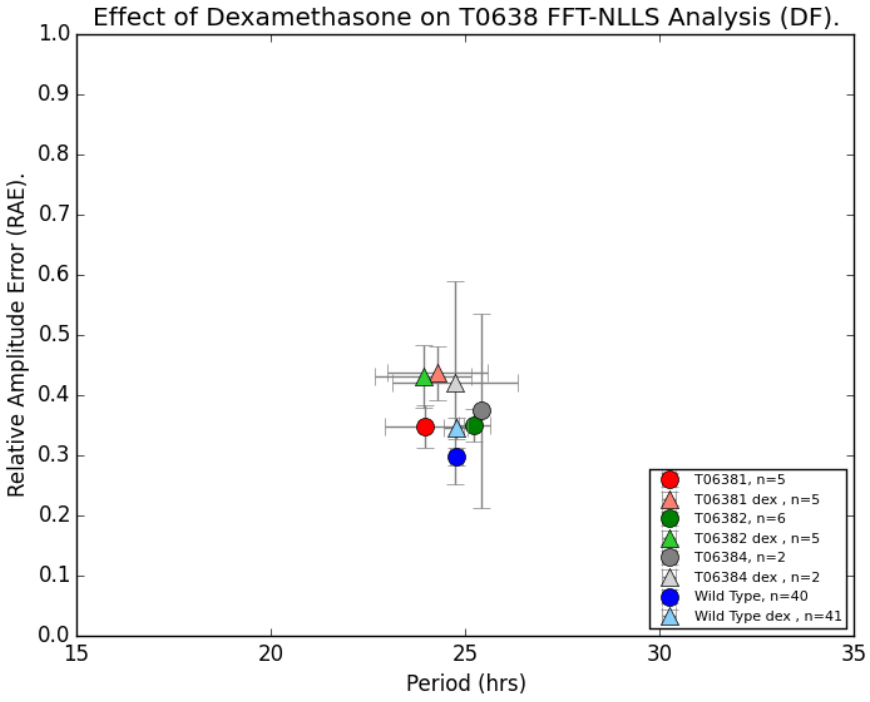

(D) DF Periods, by Independently-Transformed Lines

FIGURE 4.30: Effects of Dex-Induction of *ANAC087* (T0649) on DF Intensity

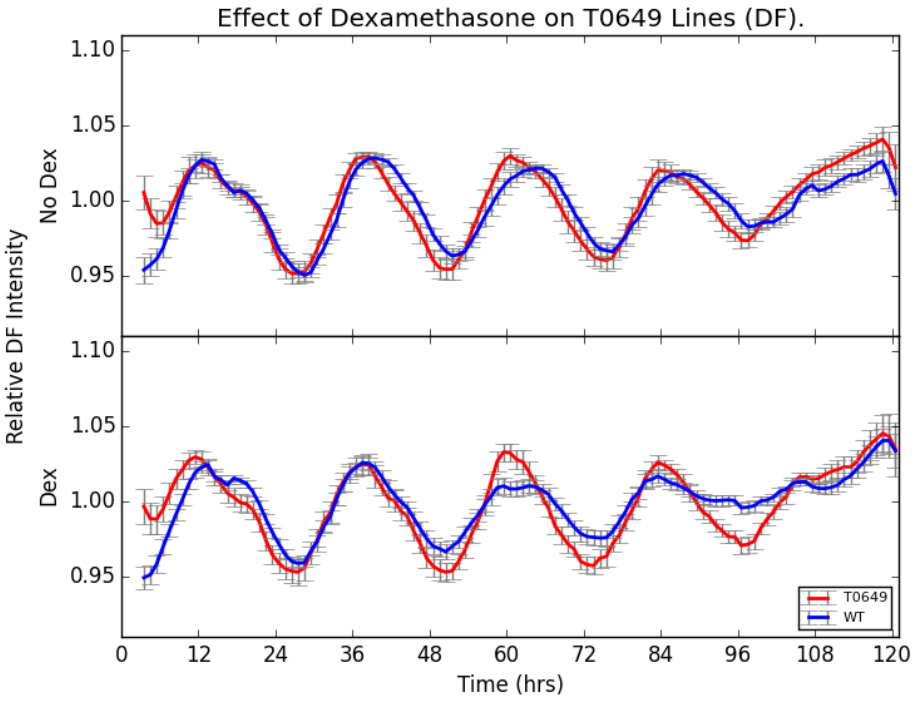

(A) DF Intensity, Averaged

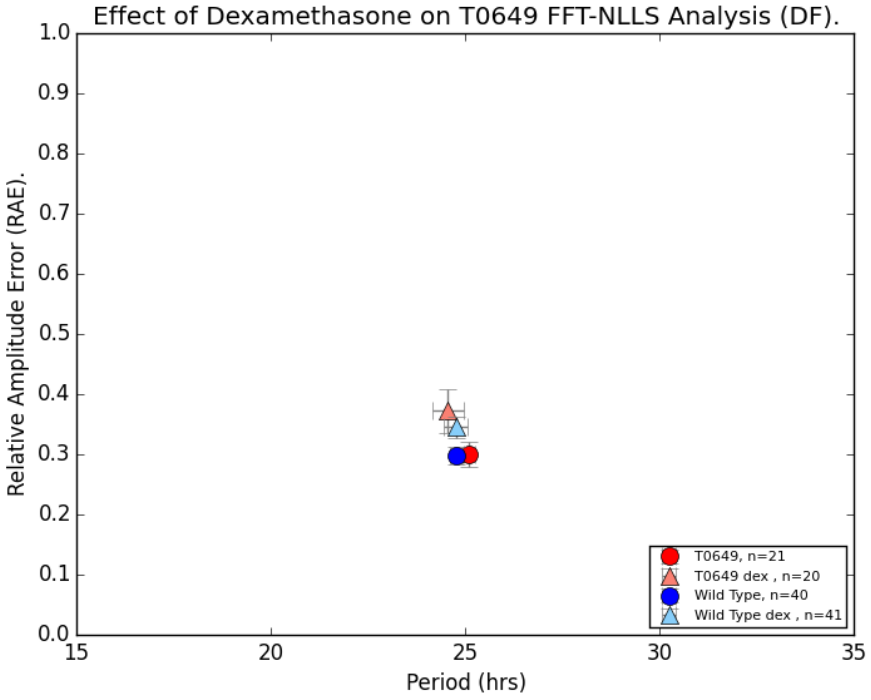

(B) DF Periods, Averaged

Seedlings were grown at a density of 15-20 per sample for a total of 15 days in 12/12 LD cycles before treatment with dexamethasone at ZT+14. Experimental imaging began at dawn day 16 with transfer into LL.

Figure 4.30, Continued...

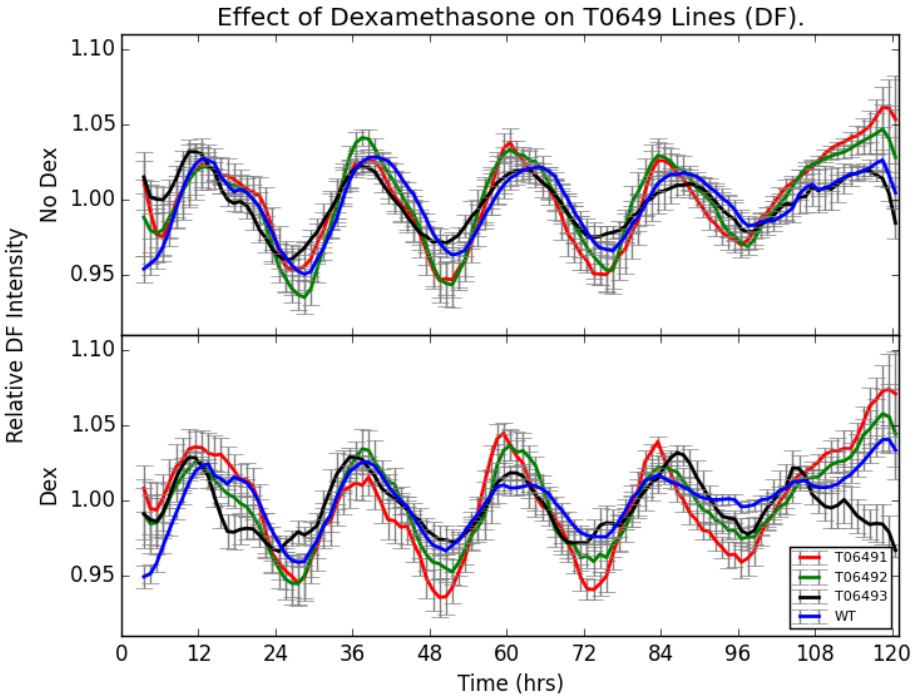

(C) DF Intensity, by Independently-Transformed Lines

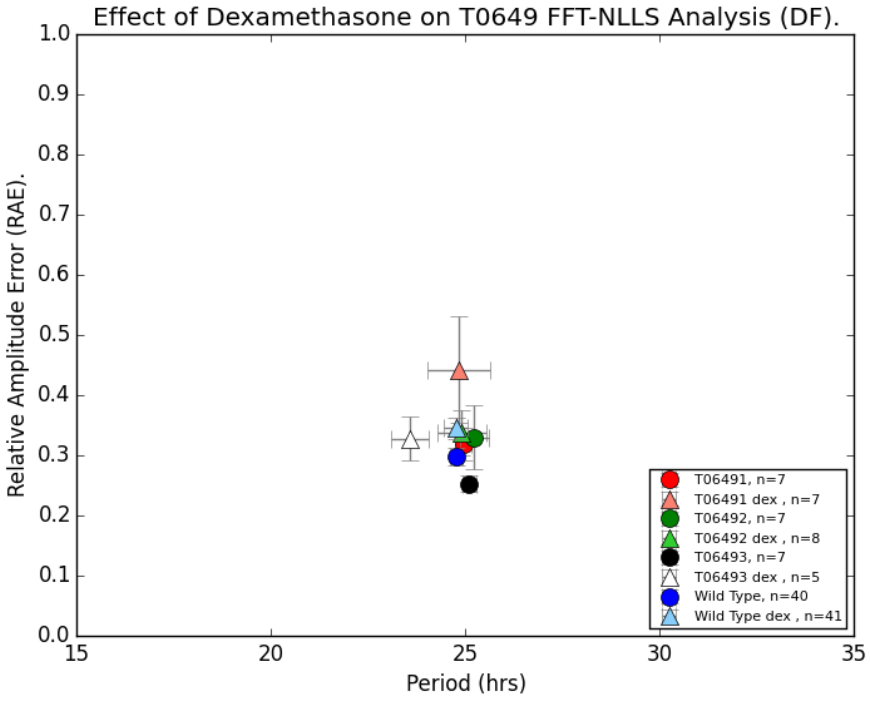

(D) DF Periods, by Independently-Transformed Lines

FIGURE 4.31: Effects of Dex-Induction of *HAP2B* (T0825) on DF Intensity

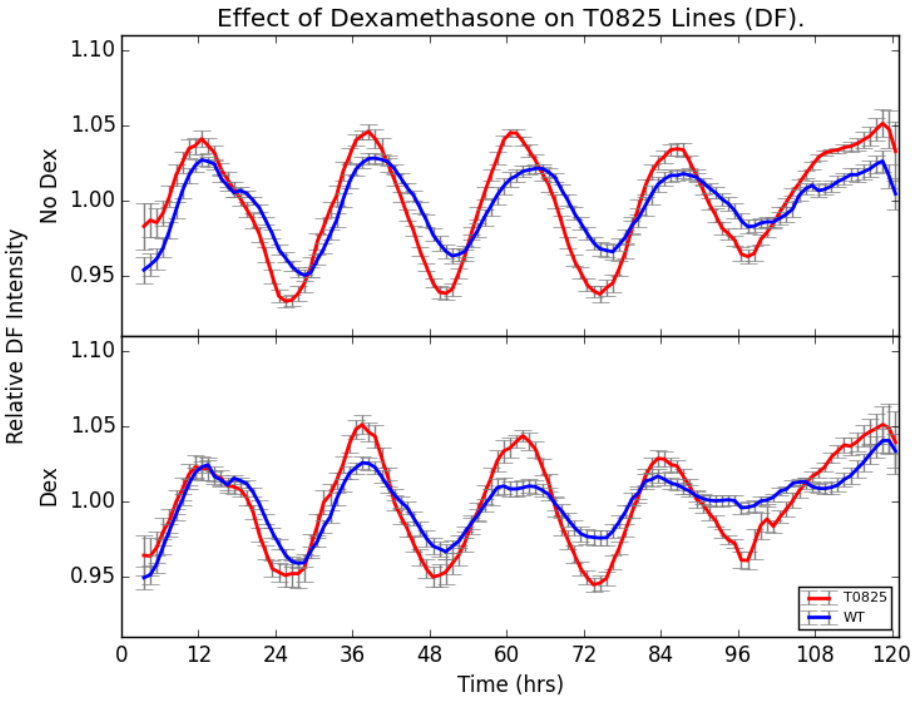

(A) DF Intensity, Averaged

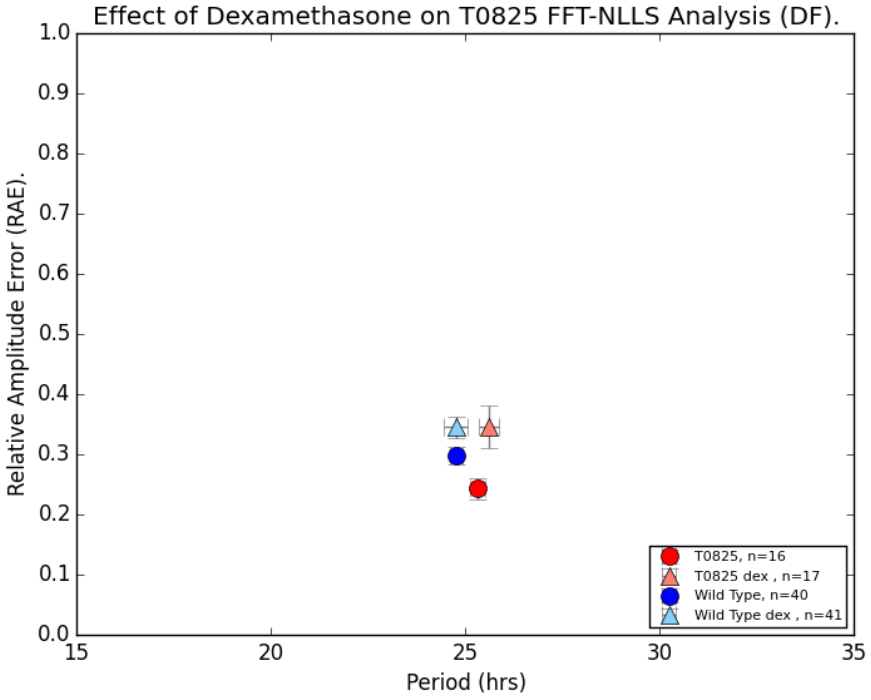

(B) DF Periods, Averaged

Seedlings were grown at a density of 15-20 per sample for a total of 15 days in 12/12 LD cycles before treatment with dexamethasone at ZT+14. Experimental imaging began at dawn day 16 with transfer into LL.

Figure 4.31, Continued...

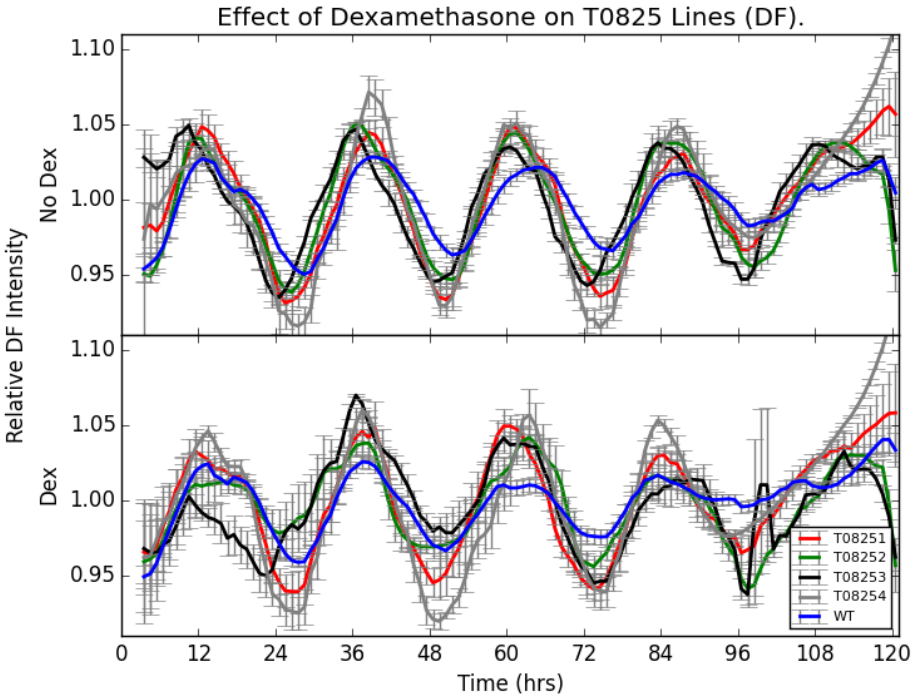

(C) DF Intensity, by Independently-Transformed Lines

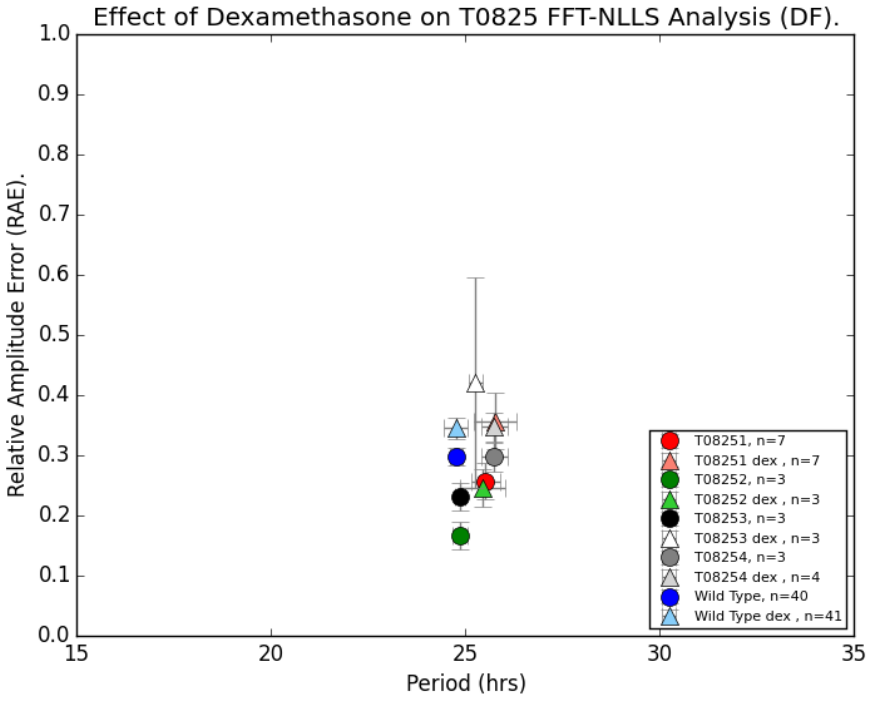

(D) DF Periods, by Independently-Transformed Lines

FIGURE 4.32: Effects of Dex-Induction of *HRS1* (T0840) on DF Intensity

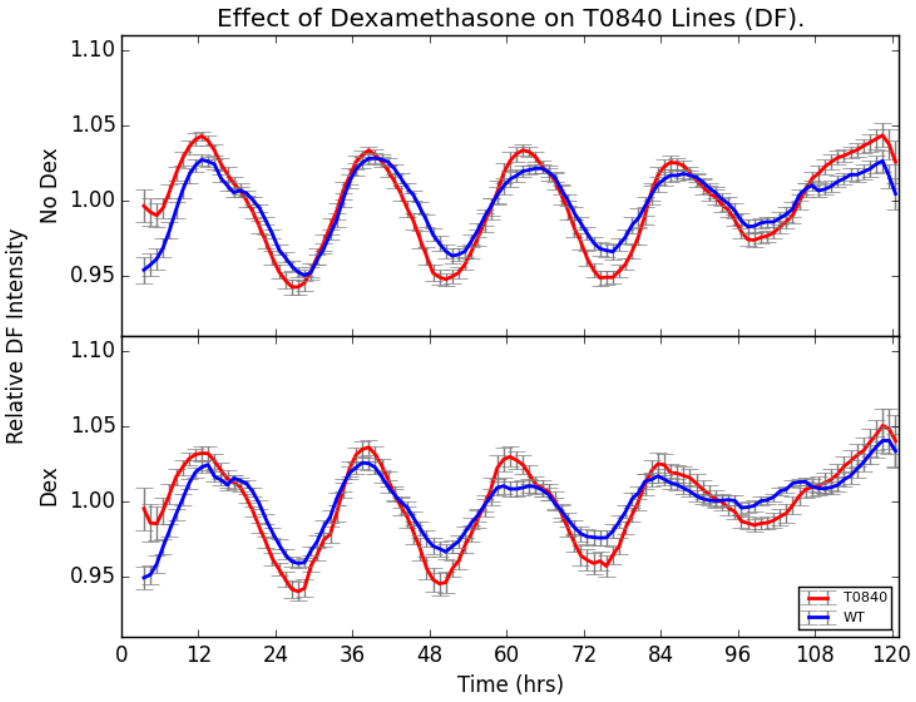

(A) DF Intensity, Averaged

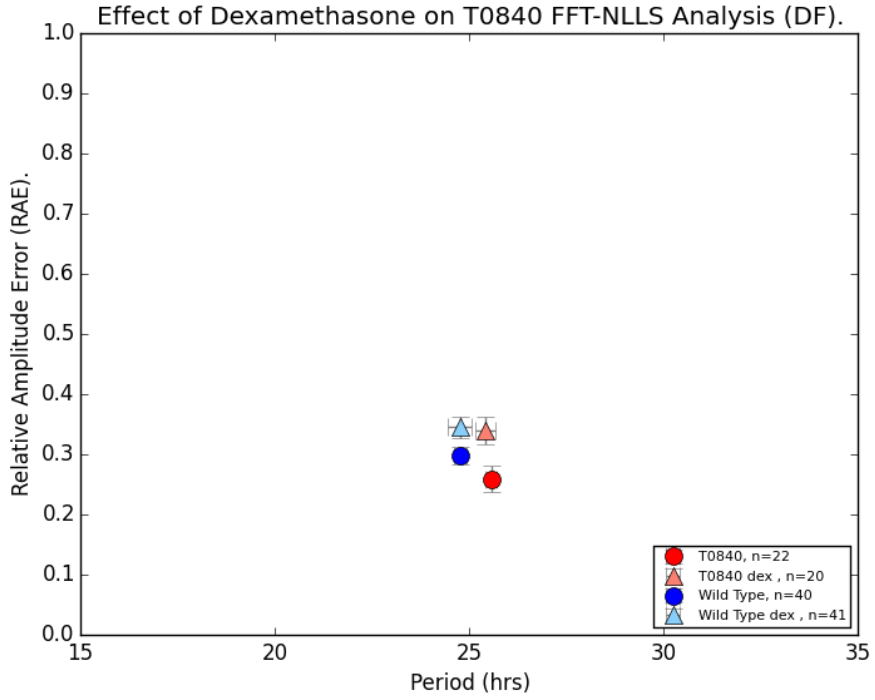

(B) DF Periods, Averaged

Seedlings were grown at a density of 15-20 per sample for a total of 15 days in 12/12 LD cycles before treatment with dexamethasone at ZT+14. Experimental imaging began at dawn day 16 with transfer into LL.

Figure 4.32, Continued...

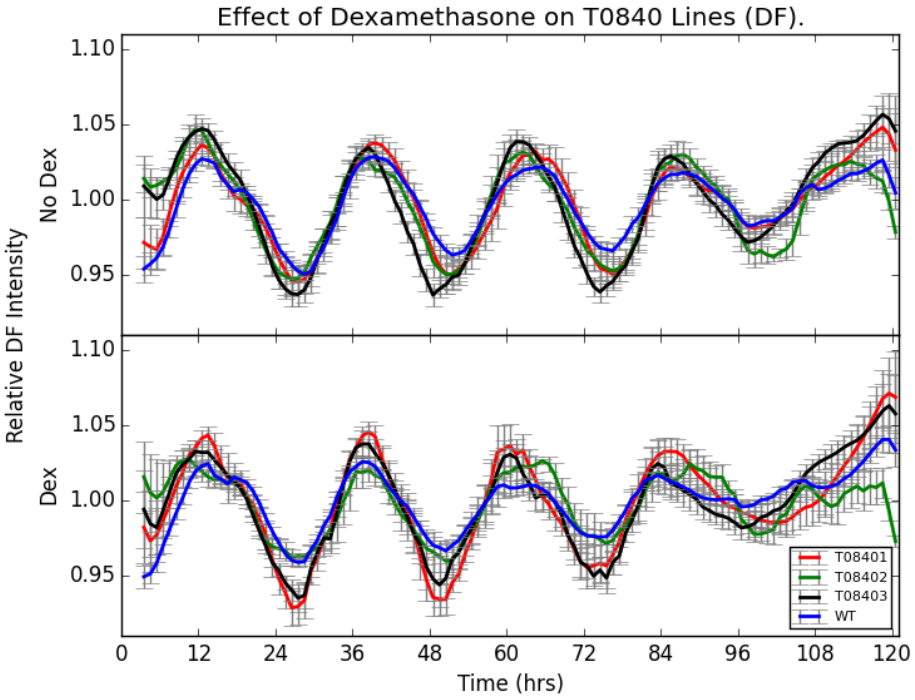

(C) DF Intensity, by Independently-Transformed Lines

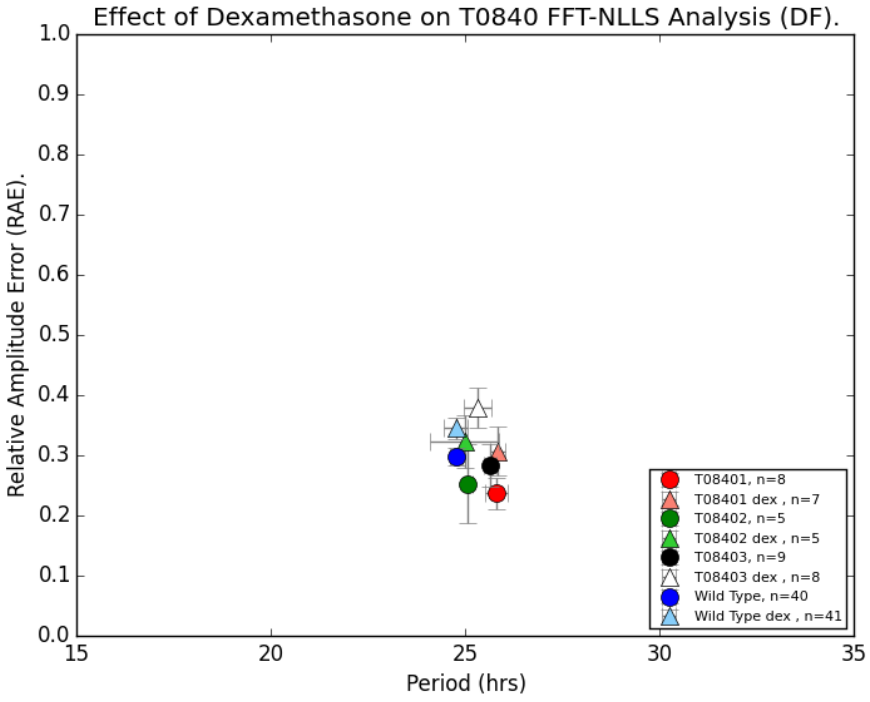

(D) DF Periods, by Independently-Transformed Lines

FIGURE 4.33: Effects of Dex-Induction of *MYBC1* (T0856) on DF Intensity

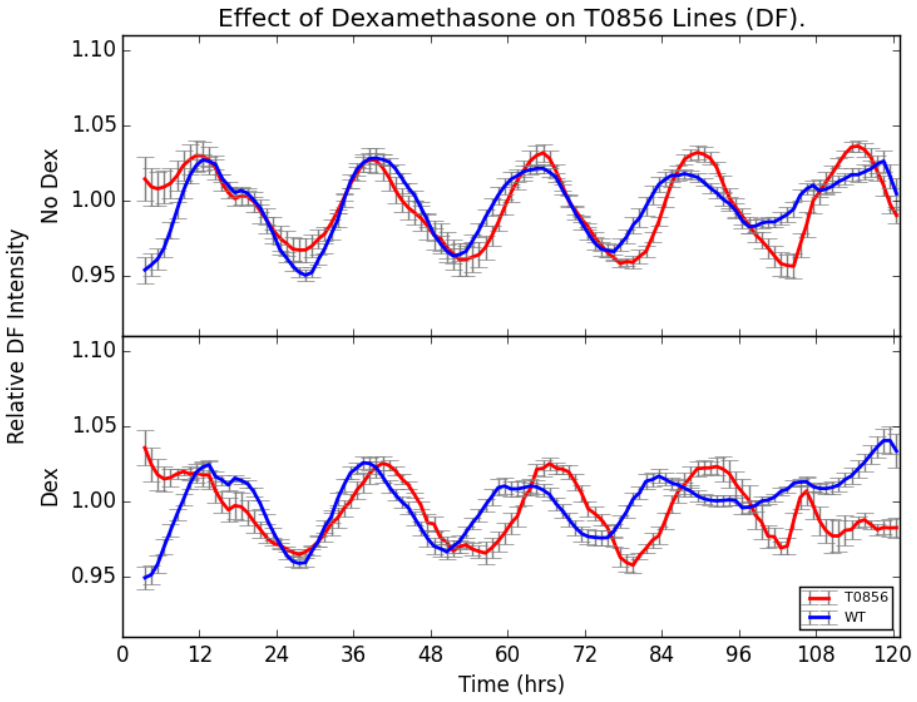

(A) DF Intensity, Averaged

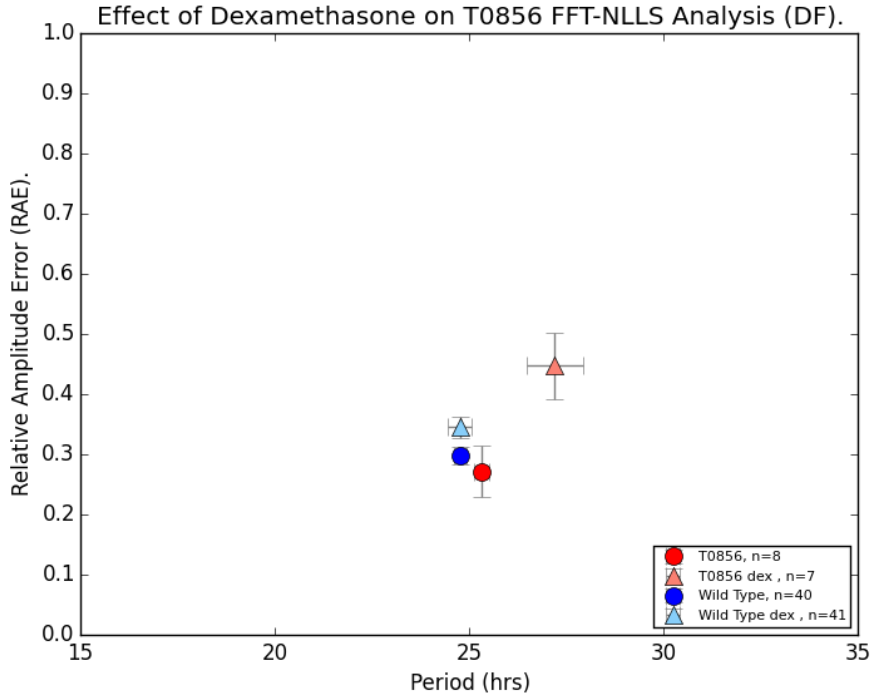

(B) DF Periods, Averaged

Seedlings were grown at a density of 15-20 per sample for a total of 15 days in 12/12 LD cycles before treatment with dexamethasone at ZT+14. Experimental imaging began at dawn day 16 with transfer into LL.

Figure 4.33, Continued...

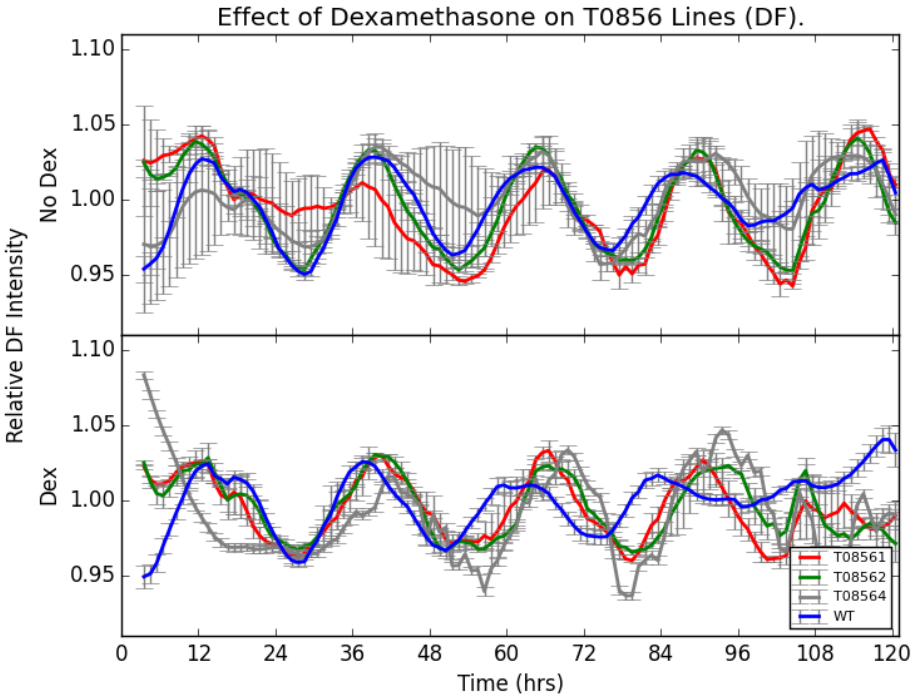

(C) DF Intensity, by Independently-Transformed Lines

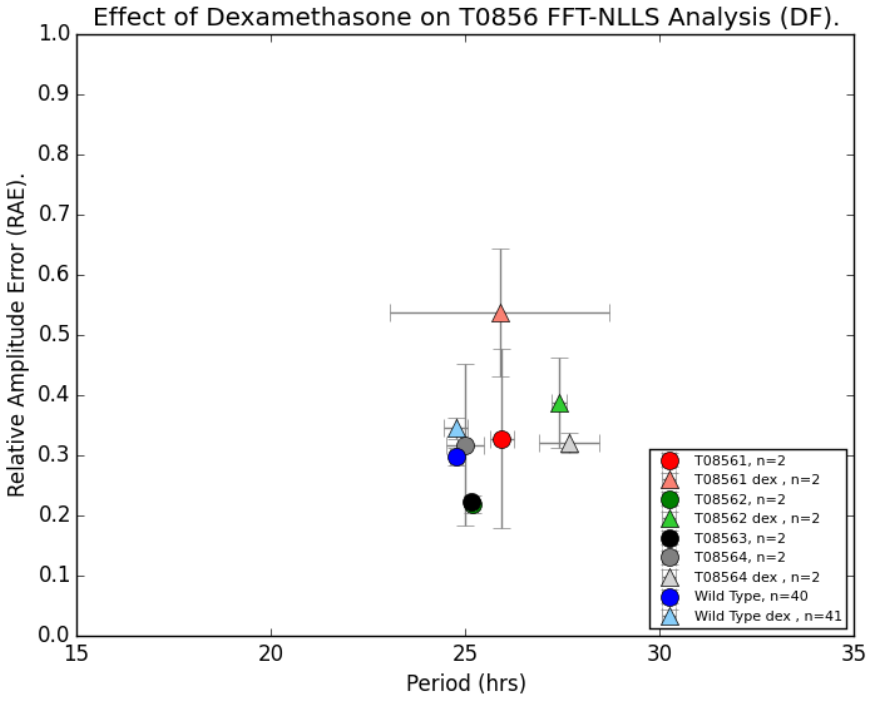

(D) DF Periods, by Independently-Transformed Lines

FIGURE 4.34: Effects of Dex-Induction of AT5G66770 (T0910) on DF Intensity

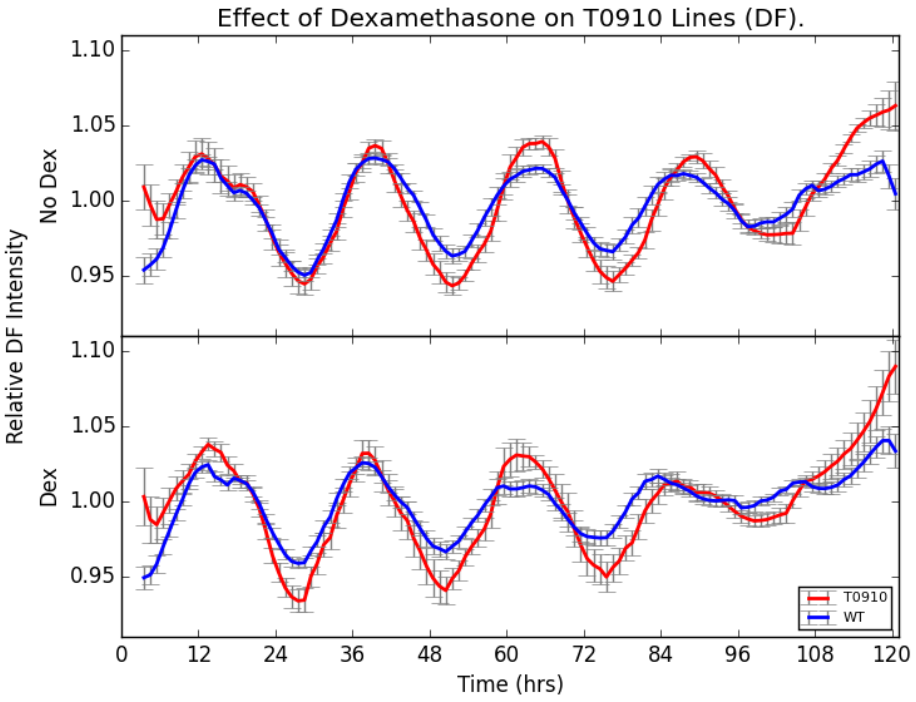

(A) DF Intensity, Averaged

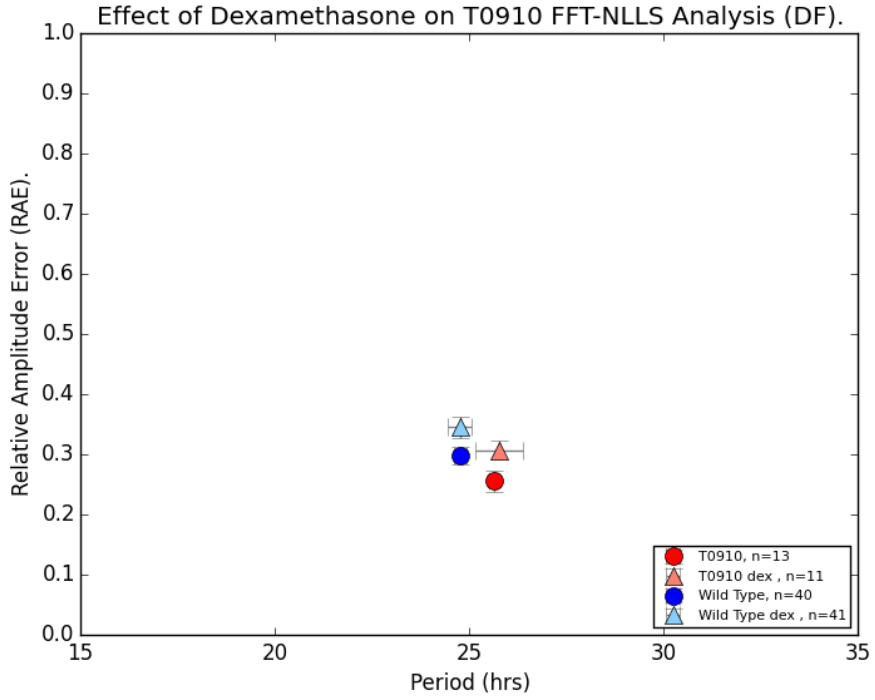

(B) DF Periods, Averaged

Seedlings were grown at a density of 15-20 per sample for a total of 15 days in 12/12 LD cycles before treatment with dexamethasone at ZT+14. Experimental imaging began at dawn day 16 with transfer into LL.

Figure 4.34, Continued...

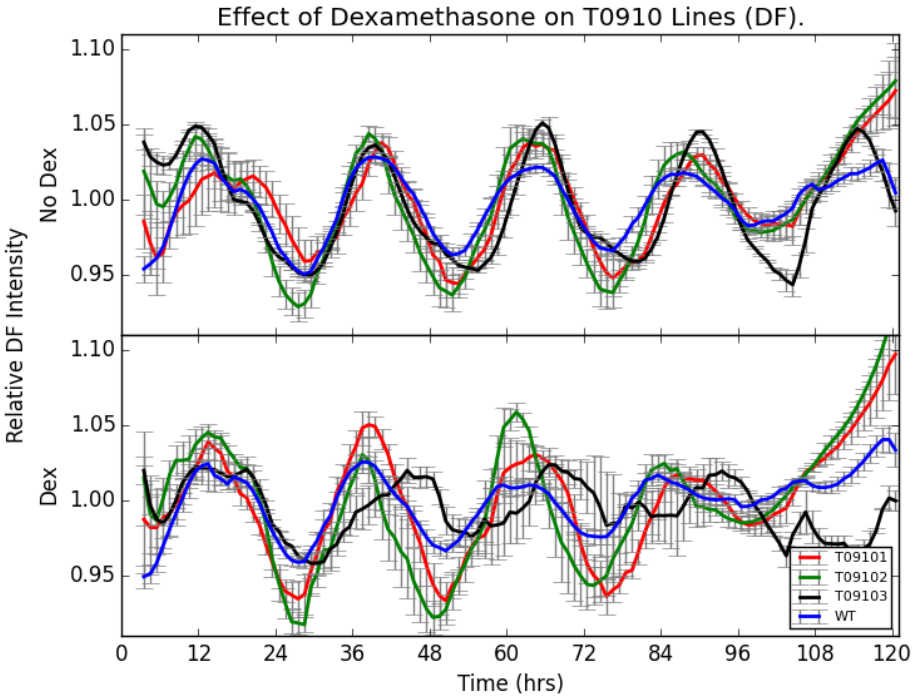

(C) DF Intensity, by Independently-Transformed Lines

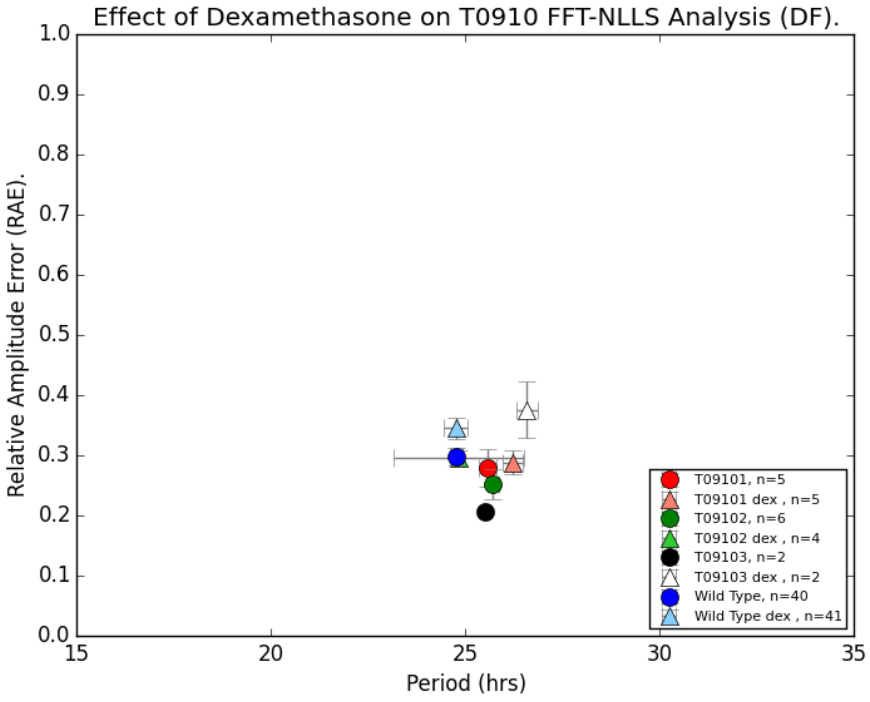

(D) DF Periods, by Independently-Transformed Lines

FIGURE 4.35: Effects of Dex-Induction of *COL15* (T1082) on DF Intensity

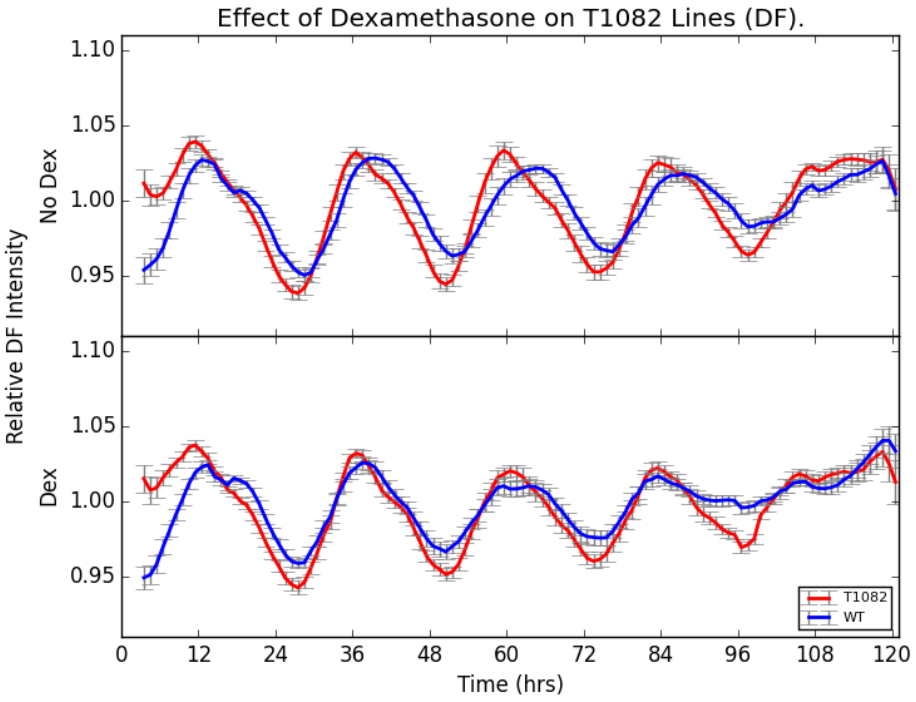

(A) DF Intensity, Averaged

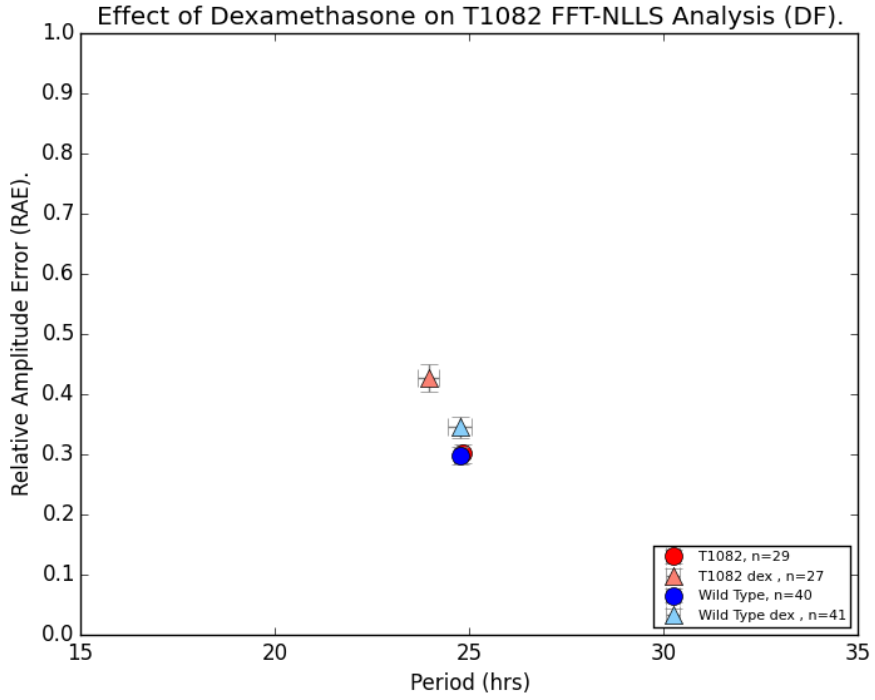

(B) DF Periods, Averaged

Seedlings were grown at a density of 15-20 per sample for a total of 15 days in 12/12 LD cycles before treatment with dexamethasone at ZT+14. Experimental imaging began at dawn day 16 with transfer into LL.

Figure 4.35, Continued...

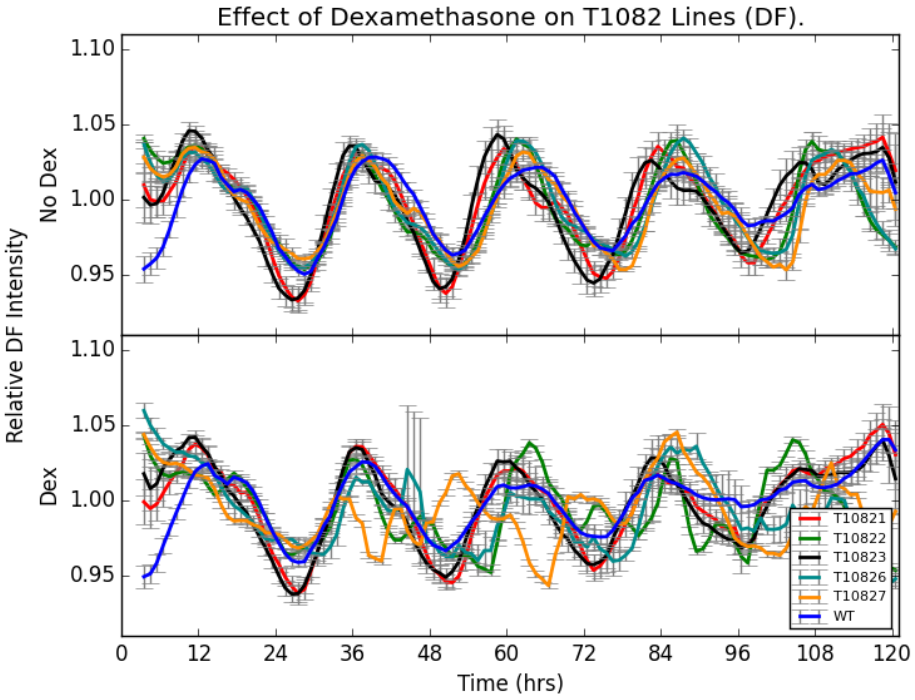

(C) DF Intensity, by Independently-Transformed Lines

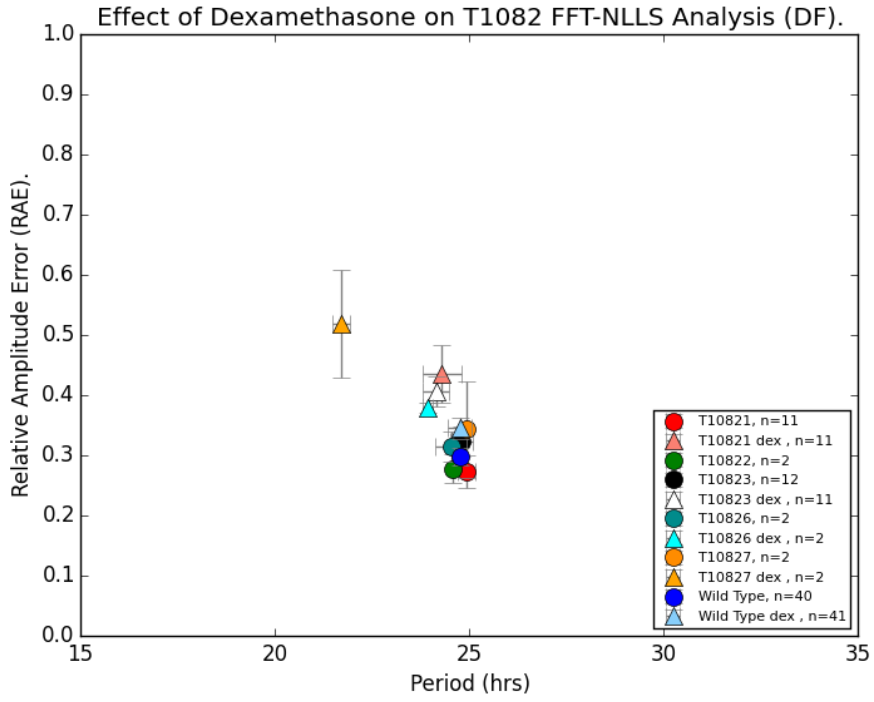

(D) DF Periods, by Independently-Transformed Lines

FIGURE 4.36: Effects of Dex-Induction of TFCCA1 on DF Intensity

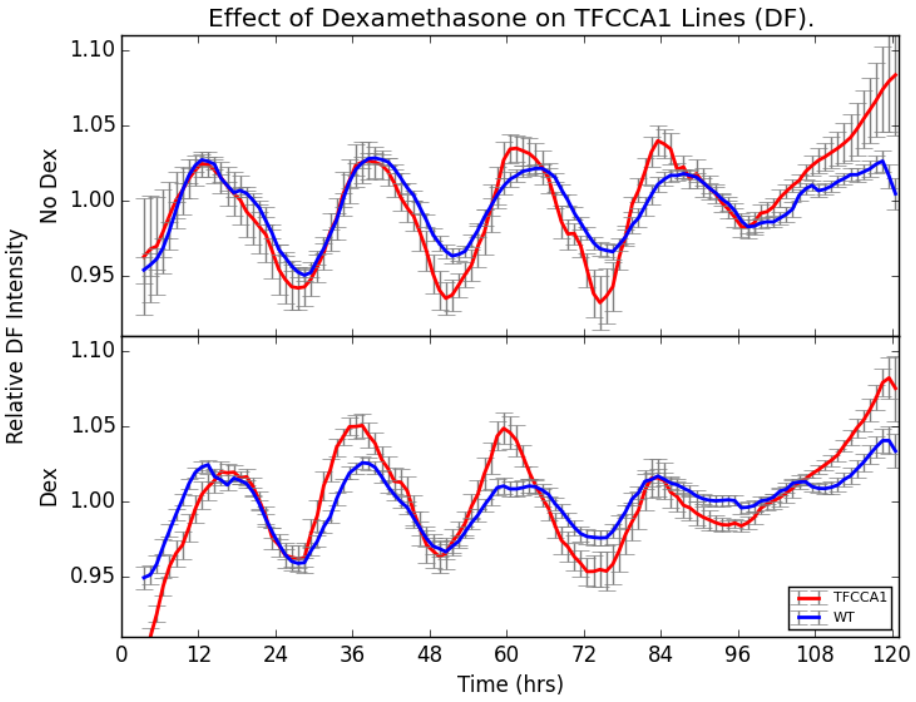

(A) DF Intensity, Averaged

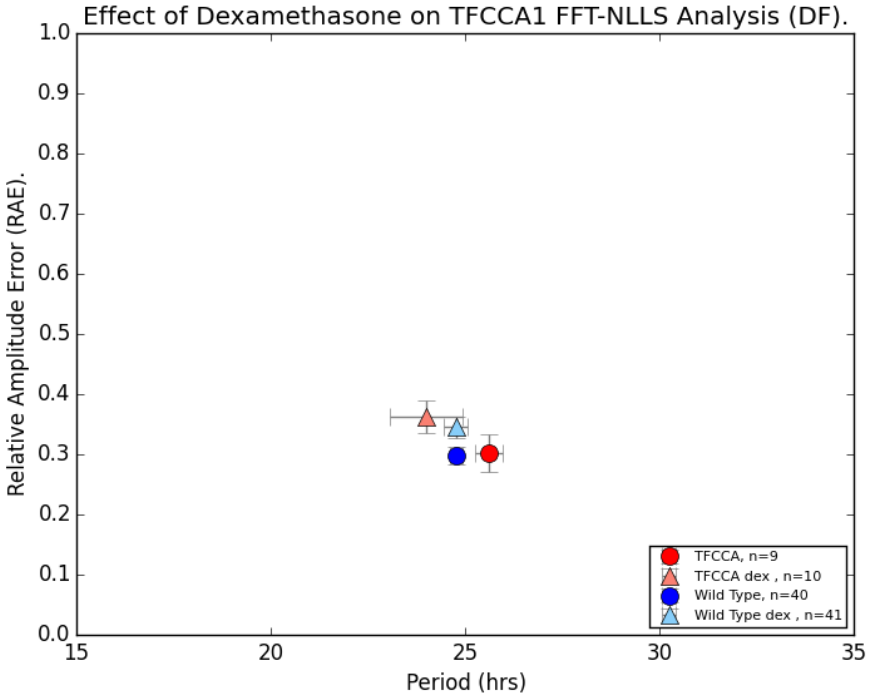

(B) DF Periods, Averaged

Seedlings were grown at a density of 15-20 per sample for a total of 15 days in 12/12 LD cycles before treatment with dexamethasone at ZT+14. Experimental imaging began at dawn day 16 with transfer into LL.

4.5 Hypocotyl Phenotypes Under Monochromatic Light

Circadian dysfunction frequently results in aberrant hypocotyl elongation, as outlined in Chapter 1.3.2.1. It is a well-characterised phenomena occurring in seedlings in the first few days following dormancy. It has widely been studied due to its sensitivity to a large number of stimuli - elongation is controlled by an coincidence mechanism between several different signalling pathways (Nozue et al., 2007). Foremost amongst these is light, perceived by the red-light sensitive phytochomes and blue light sensitive cytochromes, which severely suppresses extension(Chen et al., 2004). Additionally, the phytohormones ethylene, cytokinin (Cary et al., 1995), auxin (Jensen et al., 1998), giberellins and brassinosteroids (Chory and Li, 1997) all have regulatory roles on hypocotyl elongation. Finally, this growth is gated by the circadian clock (Dowson-Day and Millar, 1999).

Light, of both red and blue wavelengths, has a central role in controlling hypocotyl elongation (Chen et al., 2004). Red light acts through the *PHYTOCHROME* light receptor gene family (Clack et al., 1994, Kendrick and G. H. M. Kronemberg, 1994, Sharrock and Quail, 1989), which regulates de-etiolation of seedlings (a suite of developmental responses including hypocotyl elongation). Under constant red light conditions, de-etiolation is primarily mediated through *PHYB* and, to a lesser extent, *PHYA* (Cerdán et al., 1999, Mazzella et al., 1997), which are partially redundant in this (Cerdán et al., 1999, Mazzella et al., 1997). Blue light is perceived in *Arabidopsis* by the partially redundant *CRYPTOCHROME1/2* receptors. Under constant blue light, *cry1* mutants exhibit elongated hypocotyls relative to wild type, whilst *CRY1* OX is hypersensitive to blue light and displays a significantly shortened (Cashmore et al., 1999). Under red light, there is no difference relative to the wild type. Cryptochromes are also key inputs

to the circadian clockwork, and are required for phytochrome signalling into the clock (Devlin and Kay, 2000).

Circadian dysfunction frequently results in aberrant hypocotyl elongation phenotypes under constant light - elongation is rhythmically controlled, with a daily growth arrest coinciding with perceived dawn and a rapid growth phase at subjective dusk (Dowson-Day and Millar, 1999). Many canonical circadian genes are implicated in the control of hypocotyl elongation, including *LHY*, (Schaffer et al., 1998), *TOC1*,(Somers et al., 1998b), and *ELF3* (Dowson-Day and Millar, 1999). Mutations that affect the circadian system have wide-reaching effects on regulating the signalling pathways that control hypocotyl elongation, making it a key phenotype for prospective circadian mutants.

In this section, the hypocotyl elongation phenotypes of TF lines were analysed under three monochromatic light regimes: constant red (1μmol m^{-2}), constant blue (10μmol m^{-2}) and constant dark (wrapped in foil), as per the method in Chapter 2. Heterozygous seed was used for this experiment. *COL15* and *IAA11* were selected as the leading candidate genes following luciferase phenotyping. *ANAC087* and *NF-YA2* were added on the request of Prof Matsui from the 21 TF line long-list.

Three additional lines were added as controls. Two of these were light signalling mutants, expected to give phenotypes in the different growth conditions. The *cry1cry2* double mutant is expected to give elongated hypocotyls under blue light (Cashmore et al., 1999). The *phyB* mutant is a control for red light elongation, with long hypocotyls expected under red light (Reed et al., 1994) Finally, T1368 (*MYB70*) was also included. This TF line was previously found to give a dexamethasone dependent long hypocotyl phenotype under blue light (Unpublished). This line was included to demonstrate that

dexamethasone-dependent TF induction was working effectively. A homozygous stock was kindly donated by Dr Setsuko Shimada.

4.5.1 Results

Measurements were taken after 11 days of growth. As expected, hypocotyl elongaiton was suppressed in the wild type in both conditions where light was present (Mean wild type extension: Blue = 4.21mm, Dark = 17.89, Red = 6.50mm). Data were normalised to the wild type , and then expressed in terms of percent relative change. This was chosen as, otherwise, the sheer size of the extensions of red light mutants would make visualising the data difficult; also it is difficult to view any mutants with suppressed hypocotyl elongation as, whilst a hypocotyl could easily be double that of the wild type (i.e. 40mm vs 20mm), a similar shortening (0mm) would be scored as non-germinating. Normalising the data this way allows it to be viewed and analysed side by side with ease.

The three controls gave phenotypes as expected. *phyB* has elongated hypocotyls in red light but not in the blue light or dark treated plants (WT+140.92%, $p < 0.001$, 4.23). Similarly, *cry1cry2* exhibits severe lengthening relative to the wild type in blue light (WT+127.13%), but not dark or red light treated conditions. The dark and red light conditions are, indeed, slightly shorter than the wild types. This is not a concern - short hypocotyl phenotypes are not of particular interest, unless they are severe. Short hypocotyls can be explained by late germination, or slowed growth, rather than any effect on the hypocotyl elongation controlling pathways *per se*. Statistically significant elongation of hypocotyls, representing changes of more than 25%, where the interquartile ranges do not overlap in Figure 4.37, is the criteria for a phenotype of interest in this experiment.

MYB70 shows an average increase in hypocotyl length in blue light, however as the boxplot in Figure 4.37 shows there is a large distribution in these lengths. This is possibly a result of the seed stock provided not being homozygous, despite the assurance of Dr Shimada - this would result in a segregating phenotype. Regardless, there is an elongated hypocotyl phenotype in this line (Average = WT+39.08%, $p < 0.001$), indicating that the dexamethasone treatment was sufficient to induce nuclear import. It also shows a smaller (WT+17.7%) statistically significant hypocotyl lengthening under red light conditions. This was unexpected, as the lengthening phenotype was believed to be blue-light dependent, however the Matsui team had not investigated *MYB70* under red light. Future work by the Matsui team will investigate this.

Of the test lines, neither *ANAC087* or *IAA11* have any abnormal hypocotyl elongation, with none of the conditions being longer than the wild type (Table 4.23). *IAA11* is slightly shorter all three conditions, whilst *ANAC087* is slightly shorter under blue light and dark conditions; however in all these, the difference is small (all represent less than 25% change relative to the wild type).

NF-YA2 exhibits hypocotyl elongation under red light (WT + 66.34%). This change is statistically significant ($p < 0.001$, Table 4.23). Additionally, *COL15* appears to show a statistically significant lengthening under red light conditions (WT + 26.49%). This is of a comparable size to that of the dexamethasone control; however there is a large distribution of hypocotyl lengths recorded (Figure 4.37). This may be due to the distribution of homo-, hetero- and wild type seed.

In summary, the hypocotyl elongation assays are limited by the lack of homozygous seed, their limited scope, and the lack of follow-up to elucidate whether these phenotypes are a result of circadian defects or perturbation of light-signalling pathways.

FIGURE 4.37: Light-Dependent Hypocotyl Elongations Under Three Light Regimes, With Dexamethasone

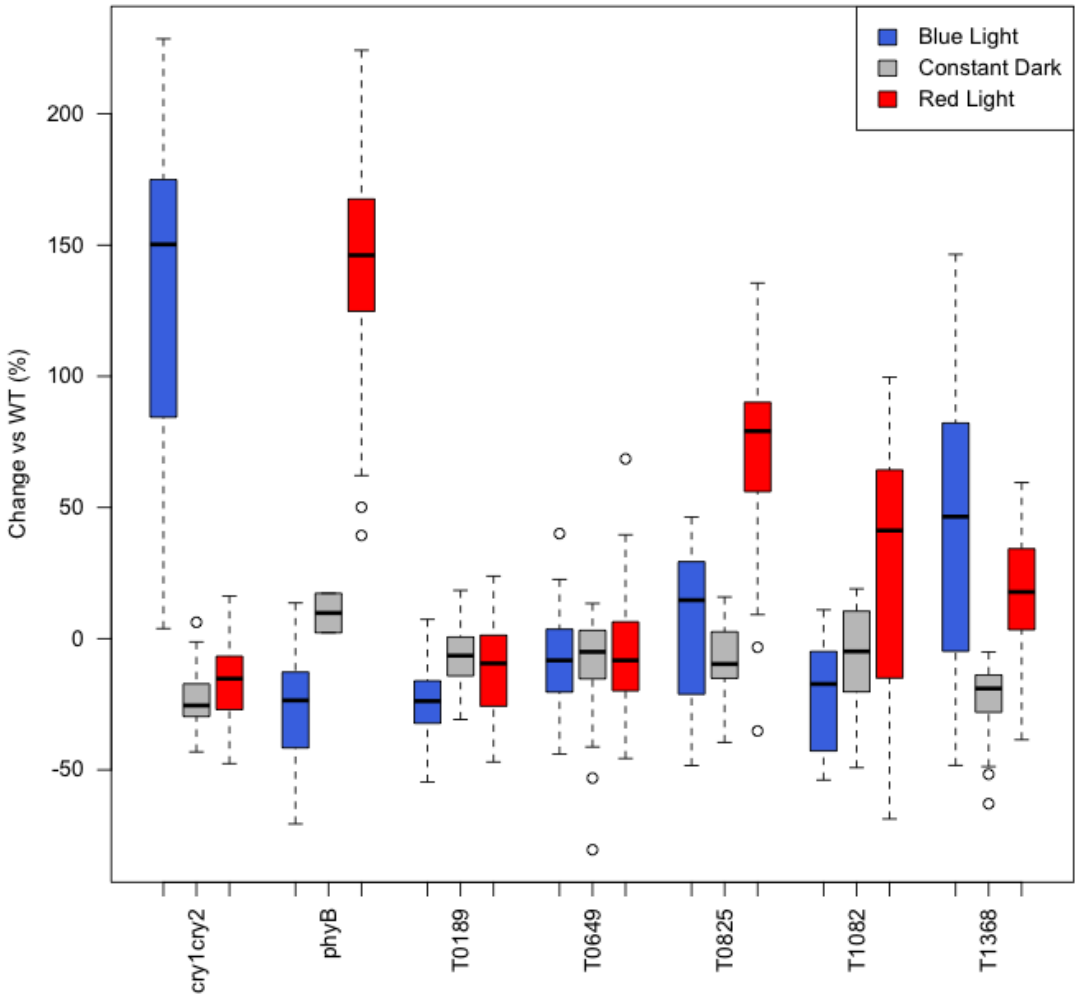

Seeds were liquid-phase surface sterilised and planted on GM agar plates + 5μM dexamethasone, stratified in the dark for 3 days at 4°C before exposure to red light (1μmol m^{-2}) for 3 hours to induce germination. Plants were then transferred to the test light conditions and grown for 11 days. These were: constant red (1μmol m^{-2}), constant blue (10μmol m^{-2}) and constant dark, all at 22°C . Hypocotyls were photographed and measured in ImageJ. Lengths were normalised to the wild type and are plotted as percentage change.

TABLE 4.23: Hypocotyl Extension in 3 Light Conditions.

Blue

	Length(mm)	Normalised (mm)	% v WT	p=
WT	4.21			
cry1cry2	9.56	5.35	127.13	<0.001
phyB	3.08	-1.12	-26.70	<0.001
IAA11	3.24	-0.97	-22.93	<0.001
ANAC087	3.85	-0.36	-8.52	0.015
NF-YA2	4.45	0.24	5.69	0.332
COL15	3.24	-0.97	-22.93	<0.001
MYB70	5.85	1.64	39.08	<0.001

Red

	Length(mm)	Normalised (mm)	% v WT	p=
WT	6.50			
cry1cry2	5.44	-1.06	-16.35	<0.001
phyB	15.66	9.16	140.92	<0.001
IAA11	5.78	-0.72	-11.04	0.003
ANAC087	6.13	-0.37	-5.73	0.136
NF-YA2	10.81	4.31	66.34	<0.001
COL15	8.22	1.72	26.49	<0.001
MYB70	7.65	1.15	17.70	0.001

Dark

	Length(mm)	Normalised (mm)	% v WT	p=
WT	17.90			
cry1cry2	13.70	-4.20	-23.48	<0.001
phyB	19.40	1.50	8.40	0.456
IAA11	16.32	-1.58	-8.82	0.001
ANAC087	16.81	-1.09	-6.08	0.001
NF-YA2	16.79	-1.11	-6.19	0.011
COL15	16.32	-1.58	-8.82	0.011
MYB70	14.27	-3.63	-20.29	<0.001

Seeds were liquid-phase surface sterilised and planted on GM agar plates + 5μM dexamethasone, stratified in the dark for 3 days at 4°C before exposure to red light (1μmol m^{-2}) for 3 hours to induce germination. Plants were then transferred to the test light conditions and grown for 11 days. These were: constant red (1μmol m^{-2}), constant blue (10μmol m^{-2}) and constant dark, all at 22°C . Hypocotyls were photographed and measured in ImageJ. All statistical tests are Student's T-Test (heteroscedastic, 2-tailed).

4.6 Effects of Timing of Dexamethasone Treatment on the Induced Phenotype

So far, dexamethasone was applied in the afternoon, at 7hrs after subjective dawn (ZT+7). In part, this choice of time points was made for practical reasons - it allows applications to be made in a normal working day, and is the same approximate time as luciferase applications, reducing the stress of treatment on the plants. For screening, confirmation and characterisation of phenotypes, the choice of time point of dexamethasone is relatively unimportant, provided that it is the same between experiments, as it is likely that despite missing phenotypes that would only emerge following morning treatment, there are a comparable number of phenotypes that are more severe following an evening treatment. However, it is possible that the timing of dexamethasone treatment has greater effects on the circadian phenotypes.

Seeds were gas sterilised, imbibed, sown on MS agar and grown for DF imaging as outlined previously in Chapter 2. After 14 days of growth in diurnal light conditions (12:12 LD), dexamethasone treatments were administered at ZT+0, ZT+7 and ZT+24 i.e. at dawn the following day, immediately prior to transfer to free-run (LL) in the CCD cabinets for imaging. Plants were then imaged and analysed as previously.

Heterozygous-Homozygous-Wild Type seeds stocks were surface sterilised and 3 replicates planted for each independently transformed TF line.

4.6.1 Results

There is a general increase in RAE between the mock and dexamethasone-treated wild type plants. This increase is statistically significant for all treatment conditions. This

may possibly be due to increases in humidity from treatment, a relatively small sample set, or problems introduced at the treatment stage. However, this trend does not seem to greatly affect period (Mean period across all conditions = 24.3hrs Table 4.24).

There is no general trend in periods. Period phenotypes are generally more severe when treated with dexamethasone at ZT +7 than ZT+0. Whilst this might have been expected for the TF lines, as the genes of interest were identified as yielding phenotypes following this treatment, this holds true for TF-CCA1. This runs against our expectations. The sample appears to have a larger increase in RAE value and a wide range of periods, indicating a loss of robustness. This is especially clear in Figure 4.39a, where there appears to be an abolition of rhythms by 72hrs, as well as in the RAE plot in Figure 4.39b.

From the period data alone, it appears that treatment with dexamethasone at ZT+24 has little mean effect on period data, with the mean periods of COL15 and TF-CCA1 in this condition being within 0.1hr of the wild type. However, this is not the case for the RAE values, and especially not the case for TF-CCA1. There is a very large increase in mean RAE following dexamethasone treatment at ZT+24, which has a large standard error (Figure 4.39b). There is also larger degree of noise in the intensity line graph, characterised by a increase in "spiky-ness" (Figure 4.39a). Taken together, it is possible that this effect is a result of the short time between spray treatment and imaging, as it affects all samples.

FIGURE 4.38: Effects of Dexamethasone Timing on DF Periods in COL15

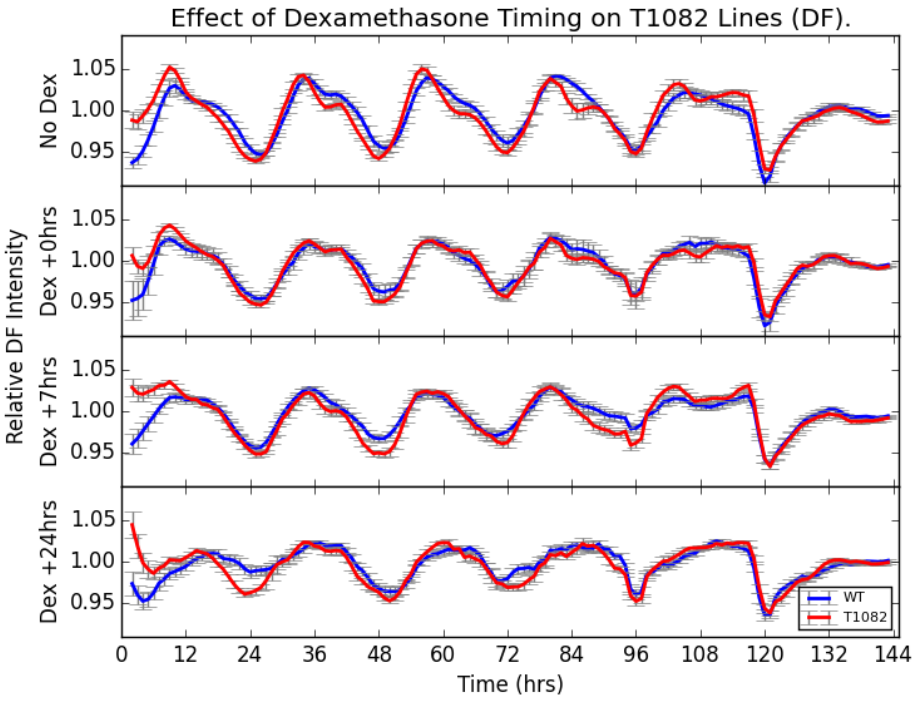

(A) Relative Intensity

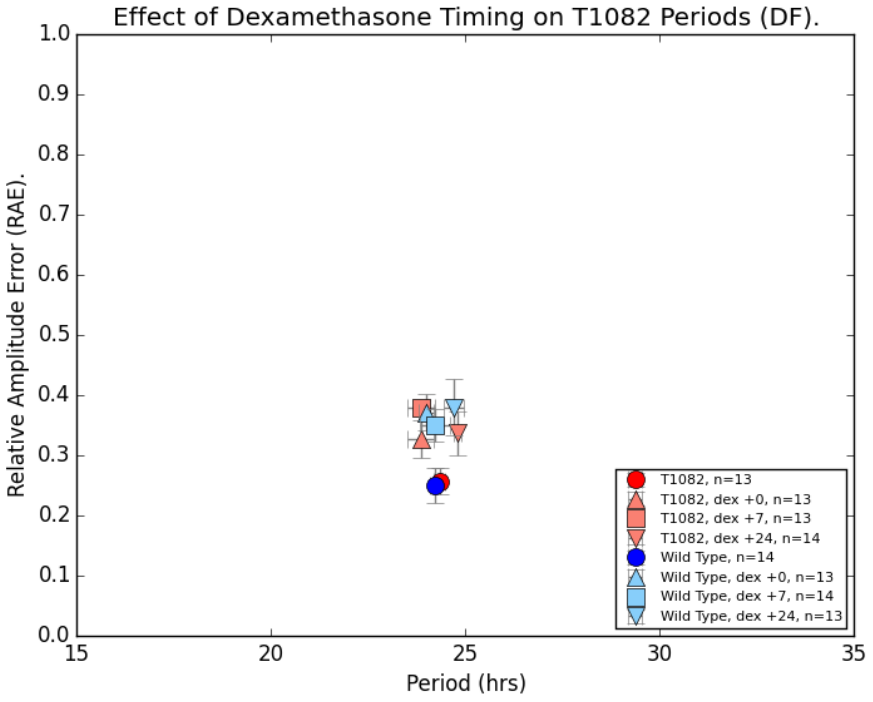

(B) Periods

Seedlings were grown at a density of 15-20 per sample for a total of 14 days in 12/12 LD cycles before treatment with dexamethasone at intervals beginning at ZT+0 on day 14. Experimental imaging began at dawn day 15 (i.e. ZT+24) with transfer into LL.

FIGURE 4.39: Effects of Dexamethasone Timing on DF Periods in TF-CCA1

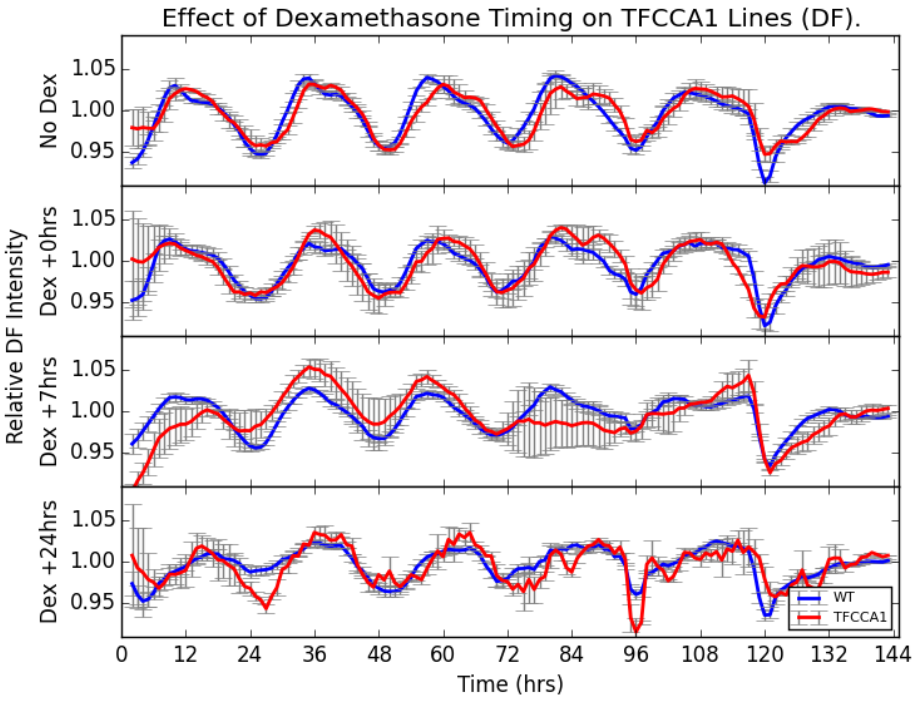

(A) Relative Intensity

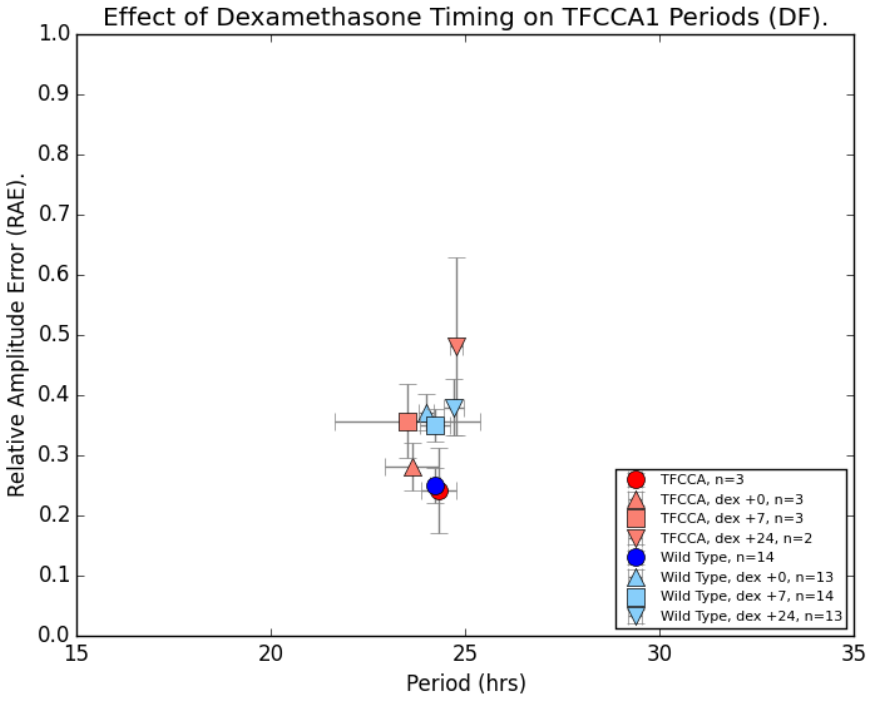

(B) Periods

Seedlings were grown at a density of 15-20 per sample for a total of 14 days in 12/12 LD cycles before treatment with dexamethasone at intervals beginning at ZT+0 on day 14. Experimental imaging began at dawn day 15 (i.e. ZT+24) with transfer into LL.

TABLE 4.24: Effects of Timing of Dexamethasone Application on the TF line phenotype

		Period Changes, vs WT (hrs)				RAE Changes, vs WT			
Line	n	Mock	ZT+0	ZT+7	ZT+24	Mock	ZT+0	ZT+7	ZT+24
COL15	13	+0.10	-0.15	-0.36	+0.09	+0.01	+0.08	+0.13	+0.09
TFCCA1	3	+0.09	-0.37	-0.70	+0.05	-0.01	+0.03	+0.11	+0.23
Wild Type	14	**24.24**	-0.23	-0.01	+0.01	**0.37**	+0.12 **	+0.10 *	+0.13 *

Plants were analysed in LL conditions following 12:12 LD entrainment. Dexamethasone treatment was performed at time points starting from dawn (ZT+0) the day prior to the start of imaging imaging as outlined previously. Images were captured and period analysis was performed on baseline detrended data, normalised to the mean, as outlined in Section 2. Comparisons are calculated against the wild type references in the same dexamethasone treatment regime. Values in **bold** are the mean values for the wild types, against which other values are calculated. All statistical tests are Student's T-Test (two-tailed, unpaired); significance thresholds: $p \leq 0.001$ ***, $p \leq 0.01$ **, $p \leq 0.05$ *

4.7 Discussion

The goal of the experiments in this chapter was to sift through the list of genes of interest identified by the initial DF screen, identifying lines with reproducible, dexamethasone-dependent phenotypes. Additionally, knockout lines were assayed, hypocotyl elongation under monochromatic light was recorded and the effects of time of dexamethasone treatment on the clock was investigated in order to fully describe the phenotype of these genes.

In this section, DF and luciferase data were amplitude normalised. The rationale for performing this was to counteract dampening of intensity throughout the experiment. However, this renders it difficult to use low amplitude as a quality control threshold. Additionally, the original screen did not focus on amplitude as a selection criteria, so there was no hypothesis to confirm. It would be interesting (although outside the scope of this project) to evaluate the amplitudes of these lines for phenotypes. Additional shortcomings of the experiments include the failures to genotype and generate homozygous lines. For further discussion of these issues, see Chapter 6.

In total, 18 genes were re-phenotyped in the presence and absence of dexamethasone - 11 by both luciferase and DF, 7 by DF alone. As a general rule, in the replications through DF, the direction of the period changes following dexamethasone treatment seemed to match that expected from the initial screen - that is to say, periods shortened or lengthened in line with the original experiment. However, again in general, these changes were not statistically significant. This could be due to a dosage response effect, whereby the level of expression conveyed by the 35S promoter leads to some low-level of phenotypic induction even in the mock-treated plants. Alternatively, the level of applied

dexamethasone might be insufficient to fully induce the sustained nuclear import of the transcription factor. 50μM dexamethasone was applied to seedlings as before, albeit from a freshly made master stock. Previous evidence suggests that topical application of dexamethasone as a mist in concentrations of 20-200μM is sufficient to induce high levels of protein expression of downstream targets of a 35S-driven gene (Kemen et al., 2011), with no difference in induction between 20 and 200μM treatments, although these studies were carried out on adult whole plants and included Silwet rather than Tween 20 as a surfactant. Unfortunately, due to time and throughput constraints on the imaging cabinets, there was no investigation into the dexamethasone dosage response curve for the TF-GR system.

Additionally, 14 genes were phenotyped as SALK knock-outs by delayed fluorescence. These experiments were not especially expected to give lots of strong phenotypes. There is a great deal of partial and total redundancy within the genome of *Arabidopsis* and, as such, a large number of gene knock outs do not give phenotypes of any kind in normal experimental conditions (Bouché and Bouchez, 2001). Indeed, partial redundancy has already been described in the core circadian oscillator by Mizoguchi et al. (2002), who observed that *cca1* and *lhy* double mutants are far more severe than single mutants, and this severity of phenotype increases in a non-additive manner. It seems possible that this effect will be even more pronounced in peripheral components; indeed it is perhaps even likely given that any immediately apparent circadian phenotypes in null mutants would have already been identified, whether through circadian studies or through hypocotyl or flowering time phenotypes.

A putative experiment was carried out in order to investigate whether the timing of dexamethasone treatment affected the eventual delayed fluorescence phenotype. This was inconclusive - it suggests that timing of transcription factor function may affect the

severity of the phenotype, but this is far from conclusive. This is complicated by the TF-CCA1, which appeared to have in profoundly different phenotypes following different treatments. Unfortunately, this experiment was carried out with a small selection of genes, with low replication, and relatively few time points compared to the other DF and luciferase phenotyping experiments in this section. In the future, this would need to be extended to more TF lines, more time points, and the level of replication increased.

In the luciferase experiments, there is a tendency in all conditions for shorter periods than the wild type regardless of treatment regime or expected phenotype. Conversely, in the delayed fluorescence experiments, this tendency is inverted with TF lines typically being longer than the wild type. In contrast, however, the wild type periods were broadly the same across the experiments regardless of phenotyping method - indeed, the seed used for both experiments was the same WT/*pCAB2:LUC+* stock as it was of a similar age to the TF lines, and germinated at a comparable rate. Other wild type seed stocks grown at Liverpool proved to have poor germination compared to the TF lines, likely due to their age and problems with seed storage. The results from the wild type seeds were satisfactory - there is no significant difference in period or RAE between the mock- and dex-treated plants (see Section 4.4.3). Differences between the TF and TF-LUC lines may be a result of seed storage or preparation. TF lines were shipped from Japan to Liverpool as T1 seed, whilst luciferase stocks were sent predominantly as T0 stocks which required selection and harvest under necessarily different conditions. As such, it is the differences between the TF line plants in the two conditions that will be primarily considered to identify interesting lines.

As a result of this investigation, three genes stand out as having especially interesting circadian phenotypes:

T0856 (*MYBC1)* was identified first amongst these. In the DF experiments, there is a large period lengthening as observed in the original screen. Furthermore, unlike the majority of TF lines, this lengthening appears to be dexamethasone-dependent (there is a +1.89hr difference between the two conditions) and is statistically significant (p= 0.02). Unfortunately, neither luciferase nor SALK knock-out phenotypes were available for this line.

T0189 (*IAA11*) also gave interesting results. The luciferase and DF experiments both show dexamethasone-dependent shortening (although only the difference between the dex-treated luciferase plants and the wild type is statistically significant), which agrees with the phenotype expected from the screen. There's a clear phase-shifting in the luciferase line graphs, and towards the end of the DF experiment (especially for T0189-3). Furthermore, the SALK lines show the converse phenotype, lengthening by +0.66hrs. Whilst this is not statistically significant (p= 0.057), it is when measured by spectrum resampling (p= 0.039).

T1082 (*COL15/BBX13*), however, has perhaps the greatest body of evidence supporting its selection. Both the delayed fluorescence and luciferase experiments show period shortening, which agrees with the phenotype of the initial screen. In the DF experiments, this shortening is dexamethasone dependent; indeed, the mean mock-treated period is within 0.06hrs of the wild type, whilst the treated condition is 0.8hrs shorter. Furthermore, this effect appears to be statistically significant (p= 0.006). In the luciferase experiments, there is no difference in shortening between the two treatment conditions. This may be due to a dose-dependent effect: the luciferase lines are necessarily of later generations due to the requirements of the transformation protocol, which, with the multiple parallel insertions typical of *Agrobacterium* transformation (Gelvin, 2003), may have led to a far higher copy number and hence expression level of COL15/BBX13. In addition, one (but

not both) SALK knock-out lines gives the converse statistically-significant long period phenotype.

In silico, *COL15* was identified as co-expressed alongside known circadian genes across published microarray experiments (Figures 4.1, 4.2) and was predicted to have evening elements in its promoter (Figure 4.3e). *DIURNAL* data suggest that *COL15/BBX13* is typically expressed in the evenings, and taken together this suggests that *COL15* may be under transcriptional control mediated by the evening-element binding repressors *CCA1* and *LHY* (Alabadí et al., 2001, Harmer et al., 2000). It would be interesting to see how *COL15* mRNA expression patterns are altered in *cca1/lhy* mutants.

In published literature, COL15/BBX13 protein has been shown to interact with the circadian-related E3 ubiquitin ligase SCF factors LKP2 and, to a lesser extent, ZTL (Fukamatsu et al., 2005). It should be noted that affinity of genes for ZTL is dependent in part by their level of phosphorylation (Fujiwara et al., 2008); it is therefore possible that this binding affinity will change at different circadian time points and under different conditions (neither of which were studied in that particular investigation). This is intriguing, and suggests that *COL15* may be a target of ZTL- or LKP2-mediated degradation, gating its expression at the protein level in a circadian manner in addition to the diurnal rhythms of transcription . The data in this investigation have shown that *COL15* over-expression results in period shortening, with a converse long period in the knock out - which is striking as the reverse phenotypes of *TOC1*, another ZTL-targeting, CCT domain-containing gene (Millar et al., 1995a). This could be a result of competitive inhibition of the TOC1/ZTL interaction, or it could be a genuine circadian effect. It has also been found that cADPR upregulates expression of *COL15/BBX13* (Sánchez et al., 2004), indicating there may possibly be a site of circadian crosstalk with the non-transcriptional circadian cADPR circadian feedback loop (Dodd et al., 2009).

Taken as a whole, there is a body of encouraging experimental evidence as well as clues from the literatue that *COL15/BBX13* is involved in the circadian clock. It is this gene that is the best candidate to emerge from this study.

TABLE 4.25: Summary of Dexamethasone Induction Phenotypes

	DF				Luc				SALK	
Line	Period (NoDex)	Period (Dex)	Diff.	P=	Period (NoDex)	Period (Dex)	Diff.	P=	Period	P=
T0189	25.27 (+0.84)	24.82 (+0.07)	-0.44	0.464	24.00 (-0.46)	23.46 (-1.01)	-0.53	0.586	24.21 (+0.66)	0.057
T0856	25.32 (+0.56)	27.21 (+2.45)	1.89	0.02						
T1082	24.83 (+0.06)	23.96 (-0.80)	-0.87	0.006	23.95 (-0.50)	23.92 (-0.56)	-0.03	0.780	25.66 (+1.60)	0.039

All mean periods are calculated through FFT-NLLS analysis and are given in hours (bracketed numbers are mean period differences from the wild type, in hours). Statistical tests are Student's T-Test (two-tailed, unpaired). Lines were selected as giving interesting phenotypes depending on the size and statistical significance of their period shifts, as well as a qualitative review of their waveforms and RAE graphs.

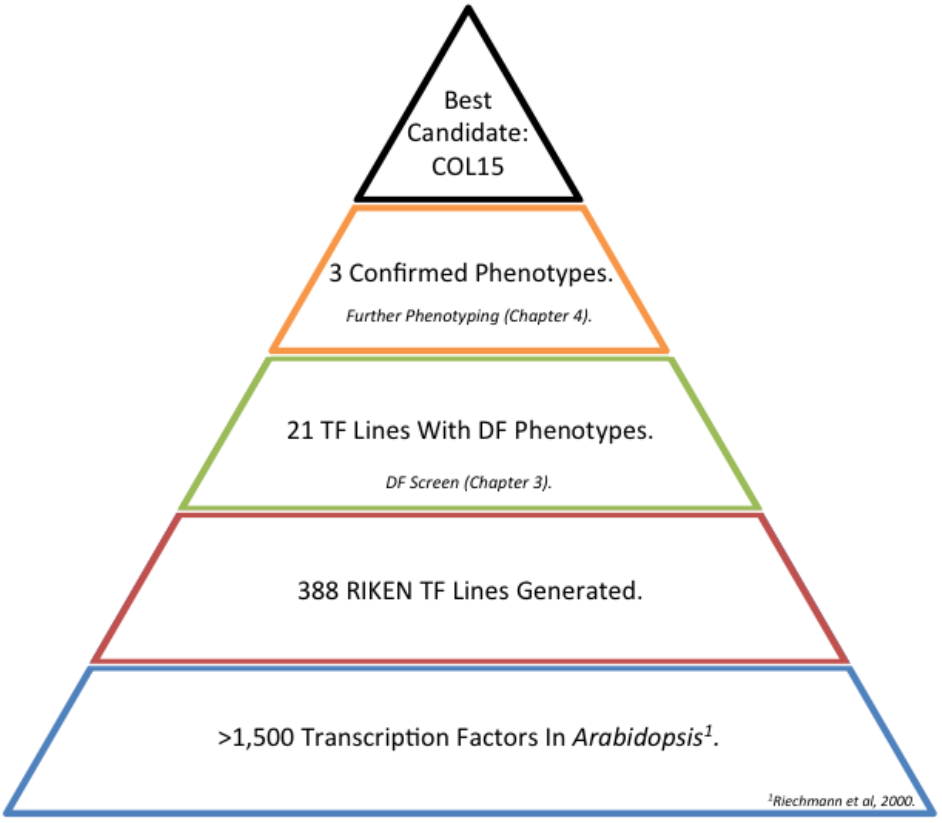

FIGURE 4.40: Project Overview

Three Tf line phenotypes were confirmed through LUC and DF screening. Factoring in SALK-DF, *in silico* and literature investigations, *COL15/BBX13* emerged as the best candidate for further study.

Chapter 5

Work at RIKEN

5.1 Introduction

During years two and three of the PhD project, I spent the time on a placement in Prof. Matsui's lab at RIKEN Yokohama. During this placement the luciferase transgenic lines were produced and much of the *in silico* work was carried out. Additionally, multiple experiments were attempted, including the monochromatic hypocotyl assay experiments outlined in Chapter 4.5. Other experiments were less successful. In this chapter the rationale, design, and outcomes of these experiments is outlined. It is envisioned that this chapter will show potential starting points for further work, as well as provide a record of the placement in Japan.

5.2 GFP Fusion

It was desirable to generate plants expressing GFP-tagged versions of COL15 (as well as the other genes of interest) for several reasons. As GFP fluoresces under light, and

several versions of GFP such as sGFP have been engineered to give higher fluorescence when expressed in plants Chiu et al. (1996), NIWA (2003), a tagged line would allow the study of protein dynamics and localisation.

There is some indication from the literature that COL15 is degraded by members of the LOV-KETCH PROTEIN family, which includes ZTL. COL15 is known to exhibit protein-protein interactions with the circadian regulators and F-box proteins LKP2 and ZTL (Fukamatsu et al., 2005). We hypothesise that COL15 interacts with ZTL *in planta*, and the colocalisation of COL15 with ZTL (as demonstrated, for example, through the use of a GFP-tagged COL15 in a YFP-tagged ZTL background) would further support this hypothesis.

The GFP-tag can also be used for antibody binding experiments using the engineered antibody anti-GFP Wang et al. (2014b). The Matsui lab recommended this moiety as an antibody target, and report successful use of GFP fusions for antibody pull down. Such a tag would allow the post-transcriptional dynamics of COL15 to be studied. As LKP2 and ZTL are mediators of protein degradation, we hypothesise that COL15 is regulated on the post transcriptional level. The GFP tag would allow the relative expression levels of COL15 throughout the circadian cycle in wild type and ZTL/LKP2-deficient varieties through Western blotting. Antibody binding would also allow investigation of COL15 transcription factor binding sites through Chromatin Immuno-Precipitation Sequencing (ChIP-Seq) and, hence, allow us to view the downstream COL15 regulome.

Additionally, developing a COL15-GFP fusion under the control of a GR cassette would allow us to view the effects of dexamethasone treatment and to study the dynamics of dexamethasone-mediated nuclear import, which is currently lacking in this study.

Due to resource constraints, a single gene was initially selected as a pilot for GFP-line generation. COL15 was selected for this experiment. After successful generation of a COL15-GFP line, it was was envisioned that the technique would be rolled out to other genes of interest. A COL15-GFP fusion protein under the control of a native promoter was selected as the goal of this work, as study of subcellular dynamics and degradation is needed the aforementioned experiments. The goal of the pilot was optimisation and proof-of-concept for the cloning techniques. It was envisioned that, once this line had been generated, a version under the control of the GR cassette could be made - for example, through introducing a GR cassette by restriction cloning at the start or end of the process.

5.2.1 Introduction to GATEWAY Cloning

The GATEWAY®cloning system developed by Invitrogen was chosen as the method of vector construction. The Matsui team had already used this technique successfully to create GFP fusion protein vectors (Shimada et al., 2015). GATEWAY cloning takes advantage of the integrases and recombinases used by bacteriophage lambda. The phage carries a DNA vector including a recombination site "attP". This is recognised by a recombinase, carried by the phage virion and encoded for by the phage vector), which catalyses the recombination with a recombination site "attB" found in the host genome. The vector is therefore inserted into the host genome, flanked by a new pair of recombination sites (attL and attR). This reaction is reverisble, as an attL and attR site can recombine to form an attB and attP site. The equilibrium of this reaction shifts throughout the phage infection cycle (Gottesman, 1999, Nash, 1977)

In the GATEWAY system, a DNA molecule of interest (for example, a gene) is flanked by two recombination sites - for example, a segment flanked by two attL sites. The sites

are directional and identical - unlike in the lambda phage, they cannot recombine with each other. This is mixed with a second DNA molecule carrying a corresponding pair of recombination sites - in our example, this would be two attR sites - and incubated with a recombinase. The recombinase catalyses the recombination between the two molecules and results in the intra-site regions switching. Often in GATEWAY cloning, the DNA molecules are circular vectors carrying selection markers, allowing the products to be sorted after recombination Hartley et al. (2000). This method is advantageous over traditional restriction-ligation mixes as it allows simple one-step recombinations.

Another advantage of GATEWAY cloning is that it is modular. In a first step, a PCR fragment encoding a gene of interest (or fragment thereof) flanked with attB sites is incorporated into a vector carrying a pair of attP sites. This is the "BP" or "TOPO cloning" step, as the recombinase mixture includes a topoisomerase. As attB and attP recombination results in attL and attR sites, the resulting "Entry vector" carries the gene of interest flanked by attL sites (the attR sites are on the PCR fragment). The Entry vector is then introduced into a "Destination vector" carrying attR sites. As the Entry vector is stable and can be stored in and generated from transformed bacteria, it can be used to introduce a gene of interest into multiple Destination vectors. In this way, generation of a suitable native promoter driven COL15 entry vector could be used to generate a variety of different fusion proteins through GATEWAY cloning.

The goal of the assembly was to generate a native promoter-driven COL15-GFP fusion protein. A *pCOL15:COL15* gene fragment lacking a STOP codon was generated through PCR and introduced into the GATEWAY Entry vector pDONR201 (Thermo Fisher Scientfic) This vector was used in experiments to introduce the fragment into GATEWAY Destination vector pGWB4, which incorporates an sGFP sequence immediately after the recombination site. The resulting target vector would be selected from the reaction

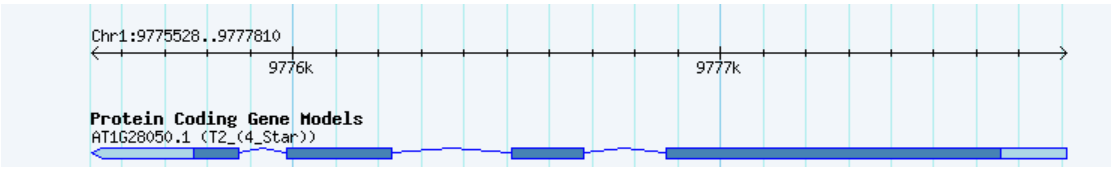

FIGURE 5.1: Genomic DNA sequence of *COL15 (AT1G28050.1)*.

Dark blue regions are coding sequence. Light blue regions are the 5'- and 3'-UTRs.

mix through positive and negative selection markers, isolated and confirmed. The target vector is suitable for transformation into *Arabidopsis*, particularly into a *col15* null mutant.

5.2.2 Generation of COL15 Gene Fragment

The first step in preparing the required construct is to design primers to isolate the sequence of interest for BP-TOPO cloning. This region consists of the stretch of *COL15* sequence including the promoter, but it is vital that is does not include the stop codon in the 3' UTR in order to generate a fusion protein.

First, the native promoter was identified. Genomic data for *COL15* was obtained from TAIR. The genomic DNA coding region for *COL15* has a length of 2283bp, with the open reading frame stretching from 154bp to 2043bp and the TAA stop codon lying at 2044-6bp. The promoter prediction tool ATHENA suggests that the first 500bp is enough to incorporate the TATA box, the Evening Element Binding Motif and the entire CpG island (see Figure 4.3e). On the advice of Dr Shimada, a 1000bp upstream region was selected as the promoter region - this region would definitely include the promoter and would offer a margin of safety if the predictions were wrong. Primers were designed using Primer3 (Untergasser et al., 2007).

The reverse primer (TopoCOL15R, 5.5) was generated first, as it is the least flexible in its positioning. A reverse complement of the 50bp upstream region of the target sequence

(i.e. the genomic sequence leading up to but not including the stop codon, from 1993-2043bp) was generated as a proto-primer. This primer was tested using PrimerBLAST and Tm Calculator. Bases were removed at the primer's 3' end (i.e. the 5' of the complementary target) until the Tm of the primer was approximately 60°C and, therefore, suitable for PCR.

The forward primer (TopoCOL15F, 5.5) was generated by designing a primer via Primer3 with a Tm of 60°C of (i.e. close to that of the reverse primer) that binds within the -3000bp and -1000bp region. This forward primer was prefaced by the 5' CACC- sequence needed for BP clonase-mediated TOPO cloning. The primers were tested with BLAST (blastn) against the *Arabidopsis* genome in order to show predicted binding sites, and to ensure that only one product will be amplified. The desired size of the amplified product is 3,358bp.

Full-length genomic DNA was extracted from wild type *Arabidopsis* plants and the resulting extraction cleaned through ethanol precipitation as outlined in the methods section. This DNA was used as a template for COL15 amplification using the high-fidelity proof-reading polymerase KOD-Plus-Neo (Toyobo Biosciences), with an annealing temperature of 59°C for a total of 45 cycles. The product was run out on agarose gel, and the gel band of the correct weight excised and purified using the Wizard SV gel cleanup kit 5.2.

5.2.3 BP/TOPO Cloning of COL15 Entry Vector

BP-Clonase TOPO cloning was carried out according to manufacturer's instructions (and as outlined in the methods section). The supplied controls were performed - the kit provides template DNA and primers, as well as primers for confirmation of the resulting

FIGURE 5.2: PCR to Obtain *pCOL15:COL15* Fragment

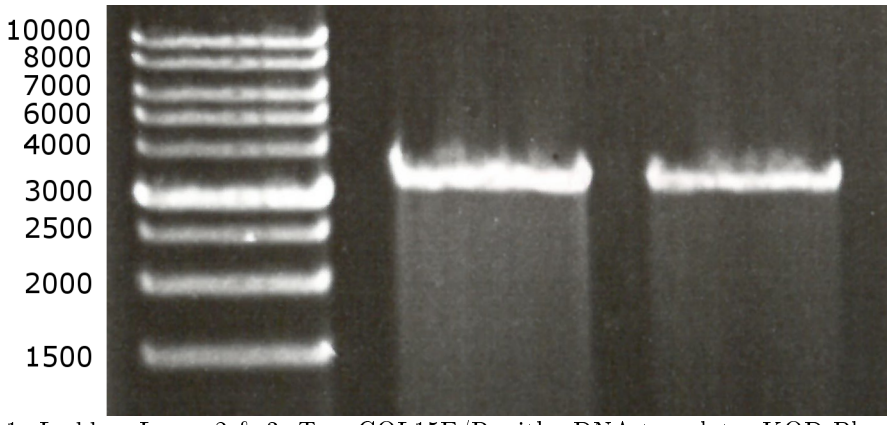

Lane 1: Ladder. Lanes 2 & 3: TopoCOL15F/R with gDNA template. KOD-Plus-Neo, 45 cycles, run on 1.5% agarose gel for 30 minutes. Target product size = 3,358bp. Gel bands were then excised and cleaned-up via Wizard SV Gel Cleanup Kit.

vectors. Following the BP-clonase reaction he molar ratio of pDONR201:PCR product was adjusted to 2:1 in a 2.5μl reaction volume.

The whole reaction transformed into *E. coli*and plated onto 50μg /ml kanamycin selection plates to select for pDONR201, which carries a kanamycin resistance gene. Unreacted pDONR201 was not transformed into the bacteria, as the TOPO cloning reaction does not produce a viable vector in the absence of recombination.

The resulting reaction gave a total of 24 colonies on the test plate (and 31 colonies on the in-kit control plates). These colonies were grown overnight in kanamycin-laced media before vector recovery through miniprep.

Seventeen of these samples were sent for sequencing with the M13F and M13R primers supplied in the kit, as well as with a forward primer which bound in the COL15 sequence (TOPOcheckF2).

Sequencing was carried out through RIKEN's in-house sequencing service. On receiving the results, the quality of the sequence was analysed through viewing the spectrum trace in the BioEdit software suite and the sequences were analysed through BLAST

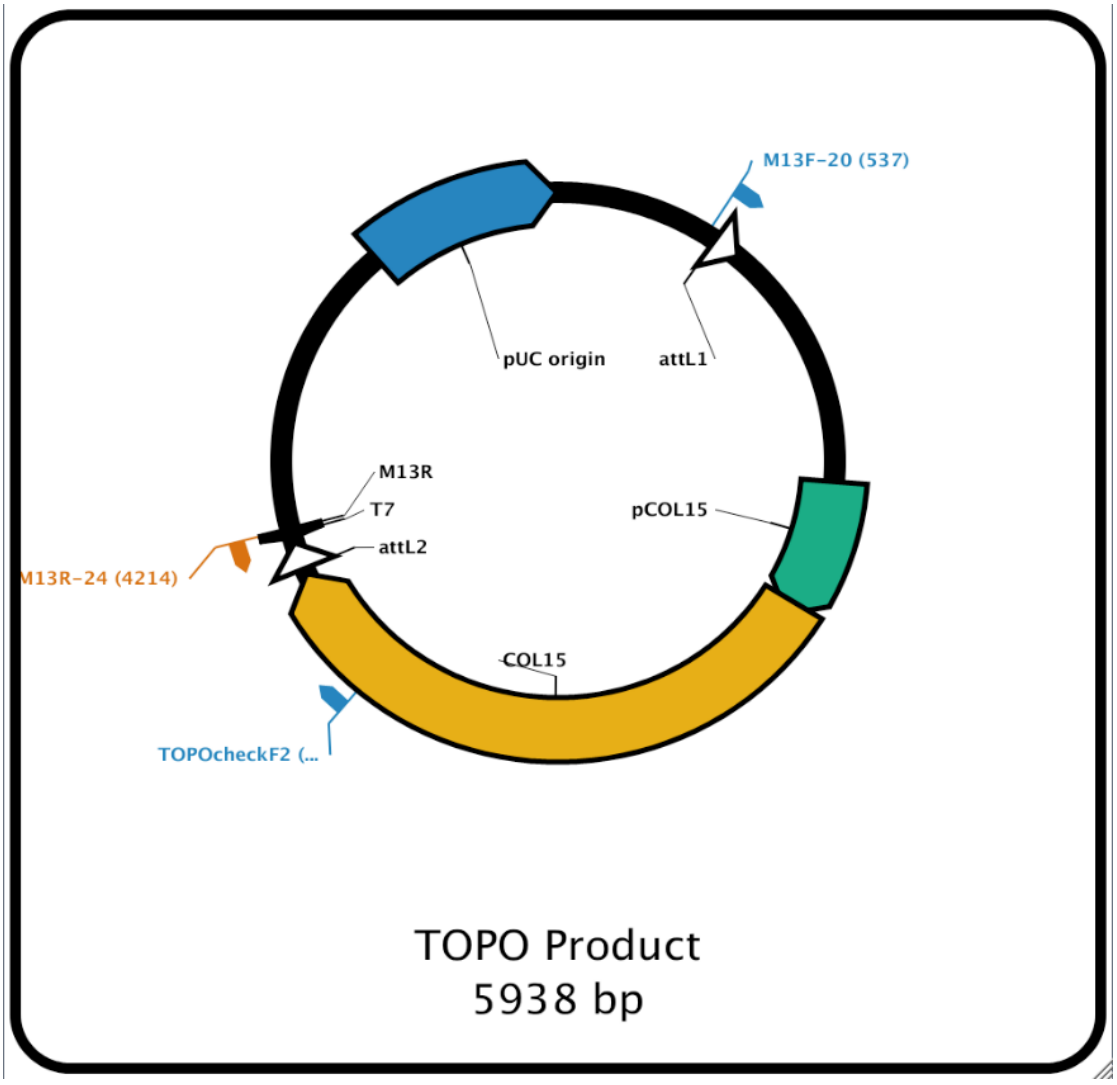

FIGURE 5.3: Binding Sites of Sequencing Primers on the TOPO-Cloning Product.

(megablast, optimised for highly similar sequences). Sequences were initially compared against the full nucleotide collection. Results of the sequencing can be seen in Tables 5.1 and 5.2.

Of the 17 colonies sequenced, four produced sequencing results that matched all four expected sequences. Of these, one contained a deletion in the sequence (Topo17) and was therefore omitted as unreliable. The sequencing results for the remaining three candidates, along with the target *pCOL15:COL15* sequence, were aligned with the target vector backbone. As is clear from the vector map (Figure 5.3), a correctly-orientated

vector should have the sequences generated from the M13F primer aligning 5'-3' at the 5' end, sequences generated from M13R/M13Rss aligning 3'-5' at the 3' end, and TopoCheckF2 aligning 5'-3 at the 3' end.

TABLE 5.1: Results of TOPO-Product Sequencing, Aligned Against Full Nucleotide Collection Via BLAST (blastn).

ID	Template	Primer	Hits	Identity
1	Topo1	M13R	Vectors	
2	Topo2	M13R	Vectors	
3	Topo3	M13R	Vectors	
4	Topo4	M13R	Vectors	
5	Topo5	M13R	COL15	100.00%
6	Topo6	M13R	Vectors	
7	Topo7	M13R	NNNN	
8	Topo8	M13R	Vectors	
9	Topo9	M13R	Vectors	
10	Topo10	M13R	Vectors	
11	Topo11	M13R	COL15	99% (mismatch one base)
12	Topo12	M13R	COL15	100.00%
13	Topo13	M13R	COL15	99% (mismatch one base)
14	Topo14	M13R	Vectors	
15	Topo15	M13R	Vectors	
16	Topo16	M13R	Vectors	
17	Topo1	M13F	Vectors	
18	Topo2	M13F	Vectors	
19	Topo3	M13F	Vectors	
20	Topo4	M13F	Vectors	
21	Topo5	M13F	NNNN	
22	Topo6	M13F	Vectors	
23	Topo7	M13F	NNNN	
24	Topo8	M13F	Vectors	

Continued on next page

Table 5.1 – *Continued from previous page*

ID	Template	Primer	Hits	Identity
25	Topo9	M13F	Vectors	
26	Topo10	M13F	Vectors	
27	Topo11	M13F	COL15	100.00%
28	Topo12	M13F	COL15	100.00%
29	Topo13	M13F	COL15	93% (67/72, mismatches)
30	Topo14	M13F	Vectors	
31	Topo15	M13F	Vectors	
32	Topo16	M13F	Vectors	
33	Topo1	M13Rss	Vectors	
34	Topo2	M13Rss	Vectors	
35	Topo3	M13Rss	Vectors	
36	Topo4	M13Rss	Vectors	
37	Topo5	M13Rss	COL15	100% (436/436)
38	Topo6	M13Rss	Vectors	
39	Topo7	M13Rss	Vectors	
40	Topo8	M13Rss	Vectors	
41	Topo9	M13Rss	Vectors	
42	Topo10	M13Rss	Vectors	
43	Topo11	M13Rss	COL15	99% (mismatch one base)
44	Topo12	M13Rss	COL15	100.00%
45	Topo13	M13Rss	COL15	99% (mismatch one base)
46	Topo14	M13Rss	Vectors	
47	Topo15	M13Rss	Vectors	
48	Topo16	M13Rss	Vectors	
49	Topo1	TopoCheckF2	Vectors	
50	Topo2	TopoCheckF2	NNNN	
51	Topo3	TopoCheckF2	NNNN	
52	Topo4	TopoCheckF2	NNNN	

Continued on next page

Table 5.1 – *Continued from previous page*

ID	Template	Primer	Hits	Identity
53	Topo5	TopoCheckF2	Vectors	
54	Topo6	TopoCheckF2	Vectors	
55	Topo7	TopoCheckF2	Vectors	
56	Topo8	TopoCheckF2	NNNN	
57	Topo9	TopoCheckF2	NNNN	
58	Topo10	TopoCheckF2	NNNN	
59	Topo11	TopoCheckF2	Vectors	
60	Topo12	TopoCheckF2	Vectors	
61	Topo13	TopoCheckF2	Vectors	
62	Topo14	TopoCheckF2	NNNN	
63	Topo15	TopoCheckF2	NNNN	
64	Topo16	TopoCheckF2	NNNN	
65	Topo17	M13R	COL15	99% (deletion, one base in insert)
66	Topo17	M13F	COL15	100% (449/449)
67	Topo17	M13Rss	COL15	99% (deletion, one base, same as 65)
68	Topo17	TopoCheckF2	Vectors	
69	dH2O	M13R	NNNN	
70	dH2O	M13F	NNNN	
71	dH2O	M13Rss	NNNN	
72	dH2O	TopoCheckF2	NNNN	

Table 5.2: Grid-View of Results of TOPO-Product Sequencing.

Topo Vector:	1	2	3	4	5	6	7	8	9	10	11	12	13	14	15	16	17
M13R	V	V	V	V	C	V	N	V	V	V	C	C	C	V	V	V	C
M13F	V	V	V	V	N	V	V	V	V	V	C	C	C	V	V	V	C
M13Rss	V	V	V	V	C	V	V	V	V	V	C	C	C	V	V	V	C
TopoCheckF2	V	N	N	N	V	N	V	N	N	N	V	V	V	N	N	N	V
Result:	1/4	0/4	0/4	0/4	3/4	0/4	0/4	0/4	0/4	0/4	4/4	4/4	4/4	0/4	0/4	0/4	4/4

Methodology as per Table 5.1. Key: V = Vector, C= Col15 N = No Result.

As we can see, the candidate Topo12 fulfils these criteria. Topo12 also shares 100% identity with the target sequence, with no deletions, substitutions or insertions, unlike the other candidates (see Table 5.1). Topo12 was selected for further analysis and is suitable for LR Recombination (Figure 5.4b).

5.2.4 Destination Vector pGWB4

The pGWB4 vector is a GATEWAY binary vector for the generation of sGFP-tagged genes in a T-DNA vector suitable for transformation of plants Nakagawa et al. (2007) (Figure 5.4c). A vector resulting from the LR reaction with this vector carries would be suitable for expression in *Agrobacterium* and transformation of the COL15 sequence into *Arabidopsis* as it carries T-DNA sites (Figure 5.4d).

The destination vector pGWB4 carries hygromycin (HygR) and kanamycin (TrfA) resistance genes as positive selection markers. It also carries a ccdB negative selection marker between the two attR sites. Recombination of the Entry vector with pGWB4 results in an Entry vector which is lethal in bacteria lacking the "antidote" gene ccdA (Wang et al., 2014a). As a result, recombined pGWB4 carrying the COL15 insert can be separated from un-recombined pGWB4, un-recombined Entry vector, and recombined Entry vector carrying ccdB by transformation into a ccdA-negative *E. coli*strain and plating on hygromycin-kanamycin dual selection media.

Stocks of destination vector were made through transformation into OneShot®ccdB Survival *E.coli* (Invitrogen). These cells do not find ccdB lethal. The transformed bacteria were plated onto hygromycin-kanamycin selection media and incubated for 2 days at 38°C before isolating individual colonies. Overnight culture of 5 colonies were made

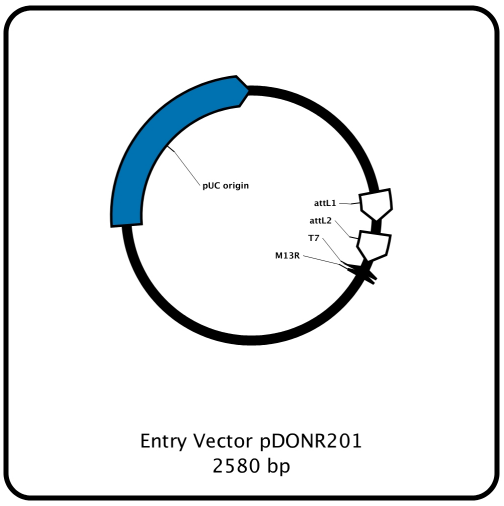

(A) Empty Entry vector pDONR201.

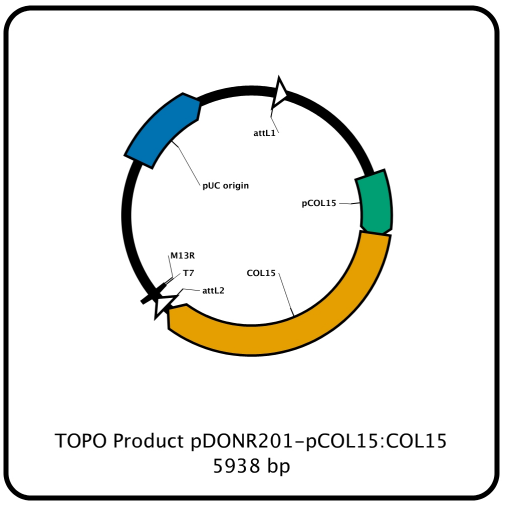

(B) Result of BP-TOPO cloning.

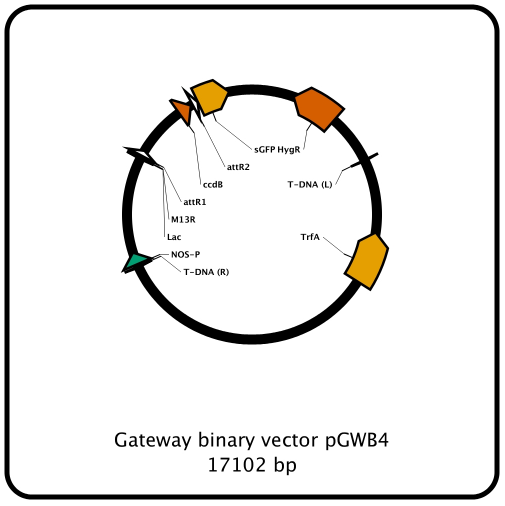

(C) pGWB4 Destination vector as described in Nakagawa et al. (2007)

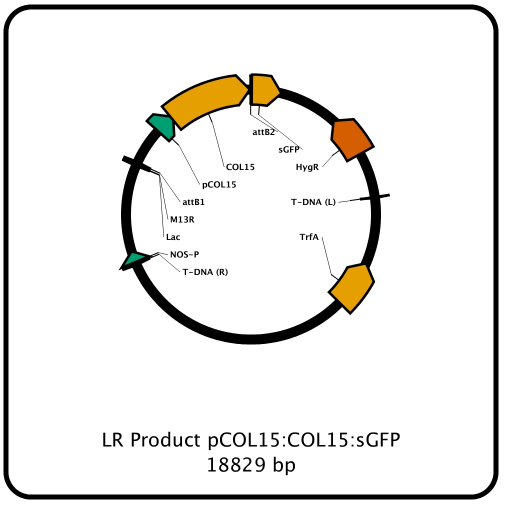

(D) Final Vector, pCOL15:COL15:sGFP, following GATEWAY Cloning.

FIGURE 5.4: Overview of GATEWAY Cloning.

Through BP-cloning, a target PCR product is incorporated into the Entry vector pDONR201 (5.4a). This vector (5.4b) can recombine with the Destination vector pGWB4 (5.4c) through LR cloning to produce a vector containing a sGFP-fusion protein (5.4d).

in LB media with antibiotics. Vectors were isolated by miniprep, and their identity confirmed by PCR (Figure 5.5).

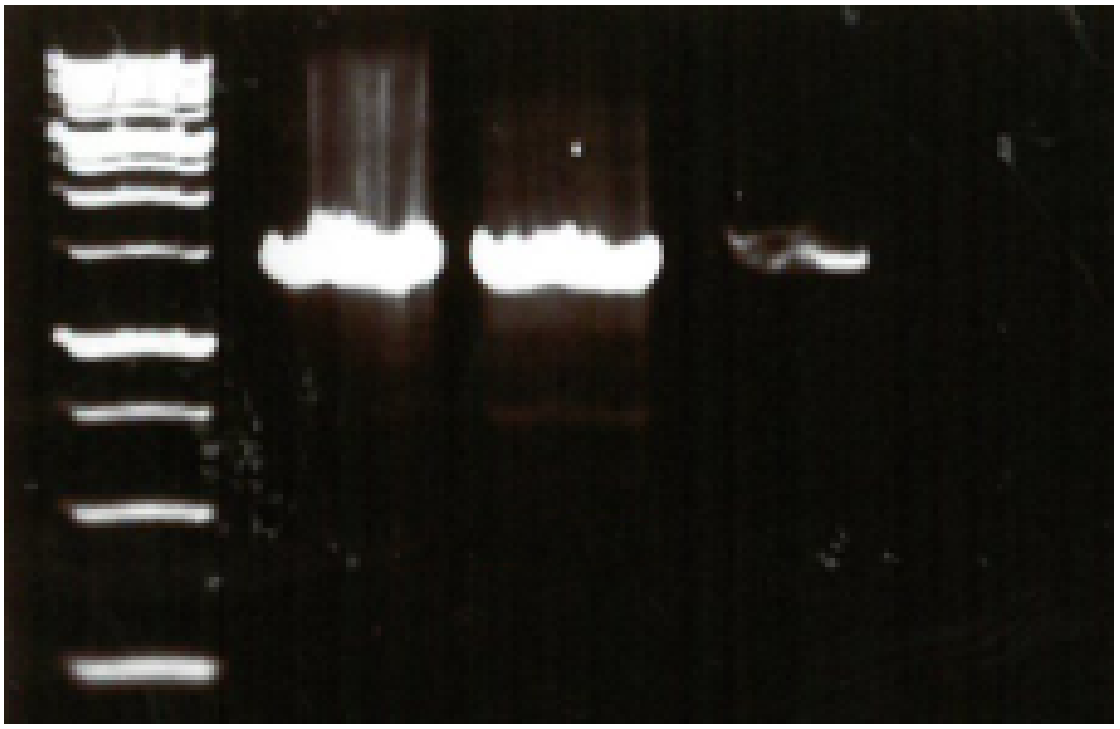

FIGURE 5.5: Confirmation PCR of pGWB4 miniprep.

DNA samples were obtained from plasmid Miniprep and PCR performed, as outlined in Chapter 2. Samples left to right are: lane 1 - ladder; lane 2 - pGWB4 colony 1; lane 3 - pGWB4 colony 2; lane 4 - pGWB4 colony 1 + 2, combined and cleaned-up using the ethanol precipitation method in Chapter 2. Primers were "CheckF/CheckR", expected product length = 1570bp. 1kb Ladder, weights from bottom: 250bp, 500bo, 1000bp, 1500bp, 2000bp, 2500bp, 3000bp.

5.2.5 LR Reaction

The LR reaction was performed by mixing the entry and destination vectors, and incubating in the presence of LR clonase. pENTR-GUS LR reaction control were performed, as per the manufacturer's instructions. Reactions were terminated by treatment with Proteinase K, and the whole resulting reaction mixture transformed into DH5α *E.coli*, which is ccdB-sensitive. Transformants were plated onto Kanamycin-Hygromycin selection media and incubated as before. Resulting colonies were restreaked onto selection plates, grown in culture and the plasmids recovered by Miniprep. The resulting plasmids were sequenced in-house using the TOPOCheckF2 primer described previously, as well as with the sequencing primers from Nakagawa et al. (2007).

A general LR protocol is given in Chapter 2, however a variety of reaction conditions were attempted as reproduced in Table 5.3).

The experiment was initially attempted according to the manufacturer's instructions. Invitrogen recommend using between 100 and 300ng of entry vector to 300ng of destination vector, in a 20μl reaction volume. In subsequent reactions, the protocol used at RIKEN was consulted. Dr Shimada frequently extended the reaction time for Gateway reactions involving large vectors. She also performed these experiments in a smaller reaction volume, with 1:3 ration Entry:Destination vector, in order to increase the transformation rate (conditions 3-5). Additionally, the protocol provided by Dr Shimada was adapted to correct for the differences in relative size between the two vectors (Conditions 6-8). As the Entry vector is 6kbp, and the destination vector 17kbp, a 1:3 molar ratio is closer to a 1:10 ratio by weight. Many of these reactions were attempted several times.

Finally, and additionally, conditions 6-8 were also performed with a linearised pGWB4. Whilst the current protocols supplied with Gateway kits note that linearisation does not have a significant effect on efficiency, previous versions included this step. As many protocols and practitioners still reccommend destination vector linearisation for increasing efficiency, *XhoI* was used to digest pGWB4 a the site outlined in Nakagawa et al. (2007).

Table 5.3: LR Reaction conditions

Exp.	Entry:Dest.	Reaction vol.	Incubation (25°C)	Notes
1	300ng:300ng	20μl	1hr	As manual
2	100ng:300ng	20μl	1hr	As manual
3	25ng:75ng	5μl	1hr	
4	25ng:75ng	5μl	2hr	
5	25ng:75ng	5μl	Overnight	Shimada protocol
6	10ng:90ng	5μl	1hr	Equimolar
7	10ng:90ng	5μl	2hr	Equimolar
8	10ng:90ng	5μl	Overnight	Equimolar

On the vast majority of plates, no colonies at all could be found. The plates that did yield colonies had very few - typically < 10, whilst the Gateway manual indicates 10-100 colonies are typical - however this is not atypical when working with large Entry vectors. This low colony count was observed with all reaction conditions, both for the experimental and control reactions. There was no observable effect on colony number of increasing incubation time or of performing restriction digest. As the transformation control (pUC19, plated onto kanamycin, as supplied in the Gateway kit) had a high transformation rate with hundreds of colonies, and the mock transformation (with an equal volume of water) yielded none, the transformation protocol was shown to be successful.

In total, 23 colonies were recovered and sequenced. Of these, eight were from the LR control reactions (i.e. pENTR-GUS x pGWB4) None returned sequences indicating that they were successful LR reaction products.

5.3 Yeast 2-Hybrid

Another line of inquiry explored in RIKEN was the protein-protein interactions of the genes of interest. Many plant transcription factors function in protein complexes (Gonzalez, 2016). These complexes rely on protein-protein interactions for proper formation and, hence, function. Within the circadian clock, LHY and CCA1 physically interact (Lu et al., 2009). Similarly, PRR9, PRR7, and PRR5 physically interact with a transcriptional corepressor, TOPLESS, to inhibit expression of CCA1 and LHY (Wang et al., 2013). Additionally, ZTL regulates TOC1 protein levels through protein-protein interactions, and is in turn regulated by physical interaction with PRR3 (Más et al., 2003, Para et al., 2007). As mentioned previously, there is putative evidence that COL15 interacts

with LKP2 and/or ZTL *in vivo* (Fukamatsu et al., 2005). Identifying protein binding partners of the genes of interest in order to gain clues to their mechanism of circadian regulation was therefore seen a potentially fruitful avenue of research.

Yeast 2-Hybrid screening was selected as an assay for investigating these interactions. The basic premise of Yeast 2-Hybrid relies on the fact that the DNA binding and transcription-activation domains of the yeast transcription factor *GAL-4* can function in close proximity even if they are not physically connected within a contiguous protein. The *GAL-4* DNA binding domain is fused to a "bait" protein. This fusion can bind the GAL4 promoter, but does not drive transcription. The activation domain is fused to "prey" proteins - this second fusion cannot bind the promoter but is capable of driving transcription. When the bait and prey proteins interact physically - for example, when they represent factors which form a heterodimer *in vivo* - the activation and DNA binding domains are brought into close enough proximity that transcription is possible. The yeast cells are engineered such that transcription from the GAL4 promoter drives one or more selection markers - typically survival markers such as the ability to synthesise certain amino acids.

A useful feature of the yeast *Saccharomyces cerevisiae* utilised by the screening technique is that it ie capable of mating. Haploid yeasts have of two "mating types", denoted a or α. Essentially, cells of each type express a mating pheromone and a surface receptor for the pheromone of the opposite mating type. When combined, the two mating types combine to form a diploid yeast. In 2-hybrid screening, the bait fusion protein is introduced in one mating type, whilst a library of prey proteins is expressed in the opposite type. By combining and mating the two strains, then selecting for GAL-promoter driven survival factors, it is possible to assay a large library of prey proteins in a single reaction.

The surviving yeasts can then be identified by DNA sequencing.

5.3.1 Generation of Bait Plasmids

Bait plasmids were generated through Gateway cloning. The destination vector pGBD is a modified pGBKT7 vector incorporating a Gateway cloning site and ccdB negative selection marker. It was generated at RIKEN previously, and carries chloramphenicol and kanamycin resistance markers for positive selection in *E.coli*, as well as a ccdB selection marker for negative selection of non-recombined vectors. In yeast, the plasmid carries a tryptophan survival marker - that is to say, it is capable of growing on media lacking tryptophan.

An initial five lines were used as a proof-of-concept, selected from the genes of interest identified by DF screening. These lines were chosen as there were large amounts of cDNA entry vector stocks in storage. These experiments were carried out before the further phenotyping in Chapter 4. The lines used were*IAA11* (T0189), *ANAC087* (T0649), *HAP2B* (T0825), *HRS1* (T0840) and BBX13/COL15 (T1082).

Gateway LR cloning was performed according to the manufacturer's instructions (as outlined in Chapter 2). The reaction was terminated with Proteinase K and transformed into DH5α *E.coli* for selection on plates laced with chloramphenicol and kanamycin. Bait fusion vectors were recovered by miniprep and confirmed by sequencing with M13R and F sequencing primers. All five genes were successfully cloned (Table 5.4).

TABLE 5.4: Sequencing Results for Yeast Bait Plasmid LR Gateway Reaction

Entry Vectors	Primer	Lower c/o	Upper c/o	BLAST Hits	Success?
IAA11	M13F	50	700	Arabidopsis thaliana auxin-responsive protein IAA11 (AT4G28640) mRNA, complete cds	Y
IAA11	M13R	60	600	Arabidopsis thaliana auxin-responsive protein IAA11 (AT4G28640) mRNA, complete cds	Y
ANAC087	M13F	30	800	Arabidopsis thaliana NAC domain containing protein 87 (AT5G18270) mRNA, complete cds	Y
ANAC087	M13R	80	480	Arabidopsis thaliana NAC domain containing protein 87 (AT5G18270) mRNA, complete cds	Y
HAP2B	M13F	60	700	Arabidopsis thaliana heme activator protein (yeast) homolog 2b (HAB2B, At3g05690) mRNA, complete cds	Y
HAP2B	M13R	30	550	Arabidopsis thaliana heme activator protein (yeast) homolog 2b (HAB2B, At3g05690) mRNA, complete cds	Y
HRS1	M13F	50	730	Arabidopsis thaliana myb-like transcription factor family protein (HRS1, AT1G13300) mRNA, complete cds	Y
HRS1	M13R	50	750	Arabidopsis thaliana myb-like transcription factor family protein (HRS1, AT1G13300) mRNA, complete cds	Y
COL15	M13F	40	730	Arabidopsis thaliana zinc finger protein CONSTANS-LIKE 15 (AT1G28050) mRNA, complete cds	Y
COL15	M13R	50	900	Arabidopsis thaliana zinc finger protein CONSTANS-LIKE 15 (AT1G28050) mRNA, complete cds	Y

Samples were sent for sequencing at RIKEN's in-house service. 500ng of plasmid was combined with 3.2 pm primer and 1μl reaction enzyme mix in a 10μl sample. Results were visualised with BioEdit, and the upper and lower cut offs set where the amplitude of signal intensity dropped below the noise line (set at 50 relative intensity units). The remaining sequence data was analysed with BLAST to find the gene with closest homology *Arabidopsis*. All samples had at least 99% homology with their closest hit sequence.

5.3.2 Transformation into Yeast

The bait fusion vectors were transformed into the yeast strain AH109 (James et al., 1996). This strain is provided by Clontech for use with their Matchmaker Gold®Mate and Plate system. It carries survival selection markers for methionine and uracil deficient SD minimal media, and is ampicillin resistant. It carries *ADE2*, *HIS3* and *MEL1* are under the control of GAL4. These genes are activated by binding of bait and prey following mating. They provide survival on adenine and histadine deficient media, as well as *alpha*-galactosidase as a positive selection marker. Clontech also provide a library comprising *Arabidopsis* transcription factor cDNAs fusions in the yeast strain Y187, for use as prey in screening.

Transformed yeast was plated onto SD -Trp media to select for transformants. Media was supplemented with ampicillin to prevent growth of bacteria during incubation. These plates were infused with the chromogenic substance 5-bromo-4-chloro-3-indolyl alpha-D-galactopyranoside (X-α-gal) which has a distinctive blue colour when hydrolised by MEL1. X-α-gal was included to confirm that the bait plasmids were not self-activating.

The destination vector pGBD was used as a positive control for transformation, as it carries the same tryptophan survival phenotype as the recombined vectors. A volume of water was used as a negative control for nutrient selection. If plates had no colonies, transformation did not occur. If colonies grew on plates, then the transformation was successful. If the colonies turned blue, the construct is auto-activating in yeast and therefore cannot be used for library screening. As can be seen in Figure 5.6, the COL15 bait plasmid was auto-activating in yeast. Despite the fact that all other lines were successfully transformed and not shown to be auto-activating, the decision was taken not to pursue the experiment further. Without the primary gene of interest, the cost of the

FIGURE 5.6: Auto-activation of COL15 (T1082) Bait Plasmids.

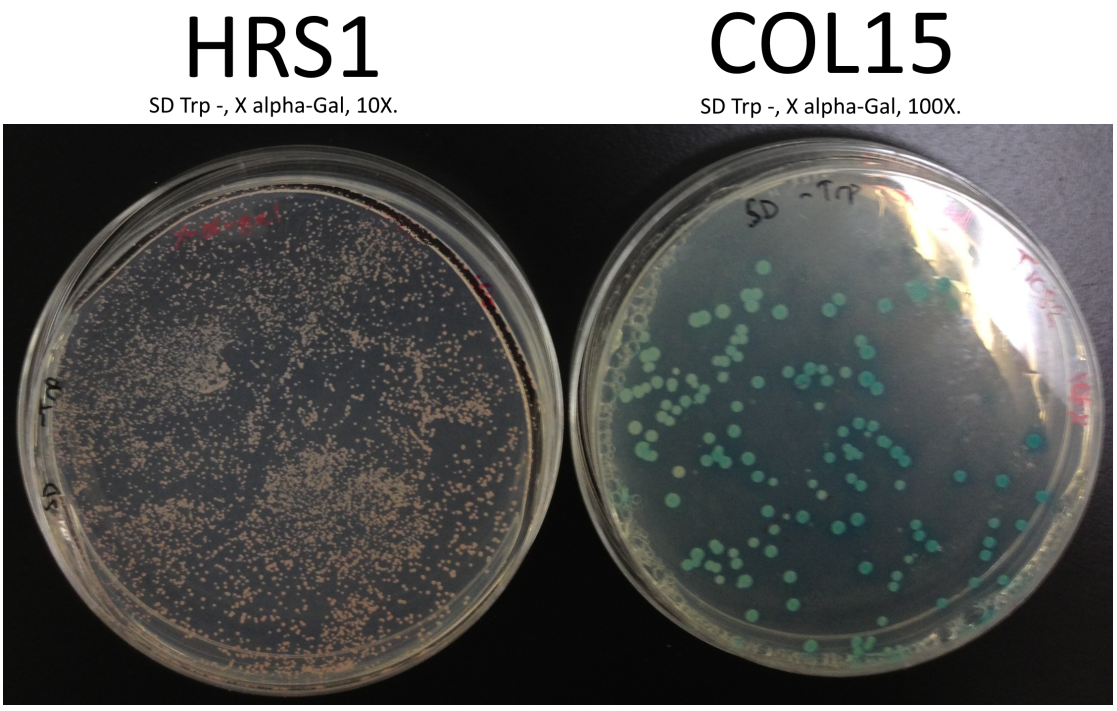

Yeast strains were plated onto SD -Trp media supplemented with ampicillin and incubated at 30°C for 72hrs. Prior to plating and incubation, plates were surface-infused with 100μl of 4mg/ml X-α-gal dissolved in dimethylformamide and incubated overnight at 30°C to drive off solvent. Blue colonies indicate that COL15 (T1082) is auto-activating in AH109, whilst HRS1 (T0840) is not. Remaining lines are omitted for clarity.

prey plasmid libraries could not be justified by the lab in RIKEN and the experiment was deemed no longer viable.

5.4 RNA Microarray

In addition to the protein dynamics of COL15, the transcription factor activity was investigated. Transcription factors regulate the transcription of distinct sets of genes, through which they exert their effect. By identifying the genes whose expression is affected in COL15 over-expression and knock outs, we can hopefully identify the causal agents of its observed circadian effect.

Microarray analysis was chosen as a technique for investigating this aspect. Microarrays allow the simultaneous measurement of tens of thousands of messenger RNA (mRNA) transcripts for gene expression. The intention was to cast an initial "wide net", covering all genes whose expression is perturbed when COL15 levels are altered. This would identify genes which are regulated by COL15, as well as genes several stages downstream. Once genes are identified, the nature of their regulation can be investigated by, for example, demonstrating direct COL15 promoter binding by DNA pulldown and EMS (Electrophoretic Mobility Shift Assay), or investigating transcriptional ability through reporter assays.

The intention was to perform the experiment for five genetic conditions (a wild type, two independently transformed COL15-GR lines, and two independent SALK *col15* lines), in both dexamethasone treated and untreated conditions, in triplicate. However, RIKEN initially allocated funds that would allow just eight samples to be investigated. Therefore, the five genetic conditions were selected, with a single repeat, in dexamethasone treated conditions. The hope was that, upon seeing evidence that the techniques could be carried out, and preliminary results showing a putative transcription factor regulome, RIKEN would allocate more funds to allow further replication.

5.4.1 Plant Material and Sampling

Five plant ecotypes were used. A wild type (Col-0) was used as a reference. Two *col15* null lines (the SALK lines N655685 and N666438) were used to investigate the effect of knocking out *COL15*. Finally, two *COL15* GR/TF lines were used. These were grown to T3 non-segregating seed (as verified through kanamycin resistance screening). To induce the transcription factors, the lines sprayed with dexamethasone as outlined before. Samples were treated with dexamethasone at ZT+7 of the 13th day of growth and harvested

at the same time as the 14th day, as this was analogous to the timing of dexamethasone application in the initial screening experiments (which, at this point, were the only data available). Six samples of each condition were harvested, of these three were RNA extracted.

5.4.2 RNA Extraction and Quality Control

RNA was extracted using the RNeasy kits, as outlined in Chapter 2. Clean-up was performed first using DNase I digest in order to remove DNA from the samples. A second clean-up to remove carbohydrates and proteins was performed using phenol chloroform. The concentration of the thoroughly cleaned RNA was checked by nanodrop as an indicator of stability before carrying out the protocols in the Agilent One Color RNA Spike-In Kit. This kit provide positive controls for monitoring RNA levels and integrity from sample amplification and labeling all the way to microarray processing. It consists of a set of positive control transcripts optimized to anneal to complementary probes on the microarray, providing a sample reference.

Following Spike-In labelling, RNA quality was analysed through BioAnalyser (Agilent) chip-based capillary electrophoresis. This gives an indication of RNA degradation, as well as of the efficiency of the Spike-In reaction. However, as can be seen in Figure 5.7a, the resulting RNA was degraded.

On the second attempt, the techniques were modified to increase RNA fidelity. During extraction, the quantity of plant material was increased , and an additional ethanol wash of the RNA pellet introduced. The total amount of RNA used for labelling was increased to 1000ng on the recommendation of Dr Kurihara, a member of Prof. Matsui's lab with

experience in microarrays. Despite increasing the amount of RNA, the protocol for 200ng RNA labelling was used unchanged. Normally, the protocol uses 1μl of Spike-Mix RNA for every 100ng of total RNA in the labelling reaction up to 500 ng, with an additional 0.5μl for every 100ng total RNA above 500ng. As such, Dr Kurihara recommends using approximately four times as much RNA for the amount of spike in mix as recommended by the kit manufacturer. The rest of the protocol remained unchanged. As can be seen in Figure 5.7b, the resulting RNA was of much higher quality than previously obtained.

5.4.3 Microarray Pilot

RNA samples were labelled and the microarray performed. Due to a limited availability of microarray chips, only the dexamethasone treated samples were used, with two biological replicates of each biological condition. No technical replicates were performed at this time - the intention was to subsequently repeat the experiment to add further replication. Data were analysed with Genespring GX (Agilent Technologies). The first stage in the analysis pipeline is a quality control stage. The controls introduced in the Spike-In reaction are analysed in six categories, as outlined in methods. This immediately flagged one repeat of *col15-1* as falling outside the acceptable range of all five quality controls (detection limit = 4.1, abs. Ela slope = 0.78, gSpatial = 246, gNeg CH/Met = 149, gNeg CH Sub Sig. = 158). This was corroborated by the intensity Box Whisker plot (Figure 5.8). In this plot, normalised intensity values for each sample are displayed, in order to investigate their distibution. A tight interquartile range is expected, indicating a cluster of housekeeping genes, with a number of individual transcripts outside the box highlighted in red, indicating transcripts which are up- or down- regulated. The broad interquartile range observed for the first repeat of *col15-1* is atypical for intact RNA. It

FIGURE 5.7: Analysis of RNA Integrity With BioAnalyser

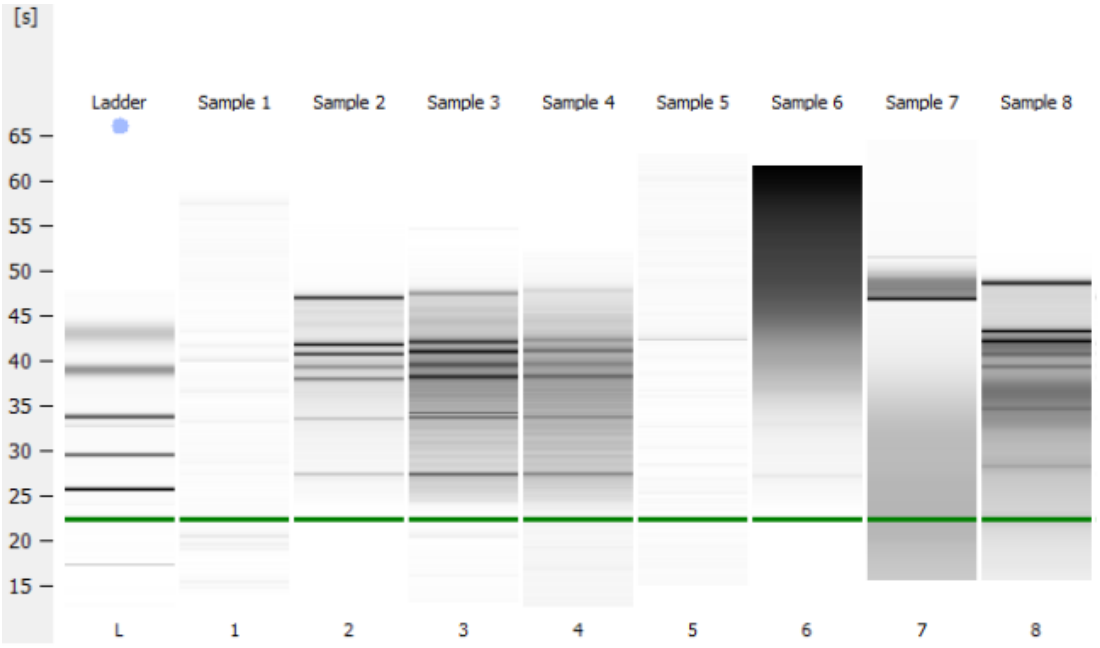

(A) First Attempt, Normal Protocol

(B) Second Attempt, Modified Protocol

Samples for Gel 1 were run following RNA extraction, DNase I and Phenochloroform clean-ups, and One Color Spike-In reaction. "Pre-clean" samples (Second Attempt) were run following RNA extraction, in order to elucidate whether RNA degradation occurred during extraction or subsequent sample processing. All samples were dexamethasone treated and harvested as outlined above. Clear, crisp bands show high quality RNA with little degradation.

Lane IDs - Figure A: Wild type x2, *COL15*-TF1, *COL15*-TF2, *col15-1*, *col15-2*. Figure B: Wild type pre-clean, *COL15*-TF1 pre-clean, *COL15*-TF2 pre-clean, *col15-1* pre-clean, *col15-2* pre-clean, dH20 negative control, Wild type, *COL15*-TF1, *COL15*-TF2, *col15-1*. Replicates have been ommitted for clarity.

FIGURE 5.8: Microarray Quality Control Boxplots.

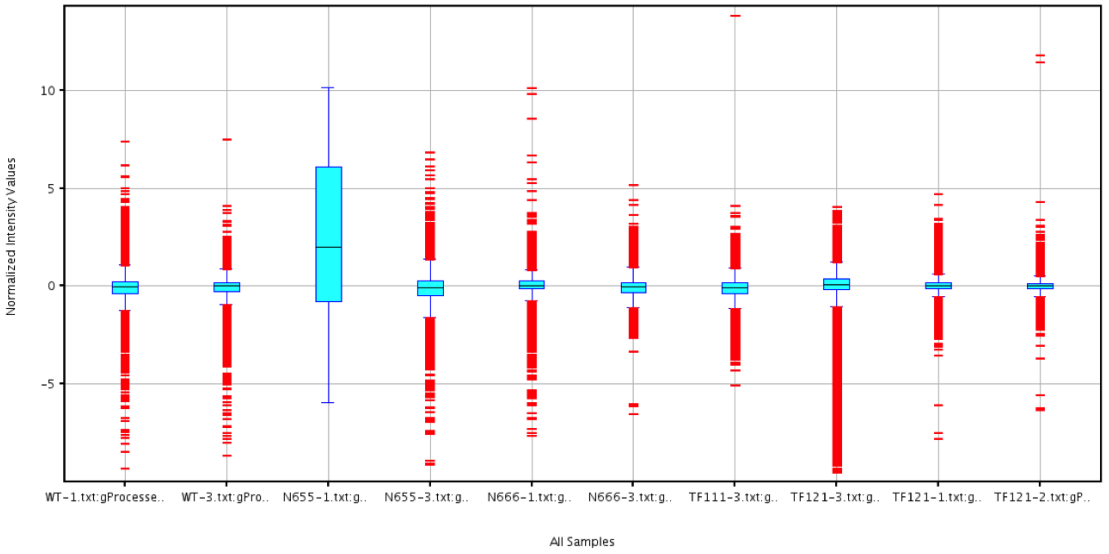

The distribution of normalised intensity values for each sample is displayed in the box-whisker plot. Samples are base-lined to the median of all samples. Entities with intensity values beyond 1.5 times the inter-quartile range are shown in red. Samples left to right are: WT repeats 1 & 2, *col15-1* repeats 1 & 2, *col15-2* repeats 1 & 2, *COL15*-TF1 repeats 1 & 2, *COL15*-TF2 repeats 1 & 2.

indicates degradation in the sample preparation, and as such this sample was omitted from further analysis.

An initial analysis was performed using One-Way ANOVA with a p value cut off of p=0.05. Three groups were compared to each other - the TF lines, the SALK lines, and the wild types. This comparison was expected to show a host of transcripts which are differentially expressed as a result of *COL15* over-expression and knock out. However, instead, only two probe identities were returned as significantly differentially regulated in the conditions:AT5G24240 (Phosphatidylinositol 3-& 4- kinase; a ubiquitin family protein involved in protein degradation) and AT1G22790 (unknown protein).

By this time, the placement in Japan was drawing to an end. The data were transferred to Liverpool for further analysis. It was felt, upon return to Liverpool, that the amount of time and resources required to perform more microarray experiments and to carry out

the analysis far outstripped their merits. This was especially true as the remaining plant and RNA samples could not be brought back from Japan.

5.5 Discussion

Unfortunately, a successful COL15-GFP fusion could not be generated during the placement in Japan, despite multiple attempts. On return to Liverpool in the final year of the project, it was decided that the timeframe was too tight to perform the experiments due to the significant amount time required to generate a fusion and a stable T2 line for the envisaged experiments. However, the results of these experiments provide several pointers for future generation of fusion proteins. The lack of success in generating GFP fusions could at least partially be a consequence of the large Gateway destination vectors used. Indeed, a similar low efficiency was observed during the generation of *35S:BSP1:GFP* vectors by Shimada et al. (2015), as reported by the author. Dr Shimada shared her protocol and optimisation techniques; however she warned of low success rates that in her previous experiments only a single colony in eight experiments carried the insert. As such, future attempts to generate plant gene-GFP fusion vectors should utilise smaller vectors, perform the recombination in several stages, or use alternative techniques such as restriction cloning, solid-state synthesis, Golden Gate cloning or the GeneMill system developed at Liverpool.

Additionally, the high rate of success of Gateway cloning in generating vectors for Yeast 2-Hybrid shows that Gateway cloning could indeed be successfully carried out. It was unfortunate that COL15 bait plasmids were auto-activating, as this was the primary motivation for the experiments. In the absence of the lead compound, the experiment

was cut short. However, the remaining bait vectors were deposited in the long-term storage freezers at RIKEN should this avenue prove interesting for exploration in the future.

The microarray project was, in hindsight, ambitious. It took multiple attempts to gather substantial quantities of high quality RNA and, when RNA was obtained, there were long waits for access to machines. Whilst cost considerations significantly reduced the scope of the experiments, the ultimate obstacle was time. By the time the first dataset was complete, the placement at RIKEN was over. Needless to say, this dataset is too small to allow any meaningful conclusions. It was frustrating that the lack of promising results prevented the expansion of the experiment to perform greater replication and carry out more complicated analysis, yet this limited scale was in part responsible for the lack of data.

The lack of putative results may be due to a lack of replication. However, there are other possibilities. The lack of geneotyping, again, presents an issue for the interpretation of null results in allegedly TF-GR plants. It is also possible that the dexamethasone treatment did not work - whether due to the fact that the delay between treatment and sampling was too short to see an effect, or whether the dexamethasone treatment worked at all. In the absence of a positive control for dexamethasone induction, in this experiment and in the project as a whole, there is no way of knowing. Another explanation is that COL15 simply does not affect gene expression, at least at the time point studied here - and perhaps, even, that it was identified erroneously as a circadian related gene in the first place. In the absence of greater replication and proper controls, it is impossible to say.

Given more time, or more success early on, the experiment could have been expanded

Table 5.5: List of Primers

Primer Name	Sequence (5'-3')
TopoCOL15F	CACCCGTATTCGCCGGTCCTATAA
TopoCOL15R	AGGGTAAGGAGCTTCACTAGCTTT
M13F	GTAAAACGACGGCCAGT
M13R	AACAGCTATGACCATG

to provide relevant transcriptomic data for *COL15*, both in the envisioned experiments and even across different points in the circadian time course.

Chapter 6

Discussion And Future Work

Whilst, throughout the last 20 years, an outline of the *Arabidopsis* circadian oscillator mechanism has emerged, it remains incomplete. Although we can state that the general schema of interlocked feedback loops forming a circadian oscillator is conserved in plants, not all the components have yet been identified, and the mechanistic details of many steps are only partially understood. Many of the core genes regulating the transcriptional circadian oscillator - those which are required for the proper phasing and period of gene transcription - do not appear to have functional transcription factor domains. In particular, the regulation of *CCA1* and *LHY* remains incompletely resolved, with no activators as yet identified for these genes. Similarly, whilst *TOC1* has recently been demonstrated to possess transcriptional repressor ability akin to its *PRR* family members (Gendron et al., 2012), no co-repressors, akin to *TOPLESS* with the other *PRR* proteins have been identified for it (Wang et al., 2013). Regulation of the Evening Complex is better characterised (Chow et al., 2012), however none of the genes known in the EC are in themselves transcription factors. Recent expansions of the circadian clock to include post-transcriptional and chromatin remodelling pathways further complicate

the picture, with yet more processes feeding back to regulate transcription in as-yet unknown manners.

6.1 COL15 in the Circadian clock

The gene with the most convincing identified phenotype identified by this study was *COL15*. It has a dexamethasone-inducible DF period shortening, a *pCAB2:LUC* period shortening, a phenotype in a SALK knock-out, and a red light-dependent overexpression hypocotyl elongation phenotype. It is coexpressed with *LUX, TOC1, ELF4* and *PRR3/5*. This phenotype has several possible explanations. COL15 could be a DNA-binding transcription factor, directly affecting the expression level of circadian genes. It could be a regulator of a clock input. Additionally, COL15 could be interacting with and disrupting other circadian factors, or competing with them for binding sites or spaces in protein complexes. In order to unpack this, and confirm that the phenotypes are genuine and reproducible, further work focussing on COL15 is necessary.

As previously mentioned, COL15 expression is diurnally regulated in normal and free run (LL) conditions, as can be seen in the timecourse microarray data made available through DIURNAL by Mockler et al. (2007). In wild type plants, *COL15* mRNA expression is rhythmic, peaking in the late afternoon at ZT+8 (Figure 6.1). This is perhaps surprising - one might expect a screen where gene function is induced by dexamethasone treatment in the afternoon at ZT+7 would identify mostly normally morning expressed genes as there are more severely mis-expressed by afternoon or evening induction. One might expected the dexamethasone induction technique used in this studt to have a weaker

effect on evening phased genes as they are already active at the time of dexamethasone treatment. This expression level profile persists in free-run (Figure 6.1a). In short day cycles (8hrs light), *COL15* mRNA is still rhythmic with a 12hr cycle, albeit with a lower expression level (Figure 6.1b). However, interestingly, this rhythm is abolished in *lhy* null mutants. There is a slight peak around dawn in these plants, possibly indicating a breakdown in proper circadian phasing. Together, this data suggests that *COL15* is under circadian and not merely diurnal regulation.

If COL15 truly does affect the circadian clock, the question remains - why has this gene, which gives a circadian phenotype, remained unidentified thusfar?

The CONSTANS-LIKE family is large, consisting of 17 genes in *Arabidopsis* (Griffiths et al., 2003, Robson et al., 2001). The family contains two signature domains - the nuclear localising CCT (CO, CO-like, TOC1) domain and the protein-protein interaction mediating B-box domain. The family has been implicated in multiple developmental processes including seedling photomorphogenesis, photoperiodic regulation of flowering, shade avoidance, and responses to biotic and abiotic stresses (Gangappa and Botto, 2014). COL15 is a poorly characterised gene, with relatively few pertinent publications focusing on it - the majority of papers cited in this section mention it only in passing and, instead, focus on other genes.

The current literature shows that *COL15* is capable of forming a complex with HEME ACTIVATOR PROTEIN (HAP) subunits (Wenkel et al., 2006b), basal transcription factors which bind CCAAT boxes in eukaryotic promoters. Indeed this has been proposed as a mechanism by which all CONSTANS-like genes are correctly targeted to their promoters (Ben-Naim et al., 2006). It has been proposed that there is a degree

of functional redundancy between these genes and, as outlined in the introduction to the project, the use of a 35S-driven library allows identification of phenotypes in such partially overlapping genes.

Previously, COL15/BBX13 protein was shown to physically interact with the circadian-related E3 ubiquitin ligase SCF factors LKP2 and ZTL by Fukamatsu et al. (2005). COL15 protein is primarily found in the nucleus, unlike ZTL and FKP2 which are additionally found in the cytoplasm (Figure 6.2). ZTL and FKP2-degradation occurs in the cytoplasm - whilst this could indicate that the reported interaction is not biologically significant, it could also be indicative of effective ZTL-mediated degradation excluding COL15 from the cytoplasm. In this study, *COL15* was shown to have similar short-period OX phenotypes to those of other known ZTL targets such as *TOC1* (Millar et al., 1995a). The phenotype could be a result of competitive inhibition of the TOC1/ZTL interaction, or it could be a genuine circadian effect - where, in normal plants, COL15 levels are normally kept under control by ZTL and, in the TF line plants, this regulation was broken. Confirmation of this hypothetical interaction was a goal of the work in Japan, although this was not successful.

A genetic cross between *pCAB2:LUC+, ztl* knockout plants and *T1082* lines could be performed in order to investigate any epistasis between these two genes. The genetic interaction of COL15-OX and mutants in *ZTL* would provide clues as to the interaction between these two genes. Construction of an antibody-tagged COL15 vector would be integral to future investigation, whilst fluorescence-resonance energy transfer (FRET) experiments could confirm any physical associations *in planta*. This interaction between ZTL and COL15 would implicate the latter further within the circadian clockwork and provide a molecular mechanism for its action. It has also been found that cADPR upregulates expression of *COL15/BBX13* (Sánchez et al., 2004), indicating there may possibly

FIGURE 6.1: COL15 Expression with Diurnal

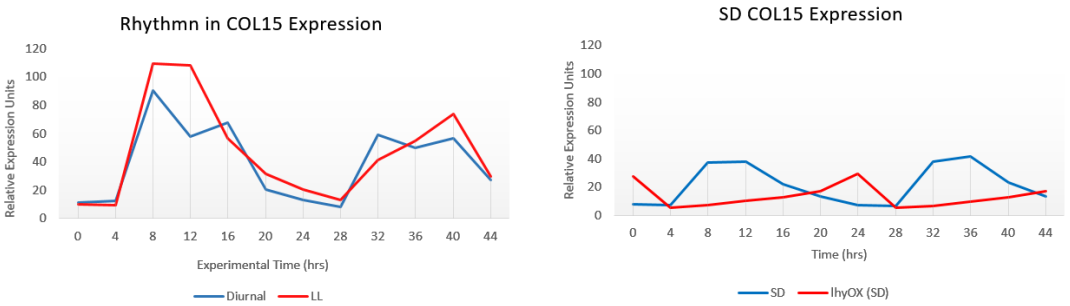

(A) Wild type plants, diurnal and free-run. (B) Wild type and *lhy-OX* plants, short days.

Timecourse microarray data were obtained from DIURNAL (Mockler et al., 2007). Cut off value = 0.8. Diurnal = LD photocycles and 22/12°C thermocycles, 12hr cycles. Free-run plants were entrained in these conditions before transfer to LL (22°C). SD = 8hrs light, 16hrs dark cycles at constant 22°C temperature.

FIGURE 6.2: Subcellular Expression of COL15, LKP2 and ZTL

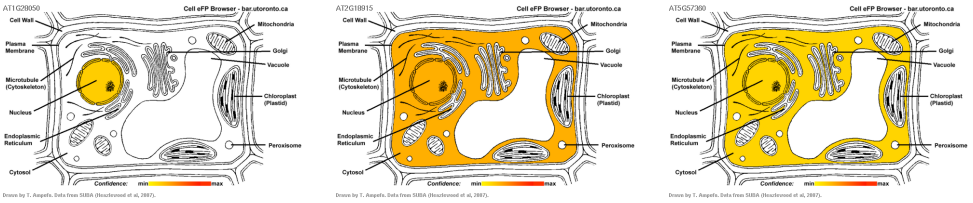

(A) COL15 (B) LKP2 (C) ZTL

Visualisations via electronic Fluorescent Pictograph (eFP Browser, Winter et al. (2007))

be more circadian crosstalk in its regulation, seeing that the circadian clock includes a cADPR circadian feedback loop (Dodd et al., 2009).

In this investigation, a single luciferase reporter was introduced into TF lines as a result of time and space constraints during transformation. This was unfortunate; ideally, as *pCAB2:LUC+* is a morning-expressed output of the circadian clock, an evening-phased output (such as *CCR2*) would have also been generated. In the future, luciferase reporters under the control of promoters from circadian clock genes could be introduced into the RIKEN TF lines in order to directly investigate the action of the TF lines on the

core oscillator, and furthermore to identify their sites of action. Following dexamethasone induction TF lines that, for example, increase expression of the morning loop genes may be identified as inducers of CCA1/LHY. The use of the GR system would allow this to be carried out in near-real time, especially if investigating whole plants. Differential regulation of different transcriptional loops would help identify the site of TF action on the clock.

However, there is an alternative explanation. Whilst primarily discussed in relation to their effects on flowering time, the CONSTANS-LIKE gene family has been previously linked with the circadian clock. It has been show that *COL1* overexpressors have shortened periods of leaf movement and *CAB2* expression (Ledger et al., 2001). This shortening occurred in a fluence rate–dependent manner, suggesting that *COL1* exerts its influence on a light-input pathway to the circadian clock. There is considerable evidence in the gene family for control over light signalling pathways. Red light-dependent hypocotyl elongation phenotypes have been reported in *COL3* knockouts and *COL7* overexpressors (Datta et al., 2006, Wang et al., 2013) and, indeed, in this investigation COL15 was reported to have a similar red light dependent hypocotyl elongation phenotype (see 4.5, Figure 4.37 and Table 4.23). It seems possible, therefore, that COL15's effects on the circadian clock are through a light-input pathway, in which it acts as a negative regulator.

6.2 Criticisms & Weaknesses of the Project

It would be patently untrue to claim that this project went according to plan. As alluded to in Chapter 5, the experimental outcomes of the Japan project were limited by

a shortage of funds, a lack of time and, on occasion, bad luck. However, it would also be unfair to blame all the shortcomings of the project on factors beyond control. There are several areas in which the project is lacking, which are discussed herein along with suggestions as to how they could be improved if the work were repeated or extended in the future.

The first, and perhaps most glaring, shortcoming is the lack of confirmation for the dexamethasone treatment regimens. As it stands, there is no solid confirmation that dexamethasone treatment works. This is made worse by the fact that the group at RIKEN grows TF line plants on dexamethasone supplemented media and has no protocols for topical or otherwise inducible treatment. In part, this was due to a lack of suitable lines to perform experiments on. The RIKEN TF library lacked GR fusions of any canonical clock genes - *TOC1* was not identified as a transcription factor at the time of library construction, both *CCA1* and *LHY* were attempted, but the transformation failed. Whilst I attempted to construct these lines, the phenotypes of *35S:GR:CCA1* lines did not match those predicted in the literature, bringing into question the effectiveness of the dexamethasone treatment.

If the work were to be repeated or extended, confirming the efficacy of the dexamethasone treatment would be of primary importance. One way to achieve this would be to generate and confirm *35S:GR:CCA1*, *35S:GR:LHY* and/or *35S:GR:TOC1* fusions. A three way comparison could be carried out - phenotyping the lines grown on MS media and mock-sprayed, grown on MS media and sprayed with dexamethasone as in this report, and grown on dexamethasone-supplemented MS media and mock-sprayed. This would provide answers to two key questions. Comparison of the circadian phenotypes of MS-grown mock-sprayed plants to those sprayed with dexamethasone would definitively

show whether the dexamethasone treatment in this study is effective at inducing clock transcription factor activity. If the answer to this question is negative, comparison of mock-sprayed plants grown on MS and dexamethasone-supplemented media would show whether dexamethasone is capable of inducing plant transcription factor function at all.

An alternative solution would be to construct a *35S:GR:GFP* fusion. Unsucessful attempts were made to obtain a suitable Entry vector, or the resources to generate one, at RIKEN. Such a construct would, through confocal microscopy, allow the effectiveness of dexamethasone treatment to be studied in real time. In addition to the basic question of whether or not the treatment regimen is effective, this would reveal just how long the dexamethasone treatment lasts for. Does dexamethasone spray administed a "pulse" of transcription factor activity, eventually returning to the baseline level, or are the dexamethasone sprays sufficient enough to maintain high levels of transcription factor activity throughout the experiment? If the former is true, this could also provide tools for fine manipulation of the clock, through altering the timing and/or duration of dexamethasone treatment.

If the work were to be repeated, a preliminary stage where the dexamethasone treatment regimen was robustly studied should be undertaken. Using a known dexamethasone-responsive line, different timings and quantities of dexamethasone should be applied and the effects studied in order to find a suitable treatment. This work would be carried out in Liverpool, perhaps as a precursor to the PhD project proper, in order to allow a full TF library screen before the commencement of the Japanese phase of the project, where no more DF or luciferase phenotyping can be performed.

Another major fault of this study was the lack of genotyping of lines. Failure to generate

and identify homozygous TF lines means that the reproducibility of the experiments is poor and their results have to be taken with a degree of scepticism. Furthermore, the insert sites of the GR-TF constructs was not confirmed. It is possible that observed phenotypes may be as likely due to knocking out of genes through insertional mutagenesis, rather than GR-TF activity.

A similar criticism applies to the SALK lines. Whilst the NASC repository stated that the lines were homozygous, this should have been confirmed. Furthermore, the insert sites should have been sequenced in order to distinguish between full knock-outs, truncated genes, multiple T-DNA insertions, and similar insertional mutants.

Homozygocity can be confirmed through PCR. Such techniques are widely reported which allow the zygocity of a known insert in a known position to be characterised (Kihara et al., 2006). In such an approach, two sets of primer pairs with the same melting temperature are used in a PCR reaction with a precisely known quantity of DNA. A first pair bind targets within the integrated T-DNA, whilst the second targets an endogenous gene as a reference. The resulting PCR product band intensities are compared, allowing the ploidy of the insert to be known.

In addition, it would be prudent to investigate the level of gene expression through QPCR. Quantifying the level of GR-TF transgene transcription would allow us to control for inserts into islands of especially high or low transcriptional activity.

The experimental design of the initial screen would be reworked if the investigation were to be repeated (Chapter 3.5.1). Dexamethasone was applied in the afternoon. The rationale was that the timing of dexamethasone treatment was essentially arbitrary - on the assumption that a similar number of genes are normally phased to dawn as to dusk,

dexamethasone treatment will induce similar numbers of circadian phenotypes regardless of timing. If the assumption is true, then the identity of the genes selected by the screen may change, but their numbers will be similar. However, this assumption likely does not hold. A large number of circadian regulated genes are evening phased (Harmer and Kay, 2005). As such, inducing the over expression of these transcription factors at the time where the endogenous levels would peak is less likely to reveal strong phenotypes. If the work were to be extended, a repeat of the screening experiment with a morning induction would provide an interesting comparison.

The return of the treated samples to the diurnal growth condition likely reduced the efficacy of the screen. As discussed above, it is currently unknown how long transcription factors are induced following dexamethasone treatment. By inducing the transcription factors in the evening, then returning them to the diurnally oscillating entrainment conditions, the clock is able to reset. This would smother many circadian phenotypes. If the experiment were repeated, the plants would be placed in free-run immediately after treatment. This would allow clock phenotypes to manifest, without resetting, allowing more key genes to be identified.

The selection criteria were chosen to select genes that showed measurable divergence from the expected period of the wild type (Chapter 3.5.2). As the study progressed, it became clear that this semi-quantitative method was less than ideal. Statistical comparison of periods to those of the wild type was later carried out using a two-tailed Student's T-Test. As mentioned in Table 3.8, all of the genes of interest selected except one had statistically significant period differences, and this exception (MYBC1/T0856) was selected due to its loss of robustness (RAE = WT + 0.2, $p < 0.001$, Figure 3.20b). If the experiment

was to be performed again, relying on statistical methods first and foremost may lead to better selection of TF lines.

Unfortunately by the time this analysis was carried out the subsequent transformation and investigation of the genes of interest had been carried out and, sadly, time constraints prevented these experiments being repeated on the new selection. Ideally, there would be the time and resources to generate the subsequent transgenic libraries and carry over the molecular work with these lines, however this was not possible due to the nature of this project. During the 2 year placement in RIKEN Yokohama, without access to DF phenotyping equipment but with access to the entire seed library and transgenic generation facilities, the project proceeded ahead and it was not until the final year that the data was re-analysed. In the future, it would be good to take these missing lines and subject them to the experimental work the rest of the lines underwent. In subsequent experiments, it would be prudent to use a statistical threshold to pre-select lines, then assess their phenotypes manually, and use these as the foundation of further investigation.

The over-expression system used by the TF lines offered an excellent opportunity to screen a large number of lines. Although it turned out not to be as complete as initially thought (as many lines were missing), the library offered a large number of transcription factors as T1 seed. As the TF lines are driven by a 35S promoter, it is possible to phenotype the pooled mix of heterzygous, homozygous and wild type seed. However, the over expression system is not without shortcomings. The RIKEN TF constructs are inserted into wild type plants. Therefore, in addition to the gene that is over-expressed, TF plants carry two functional copies of the same gene under normal regulation. Homozygous TF lines, even if grown on dexamethasone-supplemented media, are not analogous to over expression lines as there is still regular, diurnal expression of the genes. In the future,

it would be desirable to introduce the *COL15-GR* construct into a *col15* null mutant, as well as to introduce those of the TF line vectors for known circadian genes into their respective null mutants, in order to view the complementation phenotype.

Over expression is also a "blunt tool". Over expression phenotypes are highly artificial models with an unphysiologically high expression level. Furthermore, the assays can be affected by different transfection efficiencies, multiple insertion and insertion site. Different regions of the genome have varying degrees of transcriptional activity. Similarly, transformation of *Arabidopsis* may insert multiple copies of the vector into the genome. These effects mean that the actual levels of transcription faction are variable between individual TF lines. This limits the effectiveness of the screen.

The TF lines contain cDNAs under the control of two different components - the 35S promoter and the GR cassette - which both bring potential problems. 35S promoter of cauliflower mosaic virus confers a high level of gene expression when transferred to plants (Benfey and Chua, 1990, Jefferson et al., 1987, Odell et al., 1985). The GR cassette does not perfectly exclude components from the nucleus - rather, the subcellular localisation of GR is determined by the balance between its rates of nuclear import and export. Native GR in mammals shuttles continuously between cytoplasm and nucleus via the nuclear pore complex (NPC) with glucocorticoid treatment moving the equilibria and resulting in a net shift from cytoplasm to nucleus (Madan and DeFranco, 1993, Savory et al., 1999). As such, the combination of high transcriptional expression from the 35S promoter (potentially transcribed from multiple copies) combined with this nuclear pore "leak" may result in nuclear TF levels sufficient to induce transcription in the absence of dexamethasone. This is particularly possible for genes that are normally expressed at low copy number - which includes many diurnally oscillating genes in their "trough" phase. As a consequence, it is important to compare the phenotypes of the dex-treated

TF lines not only to the wild type but to untreated lines. Genes may show induction in both conditions, they may have partial induction when untreated with phenotype severity increasing with dexamethasone treatment (i.e. a TF dose-dependent effect), or they may show the binary on/off induction previously assumed.

Finally, the screen is unable to distinguish between true circadian acting genes and pleiotropy. Pleiotropy occurs when one gene influences two or more seemingly unrelated phenotypic traits. Consequently, a mutation in a pleiotropic gene may have an effect on some or all traits simultaneously. The screen aims to select genes that, when over expressed, result in a circadian phenotype. This includes genes which regulate circadian input pathways. It also includes genes which cause widespread changes in expression. Severe stress responses could perturb the clock, not through a specific pathway but through a series of general stress mechanisms. In future work, the expression level of genes must be quantified, and pleiotropic effects distinguished from true circadian phenotypes. These latter effects can be distinguished by, for example, investigating the gene functions on the molecular level, introducing the TF construct into mutants deficient in clock components and entrainment pathways, and performing more hypocotyl elongation experiments.

6.3 Horizons & Future Work

A significant amount of work would need to be carried out to turn the data in this report into a publication. This work could be carried out and expanded over a 6-12 month period. However, it is this researcher's intention to leave research science after

the cessation of this project. As such, the following outline of work needed for publication is accompanied by suggestions of how it could be divided amongst future researchers.

As highlighted above, there is a need for control experiments. Confirmation of the identity of COL15 TF lines - of their ploidy, their expression levels, and the sites of their T-DNA insertion - are vital. Without a clear genetic characterisation of the seed, the data can not meet the standard for publication. Fortunately, there are several TF T2 seed stocks in the collection at Liverpool. It would be relatively straightforward to grow these stocks, extract DNA and RNA, and analyse them according to the techniques highlighted above. Indeed, this could be carried out as part of a research student summer project.

Once characterised, the circadian phenotype of these lines could be confirmed. The experimental protocol could be reconsidered at this time - dexamethasone treatment could be applied in the evening as normal, and the plants immediately transferred to free-run.

Similar experiments would need to be performed with TF-CCA1 seed. The clock phenotype - or absence thereof - of TF-CCA1 would need to be investigated and explained.

Ideally, further substantive work would be performed. Replicating the experiments would be valuable - both for circadian imaging and the hypocotyl elongation experiments - to improve the confidence of our conclusions. The use of more independently transformed lines would be desirable, as it would help compensate for the different transcriptional activity at the sites of insertion that may affect the results. The pilot work investigating timing of dexamethasone could be expanded upon, to further investigate the effects of misregulating and misexpressing *COL15* and its downstream targets. These experiments

could quite easily be divided up into small chunks, each of which could form an honours student project.

An interesting avenue to explore would be circadian imaging under monochromatic light. COL15 TF lines were demonstrated to give a red-light dependent hypocotyl elongation phenotype. In tandem with the existing literature, it is hypothesised that *COL15* is responsible for mediating red light signalling in a manner than affects the clock. This could be investigated through delayed fluorescence or luciferase imaging under monochromatic light regimes. If this hypothesis is true, it would be expected that the short period T1082 phenotype is exacerbated in red-light, and attenuated in blue light.

If there was sufficient interest, time, and budget, the molecular work could be expanded upon. The University of Liverpool has recently begun its GeneMill service, specialising in generating synthetic DNA vectors and reporters. This service could be used to quickly and efficiently generate the COL15-GFP vectors that proved so difficult at RIKEN. The GFP-GR vector discussed above could also be generated for the study of dexamethasone treatments. These vectors, once generated, would be relatively straightforward to transform into *Arabidopsis*. Whilst generating stable homozygous transgenic lines can be time consuming, it is not especially arduous. The experiments that these two plant lines would open up would greatly expand the scope and impact of the project, however they would also require significant amounts of time - perhaps best suited as a Masters project or as part of a future doctoral candidate student's work.

6.4 Conclusion

In conclusion, the wholescale circadian screening of transcription factors in *Arabidopsis* has provided the first evidence identifying *COL15* as a novel, putative circadian affecting

gene. The data in this report are preliminary and not without flaws. A significant amount of work remains to be performed in order to bring the results and conclusions up to the standards required for publication. However, the data are not entirely without value, and provide a valuable starting point for further work. With confirmation of the phenotypes in this report with genotyped, known lines, and expansion of the investigation into the molecular characterisation of COL15 proteins, *COL15* can perhaps one day be confirmed as a circadian transcription factor. Through this work whittling down the large RIKEN library to a single transcription factor of interest, detailed molecular work is now feasible to characterise the expression, regulation, and downstream components of this putative circadian gene.

Appendix A

Comparison of Period Prediction Techniques

FIGURE A.1: Comparison of Period Prediction Methods on *pCAB2:LUC+* Samples.

Comparison of the same set of previously published luciferase data (for provenance, see Section 3.3.1). Seeds were surface-sterilised, vernalised for 2 days in constant darkness at 4°C before being planted on MS + 1.5% agar in 96-well plates at a density of c 10 seeds per sample, sealed with micropore tape and grown under 100μmol m^{-2} s^{-1} 12:12 22°C conditions for 7 days. Samples were saturated with luciferase through topical application on the evening of day 7 before transfer to the CCD imaging camera. Intensity traces are made through binning the relative intesnity values to smooth, averaging across all replicate samples and plotting the results across the experimental timecourse. Period prediction was performed through four period estimation methods hosted on BioDARE and the predicted periods plotted against error. Data is presented without cleaning. For all samples, n = 8.

Fig 1.1.1: Intensity Plot of prr51:CAB.

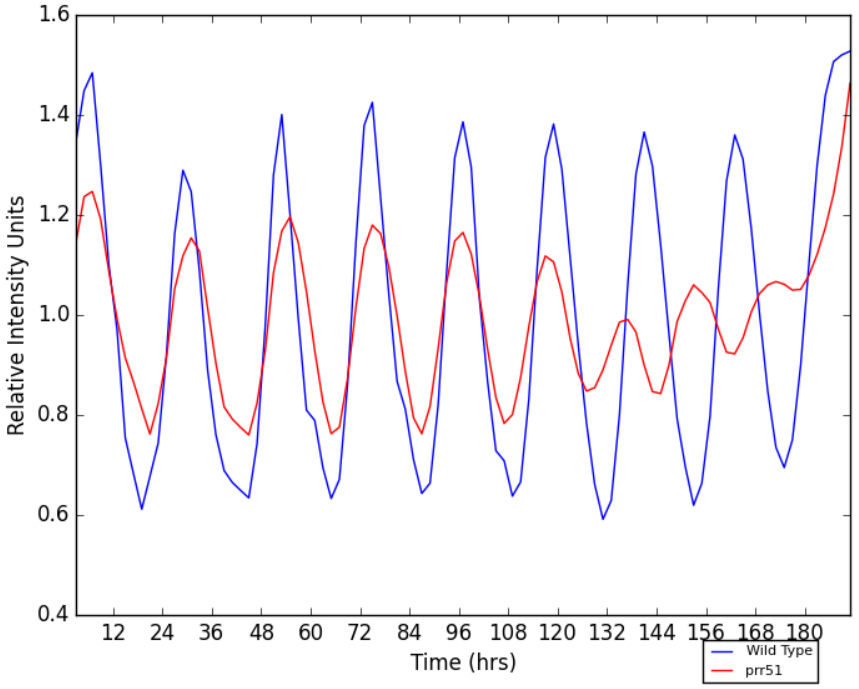

Fig 1.1.2: Period Analysis of prr51:CAB.

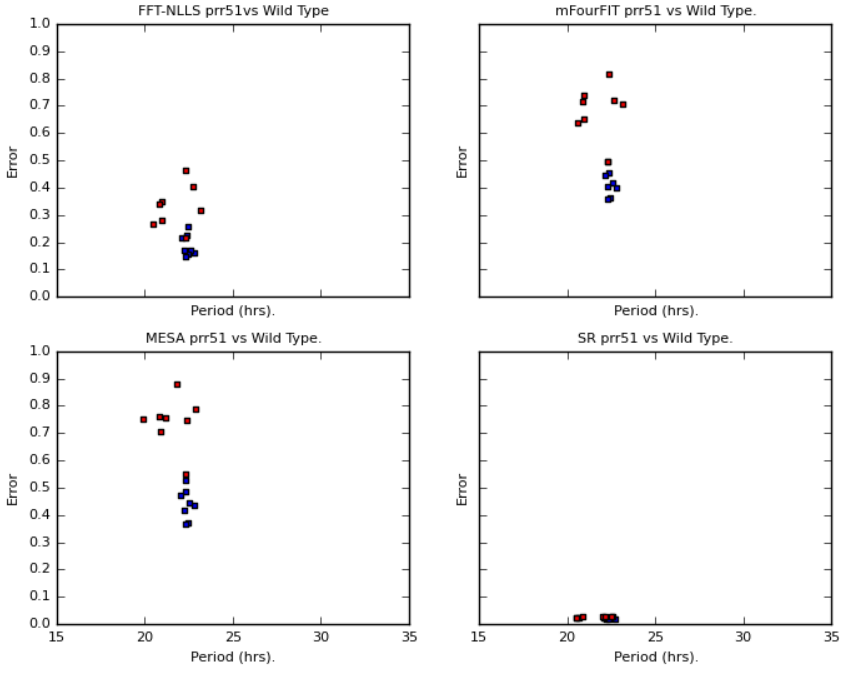

Figure A.1, Continued...

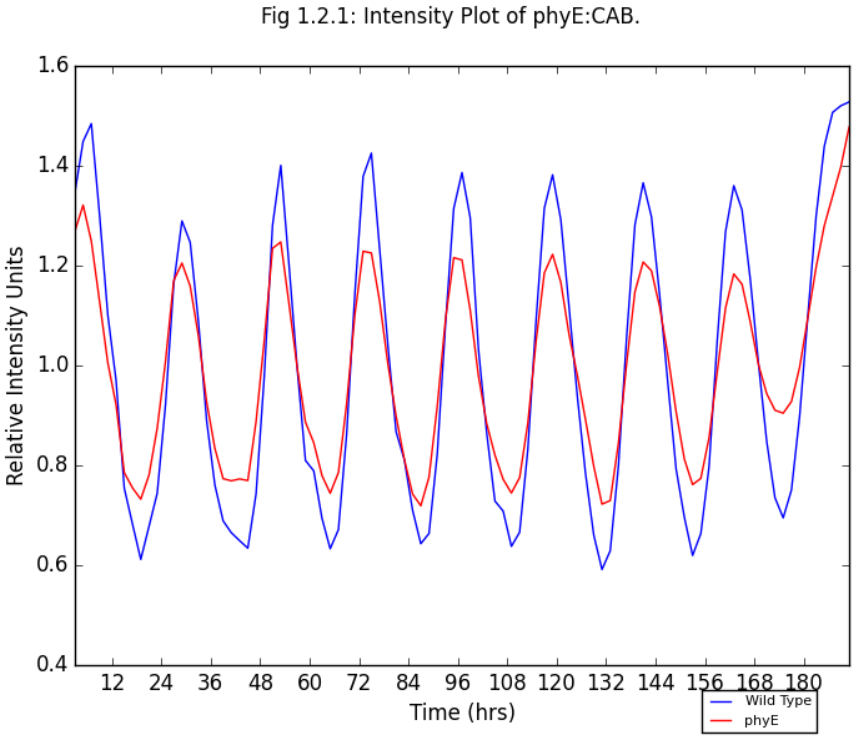

Figure A.1, Continued...

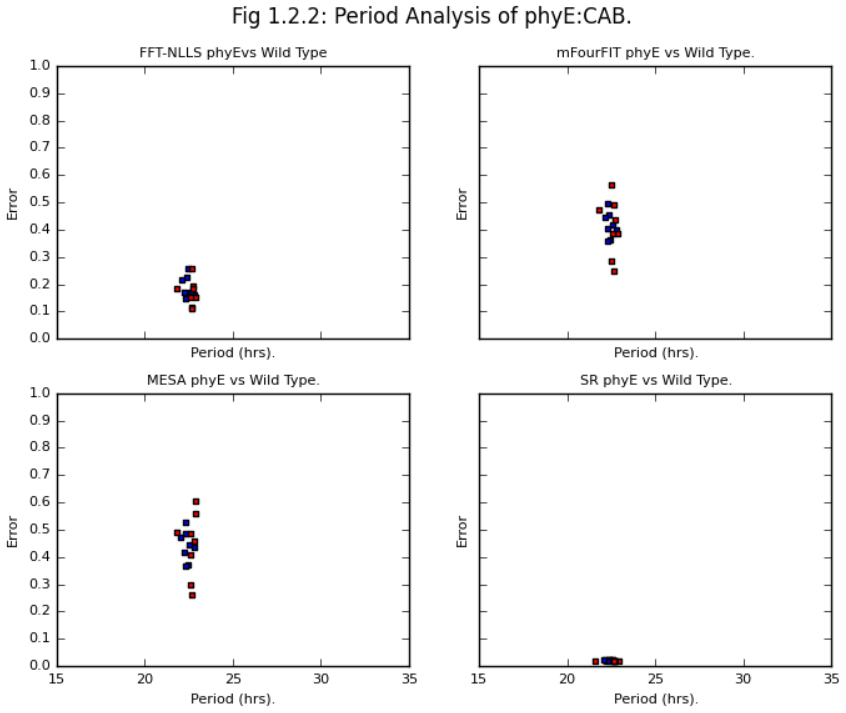

Figure A.1, Continued...

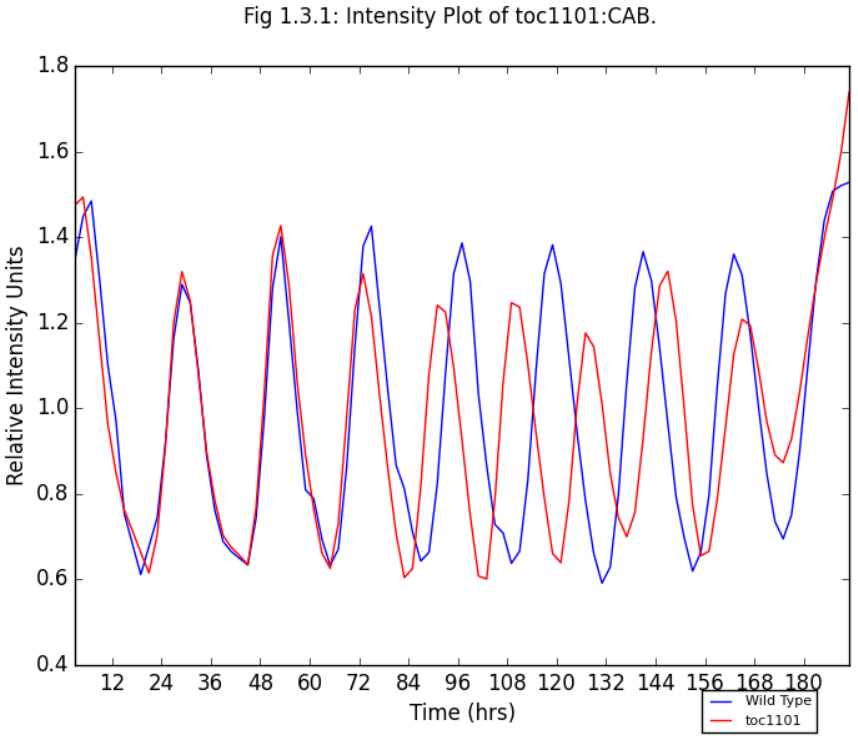

Figure A.1, Continued...

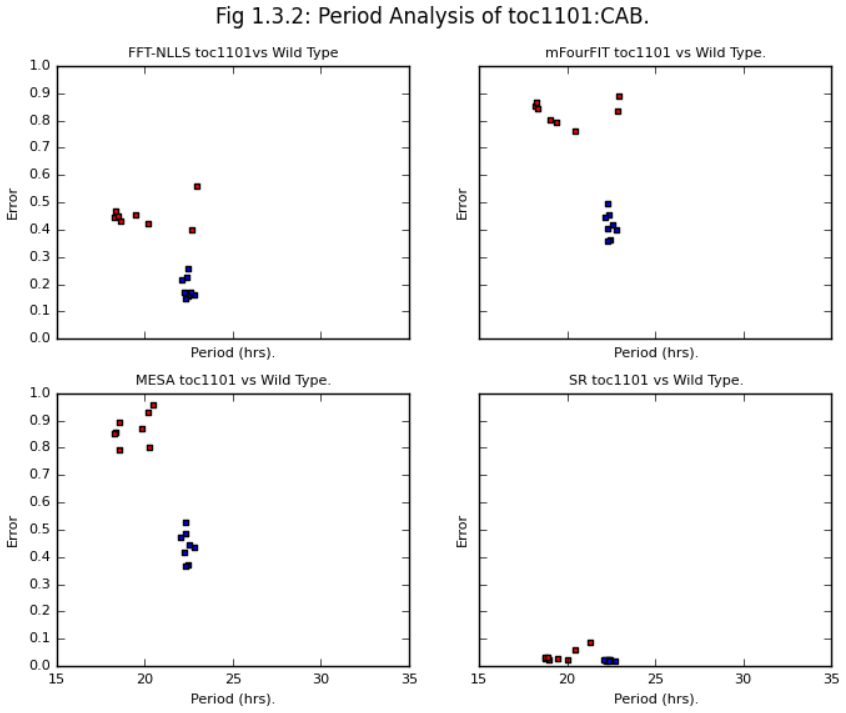

FIGURE A.2: Comparison of Period Prediction Methods on *pCCR2:LUC+* Samples.

Comparison of the same set of previously published luciferase data (for provenance, see Section 3.3.1). Seeds were surface-sterilised, vernalised for 2 days in constant darkness at 4°C before being planted on MS + 1.5% agar in 96-well plates at a density of c 10 seeds per sample, sealed with micropore tape and grown under 100μmol m^{-2} s^{-1} 12:12 22°C conditions for 7 days. Samples were saturated with luciferase through topical application on the evening of day 7 before transfer to the CCD imaging camera. Intensity traces are made through binning the relative intesnity values to smooth, averaging across all replicate samples and plotting the results across the experimental timecourse. Period prediction was performed through four period estimation methods hosted on BioDARE and the predicted periods plotted against error. Data is presented without cleaning. For all samples, n = 8.

Fig 2.1.1: Intensity Plot of toc1101:CCR2.

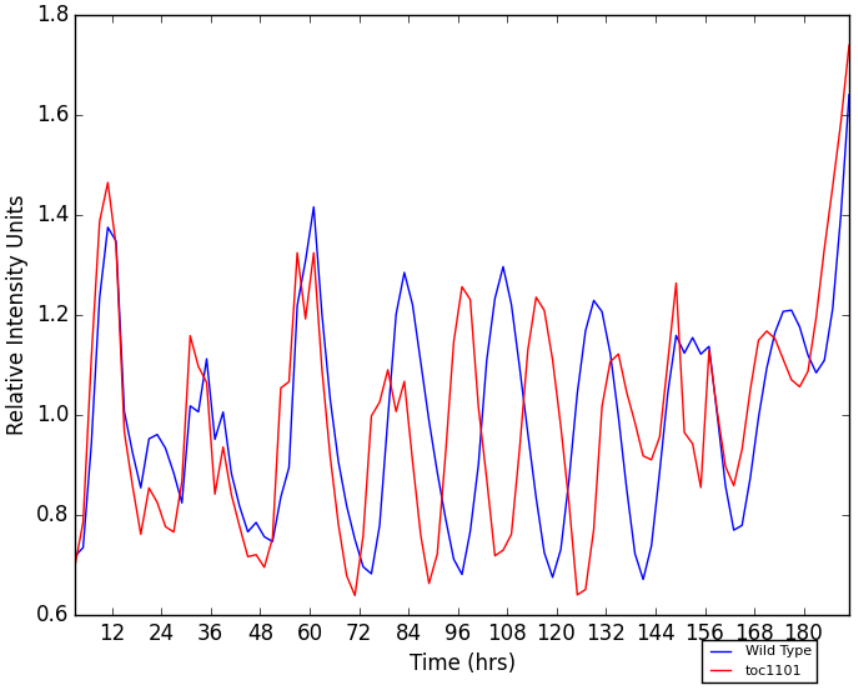

Fig 2.1.2: Period Analysis of toc1101:CCR2.

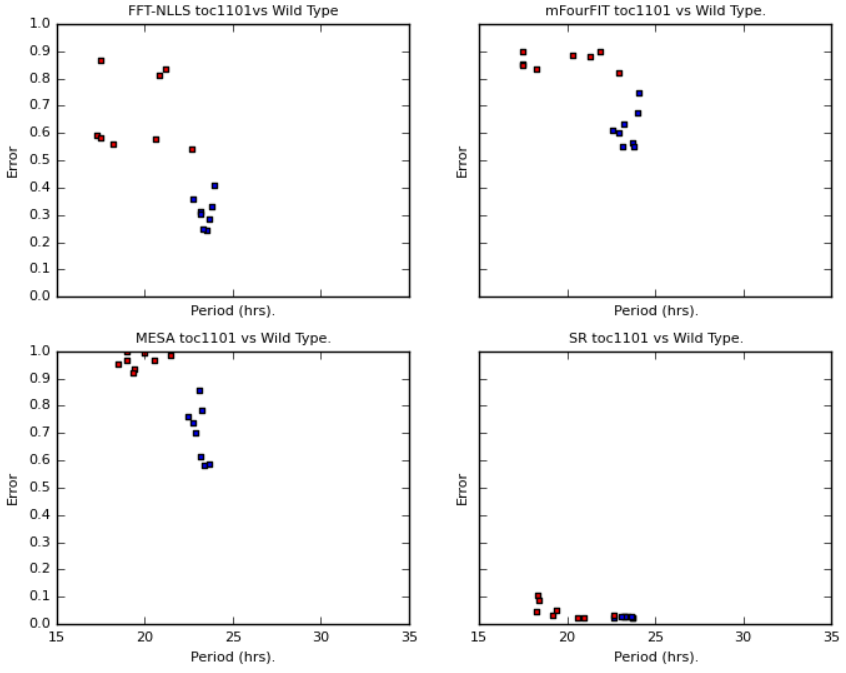

Figure A.2, Continued...

Fig 2.2.1: Intensity Plot of prr51:CCR2.

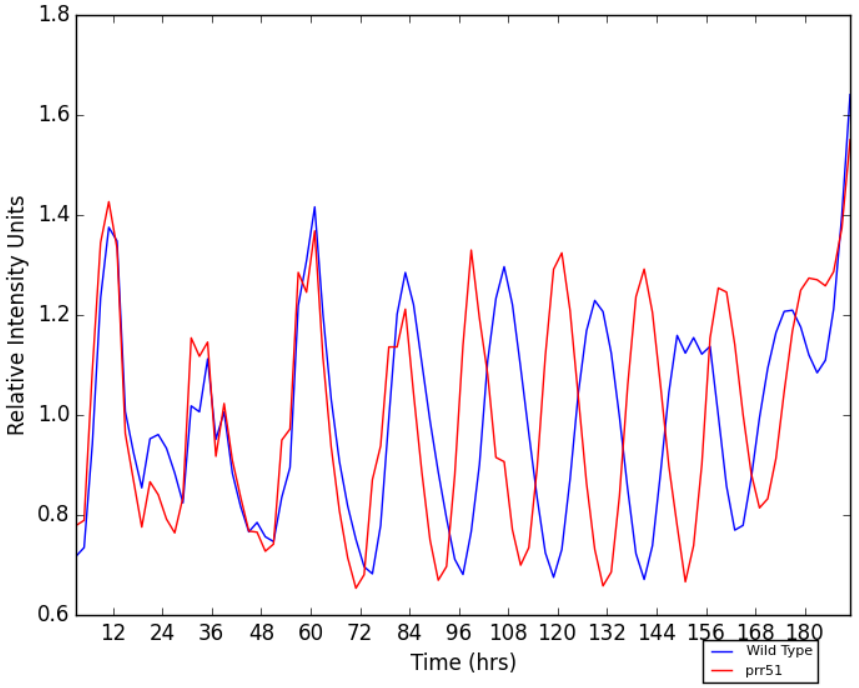

Fig 2.2.2: Period Analysis of prr51:CCR2.

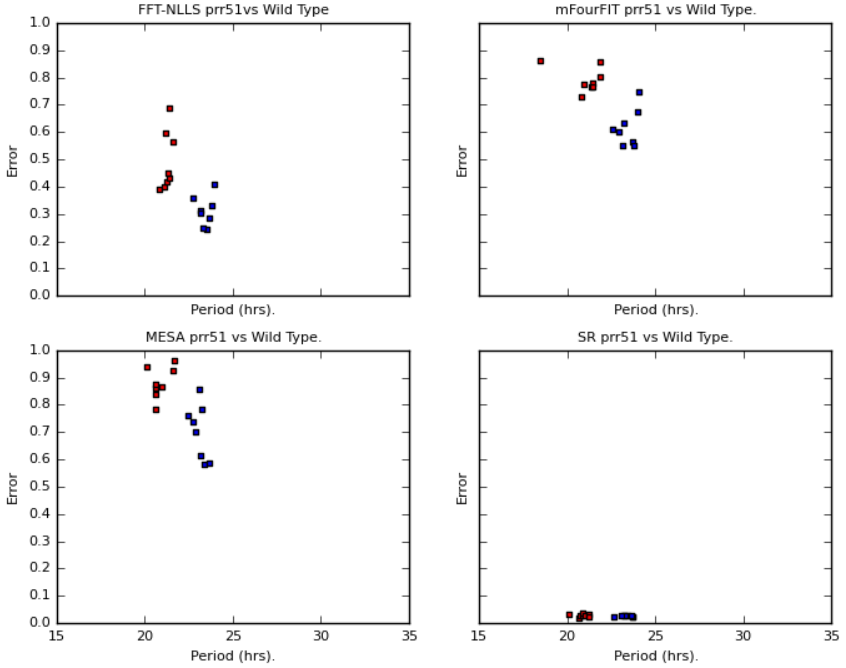

Figure A.2, Continued...

Fig 2.3.1: Intensity Plot of ztl105:CCR2.

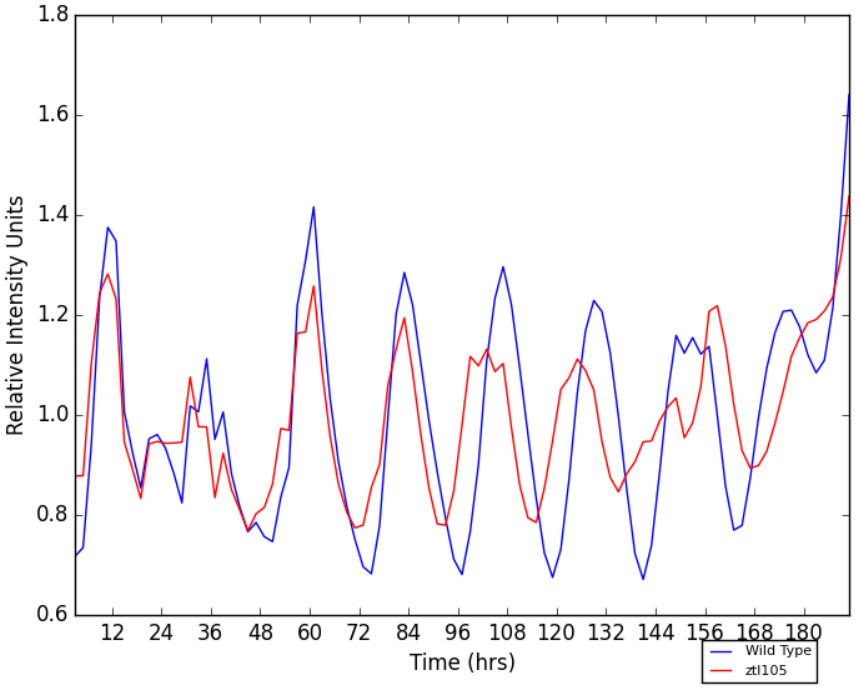

Fig 2.3.2: Period Analysis of ztl105:CCR2.

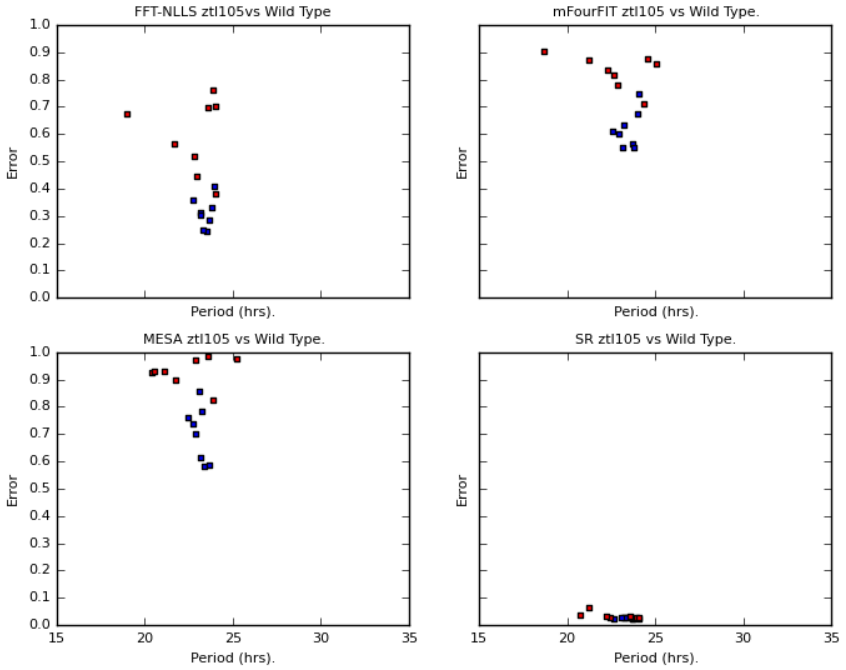

Figure A.2, Continued...

Fig 2.4.1: Intensity Plot of lhy:CCR2.

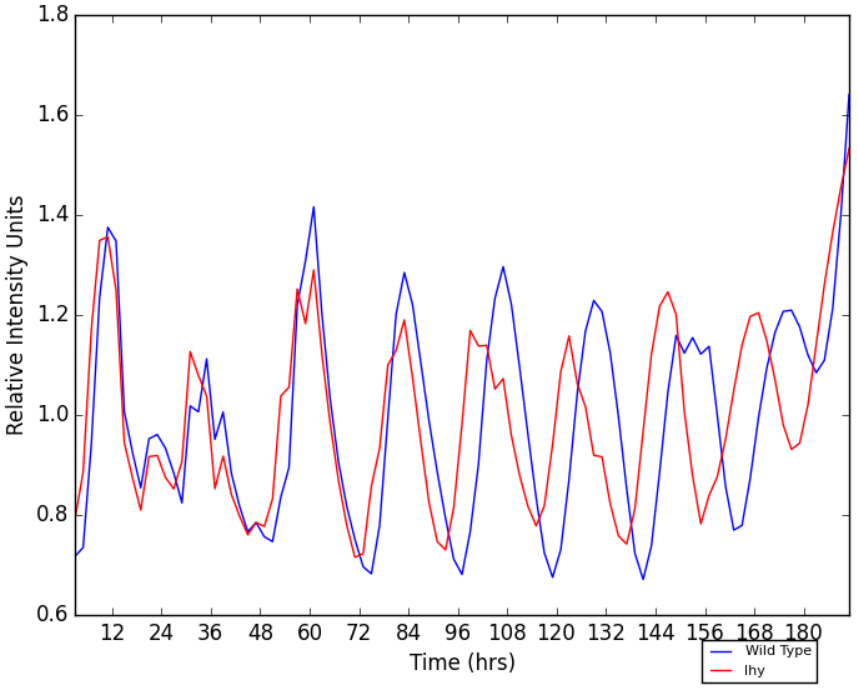

Fig 2.4.2: Period Analysis of lhy:CCR2.

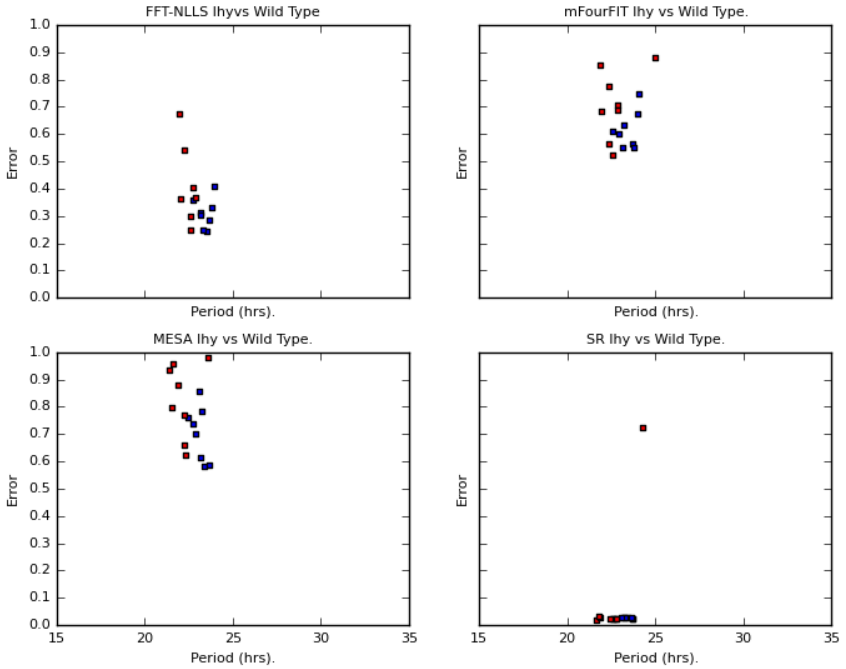

Figure A.2, Continued...

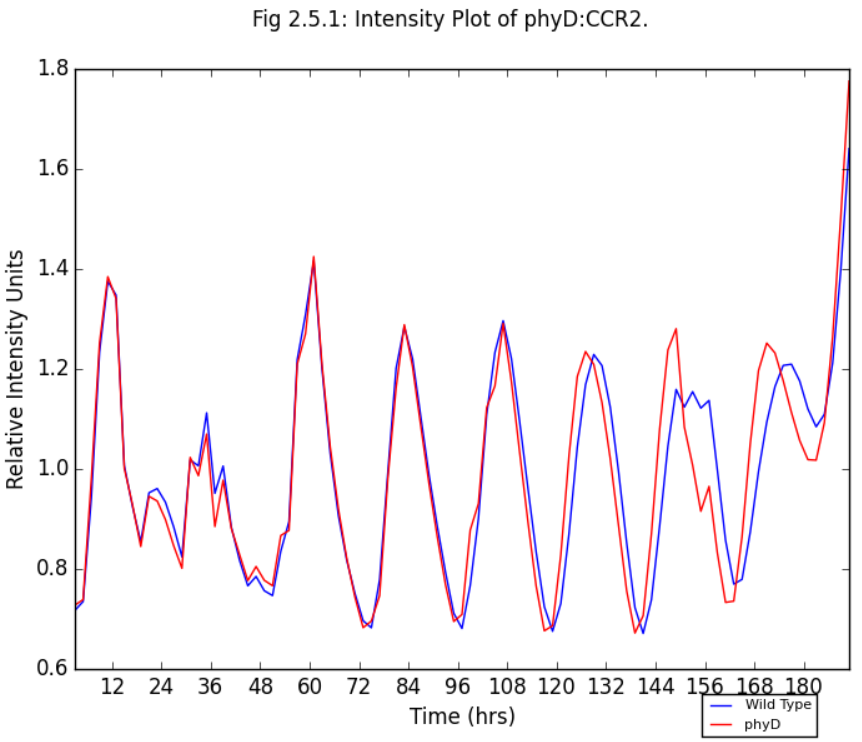

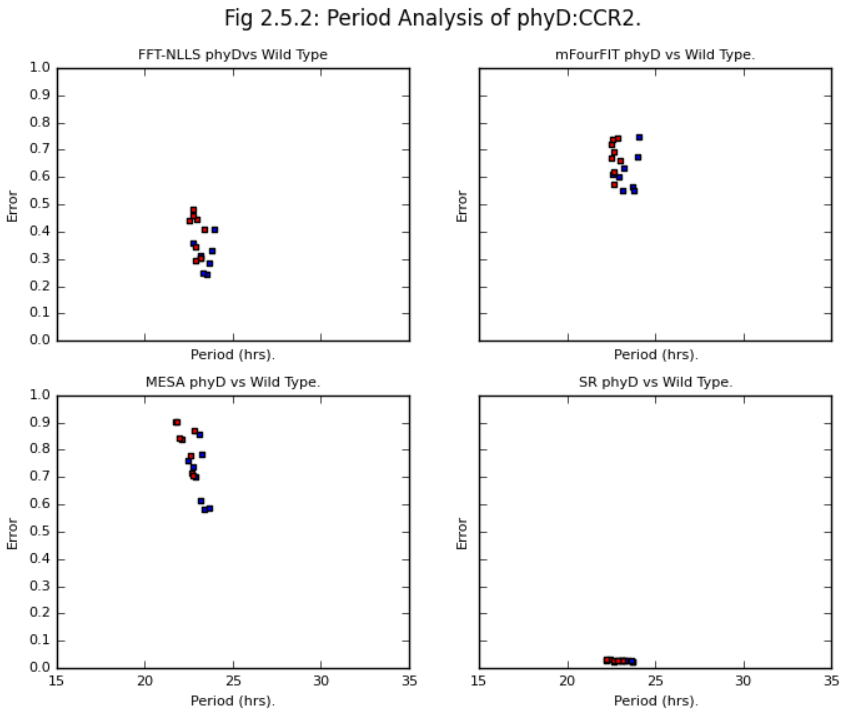

Appendix B

Further DF Screening Results

In addition to the lines selected for further study, multiple other TF lines were screened by DF in the original experiments outlined in Chapter 3.5. In this appendix, the data for the rest of the TF lines not selected are provided below in Table B for completeness.

Plant growth conditions and dexamethasone treatment regimes were identical to those described in Chapter 3.5.1. All samples are groups of dexamethasone treated seedlings as previously outlined. The screening was performed in eight batches (each consisting of a single experimental run in an ORCA-II growth chamber). Data analysis in this section is performed by Student's T-Test, comparing the FFT period estimates to that of the wild type of the same experimental run.

TABLE B.1: Additional results of TF line Screening for lines not selected for further analysis

Line	AtG	n(fft)=	Mean Period (FFT)	Mean Diff v WT	P(period) =
T0002	AT2G30470	8	24.39	-0.721	0.385
T0004	AT2G30470	15	23.35	-2.478	<0.001 ***
T0005	AT2G30470	12	23.61	0.191	0.658

Continued on next page

Table B.1 – *Continued from previous page*

Line	AtG	n(fft)=	Mean Period (FFT)	Mean Diff v WT	P(period) =	
T0011	AT2G30470	15	25.97	0.143	0.465	
T0012	AT3G42790	16	23.40	-1.703	0.006	**
T0018	AT3G42790	15	24.50	-1.328	<0.001	***
T0019	AT3G42790	16	24.63	-1.202	0.001	***
T0025	AT1G16060	8	22.84	-2.270	0.006	**
T0026	AT1G16060	13	22.67	-0.745	0.091	
T0027	AT1G21910	8	23.57	-1.535	0.058	
T0028	AT1G21910	15	25.52	-0.311	0.164	
T0029	AT1G22810	8	23.40	-1.706	0.035	*
T0030	AT1G22985	8	23.66	-1.451	0.072	
T0032	AT1G25470	8	23.66	-1.442	0.081	
T0035	AT1G28360	8	23.89	-1.216	0.132	
T0036	AT1G28370	8	23.36	-1.747	0.034	*
T0037	AT1G33760	21	23.77	-0.307	0.237	
T0039	AT1G33760	10	22.87	-0.544	0.249	
T0040	AT1G44830	8	23.39	-1.712	0.040	*
T0041	AT1G46768	8	23.97	-1.134	0.165	
T0046	AT1G53170	8	24.60	-0.509	0.526	
T0049	AT1G64380	8	23.54	-1.565	0.053	
T0050	AT1G68550	8	23.08	-2.026	0.013	*
T0051	AT1G68840	8	23.44	-1.667	0.043	*
T0054	AT1G71520	8	23.44	-1.667	0.041	*
T0057	AT1G74930	8	24.03	-1.080	0.182	
T0058	AT1G75490	8	23.88	-1.224	0.128	
T0060	AT1G77640	18	24.19	0.113	0.726	
T0061	AT1G77640	15	24.99	-0.832	0.009	**
T0064	AT2G20880	7	24.59	-0.520	0.544	

Continued on next page

Table B.1 – *Continued from previous page*

Line	AtG	n(fft)=	Mean Period (FFT)	Mean Diff v WT	P(period) =	
T0065	AT2G22200	8	25.54	0.431	0.594	
T0068	AT2G28550	8	25.22	0.111	0.894	
T0069	AT2G31230	8	24.51	-0.595	0.453	
T0069	AT2G31230	14	24.42	-1.412	0.002	**
T0071	AT2G31230	15	24.61	-1.215	0.002	**
T0076	AT2G40340	8	23.85	-1.256	0.118	
T0077	AT2G40340	12	23.24	-0.182	0.669	
T0078	AT2G44840	8	23.49	-1.615	0.049	*
T0079	AT2G44940	8	23.33	-1.781	0.036	*
T0080	AT2G46310	8	22.81	-2.294	0.006	**
T0083	AT3G14230	8	26.78	1.912	0.016	*
T0084	AT3G15210	8	25.19	0.081	0.932	
T0086	AT3G15210	14	24.92	-0.903	0.001	**
T0089	AT3G23230	7	23.75	-1.352	0.116	
T0091	AT3G23230	10	22.97	-0.451	0.340	
T0092	AT3G25890	7	24.06	-0.811	0.387	
T0093	AT3G25890	8	26.93	2.062	0.010	**
T0095	AT3G57600	8	23.72	-1.387	0.088	
T0096	AT3G60490	8	23.12	-1.985	0.016	*
T0097	AT3G61630	8	23.11	-1.996	0.015	*
T0098	AT4G06746	8	22.89	-2.219	0.007	**
T0106	AT4G25480	6	28.29	3.417	0.001	***
T0112	AT4G25480	12	23.12	-0.294	0.493	
T0115	AT4G36920	8	24.22	-0.889	0.264	
T0116	AT4G39780	15	23.19	-0.228	0.553	
T0132	AT5G25810	12	22.84	-0.579	0.181	
T0142	AT5G61590	13	23.18	-0.233	0.570	

Continued on next page

Table B.1 – *Continued from previous page*

Line	AtG	n(fft)=	Mean Period (FFT)	Mean Diff v WT	P(period) =	
T0143	AT5G61590	8	24.78	-0.093	0.905	
T0159	AT5G67190	8	23.36	-1.742	0.031	*
T0161	AT5G67190	8	24.14	-0.965	0.287	
T0162	AT2G46530	8	24.64	-0.233	0.746	
T0166	AT4G30080	8	23.60	-1.510	0.065	
T0168	AT5G62000	8	25.42	0.310	0.740	
T0169	AT1G04240	8	24.87	-0.241	0.768	
T0170	AT1G04240	8	23.88	-1.225	0.131	
T0171	AT1G04240	8	23.26	-1.847	0.023	*
T0173	AT1G04240	8	23.12	-1.985	0.015	*
T0179	AT3G04730	15	25.26	-0.571	0.080	
T0181	AT3G15540	7	24.82	-0.045	0.958	
T0183	AT3G17600	8	23.71	-1.397	0.083	
T0184	AT3G17600	8	23.63	-1.479	0.067	
T0186	AT4G28640	13	23.11	-0.305	0.461	
T0188	AT4G29080	8	24.05	-1.059	0.185	
T0191	AT1G01260	11	23.35	-0.068	0.879	
T0193	AT1G03040	8	23.73	0.597	0.248	
T0194	AT1G03040	8	23.66	-1.450	0.072	
T0195	AT1G03040	8	23.72	-1.390	0.086	
T0197	AT1G09530	14	22.75	-0.664	0.101	
T0198	AT1G10120	8	23.12	-0.014	0.978	
T0201	AT1G18400	12	24.14	0.727	0.179	
T0209	AT1G26260	8	24.31	-0.797	0.318	
T0212	AT1G35460	8	24.03	-0.756	0.636	
T0214	AT1G59640	8	23.85	-0.935	0.557	
T0217	AT1G68810	8	22.94	-0.197	0.624	

Continued on next page

Table B.1 – *Continued from previous page*

Line	AtG	n(fft)=	Mean Period (FFT)	Mean Diff v WT	P(period) =	
T0218	AT1G68810	8	23.67	-1.437	0.077	
T0219	AT1G68810	8	24.78	0.003	0.998	
T0221	AT1G72210	8	24.49	-0.292	0.854	
T0222	AT2G18300	10	23.42	-0.001	0.998	
T0223	AT2G18300	8	24.76	-0.351	0.657	
T0227	AT2G31210	8	22.77	-0.365	0.376	
T0238	AT2G46510	8	24.60	-0.509	0.522	
T0241	AT3G17100	8	24.99	-0.112	0.892	
T0242	AT3G20640	11	23.32	-0.099	0.827	
T0243	AT3G21330	8	23.14	0.004	0.993	
T0245	AT3G21330	31	22.62	-1.456	<0.001	***
T0247	AT3G21330	19	22.48	-1.597	<0.001	***
T0248	AT3G47640	8	23.39	-0.026	0.960	
T0259	AT4G00870	8	23.00	-0.138	0.736	
T0266	AT4G17880	7	23.40	-0.022	0.969	
T0272	AT4G30980	7	23.10	-0.032	0.943	
T0279	AT5G09750	8	23.15	-0.265	0.612	
T0281	AT5G12330	8	22.94	-0.194	0.633	
T0284	AT5G43650	7	21.95	-1.189	0.041	*
T0291	AT5G54680	8	22.87	-0.264	0.520	
T0294	AT5G58010	17	22.32	-1.757	<0.001	***
T0295	AT5G64340	6	23.23	0.095	0.840	
T0296	AT5G64980	14	22.72	-0.695	0.086	
T0301	AT5G67110	8	22.93	-1.854	0.251	
T0302	AT1G06070	13	22.96	-0.457	0.273	
T0306	AT1G06850	20	23.85	-0.234	0.374	
T0309	AT1G22070	20	23.64	-0.442	0.170	

Continued on next page

Table B.1 – *Continued from previous page*

Line	AtG	n(fft)=	Mean Period (FFT)	Mean Diff v WT	P(period) =	
T0310	AT1G22070	17	23.97	-0.114	0.694	
T0312	AT1G22070	7	24.28	-0.500	0.769	
T0315	AT1G58110	13	24.80	-1.030	0.014	*
T0318	AT1G58110	20	24.39	0.308	0.320	
T0327	AT2G18160	16	23.45	-0.631	0.035	*
T0329	AT2G35530	15	23.10	-0.317	0.408	
T0345	AT3G54620	21	23.93	-0.147	0.686	
T0349	AT3G62420	20	23.96	-0.123	0.688	
T0350	AT3G62420	20	23.32	-0.763	0.006	**
T0366	AT5G10030	21	23.30	-0.777	0.004	**
T0367	AT5G10030	20	23.11	-0.974	<0.001	***
T0368	AT5G10030	19	23.44	-0.640	0.031	*
T0377	AT1G04445	14	23.15	-0.263	0.506	
T0378	AT1G08290	17	23.75	-0.330	0.279	
T0380	AT1G14580	17	23.92	-0.161	0.661	
T0381	AT1G14580	13	56.11	32.031	0.002	**
T0388	AT1G66140	8	24.22	-0.522	0.418	
T0389	AT1G66140	16	23.08	-1.000	0.001	**
T0390	AT1G66140	15	23.77	-2.059	<0.001	***
T0393	AT2G02070	19	23.61	-0.467	0.136	
T0397	AT2G18490	21	23.46	-0.619	0.022	*
T0433	AT5G16470	21	23.31	-0.767	0.004	**
T0444	AT5G59820	7	24.87	0.135	0.854	
T0465	AT2G41900	21	23.79	-0.292	0.259	
T0468	AT1G28310	21	24.06	-0.017	0.952	
T0469	AT1G51700	15	24.88	-0.945	0.116	
T0470	AT1G51700	21	23.99	-0.085	0.751	

Continued on next page

Table B.1 – *Continued from previous page*

Line	AtG	n(fft)=	Mean Period (FFT)	Mean Diff v WT	P(period) =	
T0471	AT1G51700	20	24.13	0.051	0.900	
T0478	AT3G45610	20	23.45	-0.635	0.017	*
T0490	AT5G39660	18	23.91	-0.169	0.556	
T0491	AT5G39660	8	25.03	0.296	0.644	
T0492	AT5G62940	8	22.41	-0.728	0.081	
T0493	AT5G65590	7	22.46	-0.680	0.129	
T0494	AT5G65590	22	23.62	-0.462	0.090	
T0498	AT3G06740	19	23.73	-0.351	0.210	
T0500	AT3G21175	8	22.99	-0.143	0.722	
T0501	AT3G21175	22	23.79	-0.287	0.257	
T0505	AT3G54810	23	23.92	-0.156	0.529	
T0507	AT4G24470	8	24.19	-0.547	0.397	
T0509	AT4G26150	20	23.69	-0.392	0.165	
T0518	AT5G56860	8	25.12	0.379	0.544	
T0520	AT1G05230	8	24.18	-0.602	0.704	
T0520	AT1G05230	15	23.87	-1.958	<0.001	***
T0523	AT1G23380	18	23.66	-0.417	0.149	
T0525	AT1G30490	8	27.45	2.665	0.122	
T0528	AT1G52150	17	24.62	0.539	0.105	
T0529	AT1G69780	14	24.03	-1.801	<0.001	***
T0531	AT1G69780	18	23.77	-0.313	0.274	
T0534	AT1G75410	20	23.89	-0.195	0.477	
T0539	AT2G18550	20	23.26	-0.816	0.003	**
T0541	AT2G22800	21	23.26	-0.821	0.002	**
T0548	AT2G35940	21	23.70	-0.380	0.146	
T0549	AT3G01220	5	23.41	0.278	0.586	
T0555	AT3G61150	20	23.74	-0.338	0.280	

Continued on next page

Table B.1 – *Continued from previous page*

Line	AtG	n(fft)=	Mean Period (FFT)	Mean Diff v WT	P(period) =	
T0557	AT4G04890	14	22.90	-0.518	0.193	
T0560	AT4G16780	19	24.27	0.189	0.589	
T0562	AT4G32040	6	23.73	0.593	0.207	
T0564	AT4G32980	6	23.39	0.254	0.589	
T0565	AT4G34610	7	22.81	-0.327	0.452	
T0566	AT4G35550	7	23.73	-1.011	0.144	
T0568	AT4G37790	8	22.88	-0.253	0.530	
T0575	AT5G25220	8	24.29	-0.448	0.490	
T0580	AT5G25220	17	24.76	0.682	0.066	
T0589	AT2G38950	18	23.69	-0.393	0.195	
T0596	AT1G34190	7	23.34	0.201	0.641	
T0598	AT1G52890	21	23.26	-0.815	0.009	**
T0602	AT1G52890	19	23.69	-0.385	0.204	
T0603	AT1G52890	22	23.53	-0.551	0.037	*
T0604	AT1G52890	8	23.22	-1.559	0.328	
T0606	AT1G71930	5	22.59	-0.548	0.284	
T0608	AT1G71930	19	24.18	0.105	0.749	
T0610	AT1G71930	8	24.57	-0.208	0.899	
T0613	AT2G24430	8	24.46	-0.319	0.841	
T0615	AT2G33480	8	23.37	0.237	0.555	
T0618	AT2G46770	9	28.11	4.029	$<$0.001	***
T0619	AT2G46770	8	24.08	-0.658	0.311	
T0622	AT3G10490	7	23.12	-1.617	0.025	*
T0627	AT3G12910	8	23.19	-1.118	0.104	
T0630	AT3G18400	6	22.44	-0.695	0.145	
T0631	AT3G29035	8	23.23	0.092	0.825	
T0635	AT3G29035	8	23.85	-0.889	0.160	

Continued on next page

Table B.1 – *Continued from previous page*

Line	AtG	n(fft)=	Mean Period (FFT)	Mean Diff v WT	P(period) =
T0642	AT4G36160	8	23.15	0.015	0.971
T0644	AT5G04410	7	24.91	0.175	0.793
T0645	AT5G08790	8	22.52	-0.616	0.164
T0646	AT5G09330	8	23.04	-0.096	0.809
T0652	AT5G22380	8	23.20	0.064	0.873
T0654	AT5G22380	8	25.07	0.332	0.618
T0662	AT5G66300	8	23.12	-0.016	0.968
T0663	AT1G64280	8	22.83	-0.304	0.449
T0669	AT2G41370	8	24.90	0.122	0.941
T0670	AT2G41370	8	23.86	-0.918	0.564
T0690	AT2G41370	8	23.21	-1.101	0.123
T0700	AT2G41370	8	23.90	-0.879	0.580
T0701	AT2G41370	8	23.31	-1.473	0.357
T0702	AT1G63480	8	23.67	-1.112	0.484
T0724	AT4G39100	8	24.64	0.334	0.677
T0755	AT3G43240	8	23.56	-0.749	0.285
T0756	AT3G43240	8	23.22	-1.087	0.118
T0758	AT3G43240	8	23.30	-1.012	0.157
T0759	AT3G43240	8	23.81	-0.496	0.496
T0761	AT3G43240	8	24.67	-0.064	0.924
T0794	AT5G56270	7	24.68	-0.103	0.952
T0798	AT2G35310	8	24.28	-0.026	0.970
T0812	AT5G60140	8	23.31	-1.476	0.361
T0815	AT1G17590	8	28.84	4.056	0.129
T0816	AT1G17590	8	24.18	-0.127	0.854
T0816	AT1G17590	8	25.44	0.656	0.700
T0817	AT1G17590	14	24.97	-0.860	0.024 *

Continued on next page

Table B.1 – *Continued from previous page*

Line	AtG	n(fft)=	Mean Period (FFT)	Mean Diff v WT	P(period) =	
T0818	AT1G17590	8	23.09	-1.214	0.083	
T0828	AT3G14020	8	23.74	-0.569	0.407	
T0832	AT4G14540	8	25.44	0.702	0.320	
T0844	AT1G49560	8	24.48	-0.302	0.852	
T0847	AT1G68670	8	22.86	-1.452	0.038	*
T0849	AT1G79430	8	24.45	0.139	0.860	
T0853	AT2G03500	7	24.62	-0.118	0.860	
T0862	AT3G12730	8	24.56	-0.176	0.821	
T0868	AT3G46640	8	24.89	0.156	0.804	
T0874	AT4G31920	8	25.71	0.968	0.152	
T0875	AT4G31920	8	24.17	-0.569	0.385	
T0886	AT1G14920	14	22.81	-0.609	0.129	
T0887	AT1G14920	8	23.96	-0.823	0.605	
T0893	AT1G66350	8	23.61	-0.702	0.378	
T0895	AT2G04890	8	23.05	-1.256	0.069	
T0896	AT2G04890	8	23.77	-0.534	0.443	
T0898	AT2G04890	8	23.88	-0.428	0.542	
T0909	AT5G41920	7	24.22	-0.083	0.911	
T0923	AT1G76510	8	22.97	-1.334	0.058	
T0925	AT1G76500	8	23.90	-0.408	0.558	
T0945	AT1G67970	8	22.96	-1.351	0.056	
T0949	AT3G24520	7	24.81	-0.055	0.944	
T0954	AT4G17750	8	23.95	-0.361	0.611	
T0958	AT4G17750	8	23.78	-0.532	0.448	
T0962	AT5G54070	8	25.18	0.873	0.273	
T0963	AT5G54070	8	23.63	-0.678	0.342	
T0968	AT2G33810	8	24.42	-0.451	0.525	

Continued on next page

Table B.1 – *Continued from previous page*

Line	AtG	n(fft)=	Mean Period (FFT)	Mean Diff v WT	P(period) =
T0972	AT5G18830	8	24.08	-0.223	0.746
T1005	AT5G08330	12	22.68	-0.736	0.091
T1006	AT5G23280	6	23.59	0.457	0.332
T1008	AT5G51910	10	22.84	-0.577	0.227
T1009	AT5G60970	8	23.11	-0.030	0.942
T1010	AT1G13450	11	22.94	-0.477	0.293
T1011	AT1G21200	7	24.29	1.157	0.066
T1012	AT1G54060	10	23.02	-0.394	0.414
T1017	AT2G35640	8	22.88	-0.259	0.524
T1018	AT2G38250	13	23.14	-0.282	0.505
T1021	AT3G10030	7	22.17	-0.965	0.071
T1023	AT3G11100	12	22.75	-0.665	0.132
T1028	AT3G58630	8	22.94	-0.195	0.638
T1029	AT4G17050	11	23.87	0.451	0.402
T1033	AT5G05550	8	23.02	-0.114	0.778
T1034	AT5G28300	13	22.66	-0.758	0.072
T1035	AT5G47660	8	22.99	-0.142	0.728
T1038	AT1G07470	11	22.60	-0.820	0.072
T1039	AT1G07900	7	22.79	-0.341	0.431
T1040	AT1G16530	14	23.10	-0.319	0.428
T1041	AT1G31320	7	22.67	-0.470	0.288
T1042	AT1G31320	8	23.98	-0.326	0.644
T1043	AT1G31320	7	25.23	0.925	0.212
T1044	AT1G75510	13	24.13	0.710	0.173
T1045	AT1G75510	8	25.52	1.209	0.114
T1046	AT1G78420	5	22.99	-0.143	0.784
T1050	AT2G37120	10	23.07	-0.350	0.455

Continued on next page

Table B.1 – *Continued from previous page*

Line	AtG	n(fft)=	Mean Period (FFT)	Mean Diff v WT	P(period) =	
T1058	AT3G03760	16	23.00	-0.415	0.265	
T1060	AT3G10330	13	23.05	-0.369	0.375	
T1071	AT4G24440	16	22.85	-0.563	0.133	
T1074	AT4G37540	7	24.44	0.135	0.854	
T1080	AT5G67420	8	24.22	-0.084	0.902	
T1081	AT5G67420	8	23.91	-0.398	0.561	
T1083	AT1G49130	15	23.22	-0.201	0.603	
T1085	AT1G60250	8	23.23	-1.076	0.117	
T1086	AT1G60250	8	24.40	-0.468	0.534	
T1087	AT1G60250	8	23.48	-0.832	0.224	
T1090	AT2G21320	8	23.65	-0.656	0.339	
T1091	AT2G31380	13	23.06	-0.361	0.384	
T1092	AT2G47890	15	24.30	-0.566	0.366	
T1093	AT3G02380	9	22.77	-0.646	0.206	
T1094	AT3G07650	11	22.86	-0.562	0.229	
T1095	AT3G21150	9	23.28	-0.136	0.788	
T1101	AT4G39070	12	23.20	-0.220	0.622	
T1103	AT5G15840	7	23.70	-1.168	0.132	
T1104	AT5G48250	8	22.81	-2.063	0.005	**
T1105	AT5G54470	16	23.08	-0.336	0.367	
T1106	AT5G57660	8	23.60	-1.272	0.103	
T1108	AT3G22760	13	23.28	-0.140	0.734	
T1111	AT5G66940	8	22.90	-0.240	0.564	
T1112	AT1G47870	8	24.67	-0.197	0.805	
T1116	AT5G14960	11	22.99	-0.423	0.350	
T1119	AT2G27050	7	23.07	-0.070	0.884	
T1131	AT4G00270	8	24.51	-0.356	0.624	

Continued on next page

Table B.1 – *Continued from previous page*

Line	AtG	n(fft)=	Mean Period (FFT)	Mean Diff v WT	P(period) =	
T1135	AT5G28040	8	24.09	-0.782	0.308	
T1137	AT2G36400	7	23.36	-1.421	0.405	
T1139	AT3G13960	4	23.86	0.726	0.215	
T1143	AT5G40710	8	25.28	0.494	0.769	
T1144	AT5G63280	6	22.69	-0.445	0.360	
T1146	AT1G10200	8	23.67	-1.201	0.092	
T1147	AT2G39900	8	24.75	-0.029	0.986	
T1148	AT2G45800	3	23.17	0.034	0.959	
T1149	AT3G55770	5	22.56	-0.576	0.279	
T1152	AT1G17310	8	23.87	-0.999	0.160	
T1153	AT1G22590	8	23.58	-1.286	0.075	
T1154	AT1G24260	4	23.48	0.348	0.540	
T1155	AT1G26310	8	24.58	-0.293	0.676	
T1165	AT1G65300	8	24.25	-0.623	0.379	
T1168	AT1G69120	7	23.40	-1.469	0.057	
T1175	AT2G22630	3	22.86	-0.278	0.675	
T1176	AT2G45650	4	22.78	-0.355	0.542	
T1182	AT3G54340	14	23.39	-0.031	0.938	
T1185	AT5G65230	8	23.85	-1.018	0.157	
T1186	AT5G65790	7	25.38	0.512	0.552	
T1195	AT1G28520	8	24.58	-0.291	0.682	
T1203	AT1G66500	7	24.46	-0.408	0.588	
T1208	AT2G02540	7	22.97	-1.894	0.017	*
T1213	AT2G42400	8	24.54	-0.328	0.656	
T1236	AT4G26170	8	24.26	-0.525	0.741	
T1254	AT5G50010	8	25.85	0.979	0.217	
T1275	AT1G25280	14	23.83	0.410	0.322	

Continued on next page

Table B.1 – *Continued from previous page*

Line	AtG	n(fft)=	Mean Period (FFT)	Mean Diff v WT	P(period) =	
T1280	AT3G57390	8	23.10	-0.033	0.937	
T1281	AT3G58780	6	22.87	-0.266	0.564	
T1284	AT4G09960	8	22.99	-0.148	0.714	
T1287	AT4G18960	3	23.23	0.098	0.881	
T1293	AT5G10140	5	22.94	-0.195	0.702	
T1294	AT5G13790	6	22.81	-0.326	0.578	
T1295	AT5G15800	3	22.67	-0.466	0.483	
T1296	AT5G20240	5	22.49	-0.646	0.230	
T1303	AT5G26880	13	23.47	0.053	0.899	
T1315	AT5G27810	8	22.87	-1.999	0.006	**
T1316	AT5G60910	3	23.01	-0.124	0.849	
T1317	AT5G62165	5	23.22	0.084	0.869	
T1324	AT1G01520	26	23.43	0.008	0.979	
T1325	AT1G06910	6	22.95	-0.184	0.706	
T1327	AT1G09540	12	21.59	-1.831	<0.001	***
T1331	AT1G14350	13	22.69	-0.730	0.079	
T1332	AT1G15720	14	22.95	-0.469	0.242	
T1335	AT1G17950	6	22.65	-0.766	0.210	
T1336	AT1G18330	16	22.90	-0.515	0.169	
T1337	AT1G18570	13	23.64	0.225	0.676	
T1346	AT1G48000	8	23.70	-1.164	0.118	
T1347	AT1G49010	4	23.06	-0.076	0.896	
T1348	AT1G49950	8	22.51	-2.357	0.004	**
T1349	AT1G56650	13	22.78	-0.640	0.134	
T1351	AT1G63910	8	23.89	-0.977	0.173	
T1352	AT1G66230	8	25.09	0.224	0.796	
T1354	AT1G66380	10	23.07	-0.344	0.466	

Continued on next page

Table B.1 – *Continued from previous page*

Line	AtG	n(fft)=	Mean Period (FFT)	Mean Diff v WT	P(period) =	
T1355	AT1G68320	9	23.10	-0.316	0.534	
T1356	AT1G70000	7	25.00	0.128	0.870	
T1357	AT1G71030	13	23.04	-0.381	0.356	
T1360	AT1G74430	7	26.52	1.652	0.039	*
T1368	AT2G23290	8	25.99	1.117	0.129	
T1380	AT2G47190	8	23.11	-0.029	0.942	
T1381	AT2G47460	11	23.24	-0.181	0.684	
T1384	AT3G02940	9	22.50	-0.920	0.070	
T1387	AT3G09370	8	23.81	-1.057	0.140	
T1401	AT3G27785	8	26.38	1.510	0.055	
T1421	AT4G09460	8	24.17	-0.701	0.324	
T1428	AT4G34990	8	24.06	-0.812	0.281	
T1435	AT5G02840	8	22.91	-1.954	0.008	**
T1438	AT5G07690	8	23.78	-1.091	0.130	
T1440	AT5G08520	8	24.75	-0.122	0.874	

Bibliography

M. G. Aarts, W. G. Dirkse, W. J. Stiekema, and a. Pereira. Transposon tagging of a male sterility gene in Arabidopsis. *Nature*, 363(6431):715–717, 1993.

M. D. Abràmofff, P. J. Magalhães, and S. J. Ram. Image processing with ImageJ. *Biophotonics International*, 11:36–43, 2005.

D. Alabadí, T. Oyama, M. J. Yanovsky, F. G. Harmon, P. Más, and S. A. Kay. Reciprocal regulation between TOC1 and LHY/CCA1 within the Arabidopsis circadian clock. *Science*, 293(5531):880–883, aug 2001.

D. Alabadí, M. J. Yanovsky, P. Más, S. L. Harmer, and S. a. Kay. Critical Role for CCA1 and LHY in Maintaining Circadian Rhythmicity in Arabidopsis. *Current Biology*, 12 (02):757–761, 2002.

U. Albrecht and G. Eichele. The mammalian circadian clock. *Current Opinion in Genetics and Development*, 13(3):271–277, 2003.

G. J. Allen, S. R. Muir, and D. Sanders. Release of Ca2+ from individual plant vacuoles by both InsP3 and cyclic ADP-ribose. *Science*, 268(5211):735–737, 1995.

G. J. Allen, S. P. Chu, C. L. Harrington, K. Schumacher, T. Hoffmann, Y. Y. Tang, E. Grill, and J. I. Schroeder. A defined range of guard cell calcium oscillation parameters encodes stomatal movements. *Nature*, 411:1053–1057, 2001.

J. M. Alonso, A. N. Stepanova, T. J. Leisse, C. J. Kim, H. Chen, P. Shinn, D. K. Stevenson, J. Zimmerman, P. Barajas, R. Cheuk, C. Gadrinab, C. Heller, A. Jeske, E. Koesema, C. C. Meyers, H. Parker, L. Prednis, Y. Ansari, N. Choy, H. Deen, M. Geralt, N. Hazari, E. Hom, M. Karnes, C. Mulholland, R. Ndubaku, I. Schmidt, P. Guzman, L. Aguilar-Henonin, M. Schmid, D. Weigel, D. E. Carter, T. Marchand, E. Risseeuw, D. Brogden, A. Zeko, W. L. Crosby, C. C. Berry, and J. R. Ecker. Genome-wide insertional mutagenesis of Arabidopsis thaliana. *Science*, 301(5633): 653–657, 2003.

T. Altmann, G. Felix, A. Jessop, A. Kauschmann, U. Uwer, H. Peña-Cortés, and L. Willmitzer. Ac/Ds transposon mutagenesis in Arabidopsis thaliana: mutant spectrum and frequency of Ds insertion mutants. *MGG Molecular & General Genetics*, 247(5):646–652, 1995.

S. F. Altschul, W. Gish, W. Miller, E. W. Myers, and D. J. Lipman. Basic local alignment search tool. *Journal of Molecular Biology*, 215(3):403–410, 1990.

S. Aoki, T. Kondo, H. Wada, and M. Ishiura. Circadian rhythm of the cyanobacterium Synechocystis sp. strain PCC 6803 in the dark. *Journal of Bacteriology*, 179(18): 5751–5755, 1997.

T. Aoyama and N.-H. Chua. A glucocorticoid-mediated transcriptional induction system in transgenic plants. *The Plant Journal*, 11(3):605–612, mar 1997.

T. Araki and Y. Komeda. Analysis of the role of the late-flowering locus, GI, in the flowering of Arabidopsis thaliana. *Plant Journal*, 3(2):231–239, 1993.

F. D. Ariel, P. a. Manavella, C. a. Dezar, and R. L. Chan. The true story of the HD-Zip family. *Trends in Plant Science*, 12(9):419–426, 2007.

W. Arnold and J. B. Davidson. The identity of the fluorescent and delayed light emission spectra in Chlorella. *The Journal of General Physiology*, 37(5):677–684, 1954.

K. Bae and I. Edery. Regulating a circadian clock's period, phase and amplitude by phosphorylation: Insights from Drosophila. *Journal of Biochemistry*, 140(5):609–617, 2006.

I. Bancroft and C. Dean. Transposition pattern of the maize element Ds in Arabidopsis thaliana. *Genetics*, 134(4):1221–1229, 1993.

T. Barrett, D. B. Troup, S. E. Wilhite, P. Ledoux, D. Rudnev, C. Evangelista, I. F. Kim, A. Soboleva, M. Tomashevsky, and R. Edgar. NCBI GEO: Mining tens of millions of expression profiles - Database and tools update. *Nucleic Acids Research*, 35(SUPPL. 1):760–765, 2007.

A. Baudry, S. Ito, Y. H. Song, A. a. Strait, T. Kiba, S. Lu, R. Henriques, J. L. Pruneda-Paz, N. H. Chua, E. M. Tobin, S. a. Kay, and T. Imaizumi. F-Box Proteins FKF1 and LKP2 Act in Concert with ZEITLUPE to Control Arabidopsis Clock Progression. *The Plant Cell*, 22(3):606–622, mar 2010.

J. Beales, A. Turner, S. Gri, J. W. Snape, D. a. Laurie, S. Griffiths, J. W. Snape, and D. a. Laurie. A Pseudo-Response Regulator is misexpressed in the photoperiod insensitive Ppd-D1a mutant of wheat (Triticum aestivum L.). *Theoretical and Applied Genetics*, 115(5):721–733, 2007.

O. Ben-Naim, R. Eshed, A. Parnis, P. Teper-Bamnolker, A. Shalit, G. Coupland, A. Samach, and E. Lifschitz. The CCAAT binding factor can mediate interactions between CONSTANS-like proteins and DNA. *The Plant Journal*, 46(3):462–476, 2006.

C. Bendix, J. M. Mendoza, D. N. Stanley, R. Meeley, and F. G. Harmon. The circadian clock-associated gene gigantea1 affects maize developmental transitions. *Plant, Cell and Environment*, 36(7):1379–1390, 2013.

P. N. Benfey and N. H. Chua. The Cauliflower Mosaic Virus 35S Promoter: Combinatorial Regulation of Transcription in Plants. *Science*, 250(4983):959–966, 1990.

M. Berden-zrimec, L. Drinovec, and A. Zrimec. *Chlorophyll a Fluorescence in Aquatic Sciences: Methods and Applications*, volume 4. Springer Netherlands, Dordrecht, 2010. ISBN 978-90-481-9267-0.

V. Bhardwaj, S. Meier, L. N. Petersen, R. a. Ingle, and L. C. Roden. Defence responses of arabidopsis thaliana to infection by pseudomonas syringae are regulated by the circadian clock. *PLoS ONE*, 6(10):1–8, 2011.

A. M. Bhatt, T. Page, E. J. Lawson, C. Lister, and C. Dean. Use of Ac as an insertional mutagen in Arabidopsis. *The Plant Journal*, 9(6):935–945, jun 1996.

Z. Bieniawska, C. Espinoza, A. Schlereth, R. Sulpice, D. K. Hincha, and M. a. Hannah. Disruption of the Arabidopsis circadian clock is responsible for extensive variation in the cold-responsive transcriptome. *Plant physiology*, 147(1):263–79, may 2008.

R. E. Blankenship. *Molecular Mechanisms of Photosynthesis*. Blackwell Science Ltd, Oxford, UK, dec 2002. ISBN 9780470758472.

O. E. Bläsing, Y. Gibon, M. Günther, M. Höhne, R. Morcuende, D. Osuna, O. Thimm, B. Usadel, W.-R. Scheible, M. Stitt, O. E. Bla, M. Ho, and O. Thimm. Sugars and circadian regulation make major contributions to the global regulation of diurnal gene expression in Arabidopsis. *The Plant Cell*, 17(12):3257–3281, dec 2005.

M. Blazquez, R. Green, O. Nilsson, M. Sussman, and D. Weigel. Gibberellins promote flowering of arabidopsis by activating the LEAFY promoter. *The Plant Cell*, 10(5): 791–800, 1998.

L. K. Bognár, a. Hall, E. Adám, S. C. Thain, F. Nagy, and a. J. Millar. The circadian clock controls the expression pattern of the circadian input photoreceptor, phytochrome B. *Proceedings of the National Academy of Sciences of the United States of America*, 96 (25):14652–14657, 1999.

N. E. Borlaug. Contributions of conventional plant breeding to food production. *Science*, 219(4585):689–693, 1983.

J. Bou-Torrent, M. Salla-Martret, R. Brandt, T. Musielak, J.-C. Palauqui, J. F. Martinez-Garcia, and S. Wenkel. ATHB4 and HAT3, two class II HD-ZIP transcription factors, control leaf development in Arabidopsis. *Plant Signaling & Behavior*, 7(11):1382–1387, 2012.

N. Bouché and D. Bouchez. Arabidopsis gene knockout: Phenotypes wanted. *Current Opinion in Plant Biology*, 4(2):111–117, 2001.

P. Boudry, R. Wieber, P. Saumitou-Laprade, K. Pillen, H. Van Dijk, and C. Jung. Identification of RFLP markers closely linked to the bolting gene B and their significance for the study of the annual habit in beets (Beta vulgaris L.). *Theoretical and Applied Genetics*, 88(6-7):852–858, 1994.

R. Bours, M. Muthuraman, H. Bouwmeester, and A. van der Krol. OSCILLATOR: A system for analysis of diurnal leaf growth using infrared photography combined with wavelet transformation. *Plant Methods*, 8(1):29, aug 2012.

B. Brockmann, M. W. Smith, a. G. Zaraisky, K. Harrison, K. Okada, and Y. Kamiya. Subcellular localization and targeting of glucocorticoid receptor protein fusions expressed in transgenic Arabidopsis thaliana. *Plant and Cell Physiology*, 42(9):942–951, 2001.

S. a. Brown, E. Kowalska, and R. Dallmann. (Re)inventing the Circadian Feedback Loop. *Developmental Cell*, 22(3):477–487, 2012.

M. Brunner and K. Káldi. Interlocked feedback loops of the circadian clock of Neurospora crassa. *Molecular Microbiology*, 68(2):255–262, 2008.

J. C. Buckingham. Glucocorticoids: Exemplars of Multi-Tasking. *British Journal of Pharmacology*, 147(1):S258–S268, 2006.

J. P. Burg. The relationship between maximum entropy and maximum likelihood spectra. *Geophysics*, 37(2):375–276, 1972.

G. Q. Butcher, H. Dziema, M. Collamore, P. W. Burgoon, K. Obrietan, and K. Obrietani. The p42/44 mitogen-activated protein kinase pathway couples photic input to circadian clock entrainment. *Journal of Biological Chemistry*, 277(33):29519–29525, 2002.

C. Cajochen, K. Kräuchi, A. Wirz-Justice, and K. Kra. Role of melatonin in the regulation of human circadian rhythms and sleep. *Journal of Neuroendocrinology*, 15(4): 432–437, 2003.

A. J. Cary, W. Liu, and S. H. Howell. Cytokinin action is coupled to ethylene in its effects on the inhibition of root and hypocotyl elongation in Arabidopsis thaliana seedlings. *Plant Physiology*, 107(1 995):1075–1082, 1995.

A. R. Cashmore, J. A. Jarillo, Y. J. Wu, and D. Liu. Cryptochromes: blue light receptors for plants and animals. *Science*, 284(5415):760–765, apr 1999.

P. D. Cerdán and J. Chory. Regulation of flowering time by light quality. *Nature*, 423 (6942):881–885, 2003.

P. D. Cerdán, M. J. Yanovsky, F. C. Reymundo, A. Nagatani, R. J. Staneloni, G. C. Whitelam, and J. J. Casal. Regulation of phytochrome B signaling by phytochrome A and FHY1 in Arabidopsis thaliana. *The Plant Journal*, 18(5):499–507, jun 1999.

S. M. Chaw, C. C. Chang, H. L. Chen, and W. H. Li. Dating the monocot-dicot divergence and the origin of core eudicots using whole chloroplast genomes. *Journal of Molecular Evolution*, 58(4):424–441, 2004.

M. Chen, J. Chory, and C. Fankhauser. Light signal transduction in higher plants. *Annual Review of Genetics*, 38:87–117, jan 2004.

Y.-b. B. Chen, Y.-b. B. Chen, B. Dominic, B. Dominic, M. T. Mellon, M. T. Mellon, J. P. Zehr, J. P. Zehr, S. Ims, Y.-b. B. Chen, B. Dominic, M. T. Mellon, and J. P. Zehr. Circadian rhythm of nitrogenase gene expression in the diazotrophic filamentous nonheterocystous cyanobacterium Trichodesmium sp strain IMS101. *Journal of Bacteriology*, 180(14):3598–3605, 1998.

Y.-Y. Chen, Y. Wang, L.-J. Shin, J.-F. Wu, V. Shanmugam, M. Tsednee, J.-C. Lo, C.-C. Chen, S.-H. Wu, and K.-C. Yeh. Iron is involved in the maintenance of circadian period length in Arabidopsis. *Plant Physiology*, 161:1409–20, jan 2013.

P. Cheng, Y. Yang, and Y. Liu. Interlocked feedback loops contribute to the robustness of the Neurospora circadian clock. *Proceedings of the National Academy of Sciences*, 98(13):7408–7413, 2001.

W.-l. Chiu, Y. Niwa, W. Zeng, T. Hirano, H. Kobayashi, and J. Sheen. Engineered GFP as a vital reporter in plants. *Current Biology*, 6(3):325–30, mar 1996.

H. Choi, J. Hong, J. Ha, J. Kang, and S. Kim. ABFs, a family of ABA responsive element binding factors. *Journal of Biological Chemistry*, 275(3):1723–1730, 2000.

J. Chory and J. Li. Gibberellins, brassinosteroids and light-regulated development. *Plant, Cell and Environment*, 20:801–806, 1997.

M. K. Choudhary, Y. Nomura, L. Wang, H. Nakagami, and D. E. Somers. Quantitative circadian phosphoproteomic analysis of Arabidopsis reveals extensive clock control of key components in physiological, metabolic and signaling pathways. *Molecular and Cellular Proteomics*, pages 1–56, 2015.

B. Y. Chow, A. Helfer, D. A. Nusinow, and S. A. Kay. ELF3 recruitment to the PRR9 promoter requires other Evening Complex members in the Arabidopsis circadian clock. *Plant Signaling & Behavior*, 7(2):170–173, 2012.

G. Christen, R. Steffen, and G. Renger. Delayed fluorescence emitted from light harvesting complex II and photosystem II of higher plants in the 100 ns-5 μs time domain. *FEBS Letters*, 475(2):103–106, 2000.

A. R. Ciarbelli, A. Ciolfi, S. Salvucci, V. Ruzza, M. Possenti, M. Carabelli, A. Fruscalzo, G. Sessa, G. Morelli, and I. Ruberti. The Arabidopsis Homeodomain-leucine Zipper II gene family: Diversity and redundancy. *Plant Molecular Biology*, 68(4-5):465–478, 2008.

T. Clack, S. Mathews, and R. a. Sharrock. The phytochrome apoprotein family in Arabidopsis is encoded by five genes: the sequences and expression of PHYD and PHYE. *Plant Molecular Biology*, 25(3):413–427, jun 1994.

S. E. Clark, S. E. Jacobsen, J. Z. Levin, and E. M. Meyerowitz. The CLAVATA and SHOOT MERISTEMLESS loci competitively regulate meristem activity in Arabidopsis. *Development*, 122(5):1567–1575, 1996.

S. Clemens, M. G. Palmgren, U. Krämer, and U. Kr. A long way ahead: Understanding and engineering plant metal accumulation. *Trends in Plant Science*, 7(7):309–315, 2002.

S. J. Clough and A. F. Bent. Floral dip: A simplified method for Agrobacterium-mediated transformation of Arabidopsis thaliana. *The Plant Journal*, 16(6):735–743, dec 1998.

C. E. Collett, N. P. Harberd, and O. Leyser. Hormonal interactions in the control of Arabidopsis hypocotyl elongation. *Plant Physiology*, 124(2):553–562, 2000.

A. Concerte, C. Duc, F. Cellier, S. Lobréaux, J. F. Briat, and F. Gaymard. Regulation of iron homeostasis in Arabidopsis thaliana by the clock regulator time for coffee. *Journal of Biological Chemistry*, 284(52):36271–36281, 2009.

L. Corbesier and G. Coupland. The quest for florigen: a review of recent progress. *Journal of experimental botany*, 57(13):3395–3403, 2006.

M. J. Costa, B. Finkenstädt, V. Roche, F. Lévi, P. D. Gould, J. Foreman, K. Halliday, A. Hall, and D. A. Rand. Inference on periodicity of circadian time series. *Biostatistics*, 14(4):792–806, 2013.

M. F. Covington and S. L. Harmer. The circadian clock regulates auxin signaling and responses in Arabidopsis. *PLoS Biology*, 5(8):1773–1784, 2007.

M. F. Covington, J. N. Maloof, M. Straume, S. A. Kay, and S. L. Harmer. Global transcriptome analysis reveals circadian regulation of key pathways in plant growth and development. *Genome Biology*, 9(8):R130, jan 2008.

P. G. Cristiane, C. P. G. Calixto, R. Waugh, and J. W. S. Brown. Evolutionary Relationships Among Barley and Arabidopsis Core Circadian Clock and Clock-Associated Genes. *Journal of Molecular Evolution*, 80(2):108–119, 2015.

J. W. Cutcliffe, E. Hellmann, A. Heyl, and A. M. Rashotte. CRFs form protein-protein interactions with each other and with members of the cytokinin signalling pathway in Arabidopsis via the CRF domain. *Journal of Experimental Botany*, 62(14):4995–5002, 2011.

S. Dai, X. Wei, L. Pei, R. L. Thompson, Y. Liu, J. E. Heard, T. G. Ruff, and R. N. Beachy. BROTHER OF LUX ARRHYTHMO is a component of the Arabidopsis circadian clock. *The Plant Cell*, 23(March):961–972, 2011.

N. Dalchau, S. J. Baek, H. M. Briggs, F. C. Robertson, A. N. Dodd, M. J. Gardner, M. A. Stancombe, M. J. Haydon, G.-B. Stan, J. M. Gonçalves, and A. A. R. Webb. The circadian oscillator gene GIGANTEA mediates a long-term response of the Arabidopsis thaliana circadian clock to sucrose. *Proceedings of the National Academy of Sciences*, 108(12):5104–5109, mar 2011.

X. Daniel, S. Sugano, and E. M. Tobin. CK2 phosphorylation of CCA1 is necessary for its circadian oscillator function in Arabidopsis. *Proceedings of the National Academy of Sciences*, 101:3292–3297, 2004.

S. Datta, G. H. C. M. Hettiarachchi, X.-W. Deng, and M. Holm. Arabidopsis CONSTANS-LIKE3 is a positive regulator of red light signaling and root growth. *The Plant Cell*, 18(1):70–84, 2006.

A. M. Davis, A. Hall, A. J. Millar, C. Darrah, and S. J. Davis. Protocol: Streamlined sub-protocols for floral-dip transformation and selection of transformants in Arabidopsis thaliana. *Plant Methods*, 5:3, jan 2009.

R. V. Davuluri, H. Sun, S. K. Palaniswamy, N. Matthews, C. Molina, M. Kurtz, and E. Grotewold. AGRIS : Arabidopsis Gene Regulatory Information Server , an nformation resource of Arabidopsis cis-regulatory elements and transcription factors. *BMC Bioinformatics*, 4(25):1–11, 2003.

A. de Montaigu, A. Giakountis, M. Rubin, R. Tóth, F. Cremer, V. Sokolova, A. Porri, M. Reymond, C. Weinig, and G. Coupland. Natural diversity in daily rhythms of gene expression contributes to phenotypic variation. *Proceedings of the National Academy of Sciences of the United States of America*, 104:20996–21001, 2014.

I. Debeaujon, K. M. Léon-Kloosterziel, and M. Koornneef. Influence of the testa on seed dormancy, germination, and longevity in Arabidopsis. *Plant Physiology*, 122(2): 403–414, 2000.

M. Delarue, E. Prinsen, H. Van Onckelen, M. Caboche, and C. Bellini. Sur2 mutations of Arabidopsis thaliana define a new locus involved in the control of auxin homeostasis. *Plant Journal*, 14(5):603–611, 1998.

E. Demarsy and C. Fankhauser. Higher plants use LOV to perceive blue light. *Current Opinion in Plant Biology*, 12(1):69–74, 2009.

P. F. Devlin and S. A. Kay. Cryptochromes are required for phytochrome signaling to the circadian clock but not for rhythmicity. *The Plant Cell*, 12(12):2499–2510, dec 2000.

E. B. Djouani-Tahri, J.-P. Motta, F.-Y. Bouget, and F. Corellou. Insights into the regulation of the core clock component TOC1 in the green picoeukaryote Ostreococcus. *Plant signaling & behavior*, 5(April 2015):332–335, 2010.

A. N. Dodd, N. Salathia, A. Hall, E. Kévei, R. Tóth, F. Nagy, J. M. Hibberd, A. J. Millar, and A. A. R. Webb. Plant circadian clocks increase photosynthesis, growth, survival, and competitive advantage. *Science*, 309(5734):630–633, 2005.

A. N. Dodd, M. J. Gardner, C. T. Hotta, K. E. Hubbard, N. Dalchau, J. Love, J.-M. Assie, Fiona C. Robertson, M. K. Jakobsen, J. M. Gonçalves, D. Sanders, and A. A. R. Webb. The Arabidopsis circadian clock incorporates a cADPR-based feedback loop. *Science*, 318(1789):1790–1792, 2009.

A. N. Dodd, J. Kudla, and D. Sanders. The language of calcium signaling. *Annual Review of Plant Biology*, 61:593–620, jan 2010.

T. Dornbusch, O. Michaud, I. Xenarios, and C. Fankhauser. Differentially Phased Leaf Growth and Movements in Arabidopsis Depend on Coordinated Circadian and Light Regulation. *The Plant Cell*, 26(10):3911–3921, oct 2014.

J.-J. d'Ortous De Mairan. Observation botanique. In *Histoire de l'Academie Royale des Sciences*, pages 35–36. 1792.

H. B. Dowse and J. M. Ringo. The search for hidden periodicities in biological time series revisited. *Journal of Theoretical Biology*, 139:487–515, 1989.

M. J. Dowson-Day and A. J. Millar. Circadian dysfunction causes aberrant hypocotyl elongation patterns in Arabidopsis. *The Plant Journal*, 17(1):63–71, jan 1999.

M. R. Doyle, S. J. Davis, R. M. Bastow, H. G. McWatters, L. Kozma-Bognár, F. Nagy, A. J. Millar, and R. M. Amasino. The ELF4 gene controls circadian rhythms and flowering time in Arabidopsis thaliana. *Nature*, 419(6902):74–77, 2002.

V. Dvornyk, O. Vinogradova, and E. Nevo. Origin and evolution of circadian clock genes in prokaryotes. *Proceedings of the National Academy of Sciences*, 100(5):2495–2500, 2003.

A. Edelstein, N. Amodaj, K. Hoover, R. Vale, and N. Stuurman. Computer control of microscopes using manager. *Current Protocols in Molecular Biology*, pages 1–22, 2010.

R. S. Edgar, E. W. Green, Y. Zhao, G. van Ooijen, M. Olmedo, X. Qin, Y. Xu, M. Pan, U. K. Valekunja, K. A. Feeney, E. S. Maywood, M. H. Hastings, N. S. Baliga, M. Merrow, A. J. Millar, C. H. Johnson, C. P. Kyriacou, J. S. O'Neill, and A. B. Reddy. Peroxiredoxins are conserved markers of circadian rhythms. *Nature*, 485(7399):459–64, may 2012.

C. E. Edwards, B. E. Ewers, D. G. Williams, Q. Xie, P. Lou, X. Xu, C. R. Mcclung, C. Weinig, C. Robertson McClung, and C. Weinig. The genetic architecture of ecophysiological and circadian traits in Brassica rapa. *Genetics*, 189(1):375–390, 2011.

C. E. Edwards, B. E. Ewers, C. R. McClung, P. Lou, and C. Weinig. Quantitative variation in water-use efficiency across water regimes and its relationship with circadian, vegetative, reproductive, and leaf gas-exchange traits. *Molecular Plant*, 5(3):653–668, 2012.

D. Edwards, J. a. Murray, and a. G. Smith. Multiple genes encoding the conserved CCAAT-box transcription factor complex are expressed in Arabidopsis. *Plant Physiology*, 117(3):1015–1022, 1998.

K. D. Edwards and A. J. Millar. Analysis of circadian leaf movement rhythms in Arabidopsis thaliana. *Methods in Molecular Biology*, 362:103–113, jan 2007.

K. D. Edwards, J. R. Lynn, P. Gyula, F. Nagy, and A. J. Millar. Natural allelic variation in the temperature-compensation mechanisms of the Arabidopsis thaliana circadian clock. *Genetics*, 170(1):387–400, may 2005.

K. D. Edwards, O. E. Akman, K. Knox, P. J. Lumsden, A. W. Thomson, P. E. Brown, A. Pokhilko, L. Kozma-Bognar, F. Nagy, D. A. Rand, and A. J. Millar. Quantitative analysis of regulatory flexibility under changing environmental conditions. *Molecular Systems Biology*, 6(424):424, nov 2010.

Z. Eelderink-Chen, G. Mazzotta, M. Sturre, J. Bosman, T. Roenneberg, and M. Merrow. A circadian clock in Saccharomyces cerevisiae. *Proceedings of the National Academy of Sciences*, 107(5):2043–2047, 2010.

K. Eimert, S. Wang, W. Lue, and J. Chen. Monogenic Recessive Mutations Causing Both Late Floral Initiation and Excess Starch Accumulation in Arabidopsis. *The Plant Cell*, 7(10):1703–1712, 1995.

M. B. Elowitz and S. Leibler. A synthetic oscillatory network of transcriptional regulators. *Nature*, 403(6767):335–338, 2000.

M. Endo, H. Shimizu, M. A. Nohales, T. Araki, and S. A. Kay. Tissue-specific clocks in Arabidopsis show asymmetric coupling. *Nature*, 515(7527):419–422, oct 2014.

K. Endrizzi, B. Moussian, A. Haecker, J. Z. Levin, and T. Laux. The SHOOT MERISTEMLESS gene is required for maintenance of undifferentiated cells in Arabidopsis shoot and floral meristems and acts at a different regulatory level than the meristem genes WUSCHEL and ZWILLE. *The Plant Journal*, 10(6):967–979, 1996.

W. Engelmann and A. Johnsson. Rhythms in Organ Movement. In P. J. Lumsden and A. J. Millar, editors, *Biological Rhythms and Photoperiodism in Plants*, chapter 2, pages 35–48. BIOS Scientific Publishers, Oxford, UK, 1998. ISBN 1859962165.

H. a. Ernst, A. N. Olsen, S. Larsen, and L. Lo Leggio. Structure of the conserved domain of ANAC, a member of the NAC family of transcription factors. *EMBO reports*, 5(3): 297–303, 2004.

P. Facella, L. Lopez, F. Carbone, D. W. Galbraith, G. Giuliano, and G. Perrotta. Diurnal and circadian rhythms in the tomato transcriptome and their modulation by cryptochrome photoreceptors. *PLoS ONE*, 3(7), 2008.

B. Farinas and P. Mas. Functional implication of the MYB transcription factor RVE8/LCL5 in the circadian control of histone acetylation. *The Plant Journal*, 66: 318–329, 2011.

E. M. Farré. The regulation of plant growth by the circadian clock. *Plant biology (Stuttgart, Germany)*, 14(3):401–10, may 2012.

E. M. Farré and S. a. Kay. PRR7 protein levels are regulated by light and the circadian clock in Arabidopsis. *Plant Journal*, 52:548–560, 2007.

E. M. Farré, S. L. Harmer, and F. G. Harmon. Overlapping and distinct roles of PRR7 and PRR9 in the Arabidopsis circadian clock. *Current Biology*, 15:47–54, 2005.

S. A. Filichkin, H. D. Priest, S. A. Givan, R. Shen, D. W. Bryant, S. E. Fox, W.-k. K. Wong, and T. C. Mockler. Genome-wide mapping of alternative splicing in Arabidopsis thaliana. *Genome Research*, 20(1):45–58, 2010.

L. S. Fore, K. Paulsen, and K. O'Laughlin. Assessing the performance of volunteers in monitoring streams. *Freshwater Biology*, 46:109–123, 2001.

S. Fowler, K. Lee, H. Onouchi, A. Samach, K. Richardson, B. Morris, G. Coupland, and J. Putterill. GIGANTEA: A circadian clock-controlled gene that regulates photoperiodic flowering in Arabidopsis and encodes a protein with several possible membrane-spanning domains. *EMBO Journal*, 18(17):4679–4688, 1999.

S. G. Fowler, D. Cook, and M. F. Thomashow. Low temperature induction of Arabidopsis CBF1, 2, and 3 is gated by the circadian clock. *Plant Physiology*, 137(3):961–968, 2005.

M. Fujita, Y. Fujita, K. Maruyama, M. Seki, K. Hiratsu, M. Ohme-Takagi, L. S. P. Tran, K. Yamaguchi-Shinozaki, and K. Shinozaki. A dehydration-induced NAC protein, RD26, is involved in a novel ABA-dependent stress-signaling pathway. *The Plant Journal*, 39(6):863–876, 2004.

S. Fujiwara, L. Wang, L. Han, S. S. Suh, P. A. Salomé, C. R. McClung, and D. E. Somers. Post-translational regulation of the Arabidopsis circadian clock through selective proteolysis and phosphorylation of pseudo-response regulator proteins. *Journal of Biological Chemistry*, 283:23073–23083, 2008.

Y. Fukamatsu, S. Mitsui, M. Yasuhara, Y. Tokioka, N. Ihara, S. Fujita, and T. Kiyosue. Identification of LOV KELCH PROTEIN2 (LKP2)-interacting factors that can recruit LKP2 to nuclear bodies. *Plant and Cell Physiology*, 46(8):1340–1349, aug 2005.

H. Fukuda, K. Ukai, and T. Oyama. Self-arrangement of cellular circadian rhythms through phase-resetting in plant roots. *Physical Review E - Statistical, Nonlinear, and Soft Matter Physics*, 86(4):041917, oct 2012.

M. Gallego and D. M. Virshup. Post-translational modifications regulate the ticking of the circadian clock. *Nature reviews. Molecular cell biology*, 8(February):139–148, 2007.

S. N. Gangappa and J. F. Botto. The BBX family of plant transcription factors. *Trends in plant science*, 19(7):460–70, jul 2014.

P. Gawroński, R. Ariyadasa, A. Himmelbach, N. Poursarebani, B. Kilian, N. Stein, B. Steuernagel, G. Hensel, J. Kumlehn, S. K. Sehgal, B. S. Gill, P. Gould, A. Hall, and T. Schnurbusch. A distorted circadian clock causes early flowering and temperature-dependent variation in spike development in the Eps-3Am mutant of einkorn wheat. *Genetics*, 196(4):1253–1261, jan 2014.

S. B. Gelvin. Agrobacterium -Mediated Plant Transformation : the Biology behind the Agrobacterium -Mediated Plant Transformation : the Biology behind the " Gene-Jockeying " Tool. *Microbiology and Molecular Biology Reviews*, 67(1):16–37, 2003.

J. M. Gendron, J. L. Pruneda-Paz, C. J. Doherty, A. M. Gross, S. E. Kang, and S. A. Kay. Arabidopsis circadian clock protein, TOC1, is a DNA-binding transcription factor. *Proceedings of the National Academy of Sciences*, 109(8):3167–3172, feb 2012.

W. Gish and D. J. States. Identification of protein coding regions by database similarity search. *Nature Genetics*, 3(3):266–272, 1993.

C. Gleason, S. Chaudhuri, T. Yang, A. Muñoz, B. W. Poovaiah, and G. E. D. Oldroyd. Nodulation independent of rhizobia induced by a calcium-activated kinase lacking autoinhibition. *Nature*, 441(June):1149–1152, 2006.

V. Goltsev, I. Zaharieva, P. Lambrev, I. Yordanov, and R. Strasser. Simultaneous analysis of prompt and delayed chlorophyll a fluorescence in leaves during the induction period of dark to light adaptation. *Journal of Theoretical Biology*, 225(2):171–183, nov 2003.

D. H. Gonzalez. Introduction to Transcription Factor Structure and Function. In *Plant Transcription Factors*, pages 3–11. Elsevier, 2016.

D. Gonze and A. Goldbeter. Circadian rhythms and molecular noise. *Chaos*, 16(2), 2006.

D. Goodspeed, E. W. Chehab, A. Min-Venditti, J. Braam, and M. F. Covington. Arabidopsis synchronizes jasmonate-mediated defense with insect circadian behavior, mar 2012.

H. L. Gorton, W. E. Williams, M. E. Binns, C. N. Gemmell, E. a. Leheny, and a. C. Shepherd. Circadian Stomatal Rhythms in Epidermal Peels from Vicia faba. *Plant Physiology*, 90(4):1329–1334, 1989.

M. Gottesman. Bacteriophage lambda: the untold story. *Journal of molecular biology*, 293(2):177–180, 1999.

P. D. Gould, P. Diaz, C. Hogben, J. Kusakina, R. Salem, J. Hartwell, and A. Hall. Delayed fluorescence as a universal tool for the measurement of circadian rhythms in higher plants. *The Plant Journal*, 58(5):893–901, jun 2009.

A. Graf, A. Schlereth, M. Stitt, and A. M. Smith. Circadian control of carbohydrate availability for growth in Arabidopsis plants at night. *Proceedings of the National Academy of Sciences*, 107(20):9458–9463, 2010.

R. M. Green, S. Tingay, Z.-Y. Wang, and E. M. Tobin. Circadian rhythms confer a higher level of fitness to Arabidopsis plants. *Plant Physiology*, 129(2):576–584, 2002.

A. Greenup, W. J. Peacock, E. S. Dennis, and B. Trevaskis. The molecular biology of seasonal flowering-responses in Arabidopsis and the cereals. *Annals of Botany*, 103(8): 1165–1172, 2009.

S. Griffiths, R. P. Dunford, G. Coupland, and D. a. Laurie. The evolution of CONSTANS-like gene families in barley, rice, and Arabidopsis. *Plant Physiology*, 131(4):1855–1867, 2003.

A. Guo, K. He, D. Liu, S. Bai, X. Gu, L. Wei, and J. Luo. DATF: A database of Arabidopsis transcription factors. *Bioinformatics*, 21(10):2568–2569, 2005.

Z. Guo, Y. Song, R. Zhou, Z. Ren, and J. Jia. Discovery, evaluation and distribution of haplotypes of the wheat Ppd-D1 gene. *New Phytologist*, 185(3):841–851, 2010.

R. a. Gutierrez, R. M. Ewing, J. M. Cherry, and P. J. Green. Identification of unstable transcripts in Arabidopsis by cDNA microarray analysis: rapid decay is associated with a group of touch- and specific clock-controlled genes. *Proceedings of the National Academy of Sciences of the United States of America*, 99(17):11513–11518, 2002.

R. a. Gutiérrez, T. L. Stokes, K. Thum, X. Xu, M. Obertello, M. S. Katari, M. Tanurdzic, A. Dean, D. C. Nero, C. R. McClung, and G. M. Coruzzi. Systems approach identifies an organic nitrogen-responsive gene network that is regulated by the master clock control gene CCA1. *Proceedings of the National Academy of Sciences of the United States of America*, 105(12):4939–4944, 2008.

E. Gwinner and R. Brandstätter. Complex bird clocks. *Philosophical transactions of the Royal Society of London. Series B, Biological Sciences*, 356(1415):1801–1810, 2001.

N. Gyllenstrand, A. Karlgren, D. Clapham, K. Holm, A. Hall, P. D. Gould, T. Källman, and U. Lagercrantz. No time for spruce: Rapid dampening of circadian rhythms in picea abies (L. Karst). *Plant and Cell Physiology*, 55(3):535–550, mar 2014.

A. Hall and P. Brown. Monitoring circadian rhythms in Arabidopsis thaliana using luciferase reporter genes. *Methods in Molecular Biology*, 362:143–52, jan 2007.

L. Han, M. Mason, E. P. Risseeuw, W. L. Crosby, and D. E. Somers. Formation of an SCFZTL complex is required for proper regulation of circadian timing. *The Plant Journal*, 40:291–301, 2004.

S. Hanano, M. A. Domagalska, F. Nagy, and S. J. Davis. Multiple phytohormones influence distinct parameters of the plant circadian clock. *Genes to Cells*, 11(12): 1381–92, dec 2006.

S. L. Harmer. The circadian system in higher plants. *Annual Review of Plant Biology*, 60:357–377, jan 2009.

S. L. Harmer and S. A. Kay. Positive and Negative Factors Confer Phase-Specic Circadian Regulation of Transcription in Arabidopsis. *The Plant Cell*, 17(July):1926–1940, 2005.

S. L. Harmer, J. B. Hogenesch, M. Straume, H. S. Chang, B. Han, T. Zhu, X. Wang, J. A. Kreps, and S. A. Kay. Orchestrated transcription of key pathways in Arabidopsis by the circadian clock. *Science*, 290(5499):2110–2113, dec 2000.

S. J. Harrison, E. K. Mott, K. Parsley, S. Aspinall, J. C. Gray, and A. Cottage. A rapid and robust method of identifying transformed Arabidopsis thaliana seedlings following floral dip transformation. *Plant Methods*, 2:19, jan 2006.

J. L. Hartley, G. Temple, and M. A. Brasch. DNA Cloning Using In Vitro Site-Specific Recombination. *Genome Research*, (10):1788–1795, nov 2000.

K. Hasegawa, T. Saigusa, and Y. Tamai. Caenorhabditis elegans opens up new insights into circadian clock mechanisms. *Chronobiology international*, 22(1):1–19, 2005.

R. Hayama, G. Coupland, and E. Bu. The molecular basis of diversity in the photoperiodic flowering responses of Arabidopsis and rice. *Plant Physiology*, 135(2):677–684, 2004.

R. Hayashi, H. Wada, K. Ito, and I. M. Adcock. Effects of glucocorticoids on gene transcription. *European Journal of Pharmacology*, 500:51–62, 2004.

M. J. Haydon, T. J. Hearn, L. J. Bell, M. A. Hannah, and A. A. R. Webb. Metabolic regulation of circadian clocks. *Seminars in Cell and Developmental Biology*, 24(5): 414–421, may 2013a.

M. J. Haydon, O. Mielczarek, F. C. Robertson, K. E. Hubbard, and A. A. R. Webb. Photosynthetic entrainment of the Arabidopsis thaliana circadian clock. *Nature*, 502 (7473):689–92, oct 2013b.

M. J. Haydon, Á. Román, and W. Arshad. Nutrient homeostasis within the plant circadian network. *Frontiers in Plant Science*, 6, 2015.

S. P. Hazen, T. F. Schultz, J. L. Pruneda-Paz, J. O. Borevitz, J. R. Ecker, and S. a. Kay. LUX ARRHYTHMO encodes a Myb domain protein essential for circadian rhythms. *Proceedings of the National Academy of Sciences*, 102(29):10387–10392, jul 2005.

T. J. Hearn and A. A. R. Webb. Measuring Circadian Oscillations of Cytosolic-Free Calcium in Arabidopsis thaliana. In D. Staiger, editor, *Plant Circadian Networks: Methods & Protocols*, volume 1158 of *Methods in Molecular Biology*, pages 215–226. Springer New York, New York, NY, 2014. ISBN 978-1-4939-0699-4.

A. Helfer, D. A. Nusinow, B. Y. Chow, and A. R. Gehrke. LUX ARRHYTHMO Encodes a Nighttime Repressor of Circadian Gene Expression in the Arabidopsis Core Clock. *Current Biology*, 21(2):126–133, 2012.

P. K. Hepler, L. Vidali, and A. Y. Cheung. Polarized cell growth in higher plants. *Annual Review of Cell and Developmental Biology*, 17:159–187, 2001.

E. Herrero, E. Kolmos, N. Bujdoso, Y. Yuan, M. Wang, M. C. Berns, H. Uhlworm, G. Coupland, R. Saini, M. Jaskolski, A. A. R. Webb, J. M. Gonçalves, and S. J. Davis. EARLY FLOWERING4 recruitment of EARLY FLOWERING3 in the nucleus sustains the Arabidopsis circadian clock. *The Plant Cell*, 24(February):428–43, feb 2012.

H. Herzel, A. Kramer, S. Bernard, D. Gonze, C. Branka, B. Čajavec, H. Herzel, and A. Kramer. Synchronization-induced rhythmicity of circadian oscillators in the suprachiasmatic nucleus. *PLoS Computational Biology*, 3(4):667–679, 2007.

K. S. Heyndrickx and K. Vandepoele. Systematic Identification of Functional Plant Modules through the Integration of Complementary Data Sources. *Plant Physiology*, 159(3):884–901, 2012.

H. Highkin and J. Hanson. Possible interaction between light-dark cycles and endogenous daily rhythms on the growth of tomato plants. *Plant physiology*, (4):301–302, 1954.

J. Hirayama, M. Kaneko, L. Cardone, G. Cahill, and P. Sassone-Corsi. Analysis of circadian rhythms in zebrafish. *Methods in Enzymology*, 393:186–204, 2005.

K. Holm, T. Källman, N. Gyllenstrand, H. Hedman, and U. Lagercrantz. Does the core circadian clock in the moss Physcomitrella patens (Bryophyta) comprise a single loop? *BMC Plant Biology*, 10:109, 2010.

M. G. Holmes and W. H. Klein. Photocontrol of Dark Circadian Rhythms in Stomata of Phaseolus vulgaris L. *Plant Physiology*, 82(1):28–33, 1986.

M. Honda, Y. Muramoto, T. Kuzuguchi, S. Sawano, M. Machida, and H. Koyama. Determination of gene copy number and genotype of transgenic Arabidopsis thaliana by competitive PCR. *Journal of experimental botany*, 53(373):1515–1520, 2002.

J. P. Hong, Y. Takeshi, Y. Kondou, D. P. Schachtman, M. Matsui, and R. Shin. Identification and characterization of transcription factors regulating arabidopsis HAK5. *Plant and Cell Physiology*, 54(9):1478–1490, sep 2013.

T. Hruz, O. Laule, G. Szabo, F. Wessendorp, S. Bleuler, L. Oertle, P. Widmayer, W. Gruissem, and P. Zimmermann. Genevestigator v3: a reference expression database for the meta-analysis of transcriptomes. *Advances in Bioinformatics*, 2008:420747, jan 2008.

P. Y. Hsu, U. K. Devisetty, and S. L. Harmer. Accurate timekeeping is controlled by a cycling activator in Arabidopsis. *eLife*, 2013:1–20, 2013.

K. E. Hubbard, C. T. Hotta, M. J. Gardner, S. J. Baek, N. Dalchau, S. Dontamala, A. N. Dodd, and A. a. R. Webb. Circadian Rhythms in Stomata: Physiological and Molecular Aspects. In *Rhythms in Plants*, pages 157–177. Springer Berlin Heidelberg, Berlin, Heidelberg, 2007.

K. a. Hudson. The Circadian Clock-controlled Transcriptome of Developing Soybean Seeds. *The Plant Genome Journal*, 3(1):3, 2010.

T. Ichikawa, M. Nakazawa, M. Kawashima, H. Iizumi, H. Kuroda, Y. Kondou, Y. Tsuhara, K. Suzuki, A. Ishikawa, M. Seki, M. Fujita, R. Motohashi, N. Nagata, T. Takagi, K. Shinozaki, and M. Matsui. The FOX hunting system: An alternative gain-of-function gene hunting technique. *The Plant Journal*, 48(6):974–985, dec 2006.

K. Iida, M. Seki, T. Sakurai, M. Satou, K. Akiyama, T. Toyoda, A. Konagaya, and K. Shinozaki. RARTF: Database and tools for complete sets of Arabidopsis transcription factors. *DNA Research*, 12(4):247–256, 2005.

T. Imaizumi, H. G. Tran, T. E. Swartz, W. R. Briggs, and S. A. Kay. FKF1 is essential for photoperiodic-specific light signalling in Arabidopsis. *Nature*, 426(6964):302–306, 2003.

M. Ishikawa, T. Kiba, and N.-h. H. Chua. The Arabidopsis SPA1 gene is required for circadian clock function and photoperiodic flowering. *Plant Journal*, 46(5):736–746, 2006.

M. Ishiura, S. Kutsuna, S. Aoki, H. Iwasaki, C. R. Andersson, a. Tanabe, S. S. Golden, C. H. Johnson, and T. Kondo. Expression of a gene cluster kaiABC as a circadian feedback process in cyanobacteria. *Science (New York, N.Y.)*, 281(September):1519–1523, 1998.

S. Ito, Y. H. Song, a. R. Josephson-Day, R. J. Miller, G. Breton, R. G. Olmstead, and T. Imaizumi. FLOWERING BHLH transcriptional activators control expression of the photoperiodic flowering regulator CONSTANS in Arabidopsis. *Proceedings of the National Academy of Sciences*, 109(9):3582–3587, 2012.

T. Izawa, M. Mihara, Y. Suzuki, M. Gupta, H. Itoh, A. J. Nagano, R. Motoyama, Y. Sawada, M. Yano, M. Y. Hirai, A. Makino, and Y. Nagamura. Os-GIGANTEA confers robust diurnal rhythms on the global transcriptome of rice in the field. *The Plant Cell*, 23(5):1741–1755, 2011.

A. B. James, J. A. Monreal, G. A. Nimmo, C. L. Kelly, P. Herzyk, G. I. Jenkins, and H. G. Nimmo. The circadian clock in Arabidopsis roots is a simplified slave version of the clock in shoots. *Science*, 322(December):1832–1835, 2008.

A. B. James, N. H. Syed, J. W. S. Brown, and H. G. Nimmo. Thermoplasticity in the Plant Circadian Clock: How Plants tell the Time-perature. *Plant Signaling & Behavior*, 7(10):1219–1223, oct 2012.

P. James, J. Halladay, and E. A. Craig. Genomic libraries and a host strain designed for highly efficient two-hybrid selection in yeast. *Genetics*, 144(4):1425–1436, 1996.

R. a. Jefferson, T. a. Kavanagh, and M. W. Bevan. GUS fusions: beta-glucuronidase as a sensitive and versatile gene fusion marker in higher plants. *The EMBO Journal*, 6 (13):3901–3907, 1987.

P. J. Jensen, R. P. Hangarter, and M. Estelle. Auxin transport is required for hypocotyl elongation in light-grown but not dark-grown Arabidopsis. *Plant Physiology*, 116(2): 455–462, feb 1998.

M. Johansson and D. Staiger. Time to flower: interplay between photoperiod and the circadian clock. *Journal of Experimental Botany*, nov 2014.

C. H. Johnson, M. R. Knight, T. Kondo, P. Masson, J. Sedbrook, A. Haley, and A. Trewavas. Circadian oscillations of cytosolic and chloroplastic free calcium in plants. *Science*, 269(5232):1863–1865, 1995.

R. Jones. Day and night: Circadian rhythms in worms. *PLoS Biology*, 8(10):1–2, 2010.

R. Jorgensen, C. Snyder, and J. Jones. T-DNA is organized predominantly in inverted repeat structures in plants transformed with Agrobacterium tumefaciens C58 derivatives. *Molecular and General Genetics*, 207:471–477, 1987.

L. Jouve, T. Gaspar, C. Kevers, H. Greppin, and R. D. Agosti. Involvement of indole-3-acetic acid in the circadian growth of the first internode of Arabidopsis. *Planta*, 209 (1):136–142, 1999.

P. A. Jursinic. Delayed fluorescence: Current concepts and status. In J. Govindjee, Amesz and D. Fork, editors, *Light Emission by Plants and Bacteria*, pages 291–328. Academic Press, New York, NY, 1986. ISBN 978-0-12-294310-2.

H. G. Kang, Y. Fang, and K. B. Singh. A glucocorticoid-inducible transcription system causes severe growth defects in Arabidopsis and induces defense-related genes. *Plant Journal*, 20(1):127–133, 1999.

L. Kastrup, H. Oberleithner, Y. Ludwig, C. Schafer, and V. Shahin. Nuclear envelope barrier leak induced by dexamethasone. *Journal of Cellular Physiology*, 206(2):428–434, 2006.

J. Keller, E. Lim, and H. K. Dooner. Preferential transposition of Ac to linked sites in Arabidopsis. *Theoretical and Applied Genetics*, 86(5):585–588, 1993.

E. Kemen, K. Mendgen, and R. T. Voegele. Plant Immunity. *Methods*, 712(2):211–225, 2011.

R. E. Kendrick and G. H. M. Kronemberg. *Photomorphogenesis in Plants*. Kluwer Academic Publishers, 1994.

T. Kiba, R. Henriques, H. Sakakibara, and N.-H. Chua. Targeted degradation of PSEUDO-RESPONSE REGULATOR5 by an SCFZTL complex regulates clock function and photomorphogenesis in Arabidopsis thaliana. *The Plant Cell*, (8):2516–30, aug 2007.

E. Kiegle, C. a. Moore, J. Haseloff, M. a. Tester, and M. R. Knight. Cell-type-specific calcium responses to drought, salt and cold in the Arabidopsis root. *The Plant Journal*, 23:267–278, 2000.

T. Kihara, C.-R. Zhao, Y. Kobayashi, E. Takita, T. Kawazu, and H. Koyama. Simple identification of transgenic Arabidopsis plants carrying a single copy of the integrated gene. *Bioscience, biotechnology, and biochemistry*, 70(7):1780–1783, 2006.

J. Kim and H.-G. Nam. Instrumentation and Software for Analysis of Arabidopsis Circadian Leaf Movement. *Interdisciplinary Bio Central*, 1(1):22–25, mar 2009.

J. Kim, R. Geng, R. A. Gallenstein, and D. E. Somers. The F-box protein ZEITLUPE controls stability and nucleocytoplasmic partitioning of GIGANTEA. *Development*, 140(19):4060–4069, oct 2013a.

J. A. Kim, J. S. Kim, J. K. Hong, Y. H. Lee, B. S. Choi, Y. J. Seol, and C. H. Jeon. Comparative mapping, genomic structure, and expression analysis of eight pseudo-response regulator genes in Brassica rapa. *Molecular Genetics and Genomics*, 287(5): 373–388, 2012.

J. Y. Kim, H. R. Song, B. L. Taylor, and I. A. Carre. Light-regulated translation mediates gated induction of the Arabidopsis clock protein LHY. *The EMBO Journal*, 22(4):935–944, 2003.

M. H. Kim, Y. Sonoda, K. Sasaki, H. Kaminaka, and R. Imai. Interactome analysis reveals versatile functions of Arabidopsis COLD SHOCK DOMAIN PROTEIN 3 in RNA processing within the nucleus and cytoplasm. *Cell Stress and Chaperones*, 18(4): 517–525, jan 2013b.

W.-Y. Kim, S. Fujiwara, S.-S. Suh, J. Kim, Y. Kim, L. Han, K. David, J. Putterill, H. G. Nam, and D. E. Somers. ZEITLUPE is a circadian photoreceptor stabilized by GIGANTEA in blue light. *Nature*, 449(7160):356–60, sep 2007.

H. Knight, A. J. W. Thomson, and H. G. McWatters. Sensitive to freezing6 integrates cellular and environmental inputs to the plant circadian clock. *Plant Physiology*, 148 (1):293–303, sep 2008.

S. M. Knowles, S. X. Lu, and E. M. Tobin. *Plant Circadian Networks*, volume 1158 of *Methods in Molecular Biology*. Springer New York, New York, NY, 2014. ISBN 978-1-4939-0699-4.

C. H. Ko and J. S. Takahashi. Molecular components of the mammalian circadian clock. *Human molecular genetics*, 15 Spec No(2):R271–7, oct 2006.

E. Kolmos, M. Nowak, M. Werner, K. Fischer, G. Schwarz, S. Mathews, H. Schoof, F. Nagy, J. M. Bujnicki, and S. J. Davis. Integrating ELF4 into the circadian system through combined structural and functional studies. *HFSP Journal*, 3(5):350–366, 2009.

E. Kolmos, B. Y. Chow, J. L. Pruneda-Paz, and S. a. Kay. HsfB2b-mediated repression of PRR7 directs abiotic stress responses of the circadian clock. *Proceedings of the National Academy of Sciences*, 111(45):16172–16177, 2014.

T. Kondo, C. a. Strayer, R. D. Kulkarni, W. Taylor, M. Ishiura, S. S. Golden, and C. H. Johnson. Circadian rhythms in prokaryotes: luciferase as a reporter of circadian gene expression in cyanobacteria. *Proceedings of the National Academy of Sciences*, 90(12): 5672–5676, jun 1993.

B.-h. H. Koo, S.-c. C. Yoo, J.-w. W. Park, C.-t. T. Kwon, B.-d. D. Lee, G. An, Z. Zhang, J. Li, Z. Li, and N. C. Paek. Natural variation in OsPRR37 regulates heading date and contributes to rice cultivation at a wide range of latitudes. *Molecular Plant*, 6(6): 1877–1888, 2013.

R. Kumar and E. B. Thompson. Gene regulation by the glucocorticoid receptor: structure:function relationship. *The Journal of Steroid Biochemistry and Molecular Biology*, 94(5):383–394, 2005.

K. Kume, M. J. Zylka, S. Sriram, L. P. Shearman, D. R. Weaver, X. Jin, E. S. Maywood, M. H. Hastings, and S. M. Reppert. mCRY1 and mCRY2 are essential components of the negative limb of the circadian clock feedback loop. *Cell*, 98(2):193–205, 1999.

J. Kusakina, P. D. Gould, and A. Hall. A fast circadian clock at high temperatures is a conserved feature across Arabidopsis accessions and likely to be important for vegetative yield. *Plant, Cell and Environment*, 37:327–340, jun 2014.

J. Kusakina, Z. Rutterford, S. Cotter, M. C. Martí, D. a. Laurie, A. J. Greenland, A. Hall, and A. a. R. Webb. Barley Hv CIRCADIAN CLOCK ASSOCIATED 1 and Hv PHOTOPERIOD H1 Are Circadian Regulators That Can Affect Circadian Rhythms in Arabidopsis. *Plos One*, 10(6):e0127449, 2015.

Z. Lai, K. Vinod, Z. Zheng, B. Fan, and Z. Chen. Roles of Arabidopsis WRKY3 and WRKY4 transcription factors in plant responses to pathogens. *BMC Plant Biology*, 8: 68, 2008.

D. A. Laurie. Comparative genetics of flowering time. *Plant Molecular Biology*, 35(1-2): 167–177, sep 1997.

F. Le Couviour, S. Faure, B. Poupard, Y. Flodrops, P. Dubreuil, and S. Praud. Analysis of genetic structure in a panel of elite wheat varieties and relevance for association mapping. *Theoretical and Applied Genetics*, 123(5):715–727, 2011.

S. Ledger, C. Strayer, F. Ashton, S. A. Kay, and J. Putterill. Analysis of the function of two circadian-regulated CONSTANS-LIKE genes. *The Plant Journal*, 26(1):15–22, may 2001.

K. Lee, H. Onouchi, T. Mizoguchi, L. Wright, and S. Fujiwara. Distinct Roles of GIGANTEA in Promoting Flowering and Regulating Circadian Rhythms in Arabidopsis. *The Plant Cell*, 17(August):2255–2270, 2005.

T. Legnaioli, J. Cuevas, and P. Mas. TOC1 functions as a molecular switch connecting the circadian clock with plant responses to drought. *The EMBO Journal*, 28(23): 3745–57, dec 2009.

G. Li, H. Siddiqui, Y. Teng, R. Lin, X.-y. Wan, J. Li, O.-S. Lau, X. Ouyang, M. Dai, J. Wan, P. F. Devlin, X. W. Deng, and H. Wang. Coordinated transcriptional regulation underlying the circadian clock in Arabidopsis. *Nature Cell Biology*, 13(5):616–622, may 2011.

J. Li, G. Li, S. Gao, C. Martinez, G. He, Z. Zhou, X. Huang, J.-h. Lee, H. Zhang, Y. Shen, H. Wang, and X. W. Deng. Arabidopsis transcription factor ELONGATED HYPOCOTYL5 plays a role in the feedback regulation of phytochrome A signaling. *The Plant Cell*, 22(11):3634–3649, 2010.

X. Li and Y. Zhang. Reverse genetics by fast neutron mutagenesis in higher plants. *Functional and Integrative Genomics*, 2(6):254–258, 2002.

X. Li, Y. Song, K. Century, S. Straight, P. Ronald, X. Dong, M. Lassner, and Y. Zhang. A fast neutron deletion mutagenesis-based reverse genetics system for plants. *Plant Journal*, 27(3):235–242, 2001.

P. Lidder, R. A. Gutiérrez, P. A. Salomé, C. R. McClung, and P. J. Green. Circadian control of messenger RNA stability. Association with a sequence-specific messenger RNA decay pathway. *Plant Physiology*, 138(August):2374–2385, 2005.

L. C. Liew, V. Hecht, R. E. Laurie, C. L. Knowles, J. K. Vander Schoor, R. C. Macknight, J. L. Weller, K. V. Schoor, L. C. Liew, R. C. Macknight, and J. L. Weller. DIE NEUTRALIS and LATE BLOOMER 1 contribute to regulation of the pea circadian clock. *The Plant Cell*, 21(10):3198–3211, 2009.

L. C. Liew, M. B. Singh, and P. L. Bhalla. Unique and conserved features of floral evocation in legumes. *Journal of Integrative Plant Biology*, 56(8):714–728, 2014.

R. Lin, L. Ding, C. Casola, D. R. Ripoll, C. Feschotte, and H. Wang. Transposase-derived transcription factors regulate light signaling in Arabidopsis. *Science*, 318(5854):1302–1305, 2007.

E. Liscum and J. W. Reed. Genetics of Aux/IAA and ARF action in plant growth and development. *Plant Molecular Biology*, 49(3-4):387–400, 2002.

S. Litthauer, M. W. Battle, T. Lawson, and M. a. Jones. Phototropins maintain robust circadian oscillation of PSII operating efficiency under blue light. *The Plant Journal*, 83(6):1034–1045, aug 2015.

H. Liu, H. Wang, P. Gao, J. Xü, T. Xü, J. Wang, B. Wang, C. Lin, Y.-f. F. Fu, J. Xu, J. Wang, B. Wang, C. Lin, and Y.-f. F. Fu. Analysis of clock gene homologs using unifoliolates as target organs in soybean (Glycine max). *Plant Physiology*, 166(3): 278–289, 2009.

T. Liu, J. Carlsson, T. Takeuchi, L. Newton, E. Lansing, and E. M. Farré. Direct regulation of abiotic responses by the Arabidopsis circadian clock component PRR7. *Plant Journal*, 76(1):101–114, 2013.

Y. Liu and D. Bell-Pedersen. Circadian rhythms in Neurospora crassa and other filamentous fungi. *Eukaryotic Cell*, 5(8):1184–1193, 2006.

A. M. Lloyd, M. Schena, V. Walbot, and R. W. Davis. Epidermal cell fate determination in Arabidopsis: patterns defined by a steroid-inducible regulator. *Science*, 266(5184): 436–439, 1994.

J. C. W. Locke, A. J. Millar, and M. S. Turner. Modelling genetic networks with noisy and varied experimental data: the circadian clock in Arabidopsis thaliana. *Journal of Theoretical Biology*, 234(3):383–93, jun 2005a.

J. C. W. Locke, M. M. Southern, L. Kozma-Bognár, V. Hibberd, P. E. Brown, M. S. Turner, and A. J. Millar. Extension of a genetic network model by iterative experimentation and mathematical analysis. *Molecular Systems Biology*, 1:2005.0013, jan 2005b.

D. Long, M. Martin, E. Sundberg, J. Swinburne, P. Puangsomlee, and G. Coupland. The maize transposable element system Ac/Ds as a mutagen in Arabidopsis: identification of an albino mutation induced by Ds insertion. *Proceedings of the National Academy of Sciences*, 90(21):10370–10374, 1993.

D. Long, J. Goodrich, K. Wilson, E. Sundberg, M. Martin, P. Puangsomlee, and G. Coupland. DS elements on all five Arabidopsis chromosomes and assessment of their utility for transposon tagging. *Plant Journal*, 11(1):145–148, 1997.

J. a. Long, E. I. Moan, J. I. Medford, and M. K. Barton. A member of the KNOTTED class of homeodomain proteins encoded by the STM gene of Arabidopsis. *Nature*, 379 (6560):66–69, 1996.

P. Lou, Q. Xie, X. Xu, C. E. Edwards, M. T. Brock, C. Weinig, and C. R. McClung. Genetic architecture of the circadian clock and flowering time in Brassica rapa. *Theoretical and Applied Genetics*, 123(3):397–409, 2011.

P. Lou, J. Wu, F. Cheng, L. G. Cressman, X. Wang, and C. R. McClung. Preferential Retention of Circadian Clock Genes during Diploidization following Whole Genome Triplication in Brassica rapa. *The Plant Cell*, 24(6):2415–2426, 2012.

J. Love, A. N. Dodd, and A. A. R. Webb. Circadian and Diurnal Calcium Oscillations Encode Photoperiodic Information in Arabidopsis. *The Plant Cell*, 16(4):956–966, mar 2004.

S. X. Lu, S. M. Knowles, C. Andronis, M. S. Ong, and E. M. Tobin. CIRCADIAN CLOCK ASSOCIATED1 and LATE ELONGATED HYPOCOTYL function synergistically in the circadian clock of Arabidopsis. *Plant Physiology*, 150(2):834–843, jul 2009.

Y. Lu, J. P. Gehan, and T. D. Sharkey. Daylength and circadian effects on starch degradation and maltose metabolism. *Plant Physiology*, 138(4):2280–2291, 2005.

D. R. MacGregor, P. Gould, J. Foreman, J. Griffiths, S. Bird, R. Page, K. Stewart, G. Steel, J. Young, K. Paszkiewicz, A. J. Millar, K. J. Halliday, A. J. Hall, and S. Penfield. HIGH EXPRESSION OF OSMOTICALLY RESPONSIVE GENES1 is required for circadian periodicity through the promotion of nucleo-cytoplasmic mRNA export in Arabidopsis. *The Plant Cell*, pages 4391–404, nov 2013.

E. a. MacRobbie. ABA activates multiple Ca(2+) fluxes in stomatal guard cells, triggering vacuolar K(+)(Rb(+)) release. *Proceedings of the National Academy of Sciences*, 97(22):12361–12368, 2000.

a. P. Madan and D. B. DeFranco. Bidirectional transport of glucocorticoid receptors across the nuclear envelope. *Proceedings of the National Academy of Sciences*, 90(8): 3588–3592, 1993.

S. Makino, T. Kiba, A. Imamura, N. Hanaki, A. Nakamura, M. Taniguchi, C. Ueguchi, T. Sugiyama, and T. Mizuno. Genes Encoding Pseudo-Response Regulators : Insight into His-to-Asp Phosphorelay and Orcadian Rhythm in Arabidopsis thaliana. *Plant and Cell Physiology*, 41(6):791–803, 2000.

J. Malapeira, L. C. Khaitova, and P. Mas. Ordered changes in histone modifications at the core of the Arabidopsis circadian clock. *Proceedings of the National Academy of Sciences*, 109:21540–5, dec 2012.

R. Mantovani. The molecular biology of the CCAAT-binding factor NF-Y. *Gene*, 239 (1):15–27, 1999.

J. Maple and S. G. Møller. Mutagenesis in Arabidopsis. *Methods in Molecular Biology*, 362:197–206, 2007.

Martin Straume, S. G. Fraiser-Cadoret, and M. L. Johnson. Least-Squares Analysis of Fluorescence Data. In *Topics in Fluorescence Spectroscopy*, volume 2, pages 177–240. 1991. ISBN 0-306-45553-6.

P. Más, P. F. Devlin, S. Panda, and S. a. Kay. Functional interaction of phytochrome B and cryptochrome 2. *Nature*, 408(6809):207–211, 2000.

P. Más, W.-Y. Kim, D. E. Somers, and S. a. Kay. Targeted degradation of TOC1 by ZTL modulates circadian function in Arabidopsis thaliana. *Nature*, 426:567–570, 2003.

M. Mazzella, T. M. Alconada-Magliano, and J. J. Casal. Dual effect of phytochrome A on hypocotyl growth under continuous red light. *Plant, Cell and Environment*, pages 261–267, 1997.

C. R. McClung. Wheels within wheels: new transcriptional feedback loops in the Arabidopsis circadian clock. *F1000prime reports*, 6(January):2, 2014.

M. J. Mcdonald. Microarray Analysis and Organization of Circadian Gene Expression in Drosophila Cycling Circadian Genes Cycling Genes with Related. *Cell*, 107:567–578, 2001.

H. G. McWatters, E. Kolmos, A. Hall, M. R. Doyle, R. M. Amasino, P. Gyula, F. Nagy, A. J. Millar, and S. J. Davis. ELF4 is required for oscillatory properties of the circadian clock. *Plant Physiology*, 144(1):391–401, may 2007.

A. Medici, A. Marshall-Colon, E. Ronzier, W. Szponarski, R. Wang, A. Gojon, N. M. Crawford, S. Ruffel, G. M. Coruzzi, and G. Krouk. AtNIGT1/HRS1 integrates nitrate and phosphate signals at the Arabidopsis root tip. *Nature Communications*, 6:6274, 2015.

T. Michael and C. McClung. Enhancer Trapping Reveals Widespread Circadian Clock Transcriptional Control in Arabidopsis. *Plant Physiology*, 132:629–639, 2003.

T. P. Michael, T. C. Mockler, G. Breton, C. McEntee, A. Byer, J. D. Trout, S. P. Hazen, R. Shen, H. D. Priest, C. M. Sullivan, S. A. Givan, M. Yanovsky, F. Hong, S. A. Kay, and J. Chory. Network discovery pipeline elucidates conserved time-of-day-specific cis-regulatory modules. *PLoS Genetics*, 4(2):e14, feb 2008.

S. D. Michaels, Y. He, K. C. Scortecci, and R. M. Amasino. Attenuation of FLOWERING LOCUS C activity as a mechanism for the evolution of summer-annual flowering behavior in Arabidopsis. *Proceedings of the National Academy of Sciences*, 100(17): 10102–10107, 2003.

M. D. Mikkelsen and M. F. Thomashow. A role for circadian evening elements in cold-regulated gene expression in Arabidopsis. *The Plant Journal*, 60(2):328–339, oct 2009.

A. J. Millar and S. A. Kay. Circadian Control of cab Gene Transcription and mRNA Accumulation in Arabidopsis. *The Plant Cell*, 3(5):541–550, may 1991.

A. J. Millar, S. R. Short, K. Hiratsuka, N.-H. Chua, and S. a. Kay. Firefly luciferase as a reporter of regulated gene expression in higher plants. *Plant Molecular Biology Reporter*, 10(4):324–337, nov 1992.

A. J. Millar, I. A. Carré, C. A. Strayer, N. H. Chua, and S. A. Kay. Circadian clock mutants in Arabidopsis identified by luciferase imaging. *Science*, 267(5201):1161–1163, feb 1995a.

A. J. Millar, M. Straume, J. Chory, N. H. Chua, and S. A. Kay. The regulation of circadian period by phototransduction pathways in Arabidopsis. *Science*, 267(5201): 1163–1166, feb 1995b.

H. Min, H. Guo, and J. Xiong. Rhythmic gene expression in a purple photosynthetic bacterium, Rhodobacter sphaeroides. *FEBS Letters*, 579(3):808–812, 2005.

P. Mishra and K. C. Panigrahi. GIGANTEA: an emerging story. *Frontiers in Plant Science*, 6(January):1–15, 2015.

N. Mitsuda, A. Iwase, H. Yamamoto, M. Yoshida, M. Seki, K. Shinozaki, and M. Ohme-Takagi. NAC transcription factors, NST1 and NST3, are key regulators of the formation of secondary walls in woody tissues of Arabidopsis. *The Plant Cell*, 19(1):270–280, 2007.

N. Mitsuda, I. Miho, S. Takada, Y. Takiguchi, Y. Kondou, T. Yoshizumi, M. Fujita, K. Shinozaki, M. Matsui, and M. Ohme-Takagi. Efficient Yeast one-/two-hybrid screening using a library composed only of transcription factors in Arabidopsis thaliana. *Plant and Cell Physiology*, 51(12):2145–2151, dec 2010.

M. Mittag, S. Kiaulehn, and C. H. Johnson. The Circadian Clock in Chlamydomonas reinhardtii . What Is It For ? What Is It Similar To ? 1. *Plant Physiology*, 137 (February):399–409, 2005.

Y. Miyazaki, H. Abe, T. Takase, M. Kobayashi, and T. Kiyosue. Overexpression of LOV KELCH PROTEIN 2 confers dehydration tolerance and is associated with enhanced expression of dehydration-inducible genes in Arabidopsis thaliana. *Plant Cell Reports*, pages 843–852, 2015.

T. Mizoguchi, K. Wheatley, and Y. Hanzawa. LHY and CCA1 are partially redundant genes required to maintain circadian rhythms in Arabidopsis. *Developmental cell*, 2: 629–641, 2002.

T. C. Mockler, H. Guo, H. Yang, H. Duong, and C. Lin. Antagonistic actions of Arabidopsis cryptochromes and phytochrome B in the regulation of floral induction. *Development*, 126(10):2073–82, may 1999.

T. C. Mockler, T. P. Michael, H. D. Priest, R. Shen, C. M. Sullivan, S. A. Givan, C. Mcentee, S. A. Kay, and J. Chory. The diurnal project: Diurnal and circadian expression profiling, model-based pattern matching, and promoter analysis. In *Cold Spring Harbor Symposia on Quantitative Biology*, volume 72, pages 353–363, jan 2007. ISBN 9780879698232.

G. B. Monshausen, M. a. Messerli, and S. Gilroy. Imaging of the Yellow Cameleon 3.6 indicator reveals that elevations in cytosolic Ca2+ follow oscillating increases in growth in root hairs of Arabidopsis. *Plant Physiology*, 147(August):1690–1698, 2008.

M. Murakami, M. Ashikari, K. Miura, T. Yamashino, and T. Mizuno. The Evolutionarily Conserved OsPRR Quintet: Rice Pseudo-Response Regulators Implicated in Circadian Rhythm. *Plant and Cell Physiology*, 44(11):1229–1236, 2003.

M. Murakami, Y. Tago, T. Yamashino, and T. Mizuno. Comparative overviews of clock-associated genes of Arabidopsis thaliana and Oryza sativa. *Plant and Cell Physiology*, 48(1):110–121, 2007a.

M. Murakami, Y. Tago, T. Yamashino, and T. Mizuno. Characterization of the rice circadian clock-associated pseudo-response regulators in Arabidopsis thaliana. *Bioscience, Biotechnology, and Biochemistry*, 71(4):1107–1110, 2007b.

T. Muranaka, S. Kubota, and T. Oyama. A single-cell bioluminescence imaging system for monitoring cellular gene expression in a plant body. *Plant and Cell Physiology*, 54 (12):2085–2093, dec 2013.

R. L. Murphy, R. R. Klein, D. T. Morishige, J. a. Brady, W. L. Rooney, F. R. Miller, D. V. Dugas, P. E. Klein, and J. E. Mullet. Coincident light and clock regulation of pseudoresponse regulator protein 37 (PRR37) controls photoperiodic flowering in sorghum. *Proceedings of the National Academy of Sciences*, 108(39):16469–16474, 2011.

D. H. Nagel, J. L. Pruneda-Paz, and S. a. Kay. FBH1 affects warm temperature responses in the Arabidopsis circadian clock. *Proceedings of the National Academy of Sciences*, 111:14595–14600, sep 2014.

D. H. Nagel, C. J. Doherty, J. L. Pruneda-Paz, R. J. Schmitz, J. R. Ecker, and S. A. Kay. Genome-wide identification of CCA1 targets uncovers an expanded clock network in Arabidopsis. *Proceedings of the National Academy of Sciences*, 112(34): E4802–E4810, 2015.

T. Nakagawa, T. Kurose, T. Hino, K. Tanaka, M. Kawamukai, Y. Niwa, K. Toyooka, K. Matsuoka, T. Jinbo, and T. Kimura. Development of series of gateway binary vectors, pGWBs, for realizing efficient construction of fusion genes for plant transformation. *Journal of bioscience and bioengineering*, 104(1):34–41, 2007.

M. Nakajima, K. Imai, H. Ito, T. Nishiwaki, Y. Murayama, H. Iwasaki, T. Oyama, and T. Kondo. Reconstitution of circadian oscillation of cyanobacterial KaiC phosphorylation in vitro. *Science*, 308:414–415, 2005.

N. Nakamichi, T. Kiba, R. Henriques, T. Mizuno, N.-H. Chua, and H. Sakakibara. PSEUDO-RESPONSE REGULATORS 9, 7, and 5 are transcriptional repressors in the Arabidopsis circadian clock. *The Plant Cell*, (3):594–605, mar 2010.

M. Nakazawa and M. Matsui. Selection of Hygromycin-Resistant Arabidopsis Seedlings. *Biotechniques*, 34(1), 2003.

H. A. Nash. Integration and Excision of Bacteriophage λ. In *Current Topics in Microbiology and Immunology*, pages 171–199. Heidelberg, 1977.

D. C. Nelson, J. Lasswell, L. E. Rogg, M. a. Cohen, and B. Bartel. FKF1, a clock-controlled gene that regulates the transition to flowering in Arabidopsis. *Cell*, 101: 331–340, 2000.

N. Nelson, A. Ben-Shem, and T. G. S. Wise. The complex architecture of oxygenic photosynthesis. *Nature Reviews: Molecular Cell Biology*, 5(12):971–982, 2004.

Y. NIWA. A Synthetic Green Fluorescent Protein Gene for Plant Biotechnology., 2003.

Z. B. Noordally, K. Ishii, K. A. Atkins, S. J. Wetherill, J. Kusakina, E. J. Walton, M. Kato, M. Azuma, K. Tanaka, M. Hanaoka, and A. N. Dodd. Circadian control of chloroplast transcription by a nuclear-encoded timing signal. *Science*, 339(6125): 1316–9, mar 2013.

K. Nozue, M. F. Covington, P. D. Duek, S. Lorrain, C. Fankhauser, S. L. Harmer, and J. N. Maloof. Rhythmic growth explained by coincidence between internal and external cues. *Nature*, 448(7151):358–61, jul 2007.

D. a. Nusinow, A. Helfer, E. E. Hamilton, J. J. King, T. Imaizumi, T. F. Schultz, E. M. Farré, and S. a. Kay. The ELF4-ELF3-LUX complex links the circadian clock to diurnal control of hypocotyl growth. *Nature*, 475(7356):398–402, jul 2011.

T. R. O'Connor, C. Dyreson, and J. J. Wyrick. Athena: a resource for rapid visualization and systematic analysis of Arabidopsis promoter sequences. *Bioinformatics*, 21(24): 4411–3, dec 2005.

J. T. Odell, F. Nagy, and N.-H. Chua. Identification of DNA sequences required for activity of the cauliflower mosaic virus 35S promoter, 1985.

R. Okada, S. Kondo, S. B. Satbhai, N. Yamaguchi, M. Tsukuda, and S. Aoki. Functional characterization of CCA1/LHY homolog genes, PpCCA1a and PpCCA1b, in the moss Physcomitrella patens. *Plant Journal*, 60(3):551–563, 2009.

K. Onai and M. Ishiura. PHYTOCLOCK 1 encoding a novel GARP protein essential for the Arabidopsis circadian clock. *Genes to Cells*, 10(10):963–972, oct 2005.

K. Onai, K. Okamoto, H. Nishimoto, C. Morioka, M. Hirano, N. Kami-ike, and M. Ishiura. Large-scale screening of Arabidopsis circadian clock mutants by a high-throughput real-time bioluminescence monitoring system. *Plant Journal*, 40(1):1–11, 2004.

J. S. O'Neill and A. B. Reddy. Circadian clocks in human red blood cells. *Nature*, 469 (7331):498–503, jan 2011.

J. S. O'Neill, G. van Ooijen, L. E. Dixon, C. Troein, F. Corellou, F.-Y. Bouget, A. B. Reddy, and A. J. Millar. Circadian rhythms persist without transcription in a eukaryote. *Nature*, 469(7331):554–8, jan 2011.

H. Onouchi, M. I. Igeño, C. Périlleux, K. Graves, G. Coupland, J. I. Centre, C. Lane, N. Nr, and U. Kingdom. Mutagenesis of plants overexpressing CONSTANS demonstrates novel interactions among Arabidopsis flowering-time genes. *The Plant Cell*, 12 (6):885–900, 2000.

Y. Ouyang, C. R. Andersson, T. Kondo, S. S. Golden, and C. H. Johnson. Resonating circadian clocks enhance fitness in cyanobacteria in silico. *Proceedings of the National Academy of Sciences*, 95(15):8660–4, 1998.

D. W. D. Ow, K. V. Wood, M. Deluca, J. R. D. J. D. WET, D. D. R. Helinski, H. Howell, S. H. HOWELL, J. R. DE Wet, D. D. R. Helinski, S. H. HOWELL, K. V. Wood, and M. Deluca. Transient and stable expression of the firefly luciferase gene in plant cells and transgenic plants. *Science (New York, N.Y.)*, 234(4778):856–859, 1986.

A. Para, E. M. Farré, T. Imaizumi, J. L. Pruneda-Paz, F. G. Harmon, and S. a. Kay. PRR3 Is a vascular regulator of TOC1 stability in the Arabidopsis circadian clock. *The Plant Cell*, (November):3462–3473, 2007.

D. H. Park, D. E. Somers, Y. S. Kim, Y. H. Choy, H. K. Lim, M. S. Soh, H. J. Kim, S. A. Kay, and H. G. Nam. Control of circadian rhythms and photoperiodic flowering by the Arabidopsis GIGANTEA gene. *Science*, 285(September):1579–1582, 1999.

V. Pautot, J. Dockx, O. Hamant, J. Kronenberger, O. Grandjean, D. Jublot, and J. Traas. KNAT2: evidence for a link between knotted-like genes and carpel development. *The Plant Cell*, 13(8):1719–1734, 2001.

A. Pokhilko, S. K. Hodge, K. Stratford, K. Knox, K. D. Edwards, A. W. Thomson, T. Mizuno, and A. J. Millar. Data assimilation constrains new connections and components in a complex, eukaryotic circadian clock model. *Molecular Systems Biology*, 6 (1):416, sep 2010.

S. Portolés and P. Más. Altered oscillator function affects clock resonance and is responsible for the reduced day-length sensitivity of CKB4 overexpressing plants. *The Plant Journal*, 51:966–977, 2007.

W. B. Pratt, Y. Morishima, M. Murphy, and M. Harrell. Chaperoning of glucocorticoid receptors. *Handbook of Experimental Pharmacology*, 172:111–138, 2006.

S. B. Preuss, R. Meister, Q. Xu, C. P. Urwin, F. a. Tripodi, S. E. Screen, V. S. Anil, S. Zhu, J. a. Morrell, G. Liu, O. J. Ratcliffe, T. L. Reuber, R. Khanna, B. S. Goldman, E. Bell, T. E. Ziegler, A. L. McClerren, T. G. Ruff, and M. E. Petracek. Expression of the Arabidopsis thaliana BBX32 gene in soybean increases grain yield. *PLoS ONE*, 7(2):e30717, jan 2012.

J. L. Pruneda-Paz, G. Breton, A. Para, and S. A. Kay. A functional genomics approach reveals CHE as a component of the Arabidopsis circadian clock. *Science*, 323(5920): 1481–1485, mar 2009.

J. Putterill, F. Robson, K. Lee, R. Simon, and G. Coupland. The CONSTANS gene of Arabidopsis promotes flowering and encodes a protein showing similarities to zinc finger transcription factors. *Cell*, 80(6):847–857, 1995.

M. Ramaiah, a. Jain, and K. G. Raghothama. ETHYLENE RESPONSE FACTOR070 Regulates Root Development and Phosphate Starvation-Mediated Responses. *Plant Physiology*, 164(3):1484–1498, 2014.

U. Rascher, M. T. Hütt, K. Siebke, B. Osmond, F. Beck, and U. Lüttge. Spatiotemporal variation of metabolism in a plant circadian rhythm: the biological clock as an assembly of coupled individual oscillators. *Proceedings of the National Academy of Sciences of the United States of America*, 98(20):11801–11805, 2001.

R. Rawat, N. Takahashi, P. Y. Hsu, M. A. Jones, J. Schwartz, M. R. Salemi, B. S. Phinney, and S. L. Harmer. REVEILLE8 and PSEUDO-REPONSE REGULATOR5 form a negative feedback loop within the arabidopsis circadian clock. *PLoS Genetics*, 7(3):e1001350, mar 2011.

G. P. Rédei. Supervital Mutants of Arabidopsis. *Genetics*, 47(4):443–460, 1962.

J. W. Reed, A. Nagatani, T. D. Elich, M. Fagan, and J. Chory. Phytochrome A and Phytochrome B Have Overlapping but Distinct Functions in Arabidopsis Development. *Plant Physiology*, 104(4):1139–1149, 1994.

B. A. Reyes, J. S. Pendergast, and S. Yamazaki. Mammalian Peripheral Circadian Oscillators Are Temperature Compensated. *Journal of Biological Rhythms*, 23(1):95–98, 2008.

T. Rhen and J. A. Cidlowski. Antiinflammatory action of glucocorticoids–new mechanisms for old drugs. *The New England Journal of Medicine*, 353:1711–1723, 2005.

D. M. Riaño-Pachón, S. Ruzicic, I. Dreyer, and B. Mueller-Roeber. PlnTFDB: an integrative plant transcription factor database. *BMC Bioinformatics*, 8:42, 2007.

J. L. Riechmann, J. Heard, G. Martin, L. Reuber, C. Jiang, J. Keddie, L. Adam, O. Pineda, O. J. Ratcliffe, R. R. Samaha, R. Creelman, M. Pilgrim, P. Broun, J. Z. Zhang, D. Ghandehari, B. K. Sherman, and G. Yu. Arabidopsis transcription factors: genome-wide comparative analysis among eukaryotes. *Science*, 290(5499):2105–2110, dec 2000.

A. Rikin. Circadian rhythm of heat resistance in cotton seedlings: synthesis of heat-shock proteins. *European Journal of Cell Biology*, 59(1):160–5, 1992.

A. Rikin, J. W. Dillwith, and D. K. Bergman. Correlation between the Circadian Rhythm of Resistance to Extreme Temperatures and Changes in Fatty Acid Composition in Cotton Seedlings. *Plant Physiology*, 101(1):31–36, 1993.

F. Robson, M. M. R. Costa, S. R. Hepworth, I. Vizir, M. Piñeiro, P. H. Reeves, J. Putterill, and G. Coupland. Functional importance of conserved domains in the flowering-time gene CONSTANS demonstrated by analysis of mutant alleles and transgenic plants. *Plant Journal*, 28(6):619–631, 2001.

T. Roenneberg, S. Daan, and M. Merrow. The Art of Entrainment. *Journal of Biological Rhythms*, 18(3):183–194, 2003.

C. P. Romano, P. R. Robson, H. Smith, M. Estelle, and H. Klee. Transgene-mediated auxin overproduction in Arabidopsis: hypocotyl elongation phenotype and interactions with the hy6-1 hypocotyl elongation and axr1 auxin-resistant mutants. *Plant Molecular Biology*, 27(6):1071–1083, 1995.

S. Rusconi and K. R. Yamamoto. Functional dissection of the hormone and DNA binding activities of the glucocorticoid receptor. *The EMBO Journal*, 6(5):1309–1315, 1987.

A. W. Rutherford, Govindjee, and Y. Inoue. Charge accumulation and photochemistry in leaves studied by thermoluminescence and delayed light emission. *Proceedings of the National Academy of Sciences*, 81(4):1107–1111, feb 1984.

M. Rutitzky, H. O. Ghiglione, J. a. Curá, J. J. Casal, and M. J. Yanovsky. Comparative genomic analysis of light-regulated transcripts in the Solanaceae. *BMC Genomics*, 10: 60, 2009.

R. W. Sablowski and E. M. Meyerowitz. A homolog of NO APICAL MERISTEM is an immediate target of the floral homeotic genes APETALA3/PISTILLATA. *Cell*, 92(1): 93–103, jan 1998.

Y. Saidi, A. Finka, M. Muriset, Z. Bromberg, Y. G. Weiss, F. J. M. Maathuis, and P. Goloubinoff. The heat shock response in moss plants is regulated by specific calcium-permeable channels in the plasma membrane. *The Plant Cell*, (September):2829–2843, 2009.

Y. Saijo, D. Zhu, J. Li, V. Rubio, Z. Zhou, Y. Shen, U. Hoecker, H. Wang, and X. W. Deng. Arabidopsis COP1/SPA1 Complex and FHY1/FHY3 Associate with Distinct Phosphorylated Forms of Phytochrome A in Balancing Light Signaling. *Molecular Cell*, 31(4):607–613, 2008.

T. Saithong, K. J. Painter, and A. J. Millar. The contributions of interlocking loops and extensive nonlinearity to the properties of circadian clock models. *PLoS ONE*, 5(11): 1–11, 2010.

L. Salichos and A. Rokas. The diversity and evolution of circadian clock proteins in fungi. *Mycologia*, 102(2):269–278, 2010.

P. A. Salomé and C. R. McClung. PSEUDO-RESPONSE REGULATOR 7 and 9 are partially redundant genes essential for the temperature responsiveness of the Arabidopsis circadian clock. *The Plant Cell*, 17(3):791–803, 2005.

P. A. Salomé, M. Oliva, D. Weigel, and U. Krämer. Circadian clock adjustment to plant iron status depends on chloroplast and phytochrome function. *The EMBO journal*, 32 (4):1–13, dec 2012.

A. Samach and A. Gover. Photoperiodism: The consistent use of CONSTANS. *Current Biology*, 11(16):651–654, 2001.

A. Samach, H. Onouchi, S. E. Gold, G. S. Ditta, Z. Schwarz-Sommer, M. F. Yanofsky, and G. Coupland. Distinct roles of CONSTANS target genes in reproductive development of Arabidopsis. *Science*, 288(June):1613–1616, 2000.

J. P. Sánchez, P. Duque, and N. H. Chua. ABA activates ADPR cyclase and cADPR induces a subset of ABA-responsive genes in Arabidopsis. *Plant Journal*, 38(3):381–395, 2004.

D. Sanders, C. Brownlee, and J. F. Harper. Communicating with calcium. *The Plant Cell*, 11(April):691–706, 1999.

D. Sanders, J. Pelloux, C. Brownlee, and J. F. Harper. Calcium at the crossroads of signaling. *The Plant Cell*, pages S401–S417, 2002.

A. Sarker, W. Erskine, B. Sharma, and M. C. Tyagi. Inheritance and linkage relationship of days to flower and morphological loci in lentil (Lens culinaris Medikus subsp. culinaris). *Journal of Heredity*, 90(2):270–275, 1999.

J. G. Savory, B. Hsu, I. R. Laquian, W. Giffin, T. Reich, R. J. Haché, and Y. a. Lefebvre. Discrimination between NL1- and NL2-mediated nuclear localization of the glucocorticoid receptor. *Molecular and cellular biology*, 19(2):1025–1037, 1999.

M. Sawa, S. a. Kay, and T. Imaizumi. Photoperiodic flowering occurs under internal and external coincidence. *Plant Signaling & Behavior*, 3(4):269–271, 2008.

S. Sawa, M. Ohgishi, H. Goda, K. Higuchi, Y. Shimada, S. Yoshida, and T. Koshiba. The HAT2 gene, a member of the HD-Zip gene family, isolated as an auxin inducible gene by DNA microarray screening, affects auxin response in Arabidopsis. *Plant Journal*, 32(6):1011–1022, 2002.

R. Schaffer, N. Ramsay, A. Samach, S. Corden, J. Putterill, I. A. Carré, and G. Coupland. The late elongated hypocotyl mutation of Arabidopsis disrupts circadian rhythms and the photoperiodic control of flowering. *Cell*, 93(7):1219–1229, jun 1998.

R. Schaffer, J. Landgraf, M. Accerbi, V. Simon, M. Larson, and E. Wisman. Microarray analysis of diurnal and circadian-regulated genes in Arabidopsis. *The Plant Cell*, 13 (1):113–123, 2001.

M. Schmid, T. S. Davison, S. R. Henz, U. J. Pape, M. Demar, M. Vingron, B. Schölkopf, D. Weigel, and J. U. Lohmann. A gene expression map of Arabidopsis thaliana development. *Nature Genetics*, 37(5):501–506, 2005.

R. J. Schmitz and R. M. Amasino. Vernalization: A model for investigating epigenetics and eukaryotic gene regulation in plants. *Biochimica et Biophysica Acta - Gene Structure and Expression*, 1769(5-6):269–275, 2007.

J. I. Schroeder, J. M. Kwak, and G. J. Allen. Guard cell abscisic acid signalling and engineering drought hardiness in plants. *Nature*, 410(6826):327–330, 2001.

T. F. Schultz, T. Kiyosue, M. Yanovsky, M. Wada, and S. A. Kay. A Role for LKP2 in the Circadian Clock of Arabidopsis. 13(December):2659–2670, 2001.

S. Scofield, W. Dewitte, and J. a. H. Murray. The KNOX gene SHOOT MERISTEMLESS is required for the development of reproductive meristematic tissues in Arabidopsis. *Plant Journal*, 50(5):767–781, 2007.

M. Seki, M. Chono, H. Matsunaka, M. Fujita, S. Oda, K. Kubo, C. Kiribuchi-Otobe, H. Kojima, H. Nishida, and K. Kato. Distribution of photoperiod-insensitive alleles Ppd-B1a and Ppd-D1a and their effect on heading time in Japanese wheat cultivars. *Breeding Science*, 61(4):405–412, 2011.

P. J. Seo and P. Mas. Multiple layers of posttranslational regulation refine circadian clock activity in Arabidopsis. *The Plant Cell*, 26(1):79–87, 2014.

P. J. Seo, M.-J. Park, M.-H. Lim, S.-G. Kim, M. Lee, I. T. Baldwin, and C.-M. Park. A self-regulatory circuit of CIRCADIAN CLOCK-ASSOCIATED1 underlies the circadian clock regulation of temperature responses in Arabidopsis. *The Plant Cell*, 24 (6):2427–42, jun 2012.

P. D. Sharma, N. Singh, P. S. Ahuja, and T. V. Reddy. Abscisic acid response element binding factor 1 is required for establishment of Arabidopsis seedlings during winter. *Molecular Biology Reports*, 38(8):5147–5159, 2011.

R. A. Sharrock and P. H. Quail. Novel phytochrome sequences in Arabidopsis thaliana: structure, evolution, and differential expression of a plant regulatory photoreceptor family. *Genes & Development*, 3(11):1745–1757, nov 1989.

L. M. Shaw, A. S. Turner, L. Herry, S. Griffiths, and D. a. Laurie. Mutant alleles of Photoperiod-1 in Wheat (Triticum aestivum L.) that confer a late flowering phenotype in long days. *PLoS ONE*, 8(11), 2013.

S. L. Shaw and S. R. Long. Nod factor elicits two separable calcium responses in Medicago truncatula root hair cells. *Plant Physiology*, 131:976–984, 2003.

S. Shcolnick and N. Keren. Metal homeostasis in cyanobacteria and chloroplasts. Balancing benefits and risks to the photosynthetic apparatus. *Plant Physiology*, 141(3): 805–810, 2006.

C. C. Sheldon, E. J. Finnegan, D. T. Rouse, M. Tadege, D. J. Bagnall, C. a. Helliwell, W. J. Peacock, and E. S. Dennis. The control of flowering by vernalization. *Current Opinion in Plant Biology*, 3(5):418–422, 2000a.

C. C. Sheldon, D. T. Rouse, E. J. Finnegan, W. J. Peacock, and E. S. Dennis. The molecular basis of vernalization: the central role of FLOWERING LOCUS C (FLC). *Proceedings of the National Academy of Sciences*, 97(7):3753–3758, 2000b.

B. A. Sherf and K. V. Wood. Firefly Luciferase Engineered for Improved Genetic Reporting. *Promega Notes Magazine*, (49):14–21, 1994.

S. Shimada, T. Komatsu, A. Yamagami, M. Nakazawa, M. Matsui, H. Kawaide, M. Natsume, H. Osada, T. Asami, and T. Nakano. Formation and Dissociation of the BSS1 Protein Complex Regulates Plant Development via Brassinosteroid Signaling. *The Plant Cell Online*, 27(February):tpc.114.131508, 2015.

J. Shin, K. Heidrich, A. Sanchez-Villarreal, J. E. Parker, and S. J. Davis. TIME FOR COFFEE represses accumulation of the MYC2 transcription factor to provide time-of-day regulation of jasmonate signaling in Arabidopsis. *The Plant Cell*, (6):2470–82, jun 2012.

G. G. Simpson. The autonomous pathway: Epigenetic and post-transcriptional gene regulation in the control of Arabidopsis flowering time. *Current Opinion in Plant Biology*, 7(5):570–574, 2004.

M. Skibbe, N. Qu, I. Galis, and I. T. Baldwin. Induced plant defenses in the natural environment: Nicotiana attenuata WRKY3 and WRKY6 coordinate responses to herbivory. *The Plant Cell*, 20(7):1984–2000, 2008.

D. E. Somers, P. F. Devlin, and S. A. Kay. Phytochromes and cryptochromes in the entrainment of the Arabidopsis circadian clock. *Science*, 282(5393):1488–1490, nov 1998a.

D. E. Somers, A. A. Webb, M. Pearson, and S. A. Kay. The short-period mutant, toc1-1, alters circadian clock regulation of multiple outputs throughout development in Arabidopsis thaliana. *Development*, 125(3):485–494, feb 1998b.

G. S. Song, H. L. Zhai, Y. G. Peng, L. Zhang, G. Wei, X. Y. Chen, Y. G. Xiao, L. Wang, Y. J. Chen, B. Wu, B. Chen, Y. Zhang, H. Chen, X. J. Feng, W. K. Gong, Y. Liu, Z. J. Yin, F. Wang, G. Z. Liu, H. L. Xu, X. L. Wei, X. L. Zhao, P. B. F. Ouwerkerk, T. Hankemeier, T. Reijmers, R. Van Der Heijden, C. M. Lu, M. Wang, J. Van Der Greef, and Z. Zhu. Comparative transcriptional profiling and preliminary study on heterosis mechanism of super-hybrid rice. *Molecular Plant*, 3(6):1012–1025, nov 2010a.

H. R. Song and Y. S. Noh. Rhythmic oscillation of histone acetylation and methylation at the arabidopsis central clock loci. *Molecules and Cells*, 34:279–287, aug 2012.

Y. H. Song, S. Ito, and T. Imaizumi. Similarities in the circadian clock and photoperiodism in plants. *Current Opinion in Plant Biology*, 13(5):594–603, 2010b.

M. M. Southern, P. E. Brown, and A. Hall. Luciferases as Reporter Genes. In *Arabidopsis Methods*, volume 323, chapter 24, pages 293–305. 2006.

D. Staiger and T. Köster. Spotlight on post-transcriptional control in the circadian system, jan 2011.

J. L. Stewart, J. N. Maloof, and J. L. Nemhauser. PIF genes mediate the effect of sucrose on seedling growth dynamics. *PLoS ONE*, 6(5):1–8, 2011.

M. Stitt and S. C. Zeeman. Starch turnover: Pathways, regulation and role in growth. *Current Opinion in Plant Biology*, 15(3):282–292, 2012.

C. Strayer, T. Oyama, T. F. Schultz, R. Raman, D. E. Somers, P. Más, S. Panda, J. A. Kreps, and S. A. Kay. Cloning of the Arabidopsis clock gene TOC1, an autoregulatory response regulator homolog. *Science*, 289(1989):768–771, 2000.

B. L. Strehler and W. Arnold. Light Production By Green Plants. *The Journal of General Physiology*, 34(6):809–820, 1951.

W. Su and S. H. Howell. The Effects of Cytokinin and Light on Hypocotyl Elongation in Arabidopsis Seedlings Are Independent and Additive. *Plant Physiology*, 108(4): 1423–1430, 1995.

S. Sugano, C. Andronis, R. M. Green, Z. Y. Wang, and E. M. Tobin. Protein kinase CK2 interacts with and phosphorylates the Arabidopsis circadian clock-associated 1 protein. *Proceedings of the National Academy of Sciences*, 95(September):11020–11025, 1998.

S. Sugano, C. Andronis, M. S. Ong, R. M. Green, and E. M. Tobin. The protein kinase CK2 is involved in regulation of circadian rhythms in Arabidopsis. *Proceedings of the National Academy of Sciences of the United States of America*, 96(22):12362–12366, 1999.

N. Sugiyama, T. Izawa, and T. Oikawa. Light regulation of circadian clock-controlled gene expression in rice. *The Plant Journal*, 26(6):607–615, dec 2001.

N. Takahashi, Y. Hirata, K. Aihara, and P. Mas. A Hierarchical Multi-oscillator Network Orchestrates the Arabidopsis Circadian System. *Cell*, 163(1):148–159, 2015.

Y. Takahashi, Y. Ebisu, T. Kinoshita, M. notdoi, E. Okuma, Y. Murata, and K.-I. Shimazaki. bHLH transcription factors that facilitate K+ uptake during stomatal opening are repressed by abscisic acid through phosphorylation. *Science Signaling*, 6 (280):ra48, 2013.

N. Takata, S. Saito, C. T. Saito, T. Nanjo, K. Shinohara, and M. Uemura. Molecular phylogeny and expression of poplar circadian clock genes, LHY1 and LHY2. *New Phytologist*, 9999(9999):808–819, 2008.

N. Takata, S. Saito, C. T. Saito, and M. Uemura. Phylogenetic footprint of the plant clock system in angiosperms: evolutionary processes of pseudo-response regulators. *BMC Evolutionary Biology*, 10(Loop I):126, 2010.

S. C. Thain, A. Hall, and A. J. Millar. Functional independence of circadian clocks that regulate plant gene expression. *Current Biology*, 10(16):951–956, aug 2000.

S. C. Thain, F. Vandenbussche, L. J. J. Laarhoven, M. J. Dowson-Day, Z.-Y. Wang, E. M. Tobin, F. J. M. Harren, A. J. Millar, D. Van Der Straeten, and D. V. D. Straeten. Circadian rhythms of ethylene emission in Arabidopsis. *Plant Physiology*, 136(3):3751–3761, 2004.

The Arabidopsis Genome Initiative. Analysis of the genome sequence of the flowering plant Arabidopsis thaliana. *Nature*, 408(6814):796–815, 2000.

B. Thines and F. G. Harmon. Ambient temperature response establishes ELF3 as a required component of the core Arabidopsis circadian clock. *Proceedings of the National Academy of Sciences*, 107(7):3257–3262, feb 2010.

K. Tomioka and A. Matsumoto. A comparative view of insect circadian clock systems. *Cellular and Molecular Life Sciences*, 67(9):1397–1406, 2010.

R. Toth, E. Kevei, A. Hall, A. J. Millar, and F. Nagy. Circadian Clock-Regulated Expression of Phytochrome and Cryptochrome Genes in Arabidopsis. *Plant Physiology*, 127(December):1607–1616, 2001.

F. E. Tracy, M. Gilliham, A. N. Dodd, A. A. R. Webb, and M. Tester. NaCl-induced changes in cytosolic free Ca2+ in Arabidopsis thaliana are heterogeneous and modified by external ionic composition. *Plant, Cell and Environment*, 31:1063–1073, 2008.

L.-S. P. Tran, K. Nakashima, Y. Sakuma, S. D. Simpson, Y. Fujita, K. Maruyama, M. Fujita, M. Seki, K. Shinozaki, and K. Yamaguchi-Shinozaki. Isolation and functional analysis of Arabidopsis stress-inducible NAC transcription factors that bind to a drought-responsive cis-element in the early responsive to dehydration stress 1 promoter. *The Plant Cell*, 16(9):2481–2498, 2004.

L. S. P. Tran, K. Nakashima, Y. Sakuma, Y. Osakabe, F. Qin, S. D. Simpson, K. Maruyama, Y. Fujita, K. Shinozaki, and K. Yamaguchi-Shinozaki. Co-expression of the stress-inducible zinc finger homeodomain ZFHD1 and NAC transcription factors enhances expression of the ERD1 gene in Arabidopsis. *The Plant Journal*, 49(1): 46–63, 2007.

A. Turner, J. Beales, S. Faure, R. P. Dunford, and D. A. Laurie. The pseudo-response regulator Ppd-H1 provides adaptation to photoperiod in barley. *Science*, 310(5750): 1031–1034, 2005.

A. Untergasser, H. Nijveen, X. Rao, T. Bisseling, R. Geurts, and J. A. M. Leunissen. Primer3Plus, an enhanced web interface to Primer3. *Nucleic Acids Research*, 35 (SUPPL.2), 2007.

A. Untergasser, I. Cutcutache, T. Koressaar, J. Ye, B. C. Faircloth, M. Remm, and S. G. Rozen. Primer3-new capabilities and interfaces. *Nucleic Acids Research*, 40(15):1–12, 2012.

F. Valverde, A. Mouradov, W. Soppe, D. Ravenscroft, A. Samach, and G. Coupland. Photoreceptor regulation of CONSTANS protein in photoperiodic flowering. *Science*, 303(5660):1003–1006, 2004.

G. T. van der Horst, M. Muijtjens, K. Kobayashi, R. Takano, S. Kanno, M. Takao, J. de Wit, a. Verkerk, a. P. Eker, D. van Leenen, R. Buijs, D. Bootsma, J. H. Hoeijmakers, and a. Yasui. Mammalian Cry1 and Cry2 are essential for maintenance of circadian rhythms. *Nature*, 398(6728):627–630, 1999.

W. Van Leeuwen, M. J. M. Hagendoorn, T. Ruttink, R. Van Poecke, L. H. W. Van der Plas, and a. R. Van der Krol. The Use of the Luciferase Reporter System for in Planta Gene Expression Studies. *Plant Molecular Biology Reporter*, 18:143a–143t, 2000.

E. Van Praag, R. Degli Agosti, and R. Bachofen. Rhythmic activity of uptake hydrogenase in the prokaryote Rhodospirillum rubrum. *Journal of biological rhythms*, 15(3): 218–224, 2000.

R. Van Wijk, A. Scordino, A. Triglia, and F. Musumeci. 'Simultaneous' measurements of delayed luminescence and chloroplast organization in Acetabularia acetabulum. *Journal of Photochemistry and Photobiology B: Biology*, 49(2-3):142–149, apr 1999.

S. Vandevyver, L. Dejager, and C. Libert. On the Trail of the Glucocorticoid Receptor: Into the Nucleus and Back. *Traffic*, 13(3):364–374, 2012.

U. Voß, M. H. Wilson, K. Kenobi, P. D. Gould, F. C. Robertson, W. a. Peer, M. Lucas, K. Swarup, I. Casimiro, T. J. Holman, D. M. Wells, B. Péret, T. Goh, H. Fukaki, T. C. Hodgman, L. Laplaze, K. J. Halliday, K. Ljung, A. S. Murphy, A. J. Hall, A. a. R. Webb, and M. J. Bennett. The circadian clock rephases during lateral root organ initiation in Arabidopsis thaliana. *Nature Communications*, 6(May):7641, 2015.

H. Wang, X. Bian, L. Xia, X. Ding, R. Muller, Y. Zhang, J. Fu, and A. F. Stewart. Improved seamless mutagenesis by recombineering using ccdB for counterselection. *Nucleic Acids Research*, 42(5), 2014a.

L. Wang, J. Kim, and D. E. Somers. Transcriptional corepressor TOPLESS complexes with pseudoresponse regulator proteins and histone deacetylases to regulate circadian transcription. *Proceedings of the National Academy of Sciences*, 110(2):761–766, jan 2013.

R. Wang, S. Xiang, Y. Zhang, Q. Chen, Y. Zhong, and S. Wang. Development of a functional antibody by using a green fluorescent protein frame as the template. *Applied and Environmental Microbiology*, 80(14):4126–37, jul 2014b.

W. Wang, J. Y. Barnaby, Y. Tada, H. Li, M. Tör, D. Caldelari, D.-u. Lee, X.-D. Fu, and X. Dong. Timing of plant immune responses by a central circadian regulator. *Nature*, 470(7332):110–4, mar 2011.

Z. Y. Wang and E. M. Tobin. Constitutive expression of the CIRCADIAN CLOCK ASSOCIATED 1 (CCA1) gene disrupts circadian rhythms and suppresses its own expression. *Cell*, 93(7):1207–1217, jun 1998.

D. Weigel and J. Glazebrook. Transformation of Agrobacterium Using the Freeze-Thaw Method. *Cold Spring Harbor Protocols*, 2006(30):pdb.prot4666–pdb.prot4666, dec 2006.

J. L. Weller, L. Chee, V. F. G. Hecht, V. Rajandran, R. E. Laurie, S. Ridge, L. C. Liew, V. F. G. Hecht, V. Rajandran, R. E. Laurie, S. Ridge, B. Wenden, J. K. Vander Schoor, O. Jaminon, C. Blassiau, M. Dalmais, C. Rameau, A. Bendahmane, R. C. Macknight, and I. Lejeune-Hénaut. A conserved molecular basis for photoperiod adaptation in two temperate legumes. *Proceedings of the National Academy of Sciences*, 109(51): 21158–63, 2012.

B. Wenden, D. L. K. Toner, S. K. Hodge, R. Grima, and A. J. Millar. Spontaneous spatiotemporal waves of gene expression from biological clocks in the leaf, apr 2012.

S. Wenkel, F. Turck, K. Singer, L. Gissot, J. Le Gourrierec, A. Samach, and G. Coupland. CONSTANS and the CCAAT box binding complex share a functionally important domain and interact to regulate flowering of Arabidopsis. *The Plant Cell*, 18(11): 2971–2984, nov 2006a.

S. Wenkel, F. Turck, K. Singer, L. Gissot, J. Le Gourrierec, A. Samach, and G. Coupland. CONSTANS and the CCAAT box binding complex share a functionally important domain and interact to regulate flowering of Arabidopsis. *The Plant Cell*, 18(11): 2971–2984, 2006b.

F. Went and K. V. Thimann. *Phytohormones*. The Macmillan Company, New York, NY, 1937.

D. Winter, B. Vinegar, H. Nahal, R. Ammar, G. V. Wilson, and N. J. Provart. An "electronic fluorescent pictograph" Browser for exploring and analyzing large-scale biological data sets. *PLoS ONE*, 2(8):1–12, 2007.

M. A. Woelfle, Y. Ouyang, K. Phanvijhitsiri, and C. H. Johnson. The adaptive value of circadian clocks: An experimental assessment in cyanobacteria. *Current Biology*, 14: 1481–1486, 2004.

Q. Xie, P. Lou, V. Hermand, R. Aman, H. J. Park, D.-j. Yun, W. Y. Kim, M. J. Salmela, B. E. Ewers, C. Weinig, S. L. Khan, D. L. P. Schaible, C. R. McClung, H. Jin, D.-j. Yun, and W. Yeon. Allelic polymorphism of GIGANTEA is responsible for naturally occurring variation in circadian period in Brassica rapa. *Proceedings of the National Academy of Sciences*, 112(12):201421803, 2015.

X. Xu, C. T. Hotta, A. N. Dodd, J. Love, R. Sharrock, Y. W. Lee, Q. Xie, C. H. Johnson, and A. A. Webb. Distinct Light and Clock Modulation of Cytosolic Free Ca2+ Oscillations and Rhythmic CHLOROPHYLL A/B BINDING PROTEIN2 Promoter Activity in Arabidopsis. *The Plant Cell*, 19(11):3474–3490, nov 2007.

Y. Xu, T. Mori, and C. H. Johnson. Cyanobacterial circadian clockwork: roles of KaiA, KaiB and the kaiBC promoter in regulating KaiC. *The EMBO Journal*, 22(9):2117–26, may 2003.

E. Yakir, D. Hilman, I. Kron, M. Hassidim, N. Melamed-Book, and R. M. Green. Post-translational regulation of CIRCADIAN CLOCK ASSOCIATED1 in the circadian oscillator of Arabidopsis. *Plant Physiology*, 150(2):844–857, jun 2009.

T. Yamashino, A. Matsushika, T. Fujimori, S. Sato, T. Kato, S. Tabata, and T. Mizuno. A link between circadian-controlled bHLH factors and the APRR1/TOC1 quintet in Arabidopsis thaliana. *Plant and Cell Physiology*, 44(6):619–629, 2003.

Y. Yang, Q. Peng, G.-x. X. Chen, X.-h. H. Li, and C.-y. Y. Wu. OsELF3 Is involved in circadian clock regulation for promoting flowering under long-day conditions in rice. *Molecular Plant*, 6(1):202–215, aug 2013.

M. J. Yanovsky and S. a. Kay. Living by the calendar: how plants know when to flower. *Nature reviews. Molecular cell biology*, 4(4):265–275, 2003.

M. J. Yanovsky, G. C. Whitelam, and J. J. Casal. fhy3-1 retains inductive responses of phytochrome A. *Plant Physiology*, 123(1):235–242, 2000.

M. J. Yanovsky, M. A. Mazzella, G. C. Whitelam, and J. J. Casal. Resetting of the circadian clock by phytochromes and cryptochromes in Arabidopsis. *Journal of Biological Rhythms*, 16(6):523–530, 2001.

M. Yasuhara, S. Mitsui, H. Hirano, R. Takanabe, Y. Tokioka, N. Ihara, A. Komatsu, M. Seki, K. Shinozaki, and T. Kiyosue. Identification of ASK and clock-associated proteins as molecular partners of LKP2 (LOV kelch protein 2) in Arabidopsis. *Journal of Experimental Botany*, 55(405):2015–27, sep 2004.

K. Yoshiyama, P. a. Conklin, N. D. Huefner, and A. B. Britt. Suppressor of gamma response 1 (SOG1) encodes a putative transcription factor governing multiple responses to DNA damage. *Proceedings of the National Academy of Sciences*, 106(31):12843–12848, 2009.

K. O. Yoshiyama, S. Kimura, H. Maki, A. B. Britt, and M. Umeda. The role of SOG1, a plant-specific transcriptional regulator, in the DNA damage response. *Plant Signaling & Behavior*, 9:e28889, 2014.

M. T. Zagotta, K. a. Hicks, C. I. Jacobs, J. C. Young, R. P. Hangarter, and D. R. Meeks-Wagner. The Arabidopsis ELF3 gene regulates vegetative photomorphogenesis and the photoperiodic induction of flowering. *Plant Journal*, 10(4):691–702, 1996.

S. Zakhrabekova, S. P. Gough, I. Braumann, a. H. Muller, J. Lundqvist, K. Ahmann, C. Dockter, I. Matyszczak, M. Kurowska, a. Druka, R. Waugh, a. Graner, N. Stein, B. Steuernagel, U. Lundqvist, and M. Hansson. Induced mutations in circadian clock regulator Mat-a facilitated short-season adaptation and range extension in cultivated barley. *Proceedings of the National Academy of Sciences*, 109(11):4326–4331, 2012.

M. N. Zeilinger, E. M. Farré, S. R. Taylor, S. A. Kay, and F. J. Doyle. A novel computational model of the circadian clock in Arabidopsis that incorporates PRR7 and PRR9. *Molecular Systems Biology*, 2:58, nov 2006.

H. Zhai, X. Bai, Y. Zhu, Y. Li, H. Cai, W. Ji, Z. Ji, X. Liu, X. Liu, and J. Li. A single-repeat R3-MYB transcription factor MYBC1 negatively regulates freezing tolerance in Arabidopsis. *Biochemical and Biophysical Research Communications*, 394(4):1018–1023, 2010.

C. Zhang, Q. Xie, R. G. Anderson, G. Ng, N. C. Seitz, T. Peterson, C. R. McClung, J. M. McDowell, D. Kong, J. M. Kwak, and H. Lu. Crosstalk between the Circadian Clock and Innate Immunity in Arabidopsis. *PLoS Pathogens*, 9(6), jan 2013.

W. Zhang, R.-G. Zhou, Y.-J. Gao, S.-Z. Zheng, P. Xu, S.-Q. Zhang, and D.-Y. Sun. Molecular and genetic evidence for the key role of AtCaM3 in heat-shock signal transduction in Arabidopsis. *Plant Physiology*, 149(April):1773–1784, 2009.

Y. Zhang, Z. Liu, L. Wang, S. Zheng, J. Xie, and Y. Bi. Sucrose-induced hypocotyl elongation of Arabidopsis seedlings in darkness depends on the presence of gibberellins. *Journal of Plant Physiology*, 167(14):1130–1136, 2010.

J. Zhao, X. Huang, X. Ouyang, W. Chen, A. Du, L. Zhu, S. Wang, X. W. Deng, and S. Li. OsELF3-1, an ortholog of arabidopsis EARLY FLOWERING 3, regulates rice circadian rhythm and photoperiodic flowering. *PLoS ONE*, 7(8):e43705, aug 2012.

Y. Zhao, S. K. Christensen, C. Fankhauser, J. R. Cashman, J. D. Cohen, D. Weigel, and J. Chory. A role for flavin monooxygenase-like enzymes in auxin biosynthesis. *Science*, 291(5502):306–309, 2001.

M. Zhou, W. Wang, S. Karapetyan, M. Mwimba, J. Marqués, N. E. Buchler, and X. Dong. Redox rhythm reinforces the circadian clock to gate immune response. *Nature*, 2015.

T. Zielinski, A. M. Moore, E. Troup, K. J. Halliday, and A. J. Millar. Strengths and limitations of period estimation methods for circadian data. *PLoS ONE*, 9(5):e85754, jan 2014.

P. Zimmermann, M. Hirsch-hoffmann, L. Hennig, and W. Gruissem. GENEVESTIGATOR. Arabidopsis Microarray Database and Analysis Toolbox. *Plant Physiology*, 136 (September):2621–2632, 2004.